Handbook of Green Chemistry

Edited by Paul T. Anastas

WILEY-VCH

Green Catalysis

Volume 1: Homogeneous Catalysis

Volume Editor:
Robert H. Crabtree

Handbook of Green Chemistry

Volume 1
Homogeneous Catalysis

Volume Edited by
Robert H. Crabtree

Related Titles

Wasserscheid, P., Welton, T. (eds.)

Ionic Liquids in Synthesis

2nd Edition
2008
ISBN: 978-3-527-31239-9

Sheldon, R. A., Arends, I., Hanefeld, U.

Green Chemistry and Catalysis

2007
ISBN: 978-3-527-30715-9

Cornils, B., Herrmann, W. A., Muhler, M., Wong, C.-H. (eds.)

Catalysis from A - Z

A Concise Encyclopedia

3rd Edition
2007
ISBN: 978-3-527-31438-6

Loupy, A. (ed.)

Microwaves in Organic Synthesis

2nd Edition
2006
ISBN: 978-3-527-31452-2

Kappe, C. O., Stadler, A., Mannhold, R., Kubinyi, H., Folkers, G. (eds.)

Microwaves in Organic and Medicinal Chemistry

2005
ISBN: 978-3-527-31210-8

Copyrighted Material

Handbook of Green Chemistry

Volume 1
Homogeneous Catalysis

Volume Edited by Robert H. Crabtree

WILEY-VCH Verlag GmbH & Co. KGaA

The Editor

Prof. Dr. Paul T. Anastas
Yale University
Center for Green Chemistry & Green Engineering
225 Prospect Street
New Haven, CT 06520
USA

Volume Editor

Prof. Dr. Robert H. Crabtree
Yale University
Department of Chemistry
225 Prospect St.
New Haven, CT 06520-8107
USA

Handbook of Green Chemistry – Green Catalysis
Vol. 1: Homogenous Catalysis
ISBN: 978-3-527-32496-5
Vol. 2: Heterogenous Catalysis
ISBN: 978-3-527-32497-2
Vol. 3: Biocatalysis
ISBN: 978-3-527-32498-9

Set I (3 volumes):
ISBN: 978-3-527-31577-2

Handbook of Green Chemistry
Set (12 volumes):
ISBN: 978-3-527-31404-1

Library of Congress Card No.:
applied for

British Library Cataloguing-in-Publication Data
A catalogue record for this book is available from the British Library.

Bibliographic information published by the Deutsche Nationalbibliothek
The Deutsche Nationalbibliothek lists this publication in the Deutsche Nationalbibliografie; detailed bibliographic data are available on the Internet at http://dnb.d-nb.de.

Typesetting Thomson Digital, Noida, India
Printing betz-druck GmbH, Darmstadt
Binding Litges & Dopf GmbH, Heppenheim
Cover Design Adam-Design, Weinheim

Printed in the Federal Republic of Germany
Printed on acid-free paper

ISBN: 978-3-527-32496-5

Contents

Handbook of Green Chemistry, Volume 1: Homogeneous Catalysis. Edited by Robert H. Crabtree

ISBN: 978-3-527-32496-5

About the Editors

Series Editor

Paul T. Anastas joined Yale University as Professor and serves as the Director of the Center for Green Chemistry and Green Engineering there. From 2004–2006, Paul was the Director of the Green Chemistry Institute in Washington, D.C. Until June 2004 he served as Assistant Director for Environment at the White House Office of Science and Technology Policy where his responsibilities included a wide range of environmental science issues including furthering international public-private cooperation in areas of Science for Sustainability such as Green Chemistry. In 1991, he established the industry-government-university partnership Green Chemistry Program, which was expanded to include basic research, and the Presidential Green Chemistry Challenge Awards. He has published and edited several books in the field of Green Chemistry and developed the 12 Principles of Green Chemistry.

Volume Editor

Robert Crabtree took his first degree at Oxford, did his Ph.D. at Sussex and spent four years in Paris at the CNRS. He has been at Yale since 1977. He has chaired the Inorganic Division at ACS, and won the ACS and RSC organometallic chemistry prizes. He is the author of an organometallic textbook, and is the editor-in-chief of the Encyclopedia of Inorganic Chemistry and Comprehensive Organometallic Chemistry. He has contributed to C-H activation, H_2 complexes, dihydrogen bonding, and his homogeneous tritiation and hydrogenation catalyst is in wide use. More recently, he has combined molecular recognition with CH hydroxylation to obtain high selectivity with a biomimetic strategy.

Handbook of Green Chemistry, Volume 1: Homogeneous Catalysis. Edited by Robert H. Crabtree

ISBN: 978-3-527-32496-5

List of Contributors

Hans-Ulrich Blaser
Solvias AG
P.O. Box 4002
Basel
Switzerland

John F. Bower
University of Texas at Austin
Department of Chemistry and Biochemistry
1 University Station A5300
Austin, TX 78712
USA

Geoffrey W. Coates
Cornell University
Department of Chemistry and Chemical Biology
Ithaca, NY 14853
USA

Terrence J. Collins
Carnegie Mellon University
Institute for Green Science
4400 Fifth Avenue
Pittsburgh, PA 15213
USA

Peter I. Dalko
Université Paris Descartes
Laboratoire de Chimie et Biochimie Pharmacologiques et Toxicologiques
UMR 8601
75270 Paris
France

Jairton Dupont
UFRGS
Institute of Chemistry
Laboratory of Molecular Catalysis
avenue Bento Goncalves
9500 Porto Alegre
France

Frédéric Favre
IFP-Lyon
Rond Point de l'Échangeur de Solaize – BP 3
69360 Solaize
France

Fabricio R. Flores
UFRGS
Institute of Chemistry
Laboratory of Molecular Catalysis
avenue Bento Goncalves
9500 Porto Alegre
France

Handbook of Green Chemistry, Volume 1: Homogeneous Catalysis. Edited by Robert H. Crabtree

ISBN: 978-3-527-32496-5

Alain Forestière
IFP-Lyon
Rond Point de l'Échangeur de Solaize – BP 3
69360 Solaize
France

John A. Gladysz
Texas A&M University
Department of Chemistry
P.O. Box 30012
College Station, TX 77842-3012
USA

Garrett Hoge
Solvias AG
P.O. Box 4002
Basel
Switzerland

François Hugues
IFP-Lyon
Rond Point de l'Échangeur de Solaize – BP 3
69360 Solaize
France

Ryan C. Jeske
Cornell University
Department of Chemistry and Chemical Biology
Ithaca, NY 14853
USA

Sushil K. Khetan
Carnegie Mellon University
Institute for Green Science
4400 Fifth Avenue
Pittsburgh, PA 15213
USA

Michael J. Krische
University of Texas at Austin
Department of Chemistry and Biochemistry
1 University Station A5300
Austin, TX 78712
USA

Mats Larhed
Uppsala University
Department of Medicinal Chemistry
Organic Pharmaceutical Chemistry
BMC
Box 574
75123 Uppsala
Sweden

Isabelle McCort-Tranchepain
Université Paris Descartes
Laboratoire de Chimie et Biochimie Pharmacologiques et Toxicologiques
UMR 8601
75270 Paris
France

Audrey Moores
McGill University
Department of Chemistry
801 Sherbrooke Street West
Montreal
QC, H3A 2K6
Canada

Christian Müller
Eindhoven University of Technology
Schuit Institute of Catalysis
Laboratory of Homogeneous Catalysis
Den Dolech 2
P.O. Box 513
5600 MB Eindhoven
The Netherlands

Luke R Odell
Uppsala University
Department of Medicinal Chemistry
Organic Pharmaceutical Chemistry
BMC
Box 574
75123 Uppsala
Sweden

Hélène Olivier-Bourbigou
IFP-Lyon
Rond Point de l'Échangeur de Solaize – BP 3
69360 Solaize
France

Walt Partenheimer
E.I. DuPont de Nemours & Co., Inc.
Central Research and Development
Experimental Station
Wilmington, DE 19880-0328
USA

Morgane Petit
Université Paris Descartes
Laboratoire de Chimie et Biochimie
Pharmacologiques et Toxicologiques
UMR 8601
75270 Paris
France

Martyn Poliakoff
University of Nottingham
School of Chemistry
University Park
Nottingham, NG7 2RD
UK

Benoît Pugin
Solvias AG
P.O. Box 4002
Basel
Switzerland

Alexander D. Ryabov
Carnegie Mellon University
Institute for Green Science
4400 Fifth Avenue
Pittsburgh, PA 15213
USA

Felix Spindler
Solvias AG
P.O. Box 4002
Basel
Switzerland

Dieter Vogt
Eindhoven University of Technology
Schuit Institute of Catalysis
Laboratory of Homogeneous Catalysis
Den Dolech 2
P.O. Box 513
5600 MB Eindhoven
The Netherlands

1
Atom Economy – Principles and Some Examples

Audrey Moores

1.1
Introduction

As many other human activities, chemistry has seen most of its progress being triggered by a constant desire to do things *better*. The word 'better' here is a general term that can encompass concepts as varied as 'that allows better theoretical understanding', 'that allows companies to make significant savings when they use the process in question' or 'that saves the experimentalist a lot of strenuous steps in a given synthesis'. Environmental and health-related issues have also been a major drive, in addition to the desire to reduce waste. The Leblanc process [1], one of the first industrial chemical processes, is a good example of this early concern. It provided a route to sodium carbonate, a vital chemical for the development of the textile industry in the early nineteenth century. It was phased out half a century later, due to the combined action of a legislation restricting the right to produce the wasteful hydrochloric acid and calcium sulfide provided by the process, but also to the finding of a cost-effective and less wasteful solution: the Solvay process. The history of chemistry is full of such examples where new methodologies would bring about significant improvements to existing ones. Yet, the main focus of chemists' attention has varied over time, in other words, *better* has not always meant exactly the same thing. The constant pressure to reach new molecular targets has led to a lot of effort being put into seeking high yields. Activation of specific sites, chemo- and regioselectivity, is also a crucial quality in a process. Synthetic challenges were indeed justifying this trend. 'Make it work' was the motto. No doubt it was often followed by 'make it good, too' but only 'if you can'. In 1991, though, Trost suggested starting to look at things with a different approach [2]. He presented a set of guidelines to assess the efficiency of a given process, by looking at the number of atoms of the reagent(s) actually ending up in the desired product(s). Atom economy was introduced. In addition to good yield and selectivity (regio-, chemo- and enantioselectivity), atom economy became the third element of the triadic goal that any synthetic chemist should seek. By analogy with the yield, which is an absolute measure, atom economy

Green Catalysis, Volume 1: Homogeneous Catalysis.
Edited by Robert H. Crabtree

ISBN: 978-3-527-32496-5

needed a quantitative criterion to allow comparison and discussion. In Section 1.2.2, some of the proposed criteria will be introduced. Although atom economy is a very simple concept, it nonetheless implied the development of a new and ambitious chemistry [3]. Making it happen involves a fresh look at molecular reactivity: activating groups should be minimized, such as stoichiometric reagents. In this chapter, the principle of atom economy is first presented. A scientific context will provide an avenue to the definition of its criteria. Impact on industry and the tool box of atom economy will also be discussed. Second, some examples using C–H activation will be described.

1.2
Principle of Atom Economy

1.2.1
Atom Economy: a Pillar of Green Chemistry

The concept of atom economy [4], and the idea of making it a primary criterion for improvement in chemistry, is a part of the green chemistry movement that was impulsed by Anastas from the early 1990s [5–7]. Then, growing environmental awareness pushed chemists to question their practice and led them to reassess the criteria of chemistry evaluation: it then obviously became necessary to look at a chemical reaction in a more global manner [8], considering aspects such as the origin of the reactants, the amount of energy necessary to make it work and the outcome of the generated waste. Thus 12 principles of green chemistry [6] were enounced, and since then chemists have used them as guidelines. The 12 principles as worded by Sheldon *et al*. [4] are as follows:

1. waste prevention instead of remediation
2. atom efficiency
3. less hazardous/toxic chemicals
4. safer products by design
5. innocuous solvents and auxiliaries
6. energy efficiency by design
7. preferably renewable materials
8. shorter synthesis – avoiding derivatization
9. catalytic rather than stoichiometric reagents
10. designing products for degradation
11. analytical methodologies for pollution prevention
12. inherently safer processes.

Waste minimization (principle 1) stands as one of the pillars of these principles, because it proposes to reduce the amount of 'unused' matter – i.e. matter that will not end up in the desired product – in a given process. 'Unused' matter, or waste, is of various natures. Solvents (principle 5) fall in that category and research on greener solvents and solventless processes is therefore a significant part of green chemistry.

However, waste also comes from the stoichiometric reagents (principle 9) necessary to promote chemical reactions and from the activating groups on reagents (principle 8). This analysis reveals how several of the 12 principles can be intertwined and beneficially interact with one another. In the frame of atom economy (principle 2), we propose to tackle these sources of waste, so that most of the matter introduced in a process is actually present in the final product. By doing that, we obviously reduce the waste generated, but we also improve the process at other levels: having less matter to manipulate diminishes the energy input (no need to heat up an atom that will not be in the product . . .), the size of the batches, the required amount of solvent, etc.

1.2.2
Principle and Criteria [4]

Atom economy demands minimization of the quantity of matter that will not be in the desired product at the end. Several criteria exist to assess how atom economical a given chemical reaction can be. They differ in what they take into account to evaluate the reaction efficiency. The simplest one was introduced by Trost in 1991 and is called simply, atom economy (AE) [2, 9]. This criterion can be assessed simply by looking at a chemical reaction on paper. It is the ratio between the mass of desired product to the total mass of products, expressed as a percentage (Scheme 1.1). The second is called the *E*-factor and was devised by Sheldon in 1992 [10]. It is the ratio between the mass

Considered reaction:

$$A + B \xrightarrow[\text{Solvents}]{\text{Additives}} C + D$$

C is the desired product

$$\textbf{Atom economy} = \frac{\text{Mass of C}}{\text{Mass of C + D}} \%$$

Optimal atom economy is 100%

$$\textbf{\textit{E}-factor} = \frac{\text{Mass of waste}}{\text{Mass of desired product}}$$

Optimal *E*-factor is 0

Waste = D + unconverted A and B + additives and solvent losses + fuel...

$$\textbf{Mass intensity} = \frac{\text{Total mass of material used}}{\text{Mass of desired product}}$$

Optimal MI is 1

$$\textbf{Effective mass yield} = \frac{\text{Mass of desired product}}{\text{Total mass of material used}} \%$$

Optimal EMY is 100%

Scheme 1.1 Selected atom economy criteria.

of all the generated waste to the mass of desired product (Scheme 1.1). This criterion takes into account anything that is not the desired product: from stoichiometric waste to solvent losses, additives and even the fuel required for energy input when it is possible to have access to this data. It also takes into account the losses due to imperfect yield. It is important to point out that water is not considered in the calculation of the *E*-factor, since it is considered innocuous. In principle, it sounds fair to ignore water, although one should keep in mind that a significant source of pollution rises from waste water streams that have not been properly depolluted prior to release into the environment

In contrast to AE, it is often challenging to evaluate the *E*-factor of a given reaction, since it necessitates being aware of many of the industrial features of a process. In addition, for a given process, it can also vary from one plant to another, due to technical variations. On the other hand, the *E*-factor constitutes a more meaningful criterion of the environmental friendliness of an industrial process. By construction, the smaller the *E*-factor, the better is the process. Table 1.1 summarizes orders of magnitude for the *E*-factors obtained for various sectors of industry. The *E*-factor is a maximum for pharmaceutical production. The number of steps involved in such syntheses substantially justifies this trend. As a consequence, the study of reactions that are both selective and designed for unactivated and unprotected reagents concentrates many efforts (see the examples presented in Section 1.3). Curzons and co-workers introduced another criterion called mass intensity (MI) [11, 12]. This is defined as the ratio of all the material used to the mass of desired product (Scheme 1.1). This criterion is equal to the *E*-factor + 1.

The effective mass yield (EMY) was introduced by Hudlicky *et al.* [13]. It is the percentage of desired product of the material introduced in the process (Scheme 1.1). It is exactly equal to the inverse of MI, expressed as a percentage. Other authors call this criterion reaction mass efficiency (RME). In their criterion, however, Hudlicky *et al.* propose not to consider just benign waste, such as water, but also alcohols, acetone, acetic acid and NaCl [13]. This proposal has been questioned by others [4] and it illustrates well a limitation of any environmental criterion: these metrics only allow one to consider an unused material as either a waste, with a weight of 1, or as innocuous, with a weight of 0. In fact, reality is more subtle: although environmentally benign in small quantity, some materials might constitute a threat in large bulk quantities; in more general terms, the relative toxicity of waste is ignored by these criteria. None of the above-mentioned criteria assesses this point properly and there

Table 1.1 *E*-factor for various sectors of industry [4].

Industry sector	Product tonnage	*E*-factor
Oil refining	10^6–10^8	<0.1
Bulk chemicals	10^4–10^6	<1–5
Fine chemicals	10^2–10^4	5–50
Pharmaceuticals	10–10^3	25–100

is a need to improve the concept in that direction. An attempt to tackle this issue led to the introduction of an unfriendliness quotient, *Q*, that can be multiplied with the *E*-factor [14]. The resulting environmental quotient takes into account the toxicity and hazards associated with waste. Several other criteria have been suggested, such as carbon efficiency (CE), atom utilization (AU) and environmental or elegance quotient (EQ). Andraos, in a review, proposed a unified view of these factors [15].

Like a yield, atom economy criteria provide a simple metric to assess a chemical reaction or process. By construction, they evaluate environmental impact and thus promote greener methodologies. However, as with any simple metric, they also lack the breadth of a more thorough analysis where toxicity and energy issues, catalyst recovery and renewable feedstock for reagents are also taken into account. Atom economy is one of the many factors to consider while assessing the greenness of a process.

1.2.3
Impact of Atom Economy on the Chemical Industry [16]

Although some ideas behind green chemistry are almost as old as chemistry itself, the momentum around the green chemistry movement initiated in the 1990s has really impressed a shift towards better practice in industry. Interestingly, chemical companies are starting to advertise green chemistry in their communication strategies (L'Oréal, for instance, currently advertise a cosmetic claiming it was produced in accordance with the principles of 'green chemistry' [17]). As chemists, we should be both satisfied that green chemistry is becoming a widespread concern and cautious because impartial criteria are necessary to award 'green' labels properly. The atom economy concept and the criteria developed with it have undoubtedly played a role in this evolution. In addition, green chemistry often offered a frame to improve the chemical industry that was highly beneficial to itself. Industries saw quickly their interest in promoting atom economy: minimizing the waste diminishes costs associated with treatment, storage and transportation, minimizing potential pollution prevents companies from legal pursuits, regulations become increasingly demanding, diminishing energy input is desirable . . . It is therefore not a surprise if one of the criteria mentioned above was found by Curzons and co-workers at the pharmaceutical company GlaxoSmithKline [11, 12]. A quick survey of the list of the Presidential Green Chemistry Challenge awardees in the category 'Industry sponsor/synthetic pathways' suffices to realize the achievements of atom economical strategies made by chemical companies, for their own benefit, but also for that of consumers and the society overall [18].

1.2.4
Atom Economy Tool Box

As a part of the green chemistry endeavor, atom economy benefits from a tool box of techniques such as catalysis, neotenic solvents and alternative energy. The input of catalysis [4, 19, 20] in the scope of atom economy is almost self-explanatory: all the

stoichiometric additives used to activate a substrate constitute a large part of the waste produced along with solvents and work-up auxiliaries. Catalytic activation was the first big step made for atom economy and continues to prove its power more than half a century after the discovery of Wilkinson's catalyst. [21] The examples proposed in the following are just a few among the myriad of potential possibilities. More recently, researchers have focused their attention on the solvent, as a part of what constitutes a waste in a chemical process. The idea of using more benign solvents [22], such as water [23–27] or supercritical fluids [28, 29], or easily recyclable solvents, such as ionic liquids [30–32], have concentrated an intense research effort. Interestingly, the development of these new reaction media has allowed the discovery of new reactivity and thus new ideas for atom economy. Rideout and Breslow showed, for instance, that the Diels–Alder reaction could be tremendously accelerated in water, compared with the same reaction in organic solvents [33]. This effect is due to the hydrophobicity of the substrates in an aqueous environment. Recently, a C–C cross-coupling reaction between indoles and quinines was obtained in absence of any catalyst, thanks to this effect (Scheme 1.2). This reaction, explained further in Section 1.2.2, occurs through sp^2 C–H activation. Such reactions, where water acts in effect as the catalyst of the reaction, are referred to as 'on-water' [34] and constitute textbook examples of atom economy.

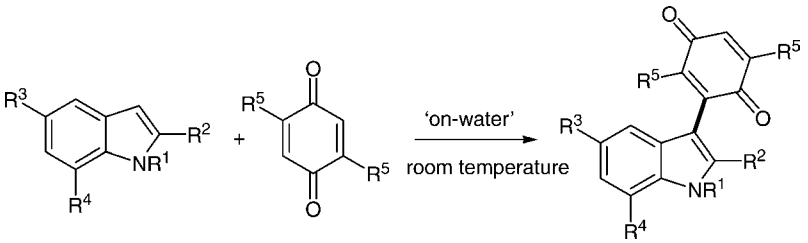

R^1 = H or Me, R^2 = H or alkyl, R^3 = H, OMe or Cl, R^4 = H or Me, R^5 = H, OMe or Cl

Scheme 1.2 'On water'-promoted direct coupling of indoles with quinines (the created bond is highlighted in bold). Adapted from [34].

Sources of energy alternative to conventional heating have also proved interesting. Under microwave heating [35], some reactions can be performed in the absence of a solvent that would be otherwise required for heat transfer [36]. Sonochemistry [37] is also a way to enhance, for instance, Diels–Alder reactions, which are very atom economical reactions [38, 39].

1.3 Atom Economical by Design: Examples of Reactions Relying on C–H Activation

The power of atom economy is to provide processes with as little waste as possible. It often requires the re-invention of *de novo* classical reactions [3]. In the following are presented some examples of recent chemical reactions that exemplify atom economy.

C–H activation is chosen here as the conduct line of this mini-review, although very interesting atom economical processes are of great interest and have been reviewed elsewhere [4, 6, 40], such as Diels–Alder reactions, pericyclic reactions, addition reactions and many others [41, 42]. Two main reaction types will be presented in this section: first, the tandem reaction involving hydrogen transfer, and second, C–C coupling allowed by direct C–H activation.

1.3.1
Tandem Reactions Involving Hydrogen Transfer

A 'tandem reaction' is a 'one-pot' process involving coupled catalyses that occur sequentially and via two (or more) mechanistically distinct processes [43]. Such reactions are of great interest for green chemistry, since they limit the number of work-up steps in a synthesis. In the scope of this chapter, it seemed interesting also to point out their great interest for atom economical applications. In a recent article, Crabtree referred to tandem reactions as being like a 'knight move' in chess: they include several steps in one process and they afford unexpected results [44]. In the following, selected examples of tandem reactions involving hydrogen transfer are presented.

Hydrogen transfer reactions are not naturally associated with the concept of atom economy: typically they are used for a hydrogenation process where the H_2 molecule is provided by an alcohol or another hydrogen-containing substrate. In strict terms, such a reaction is less atom economical than direct hydrogenation with H_2, as can be seen in Scheme 1.3, due to the generation of a wasteful carbonyl compound.

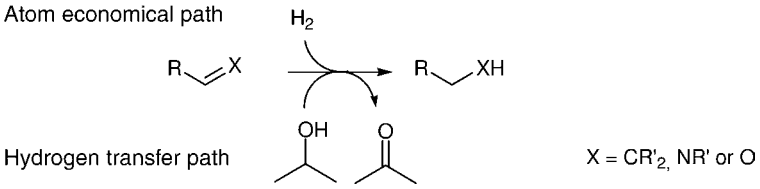

Scheme 1.3 Hydrogen transfer reaction.

However, dihydrogen is a hazardous gas and, even though large chemical companies have experience in handling it, hydrogen transfer constitutes a safe alternative for small-scale applications and academic laboratories [45].

But more interestingly, hydrogen transfer has led in recent years to the development of true atom economical pathways for interesting reactions such as alkylation of amines and C–C couplings. In these strategies, hydrogen transfer processes constitute the first and last steps of a tandem reaction. Williams and co-workers, in a recent review on the concept, denoted this idea 'hydrogen borrowing' [46]. Classically, the series of reactions involves oxidation of a substrate **A**, then the transformation of the resulting unsaturated compound **B** affording **C**, and finally hydrogenation of **C** to furnish the desired product **D** (see Scheme 1.4). This strategy may require the use of an auxiliary to sequester an H_2 molecule in the first step and

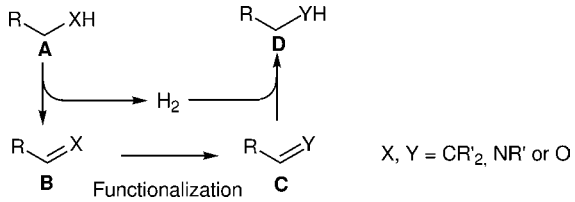

Scheme 1.4 Principle of the tandem hydrogen transfer process.

release it in the last, but most of the time the substrate itself play this role, **C** being able to trap the H_2 release by **A**.

Tandem reactions involving hydrogen transfer have been used to alkylate amines with alcohols. The process relies on the following steps: oxidation of an alcohol into an aldehyde or a ketone, condensation of an amine on to the carbonyl functionality and hydrogenation of the produced imine (Scheme 1.5a). The overall process provides a secondary [47] (tertiary [48]) amine from a primary (secondary) alcohol. This reaction requires the presence of a single catalyst which acts for both the hydrogenation and the dehydrogenation steps: Rh [49], Ir [49, 50] and Ru [47, 48, 51] complexes and heterogeneous catalysts [52] have proved efficient for this reaction. The intermediate dehydration step occurs spontaneously in the reaction medium. With this methodology, alcohols appear as a viable alternative to more toxic alkylating reagents such as halides [46]. It is also possible to create C−N bonds with a similar strategy, by using the power of the aza-Wittig reaction [53]. Similarly, C−C bond formation from alcohols has been achieved by Williams' group [54]. After the first dehydrogenation step, a Wadsworth–Emmons step occurs between the aldehyde and a phosphine oxide to provide an alkene that is then hydrogenated. An Ir complex and cesium carbonate are used as catalysts in this process, respectively.

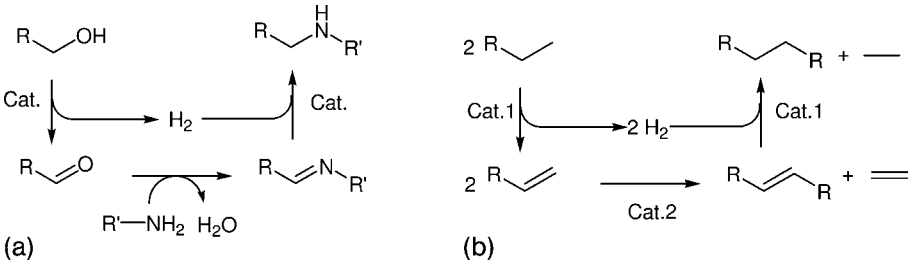

Scheme 1.5 Tandem hydrogen transfer process for (a) a reaction of alkylation of an amine and (b) a reaction of metathesis of an alkane.

In a very elegant manner, Goldman *et al.* used such a strategy to design the long-sought metathesis of alkanes (Scheme 1.5b) [55]. This reaction allows the distribution in weight of mixtures of alkanes that the petroleum industry usually produces to be considerably narrowed. In this example, the alkane is dehydrogenated thanks to an Ir (I)-pincer complex (Cat. 1). A second complex, an Mo Schrock-type catalyst (Cat. 2), is present in the reaction medium and performs a metathesis of the provided alkene.

The third step is hydrogenation of the product of the metathesis, catalyzed by Cat. 1. The whole reaction process is carried out at the moderate temperature of 125 °C. This process converts *n*-hexane into a range of alkanes from C_2 to C_{15}.

1.3.2 Selective C−H Activation for C−C Bond Formation

C−H activation has long been referred to as the Holy Grail of organic chemistry [56]. Among the many applications possible for direct C−H activation, two projects appear as crucial goals for green chemistry. The first is the use of alkanes as a pool of starting material despite their intrinsic stability [57]. The second is the capacity to activate specifically a given C−H bond in a complex and functionalized molecules, without having to use protecting and/or activating groups. From the atom economy perspective, the second point is of great potential and many reviews have covered the numerous advances in this domain [56, 58, 59]. Virtually the history of C−H activation started with transition metal activation of a C−H bond [60–62], followed by catalytic applications of these properties [63, 64], where the activated position could be reacted with a halide [65], an alkene, etc. [58, 59, 66]. More recently, the more challenging activation of two C−H functionalities to C−C couple them in an oxidative fashion was developed (Scheme 1.6): in this strategy, called by Li and co-workers cross-dehydrogenative coupling (CDC) [67, 68], the coupling of the two unactivated carbon centers goes along with elimination of one equivalent of dihydrogen (Scheme 1.6). This reaction is thus facilitated by the presence in the reaction medium of an oxidant to afford water as a side product. Ideally, this oxidant should be molecular oxygen [69], but in many cases oxidants such as peroxides are still necessary [70]. Metal complexes of Cu(I) [67], Pd(II) [71], Fe(II) [72], Au(I/III) [73] and Ru(III) [74] were demonstrated to be active in the catalysis of coupling between sp, sp^2 or sp^3 hybridized carbon centers. Since C−C-forming reactions are of crucial importance in order to set up the backbone of organic compounds [75], this reaction appears as a tremendous breakthrough for atom economical chemistry.

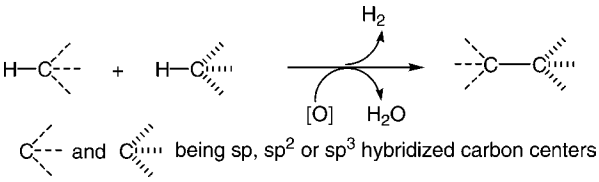

Scheme 1.6 General scheme of cross-dehydrogenative coupling (CDC).

Li and co-workers have published many results in this field, some of which are illustrated in Schemes 1.7 and 1.8, and exemplify couplings of sp–sp^3, sp^2–sp^3 and sp^3–sp^3 carbon atoms [67, 68]. sp–sp^3 coupling proved a successful route to propargylic amines, molecules of interest as synthetic intermediates. CuBr catalyzes the coupling between the sp^3 C−H adjacent to the nitrogen atom and the terminal C−H of an alkyne in the presence of a slight excess of an oxidant, *tert*-butyl hydroperoxide

sp–sp^3 CDC

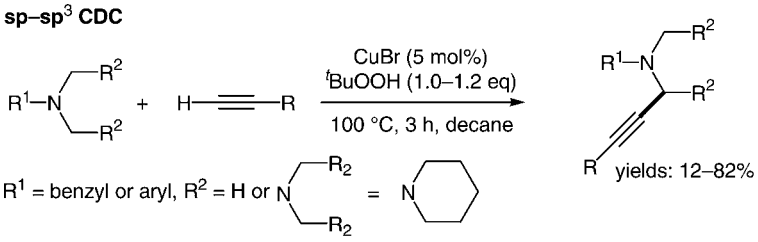

sp^2–sp^3 CDC

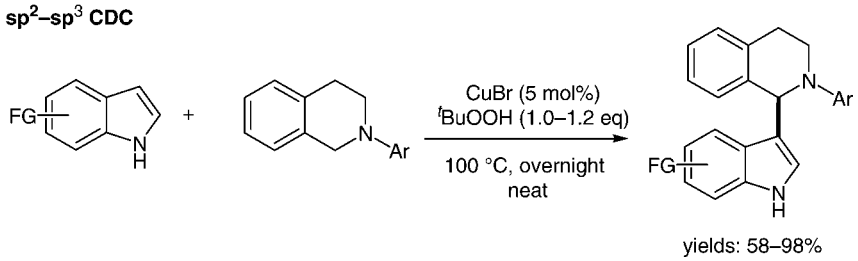

Scheme 1.7 sp–sp^3 and sp^2–sp^{3}cross-dehydrogenative coupling (CDC). (the created bond is highlighted in bold). From [67].

sp^3–sp^3 CDC

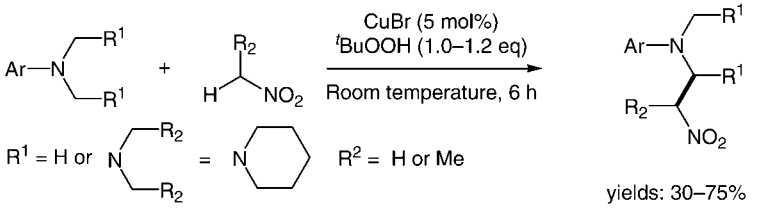

(a)

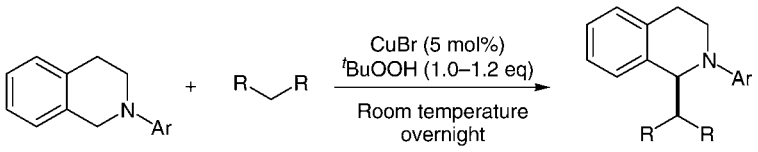

R = CN, COOMe or COOEt

(b)

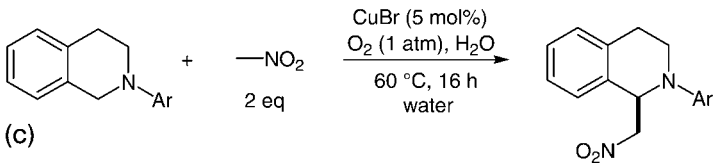

(c)

Scheme 1.8 sp^3–sp^{3}cross-dehydrogenative coupling (CDC) (the created bond is highlighted in bold). From [67].

(TBHP) (Scheme 1.7) [70]. A comparable coupling where the sp substrate is H−CN was published by Murahashi's group using an Ru(III) complex [74, 76].

Li and Li used their CuBr–HBHP system to achieve the coupling of the sp^2 C−H adjacent to the nitrogen atom of an indole with the sp^3 C−H adjacent to the nitrogen of an anime (Scheme 1.7b) [77]. The same group investigated the possibilities of coupling the sp^3 C−H adjacent to the nitrogen of an anime with another sp^3 carbon atom. To achieve this, they chose electron-deficient sp^3 centers, such as the carbon adjacent to a nitro [78], a cyanide or an ester [72] functionality (Scheme 1.8a and b). The reaction is catalyzed by CuBr in the presence of *tert*-butyl hydroperoxide as an oxidant. In a more recent version of this sp^3–sp^3 coupling, molecular oxygen was successfully used as an oxidant and with water as a solvent (Scheme 1.7c) [69], which make this reaction particularly attractive for green chemistry purposes. Finally, coupling of an alkane and sp^3 C−H adjacent to an ester group was made possible using $FeCl_2$ as a catalyst [72].

The next challenge was sp^2–sp^2 cross-coupling and especially the fusion of aromatic rings, a crucial step for the synthesis of pharmaceuticals, natural products and material compounds. The Suzuki reaction has for a long time been the method of choice, despite its limitations in terms of atom economy [79]. In recent work, Fagnou and co-workers demonstrated the feasibility of cross-coupling unactivated arenes (Scheme 1.9a) [71, 80]. The reaction proceeds via C−H activation of two distinct sp^2–sp^2 carbon centers. They used Pd(II) as a catalyst and substrates that have distinct electronic properties, so that they enter the catalytic cycle stepwise, avoiding homocoupling. For this reaction, microwave heating was employed successfully [71]. Hull and Sanford also utilized a Pd(II) complex to catalyze unactivated arene cross-coupling successfully [81]. In this example, C−H activation and regioselectivity are directed by the presence of a pyridine functionality in the substrate. Tse and co-workers evidenced the activity of Au(I/III) complexes for a similar reaction: the homocoupling of arenes with various substitution schemes (Scheme 1.9b) [73].

In the frame of C−H activation, metal carbenoid and nitrenoid insertion have led to very interesting results, as pointed out in a recent review [82]. In this strategy, a

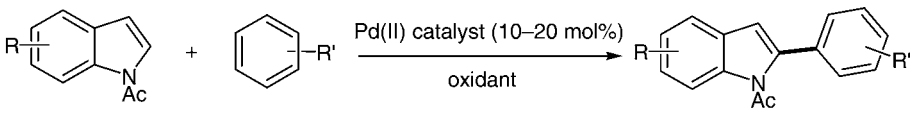

R = H, Me, OMe, Cl, COOMe R' = H, Me, OMe, F Yields: 42–84%

(a)

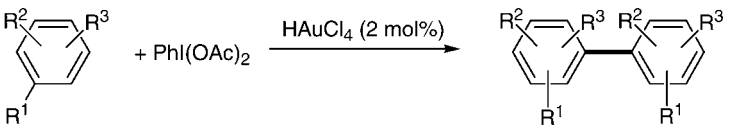

(b)

Scheme 1.9 Principle of carbenoid insertion in C−H bonds. From [81] and [73].

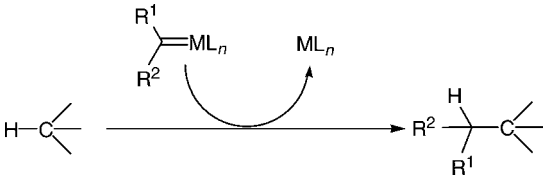

Scheme 1.10 Principle of carbenoid insertion in C−H bonds.

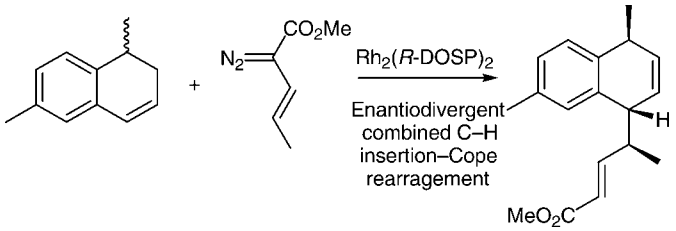

Scheme 1.11 Synthesis of an elisabethatriene precursor by a combined enantiodivergent C−H carbenoid insertion–Cope rearrangement. Adapted from [86].

metal carbenoid was shown to insert into a C−H bond, as presented in Scheme 1.10, without the need for a formal activation of the C−H bond by the metal center.

Early achievements in this field focused on intramolecular reactions, since selectivity was a great challenge. Thus cyclization, involved in biologically active molecule syntheses, was first developed [83, 84]. In 1999, Davies *et al*. reported the direct synthesis of Ritalin (methylphenidate), a treatment for attention deficit hyperactivity disorder, using a dirhodium(II) complex as catalyst [85]. In 2005, the same group developed a combined C−H carbenoid insertion–Cope rearrangement that opens an atom economical path towards *elisabethatrienes*, a family of biologically active compounds(Scheme 1.11). This reaction, catalyzed by an enantiomerically pure dirhodium(II) complex, is remarkable because it allows the introduction of three stereoselective centers in one step [86].

1.4 Conclusion

This chapter has covered only a fraction of the numerous recent advances in the field of atom economy. It is hoped that these examples have demonstrated how boldness in tackling challenging problems, in changing altogether the solvent medium, the reagent utilized and the catalyst, is key to inventing the new methodology that will solely assure progress towards atom economy.

Acknowledgments

I thank the Canada Research Chair Foundation, the Canadian Foundation for Innovation and McGill University for their support.

References

1 Lancaster, M. (2002) *Green Chemistry, an Introductory Text*, Royal Society of Chemistry, Cambridge, p. 22.
2 Trost, B.M. (1991) *Science*, **254** (5037), 1471–1477.
3 Keh, C.C.K. and Li, C.J. (2005) Atom economy, in *Yearbook of Science and Technology*, (ed. M. Licker), McGraw-Hill, New York, pp. 21–23.
4 Sheldon, R.A., Arends, I. and Hanefeld, U. (2007) *Green Chemistry and Catalysis*, Wiley-VCH Verlag GmbH, Weinheim, pp. 1–47.
5 Anastas, P.T. and Kirchhoff, M.M. (2002) *Accounts of Chemical Research*, **35** (9), 686–694.
6 Anastas, P.T. and Warner, J.C. (1998) *Green Chemistry: Theory and Practice*, Oxford University Press, New York.
7 Anastas, P.T. and Williamson, T.C. (1998) *Green Chemistry: Frontiers in Chemical Synthesis and Processes*, Oxford University Press, Oxford.
8 Anastas, P.T. and Kirchhoff, M.M. (2002) *Accounts of Chemical Research*, **35**, 686–693.
9 Trost, B.M. (1995) *Angewandte Chemie (International Edition in English)*, **34** (3), 259–281.
10 Sheldon, R.A. (1992) *Chemistry and Industry*, London (23), 903–906.
11 Curzons, A.D., Constable, D.J.C., Mortimer, D.N. and Cunningham, V.L. (2001) *Green Chemistry*, **3** (1), 1–6.
12 Constable, D.J.C., Curzons, A.D., dos Santos, L.M.F., Geen, G.R., Hannah, R.E., Hayler, J.D., Kitteringham, J., McGuire, M.A., Richardson, J.E., Smith, P., Webb, R.L. and Yu, M. (2001) *Green Chemistry*, **3** (1), 7–9.
13 Hudlicky, T., Frey, D.A., Koroniak, L., Claeboe, C.D. and Brammer, L.E. (1999) *Green Chemistry*, **1** (2), 57–59.
14 Sheldon, R.A. (1994) *Chemotherapy*, 38–47.
15 Andraos, J. (2005) *Organic Process Research & Development*, **9** (2), 149–163.
16 Sheldon, R.A. (2007) *Green Chemistry*, **9** (12), 1273–1283.
17 L'Oréal's marketing campaign for product Skin Genesis© specifically refers to the term Green Chemistry, see for instance www.lorealskin genesis.com (23 October 2008).
18 Lists of Presidential Green Chemistry Challenge awardees are available on the US EPA website, http://www.epa.gov/greenchemistry/pubs/pgcc/past.html.
19 Anastas, P.T., Bartlett, L.B., Kirchhoff, M.M. and Williamson, T.C. (2000) *Catalysis Today*, **55**, (1–2), 11–22.
20 Anastas, P.T., Kirchhoff, M.M. and Williamson, T.C. (2001) *Applied Catalysis A-General*, **221** (1–2), 3–13.
21 Osborn, J.A., Jardine, F.H., Young, J.F. and Wilkinson, G. (1966) *Journal of the Chemical Society A: Inorganic, Physical, Theoretical*, (12), 1711–1732.
22 Andrade, C.K.Z. and Alves, L.M. (2005) *Current Organic Chemistry*, **9** (2), 195–218.
23 Li, C.J. and Chan, T.H. (1997) *Organic Reactions in Aqueous Media*, John Wiley & Sons, Inc, New York.
24 Lindström, U.M. (2007) *Organic Reactions in Water: Principles, Strategies and Applications*, Blackwell, Oxford.
25 Herrerias, C.I., Yao, X., Li, Z. and Li, C.J. (2007) *Chemical Reviews*, **107** (6), 2546–2562.
26 Li, C.J. and Chen, L. (2006) *Chemical Society Reviews*, **35** (1), 68–82.
27 Engberts, J.B.F.N. (2007) Organic Chemistry in water: green and fast, in *Methods and Reagents for Green Chemistry*, (eds P. Tundo, A. Perosa and F. Zecchini), John Wiley & Sons, Inc, Hoboken, NJ, pp. 159–170.
28 Jessop, P.G. and Leitner, W. (1999) *Chemical Synthesis Using Supercritical Fluids*, Wiley-VCH Verlag GmbH, Weinheim.
29 Jessop, P.G. (2006) *Journal of Supercritical Fluids*, **38** (2), 211–231.

30 Miao, W.S. and Chan, T.H. (2006) *Accounts of Chemical Research*, **39** (12), 897–908.

31 Jain, N., Kumar, A., Chauhan, S. and Chauhan, S.M.S. (2005) *Tetrahedron*, **61** (5), 1015–1060.

32 Plechkova, N.V. and Seddon, K.R. (2007) Ionic liquids: 'designer' solvents for green chemistry, in *Methods and Reagents for Green Chemistry,* (eds P. Tundo, A. Perosa and F. Zecchini), John Wiley & Sons, Inc, Hoboken, NJ, pp. 105–130.

33 Rideout, D.C. and Breslow, R. (1980) *Journal of the American Chemical Society*, **102** (26), 7816–7817.

34 Zhang, H.B., Liu, L., Chen, Y.J., Wang, D. and Li, C.J. (2006) *European Journal of Organic Chemistry*, (4), 869–873.

35 Strauss, C.R. and Varma, R.S. (2006) *Microwave Methods in Organic Synthesis*, **266**, 199–231.

36 Cave, G.W.V., Raston, C.L. and Scott, J.L. (2001) *Chemical Communications*, (21), 2159–2169.

37 Mason, T.J. (2007) *Ultrasonics Sonochemistry*, **14** (4), 476–483.

38 Avalos, M., Babiano, R., Cabello, N., Cintas, P., Hursthouse, M.B., Jimenez, J.L., Light, M.E. and Palacios, J.C. (2003) *The Journal of Organic Chemistry*, **68** (19), 7193–7203.

39 Lancaster, M. (2002) *Green Chemistry, an Introductory Text*, Royal Society of Chemistry, Cambridge, pp. 225–228.

40 Lancaster, M. (2002) *Green Chemistry, an Introductory Text*, Royal Society of Chemistry, Cambridge, pp. 8–13.

41 Trost, B.M., Frederiksen, M.U. and Rudd, M.T. (2005) *Angewandte Chemie-International Edition*, **44** (41), 6630–6666.

42 Trost, B.M. (2002) *Accounts of Chemical Research*, **35** (9), 695–705.

43 Fogg, D.E. and dos Santos, E.N. (2004) *Coordination Chemistry Reviews*, **248** (21–24), 2365–2379.

44 Crabtree, R.H. (2006) *Nature*, **441** (7090), 165–166.

45 Gnanamgari, D., Moores, A., Rajaseelan, E. and Crabtree, R.H. (2007) *Organometallics*, **26** (5), 1226–1230.

46 Hamid, M., Slatford, P.A. and Williams, J.M.J. (2007) *Advanced Synthesis and Catalysis*, **349** (10), 1555–1575.

47 Hamid, M.H.S.A. and Williams, J.M.J. (2007) *Chemical Communications*, (7), 725–727.

48 Haniti, M., Hamid, S.A. and Williams, J.M.J. (2007) *Tetrahedron Letters*, **48** (47), 8263–8265.

49 Grigg, R., Mitchell, T.R.B., Sutthivaiyakit, S. and Tongpenyai, N. (1981) *Journal of the Chemical Society. Chemical Communications*, (12), 611–612.

50 Fujita, K., Li, Z.Z., Ozeki, N. and Yamaguchi, R. (2003) *Tetrahedron Letters*, **44** (13), 2687–2690.

51 Hollmann, D., Tillack, A., Michalik, D., Jackstell, R. and Beller, M. (2007) *Chemistry, an Asian Journal*, **2** (3), 403–410.

52 Murahashi, S.I., Shimamura, T. and Moritani, I. (1974) *Journal of the Chemical Society. Chemical Communications*, (22), 931–932.

53 Cami-Kobeci, G. and Williams, J.M.J. (2004) *Chemical Communications*, (9), 1072–1073.

54 Black, P.J., Cami-Kobeci, G., Edwards, M.G., Slatford, P.A., Whittlesey, M.K. and Williams, J.M.J. (2006) *Organic & Biomolecular Chemistry*, **4** (1), 116–125.

55 Goldman, A.S., Roy, A.H., Huang, Z., Ahuja, R., Schinski, W. and Brookhart, M. (2006) *Science*, **312** (5771), 257–261.

56 Arndtsen, B.A., Bergman, R.G., Mobley, T.A. and Peterson, T.H. (1995) *Accounts of Chemical Research*, **28** (3), 154–162.

57 Chen, H.Y., Schlecht, S., Semple, T.C. and Hartwig, J.F. (2000) *Science*, **287** (5460), 1995–1997.

58 Ritleng, V., Sirlin, C. and Pfeffer, M. (2002) *Chemical Reviews*, **102** (5), 1731–1769.

59 Dyker, G. (1999) *Angewandte Chemie-International Edition*, **38** (12), 1699–1712.

60 Crabtree, R.H. (1995) *Chemical Reviews*, **95** (4), 987–1007.

61 Goldman, A.S. (1993) *Nature*, **366** (6455), 514–514.

62 Crabtree, R.H. (1985) *Chemical Reviews*, **85** (4), 245–269.
63 Crabtree, R.H. (2001) *Journal of the Chemical Society-Dalton Transactions*, (17), 2437–2450.
64 Crabtree, R.H. (2004) *Journal of Organometallic Chemistry*, **689** (24), 4083–4091.
65 Daugulis, O., Zaitsev, V.G., Shabashov, D., Pham, Q.N. and Lazareva, A. (2006) *Synlett*, (20), 3382–3388.
66 Murai, S., Kakiuchi, F., Sekine, S., Tanaka, Y., Kamatani, A., Sonoda, M. and Chatani, N. (1993) *Nature*, **366** (6455), 529–531.
67 Li, C.J. and Li, Z.P. (2006) *Pure and Applied Chemistry*, **78** (5), 935–945.
68 Li, Z.P., Bohle, D.S. and Li, C.J. (2006) *Proceedings of the National Academy of Sciences of the United States of America*, **103** (24), 8928–8933.
69 Basle, O. and Li, C.J. (2007) *Green Chemistry*, **9** (10), 1047–1050.
70 Li, Z.P. and Li, C.J. (2004) *Journal of the American Chemical Society*, **126** (38), 11810–11811.
71 Stuart, D.R. and Fagnou, K. (2007) *Science*, **316** (5828), 1172–1175.
72 Zhang, Y.H. and Li, C.J. (2007) *European Journal of Organic Chemistry*, (28), 4654–4657.
73 Kar, A., Mangu, N., Kaiser, H.M., Beller, M. and Tse, M.K. (2008) *Chemical Communications*, (3), 386–388.
74 Murahashi, S.I., Komiya, N., Terai, H. and Nakae, T. (2003) *Journal of the American Chemical Society*, **125** (50), 15312–15313.
75 Ellman, J.A. (2007) *Science*, **316** (5828), 1131–1132.
76 Murahashi, S.I., Komiya, N. and Terai, H. (2005) *Angewandte Chemie-International Edition*, **44** (42), 6931–6933.
77 Li, Z.P. and Li, C.J. (2005) *Journal of the American Chemical Society*, **127** (19), 6968–6969.
78 Li, Z.P. and Li, C.J. (2005) *Journal of the American Chemical Society*, **127** (11), 3672–3673.
79 Suzuki, A. (1999) *Journal of Organometallic Chemistry*, **576** (1–2), 147–168.
80 Stuart, D.R., Villemure, E. and Fagnou, K. (2007) *Journal of the American Chemical Society*, **129** (40), 12072–12073.
81 Hull, K.L. and Sanford, M.S. (2007) *Journal of the American Chemical Society*, **129** (39), 11904–11905.
82 Davies, H.M.L. and Manning, J.R. (2008) *Nature*, **451** (7177), 417–424.
83 Anada, M., Mita, O., Watanabe, H., Kitagaki, S. and Hashimoto, S. (1999) *Synlett*, (11), 1775–1777.
84 Doyle, M.P. and Hu, W.H. (2002) *Chirality*, **14** (2–3), 169–172.
85 Davies, H.M.L., Hansen, T., Hopper, D.W. and Panaro, S.A. (1999) *Journal of the American Chemical Society*, **121** (27), 6509–6510.
86 Davies, H.M.L. and Walji, A.M. (2005) *Angewandte Chemie-International Edition*, **44** (11), 1733–1735.

2
Catalysis Involving Fluorous Phases: Fundamentals and Directions for Greener Methodologies

John A. Gladysz

2.1
Introduction

The title of this chapter features an adjective, fluorous, that was introduced in a seminal 1994 paper by Horváth and Rábai [1], and further analyzed by the present author in an accompanying perspective [2]. The former publication launched a new discipline, fluorous chemistry [3], one aspect of which involves catalyst and reagent recovery. The obvious connection with green chemistry is elaborated below. Over the intervening years, the following general definition of fluorous has evolved [3, 4]: '*of, relating to, or having the characteristics of, highly fluorinated saturated organic materials, molecules or molecular fragments*. Or, more simply (but less precisely): 'highly fluorinated' or 'rich in fluorine atoms' and based upon sp^3-hybridized carbon.

Separation science makes extensive use of orthogonal phases, and the incompatibility of water and many organic solvents. i.e. aqueous and lipophilic phases, is common knowledge for all scientists and anyone who has applied oil and vinegar dressing to their salads. However, prior to the 1994 paper, only a small fraction of chemists were aware that organic solvents and saturated fluorocarbons (e.g. perfluorohexane and perfluoromethylcyclohexane, which exemplify one obvious category of fluorous substances) are not normally miscible at room temperature. One might view fluorous solvents as lipophobic, but so is water, and water is similarly immiscible with saturated fluorocarbons. Hence fluorous substances can be viewed as those that are simultaneously lipophobic and hydrophobic, as per the diagram and photograph with dye-containing phases in Figure 2.1. To the author's knowledge, there are no such carbon-based, non-fluorinated materials.

Although the preceding illustration involves liquid phases, this incompatibility extends to combinations of liquid and solid phases, such as the familiar Teflon-coated frying pan. Related phenomena involving fluorous and non-fluorous domains of solids are described below.

The 1994 paper also introduced the concept of a 'ponytail', an example of what is often today termed a 'phase label' or tag [5]. However, labels and tags are normally considered to be removable, whereas ponytails are permanently affixed. In current

Handbook of Green Chemistry, Volume 1: Homogeneous Catalysis. Edited by Robert H. Crabtree

ISBN: 978-3-527-32496-5

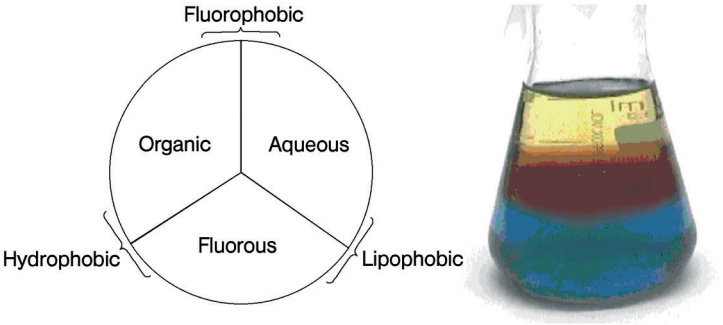

Figure 2.1 Three orthogonal (liquid) phases.

practice, these are most commonly *n*-fluoroalkyl moieties of the formula $(CH_2)_m(CF_2)_{n-1}CF_3$, often abbreviated $(CH_2)_mR_{fn}$. In future practice, other motifs are likely to become increasingly important, as described below. Depending on the quantity and lengths of the fluorous segments, they can render molecules partially, preferentially or even exclusively soluble in a fluorous liquid phase. This reflects a simple 'like dissolves like' effect. Common organic molecules show a marked preference for partitioning into organic phases (>95 : <5).

Importantly, fluorous and organic solvents usually mix at elevated temperatures. Alternatively, CO_2 pressure can be applied [6]. Either approach allows the facile switching of reactions between heterogeneous and homogeneous conditions. Temperature-dependent miscibility represents one of many types of thermomorphic behavior. The adjective thermomorphic is applied in such broad contexts that a precise definition becomes problematic, but a physical property that is temperature dependent is always involved.

The 1994 paper culminated in an elegant 'proof of principle' that combined all of the above concepts [1]. Catalysts featuring sufficient ponytails were first combined with organic reactants in fluorous–organic solvent mixtures. As shown in Figure 2.2

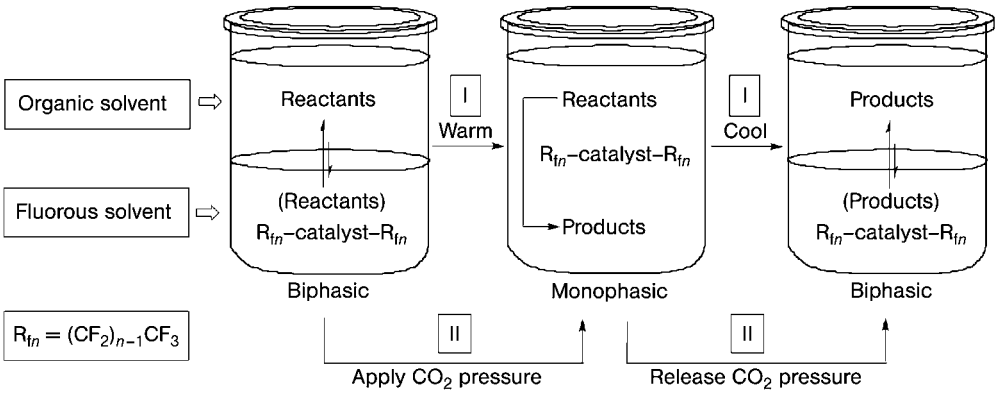

Figure 2.2 Original approach to liquid–liquid fluorous–organic biphase catalysis (I) and a modification involving CO_2 (II).

(procedure I), the samples were then warmed, achieving one-phase conditions. Homogeneous catalysis then proceeded smoothly at this high temperature limit. The samples were subsequently cooled, re-establishing two-phase conditions. Simple separation of the fluorous and organic phases simultaneously separated the organic products from the fluorous catalysts. This was termed fluorous biphase catalysis.

This broad concept was rapidly expanded to the separation of products and (spent) reagents and to the use of ponytails of varying fluorine content to label or tag libraries of compounds (for two representative applications, see [7]). Recoverable fluorous nanoparticles were also engineered [8]. Given the central importance of recoverable catalysts and reagents to green chemistry, fluorous methodologies have attracted considerable attention within this community. Fluorous solvents are furthermore included in many treatments of green solvents [9]. Nonetheless, there are a number of obvious ways in which the protocol in Figure 2.2 can be optimized from an environmental standpoint, as outlined in the following sections.

2.2
Directions for Greener Fluorous Methodologies

A number of features of the general catalyst recovery protocol in Figure 2.2 merit scrutiny from the green chemistry standpoint. First, fluorous solvents of the types mentioned above (perfluorohexane, perfluoromethylcyclohexane) are environmentally persistent [10]. However, they do not have any known toxicity *per se*, as evidenced by their clinical use as blood replacements, and do not contribute to the depletion of stratospheric ozone by any currently established mechanism [11]. Although fluorous solvents can presumably be contained by proper engineering, alternatives are obviously desirable.

Accordingly, two modifications are treated below. In one, the perfluorinated solvent is replaced with a biodegradable partially fluorinated or hybrid solvent that is still capable of phase separating from organic solvents [12, 13]. In the other, the perfluorinated solvent is simply omitted. In this case, the temperature-dependent solubility of the (solid) fluorous catalyst in the organic solvent is exploited, as per the protocol sketched in Figure 2.3a (procedure I). This is conceptually similar to the temperature-dependent liquid–liquid phase miscibilities exploited in Figure 2.2. The two phenomena likely share a common 'driving force'.

Fluorous solutes commonly show excellent solubilities in supercritical CO_2 [14]. Therefore, it is not surprising that fluorous solutes become more soluble in organic solvents when CO_2 pressure is applied [15, 16]. This constitutes an alternative, non-thermal 'solubility switch' for the protocols in Figures 2.2 and 2.3b, illustrated as procedure II.

As depicted in Figure 2.3b, the protocols in Figure 2.3a can be modified by the inclusion of a fluorous solid phase. This also facilitates the recovery of small catalyst quantities. Although enthalpic interactions between fluorous molecules are

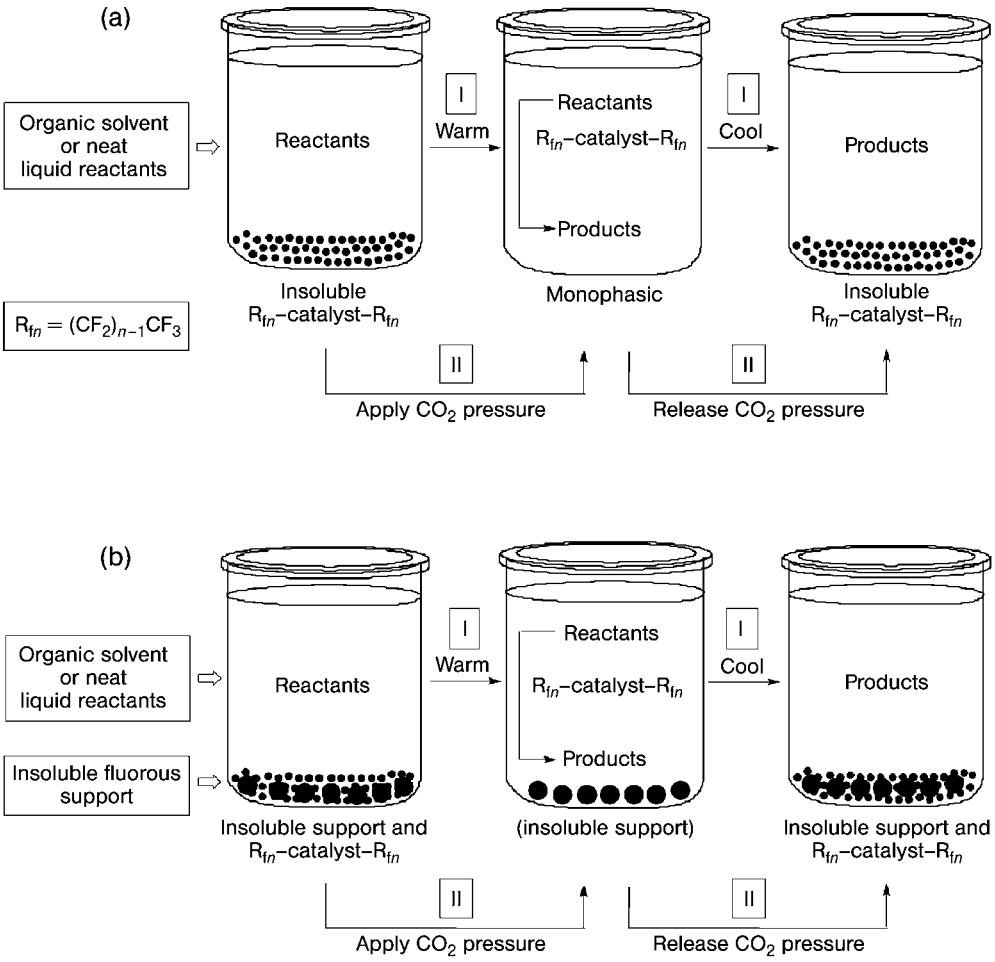

Figure 2.3 New generation solid–liquid fluorous–organic biphase protocols (a) with and (b) without an insoluble fluorous support.

extremely weak, different species often phase separate together. For example, in crystal structures of molecules with fluorous and non-fluorous segments, the latter commonly segregate into separate domains [17]. Finally, for both Figure 2.3a and b, several cases have been reported where the organic reactants can serve as there own liquid phases, thereby permitting solvent-free protocols (see below).

As would be intuitively expected, fluorous chromatographic supports preferentially retain fluorous molecules when eluted with organic solvents [18]. Although many fluorous solid phases are environmentally persistent, they are non-volatile and easier to contain than fluids. Chromatographic separations, a cartoon for which is shown in Figure 2.4, are particularly suited for lightly fluorinated ('light fluorous') catalysts and reagents that maintain good solubilities in organic solvents. These are

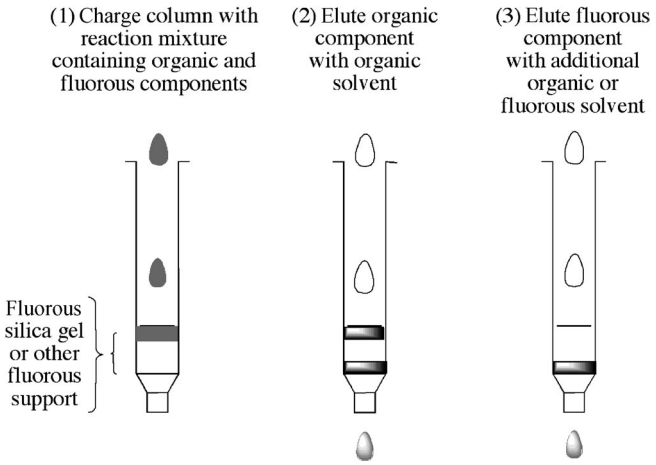

Figure 2.4 A fluorous solid-phase extraction.

often conducted as 'solid phase extractions' (SPEs), similar to 'flash chromatography'. The technical distinction between SPE and conventional column chromatography is analogous to that between purifying a two-component liquid by evaporation and distillation [18].

Another direction for greener fluorous chemistry involves ponytail design. Much recent work has unequivocally established the bioaccumulation of perfluorooctane sulfonate, $R_{f8}SO_3^-$, and also longer chain perfluoroalkyl carboxylates ($\geq R_{f7}$), in a variety of mammals, birds, fish and other biota [19, 20]. Many of the carboxylates appear to be derived by oxidative degradation of fluorotelomer alcohols $R_{fn}CH_2CH_2OH$ [21]. Consequently, there is increasing interest in the design of easily accessible, biodegradable ponytails, and/or those with shorter R_{fn} segments ($n \leq 6$). Some recent efforts are highlighted below.

However, it has recently been shown that vitamin B_{12} can serve as a catalyst for the Ti(III) citrate-promoted reductive defluorination of perfluorooctane sulfonate [22]. This has raised hopes that microorganisms will eventually be found that are capable of degrading species with R_{f6}, R_{f8}, R_{f10} and similar ponytails. The sonochemical fission of the R_{fn} chains of perfluorooctane sulfonate and perfluorooctanoic acid has also been reported [23].

2.3 Solvents for Fluorous Chemistry

Fluorous solvents have been reviewed elsewhere [24]. They are more dense than common organic solvents, including CCl_4. They are also exceedingly non-polar, as evidenced by a variety of quantitative criteria. Recently, useful two-dimensional classification schemes involving polarity and fluorophilicity axes have been devised [13a, c]. Due to the low intermolecular attractive forces, fluorous solvents cavitate easily, providing hospitable environments for small non-polar solutes (e.g. gases) and

even some polar ones. Importantly, hexafluorobenzene is not a fluorous solvent, nor is any highly fluorinated arene.

As shown in Scheme 2.1, the most common fluorous solvent is perfluorohexane or FC-72, which is sold as a mixture of isomers (b.p. 57 °C). For physical measurements or mechanistic studies, perfluoromethylcyclohexane (PFMC) (b.p. 76 °C), a more expensive but homogeneous solvent, is often favored. Other common choices for reactions include perfluorodecalin or -methyldecalin, 1-bromoperfluorooctane and perfluoro-2-butyltetrahydrofuran (all with b.p. >100 °C). Still higher boiling polyethers or polymeric fluids or greases have not yet seen application, but offer obvious advantages from the green chemistry standpoint.

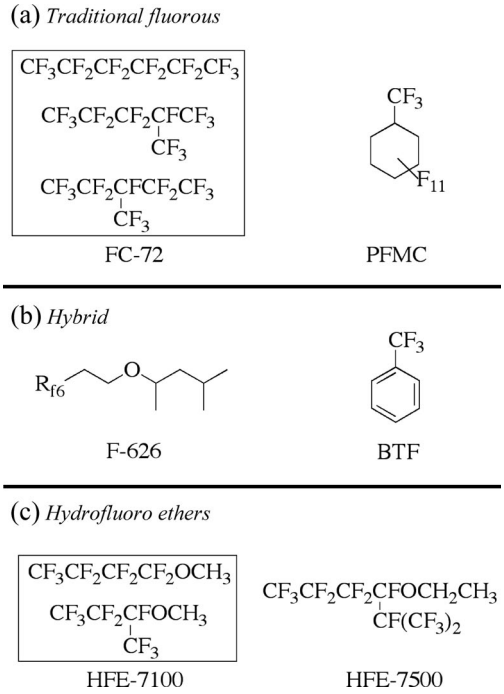

Scheme 2.1 Trends in fluorous solvents.

The solvent (trifluoromethyl)benzene (BTF) (b.p. 102 °C) [25] is able to dissolve appreciable quantities of both fluorous and non-fluorous solutes and hence is often termed 'hybrid' or 'ambiphilic'. However, it does not give biphasic systems with common organic or fluorous solvents and is strictly speaking non-fluorous. The solvent $R_{f6}(CH2)_2OCH(CH_3)CH_2CH(CH_3)_2$ (F-626; b.p. 214 °C) [12] also dissolves many organic and fluorous solutes, but would be viewed as fluorous by virtue of the R_{f6} segment. Furthermore, it gives biphasic systems with the polar organic solvents acetonitrile, DMF and methanol [13c].

Recently, much attention has been directed at methyl and ethyl ethers of shorter perfluoroalkyl segments or 'hydrofluoro ethers' (Scheme 2.1) [13]. Particularly

promising candidates include HFE-7100 (b.p. 61 °C), which is a mixture of *n*-$C_4F_9OCH_3$ and *i*-$C_4F_9OCH_3$, the corresponding ethyl ethers (HFE-7200) and HFE-7500, $CF_3(CF_2)_2CF(OCH_2CH_3)CF(CF_3)_2$ (b.p. 128 °C). In the case of HFE-7100, biphasic systems can be achieved with aqueous organic solvents (which exhibit increased fluorophobicity) or by adding a saturated fluorocarbon cosolvent (increasing lipophobicity). Similar strategies are also useful with HFE-7500, although phase separation is intrinsically easier due to its higher lipophobicity and fluorophilicity. None of these solvents are classified as volatile organic compounds (VOCs). Furthermore, extensive studies have not revealed any toxicity problems and their shorter, alkoxylated perfluoroalkyl segments are expected to be significantly more biodegradable [26].

2.4
Ponytails and Partition Coefficients

In most cases, ponytails contain an insulating group, such as a methylene chain or phenyl ring, to ameliorate the electron-withdrawing effect of the perfluoroalkyl segment. The transmission of electronic effects through various spacers has been studied in detail [27]. With only two methylene groups, a very significant effect can still be felt, especially in the case of a directly bound reaction center, such as in an amine or phosphine. The perfluoroalkyl segments are usually linear, but a few have CF_3 branches, as in HFE-7500.

One possible strategy for improving ponytail biodegradability involves alternating spacer–fluorous–spacer–fluorous segments. Towards this end, molecules with $-C(CF_3)_2OCH_2R_{f7}$ and $-C(CF_3)_2O(CH_2)_3R_{f8}$ moieties have been reported [28]. However, these feature R_{fn} groups that are particularly prone to bioaccumulation, as described above. Hence recent efforts have sought to do away with long R_{fn} ($n > 6$) segments altogether.

In this regard, the use of multiple *t*-C_4F_9 substituents, commonly as caps for ether linkages, has received attention in two groups [29–31]. This maximizes the number of CF_3 groups, which are believed to provide the greatest 'bang for the buck' (fluorine atom) in terms of fluorophilicity. For example, Mitsunobu reactions involving *t*-C_4F_9OH allow ready access to a number of building blocks of formula $XCH_2C(CH_2O\text{-}t\text{-}C_4F_9)_3$ [29, 30]. Alternatively, the alkoxide *t*-C_4F_9ONa and suitable electrophiles can be reacted [29b] In the case of the trichloride $N[(CH_2)_2Cl]_3$, the fluorous tertiary amine $N[(CH_2)_2O\text{-}t\text{-}C_4F_9]_3$ is obtained. The fluorophilicity of this species, which features three-atom spacers and an aggregate $C_{12}F_{27}$ fluorous domain, is lower than that of $N[(CH_2)_3R_{f8}]_3$, which features three-atom spacers and an aggregate $C_{24}F_{51}$ fluorous domain. However, its fluorophilicity is greater than that of the related secondary amine $CH_3N((CH_2)_3R_{f8})_2$, which features a larger, $C_{16}F_{34}$ aggregate fluorous domain [29b].

When catalogs of vendors who specialize in fluorinated chemicals are examined, many interesting future directions for ponytail design can be discerned. Some of the numerous building blocks available from ABCR (2006–2007) include the

branched terminal alkene $R_{f3}C(CF_3)_2CH{=}CH_2$, the branched carboxylic acid chloride $(CF_3)_3CC(CF_3)_2OCH_2C(=O)Cl$ and the ethereal alcohols $CF_3O(CF_2)_2OCF_2CH_2OH$, $R_{f4}O(CF_2)_2OCF_2CH_2OH$ and $HOCH_2CF_2O(CF_2)_2O(CF_2)_2OCF_2CH_2OH$. All of these could easily be elaborated or incorporated into a variety of functional groups.

With respect to liquid–liquid biphase systems, any solute, fluorous or otherwise, can be characterized by a partition coefficient. A 'higher' partition coefficient corresponds to a higher fluorophilicity or fluorous phase affinity. Obviously, for any recovery protocol involving a fluorous phase (liquid or solid), the greater the fluorophilicity of the catalyst or reagent, the greater the efficiency (the lower the leaching). Most partition coefficients, such as those of the amines mentioned above, have been measured in toluene–perfluoromethylcyclohexane mixtures. These data, which have been tabulated elsewhere [32], provide valuable guides for the design of recoverable catalysts. Reassuringly, they also indicate very low fluorous phase affinities for simple monofunctional organic molecules, as well as alkanes consisting of at least 12 carbon atoms.

2.5
Specific Examples of Catalyst Recovery that Exploit Temperature-dependent Solubilities

In this section, examples of catalyst recovery by procedure I in Figure 2.3a are collected. These involve the thermomorphic species summarized in Scheme 2.2, all of which either have longer $R_{f8}/R_{f10}/R_{f11}$ ponytails or a multitude of R_{f6} ponytails. For all studies, catalyst recoveries are quoted when available. Since the masses involved can be very small, especially for very effective catalysts, accurate determinations are not always feasible. In such cases, rate comparisons for runs conducted with recovered catalysts are given when available. The generality of all of the examples depicted below was confirmed with multiple substrates, but only those with the most extensive recycling data are depicted.

2.5.1
Two Early Examples

To the author's knowledge, the first catalyst recovered as in Figure 2.3a was perfluorinated di(*n*-octyl) ketone (**1**) [33]. Sheldon and co-workers found that this compound dissolved in refluxing 10 : 1 v/v $ClCH_2CH_2Cl$–EtOAc, under which conditions it catalyzed the epoxidation of alkenes by H_2O_2 (Scheme 2.3a). Upon cooling to 0 °C, **1** was recovered in 92% yield. In the same year, Curran, Hallberg and co-workers reported, as part of a larger study, an isolated example in which the stannane **2** (Scheme 2.2) was similarly recovered [34]. This involved the reductive addition of adamantyl bromide to acrylonitrile, with *in situ* reduction of the resulting stannyl bromide by $NaBH_3CN$. As is often the case in science, the potential generality of a phenomenon was not recognized in the initial reports.

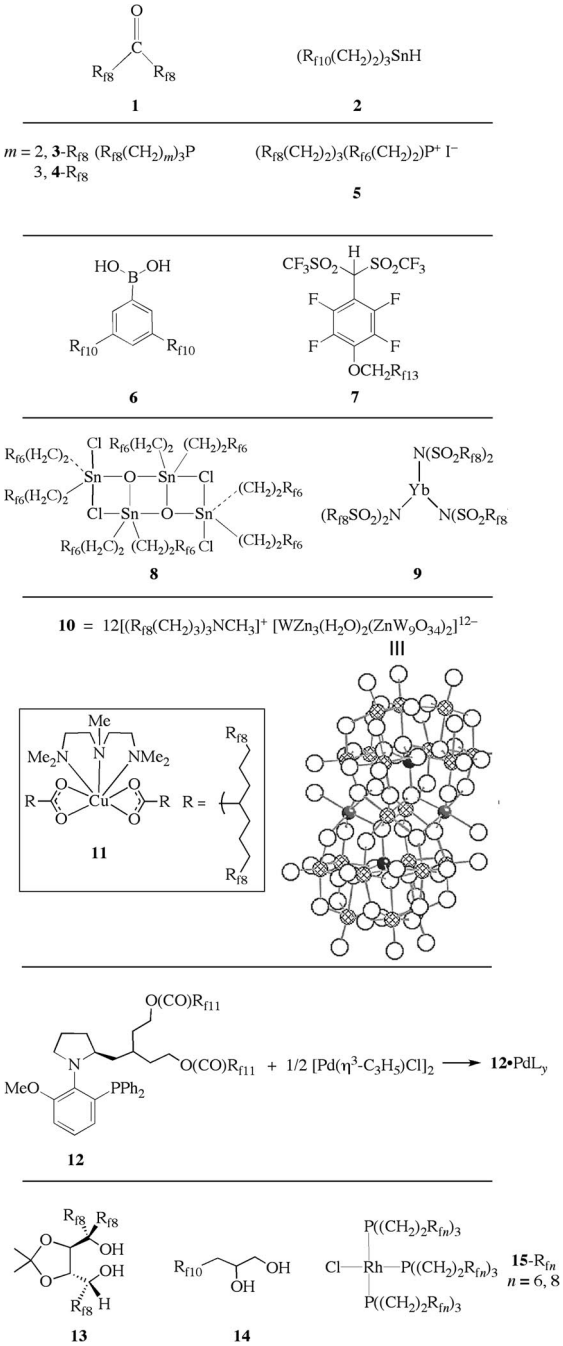

Scheme 2.2 Some thermomorphic fluorous catalysts that have been recovered by solid/liquid-phase separations.

(a)

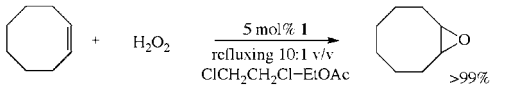

Precipitated catalyst recovered by solid/liquid phase separation; 92% recovery/cycle

(b)

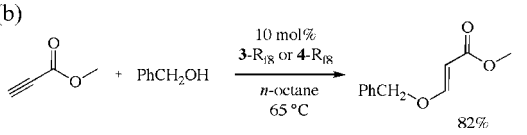

Precipitated catalyst recovered by solid/liquid phase separation; 82%, 80%, 81%, 75% yields, subsequent cycles, and additional data in the presence of supports (below)

(c)

Precipitated catalyst recovered by solid/liquid phase separation; 88% recovery/cycle (10 cycles)

(d)

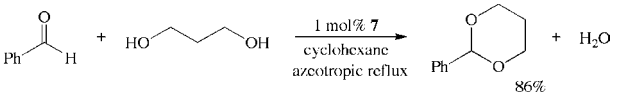

Precipitated catalyst recovered by solid/liquid phase separation; 96% recovery

(e)

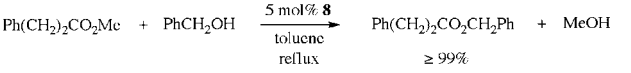

Precipitated catalyst recovered by fluorous solvent extraction; 100% recovery

(f)

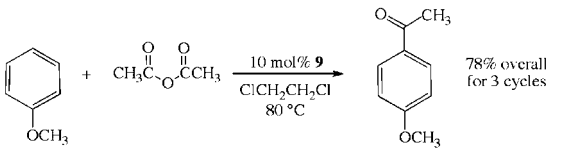

Precipitated catalyst recovered by solid/liquid phase separation

(g)

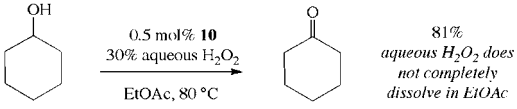

Precipitated catalyst recovered by solid/liquid phase separation; 80% and 78% yields, subsequent cycles

Scheme 2.3 Recovery of the thermomorphic catalysts in Scheme 2.2 according to procedure I in Figure 2.3a.

(h)

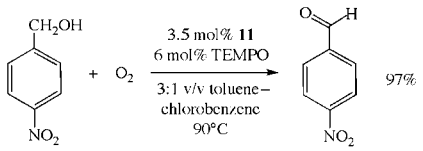

Precipitated catalyst recovered by solid/liquid phase separation; 85% recovery/cycle (4 cycles); activity recovery lower

(i)

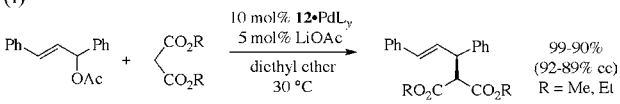

Diethyl ether is replaced by hexane and the precipitated catalyst recovered by solid/liquid phase separation; yields maintained for 4-6 cycles and activity (rate) maintained in second cycle

(j)

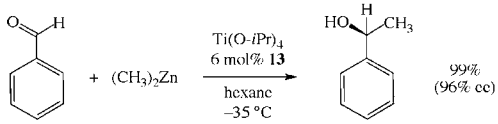

After quenching with aqueous NH_4Cl and concentrating, cold toluene is added and precipitated **13** recovered by solid/liquid phase separation; 90% recovery/cycle (6 cycles)

(k)

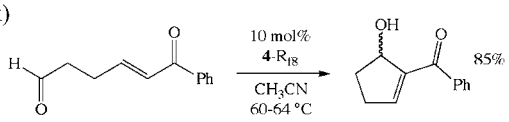

Precipitated catalyst recovered by solid/liquid phase separation; ca. 90% activity recovery/cycle (rate measurements)

(l)

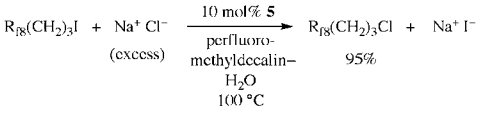

Precipitated catalyst recovered by solid/liquid phase separation after hexane addition: 82% recovery/cycle (5 cycles)

(m)

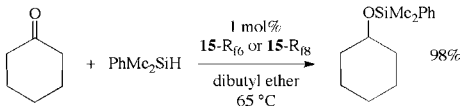

Precipitated catalyst recovered by solid/liquid phase separation; 98%, 98%, and 98% yields, subsequent cycles, and additional data in the presence of supports (below)

Scheme 2.3 *(Continued)*

2.5.2
First Examples from the Author's Laboratory [35]

The solubilities of the fluorous tertiary phosphines $[R_{fn}(CH_2)_2]_3P$ (**3**-R_{fn}, $n = 6, 8, 10$) decrease as the lengths of the R_{fn} segments increase. Quantitative data are available for **3**-R_{f8} in *n*-octane, toluene, chlorobenzene and dioxane. There is a 600-fold solubility increase between −20 °C (0.104 m*M*) and 80 °C (63.4 m*M*) and a 1500-fold solubility increase between −20 and 100 °C (151 m*M*). Data for the analogous phosphine with three methylene spacers, $[R_{f8}(CH_2)_3]_3P$ (**4**-R_{f8}), are similar. This species is much more basic and nucleophilic than **3**-R_{f8}.

The phosphines **3**-R_{f8} and **4**-R_{f8} catalyze conjugate additions of alcohols to methyl propiolate (Scheme 2.3b). They could be recovered by solid–liquid phase separation at −30 °C, under which conditions the theoretical amount of leaching due to residual solubility is <0.33%. Depending on the alcohol, 3–5 cycles were carried out, without deterioration in yield. Photographs of representative sequences have been published [35]. Interestingly, the best results were obtained under solvent-free conditions, with **3**-R_{f8} precipitating upon cooling the neat product and excess alcohol.

The leaching of degraded catalyst was assayed by both ^{31}P and ^{19}F NMR and the purity of the recovered catalyst was studied. Improved recovery protocols involving supports are described below. These phosphines can also be alkylated, allowing the preparation of phosphonium salts such as **5** (Scheme 2.2) [36]. These are in turn employed as recoverable catalysts in other types of reactions, as described below.

2.5.3
Concurrent Work by Ishihara and Yamamoto

Nearly simultaneously with our first communication, Ishihara and Yamamoto *et al.* reported that the fluorous phenylboronic acid **6** (Scheme 2.2) efficiently catalyzed condensations of carboxylic acids and amines to give amides (Scheme 2.3c) [37]. Reactions could be effected under homogeneous conditions in refluxing toluene or xylene and **6** could be recovered by precipitation at room temperature. Ten such cycles were conducted, giving the amide in 96% isolated yield (>99% conversion per cycle) and **6** in 26% yield (88% recovery per cycle). More recently, this group found that the fluorous bis(sulfone) **7**, which is a super Brønsted acid, catalyzes acetal formation (Scheme 2.3d) [38]. Reactions were effected under homogeneous conditions in refluxing hexane and **7** could be recovered in 96% yield at room temperature. Benzoylations of alcohols and esterifications of carboxylic acids were similarly conducted in toluene and methanol, with 70–68% recoveries of **7**.

2.5.4
Additional Examples from Other Research Groups

Otera has reported that fluorous distannoxanes such as **8** (Scheme 2.2), which dissociate to give Lewis acidic species, catalyze transesterifications in organic–fluorous solvent mixtures [39]. Although **8** was insoluble in toluene at room temperature, it

dissolved at reflux and efficiently promoted the transformation in Scheme 2.3e, and others. The catalyst precipitated upon cooling, but a fluorous solvent extraction was utilized for recovery (100%). Another thermomorphic fluorous Lewis acid catalyst was developed by Mikami *et al.* [40]. They found that the ytterbium tris(sulfonamide) **9** could be used for Friedel–Crafts acylations under homogeneous conditions in $ClCH_2CH_2Cl$ at 80 °C and precipitated upon cooling to −20 °C (Scheme 2.3f).

Neuman and Fish and co-workers have studied the novel polyoxometalate salt **10** (Scheme 2.2), which features 12 fluorous ammonium cations [41]. This material was insoluble in EtOAc (and toluene) at room temperature, but dissolved at 80 °C to give an effective catalyst system for the oxidation of alkenes and alcohols by 30% aqueous H_2O_2 (Scheme 2.3g). Cooling precipitated the catalyst, which was reused. Contel, Fish and co-workers have also shown that the copper(II) complex **11** (Scheme 2.2) and TEMPO give an effective catalyst system for the oxidation of *p*-nitrobenzyl alcohol by oxygen to *p*-nitrobenzaldehyde [42]. As shown in Scheme 2.3h, the copper complex is insoluble in chlorobenzene–toluene at room temperature, but dissolves at elevated temperatures and is recovered in high yields upon cooling.

Mino *et al.* [43] has described a palladium catalyst prepared from the amino phosphine **12** in Scheme 2.2 and measured its solubility in diethyl ether between −20 °C (1.14 m*M*) and 30 °C (16.7 m*M*) and in hexane between −20 °C (0.027 m*M*) and 69 °C (5.38 m*M*). This system catalyzes the enantioselective allylic alkylation shown in Scheme 2.3i. The ether solvent was replaced by cold hexane, in which the product was soluble and the catalyst rest state insoluble. Rate studies showed an induction period during the first cycle and faster conversion during the second cycle [43].

Ando and co-workers have prepared the enantiopure diol **13** (Scheme 2.2) and applied it in the enantioselective addition of dimethylzinc to aldehydes (Scheme 2.3j) [44]. The reaction mixtures were quenched with aqueous NH_4Cl and toluene was added to the residues. The samples were cooled to −40 °C and the precipitated **13** was recovered by filtration. Finally, the diol **14** in Scheme 2.2 was used to generate fluorous boronate *reagents* [45]. Palladium-catalyzed cross-couplings were conducted in aqueous dioxane. The reaction mixtures were extracted with EtOAc and upon concentration **14** could be recovered by precipitation.

2.5.5
Additional Examples from the Author's Laboratory

The phosphine **4**-R_{f8} has also proven to be an effective catalyst for the intramolecular Morita–Baylis–Hillman reaction, as shown in Scheme 2.3k. As in the case of Scheme 2.3b, it can be recovered by simple precipitation upon cooling [46]. Rate studies established an average of ca 90% activity recovery per cycle over five cycles.

The phosphonium salt **5** (Scheme 2.2) is very poorly soluble in fluorous solvents at room temperature, but appreciably soluble at elevated temperatures [36]. It has been used as a phase transfer catalyst for ionic displacements in fluorous solvents at 76–100 °C (Scheme 2.3l) [47]. It does not always spontaneously precipitate upon

cooling, perhaps in part due to partial halide anion exchange (the recovered catalyst should also contain halide anions derived from the nucleophile and leaving group). Thus, in an initial series of experiments, hexane was added after each cycle to promote precipitation. After five cycles, 38% of the original catalyst mass remained (82% recovery per cycle). Additional experiments established that most of the catalyst loss arose from incomplete precipitation. Improved recycling protocols involving the hybrid solvent (trifluoromethyl)benzene are described below [47b] There are other examples of catalysts that have been recovered by precipitation from hybrid solvents [48].

The red–orange rhodium complexes **15**-R_{f6} and **15**-R_{f8} (Scheme 2.2) are insoluble in nearly all organic solvents at room temperature [49], but often become soluble at elevated temperatures. As shown in Scheme 2.3m, they effect the hydrosilylation of ketones in dibutyl ether at 55–65 °C [50, 51]. The catalyst rest state precipitates upon cooling and can be recovered by filtration [51]. Precipitation also occurs when the reactions are run under solvent-free conditions. Four cycles can be conducted with no deterioration in yield and more diagnostic rate studies are conducted with modified protocols described below.

2.6
Specific Examples of Catalyst Recovery that Exploit Fluorous Solid Phases

Developments in this area can be grouped as follows: (a) the use of fluoropolymer supports as exemplified by procedure I in Figure 2.3b; (b) the analogous use of fluorous silica gel supports; (c) the use of supercritical CO_2 in place of temperature as a solubility trigger, as exemplified by procedure II in Figure 2.3b; (d) the use of fluorous silica gel for solid-phase extractions (SPE), as exemplified by Figure 2.4.

2.6.1
Fluoropolymer Supports

To the author's knowledge, the first use of a fluoropolymer support was in conjunction with the addition reactions in Scheme 2.3b. When the catalysts **3**-R_{f8} and **4**-R_{f8} were recycled in the presence of Teflon shavings, recoveries improved significantly [35]. Rate studies showed an approximately 10% decrease in activity from cycle to cycle.

These results were extended to the ketone hydrosilylations in Scheme 2.3m. Here common commercial Teflon tape was employed, and also somewhat lower loadings of the red–orange catalyst **15**-R_{f6} (0.15 mol%) and a temperature of 55 °C [51]. Interestingly, after cooling the catalyst rest state precipitated on to the tape ($50 \times 12 \times 0.0075$ mm) and not the stir bar (perhaps due to a processing step or coating). The tape was removed and used for subsequent cycles, the rates of which were monitored. As in earlier work, the first cycle exhibited an induction period. Retention of activity was excellent in the second and third cycles, but there was substantial loss in the fourth. In view of the similar rates of the first three cycles, this

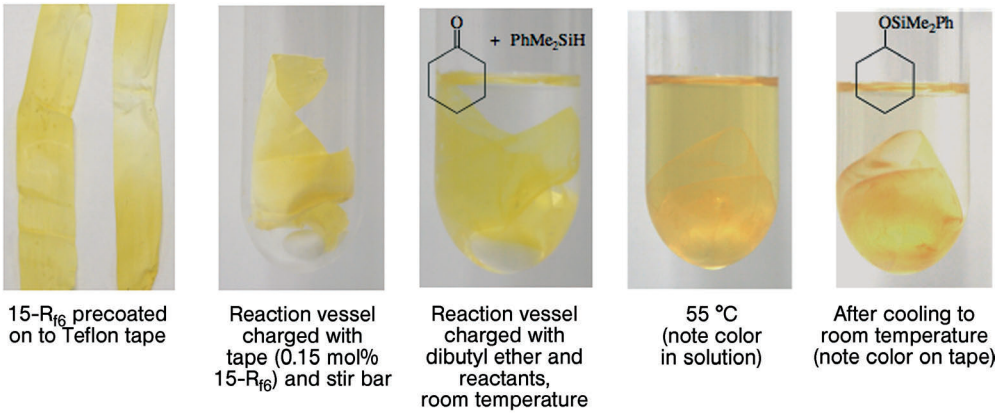

Figure 2.5 Photographs of one version of procedure I in Figure 2.3b: desorption of rhodium hydrosilylation catalyst precursor **15**-R_{f6} from Teflon tape and adsorption of the rest state upon cooling.

can be attributed to catalyst deactivation. A problem intrinsic to the recycling protocol, such as leaching, should afford a relatively constant loss of activity per cycle.

Leaching was probed in two ways. First, the dibutyl ether supernatants from the first three cycles were combined and the total ponytail leaching was assayed by ^{19}F NMR. A signal corresponding to 11.4% of the phosphine ligands of **15**-R_{f6} was observed. Since the active and resting states of the catalyst likely involve two phosphine ligands, some extraction is not surprising. Second, the supernatants were analyzed for rhodium. The first cycle showed leaching corresponding to 0.57% of the original charge and the second cycle 5.3%. The increased was attributed to the onset of catalyst degradation.

One obvious procedural refinement would be to precoat the catalyst on the Teflon tape. This would allow low loadings to be delivered by *length* as opposed to mass measurements or the tedious preparation of standard solutions. Accordingly, strips of tape were added to a solution of **15**-R_{f6} in perfluoromethylcyclohexane. The solvent was removed under an inert gas stream to give a yellowish catalyst-coated tape. This could be applied in a three-cycle sequence with results similar to those above. Photographs of the first cycle, which are representative of all the protocols in this section, are collected in Figure 2.5.

When catalysts are recycled as solid residues, it is important to exclude impurities that may 'piggyback' – such as metal particles – as the active species. This was probed in two ways. First, the tape was removed after the first cycle, rinsed and transferred to a new vessel. A second charge of ketone and dibutyl ether was added, but *not* the $PhMe_2SiH$. The sample was warmed to 55 °C, the now off-white tape was removed and $PhMe_2SiH$ was added. The rate profile was similar to the first cycle (ca 20% slower at higher conversions), consistent with predominant homogeneous catalysis by desorbed fluorous species. Second, the second cycle of a sequence was conducted in the presence of elemental mercury, which inhibits catalysis by

elemental rhodium. However, the rate profile was the same as a sequence in the absence of mercury.

These efforts were next extended to the Morita–Baylis–Hillman reaction in Scheme 2.3k. The white phosphine **4**-R_{f8} could similarly be coated onto Teflon tape [46]. However, recycling (as assayed by rate measurements) was somewhat less efficient than that achieved by simple solid–liquid phase separation (procedure I, Figure 2.3a). Note that this reaction uses a much higher catalyst loading than the ketone hydrosilylation (10 mol% **4**-R_{f8} vs 0.15 mol% **15**-R_{f6}). Perhaps the available surface area of the fluoropolymer becomes saturated or adsorption efficiency is otherwise decreased.

In an attempt to address this issue, the tape was replaced with Gore-Rastex fiber. Gore-Tex products can be viewed as porous forms of Teflon. Indeed, the recycling efficiency increased, but it still remained below that without achieved by solid–liquid phase separation without a support.

This procedure has also been extended to the ionic displacement reactions in Scheme 2.3l, which are catalyzed by the fluorous phosphonium salt **5** (Scheme 2.2). In this case, reactions were conducted in (trifluoromethyl)benzene–water mixtures. The salt **5** is less soluble in the hybrid solvent (trifluoromethyl)benzene than perfluoromethylcyclohexane and cleanly precipitates onto Teflon tape. Rate experiments show excellent retention of activity (>95% per cycle). However, in the author's experience, some fluorous catalysts more readily adsorb on fluoropolymers than others and studies of the controlling factors remain in progress [47b]. Preliminary data are beginning to appear from other investigators [52].

2.6.2 Fluorous Silica Gel Supports

Fluorous compounds and catalysts are readily adsorbed on fluorous silica gel, some forms of which are depicted in Scheme 2.4. (**18**-R_{fn}-**21**) Owing to the presence of both fluorous and non-fluorous domains, such supports are probably capable of much stronger interactions with many fluorous molecules than Teflon. These materials have been applied to reactions in organic solvents and water, both at room temperature and above [52–56]. The investigators have often interpreted the transformations as 'bonded fluorous phase catalysis', as opposed to desorption processes as exemplified by procedure I in Figure 2.3b. However, there remains the possibility that at least some catalysis takes place in the bulk solvent for the non-aqueous systems. It would be a simple matter to remove the support after warming the reaction (but before adding all substrates) and measure the rate of product formation.

To date, reports have involved palladium catalysts for Suzuki and Sonogashira coupling reactions (Bannwarth and co-workers; Scheme 2.4a) [53], rhodium catalysts for silylations of alcohols by trialkylsilanes (Biffis and co-workers; Scheme 2.4b) [54], tin-, hafnium- and scandium-based Lewis acid catalysts for Baeyer–Villiger, Diels–Alder and esterification reactions (Nishikido and co-workers; Scheme 2.4c) [55], tin catalysts for reductive free radical cyclizations (Tsang and co-workers; Scheme 2.4-D) [56] and other processes [52]. Spectroscopic and GC data established that most of the tin species desorbed at the reaction temperature (60 °C).

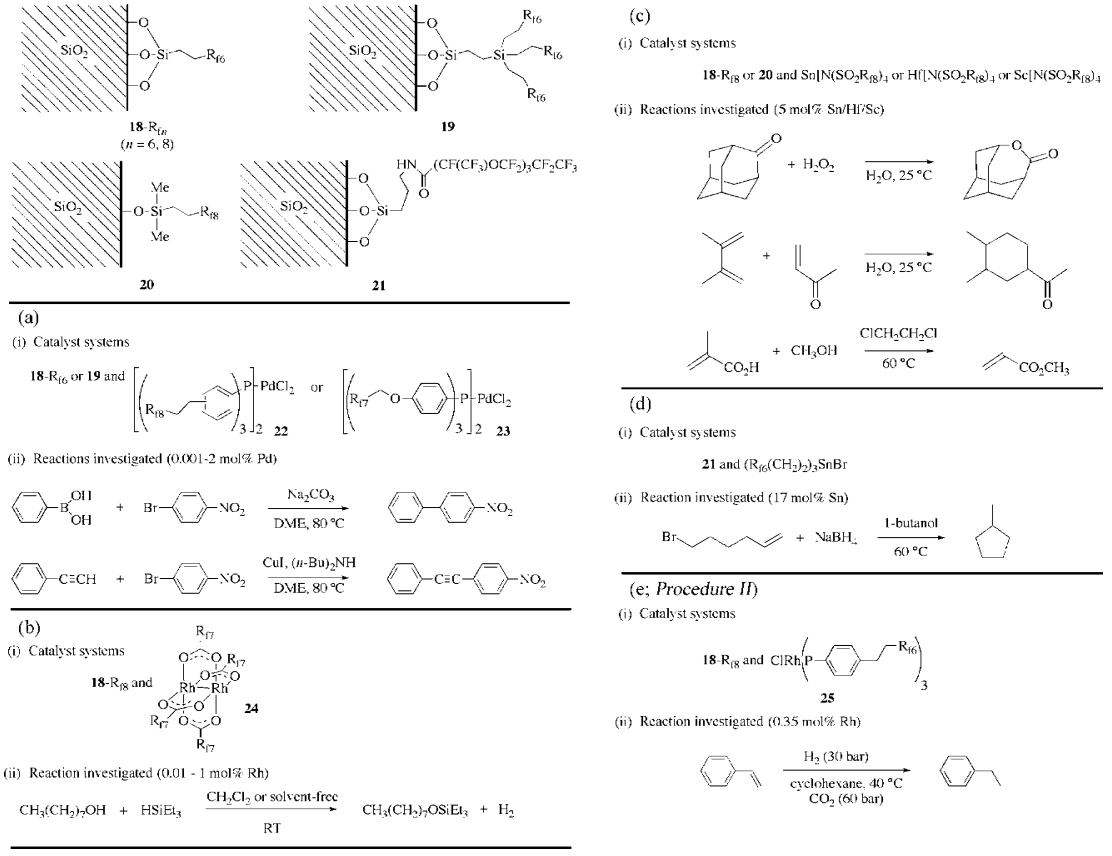

Scheme 2.4 Recovery of fluorous catalysts using fluorous silica gel, including procedures I and II in Figure 2.3b.

With the silylations, rhodium loss was 2.5–2.6% per cycle and the activity loss was ca 10% per cycle, as determined by rate measurements. Another catalyst prepared from the R_{f11} homolog of **24** was also investigated. Later studies involving the systems in Scheme 2.4a have implicated a substantial role for non-fluorous, possibly metallic, palladium catalysts derived from **22** and **23** [53c]. Such possibilities deserve particular scrutiny for any type of metal-catalyzed reaction in which catalyst recovery involves collecting a residue.

2.6.3
Approaches Involving CO_2 Pressure

Although special attention was given to CO_2 gas pressures as non-thermal miscibility or solubility switches in Figures 2.2 and 2.3, there has so far been only a single application to the recovery of a fluorous catalyst. As depicted in Scheme 2.4e, Jessop, Eckert, Liotta and co-workers adsorbed the fluorous rhodium tris(triarylphosphine) complex **25** – an analog of Wilkinson's catalyst – on fluorous silica gel [16]. Hydrogenations were subsequently carried out in cyclohexane slightly above room temperature under 60 bar of CO_2 – far from the supercritical regime. Under these conditions, **25** completely solubilized, as confirmed by independent high-pressure spectroscopic measurements. The catalyst rest state adsorbed when the pressure was released. Five cycles were conducted with essentially quantitative conversions. In a separate set of experiments, each cycle was taken to partial conversion (lower catalyst loadings, shorter reaction times). The reasonably constant yield data (72–46%) established good retention of activity.

This simple and elegant procedure is richly deserving of further study. Roughly comparable hydrogenations have been conducted at 60 °C in toluene, but using fluorous silica gel in place of CO_2 and the analog of **25** without the $(CH_2)_2$ spacers. Interestingly, rhodium leaching levels were substantial (12–25%), with even greater losses of activities in subsequent cycles [52].

2.6.4
Fluorous Solid-phase Extractions

Although this recovery procedure, shown schematically in Figure 2.4, gives the impression of being solvent intensive, there are several compensating features. First, relatively short perfluoroalkyl segments confer retention times considerably longer than those of organic compounds. Thus, R_{f6} and the newer generation non-bioaccumulative ponytails described above can be employed. Second, since such catalysts often retain appreciable solubilities in organic solvents, they can be synthesized and applied in reactions analogously to non-fluorinated analogs. Given the considerable generality of this recovery procedure, a collage of representative catalysts is depicted in Scheme 2.5, taken largely from studies by Curran, Zhang, Hope, Stuart and co-workers. [58, 59] No attempt has been made to be comprehensive. These have seen use in alkene metathesis (**26**), Heck reactions (**27**), condensations of β-diketones and ethyl cyanoformate (**28**), ligands for

ruthenium-catalyzed enantioselective hydrogenations (**29**), phase transfer catalysis (**30**) and Diels–Alder reactions (**31**).

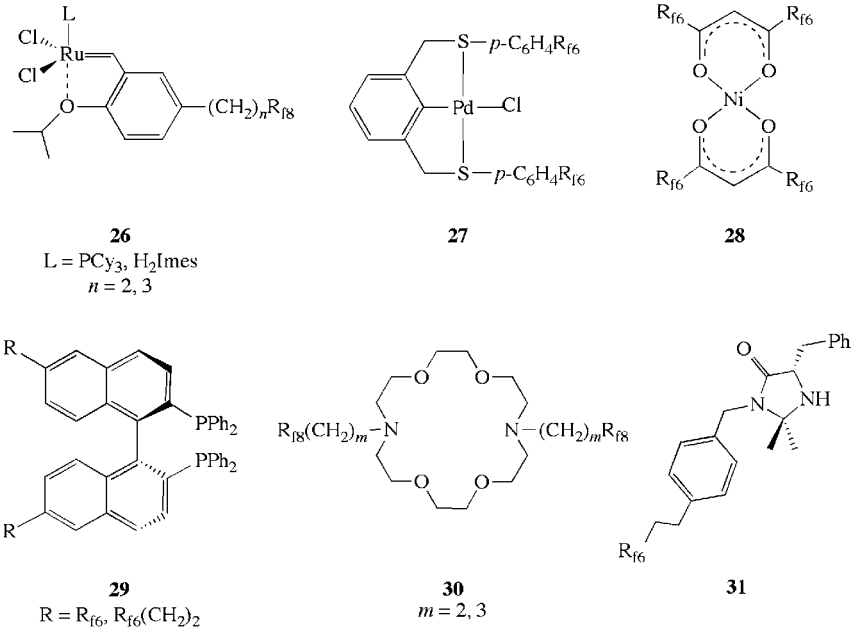

26
L = PCy_3, H_2Imes
$n = 2, 3$

27

28

29
R = R_{f6}, $R_{f6}(CH_2)_2$

30
$m = 2, 3$

31

Scheme 2.5 Representative catalysts recovered by fluorous solid-phase extraction (Figure 2.4).

2.7
Summary and Perspective

In this chapter, the essential features of fluorous chemistry have been reviewed and the evolution of catalyst recovery protocols has been traced from the initial fluorous–organic liquid–liquid biphase approach of Horváth and Rábai to various methods that substitute fluorous solid phases for fluorous liquid phases. In a few cases, even organic solvents prove unnecessary.

From a green chemistry standpoint, there are clearly additional frontiers for optimization. One involves the design and application of ponytails that do not persist in the environment – due either to abiological or biological degradation pathways – or at least do not bioaccumulate. Advances here may also be extendable to fluorous solid phases. Another involves the development and popularization of fluorous solvents, or sufficiently lipophobic and hydrophobic substitutes, which are similarly less environmentally persistent. This would give fresh impetus to liquid–liquid biphase protocols. In view of the rapid ongoing development of diverse applications for fluorous chemistry, these topics are certain to garner intense interest in the near future.

Acknowledgments

The Deutsche Forschungsgemeinschaft (DFG, GL 300/3-3) and the Welch Foundation are warmly thanked for financial support and Dr. József Rábai for helpful discussions.

References

1 Horváth, I.T. and Rábai, J. (1994) *Science*, **266**, 72.
2 Gladysz, J.A. (1994) *Science*, **266**, 55.
3 Gladysz, J.A., Curran, D.P. and Horváth, I.T. (eds) (2004) *Handbook of Fluorous Chemistry*, Wiley-VCH Verlag GmbH, Weinheim.
4 Gladysz, J.A. and Curran, D.P. (2002) *Tetrahedron*, **58**, 3823.
5 Yoshida, J.-i. and Itami, K. (2002) *Chemical Reviews*, **102**, 3693.
6 West, K.N., Hallett, J.P., Jones, R.S., Bush, D., Liotta, C.L. and Eckert, C.A. (2004) *Industrial & Engineering Chemistry Research*, **43**, 4827.
7 (a) Zhang, W., Luo, Z., Chen, C.H.-T. and Curran, D.P. (2002) *Journal of the American Chemical Society*, **124**, 10443; (b) Yang, F., Newsome, J.J. and Curran, D.P. (2006) *Journal of the American Chemical Society*, **128**, 14200.
8 Moreno-Mañas, M. and Pleixats, R. (2004) Fluorous nanoparticles, in *Handbook of Fluorous Chemistry* (eds J.A. Gladysz, D.P. Curran and I.T. Horváth), Wiley-VCH Verlag GmbH, Weinheim, p. 491.
9 Sheldon, R.A. (2005) *Green Chemistry*, **7**, 267.
10 Ravishankara, A.R., Solomon, S., Turnipseed, A.A. and Warren, R.F. (1993) *Science*, **259**, 194.
11 Ravishankara, A.R., Turnipseed, A.A., Jensen, N.R., Barone, S., Mills, M., Howard, C.J. and Solomon, S. (1994) *Science*, **263**, 71.
12 (a) Matsubara, H., Yasuda, S., Sugiyama, H., Ryu, L., Fujii, Y. and Kita, K. (2002) *Tetrahedron*, **58**, 4071; (b) Fukuyama, T., Arai, M., Matsubara, H. and Ryi, I. (2004) *The Journal of Organic Chemistry*, **69**, 8105.
13 (a) Yu, M.S., Curran, D.P. and Nagashima, T. (2005) *Organic Letters*, **7**, 3677; (b) Curran, D.P., Bajpai, R. and Sanger, E. (2006) *Advanced Synthesis and Catalysis*, **348**, 1621; (c) Chu, Q., Yu, M.S. and Curran, D.P. (2007) *Tetrahedron*, **63**, 9890; (d) Chu, Q., Yu, M.S. and Curran, D.P. (2008) *Organic Letters*, **10** 749.
14 Jessop, P.G., Ikariya, T. and Noyori, R. (1999) *Chemical Reviews*, **99**, 475.
15 Jessop, P.G., Olmstead, M.M., Ablan, C.D., Grabenauer, M., Sheppard, D., Eckert, C.A. and Liotta, C.L. (2002) *Inorganic Chemistry*, **41**, 3463.
16 Ablan, C.D., Hallett, J.P., West, K.N., Jones, R.S., Eckert, C.A., Liotta, C.L. and Jessop, P.G. (2003) *Chemical Communications*, 2972.
17 da Costa, R.C., Hampel, F. and Gladysz, J. (2007) *Polyhedron*, **26**, 581 and references therein.
18 Curran, D.P. (2004) Separations with fluorous silica gel and related materials, in *Handbook of Fluorous Chemistry* (eds J.A. Gladysz, D.P. Curran and I.T. Horváth), Wiley-VCH Verlag GmbH, Weinheim, p. 101.
19 (a) Giesy, J.P. and Kannan, K. (2001) *Environmental Science & Technology*, **35** 1339; (b) Kannan, K., Koistinen, J., Beckmen, K., Evans, T., Gorzelny, J.F., Hansen, K.J., Jones, P.D., Helle, E., Nman, M. and Giesy, J.P. (2001) *Environmental Science & Technology*, **35**, 1593.
20 (a) Moody, C.A., Martin, J.W., Kwan, W.C., Muir, D.C.G. and Marbury, S.A. (2002) *Environmental Science & Technology*, **36**,

545; (b) Martin, J.W., Smithwick, M.A., Braune, B.M., Hoekstra, P.F., Muir, D.C.G. and Marbury, S.A. (2004) *Environmental Science & Technology*, **38**, 373.

21 Hurley, M.D., Ball, J.C., Wallington, T.J., Andersen, M.P.S., Nielsen, O.J., Ellis, D.A., Martin, J.W. and Marbury, S.A. (2006) *Journal of Physical Chemistry A*, **110**, 12443, and references cited therein.

22 Ochoa-Herrera, V., Sierra-Alvarez, R., Somogyi, A., Jacobsen, N.E., Wysocki, V.H. and Field, J.A. (2008) *Environmental Science & Technology*, **42**, 3260.

23 Moriwaki, H., Takagi, Y., Tanaka, M., Tsuruho, K., Okitsu, K. and Maeda, Y. (2005) *Environmental Science & Technology*, **39**, 3388.

24 Gladysz, J.A. and Emnet, C. (2004) Fluorous solvents and related media, in *Handbook of Fluorous Chemistry* (eds J.A. Gladysz, D.P. Curran and I.T. Horváth), Wiley-VCH Verlag GmbH, Weinheim, pp. 11–23.

25 Maul, J.J., Ostrowski, P.J., Ublacker, G.A., Linclau, B. and Curran, D.P. (1999) *Topics in Current Chemistry*, **206**, 79.

26 Malinverno, G., Comombo, I. and Visca, M. (2005) *Regulatory Toxicology and Pharmacology*, **41**, 228.

27 Gladysz, J.A. (2004) Ponytails: structural and electronic considerations, in *Handbook of Fluorous Chemistry* (eds J.A. Gladysz, D.P. Curran and I.T. Horváth), Wiley-VCH Verlag GmbH, Weinheim,pp. 41–55.

28 Rábai, J., Szabó, D., Borbás, E.K., Kövesi, I., Kövesdi, I., Csámpai, A., Gömöry, Á., Pashinnik, V.E. and Shermolovich, Y.G. (2002) *Journal of Fluorine Chemistry*, **114**, 199.

29 (a) Szabó, D., Bonto, A.-M., Kövesdi, I., Gömöry, A. and Rábai, J. (2005) *Journal of Fluorine Chemistry*, **126**, 641; (b) Szabó, D., Mohl, J., Bálint, A.-M., Bodor, A. and Rábai, J. (2006) *Journal of Fluorine Chemistry*, **127**, 1496.

30 (a) Jiang, Z.-X. and Yu, Y.B. (2007) *Tetrahedron*, **63**, 3982; (b) Jiang, Z.-X. and Yu, Y.B. (2007) *The Journal of Organic Chemistry*, **72**, 1464.

31 Jiang, Z.-X. and Yu, Y.B. (2008) *Synthesis*, 215.

32 Gladysz, J.A., Emnet, C. and Rábai, J. (2004) Partition coefficients involving fluorous solvents, in *Handbook of Fluorous Chemistry* (eds J.A. Gladysz, D.P. Curran and I.T. Horváth), Wiley-VCH Verlag GmbH, Weinheim, pp. 56–100.

33 van Vliet, M.C.A., Arends, I.W.C.E. and Sheldon, R.A. (1999) *Chemical Communications*, 263.

34 Olofsson, K., Kim, S.-Y., Larhed, M., Curran, D.P. and Hallberg, A. (1999) *The Journal of Organic Chemistry*, **64**, 4539, (see Table 2, entry 4).

35 (a) Wende, M., Meier, R. and Gladysz, J.A. (2001) *Journal of the American Chemical Society*, **123**, 11490; (b) Wende, M. and Gladysz, J.A. (2003) *Journal of the American Chemical Society*, **125**, 5861.

36 Emnet, C., Weber, K.M., Vidal, J.A., Consorti, C.S., Stuart, A.M. and Gladysz, J.A. (2006) *Advanced Synthesis and Catalysis*, **348**, 1625.

37 Ishihara, K., Kondo, S. and Yamamoto, H. (2001) *Synlett*, 1371.

38 Ishihara, K., Hasegawa, A. and Yamamoto, H. (2002) *Synlett*, 1299.

39 (a) Xiang, J., Orita, A. and Otera, J. (2002) *Advanced Synthesis and Catalysis*, **344**, 84; (b) Otera, J. (2004) *Accounts of Chemical Research*, **37**, 288.

40 Mikami, K., Mikami, Y., Matsuzawa, H., Matsumoto, Y., Nishikido, J., Yamamoto, F. and Nakajima, H. (2002) *Tetrahedron*, **58**, 4015.

41 Maayan, G., Fish, R.H. and Neumann, R. (2003) *Organic Letters*, **5**, 3547.

42 Contel, M., Villuendas, P.R., Fernández-Galladrdo, J., Alonso, P.J., Vincent, J.-M. and Fish, R.H. (2005) *Inorganic Chemistry*, **44**, 9771.

43 Mino, R., Sato, Y., Saito, A., Tanaka, Y., Saotome, H., Sakamoto, M. and Fujita, T. (2005) *The Journal of Organic Chemistry*, **70**, 7979.

44 Sokeirik, Y.S., Mori, H., Omote, M., Sato, K., Tarui, A., Kumadaki, I. and Ando, A. (2007) *Organic Letters*, **9**, 1927.

45 Wang, C.-Y., Meng, W.-D., Huang, Y.-G. and Qing, F.-L. (2005) *Journal of Fluorine Chemistry*, **126**, 996.

46 Seidel, F. and Gladysz, J.A. (2008), *Advanced Synthesis and Catalysis*, **350**, 2443.

47 (a)Consorti, C.S., Jurisch, M. and Gladysz, J.A. (2007) *Organic Letters*, **9**, 2309; (b) Mandal, D., Jurisch, M., Consorti, C.S. and Gladysz, J.A. (2008), *Chem Asian J.*, **3**, 1772.

48 Fukuyama, T., Arai, M., Matsubara, H. and Ryu, I. (2004) *The Journal of Organic Chemistry*, **69**, 8105.

49 Juliette, J.J.J., Rutherford, D., Horváth, I.T. and Gladysz, J.A. (1999) *Journal of the American Chemical Society*, **121**, 2696.

50 (a) Dinh, L.V. and Gladysz, J.A. (1999) *Tetrahedron Letters*, **40**, 8995; (b) Dinh, L.V. and Gladysz, J.A. (2005) *New Journal of Chemistry*, **29**, 173.

51 Dinh, L.V. and Gladysz, J.A. (2005) *Angewandte Chemie-International Edition*, **44**, 4095; (2005) *Angewandte Chemie*, **117**, 4164.

52 Hope, E.G., Sherrington, J. and Stuart, A.M. (2006) *Advanced Synthesis and Catalysis*, **348**, 1635.

53 (a) Tzschucke, C.C., Markert, C., Glatz, H. and Bannwarth, W. (2002) *Angewandte Chemie-International Edition*, **41**, 4500; (2002) *Angewandte Chemie*, **114**, 4678; (b) Tzschucke, C.C. and Bannwarth, W. (2004) *Helvetica Chimica Acta*, **87**, 2882; (c) Tzschucke, C.C., Andrushko, V. and Bannwarth, W. (2005) *European Journal of Organic Chemistry*, 5248.

54 (a) Biffis, A., Zecca, M. and Basato, M. (2003) *Green Chemistry*, **5**, 170; (b) Biffis, A., Braga, M. and Basato, M. (2004) *Advanced Synthesis and Catalysis*, **346**, 451.

55 Yamazaki, O., Hao, X., Yoshida, A. and Nishikido, J. (2003) *Tetrahedron Letters*, **44**, 8791.

56 Jenkins, P.M., Steele, A.M. and Tsang, S.C. (2003) *Catalysis Communications*, **4**, 45.

57 (a) Curran, D.P., Fischer, K. and Moura-Letts, G. (2004) *Synlett*, 1379; (b) Matsugi, M. and Curran, D.P. (2005) *The Journal of Organic Chemistry*, **70**, 1636; (c) Chu, Q., Zhang, W. and Curran, D.P. (2006) *Tetrahedron Letters*, **47**, 9287.

58 (a) Croxtall, B., Hope, E.G. and Stuart, A.M. (2003) *Chemical Communications*, 2430; (b) Hope, E.G., Stuart, A.M. and West, A.J. (2004) *Green Chemistry*, **6**, 345; (c) Stuart, A.M. and Vidal, J.A. (2007) *The Journal of Organic Chemistry*, **72**, 3735

3
Chemistry and Applications of Iron–TAML Catalysts in Green Oxidation Processes Based on Hydrogen Peroxide

Terrence J. Collins, Sushil K. Khetan, and Alexander D. Ryabov

3.1
Introduction

Nature uses iron-based enzymes to catalyze oxidation reactions based upon oxygen and hydrogen peroxide, but until recently their efficiency and reactivity have stubbornly eluded replication in synthetic molecular catalysts. A series of small-molecule non-heme iron complexes denoted Fe–tetraamido macrocyclic ligand (TAML) activators (Scheme 3.1) are proving to be highly effective mimics of the peroxidase enzymes [1, 2]. Fe–TAML activators are also showing reactivity reminiscent of short-circuited catalytic cycles of the cytochrome-P450 enzymes. These enzymes usually make coordinated peroxide from oxygen at their active site and then proceed to use it, but can be short-circuited (relieve the requirement to reduce oxygen) by the use of various oxidants [3–5]. In the precatalyst forms of Fe–TAMLs, iron(III) ions are bonded to the four deprotonated amide-N atoms of macrocyclic tetraamide ligands. Fe^{III}–TAMLs use hydrogen peroxide (H_2O_2) to oxidize a broad range of substrates, exhibiting very high reactivity that is similar to the peroxidase enzymes themselves. While the relatively environmentally compatible and inexpensive H_2O_2 serves as the ultimate source of the oxygen atom as with peroxidase enzymes, Fe^{III}–TAML catalysts remain fairly stable under catalytic conditions such that they are able to achieve high turnover numbers until they eventually degrade under the potent oxidizing conditions – this designed stability is the real key to their successful mimicking properties [6, 7]. The suitability of Fe–TAML–peroxide processes for purifying water has been tested now for a wide range of organic pollutants, often ones that are highly recalcitrant and the technical performance is proving to be very impressive [6]. As we describe in this chapter, Fe–TAML activators (Scheme 3.1) catalyze the chemistry of a variety of peroxides. The reactions typically take place at room temperature under ambient conditions, although there is a pH dependence on the reactivity, with the highest rates being found under basic conditions near pH 10 for most catalysts. This chapter has been written to provide the reader with an overview of the published literature on the basic chemistry, mechanisms of catalysis and applications of Fe–TAML activators.

Green Catalysis, Volume 1: Homogeneous Catalysis.
Edited by Robert H. Crabtree

ISBN: 978-3-527-32496-5

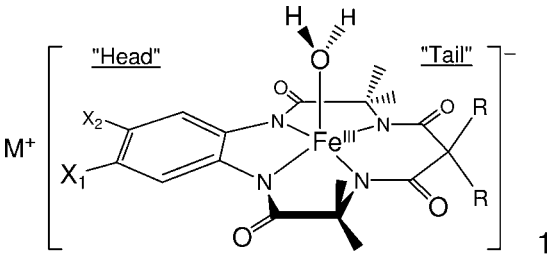

1	X_1	X_2	R
a	H	H	Me
b	Me	Me	Me
c	Me	H	Me
d	MeO	MeO	Me
e	NO_2	H	Me
f	COOMe	H	Me
g	COOH	H	Me
h	$CONH(CH_2)_2NMe_3^+$	H	Me
i	Cl	Cl	Me
j	Cl	Cl	Et
k	Cl	Cl	F
l	H	H	F
m	H	H	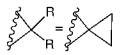
n	Cl	Cl	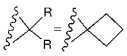

Scheme 3.1 Fe^{III}–TAML activators are pentacoordinated species, usually with an axial aqua ligand, in the solid state. The aqua complexes are synthesized as such or as the corresponding chloro species with Cl^- instead of H_2O (and with two as opposed to one $M^+ = Li^+$, Na^+, NR_4^+ counter ions). The subscript Cl as in $\mathbf{1_{Cl}}$ is employed to indicate that the corresponding chloro species to the aqua complex **1** is being discussed.

3.2
Properties of Fe–TAMLs and Mechanisms of Oxidation with Hydrogen Peroxide

3.2.1
Properties of Tetraamido Macrocyclic Iron(III) Complexes in the Solid State and in Water

3.2.1.1 Solid-State Structure and Speciation in Water

Iron(III)–TAML activators are isolated from the synthetic procedures usually as five-coordinate aqua species and occasionally as the five-coordinate chloro analogue. Representative crystal structures of $\mathbf{1i_{Cl}}$, $\mathbf{1l_{Cl}}$ and **1a** are shown in Scheme 3.2 [8].

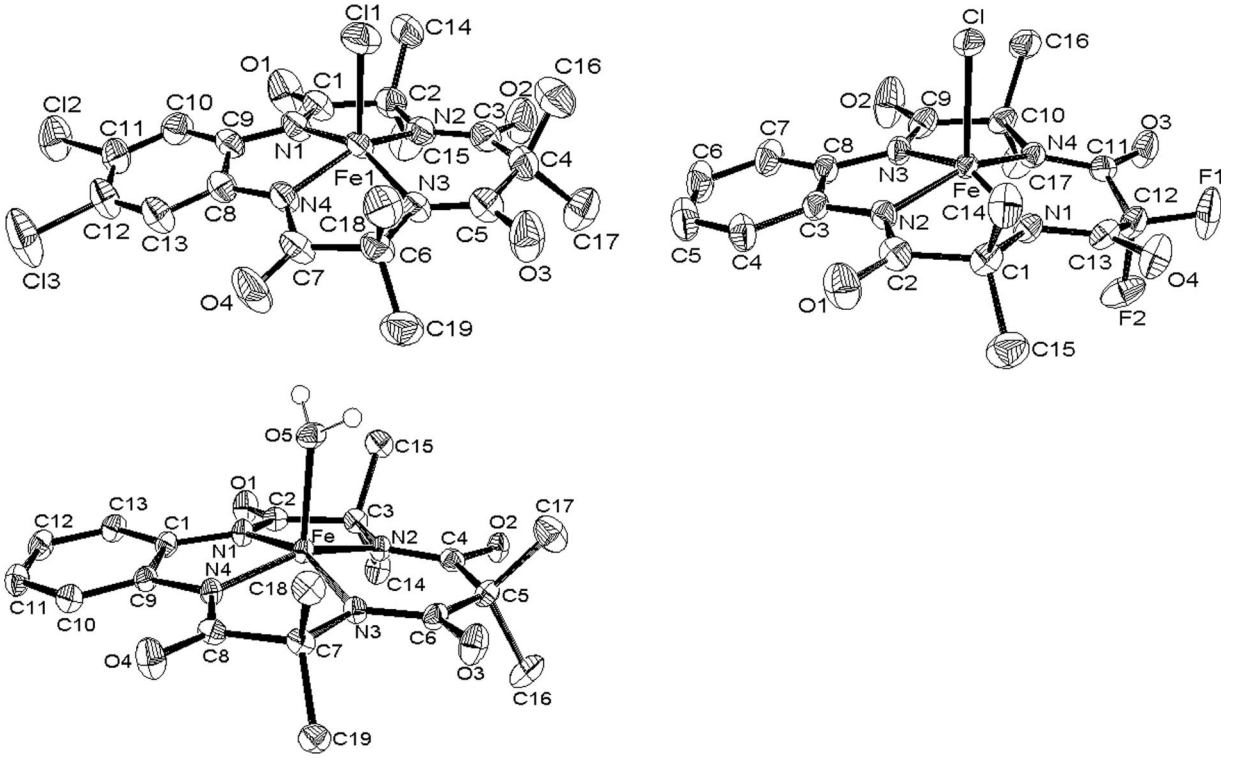

Scheme 3.2 Crystal structures of complexes $\mathbf{1i_{Cl}}$ (a dianion), $\mathbf{1l_{Cl}}$ (a dianion) and **1a** (a monoanion) [8]. H atoms are omitted for clarity.

The Fe–N bonds are short (mean 1.897, 1.894 and 1.885 Å in $\mathbf{1i_{Cl}}$, $\mathbf{1l_{Cl}}$ and **1a**, respectively) and the macrocyclic ligands have a high degree of planarity. Iron(III) is out of the plane by 0.448 and 0.403 Å toward chloride in $\mathbf{1i_{Cl}}$ and $\mathbf{1l_{Cl}}$, respectively, and 0.364 Å toward oxygen in **1a**. The Fe–Cl bond distance is much longer (2.359 and 2.361 Å in $\mathbf{1i_{Cl}}$ and $\mathbf{1l_{Cl}}$, respectively) than in $[FeCl_4]^-$ (2.182–2.187 Å) [9, 10] and Fe^{III} porphyrins (2.218 [11], 2.192 [12] and 2.223 Å [13]). The metal cation in a one-electron oxidized analogue of $\mathbf{1i_{Cl}}$ (where the oxidation site is ligand centered) is more deeply immersed into the macrocyclic cavity (0.04 Å displacement) and the Fe–Cl bond length drops to 2.203 Å [14]. The Fe^{III}–Cl bond is elongated in $\mathbf{1_{Cl}}$ due to the ground-state destabilization of the axial σ-bonding orbitals by the four deprotonated strong σ-donor amido-N ligands.

The structures in Scheme 3.2 differ in the vicinity of the 'tail' R groups. The six-membered rings in $\mathbf{1i_{Cl}}$ and **1a** have a boat conformation and the ligand plane is roughly a plane of symmetry for the methyl groups. The $\mathbf{1l_{Cl}}$ complex adopts a chair conformation. The F1 atom is virtually in the ligand plane; F2 is perpendicular to it. The separation between F1 and two adjacent amide oxygens O3 and O4 (2.550 and 2.546 Å, respectively) is lower than the sum of the van der Waals radii of O and F (2.75 Å) [15].

Elongated M–Cl bonds are usually cleaved by water to afford the corresponding aqua or hydroxo species [16–18]. This holds for complexes $\mathbf{1_{Cl}}$. The speciation of Fe^{III}–TAMLs in water studied by UV–visible and EPR spectroscopy is shown in Scheme 3.3. The chloro ligands of $\mathbf{1_{Cl}}$ undergo rapid hydrolysis; the equilibrium constants K_{Cl} (Table 3.1) indicate insignificant coordination at $[Cl^-] \leq 0.5\ M$. The complexes produced in water are six-coordinated species with two axial aqua ligands. The UV–visible and EPR spectra vary reversibly at pH 8–11 (Figure 3.1) due to deprotonation of an aqua ligand. The pK_as are in the range 9.4–10.5 (Table 3.1) [8].

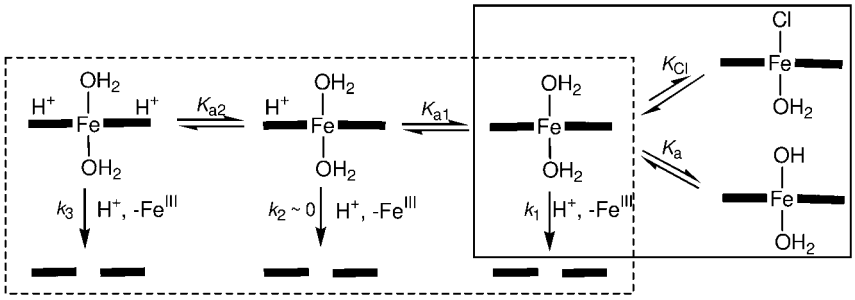

Scheme 3.3 Speciation of Fe^{III}–TAML activators in aqueous solution (solid rectangle) and suggested mechanism of the H^+-induced demetalation (dashed rectangle); ▬ ▬ = free base ligand. Charges are not shown [8].

3.2.1.2 **Binding of Axial Ligands in Water**

The spectra in Figure 3.2 obtained on addition of pyridine to an aqueous solution of **1a** indicate stepwise substitution of both aqueous ligands (Equation 3.1).

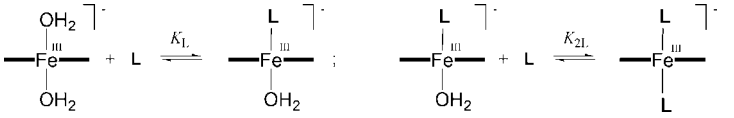

(3.1)

The py-induced spectral changes are quantifiable using Equation 3.2 (ε_M, ε_{ML} and ε_{ML2} are the respective extinction coefficients of all participants of Equation 3.1 and $[M]_t$ is the total concentration of **1**). The values of K_L and K_{2L} are summarized in Table 3.2.

$$A = \frac{\varepsilon_M + \varepsilon_{ML}K_L[L] + \varepsilon_{ML_2}K_LK_{2L}[L]^2}{1 + K_L[L] + K_LK_{2L}[L]^2}[M]_t \tag{3.2}$$

Table 3.1 Equilibrium and kinetic parameters for Fe–TAMLs at 25 °C [8].

Complex	pK_a	K_{Cl} (M^{-1})[a]	k_1^* ($M^{-1}s^{-1}$)[b]	k_3^* ($M^{-3}s^{-1}$)[b]
1a	10.1 ± 0.6	0.18 ± 0.04	2.2 ± 0.7	$(6.7 \pm 0.2) \times 10^5$
			6.1 ± 0.5[c]	$(6.4 \pm 0.3) \times 10^5$[a]
1i	10.0 ± 0.2	0.21 ± 0.09	5.19 ± 0.06	$(1.13 \pm 0.01) \times 10^6$
1d	10.5 ± 0.5	>0.05	7.1 ± 0.5	$(6.7 \pm 0.5) \times 10^5$
1j	10.4 ± 0.3		0.31 ± 0.02	$(1.03 \pm 0.05) \times 10^3$
1l	9.5 ± 0.4	1.9 ± 0.2	$(1.6 \pm 0.1) \times 10^{-4}$	$(1.6 \pm 0.2) \times 10^{-4}$
1k	9.4 ± 0.6	2.4 ± 0.4	$(3.7 \pm 0.4) \times 10^{-5}$	$(4.8 \pm 0.6) \times 10^{-5}$

[a] pH 7.
[b] 0.1 M KPF_6.
[c] In DCl–D_2O.

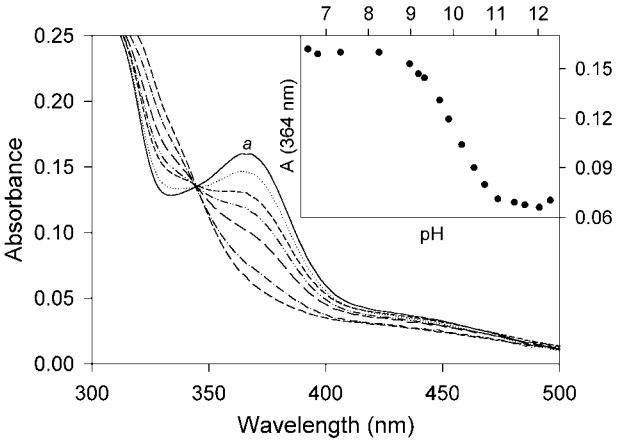

Figure 3.1 Spectra of complex **1i** at different pHs: spectrum *a* was obtained at pH 8.25 (25 °C and 0.1 *M* KPF_6); other spectra were run at pH 9.18, 9.68, 9.89, 10.2, 10.8 and 11.4. The inset shows the absorbance versus pH plot at 364 nm [8].

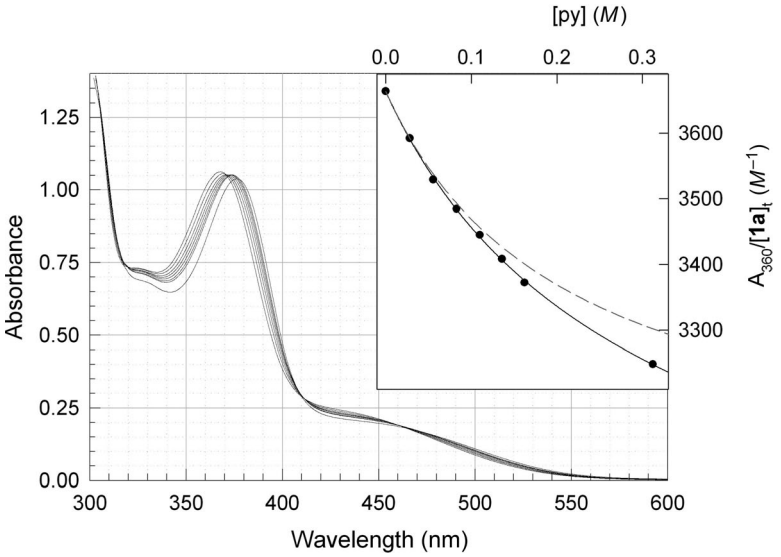

Figure 3.2 Spectral changes of **1a** (2.75×10^{-4} *M*) in the presence of pyridine: 0.1 *M* KPF_6, pH 6.3 and 25 °C. Inset: absorbance at 360 nm as a function of [py]; the solid line is the calculated curve using best-fit parameters of Equation 3.2; the broken line is a calculated curve with $K_{2L} = 0$ validating binding of the second axial ligand [19].

The data in Table 3.2 reveal that imidazole is a better ligand for **1**. The relation $K_L > K_{2L}$ holds for both ligands, but the gap between K_L and K_{2L} is larger for pyridine. An opposite trend is observed for Fe^{II} and Fe^{III} porphyrins, for which only β_2 ($K_L \times K_{2L}$) is usually determined in water [20] and non-aqueous solutions [21, 22]. In water, only bis-ligated species are observed, which are, however, formed from iron–porphyrin dimers [23, 24]. The X-ray structure of the monoligated 1-methylimidazole (MeIm) adduct (**Ia**–MeIm) is shown in Scheme 3.4 [19]. A square pyramidal environment is typical of Fe^{III}–TAMLs in the solid state [8, 14, 25]. Imidazole does not change the coordinative arrangement of Fe^{III}–TAMLs from that observed with axial water or chloride. The position of imidazole relative to four equatorial amide nitrogens, N1–N4, is interesting. The imidazole plane is close to parallel to the plane through atoms Fe1, N2 and N4 [dihedral angle 11.2(2)°].

Table 3.2 Equilibrium constants of Fe^{III}–TAMLs **1a** in aqueous solution at 25 °C, 0.1 *M* KPF_6 [19].

L	pH	K_L (M^{-1})	K_{2L} (M^{-1})
Pyridine	5.0	4.7 ± 0.1	0.42 ± 0.03
Imidazole	6.3	69 ± 10	4.7 ± 4.5

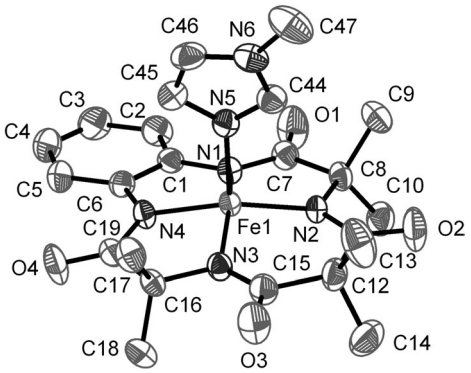

Scheme 3.4 The molecular structure of the anionic part of **1a**–MeIm. H atoms are omitted for clarity. Fe–N(1) 187.4(2) pm; Fe–N(2) 187.5(2) pm; Fe–N(3) 188.5(3) pm; Fe–N(4) 187.2 (2) pm; Fe–N(5) 212.6(2) pm. DIAMOND release 3.1e, Crystal Impact GbR, Bonn, Germany [19].

3.2.2 Demetalation of Fe–TAMLs

3.2.2.1 Induced by the Proton (Specific Acid)

At pH 3–4 and lower, compounds **1** are involved in H^+-promoted demetalation that follows the rate law $k_{obs} = k_1^*[H^+] + k_3^*[H^+]^3$ [8]. This rate law is consistent with the mechanism in Scheme 3.3 (dashed rectangle) provided that K_{a1} and K_{a2} are high ensuring $K_{a1}K_{a2} \gg (K_{a2}[H^+] + [H^+]^2)$ and k_2 is negligible compared with k_1 and k_3 [8]. The rate of acid-induced demetalation depends only slightly on the nature of the head substituents X (Table 3.1). In contrast, the tail-R groups dramatically affect k_1^* and, for the most part, k_3^*, indicating that tail amide O-atoms are sites of peripheral protonation. This was used as a strategy for producing acid tolerant Fe^{III}–TAML catalysts. Replacement of the tail groups R = Me with R = F produces a remarkable stabilization. The rate constants in Table 3.1 show that under weakly acidic conditions, where the k_1^* pathway dominates over k_3^*, fluorinated **1k** is 10^5-fold more H^+-tolerant than **1a**. Under more acidic conditions, where the k_3^* pathway contribution to the overall rate is dominant, the difference reaches a unique 11 orders of magnitude [8]. The cleavage of a single M−N bond causes a strong distortion of the planar complex and induces rapid cleavage of the remaining M−N bonds: distorted TAML ligands tend to have non-planar amides and high hydrolytic instability, e.g., **2** [8]. Complex **2** is unstable in water at pH 7. The rate constant k_1^* for **2** is >1000 times higher than for the most reactive complex in Table 3.1.

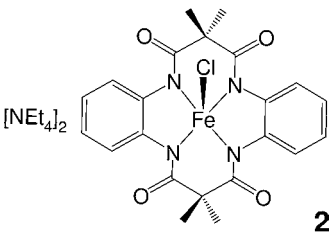

2

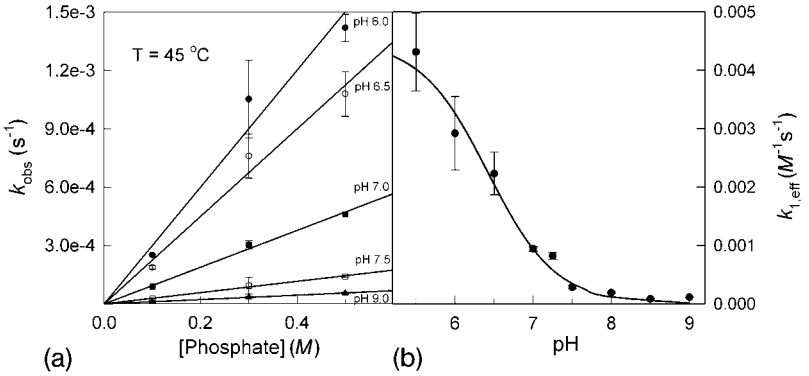

Figure 3.3 (a) Pseudo-first-order rate constants for demetalation of **1a** versus phosphate concentration at different pHs and 45 °C. (b) Second-order rate constants $k_{1,eff}$ for demetalation of **1a** as a function of pH at 45 °C. The solid line is a theoretical curve calculated using the best-fit values of the parameters of ($K_{ML} \times K_{LH}$) and K_{a2} [19].

3.2.2.2 Induced by General Acids

All the **1** activators are catalytically active in neutral and basic aqueous solutions. Under these conditions, **1** are also subject at pH 4–9 to catalyzed demetalation by Brønsted acid buffer components such as $H_2PO_4^-$, HSO_3^-, CH_3CO_2H and $HO_2CCH_2CO_2^-$. Buffers based on pyridine (py) and tris(hydroxymethyl)aminomethane (TRIS) are inactive. Pseudo-first-order rate constants for the demetalation (k_{obs}) are linear functions of total phosphate (Figure 3.3a) and the effective second-order rate constants $k_{1,eff}$ depend on pH as shown in Figure 3.3b. The inflection point at pH $\approx$ 6.5 is coincident with the pK_a of dihydrogenphosphate, implying that $H_2PO_4^-$ is reactive [19].

The data in Figure 3.3 agree with a mechanism as shown in Scheme 3.5. The rate of demetalation of **1a** in $H_2PO_4^-/HPO_4^{2-}$ buffer is appreciable, but the k_{obs} values for **1k** and **1m** are immeasurably low, showing that the rates are strongly affected by

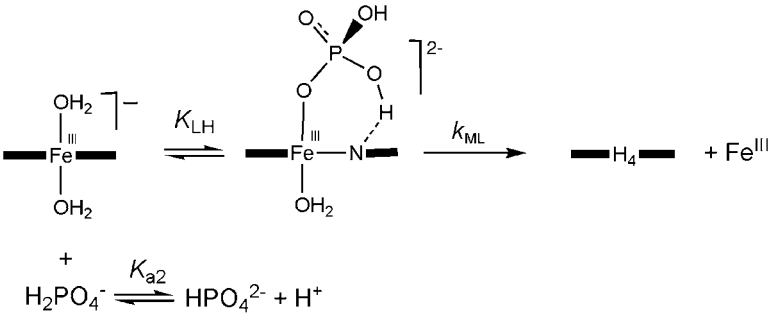

Scheme 3.5 Mechanism for the phosphate-induced demetalation of Fe^{III}–TAMLs.

the tail CR_2 fragments. The reactivities of **1** depend insignificantly on the aromatic ring or 'head' group of **1** [19].

The demetalating abilities of buffer species depend on their structures and acidities. Thus, whereas pyridine-2-carboxylic (picolinic) acid catalyzes the demetalation, its 3- and 4-isomers (nicotinic and isonicotininc acids) are inactive. The reaction order in picolinic acid is one for **1a** and two for **1m**. For **1m**, 'inactive' pyridine and nicotinic acid speed up the demetalation in the presence of picolinic acid, suggesting that the second order arises from the axial binding of two pyridine molecules, one of which must be picolinic acid for the intramolecular proton delivery to an Fe—N moiety. Mechanisms of demetalation of **1** by picolinic acid are shown in Scheme 3.6.

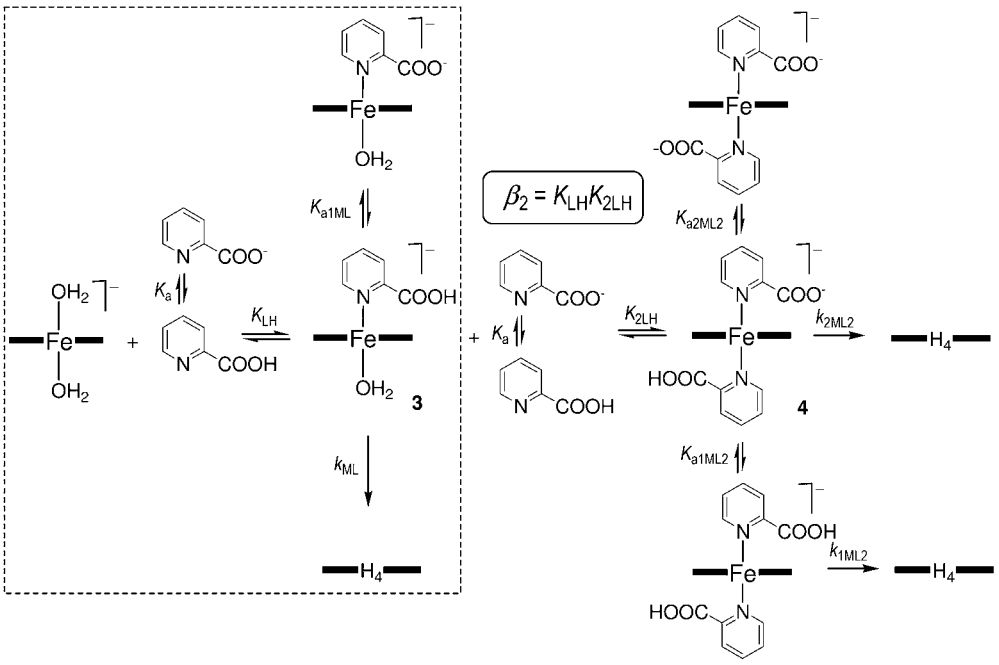

Scheme 3.6 General mechanism of demetalation of **1** by picolinic acid accounting for first (**1a**, in the box) and second (**1m**) orders in the acid. The charge of the Fe^{III}–TAML complex is shown outside the bracket and localized charges are shown for the deprotonated pyridine carboxylates [19].

Species **3** and **4** are postulated intermediates in the demetalation of **1a** and **1m**, respectively. Picolinic acid binds to the axial site of Fe^{III} and then delivers the carboxylic proton to an Fe—N bond. This is more difficult in the case of **1m**, where the amidato-N donor atoms are less basic. Therefore, the second py ligand may increase the electron density at the Fe—N bonds and it may also affect the location of the iron atom with respect to the plane of the four amidato ligands in a manner that favors the demetalation. It is significant that the picolinic acid α-carboxylic group is clearly not

essential for this second pyridine ligand because both py and nicotinic acid also accelerate the demetalation. This understanding is of real value in practical applications of Fe–TAML activators. For example, buffer systems can now be chosen that allow for long-term storage of Fe–TAML solutions at pH 4–9.

3.2.3
Understanding Mechanisms of Catalysis by Fe–TAML Activators of Hydrogen Peroxide

3.2.3.1 General Mechanism

Fe^{III}–TAML activators [**1**] of hydrogen peroxide [6, 7, 26] are valuable catalysts for a variety of environmentally important oxidation processes [27–31]. The general stoichiometric mechanism of catalysis is shown in Scheme 3.7 [31].

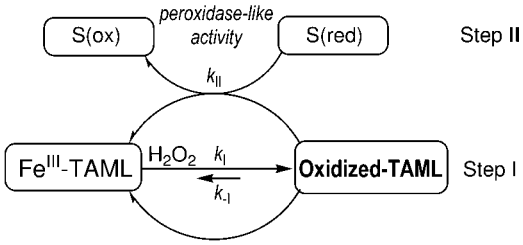

Scheme 3.7 General mechanism of catalysis by Fe^{III}–TAML activators in water. All rate constants are conditional (pH dependent).

The peroxidase-like activity of **1** is the dominating reactivity feature of the activators and therefore it has been studied kinetically [31, 32]. In terms of Scheme 3.7, the kinetic equation for the peroxidase-like activity, i.e. $-d[S(red)]/dt$, is described by Equation 3.3, meaning that under appropriate conditions the catalase-like activity (step III) is negligible.

$$-\frac{d[S(red)]}{dt} = \frac{k_I k_{II}[Fe^{III}-TAML][H_2O_2][S(red)]}{k_{-I} + k_I[H_2O_2] + k_{II}[S(red)]} \quad (3.3)$$

Evidence for the validity of Equation 3.3 with negligible k_{-I} is demonstrated in three-dimensional Figure 3.4, where the initial rates of oxidation of the commercial dye Orange II (Scheme 3.8) are plotted against concentrations of both H_2O_2 and the dye. When the concentration of H_2O_2 is low, the formation of the oxidized TAML is rate limiting and the initial rates are independent of [Orange II]. Speeding up the formation of oxidized TAML by increasing $[H_2O_2]$ moves the oxidation into a different kinetic regime where the step driven by k_{II} controls the rate and hence the rate is almost proportional to the Orange II concentration. Such 3D plots for two-substrate catalytic reactions are observed when numerical values of the products $k_I[H_2O_2]$ and $k_{II}[S(red)]$ are comparable [33].

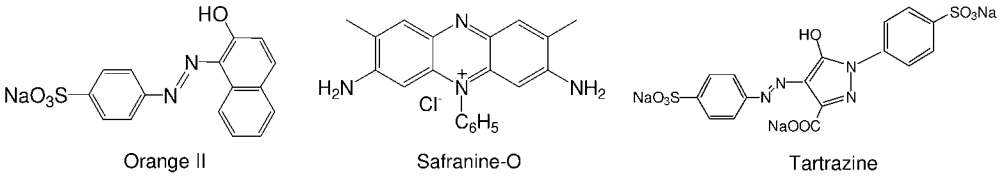

Scheme 3.8 Substrates S(red) used in kinetic measurements.

The rate constants k_I and k_{II} for **1a** calculated from the data in Figure 3.4 of ca 3.5×10^3 and $1.5 \times 10^4\ M^{-1}\,s^{-1}$ (pH 11, 25 °C) respectively, illustrate a very high activity of Fe^{III}–TAML activators, particularly in terms of k_{II}. For comparison, Oakes and Gratton reported $k_{II} = 0.08\ M^{-1}\,s^{-1}$ for the oxidation of Orange II by *p*-sulfonated perbenzoic acid under the same conditions [34]. The rate constant k_I (and also probably k_{II}) is pH dependent [31]. The maximum activity for **1l** is observed at pH $\approx$ 10 [31].

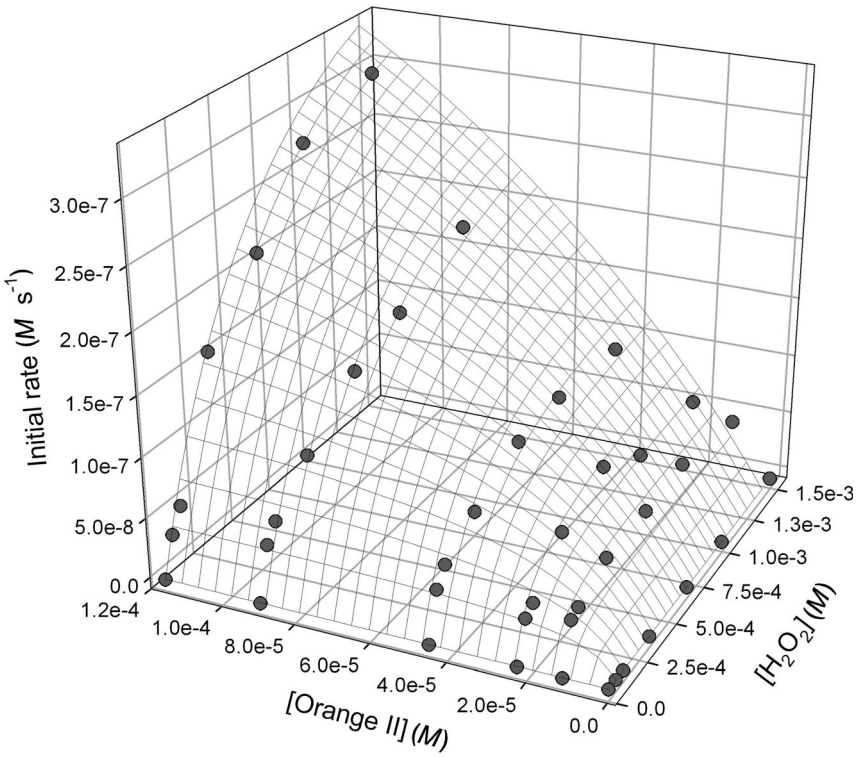

Figure 3.4 3D plot showing the dependence of initial rates of **1a**-catalyzed bleaching of Orange II by H_2O_2 as a function of [H_2O_2] and [Orange II]. Conditions: [**1a**] $2 \times 10^{-7} M$, pH 11, 25 °C [31].

Table 3.3 The rate constants k_I and k_{II} (in $M^{-1}s^{-1}$) for the **1a**-catalyzed oxidation of Orange II at pH 9 and 25 °C [31].

Peroxide	$10^{-3}k_I$	$10^{-4}k_{II}$
H_2O_2	1.40 ± 0.01	3.8 ± 0.3
Benzoyl peroxide	74 ± 3	3.7 ± 0.9
tert-Butyl hydroperoxide	0.024 ± 0.002	3.2 ± 1.5
Cumyl hydroperoxide	0.011 ± 0.001	1.8 ± 0.8

3.2.3.2 Mechanism of Benzoyl Peroxide Activation

The Fe^{III}–TAML activators catalyze oxidations by organic peroxides such as *tert*-butyl hydroperoxide, cumyl hydroperoxide and benzoyl peroxide. Equation 3.3 for the catalyzed oxidation of Orange II by organic peroxides holds at pH 9 and 25 °C [31]. The rate constants k_I and k_{II} in Table 3.3 confirm the closeness of rate constants k_{II} for all oxidants and the exceptionally large value of k_I for benzoyl peroxide, which is by a factor of 53 higher than that for H_2O_2. The reactivity of peroxides in terms of k_I decreases in the series benzoyl peroxide $(6.8 \times 10^3) > H_2O_2$ (130) > *t*-BuOOH (2) > cumyl hydroperoxide (1).

Benzoyl peroxide is much larger than H_2O_2, but the steric effect is not a factor for the highest rate constant k_I. The mechanism of reaction of benzoyl peroxide is shown in Scheme 3.9. It does not have an H−O fragment [1, 2] and therefore its coordination to iron(III) should involve either carbonyl or peroxo oxygen. According to density functional theory (DFT) [31], both oxygen atoms may coordinate to iron(III) because the effective negative charges for carbonyl and peroxo oxygen are similar, i.e. −0.38 and −0.30, respectively. We consider the peroxo oxygen to be a better candidate because the σ^* orbital of the O−O fragment is thus much closer to the reducing Fe^{III} center. However, it is also possible that the O−O bond cleavage occurs via prior coordination of a carbonyl oxygen. The DFT analysis suggests that if the carbonyl oxygen is a donor center, the complexation between **1** and benzoyl peroxide is a dead-end pathway, which does not result in O−O bond cleavage, but because of possible complications of solvation and coordination this should remain considered a possibility at this time. Assuming a peroxo oxygen coordination, intermediate **5** is on the reaction coordinate and the following energy minimum is found for the

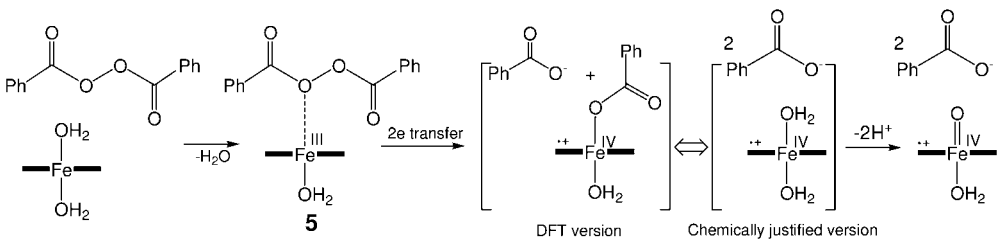

Scheme 3.9 Plausible mechanism for early steps for activation of benzoyl peroxide by Fe^{III}–TAMLs. For details, see text.

system consisting of free benzoate and benzoate coordinated to formally Fe^{V} (or $^{\bullet+}Fe^{IV}$). Benzoate coordination to iron of TAML does not occur in water [8] and the mechanism may well lead to two free benzoates per dibenzoyl peroxide.

3.2.3.3 Nature of Oxidized TAMLs: Hypotheses and Facts

Addition of peroxides to aqueous solutions of **1** produces brownish green absorbing species and less than a stoichiometric amount of peroxide causes a major increase at 350–550 nm. Minutes are needed to obtain invariable spectra at pH < 8.5; at pH > 9 the reaction is much faster. The titration experiments revealed that the absorbing species are by one oxidation equivalent above the resting state, suggesting the formation of an Fe^{IV} species [35]. The formation of the iron(IV) species may proceed via the oxidation of Fe^{III} to Fe^{V} followed by a conproportion of Fe^{V} with another Fe^{III} to produce two Fe^{IV} species. Evidence for this possibility comes from the fact that Fe^{III}–TAMLs in non-aqueous solutions are oxidized by peroxides to genuine Fe^{V}–oxo complexes, as will be described below.

The zero-field Mössbauer spectra of a frozen aqueous solution of the red compound (generated from 1×10^{-3} M ^{57}Fe–**1a** and 0.5 equiv. *t*-BuOOH) at 4.2 K consists of one doublet with a quadrupole splitting, $\Delta E_Q = 4.2\,\mathrm{mm\,s^{-1}}$ and isomer shift (versus Fe metal at 298 K) $\delta = -0.19\,\mathrm{mm\,s^{-1}}$ (Figure 3.5) [35]. This highly negative

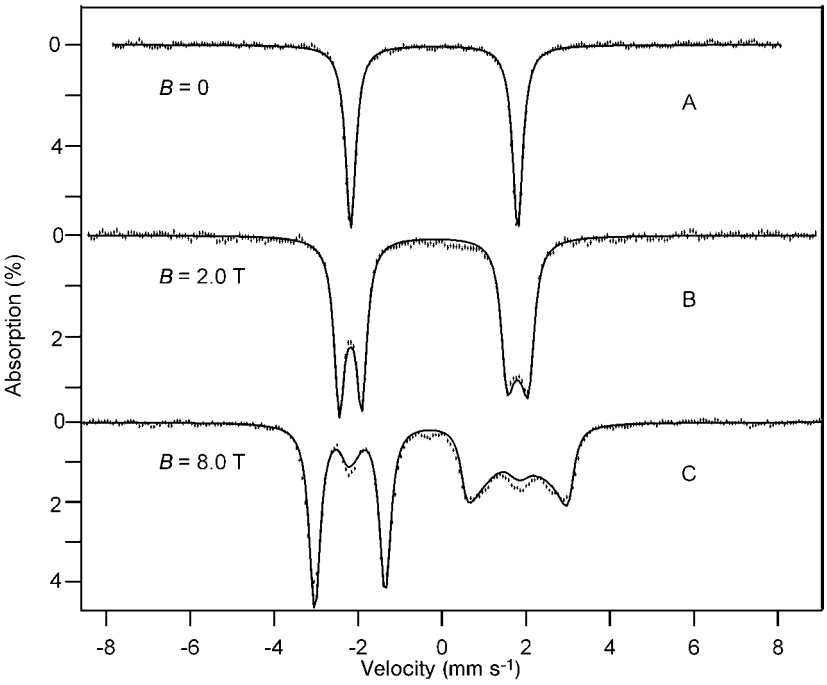

Figure 3.5 4.2 K Mössbauer spectra of ^{57}Fe–**1a** in aqueous solution, pH 14, recorded in parallel applied fields as indicated. The solid lines are spectral simulations. At least 95% of the iron in the sample belongs to ^{57}Fe–**1a** [35].

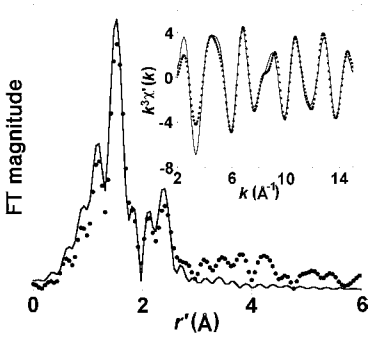

Figure 3.6 Fourier transforms of the Fe K edge EXAFS data [$k^3\chi(k)$] (dots) and the fit (solid line) with one O scatterer at 1.68 Å, five N/O scatterers at 1.89 Å and five C scatterers at 2.84 Å. The inset shows Fourier-filtered EXAFS spectra [$k^3\chi'(k)$] (dots) and the fit (solid line). Fourier transform range, $k = 2$–15 Å^{-1}; back-transform range, $r' = 0.40$–3.10 Å [35].

isomer shift is indicative of an Fe^{IV} species. Variable high-field (1.5, 6.5 and 8 T) studies at 150 K indicated an $S = 1$ species. The Mössbauer data account for ~100 and 80% of the total iron is this oxidized species at pH 14 and 12, respectively. Minor instability of the oxidized species has been detected at pH < 12.

The data [36] indicate a speciation of oxidized TAML species derived from **1** and oxidants *in aqueous solution* (Scheme 3.10). If peroxides ROOH are primary two-electron oxidants, the oxidation of **1** gives presumably the oxoiron(V) intermediate **6**, similar to $^{\bullet+}Fe^{IV}$ in Scheme 3.9. Such an Fe–TAML species has yet to be detected in water, but its existence in non-aqueous media has been established [37]. Similarly to the sterically hindered anionic porphyrin chemistry [38], if formed, highly oxidized intermediate **6** is likely to be rapidly quenched into less oxidized iron(IV) species, the speciation of which is significantly pH dependent. At pH 14, all iron (ca 95%) is monomeric oxoiron(IV) species **7′**, although theoretical DFT simulations do not exclude the aquated formulation **7″**.

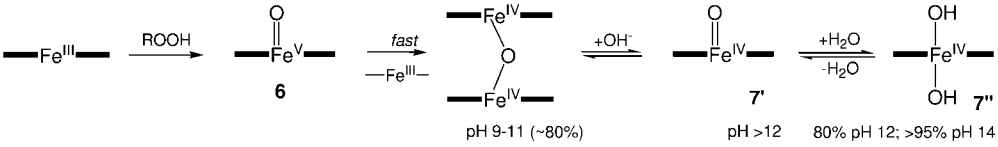

Scheme 3.10 Speciation of oxidized TAML species derived from **1** in aqueous solution. Axial aqua ligands are not shown for clarity.

The nature of **7′** and/or **7″** has been confirmed by EXAFS (Figure 3.6) and analyzed by DFT [39]. The B3LYP functional and the 6–31G level of basis function predicts reliably electronic and structural properties of complexes **1** [40]. The C_s symmetry is maintained in all cases. The Mössbauer parameters in Table 3.4 indicate that the

Table 3.4 Anticipated parameters of the Mössbauer spectra of products generated from **1** and *t*-BuOOH in basic (pH > 12) aqueous solution as calculated by DFT.

Model	OH / Fe^{IV} / OH_2	OH / Fe^{IV} / OH	O ‖ Fe^{IV} $S = 1$	O ‖ Fe^{IV} $S = 2$	O ‖ Fe^{IV} / OH	Experimentally observed
ΔE_Q (mm s^{-1})	4.4	3.6	3.5	2.5	1.8	3.9
δ (mm s^{-1})	−0.07	−0.15	−0.12	0.16	−0.07	−0.19

formulation of **7** as a **7′**/**7″** pair gives the best match with the experimental values of ΔE_Q and δ. An oxo-bridged dimer or Fe^{III} radical cation (ligand-based oxidation) [40] were ruled out at pH > 12. The $S = 1$ spin state is energetically more favorable than both high- or low-spin states. Time-dependent (TD-DFT) analysis applied to the optimized structure of **7′** (Scheme 3.11) ensures structures of the lowest energy. The theory predicts five- and six-coordinated iron(IV) in **7′** and **7″**, respectively. While the central metal in **7′** does not hold axial water due to a strong *trans* effect of the axial oxo ligand of charge −2, the six-coordinated iron with weakly bound water cannot be excluded.

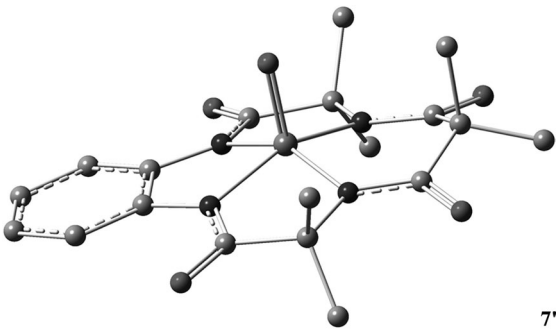

7'

Scheme 3.11 DFT-predicted lowest energy structures of oxidized species **7′**.

All oxidizing agents tested so far in water increase the oxidation state of iron in **1** by one equivalent to produce iron(IV). The iron(IV) oxidation state of in Fe–TAMLs is generated by dioxygen in non-polar organic solvents [36], but iron(V) is produced from **1** and organic peroxides in *tert*-butyronitrile [37]. Although the iron(V)–oxo complex is a species of major interest, we discuss it only lightly here because it has yet to be observed in water. The speciation of these Fe^{IV}–TAML derivatives is pH dependent. The monomeric oxoiron(IV) complexes **7** dominates at pH > 12, whereas at pH 8–10 the major species is the μ-oxo dimer, similar to that easily made from **1a** and O_2 in aprotic solvents (Scheme 3.12) [36].

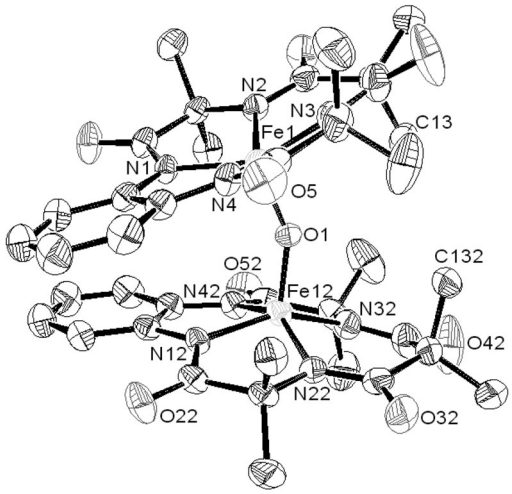

Scheme 3.12 ORTEP structure of the black, dianionic μ-oxo-bridged diiron(IV) complex that is rapidly formed in a high yield from **1a** and O_2 in CH_2Cl_2 or other weakly coordinating solvents. The ellipsoids are drawn at the 50% probability level [36].

As mentioned above, oxoiron(V) species such as **6** derived from **1** and peroxides are accessible in non-aqueous media [37]. The reaction of the tetraphenylphosphonium salt of **1a** with 2–5 equiv. of *m*-chloroperbenzoic acid (*m*CPBA) at −60 °C in *n*-butyronitrile produces within about 10 s an iron(IV) dimer followed by an as yet uncharacterized EPR-silent iron(IV) intermediate. After 15 min, a deep-green oxoiron(V) species **6** with distinct absorption maxima at 445 nm (extinction coefficient $\varepsilon = 5400\ M^{-1}\,cm^{-1}$) and 630 nm ($\varepsilon = 4200\ M^{-1}\,cm^{-1}$). At −60 °C, it decays by 10% in 90 min, but it is stable for at least 1 month at 77 K. Selected spectral data for the oxoiron(V) species are shown in Figure 3.7. DFT calculations favor the low-spin ($S = {}^1/_2$) configuration of the ground state. The calculated Fe−O bond length of 1.60 Å is in excellent agreement with the EXAFS results. The Fe atom is displaced out of the 4-N plane by 0.5 Å.

3.2.4
The Activity–Stability Parameterization of Homogeneous Green Oxidation Catalysts

3.2.4.1 Kinetic Model for Parameterization

The performance of catalysts is often characterized by the turnover number (TON) and turnover frequency (TOF) [41]. The TON is the molar ratio of a product formed compared with the amount of catalyst used. TON does not report directly on the catalyst efficacy. The TOF, expressed in s^{-1}, is the TON referred to a particular period of time, i.e. the number of catalytic turnovers per second. Estimations of the TON and the TOF can be somewhat arbitrary. For example, in the case of a self-degrading catalyst, the effective TON may be artificially increased by lowering the catalyst concentration and/or by raising the substrate concentration. The TON can also be amplified by increasing the reaction time. The TOF is less dependent upon

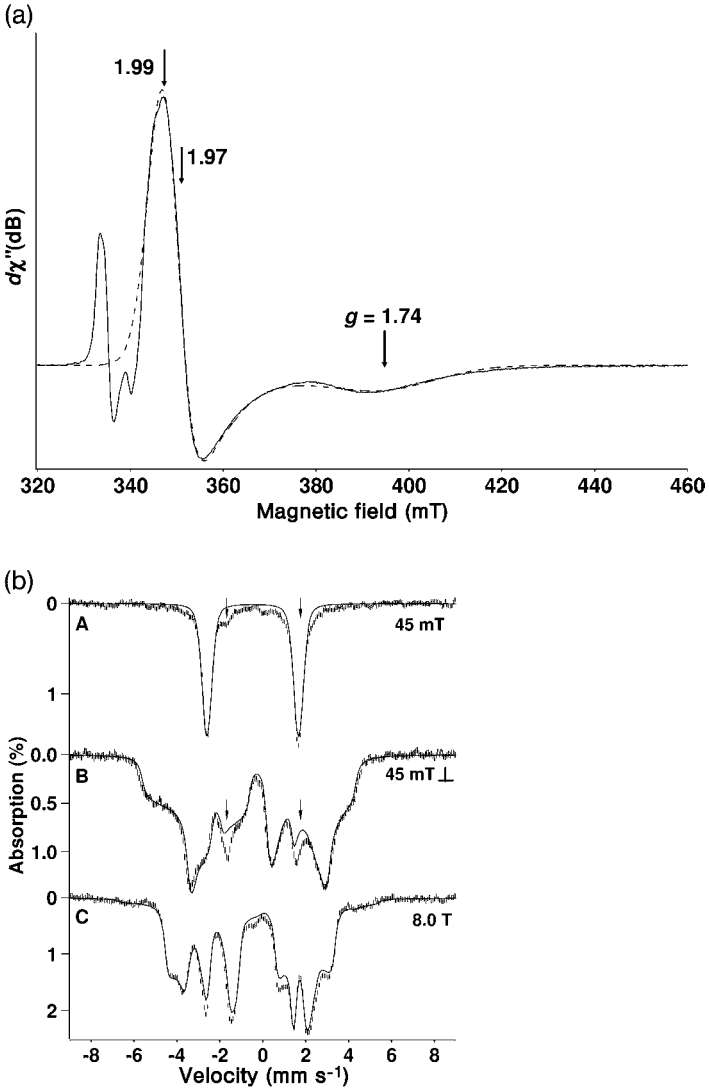

Figure 3.7 X band EPR (a) and Mössbauer (b) spectra of ca 2 mM^{57}Fe-enriched oxoiron(V) compound **6** in *n*-butyronitrile. EPR: 28 K; frequency, 9.66 GHz; microwave power, 0.02 mW, modulation, 1 mT. The dashed line is a spectral simulation. Mössbauer: 140 K (A) and 4.2 K (B, C) in magnetic fields indicated; incident γ-beam perpendicular (B) and parallel (C) to the applied field. The solid lines are spectral simulations. They represent 95% of the total absorption. Arrows (in A and B) indicate a decay product (3% of Fe) with $\Delta E_Q = 3.4\ \text{mm s}^{-1}$ and $\delta = 0.08\ \text{mm s}^{-1}$ [37].

conditions, but there is also room for manipulation. As macroscopic parameters of catalyst performance, the TON and TOF do not give a particularly deep insight into a catalytic process. They are silent with respect to the *operational stability* of the catalyst, which is influenced by both catalytic activity and stability under the operating conditions. Studies of catalytic processes involving transition metal complex catalysts

often focus on the speciation under the reaction conditions, the nature of active species and the intimate characteristics of the reaction of the active species with the substrate. The activity loss or catalyst inactivation while the catalyst is functioning is also a very important feature, but it is generally less studied. In the area of the development of peroxidase mimics, suicidal (intramolecular) and homicidal (intermolecular) self-destruction, which together can be labeled 'catalystacidal degradation', involving oxidation or reduction, attack by activated substrates, solvolysis, ligation by medium components and/or reaction product/s, etc., have received less priority by chemists. On the other hand, the kinetics and mechanisms of enzyme inactivations have been extensively investigated by biochemists, enzymologists and microbiologists. Understanding of thermal denaturing, autolysis, aggregation, chemical transformation of key functional groups, etc., has become a powerful tool for increasing the functional performance of biocatalysts [42–45].

The progress of *green chemistry* will likely bring many improvements to catalysis as it is currently practiced by the chemical industry [46, 47]. *Avant garde* catalysts are beginning to acquire features of biological systems while promising at the same time to underpin technologies that improve both economic and environmental performance. Industrial catalysts should turn enzyme-like for processes that entail release to the environment as the eventual fate, i.e. efficient, non-toxic by known standards and sufficiently fragile so as not to create a persistence problem with all that might entail for unintended toxic consequences. Ideally, a homogeneous catalyst in, say, an aqueous effluent stream should self-destruct when its intended work is done and/or be subject to biological decomposition. Nature has developed enzymes to have limited lifetimes. Industrial catalysts that are to be released to the environment as part of the technology should be similarly designed. The degradation behavior of synthetic oxidation catalysts is a particular challenge. Enzymatic oxidations are two-reagent reactions. A first reagent delivers oxidizing equivalent(s) (k_I) followed by oxidation of the targeted substrate (k_{II}) (Scheme 3.13). The active catalyst may be involved in intramolecular (k_i) or intermolecular (k_{2i}) oxidative self-destruction.

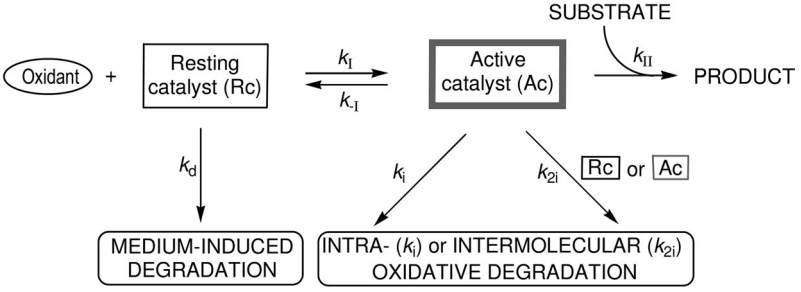

Scheme 3.13 Overview of the current mechanism of catalysis by Fe–TAML activators (not showing catalase-like activity). The rate constant k_d describes the medium-induced demetalation of **1** [8, 19]; k_i and k_{2i} refer to intra- or intermolecular catalystacidal inactivation. The catalysis is commonly run using very low concentrations of **1**, hence the k_{2i}-driven pathway is essentially negligible [32].

Enzymes are often protected from inactivation by their polypeptide containment. Low molecular weight synthetic catalysts are not, and so other design elements need to replace the features the protein brings to directing the course of the catalytic cycle and to obviating undesirable rapid catalyst degradation [48].

However, as noted above, the catalyst should degrade after the catalysis is accomplished before release to the environment. The catalyst lifetime driven by k_i and/or k_{2i} should be significantly longer than the time required for catalytic turnovers driven by k_{II}. The approach we have developed for Fe^{III}–TAMLs for assessing quantifying several key features of the pertinent kinetics allows for the simultaneous determination of k_{II} and k_i [32]. It holds when the formation of the active catalyst driven by k_I is fast and the catalyst concentration is very low such that the k_{2i} pathways can be neglected.

In studying the oxidation process spectrophotometrically, if step I (Scheme 3.7) is fast and the oxidation is set up to be *incomplete* (Figure 3.8), the kinetic trace can be analyzed using Equation 3.4, thereby allowing the determination of k_{II} and k_i:

$$\ln\left(\ln\frac{A_t}{A_\infty}\right) = \ln\left(\frac{k_{II}}{k_i}\left[Fe^{III}\right]_t\right) - k_i t \tag{3.4}$$

where A_t and A_∞ are absorbances at time t and at the end of reaction ($t = \infty$), respectively, and $[Fe^{III}]_t$ is the total catalyst concentration [32]. Note that Equation 3.4 was obtained by integration:

$$-\frac{d(D_t - x)}{dt} = k_{II}(D_t - x)([Fe^{III}]_t e^{-k_i t}) \tag{3.5}$$

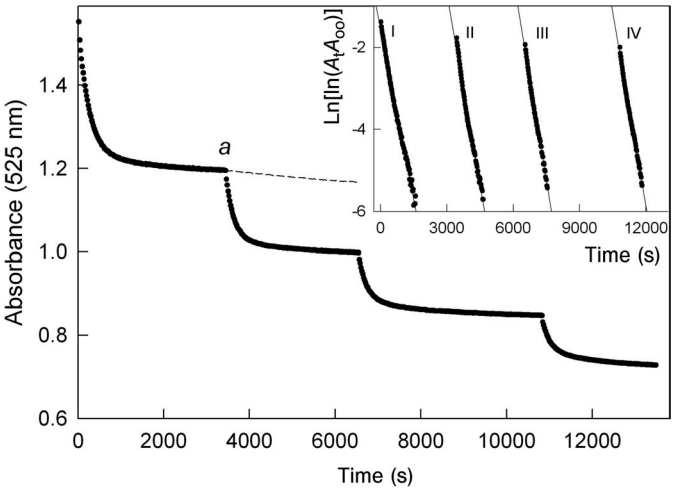

Figure 3.8 Kinetics of **1a**-catalyzed bleaching of Safranine-O (4.3×10^{-5} *M*) by 0.012 *M* H_2O_2. Initial concentration of **1a** (7.5×10^{-8} *M*); aliquots of the same amount of **1a** were added after complete inactivation of the catalyst giving rise to the stepped dependence. The dashed line shows that addition of 0.012 *M* H_2O_2 does not resume the catalytic bleaching. The inset shows the linearization of the data obtained after each addition of **1a** in terms of Equation 3.4 to give consistent values of k_i ($\sim 3.3 \times 10^{-3}\ s^{-1}$). Conditions: pH 11, 25 °C [32].

where D_t and $[Fe^{III}]_t$ are total concentrations of the dye and the Fe^{III}–TAML catalyst, respectively, and x is the concentration of a bleached dye at time t. The boundary conditions $x = x_\infty$ (x_∞ is the concentration of bleached dye obtained with single catalyst aliquot) when $t = \infty$.

The rate constants k_{II} and k_i obtained using Equation 3.4 reveal the following. (i) The activity of Fe^{III}–TAMLs in bleaching Safranine-O (k_{II}) increases more than 10-fold when the tail ethyl groups of **1a** are replaced by electron-withdrawing fluorine atoms in **1k**. The rate constant k_{II} for **1k** which equals $10^5\ M^{-1}\ s^{-1}$ at 25 °C is similar to the rate of oxidation by horseradish peroxidase Compound II of anilines and phenols [49]. (ii) The rate constants k_i also increase on going from **1a** to **1k** and a similar 10-fold gap holds. Under the operating conditions, i.e. $[H_2O_2] = 0.012\ M$, [Safranine-O] $= 4.3 \times 10^{-5}\ M$, pH 11 and 25 °C, the half-lives, $\tau_{1/2}$, for catalysts **1a** and **1k** are 7.7 and 0.88 min, respectively.

Eight structurally similar, but electronically different, Fe^{III}–TAML catalysts **1**, all with R = Me, have been investigated, ending up allowing the development of the curious LFER plot shown in Figure 3.9. Electron-withdrawing substituents (NO_2, NMe_3^+, COOEt, Cl) increase the oxidizing power of the catalysts with respect to Safranine-O (k_{II}), but retard the intramolecular inactivation (k_i). The most resistant-to-inactivation catalyst is the nitro-substituted Fe^{III}–TAML **1e**. This suggests that the aromatic components of Fe^{III}–TAML catalysts are vulnerable to oxidative degradation. The six-membered ring is the primary site for degradation in organic solvents when this is substituted with ethyl groups, which are the initiation site of degradation based on a methylene H-atom abstraction [14].

Substitution with methyl groups slows the rate significantly because the methyl C−H bonds are stronger than the methylene C−H bonds and this iteration in the design of our catalysts [7] allowed for the generation of useful catalysts. Although attack at the methyl groups may still be occurring (perhaps in the intermolecular channel), the increased catalyst stability produced by the addition of electron-

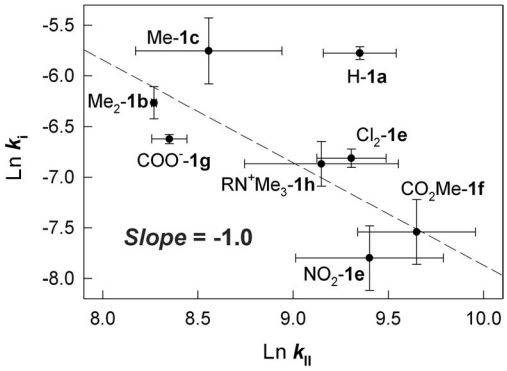

Figure 3.9 LFER between the rate constants k_{II} for bleaching Safranine-O and k_i for intramolecular inactivation in the series of 'head'-substituted Fe^{III}–TAML catalysts with methyl tail groups. Conditions: $[H_2O_2]$ 0.012 *M*, 25 °C, pH 11.0. The data point for **1a** was ignored in the linear regression [32].

withdrawing groups to the head portion of the macrocycle indicates the active catalyst destroys itself via the oxidative damage at this group and electron-withdrawing substituents protect the ligand system from whatever damage is occurring. These results pertain to very low catalyst concentrations where intramolecular or at least unimolecular catalyst degradation is occurring. The k_i value for **1a** is higher than the other data in the LFER would predict – if this datum is neglected, the slope of the resulting straight line equals -1.0 ± 0.3. This is unusual because a positive slope might be anticipated with more reactive catalysts decomposing more rapidly, but the odd behavior provides a very useful tool for thinking about tuning the catalytic activity and stability of Fe^{III}–TAML catalysts by continuing to identify the next most vulnerable site via the Collins iterative design process for achieving peroxidase mimics [7, 26].

The bleaching of Safranine-O when there is excess H_2O_2 relative to the dye is affected by the H_2O_2 concentration. Deeper **1a**-catalyzed bleaching of Safranine-O is observed at *lower* concentrations of H_2O_2. While 19% bleaching is achieved at $[H_2O_2] = 0.12\ M$, 31% is achieved at $[H_2O_2] = 0.012\ M$. Similar behavior has been observed for heme chloroperoxidase from *C. fumago*, where it has been attributed to the H_2O_2-induced irreversible inactivation of the enzyme [50]. The rate constants k_{II} are almost insensitive to $[H_2O_2]$ – the reactivity of the oxidized Fe–TAML should not depend on the H_2O_2 concentration. The rate constants k_i for **1a** and **1e** increase with increasing H_2O_2 concentration and $k_i = k_{i\alpha} + k_{i\beta}[H_2O_2]$. This two-term equation guides one to keep $[H_2O_2]$ at the lowest possible level because, in addition to the catalase-like activity displayed by Fe^{III}–TAML catalysts at high $[H_2O_2]$, resulting in waste of H_2O_2 [51], hydrogen peroxide is an inactivator of the Fe^{III}–TAML catalysts. The value of $k_{i\alpha}$ is almost six times lower for the NO_2 ring-substituted catalyst **1e** compared with the ring-unsubstituted **1a**. Hence changing the electronic properties of the head component of the catalysts is a simple tool for protection from intramolecular inactivation [32].

3.2.4.2 Model Verifications

Equation 3.4 when rearranged to Equation 3.6, describes the relative conversion of substrate (A_t/A_0) as a function of time. This equation is convenient for simulating the catalyst performance and for comparison of such simulations with experimental data. Equation 3.6. eliminates the illusion that might be gained from Figure 3.8 that **1**-catalyzed bleaching is always incomplete.

$$\frac{A_t}{A_0} = \exp\left\{\frac{k_{II}}{k_i}[Fe^{III}]_t(1-e^{-k_i t})\right\}^{-1} \tag{3.6}$$

Instead, this 'regime of incompleteness' can serve as a tool for evaluating k_i. Figure 3.10a demonstrates different regimes of bleaching calculated using Equation 3.6. The bleaching will be complete when the catalyst concentration reaches $10^{-6}\ M$ and $k_i \leq 10^{-3}\ s^{-1}$ (Figure 3.10a, *e*). At lower [Fe^{III}–TAML], the bleaching is slower and incomplete. It is also incomplete at higher catalyst concentrations ($[Fe^{III}] \geq 10^{-6}\ M$) and larger k_i values (Figure 3.10a, *c,d*).

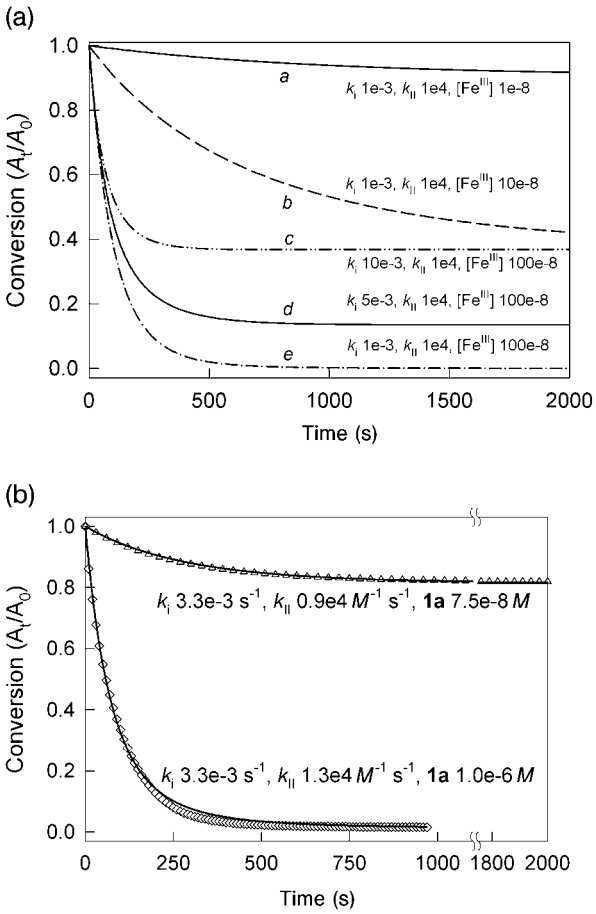

Figure 3.10 (a) Simulated bleaching of a hypothetical dye using Equation 3.6 at different concentrations of Fe^{III}–TAML catalyst (in *M*) with the rate constants k_i (in s^{-1}) and k_{II} (in $M^{-1}s^{-1}$). The numerical values are indicated on the graph. (b) Normalized experimental and simulated bleaching of Safranine-O (4.3×10^{-5} *M*) by H_2O_2 (0.012 *M*) catalyzed by **1a** at pH 11 and 25 °C. Experimental data are shown as Δ and ◇. The simulations, shown as solid lines, were made as in (a) [32].

The mechanistic hypothesis has been supported by a match between the experimental and calculated data using known k_i and k_{II} values. Figure 3.10b shows the **1a**-catalyzed bleaching of Safranine-O at different [**1a**] for comparison. The experimental and calculated curves agree and illustrate that complete bleaching of the dye is achievable by just increasing the **1a** concentration. Nevertheless, the value of the [**1a**] required for complete bleaching was found to be remarkably low at 10^{-6} *M*. Also, this very catalyst requirement was found for Safranine-O, which is a relatively difficult to oxidize dye.

Work is ongoing to quantify the relative importance of intermolecular pathways of Fe–TAML catalyst inactivation, and this should also be significant in eventual process optimization procedures. A further call for development involves the most general case without putting limitations on the rate constants k_I and k_{II}. Developing this treatment we believe will be vital when significantly higher catalyst concentrations are used and where the bimolecular suicidal oxidative inactivation of Fe–TAML catalysts is driven by k_{2i} to the point that it cannot be neglected in the modeling – an example where such conditions pertain can be found in the killing of spores by Fe–TAML–peroxide [28].

3.3
Applications of Fe–TAMLs

3.3.1
Degradation of Phosphorothioate and Phosphate Esters

3.3.1.1 Total Degradation of Organophosphorus (OP) Pesticides

Organophosphorus triesters account for an estimated 34% of worldwide insecticide sales. Their widespread use in agriculture is linked to human health and environmental concerns associated with cholinergic toxicity and, in some cases, delayed neuropathy. Some thiophosphate pesticides are endocrine disrupting chemicals (EDCs) [29]. Their pest-controlling benefits are also marred by environmental burdens. In addition to deliberate spraying, spillages resulting from farming activities often occur during filling operations of the spray equipment and subsequently during washing of the equipment after completion of spraying and these processes, which often take place in areas of farms where people and animals live, could contaminate surface or groundwater. There are also about 500 000 tonnes of unused or obsolete pesticides, including OP pesticides, scattered throughout the developing world awaiting disposal, where leaks or improper disposal can lead to severe environmental contamination [52].

The disposal of obsolete pesticides and the remediation of associated contaminated sites have become issues of worldwide concern because of the adverse implications for human health and the environment. Hydrolytic detoxification approaches for thiophosphate esters are inadequate, because these do not satisfactorily resolve concerns associated with the toxicity of the hydrolyzates. Treatment of the OP pesticides parathion, chlorpyriphos, fenitrothion and chlorpyriphos methyl with **1k** and H_2O_2 at 25 °C and pH 8 resulted in rapid total degradation within a few minutes. The **1k**: H_2O_2 ratio was of the order of 1 : 1000 to 1 : 10 000. The kinetics of fenitrothion degradation were followed by UV–visible spectroscopy at 396 nm and were found to indicate the rapid formation of the intermediate, 4-nitro-3-methylphenol, which is then more slowly degraded to completion by Fe–TAML–peroxide (Figure 3.11) [29].

Using HPLC analysis, the generation of 4-nitro-3-methylphenol as the major initial product (90%) and its concomitant degradation were confirmed, along with the

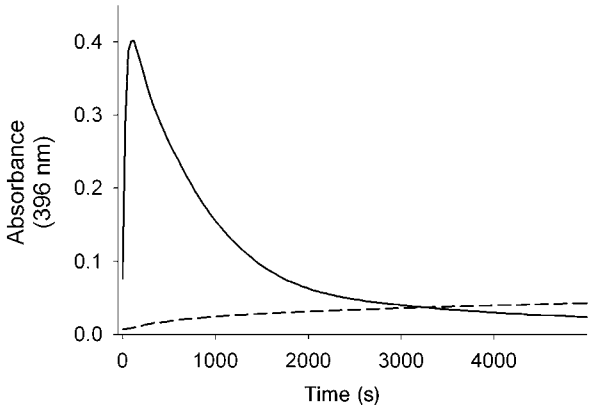

Figure 3.11 Kinetics of the decomposition of fenitrothion on treatment with **1k**–H_2O_2 followed through time-lapsed absorption at 396 nm. A very slow hydrolysis of fenitrothion (dotted line), assisted by H_2O_2 when it was added without catalyst, was observed at pH 8 [29].

identification of a minor product (10%), namely fenitrooxon, a product of oxidative desulfuration. For the reaction to proceed to complete degradation, fenitrooxon could be induced by perhydrolysis to form 4-nitro-3-methylphenol by conducting the reaction at pH 10. The Fe–TAML–peroxide approach under optimized conditions thus led to total degradation of OP pesticides to small aliphatic acids and partial mineralization, leaving little residual aquatic toxicity as determined by Microtox assays of the post-degradation mixtures (Scheme 3.14).

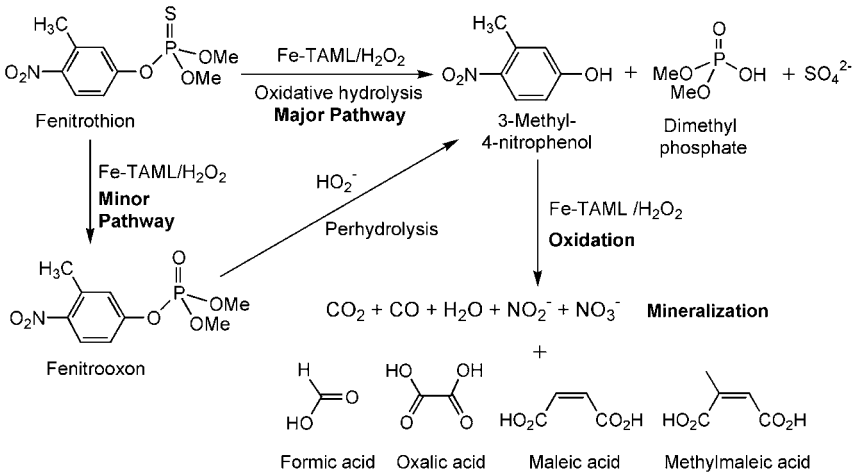

Scheme 3.14 Treatment of fenitrothion by **1k**–H_2O_2 results in its total degradation, forming some small aliphatic acids with partial mineralization [29].

Fe–TAML–H_2O_2 was also shown to degrade diazinon and quinalphos (Scheme 3.15), resulting in rapid oxidative hydrolysis forming 2-quinoxalinol and 2-isopropyl-6-methylpyrimidinol, respectively. However, these hydrolyzed products were relatively resistant to oxidative decomposition under ambient conditions, requiring that the temperature be raised to 65 °C to achieve reasonably rapid degradations.

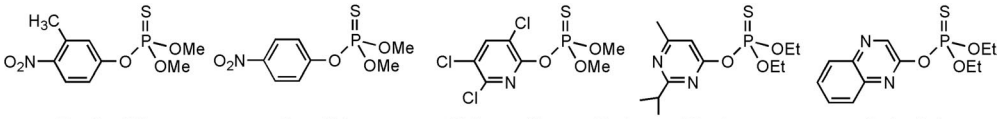

Scheme 3.15 OP pesticides studied for degradation with **1k**–H_2O_2.

3.3.1.2 Decontamination of Chemical Warfare Agents

Many chemical warfare (CW) agents are OP esters (e.g. soman and VX) (Scheme 3.16), which react irreversibly with the enzyme acetylcholinesterase. VX and other nerve agents such as tabun, sarin, soman and GF contain phosphorus centers that can be hydrolyzed leading to cleavage of P−OR or P−SR bonds to result in detoxification. New decontamination technologies that more rapidly destroy these agents rely upon a combination of hydrolysis and oxidation chemistry. The successful degradation of OP insecticides by **1**–H_2O_2 under ambient conditions suggested that these nerve agents might also be subject to rapid and complete degradation.

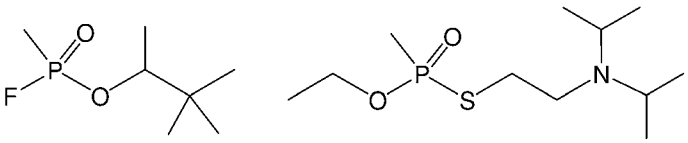

Scheme 3.16 OP chemical warfare agents GD and VX were found to degrade rapidly on treatment with a relatively non-aggressive **1b**–*t*-BuOOH system in an amine oxide-based microemulsion.

Experiments with 'live agents' (GD and VX) (Scheme 3.16) conducted at the US Navy's Surface Warfare Center at Dahlgren, VA, have shown good promise for decontamination even employing one of the least aggressive Fe–TAML catalysts such as **1b** and *tert*-butyl hydroperoxide in an amine oxide-based microemulsion [53]. It was noteworthy that the Fe–TAMLs demonstrated the highest reactivity and stability in an evaluation of over a dozen different catalysts (Fe–TAML and non-Fe–TAML) in combination with several different peroxygen compounds. The studies included systems wherein the peroxygen compounds were generated *in situ* as a method for enhancing the shelf-life and functional stability of the overall system.

3.3.2 Sulfoxidation Reactions

3.3.2.1 Reactions of Organic Sulfides

Selective oxidations of sulfur-containing compounds can be industrially significant. An example is the selective oxidation of organic sulfides to sulfoxides. Sulfoxides have several important uses as building blocks in organic synthesis and as therapeutic agents. Oxidations of sulfides to sulfoxides by hydrogen peroxide in various solvents and with several transition metal-based catalysts have been reviewed [54].

The Fe–TAML–H_2O_2 system provides a convenient, high-efficiency method for the selective oxidation of sulfides to sulfoxides or sulfones. The conditions of the Fe–TAML–H_2O_2 system can be mild with varying pH including the often desirable alkaline range, both weakly alkaline and strongly alkaline for different purposes. By all measures of toxicity and ecotoxicity to date the system is environmentally friendly. The peroxide reagents are relatively non-toxic, especially in the low concentrations required for Fe–TAML processes, and the organic products can be readily separated. Thus, Fe–TAML–H_2O_2 treatment of di-*n*-butyl sulfide under ambient conditions leads to rapid oxidation to a mixture of the sulfoxide and sulfone. The process proceeds through the sulfoxide and the reaction conditions can be designed to favor this intermediate product. Di-*n*-butyl sulfide is oxidized to di-*n*-butyl sulfoxide with equimolar aqueous H_2O_2 (supplied from 30%) alone at 35 °C in about 18 h [55]. In comparison, di-*n*-butyl sulfide, on treatment with **1a**–H_2O_2 (1 : 2000), was oxidized to predominantly di-*n*-butyl sulfoxide within 5 min at ambient temperature and neutral pH (Scheme 3.17). When hydrogen peroxide was used in significant excess (1 : 5000), the reaction proceeded predominantly to di-*n*-butyl sulfone [56]. The Fe–TAML–H_2O_2 system offers rapid reaction rates compared with a well-studied example of an analogous catalytic process based on methyltrioxorhenium(III), CH_3ReO_3 [57].

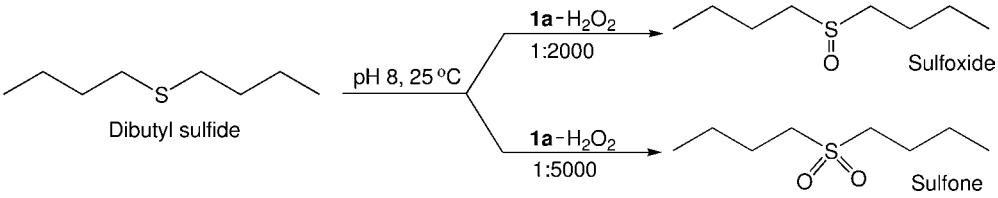

Scheme 3.17 By controlling the activator:peroxide ratio, Fe–TAML (**1a**)–H_2O_2 can be employed to oxidize di-*n*-butyl sulfide predominantly to di-*n*-butyl sulfoxide.

3.3.2.2 Decontamination of Sulfur Mustard

Sulfur mustard [bis(2-chloroethyl) sulfide, HD] is a vesicant (blistering agent), which produces chemical-induced degradation of flesh on contact. Rapid oxidation of the sulfur center plays a significant role in decontamination of sulfur-containing chemical warfare agents such as HD mustard gas. HD is an organic sulfide that is subject to detoxification by selective oxidation to the sulfoxide. The sulfoxide is

much less toxic than the parent compound, but the sulfone exhibits intermediate toxicity and so oxidative decontamination processes must be designed to avoid its production [58].

1a–H_2O_2 treatment of 2,2′-thiodiethanol, a surrogate for sulfur mustard, has been found to result in the formation of the corresponding sulfoxide in quantitative yield in 10 min. No further oxidation to the sulfone was observed even after 30 min. In the absence of **1a**, <50% conversion of thiodiethanol (0.01 *M*) to sulfoxide was observed in 1 h with H_2O_2 (0.05 *M*) alone [56]. In a live test on sulfur mustard conducted at the Defence Science and Technology Laboratory (DSTL) at Porton Down, UK, treatment with **1k**–H_2O_2 in a mixture of 30% *t*-BuOH and 70% aqueous peroxide (5%), the reaction proceeded with highly selective formation of preferred sulfoxide (Scheme 3.18), giving a measured 'half-life' of ~2 min., which represents the desired rate for a viable battlefield decontamination system [59].

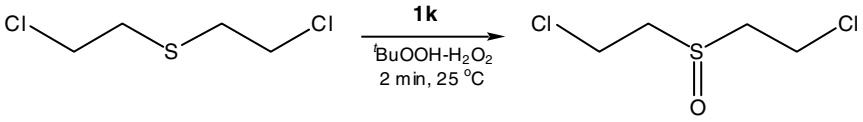

Scheme 3.18 **1k**–peroxide treatment of dichloroethyl sulfide (sulfur mustard) results in the exclusive formation of the corresponding sulfoxide.

3.3.2.3 Removal of Benzothiophene and Dibenzothiophenes from Diesel

Human health and environmental issues associated with diesel exhaust led the US Environmental Protection Agency (EPA) recently to mandate reduction of the sulfur content of diesel from 500 to 15 ppm and of gasoline from 300 to 30 ppm [60]. It is estimated that the petroleum refining industry will need to spend ca $8 billion over the next few years to meet these new EPA standards, especially, if attractive alternatives to hydrocracking are not developed.

Many oxidation approaches are focused on conversion of thiophenes to sulfoxides or sulfones, since these can be more easily separated from the petroleum base products. However, oxidation of the sulfur atom is challenging in dibenzothiophene (DBT) and its derivatives, especially when it is sterically hindered as in 4-methyldibenzothiophene (4-MDBT), and even more so in 4,6-dimethyldibenzothiophene (4,6-DMDBT) (Scheme 3.19), both of which are common sulfur contaminants fuels. One

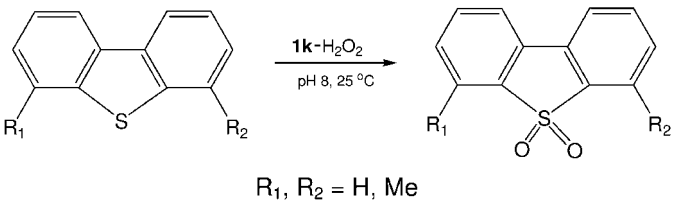

Scheme 3.19 Treatment of dibenzothiophenes with the aggressive system **1k**–H_2O_2 produces under the chosen conditions the corresponding sulfones via the sulfoxides [30].

of the significant capabilities of the **1**–peroxide system includes its ability to oxidize rapidly at the sulfurs of dibenzothiophenes, heralding a new potential technology for desulfurization of petroleum. The oxidation reactivity of **1k**–H_2O_2 to different dibenzothiophenes was found to be in the order DBT > 4-MDBT > 4,6-DMDBT, based on the time taken for 50% conversion to the corresponding sulfones [30].

3.3.3
Breaking of Disulfide Bonds and the Likely Significance for the Disinfection of Spores

Oxidative disruption of −S−S− bonds in the coats of *Bacillus* and *Clostridia* may well facilitate disinfection processes of spores and related genera based on oxidation reactions. The coat is a protein shell which encases the spores to provide protection from the environment.

3.3.3.1 Oxidative Rupture of Organic Disulfides

Oxidation of disulfides with strong oxidizing agents, such as peracids, is known to rupture disulfide bonds to produce industrially important alkanesulfonic acids. Disulfides are more resistant to oxidation in comparison with thiols and their oxidations usually require a stronger oxidant, a large excess of the oxidant, higher temperatures or a catalyst [61]. Treatment with **1k**–H_2O_2 of cystine at room temperature and pH 10 resulted in the cleavage of the disulfide bond and complete oxidation of the sulfur atoms to >90% cysteic acid within 1 h compared with <5% with H_2O_2 alone (Scheme 3.20).

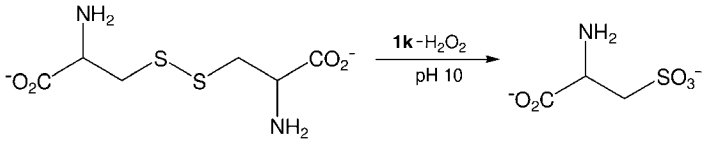

Scheme 3.20 Fe–TAML (**1k**)–H_2O_2 treatment of cystine leads to the rupture of disulfide bond resulting in near quantitative conversion to cysteic acid.

This result suggested to us that this Fe–TAML system might be useful in the disinfection of spores [61]. The need for better spore-killing systems became very apparent after the anthrax terrorist attacks of 2001 on places such as the Hart Senate Building.

3.3.3.2 Deactivation of Microbial Pathogens

Bacterial spores, which are the dormant bodies produced by a variety of *Bacillus* and *Clostridium* spp. in response to environmental stress or starvation, are well adapted for survival under adverse conditions such as heat, chemicals and radiation. As a result, *B. anthracis* spores are considered to be among the most difficult biological warfare and terrorism (BWT) agents to destroy. Spore hardiness derives in part from two structurally complex and chemically robust encapsulating layers—a multilayered

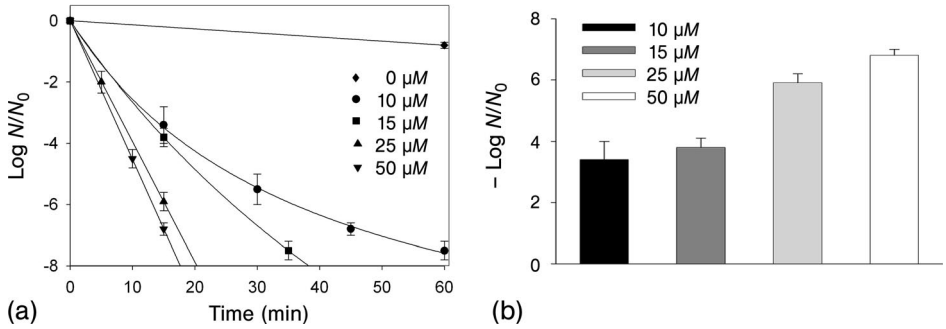

Figure 3.12 (a) Time dependence of the deactivation of *B. atrophaeus* spores with various concentrations of **1k**. (b) Bar chart showing levels of deactivation achieved in 15 min with different concentrations of **1k** [28].

protein shell known as the coat that excludes macromolecules and the peptidoglycan cortex that provides structural stability. There are in addition various membrane layers. The resistance of bacterial spores to enzymatic and chemical treatments has been attributed partly to the presence of protein disulfide cross-linkages in the spore coat that contain an unusually high content of cysteine residues [62]. On oxidation, cysteine (a thiol) forms cystine (a disulfide) [63]. The −S−S− bond can be ruptured on further oxidation leading eventually to complete oxidation of the sulfur atoms to form sulfinic and sulfonic acids [64].

Bacterial spores of *Bacillus atrophaeus* are widely accepted as non-toxigenic surrogates for exceptionally resistant *B. anthracis* spores and as indicators for water-borne protozoa such as *Cryptosporidium parvum*, a bane of drinking water treatment plants. In studies with bacterial spores of *Bacillus atrophaeus* (ATCC 9372), the **1k**–peroxide oxidant system exhibited a facility for rapid deactivation. Treatment of *B. atrophaeus* with **1k** in the presence of 0.5 *M tert*-butyl hydroperoxide (TBHP) and 0.03% cetyltrimethylammonium bromide (CTAB) at pH 10 achieved a 7-log kill in 15 min (Figure 3.12) [28].

The efficiency of Fe–TAML–TBHP with CTAB for decontaminant of bacterial spores has been separately validated by Setlow's group in deactivating *Bacillus subtilis* spores [65]. A Gram-negative bacterium *E. coli* strain DH5α was also effectively deactivated on treatment with Fe–TAML–peroxide system. Similarly, T2 phage viruses, which infect *E. coli* and are used as indicator for water-borne viruses, could be effectively deactivated with **1k**–H_2O_2, achieving a 5-log kill in just 5 min without the use of buffering salt or surfactant [28].

3.3.4 Oxidative Degradation of Phenols

3.3.4.1 Total Degradation of Trichloro- and Pentachlorophenols

A broad scientific search has been under way for almost two decades to find a facile, inexpensive, environmentally safe method for degrading chlorophenols into harmless

products. Over the past six decades, chlorophenols have found wide use in pesticides, disinfectants, wood preservatives, personal care formulations and many other products. They are significant components of the effluent streams of pulp bleaching with elemental chlorine. However, growing knowledge of the toxicities and environmental fates of specific chlorophenols has caused governments to regulate these compounds; five chlorophenols are listed by the US EPA as priority pollutants, including 2,4,6-trichlorophenol (2,4,6-TCP) and pentachlorophenol (PCP). Chlorinated phenols persist for decades in the environment because of their resistance to microbiological degradation, leading to the accumulation of these toxic molecules [66].

The electron-withdrawing substituents in the aromatic compounds make them resistant to chemical or biological oxidation and hydrolysis [67]. Nevertheless, **1a**– or **1k**–H_2O_2 treatment of chlorophenols, such as 2,4,6-trichlorophenol and pentachlorophenol, led to their total degradation mostly through an oxidative ring-opening pathway and mineralization (Scheme 3.21). In fact, an increased number of electron-withdrawing chlorine groups on the phenol ring led to an increasingly facile degradation (initial degradation rate: PCP > TCP > 2,4-DCP). A similar facile oxidative degradation of trichloro-2-pyridinol, a hydrolyzed product of methyl chlorpyrifos, described earlier, was observed on treatment with **1k**–H_2O_2 [68].

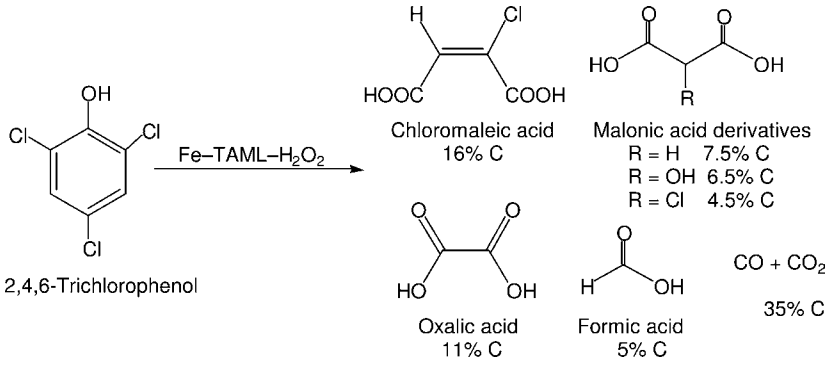

Scheme 3.21 Fe–TAML (**1a**)–H_2O_2 breaks up the persistent pollutant TCP into smaller, acyclic products, which can be consumed by microorganisms. The catalyst shows similar activity for another persistent pollutant, pentachlorophenol. The mass balance of 90% of the carbon and >95% of the chlorine was accounted for in each case. No dioxins were produced within the limits of detection of the mass spectrometers at the Institut für Ökologische Chemie, GSF-Forschungszentrum für Umwelt und Gesundheit, in Neuherberg, Germany.

3.3.4.2 **Total Degradation of Nitrophenols**

Nitroaromatic compounds, such as nitrophenols, are toxic to many aquatic organisms. These compounds are generally recalcitrant to biological treatment and remain in the biosphere, where they constitute a source of pollution due to both toxic and mutagenic effects on humans, fish, algae and microorganisms [69]. The majority of these synthetic pollutants originate from the aqueous waste of many chemical industries, namely pesticides, explosives and dyes. There is much concern over the occurrence of

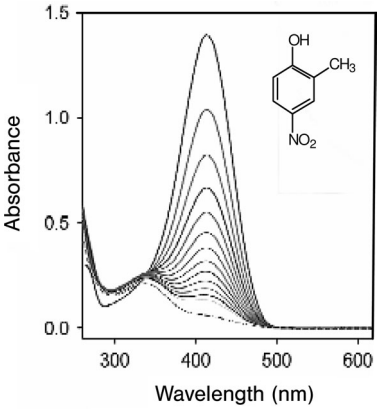

Figure 3.13 Oxidative degradation of 4-nitro-2-methyl phenol with **1l**–H_2O_2 at pH 8: time-lapsed UV–visible spectra.

the nitro compounds, their by-products and especially their biotransformation products in soil and ground water in the vicinity of former production sites [70]. The US EPA has categorized several of nitroaromatics as priority pollutants. Engineering a process for the rapid and effective removal has been of paramount concern for the environment and has remained a field of active research for some time.

The **1l**–H_2O_2 treatment of fenitrothion led to initial formation of 4-nitro-2-methylphenol as an intermediate, which proceeded to total degradation under the catalytic oxidation conditions. This observation could be reproduced on treatment of 4-nitro-2-methylphenol with **1l**–H_2O_2 (Figure 3.13). A similar observation was made with 4-nitrophenol, an intermediate formed on treatment of methyl parathion and/or parathion with **1k**–H_2O_2, which was also readily degraded [29].

The reactivity of **1l**–H_2O_2 to hydroxyaromatic compounds is characterized by facile oxidative ring cleavage of phenols with electron-withdrawing chloro and nitro substituents. However, compounds with electron-donating aryl and alkyl groups, such as 2-quinoxalinol and 2-isopropyl-6-methyl-4-pyrimidinol, which are transformed into quinoxaline and diazinone, respectively, were found to react more slowly, needing thermal activation for total degradation. We continue to pursue more aggressive Fe–TAML systems and may be able to develop systems that will reproduce the ambient reactivity found for more oxidizable substrates for these less oxidizable ones.

3.3.5
Degradation of Emerging Micropollutants

The occurrence of pharmaceuticals and personal care products in water supplies is of increasing human health and environmental concern. Conventional water treatments have a low rate of removal of these contaminants. Some pharmaceuticals are EDCs, which can impair living organisms by interfering with hormonal processes controlling cellular development [71].

3.3.5.1 Endocrine-disrupting Compounds

The active ingredient in the birth control pill 17α-ethinylestradiol (EE_2) is one such EDC, which is excreted by humans to produce a major source of artificial environmental estrogenicity. Similarly, natural estrogens found in animal waste from concentrated animal feeding operations (CAFOs) can also increase estrogenic activity of surface waters [71]. A **1a**–H_2O_2 treatment rapidly degraded 17α- and 17β-estradiol (E_2), estriol (E_3), estrone (E_1) and 17α-ethinylestradiol (EE_2) (Scheme 3.22), with apparent half-lives of approximately 5 min, and included a concomitant loss of estrogenic activity as established by E-Screen assay [72]. The study highlights the extremely low concentrations at which Fe–TAML catalysts can function, both in the amount of catalyst required and with trace quantities of substrates. Thus, the conditions employed 83 n*M* **1a** (a relatively non-aggressive Fe–TAML) and 80 μ*M* estrogen (testosterone). The H_2O_2 concentration was 4 m*M*, but this what not optimized and presumably could have been much lower. Under these non-optimized conditions, 1 kg of **1a** would be enough to treat more than 20 000 tonnes of water.

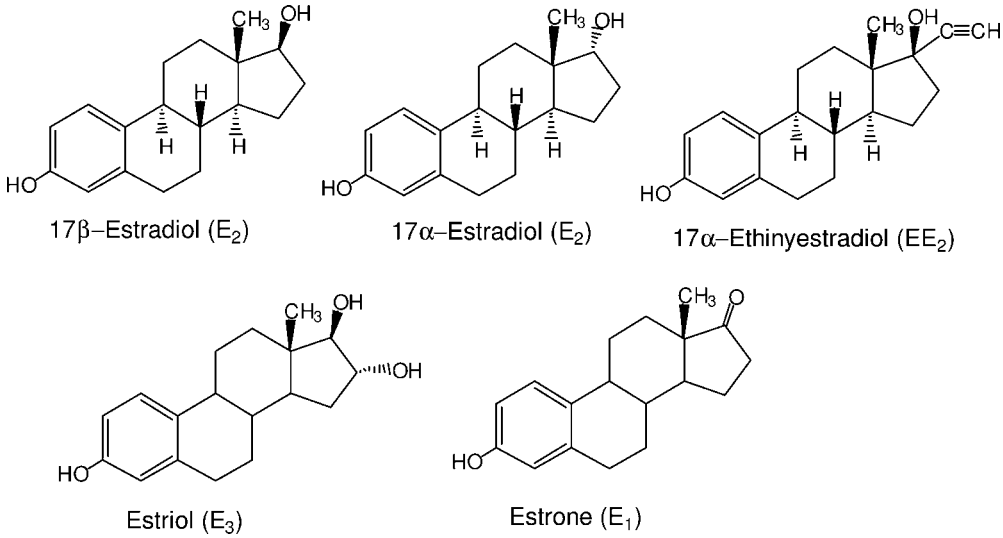

Scheme 3.22 Fe–TAML (**1a**)–H_2O_2 treatment of estrogenic steroid hormones results in their total degradation with concomitant loss of estrogenic activity.

3.3.5.2 Degradation of Pharmaceutical Active Ingredients (PAIs)

At present, there are no regulatory guidelines for the levels of pharmaceutical ingredients in drinking water. In a first attempt, Australia's national authority for regulating water quality, the Australian Environment Protection and Heritage Council, is considering proposing a daily intake of 1% of the lowest recommended therapeutic dose (LRTD) for all the drugs and 0.1% for cytotoxins and endocrine

disrupting compounds, as the new draft *Guidelines for Water Recycling* [73]. In the coming year or two, we expect to publish numerous studies indicating the effectiveness of Fe–TAML–peroxide processes for removing various emerging active pharmaceutical ingredient (API) micropollutants from the water supply.

3.3.6
Bleaching of Azo Dyes

The textile industry produces large quantities of colored effluents, presenting significant environmental problems worldwide. Approximately 80 dyes form the global industry's palette for the coloring of commercial fabrics. Modern textile dyes are chemically stable and resistant to degradation by sunlight, water, soap, bleach and perspiration. Azo dyes that incorporate the $-N=N-$ moiety constitute up to 70% of all textile dyestuffs produced [74]. They are difficult to degrade in textile wastewaters under the aerobic conditions that prevail in biological treatment plants. Dyes in wastewater create aesthetic problems, limit the possible uses of the water and reduce the efficacy of microbiological wastewater treatment because they may be toxic to microorganisms.

The complete bleaching of an extensive range of industrial dyes, which represent worldwide disposal problems because of strong resistance to oxidation, has been achieved with Fe–TAML–H_2O_2 system. For most dyes, the process proceeds rapidly at room temperature. Typical examples of azo dyes include Orange II and tartrazine (Scheme 3.8). Treatment of an aqueous solution of Orange II with **1a**–, **1k**– or **1l**–H_2O_2 at pH 9–11 led to rapid degradation with the formation of CO_2, CO, phthalic acid and smaller aliphatic carboxylic acids as major degradation products (Figure 3.14) [31]. A similar observation was made with tartrazine degradation [75].

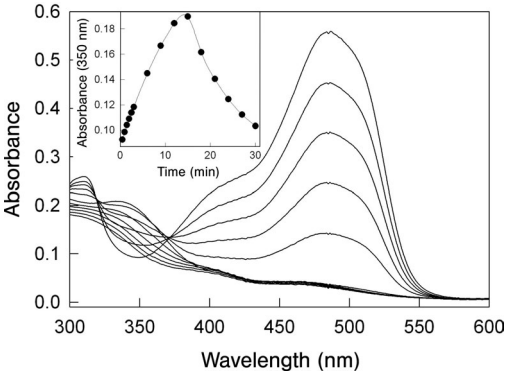

Figure 3.14 Time-lapsed changes in spectral absorbance of Orange II at 350 nm on catalytic oxidation by **1a**–H_2O_2. [**1a**] 2.6×10^{-7} *M*, [Orange II] 2.7×10^{-5} *M*, [H_2O_2] 4.4×10^{-4} *M*, pH 9, 25 °C. The inset shows changes of absorbance at 350 nm with time.

3.3.7
Pulp Bleaching and Craft Mill Effluent Treatment (P_{Fe} Process)

Paper manufacture is one of the larger industries in the USA. The bleaching of wood pulp for white paper production involves some of the largest flows of matter between the economy and the environment. Every year, the paper industry produces >100 million tonnes of bleached pulp to turn it into white paper. This industry provides a significant arena in which green chemists might improve the environmental impact of technology, but at the same profit margins are small such that any new technologies must meet demanding economic goals in addition to improving environmental performance. In pulp bleaching, the Fe–TAML peroxide process (P_{Fe}) shows high selectivity for lignin over cellulose oxidation, allowing for rapid stripping of the lignin residues from wood pulp (Figure 3.15) [76]. It is critical to the quality of the final pulp and derivative paper products that the oxidizing agent should selectively decompose the colored lignin polymer while not degrading the white cellulosic polymers.

Bleaching of the pulp with chlorine-based oxidants generates chlorophenols, dioxins (much less with ClO_2 than with Cl_2) and other potentially toxic and recalcitrant organochlorines, in addition to discharging a coffee-colored effluent that stains streams and rivers and blocks light from penetrating the water. The sources of the staining are large colored fragments of lignin, the polymer that binds the cellulose fibers in wood. **1n**–H_2O_2 treatment was able to remove color from an E_{op} filtrate by up to 78% and eliminated organochlorines (determined as AOX) by 29% (Figure 3.16) [76, 77].

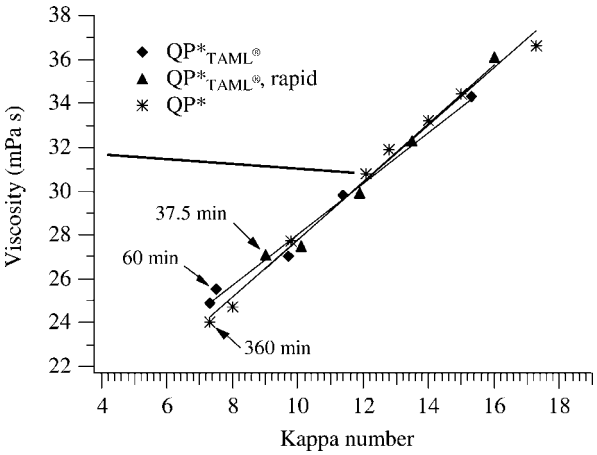

Figure 3.15 Selectivity for bleaching of kraft pulp with **1n**–H_2O_2 (4%) (each addition of 0.1 mg and data taken 7.5 min after each addition) at 90 °C. Q indicates EDTA pretreatment and * indicates treatment in the presence of diethylenetriamine pentamethylenephosphonic acid (DTMPA). DE (shown as a line) is ClO_2 treatment followed by alkaline extraction.

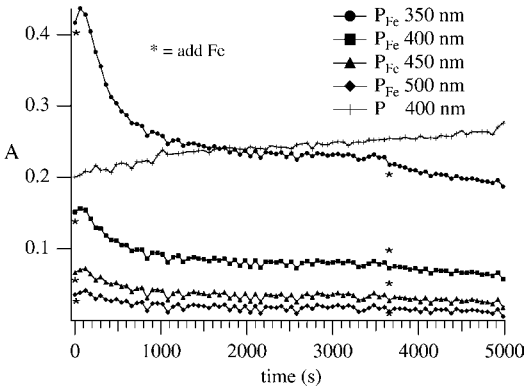

Figure 3.16 Bleaching of a kraft mill effluent by **1n**–H_2O_2 monitored by UV–visible spectroscopy at 350, 400, 450 and 500 nm. A control was monitored at 400 nm with H_2O_2 only.

3.4 Conclusion

Fe–TAMLs mimic the activity of both peroxidase [1, 2] and cytochrome P450 enzymes [3, 5]. Recent identification of stable iron(IV) species in water [35] and iron(V) oxo species in an organic solvent [37] produced from Fe–TAMLs and peroxides indicates that Fe–TAMLs do indeed substantially mimic peroxidase enzymes [1, 2] in their interaction with peroxide. For example, Fe–TAML–H_2O_2 treatment of phosphorothioate pesticides, such as fenitrothion, parathion and chlorpyrifos, has been reported to result in their total degradation [29]. However, the initial reaction produced both hydrolysis and oxidation products, which were found to be similar to the products of the reaction catalyzed by cytochrome P450 [78]. At the same time, chloroperoxidase treatment in the presence of H_2O_2 and Cl^- ions gave only oxon derivatives (phosphates) with an oxygen atom instead of sulfur atom at phosphorus [79]. Synthetic catalysts including Fe–TAMLs do not have steric limitations as imposed by the protein component of enzymes such that the close approach of substrates to the oxidized metal center is relatively unimpeded. The major structural difference between peroxidases and cytochrome P450s is that substrates can approach the heme iron only in the case of cytochrome P450. Therefore, the actual reaction between the oxidized Fe–TAML and a substrate may more closely mimic cytochrome P450 enzymes because in catalysis, peroxidase reactivity is limited by the access of the substrate to the oxidized iron [5, 80, 81]. At our present state of understanding, Fe–TAMLs are well described as being green oxidation catalysts. They have a growing number of applications for cleaning water of recalcitrant pollutants and hardy pathogens and offer a potent new tool for transforming water from polluted streams and river systems to cleaner and perhaps potable water. In the coming years, we expect to report on a large number of new such applications.

Acknowledgments

We thank for support the Heinz Endowments (T.J.C.), the Institute for Green Science (T.J.C.) and the Environmental Protection Agency (grant RD 83 to T.J.C.).

References

1 Dunford, H.B. (1982) *Advances in Inorganic Biochemistry*, **4**, 41–80.
2 Dunford, H.B. (1999) *Heme Peroxidases*, John Wiley & Sons, Inc, New York.
3 Sono, M., Roach, M.P., Coulter, E.D. and Dawson, J.H. (1996) *Chemical Reviews*, **96**, 2841–2887.
4 Solomon, E.I., Brunold, T.C., Davis, M.I., Kemsley, J.N., Lee, S.-K., Lehnert, N., Neese, F., Skulan, A.J., Yang, Y.-S. and Zhou, J. (2000) *Chemical Reviews*, **100**, 235–349.
5 Meunier, B., de Visser, S.P. and Shaik, S. (2004) *Chemical Reviews*, **104**, 3947–3980.
6 Collins, T.J. (2002) *Accounts of Chemical Research*, **35**, 782–790.
7 Collins, T.J. and Walter, C. (2006) *Scientific American*, **294** (83–88), 90.
8 Ghosh, A., Ryabov, A.D., Mayer, S.M., Horner, D.C., Prasuhn, D.E., Jr, Sen Gupta, S., Vuocolo, L., Culver, C., Hendrich, M.P., Rickard, C.E.F., Norman, R.E., Horwitz, C.P. and Collins, T.J. (2003) *Journal of the American Chemical Society*, **125**, 12378–12378.
9 Kistenmacher, T.J. and Stucky, G.D. (1968) *Inorganic Chemistry*, **7**, 2150–2155.
10 Nelson, S.M. (1987) in *Comprehensive Coordination Chemistry. The Synthesis, Reactions, Properties and Application of Coordination Compounds* (eds G. Wilkinson, R.D. Gillard and J.A. McCleverty), Vol. 4, Pergamon Press, Oxford, pp. 217–276.
11 Koenig, D.F. (1965) *Acta Crystallographica*, **18**, 663–673.
12 Hoard, J.L., Cohen, G.H. and Glick, M.D. (1967) *Journal of the American Chemical Society*, **89**, 1992–1996.
13 Ayougou, K., Mandon, D., Fischer, J., Weiss, R., Muther, M., Schunemann, V., Trautwein, A.X., Bill, E., Terner, J., Jayaraj, K., Gold, A. and Austin, R.N. (1996) *Chemistry – A European Journal*, **2**, 1159–1163.
14 Bartos, M.J., Gordon-Wylie, S.W., Fox, B.G., Wright, L.J., Weintraub, S.T., Kauffmann, K.E., Münck, E., Kostka, K.L., Uffelman, E.S., Rickard, C.E.F., Noon, K.R. and Collins, T.J. (1998) *Coordination Chemistry Reviews*, **174**, 361–390.
15 Pauling, L. (1960) *The Nature of the Chemical Bond*, 3d edn, Cornell University Press, Ithaca, NY.
16 Ryabov, A.D., Kazankov, G.M., Yatsimirsky, A.K., Kuz'mina, L.G., Burtseva, O.Y., Dvortsova, N.V. and Polyakov, V.A. (1992) *Inorganic Chemistry*, **31**, 3083–3090.
17 Schmülling, M., Ryabov, A.D. and van Eldik, R. (1994) *Journal of the Chemical Society-Dalton Transactions*, 1257–1263.
18 Schmülling, M., Grove, D.M., van Koten, G., van Eldik, R., Veldman, N. and Spek, A.L. (1996) *Organometallics*, **15**, 1384–1391.
19 Polshin, V., Popescu, D.-L., Fischer, A., Chanda, A., Horner, D.C., Beach, E.S., Henry, J., Qian, Y.-L., Horwitz, C.P., Lente, G., Fabian, I., Münck, E., Bominaar, E.L., Ryabov, A.D. and Collins, T.J. (2008) *Journal of the American Chemical Society*, **130**, 4497–4506.
20 Fleischer, E.B. and Fine, D.A. (1978) *Inorganica Chimica Acta*, **29**, 267–271.
21 Coyle, C.L., Rafson, P.A. and Abbott, E.H. (1973) *Inorganic Chemistry*, **12**, 2007–2010.

22 Nesset, M.J.M., Shokhirev, N.V., Enemark, P.D., Jacobson, S.E. and Walker, F.A. (1996) *Inorganic Chemistry*, **35**, 5188–5200.

23 Shack, J. and Clark, W.M. (1947) *The Journal of Biological Chemistry*, **171**, 143–187.

24 Cowgill, R.W. and Clark, W.M. (1952) *The Journal of Biological Chemistry*, **198**, 33–61.

25 Bartos, M.J., Kidwell, C., Kauffmann, K.E., Gordon-Wylie, S.W., Collins, T.J., Clark, G.C., Münck, E. and Weintraub, S.T. (1995) *Angewandte Chemie International Edition*, **34**, 1216–1219.

26 Collins, T.J. (1994) *Accounts of Chemical Research*, **27**, 279–285.

27 Sen Gupta, S., Stadler, M., Noser, C.A., Ghosh, A., Steinhoff, B., Lenoir, D., Horwitz, C.P., Schramm, K.-W. and Collins, T.J. (2002) *Science*, **296**, 326–328.

28 Banerjee, D., Markley, A.L., Yano, T., Ghosh, A., Berget, P.B., Minkley, E.G., Jr, Khetan, S.K. and Collins, T.J. (2006) *Angewandte Chemie-International Edition*, **45**, 3974–3977.

29 Chanda, A., Khetan, S.K., Banerjee, D., Ghosh, A. and Collins, T.J. (2006) *Journal of the American Chemical Society*, **128**, 12058–12059.

30 Mondal, S., Hangun-Balkir, Y., Alexandrova, L., Link, D., Howard, B., Zandhuis, P., Cugini, A., Horwitz, C.P. and Collins, T.J. (2006) *Catalysis Today*, **116**, 554–561.

31 Chahbane, N., Popescu, D.-L., Mitchell, D.A., Chanda, A., Lenoir, D., Ryabov, A.D., Schramm, K.-W. and Collins, T.J. (2007) *Green Chemistry*, **9**, 49–57.

32 Chanda, A., Ryabov, A.D., Mondal, S., Alexandrova, L., Ghosh, A., Hangun-Balkir, Y., Horwitz, C.P. and Collins, T.J. (2006) *Chemistry – A European Journal*, **12**, 9336–9345.

33 Ryabov, A.D., Sukharev, V.S., Alexandrova, L., Le Lagadec, R. and Pfeffer, M. (2001) *Inorganic Chemistry*, **40**, 6529–6532.

34 Oakes J. and Gratton P. (1998) *Journal of the Chemical Society-Perkin Transactions 2*, 157–164

35 Chanda, A., Shan, X., Chakrabarti, M., Ellis, W., Popescu, D., Tiago de Oliveria, F., Wang, D., Que, L., Jr., Collins, T.J., Münck, E. and Bominaar, E.L. (2008) *Inorganic Chemistry*, **47**, 3669–3678.

36 Ghosh, A., Tiago de Oliveria, F., Toshihiro Yano, T., Nishioka, T., Beach, E.S., Kinoshita, I., Münck, E., Ryabov, A.D., Horwitz, C.P. and Collins, T.J. (2005) *Journal of the American Chemical Society*, **127**, 2505–2513.

37 Tiago de Oliveira, F., Chanda, A., Banerjee, D., Shan, X., Mondal, S., Que, L., Jr., Bominaar, E.L., Muenck, E. and Collins, T.J. (2007) *Science*, **315**, 835–838.

38 Hodges, G.R., Lindsay Smith, J.R. and Oakes, J. (1998) *Journal of the Chemical Society-Perkin Transactions 2*, 617–628.

39 Frisch, M.J., Trucks, G.W., Schlegel, H.B., Scuseria, G.E., Robb, M.A., Cheeseman, J.R., Montgomery, J., Vreven, J.A.T., Kudin, K.N., Burant, J.C., Millam, J.M., Iyengar, S.S., Tomasi, J., Barone, V., Mennucci, B., Cossi, M., Scalmani, G., Rega, N., Petersson, G.A., Nakatsuji, H., Hada, M., Ehara, M., Toyota, K., Fukuda, R., Hasegawa, J., Ishida, M., Nakajima, T., Honda, Y., Kitao, O., Nakai, H., Klene, M., Li, X., Knox, J.E., Hratchian, H.P., Cross, J.B., Bakken, V., Adamo, C., Jaramillo, J., Gomperts, R., Stratmann, R.E., Yazyev, O., Austin, A.J., Cammi, R., Pomelli, C., Ochterski, J.W., Ayala, P.Y., Morokuma, K., Voth, G.A., Salvador, P., Dannenberg, J.J., Zakrzewski, V.G., Dapprich, S., Daniels, A.D., Strain, M.C., Farkas, O., Malick, D.K., Rabuck, A.D., Raghavachari, K., Foresman, J.B., Ortiz, J.V., Cui, Q., Baboul, A.G., Clifford, S., Cioslowski, J., Stefanov, B.B., Liu, G., Liashenko, A., Piskorz, P., Komaromi, I., Martin, R.L., Fox, D.J., Keith, T., Al-Laham, M.A., Peng, C.Y., Nanayakkara, A., Challacombe, M., Gill, P.M.W., Johnson, B., Chen W. Wong M.W. Gonzalez C. and Pople J.A. (2004) *Gaussian 03 (Release B05)*, Gaussian, Wallingford, CT.

40 Chanda, A., Popescu, D.-L., Tiago de Oliveira, F., Bominaar, E.L., Ryabov, A.D.,

Munck, E. and Collins, T.J. (2006) *Journal of Inorganic Biochemistry*, **100**, 606–619.
41 Beletskaya, I.P. and Cheprakov, A.V. (2000) *Chemical Reviews*, **100**, 3009–3066.
42 Dixon, M. and Webb, E.C. (1958) *Enzymes*, Academic Press, New York.
43 Dixon, M., Webb, E.C., Thorne, C.J.R. and Tipton, K.F. (1979) *Enzymes*, 3rd edn, Academic Press, New York.
44 Cornish-Bowden, A. (1995) *Fundamentals of Enzyme Kinetics*, Portland Press, London.
45 Fersht, A. (1999) *Structure and Mechanism in Protein Science: a Guide to Enzyme Catalysis and Protein Folding*, Freeman, New York.
46 Anastas, P.T. and Warner, J.C. (1998) *Green Chemistry: Theory and Practice*, Oxford University Press, Oxford.
47 Horvath, I.T. (2002) *Accounts of Chemical Research*, **35**, 685.
48 Collins, T.J., Gordon-Wylie, S.W., Bartos, M.J., Horwitz, C.P., Woomer, C.G., Williams, S.A., Patterson, R.E., Vuocolo, L.D., Paterno, S.A., Strazisar, S.A., Peraino, D.K. and Dudash, C.A. (1998) *Green Chemistry*, Oxford University Press, Oxford, pp. 46–71.
49 Job, D. and Dunford, H.B. (1976) *European Journal of Biochemistry*, **66**, 607–614.
50 Shevelkova, A.N. and Ryabov, A.D. (1996) *Biochemistry and Molecular Biology International*, **39**, 665–670.
51 Ghosh, A. (2004) Design, synthesis and mechanistic studies of iron–TAML catalytic activators of hydrogen peroxide and a new activation chemistry of dioxygen by iron, *PhD Thesis*, Department of Chemistry, Carnegie Mellon University, Pittsburgh, PA.
52 FAO Newsroom (2004), http://www.fao.org/newsroom/en/news/2004/50119/index.html (3 November 2008).
53 Brown, J.S. and Hodge, R.C. (2003) in *The Joint Service Scientific Conference on Chemical and Biological Defense Research*, Towson, MD.
54 Kaczorowska, K., Kolarska, Z., Mitka, K. and Kowalski, P. (2005) *Tetrahedron*, **61**, 8315–8327.
55 Sato, K., Hyodo, M., Aoki, M., Zheng, X.Q. and Noyori, R. (2001) *Tetrahedron*, **57**, 2469–2476.
56 Collins, T.J., Banerjee, D. and Khetan, S.K. (2004) in *228th American Chemical Society National Meeting*, Philadelphia, PA.
57 Vassell, K.A. and Espenson, J.H. (1994) *Inorganic Chemistry*, **33**, 5491–5498.
58 Amitai, G., Adani, R., Hershkovitz, M., Bel, P., Rabinovitz, I. and Meshulam, H. (2003) *Journal of Applied Toxicology*, **23**, 225–233.
59 Mitchell, S.J. (2006) DSTL, Porton Down, personal communication.
60 US EPA, *Heavy-duty Engine and Vehicle Standards and Highway Diesel Fuel Sulfur Control Requirements*, EPA420-F-00-057, Environmental Protection Agency, Washington, DC (2000).
61 Wang, Y. and Espenson, J.H. (2000) *The Journal of Organic Chemistry*, **65**, 104–107.
62 Lai, E.M., Phadke, N.D., Kachman, M.T., Giorno, R., Vazquez, S., Vazquez, J.A., Maddock, J.R. and Driks, A. (2003) *Journal of Bacteriology*, **185**, 1443–1454.
63 Regino, C.A.S. and Richardson, D.E. (2007) *Inorganica Chimica Acta*, **360**, 3971–3977.
64 Fujiwara, N., Nakano, M., Kato, S., Yoshihara, D., Ookawara, T., Eguchi, E., Taniguchi, N. and Suzuki, K. (2007) *The Journal of Biological Chemistry*, **282**, 35933–35944.
65 Paul, M., Setlow, B. and Setlow, P. (2007) *Journal of Applied Microbiology*, **102**, 954–962.
66 Meunier, B. (2002) *Science*, **296**, 270–271.
67 Rieger, P.G. and Knackmuss, H.J. (1995) in *Biodegradation of Nitroaromatic Compounds* (ed. J.C. Spain), Plenum Press, New York, pp. 1–18.
68 Chanda, A., Espinosa-Marvan, L., Khetan, S.K. and Collins, T.J. (2008) in *The 235th American Chemical Society National Meeting*, New Orleans, LA.
69 Purohit, V. and Basu, A.K. (2000) *Chemical Research in Toxicology*, **13**, 673–692.

70 Hartter, D.R. (1985) in *Toxicity of Nitroaromatic Compounds* (ed. D.E. Richard), Hemisphere Publishing, New York, pp. 1–14.

71 Khetan, S.K. and Collins, T.J. (2007) *Chemical Reviews*, **107**, 2319–2364.

72 Shappell, N.W., Vrabel, M.A., Madsen, P.J., Harrington, G., Billey, L.O., Hakk, H., Larsen, G.L., Beach, E.S., Horwitz, C.P., Ro, K., Hunt, P.G. and Collins, T.J. (2008) *Environmental Science & Technology*, **42**, 1296–1300.

73 Pomati, F. (2007) *Environmental Science & Technology*, 8204.

74 Zollinger, H. (2003) *Color Chemistry: Syntheses, Properties and Applications of Organic Dyes and Pigments*, 3rd edn, Wiley-VCH Verlag GmbH, Weinheim.

75 Beach, E.S. (2007) *PhD Thesis*, Carnegie Mellon University, Pittsburgh, PA.

76 Collins, T.J., Hall, J.J., Vuocolo, L.D., Fattaleh, N.L., Suckling, I., Horwitz, C.P., Gordon-Wylie, S.W., Allison, R.W., Fullerton, T.J. and Wright, L.J. (2000) in *Green Chemistry: Challenging Perspectives* (ed. P. Tundo), Oxford University Press, Oxgord, pp. 79–105.

77 Collins, T.J., Horwitz, C.P., Ryabov, A.D., Vuocolo, L.D., Sen Gupta, S., Ghosh, A., Fattaleh, N.L., Hangun, Y., Steinhoff, B., Noser, C.A., Beach, E., Prasuhn, D., Jr., Stuthridge, T., Wingate, K.G., Hall, J., Wright, L.J., Suckling, I. and Allison, R.W., (2002) in *Advancing Sustainability through Green Chemistry and Engineering*, (eds R.L. Lankey and P.T. Anastas), ACS Symposium Series 823, ed. R. L. a. A. Lankey, P. T., American Chemical Society, Washington, DC, pp. 47–60.

78 Levi, P.E., Hollingworth, R.M. and Hodgson, E. (1988) *Pesticide Biochemistry and Physiology*, **32**, 224–231.

79 Hernandez, J., Robledo, N.R., Velasco, L., Quintero, R., Pickard, M.A. and Vazquez-Duhalt, R. (1998) *Pesticide Biochemistry and Physiology*, **61**, 87–94.

80 Ator, M.A. and Ortiz de Montellano, P.R. (1987) *The Journal of Biological Chemistry*, **262**, 1542–1551.

81 Kumar, D., De Visser, S.P., Sharma, P.K., Derat, E. and Shaik, S. (2005) *Journal of Biological Inorganic Chemistry: JBIC: a Publication of the Society of Biological Inorganic Chemistry*, **10**, 181–189.

4
Microwave-Accelerated Homogeneous Catalysis in Water

Luke R. Odell and Mats Larhed

4.1
Introduction

The advancements in microwave-assisted metal catalysis in neat water have already been remarkable in many ways, a fact that is equally valid for the actual chemical progress made and for the sheer number of recent publications [1]. Five years ago it was possible to include all the literature in the area within the scope of a few pages. In 2007, the range of investigated transformations and the number of examples make it difficult even to include all examples in a book chapter [1]. This mini-review attempts to give an overview of microwave-promoted metal-catalyzed homogeneous transformations in neat water, providing a personal selection of both pioneering and recently published work. Covered areas include cross-couplings, Heck reactions, carbonylations, Sonogashira reactions, nucleophilic substitutions and some additional transformations. It is notable that all available published examples were conducted on the laboratory scale. After a brief background on microwaves [2–4], water as reaction medium [5] and transition metal catalysis [6], we present preparative examples and discuss the impact and future potential in both catalysis and sustainable chemistry [7, 8].

4.1.1
Microwave Heating

In principle, all metal-catalyzed organic transformations require an input of energy to proceed at a useful rate. In the correct amount and in the right form, energy drives the catalytic cycle forward, providing the desired product with high selectivity and in high yield. In the wrong amount or in the wrong form, energy can instead completely inhibit the catalytic process [9, 10]. Hence the regulation of the energy input and the choice of the energy source are of vital importance in homogeneous catalysis. Among the available alternatives, microwave irradiation has a huge potential to provide controlled energy directly to the molecules of interest [10].

Green Catalysis, Volume 1: Homogeneous Catalysis.
Edited by Robert H. Crabtree

ISBN: 978-3-527-32496-5

Microwaves are able to heat a reaction mixture by two general mechanisms, dipolar polarization and ionic conductance [2–4]. All non-crystalline solids and liquids that contain dipoles and/or charged species can absorb microwave energy and convert it into heat. This is a consequence of the fact that dipoles and ions are constantly trying to align themselves to the electric component of the oscillating electromagnetic vector of the microwave field, resulting in rotation of molecules and oscillation of ions. Hence the microwave energy absorbed in this process is first converted to kinetic energy, which is then transferred into thermal energy through molecular friction [2–4]. To accomplish efficient heating, it is important that the frequency of the applied microwave radiation is within certain limits. If the frequency is too low, the dipoles will have time to align with the electric field and smoothly follow the field fluctuations, resulting in poor heating. If instead it is too high, the dipoles will not have time to realign themselves to the quickly alternating field, which means no molecular motion is created and therefore no heat is generated [10]. The frequency used by both microwave synthesizers and domestic microwave ovens (2450 MHz, $\lambda = 12.2$ cm) is located between these extremes where dipoles have time to realign partly with the oscillating electric field but are not quite able to follow the field fluctuations. The end result is effective in-core heating [4].

Since the mid-1990s, an increasing number of research reports have indeed demonstrated that controlled microwave heating can be used to carry out almost all types of organic transformations that require thermal energy [11], including reactions catalyzed by homogeneous metal complexes [12]. Furthermore, with microwave *in situ* heating the thermal energy does not need to be transferred via the vessel wall, avoiding wall effects and the associated decomposition of sensitive catalysts. Hence this remote and volumetric heating method opens up new ways to achieve fast and selective synthesis, which is especially important in the fine-tuning and optimization of sensitive transition metal-catalyzed reactions [12].

At the beginning of the 21st century, dedicated microwave synthesizers for controlled small-scale synthesis in sealed vessels became commercially available [4]. These instruments permitted easy programming and documentation of time, temperature and irradiation power during the reactions, while at the same time providing direct reaction control, high safety, good reproducibility and straightforward operation. In addition, by using septum-sealed purpose-made closed microwave-transparent vessels, which in general could accommodate at least 20 bar of pressure, it was possible to maintain reaction solutions at temperatures much above their conventional reflux temperature. Together with high heating rates and efficient air-jet cooling systems, the overall process times were dramatically reduced. Sealed vessels permit the use of low-boiling solvents, allowing easy work-up and reduction of solvent waste. An additional environmentally friendly factor is the reduced energy consumption compared with the classical heating of small-scale reactions [13]. At present, however, it is not clear if pilot-scale or production-scale microwave processing holds this advantage compared with traditional heating [14].

4.1.2
Water as a Green Reaction Medium

In addition to finding safer and more cost-effective synthetic routes, there is also an ever growing need for more environmentally friendly methods to perform organic chemistry (the triple bottom line). Among the 12 principles of green chemistry [15], we have already touched upon the aim of reducing the energy consumption (principle 6). Two additional principles concern the desire to employ 'eco-friendly solvents' and 'catalytic protocols' (principles 5 and 9). In traditional homogeneous catalysis, organic solvents are usually utilized as the reaction media [16], often generating a number of health, safety and environmental issues. In fact, a study by Cunningham and co-workers suggests that correct solvent management could make the biggest improvement towards greener organic chemistry [17].

Although many reactions have been shown to proceed under solvent-free conditions, most catalytic transformations still require the use of solvents. Hence alternatives to standard organic solvents have been investigated, such as water, PEG, supercritical CO_2, perfluorinated hydrocarbons and ionic liquids [16]. In principle, if a solvent needs to be used, water would represent the greenest choice. In addition to being a safe, cheap and readily available environmentally friendly solvent, water at elevated temperatures has also been recognized as an effective reaction medium with unique pseudo-organic properties [2]. Interestingly, the dielectric constant of water decreases from 78 at 25 °C to 20 at 300 °C, meaning that the polarity of water will more and more resemble a typical organic solvent with higher temperature. This means that the solubility of organic compounds increases rapidly upon heating, which of course is a necessary prerequisite for an efficient reaction in a homogeneous environment [1]. In addition, once cooled to room temperature, many organic compounds will no longer be soluble and product isolation is often facilitated by precipitation. The lack of flammable properties also makes the use of water safe with pressurized exothermic reactions. However, it is important to note that any water used as a reaction medium must still be handled as reaction waste.

4.1.3
Homogeneous Transition Metal Catalysis

Reactions catalyzed by soluble transition metal complexes consist of a group of highly chemoselective transformations, which allow the formation of many kinds of carbon–carbon and carbon–heteroatom attachments that were previously very difficult to accomplish [6, 18, 19]. However, the sometimes tedious pinpointing of the appropriate reaction components, together with the long reaction times (ranging from hours to days) frequently required for full conversions, have previously limited the exploitation of these protocols in many organic synthesis applications [9]. Furthermore, the need for inert conditions under microwave irradiation has been reported to be very limited [12]. Therefore, the use of modern microwave heating equipment not only accelerates the reaction rates, but also simplifies the preparative handling.

4.1.4
Microwave-Assisted Metal Catalysis in Water

In line with the importance of biocatalysis in aqueous media, the development of metal-catalyzed organic transformations in hot water has become a vibrant research area [1, 16]. When discussing aqueous organic chemistry, it is convenient to divide the reported protocols into two broad categories: studies that involve pure water as solvent and those carried out using an organic co-solvent. We have decided, however, that the latter protocols are outside the scope of this short chapter focusing on sustainable methods and they will therefore not be discussed further. Reactions performed with heterogeneous catalysts will also not be presented.

The high-temperature water reaction range (100–200 °C) is especially well suited for microwave processing in sealed vessels with standard instruments, since higher temperatures result in pressures above the pressure limit of 20 bar [4, 20]. While pure water is difficult to heat above 130 °C due to a reduced absorbance of microwave irradiation at increasing temperature [3], in most 'real' cases the starting material, the reagent, the catalyst or the base are polar enough (or ionic) to enable microwave heating to 200 °C without the addition of 'microwave active' additives, such as salts or recently launched 'passive microwave elements' [21]. Today, the development of new methods that reduce the environmental impact is of increasing importance, not only for large-scale production, but also in the pilot- or small-scale research laboratory [7]. Thus, gradually, it has become clear that the combined approach of microwave superheating, homogeneous catalysis and aqueous conditions offers a nearly synergistic strategy as the combination may offer greater potential than the three individual components [1, 20].

4.2
Suzuki–Miyaura Reactions

The palladium-catalyzed cross-coupling of an organoboron compound and an aryl halide, known as the Suzuki–Miyaura reaction, is one of the most versatile and frequently utilized methods for C−C bond formation [12, 20, 22].

In 1999, Schotten and co-workers first reported the use of microwave irradiation, using a domestic microwave oven, to promote the cross-coupling of methyl 4-iodobenzoate and arylboronic acids in water [23]. They found that by using 0.52 equiv. of PEG 6000 as a phase transfer catalyst (PTC), the corresponding biaryl compounds could be produced in good yields and with short reaction times (Scheme 4.1).

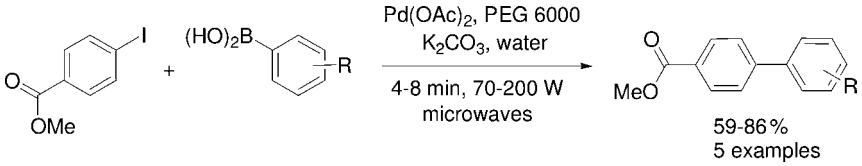

Scheme 4.1 Suzuki–Miyaura coupling of methyl 4-iodobenzoate and various arylboronic acids.

Inspired by the work of Bumagin and Bykov [24], Villemin *et al.* used the water-soluble and commercially available sodium tetraphenylborate as a phenylation agent for a range of heteroaromatic halides [25]. The reactions were performed in neat water and proceeded smoothly without the addition of any PTC.

In 2002, Leadbeater and Marco presented the first of a series of studies on the coupling of aryl halides with boronic acids in neat water [26]. Aryl iodides and bromides were rapidly coupled (5–10 min) at 150 °C, using low palladium loadings [$Pd(OAc)_2$, 0.4%], and the corresponding products were isolated in good yields (Scheme 4.2). Improved yields were obtained for non-polar aryl halides by the addition of 1 equiv. of the PTC tetrabutylammonium bromide (TBAB). TBAB was thought to facilitate the solvation of the organic substrates and enhance the reaction rate by formation of an $[ArB(OH)_3]^-[R_4N]^+$ complex. Aryl chlorides were also coupled using this simple protocol, in acceptable yields, by increasing the reaction temperature to 175 °C (Scheme 4.2). The same group subsequently discovered that electron-poor or neutral boronic acids could be coupled with various aryl bromides and aryl iodides, without the addition of a palladium source, under 'transition metal-free' conditions [27, 28]. A reassessment of these results revealed that palladium contaminants down to 50 ppb found in commercially available sodium carbonate (Na_2CO_3) were responsible for the biaryl formation [29].

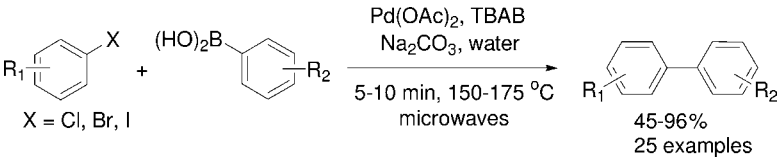

Scheme 4.2 Suzuki–Miyaura couplings of aryl halides.

Phenylboronic acid has been coupled with various aryl bromides by Zhang and co-workers using an improved domestic microwave oven [30]. A range of substituted biaryls were rapidly produced, in good yields, utilizing $Pd(PPh_3)_2Cl_2$ as catalyst and potassium carbonate (K_2CO_3) as the base.

Vanelle and co-workers described a reaction protocol comprising 10% $Pd(PPh_3)_4$, 5 equiv. of Na_2CO_3 and 1 equiv. of TBAB for the synthesis of various 6-aryl-2-arylsulfonylmethyl-3-nitroimidazo[1,2-*a*]pyridines (Scheme 4.3) [31]. The large amount of base was employed to facilitate formation of the sulfonyl anion and improve

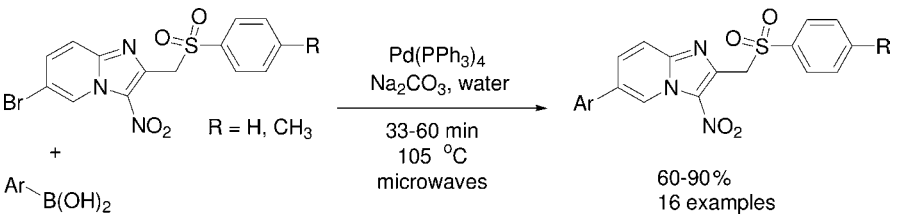

Scheme 4.3 Synthesis of 6-aryl-2-arylsulfonylmethyl-3-nitroimidazo[1,2-*a*]pyridines via Suzuki–Miyaura coupling.

aqueous solubility. Microwave irradiation was found to increase the reaction rates up to 30-fold without compromising yields and also limit the formation of aggregates, which simplified reaction workup, compared with classical oil bath heating.

A similar reaction system, utilizing standard $Pd(PPh_3)_4$, has also been employed in the cross-coupling of 4-bromo-2-chlorobenzoic acid and 3,5-dimethylphenylboronic acid [32, 33]. The reaction was found to be highly chemoselective, affording the corresponding chloro-biaryl compound in an almost quantitative yield (Scheme 4.4).

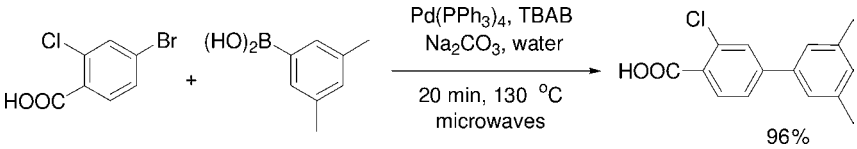

Scheme 4.4 Chemoselective Suzuki–Miyaura coupling of 4-bromo-2-chlorobenzoic acid.

The development of efficient catalytic systems for the coupling of notoriously difficult aryl chlorides has attracted the interest of several research groups [34]. Aryl chlorides are appealing coupling partners due to their lower cost and greater availability. In 2005, Anderson and Buchwald presented a highly active and general catalytic system, based on a new water-soluble biaryl-phosphine ligand [1,1′-biphenyl]-3-sulfonic acid-2′-(dicyclohexylphosphino)-2,6-dimethoxy sodium salt (**A**) [35]. With **A**, excellent yields were obtained for the coupling of functionalized aryl chlorides and aryl boronic acids (Scheme 4.5). Moreover, utilizing controlled

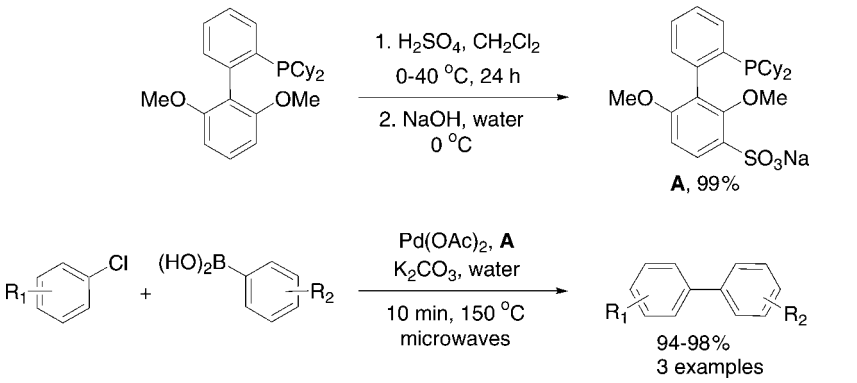

Scheme 4.5 Reactions of aryl chlorides using a biaryl-phosphine ligand.

microwave irradiation, the reaction times could be reduced from 2–8 h to just 10 min compared with the corresponding classical heating reactions conducted at 100 °C.

In 2007, Claver and co-workers described two novel air-stable and water-soluble phosphine sulfonate ligands (**B** and **C**, Scheme 4.6) [36]. These ligands were able to catalyze the cross-coupling of a small number of electron-rich aryl bromides and chlorides with various arylboronic acids. Further studies will determine the scope and general applicability of these new ligands.

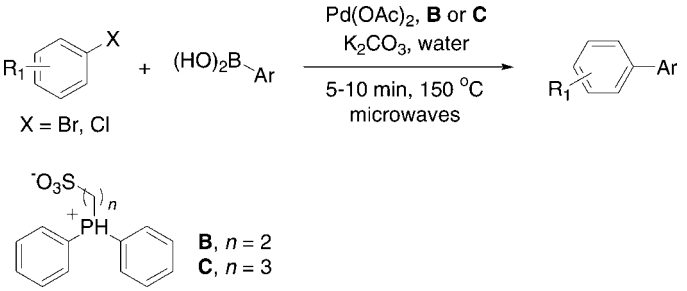

Scheme 4.6 Reactions of aryl chlorides using water-soluble phosphine sulfonate ligands.

Recently, Dawood has evaluated the catalytic activity of a new benzothiazole-oxime Pd(II) precatalyst **D**, in the coupling of aryl bromides and aryl chlorides with phenylboronic acid (Scheme 4.7) [37]. Excellent yields were obtained, using **D**, for the coupling of electron-poor and electron-rich aryl bromides. However, only electron-poor aryl chlorides gave acceptable yields, with *p*-tolyl chloride giving only 7% conversion after 30 min of irradiation at 160 °C.

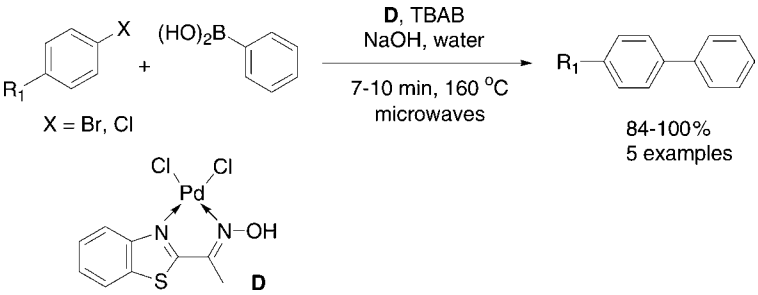

Scheme 4.7 Suzuki–Miyaura coupling of aryl bromides and chlorides with phenylboronic acid.

4.3 The Stille Reaction

The Stille reaction is a base-free cross-coupling reaction between an organotin moiety and an organohalide [38]. This reaction, like the Suzuki reaction, is very reliable, high yielding and tolerant of many functional groups [12]; however; organic stannanes are considerably more toxic than the corresponding organoboron compounds.

Van der Eycken and co-workers presented the first example of a microwave-assisted Stille reaction in neat water in 2003 [39]. They used the Stille reaction to decorate the C-3 position of the 2(1*H*)-pyrazinone scaffold with various aryl and alkyl groups (Scheme 4.8). Microwave irradiation was found to reduce the reaction time from 3 days to 15 min compared with the corresponding classical heating reactions. However, the yields obtained utilizing water as a solvent were found to be 10–20% lower than those obtained using DMF, due to hydrolysis of the sensitive imidoyl chloride moiety at elevated temperatures.

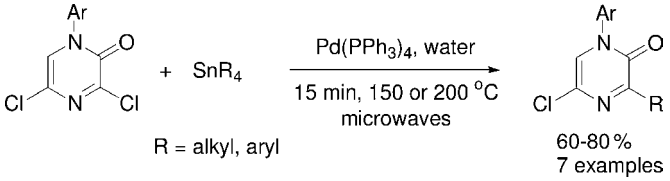

Scheme 4.8 Preparation of 2(1*H*)-pyrazinones.

4.4
The Hiyama Cross-Coupling Reaction

In 1999, DeShong and co-workers [40] found that vinyl(trimethoxy)silane could undergo a Pd(0)-catalyzed cross-coupling reaction with 4-iodotoluene in the presence of tetrabutylammonium fluoride (TBAF). Thus, upon activation by a fluoride ion, the nucleophilicity of the vinylsiloxane becomes adequate to complete the transmetalation process. In addition, hydroxide anions can also promote the Hiyama reaction with siloxanes [41]. This activation method was recently utilized by Alacid and Nájera to accomplish the first fluoride-free microwave-promoted Hiyama reactions in neat water [42]. This reaction exploited $Pd(OAc)_2$ or **E** as precatalyst and was used to produce a series of styrenes from different aryl bromides and chlorides (Scheme 4.9).

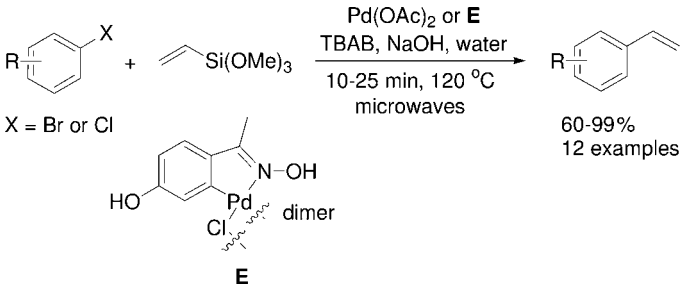

Scheme 4.9 Preparation of styrenes via Hiyama cross-coupling.

4.5
The Heck Reaction

The palladium-catalyzed arylation and alkenylation of alkenes, known today as the Heck reaction, was independently reported by Heck and Nolley [43] and Mizoroki *et al.* [44] in the early 1970s. Today, the reaction is widely recognized as one of the mildest and most versatile C–C bond-forming reactions [45–47].

In 2002, Wang *et al.* described the first microwave-assisted Heck coupling of alkenes with aryl iodides in water [48]. These high-yielding reactions (86–91%) were carried out under an argon atmosphere using $Pd(PPh_3)_2Cl_2$ and TBAB with K_2CO_3 as

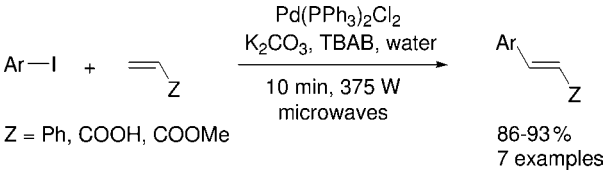

Scheme 4.10 Heck coupling of alkenes with aryl iodides.

the base (Scheme 4.10). The products were synthesized 18–42 times faster using the microwave-enhanced protocol than under conventional heating conditions.

The oxime-derived palladacycle **E** was also utilized by Botella and Nájera to catalyze the β-mono- and β,β-diarylation of terminal alkenes [49, 50]. The monoarylation of *tert*-butyl acrylate with *p*-chloroiodobenzene proceeded efficiently and rapidly under microwave conditions with both **E** (10 min, 87%) and standard $Pd(OAc)_2$ (10 min, 88%). Precatalyst **E** was found to be superior in promoting diarylation, although microwave irradiation gave a lower yield (31%) than the corresponding classical heating reaction (66%) (Scheme 4.11). In this case the microwave-promoted reaction may have benefited from a longer reaction time.

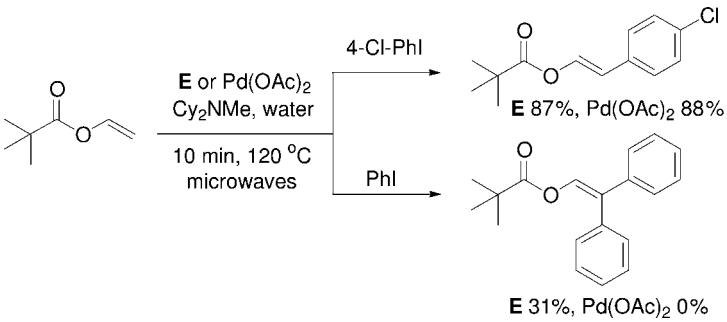

Scheme 4.11 Heck couplings using an oxime-derived palladacycle.

Arvela and Leadbeater performed microwave-assisted Heck couplings using ultra-low palladium catalyst concentrations [51]. A commercially available aqueous palladium solution was used as the catalyst source and useful product yields could be obtained, albeit for a limited range of substrates, with palladium concentrations as low as 500 ppb (Scheme 4.12).

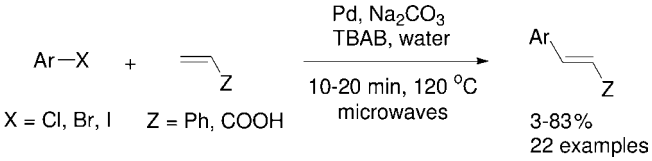

Scheme 4.12 Heck couplings using ultra-low palladium catalyst concentrations.

Hypervalent iodonium salts have recently been used as substrates in a base-free Heck coupling of acrylic acid and allyl alcohol [52]. A range of *trans*-cinnamic acids

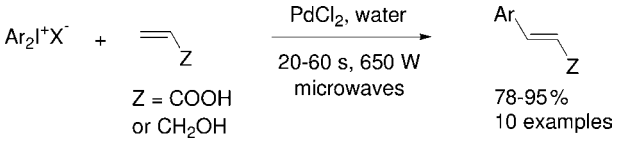

Scheme 4.13 Heck couplings using hypervalent iodonium salts.

and *trans*-cinnamyl alcohols were rapidly produced (20–60 s) in good yields (78–95%) using old-fashioned $PdCl_2$ as precatalyst in a domestic microwave oven (Scheme 4.13).

Recently, microwave irradiation has been used to promote the internal Heck arylation of ethylene glycol vinyl ether with aryl chlorides in water [53]. A regioselective reaction protocol comprising 5% of $(DIPPP)_2Pd(0)$ [DIPPP = 1,3-bis(diisopropylphosphino)propane] and K_2CO_3 provided good yields of the coupling of activated aryl chlorides; however, unactivated aryl chlorides gave poorer yields (Scheme 4.14). The products were isolated as the corresponding acetophenones after acid hydrolysis.

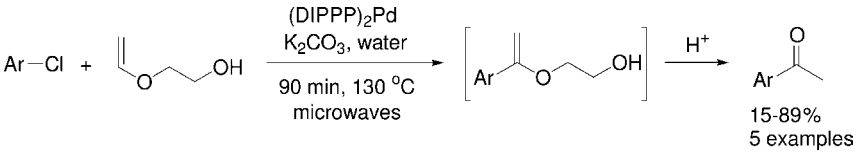

Scheme 4.14 Internal Heck arylations.

4.6
Carbonylation Reactions

Over the past years, the use of solid-phase reagents in high-throughput chemistry has been an area of rapid growth and the importance of these methods in modern chemistry is now beyond question [54, 55]. Metal-catalyzed carbonylation reactions are also of great value in organic chemistry, both in industrial processes and on the laboratory scale in the preparation of aldehydes, ketones or different carboxylic acid derivatives [56, 57]. Despite the power of carbonylative transformations, there is a considerable degree of effort required in setting up and performing reactions in sealed vessels with gaseous reactants [58]. To address this issue in carbonylation chemistry, molybdenum hexacarbonyl was identified as an easy to handle, solid reagent for the *in situ* release of carbon monoxide upon heating [59]. Applications of $Mo(CO)_6$ include palladium(0)-catalyzed aminocarbonylation, amidocarbonylation, hydrazidocarbonylation, alkoxycarbonylation and hydroxycarbonylation of aryl halides [59].

In 2006, Silvani's group presented a microwave-assisted palladium-catalyzed hydroxycarbonylation of aryl and vinyl triflates employing $Mo(CO)_6$ as the CO source [60]. They reported that organic triflates were converted to the corresponding acids in water with pyridine as base and $Pd(OAc)_2$–DPPF as the catalytic

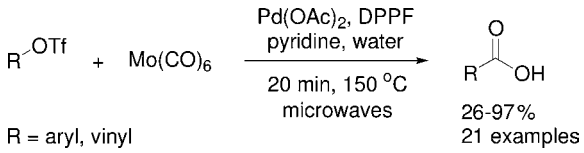

Scheme 4.15 Hydroxycarbonylation of aryl and vinyl triflates.

system within 20 min of microwave heating at 150 °C [Scheme 4.15; DPPF = 1,1′-bis(diphenylphosphino)ferrocene]. Surprisingly, 4-bromophenyl triflate was selectively converted to 4-bromobenzoic acid with no hydroxycarbonylation resulting from addition of Pd(0) into the Ar−Br bond [60].

The possibility of carrying out chemoselective $Mo(CO)_6$-promoted aminocarbonylations in pure water was examined by Wu and co-workers in two papers in 2005 [61] and 2006 [62]. Rewardingly, aryl iodides, bromides and chlorides were all transformed, within 15 min, into benzamides using an appropriate catalytic system under microwave conditions (Scheme 4.16). Aminocarbonylation strongly dominated over hydroxycarbonylation, despite the use of water as solvent, providing good yields of both secondary and tertiary amides. Impressively, more than 90 different aminocarbonylations were reported in these two investigations [61, 62].

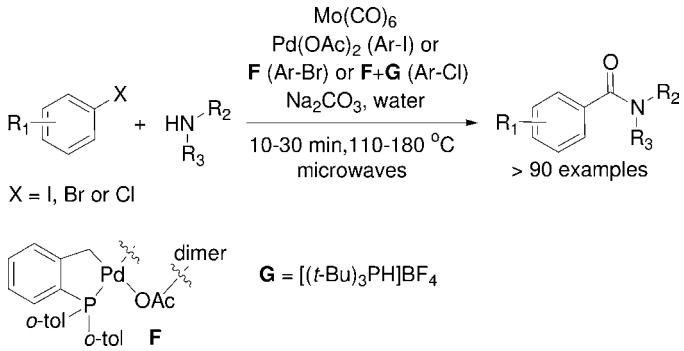

Scheme 4.16 Chemoselective $Mo(CO)_6$-promoted aminocarbonylations.

Lately, hydroxycarbonylations of aryl iodides were performed using water as both the nucleophile and the solvent in sealed microwave transparent tubes preloaded with 14 bar of CO. Microwave processing delivered high yields of benzoic acid products after 20 min of heating at 165 °C employing only 0.01% or 1 mol% of $Pd(OAc)_2$ as the catalyst (Scheme 4.17) [63].

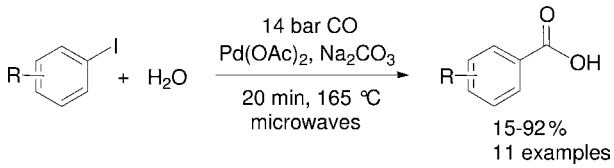

Scheme 4.17 Hydroxycarbonylations of aryl iodides.

4.7
The Sonogashira Reaction

The copper- and palladium-catalyzed cross-coupling of terminal alkynes with aryl/vinyl halides, known as the Sonogashira reaction, is a general and reliable method for the generation of substituted alkynes [64].

Similar to their reports on the Suzuki reaction (Section 4.2), Leadbeater *et al.* have also described a microwave-assisted, 'transition metal-free' Sonogashira reaction protocol [65]. They used sodium hydroxide as the base, PEG as a PTC and water as the solvent to couple a number of aryl halides with phenylacetylene and two aliphatic alkynes (Scheme 4.18). In general, aryl iodides were found to give better yields than aryl bromides and phenylacetylene was a more effective coupling partner than the aliphatic alkynes. In the light of their subsequent reassessment of the Suzuki reaction, it is likely that these Sonogashira reactions were also catalyzed by ultra-low level Pd contaminations.

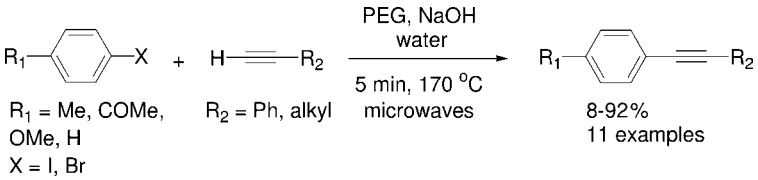

Scheme 4.18 'Transition metal-free' Sonogashira reactions.

Gil-Moltó *et al.* have used monomeric (**H**) and polymeric (**I**) di(2-pyridyl)methylamine-based $PdCl_2$ complexes to perform aqueous, copper-free Sonogashira couplings of aryl halides with phenylacetylene [66]. Specifically, microwave irradiation was utilized in the chemoselective coupling of 4-chlorobromobenzene and phenylacetylene, with higher yields obtained using the monomeric catalyst complex **H** (66% vs 47%) (Scheme 4.19).

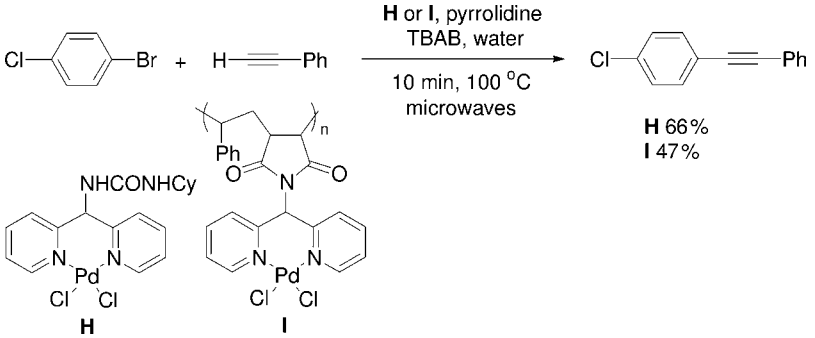

Scheme 4.19 Chemoselective coupling of 4-chlorobromobenzene and phenylacetylene.

Recently, Chen *et al.* have reported a palladium-free, copper-catalyzed method for the coupling of aryl iodides and terminal alkynes in neat water [67]. A reaction system

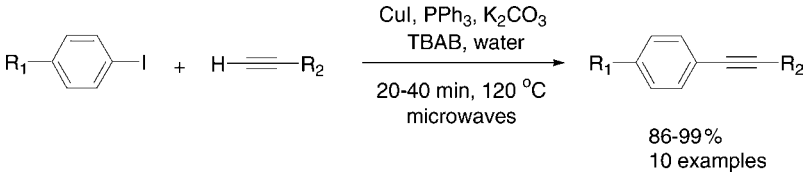

Scheme 4.20 Palladium-free copper-catalyzed coupling of aryl iodides.

comprising 10% CuI, 20% PPh_3, 1 equiv. of TBAB and 2 equiv. of K_2CO_3 was found to efficiently promote the reaction after 20–40 min of microwave irradiation at 120 °C (Scheme 4.20). The same reactions could also be carried out under classical heating conditions; however, significantly increased reaction times (16–24 h) were required.

4.8 Aryl–Nitrogen Couplings

The pioneering work by the groups of Hartwig and Buchwald in the end of the last century spurred substantial research around C–N bond formation and in particular on palladium(0)-catalyzed aryl amination chemistry [68, 69]. Today, copper-catalyzed N–aryl bond formations also rank among the most powerful methods in organic synthesis due to their mild and base-free reaction conditions [70]. Catalytic aryl amine couplings are generally slow processes, especially when copper catalysis is applied, often demanding days for completion. Thus several microwave-enhanced methods have been developed in the wake of all the newly discovered catalytic protocols in this area [12].

In the work done by Yadav *et al.*, using a single-mode cavity microwave reactor and pressurized vessels, *N*-arylations of amines, amides, imides and β-lactams with aryl halides were performed with good results in aqueous media (yields 68–91%) [71]. Active copper and a cumbersome intermittent 3–5 × 2 min irradiation–mixing cycle (with thorough mixing outside the reactor) was found to be the most efficient protocol. It is noteworthy that the method was also successful with cyclizations of β-lactam derivatives, providing sensitive penem and cephem analogues (Scheme 4.21) [71].

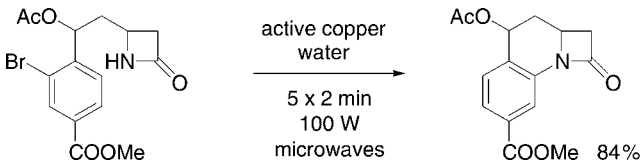

Scheme 4.21 Copper-catalyzed cyclization of a β-lactam.

In 2007, a fast copper-catalyzed process for the *N*-arylation of free and protected amino acids in water was reported [72]. Various amino acid esters could be *N*-arylated with simultaneous deprotection, generating the free acid product with less than 6% racemization (Scheme 4.22).

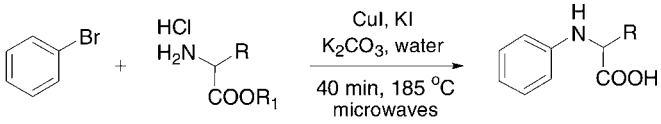

amino acid ester = L-Leu, L-Phe
R_1 = Me, Et, *t*-Bu, Bz, allyl

52-96%
6 examples

Scheme 4.22 *N*-Arylations of protected amino acids.

4.9
Aryl–Oxygen Couplings

Nowadays, the coupling of organohydroxyls with aryl halides, using copper or palladium as catalyst, is a routine method to synthesize aryl ethers [73]. In contrast, the copper salt-catalyzed direct conversion of aryl halides to the corresponding phenols in one step generally involves long reaction times and high temperatures. To improve this methodology, Kormos and Leadbeater decided to use water as both the reaction medium and the nucleophile under microwave irradiation at high-temperature (~200 °C) and at near-critical temperature (~300 C) [74]. All reactions conducted at 300 °C were processed in a dedicated multimode reactor equipped with heavy-walled quartz reaction vessels with an operating pressure limit of 80 bar. The best results were obtained with 10% CuI, 5% L-proline and 1.5 *M* NaOH at 300 °C for 30 min (ArBr and ArCl) or, alternatively, by heating the reaction cocktail to 300 °C and then allowing it to cool (ArI) (Scheme 4.23).

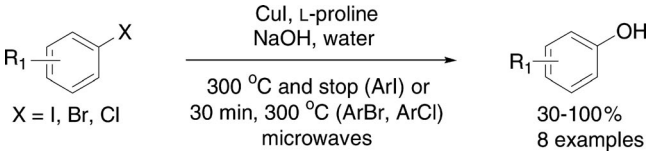

X = I, Br, Cl

30-100%
8 examples

Scheme 4.23 Direct transformation of aryl halides to phenols at 300 °C.

4.10
Miscellaneous Transformations

Matsubara and co-workers have developed a ruthenium-catalyzed protocol for the isomerization of alkenols to alkanones via a C−C double bond migration [75]. $RuCl_2(PPh_3)_3$ was found to be the most efficient catalyst and good yields of the desired products were obtained after 60 min of microwave irradiation at 185 °C (Scheme 4.24). Crucial to the success of these reactions was the use of water as solvent. An otherwise identical reaction, carried out in dioxane, failed to give any saturated ketone and only isomerization of the alkene group was observed. Acid-

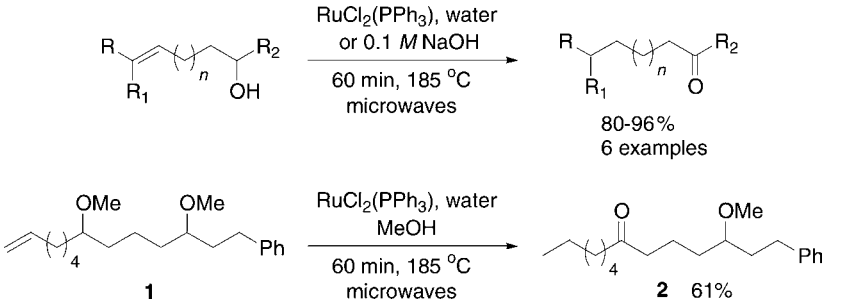

Scheme 4.24 Ruthenium-catalyzed isomerizations of alkenols and a methylated alkenol to ketones.

sensitive substrates required the use of 0.1 *M* NaOH as solvent as the catalyst was hydrolyzed under the reaction conditions to form hydrochloric acid. The authors also demonstrated that the addition of 10% MeOH was essential for the isomerization of ether-protected alcohols into their corresponding ketones. Furthermore, the dimethoxyalkene **1** could be selectively converted into the methoxy ketone **2** via this isomerization reaction (Scheme 4.24).

Tu and co-workers reported a high-yielding method to generate propargylamines via a copper-catalyzed three-component coupling of an aldehyde, an alkyne and an amine (Scheme 4.25) [76]. The reactions were conducted in an unmodified domestic oven operating at 40% power with 1 min irradiation–cooling cycles. In contrast, the corresponding classical heating reaction required more than 5 days to reach completion. Furthermore, high diastereoselectivity (95 : 5) could be obtained when (*S*)-proline methyl ester was employed as a chiral amine.

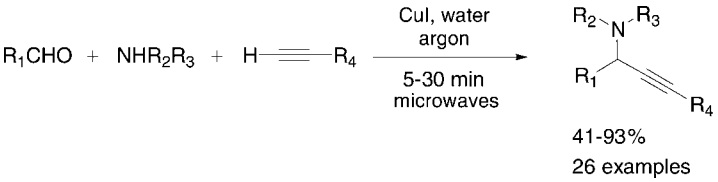

Scheme 4.25 Preparation of propargylamines via copper-catalyzed three-component reaction.

Recently, Lerebours and Wolf discovered that palladium–phosphinous acids catalyze the 1,4-addition of arylsiloxanes to α,β-unsaturated substrates [77]. Using 5 mol% of catalyst **J**, β-substituted ketones, aldehydes, esters, nitriles and nitroalkanes could be obtained, in good to excellent yields, after 4 h of microwave irradiation at 120 °C (Scheme 4.26).

More recently, Larhed's group have disclosed a microwave-enhanced method for the α-arylation of a protected glycine in neat water [78]. Using this protocol, a range of substituted phenylglycine derivatives were produced in moderate to good yields, under non-inert conditions (Scheme 4.27).

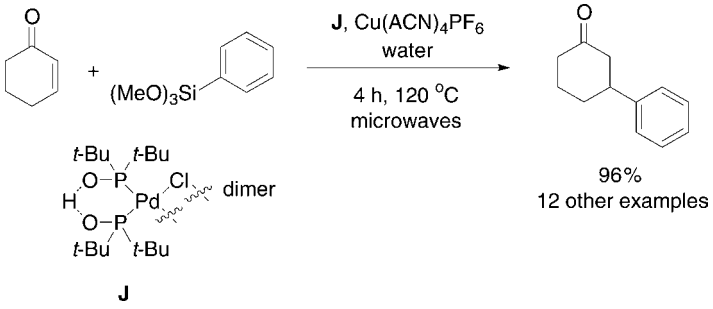

J

Scheme 4.26 Palladium-catalyzed conjugate addition of phenyltrimethoxysilane and 2-cyclohexen-1-one.

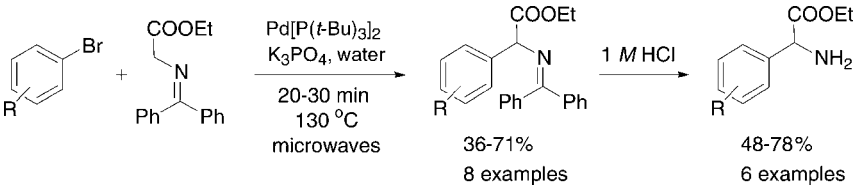

Scheme 4.27 Preparation of substituted phenylglycines.

4.11 Conclusion

The development of microwave-assisted reactions catalyzed by homogeneous metal catalysts in water has been fast during the last 5 years – from the first reports at the turn of the century, to more than 40 publications in the end of 2007. Indeed, it is possible today to perform most metal-catalyzed reactions in neat water with microwave heating provided that the substrate, base and nucleophile are stable in water. The interest has grown in parallel with the improvements in performance, control, reproducibility and safety of the marketed microwave instrumentation. There is little doubt that this development will continue, since the use of water as a non-toxic reaction medium, in combination with the employment of energy-efficient microwave heating and catalytic methods, must be considered to be both a highly promising and an enabling green alternative. Finally, although we have presented only laboratory-scale reactions, we believe the combination of energy-efficient microwave heating and metal catalysis in water also holds a large future potential for green large-scale synthesis, provided that suitable microwave reactors are developed and marketed.

Acknowledgments

We would like to thank the Knut and Alice Wallenberg Foundation and the Swedish Research Council for generous support. We also thank Riina Arvela, Jonas Sävmarker and Dr Francesco Russo for fruitful discussions.

References

1 Dallinger, D. and Kappe, C.O. (2007) Microwave-assisted synthesis in water as solvent. *Chemical Reviews*, **107**, 2563–2591.

2 Strauss, C. and Trainor, R. (1995) Developments in microwave-assisted organic chemistry. *Australian Journal of Chemistry*, **48**, 1665–1692.

3 Lidstrom, P., Tierney, J., Wathey, B. and Westman, J. (2001) Microwave assisted organic synthesis: a review. *Tetrahedron*, **57**, 9225–9283.

4 Kappe, C.O. (2004) Controlled microwave heating in modern organic synthesis. *Angewandte Chemie-International Edition*, **43**, 6250–6284.

5 Li, C.-J. (2005) Organic reactions in aqueous media with a focus on carbon–carbon bond formations. A decade update. *Chemical Reviews*, **105**, 3095–3165.

6 Xiao, J. (2005) Environmental catalysis in organic synthesis. *Environmental Catalysis*, 547–590.

7 Strauss, C.R. (1999) A combinatorial approach to the development of environmentally benign organic chemical preparations. *Australian Journal of Chemistry*, **52**, 83–96.

8 Strauss, C.R. and Varma, R.S. (2006) Microwaves in green and sustainable chemistry. *Topics in Current Chemistry*, **266**, 199–231.

9 Larhed, M., Moberg, C. and Hallberg, A. (2002) Microwave-accelerated homogeneous catalysis in organic chemistry. *Accounts of Chemical Research*, **35**, 717–727.

10 Michael, D. and Mingos, P. (2005) Theoretical aspects of microwave dielectric heating, in *Microwave Assisted Organic Synthesis* (eds J. Tierney and P. Lidström), Blackwell, Oxford, pp. 1–22.

11 Kappe, C.O. and Stadler, A. (eds) (2005) *Microwaves in Organic and Medicinal Chemistry*, Wiley-VCH Verlag GmbH, Weinheim.

12 Nilsson, P., Olofsson, K. and Larhed, M. (2006) Microwave-assisted and metal-catalyzed coupling reactions. *Topics in Current Chemistry*, **266**, 103–144.

13 Gronnow, M.J., White, R.J., Clark, J.H. and Macquarrie, D.J. (2005) Energy efficiency in chemical reactions: a comparative study of different reaction techniques. *Organic Process Research & Development*, **9**, 516–518.

14 Kremsner, J.M., Stadler, A. and Kappe, C.O. (2006) The scale-up of microwave-assisted organic synthesis. *Topics in Current Chemistry*, **266**, 233–278.

15 Anastas, P.T. and Kirchhoff, M.M. (2002) Origins, current status and future challenges of green chemistry. *Accounts of Chemical Research*, **35**, 686–694.

16 Liu, S. and Xiao, J. (2007) Toward green catalytic synthesis – transition metal-catalyzed reactions in non-conventional media. *Journal of Molecular Catalysis A-Chemical*, **270**, 1–43.

17 Jimenez-Gonzalez, C., Curzons, A.D., Constable, D.J.C. and Cunningham, V.L. (2005) Expanding GSK's Solvent Selection Guide – application of life cycle assessment to enhance solvent selections. *Journal of Clean Technology Environmental Toxicology and Occupational Medicine*, **7**, 42–50.

18 Tucker, C.E. and De Vries, J.G. (2002) Homogeneous catalysis for the production of fine chemicals. Palladium- and nickel-catalyzed aromatic carbon–carbon bond formation. *Topics in Catalysis*, **19**, 111–118.

19 Bornils, B. and Herrmann, W.A. (eds) (2002) *Applied Homogeneous Catalysis with Organometallic Compounds*, Vols 1–3, 2nd edn, Wiley-VCH Verlag GmbH, Weinheim.

20 Leadbeater, N.E. (2005) Fast, easy, clean chemistry by using water as a solvent and microwave heating: the Suzuki coupling as an illustration. *Chemical Communications*, 2881–2902.

21 Kremsner, J.M. and Kappe, C.O. (2006) Silicon carbide passive heating elements in microwave-assisted organic synthesis. *The Journal of Organic Chemistry*, **71**, 4651–4658.

22 Miyaura, N. and Suzuki, A. (1995) Palladium-catalyzed cross-coupling reactions of organoboron compounds. *Chemical Reviews*, **95**, 2457–2483.

23 Blettner, C.G., Konig, W.A., Stenzel, W. and Schotten, T. (1999) Microwave-assisted aqueous Suzuki cross-coupling reactions. *The Journal of Organic Chemistry*, **64**, 3885–3890.

24 Bumagin, N.A. and Bykov, V.V. (1997) Ligandless palladium catalyzed reactions of arylboronic acids and sodium tetraphenylborate with aryl halides in aqueous media. *Tetrahedron*, **53**, 14437–14450.

25 Villemin, D., Gomez-Escalonilla, M.J. and Saint-Clair, J.-F. (2001) Palladium-catalyzed phenylation of heteroaromatics in water or methylformamide under microwave irradiation. *Tetrahedron Letters*, **42**, 635–637.

26 Leadbeater, N.E. and Marco, M. (2002) Ligand-free palladium catalysis of the Suzuki reaction in water using microwave heating. *Organic Letters*, **4**, 2973–2976.

27 Leadbeater, N.E. and Marco, M. (2003) Transition-metal-free Suzuki-type coupling reactions: scope and limitations of the methodology. *The Journal of Organic Chemistry*, **68**, 5660–5667.

28 Leadbeater, N.E. and Marco, M. (2003) Transition-metal-free Suzuki-type coupling reactions. *Angewandte Chemie-International Edition*, **42**, 1407–1409.

29 Arvela, R.K., Leadbeater, N.E., Sangi, M.S., Williams, V.A., Granados, P. and Singer, R.D. (2005) A reassessment of the transition-metal free Suzuki-type coupling methodology. *The Journal of Organic Chemistry*, **70**, 161–168.

30 Bai, L., Wang, J.-X., and Zhang, Y. (2003) Rapid microwave-promoted Suzuki cross coupling reaction in water. *Green Chemistry*, **5**, 615–617.

31 Crozet, M.D., Castera-Ducros, C. and Vanelle, P. (2006) An efficient microwave-assisted Suzuki cross-coupling reaction of imidazo[1,2-*a*]pyridines in aqueous medium. *Tetrahedron Letters*, **47**, 7061–7065.

32 Mei, X. and Wolf, C. (2006) Determination of enantiomeric excess and concentration of chiral compounds using a 1,8-diheteroarylnaphthalene-derived fluorosensor. *Tetrahedron Letters*, **47**, 7901–7904.

33 Mei, X., Martin, R.M. and Wolf, C. (2006) Synthesis of a sterically crowded atropisomeric 1,8-diacridylnaphthalene for dual-mode enantioselective fluorosensing. *The Journal of Organic Chemistry*, **71**, 2854–2861.

34 Wu, W.-Y., Chen, S.-N. and Tsai, F.-Y. (2006) Recyclable and highly active cationic 2,2′-bipyridyl palladium(II) catalyst for Suzuki cross-coupling reaction in water. *Tetrahedron Letters*, **47**, 9267–9270.

35 Anderson, K.W. and Buchwald, S.L. (2005) General catalysts for the Suzuki–Miyaura and Sonogashira coupling reactions of aryl chlorides and for the coupling of challenging substrate combinations in water. *Angewandte Chemie-International Edition*, **44**, 6173–6177.

36 Suarez, E.J.G., Ruiz, A., Castillon, S., Oberhauser, W., Bianchini, C. and Claver, C. (2007) New alkyl derivatives phosphine sulfonate (P–O) ligands. Catalytic activity in Pd-catalysed Suzuki–Miyaura reactions in water. *Dalton Transactions*, 2859–2861.

37 Dawood, K.M. (2007) Microwave-assisted Suzuki–Miyaura and Heck–Mizoroki cross-coupling reactions of aryl chlorides and bromides in water using stable benzothiazole-based palladium(II) precatalysts. *Tetrahedron*, **63**, 9642–9651.

38 Espinet, P. and Echavarren, A.M. (2004) C−C coupling: the mechanisms of the Stille reaction. *Angewandte Chemie-International Edition*, **43**, 4704–4734.

39 Kaval, N., Bisztray, K., Dehaen, W., Kappe, C.O. and Van der Eycken, E. (2003) Microwave-enhanced transition metal-

catalyzed decoration of 2(1*H*)-pyrazinone scaffolds. *Molecular Diversity*, **7**, 125–134.

40 Mowery, M.E. and DeShong, P. (1999) Cross-coupling reactions of hypervalent siloxane derivatives: an alternative to Stille and Suzuki couplings. *The Journal of Organic Chemistry*, **64**, 1684–1688.

41 Alacid, E. and Nájera, C. (2006) Solventless and fluoride-free Hiyama reaction of arylsiloxanes with aryl bromides and chlorides promoted by sodium hydroxide: a useful protocol for palladium recycling and product isolation. *Advanced Synthesis and Catalysis*, **348**, 945–952.

42 Alacid, E. and Nájera, C. (2006) The first fluoride-free Hiyama reaction of vinylsiloxanes promoted by sodium hydroxide in water. *Advanced Synthesis and Catalysis*, **348**, 2085–2091.

43 Heck, R.F. and Nolley, J.P. (1972) Palladium-catalyzed vinylic hydrogen substitution reactions with aryl, benzyl and styryl halides. *The Journal of Organic Chemistry*, **37**, 2320–2322.

44 Mizoroki, T., Mori, K. and Ozaki, A. (1971) Arylation of olefin with aryl iodide catalyzed by palladium. *Bulletin of the Chemical Society of Japan*, **44**, 581.

45 Beletskaya, I.P. and Cheprakov, A.V. (2000) The Heck reaction as a sharpening stone of palladium catalysis. *Chemical Reviews*, **100**, 3009–3066.

46 Alonso, F., Beletskaya, I.P. and Yus, M. (2005) Non-conventional methodologies for transition metal catalysed carbon–carbon coupling: a critical overview. Part 1: the Heck reaction. *Tetrahedron*, **61**, 11771–11835.

47 Larhed, M. and Hallberg, A. (2002) The Heck reaction (alkene substitution via carbopalladation–dehydropalladation) and related carbopalladation reactions, in *Handbook of Organopalladium Chemistry for Organic Synthesis* (ed. E-i.Negishi), Vol. 1, Wiley-Interscience, New York. pp. 1133–1178.

48 Wang, J.-X., Liu, Z., Hu, Y., Wei, B. and Bai, L. (2002) Palladium and phase transfer catalyzed Heck cross coupling reaction in water under microwave irradiation. *Synthetic Communications*, **32**, 1607–1614.

49 Botella, L. and Nájera, C. (2004) Controlled mono and double Heck reactions in water catalyzed by an oxime-derived palladacycle. *Tetrahedron Letters*, **45**, 1833–1836.

50 Botella, L. and Nájera, C. (2005) Mono- and β,β-double-Heck reactions of α,β-unsaturated carbonyl compounds in aqueous media. *The Journal of Organic Chemistry*, **70**, 4360–4369.

51 Arvela, R.K. and Leadbeater, N.E. (2005) Microwave-promoted Heck coupling using ultralow metal catalyst concentrations. *The Journal of Organic Chemistry*, **70**, 1786–1790.

52 Zhu, M., Song, Y. and Cao, Y. (2007) A fast and convenient heck reaction in water under microwave irradiation. *Synthesis*, 853–856.

53 Arvela, R.K., Pasquini, S. and Larhed, M. (2007) Highly regioselective internal Heck arylation of hydroxyalkyl vinyl ethers by aryl halides in water. *The Journal of Organic Chemistry*, **72**, 6390–6396.

54 Ley, S.V., Baxendale, I.R., Bream, R.N., Jackson, P.S., Leach, A.G., Longbottom, D.A., Nesi, M., Scott, J.S., Storer, R.I. and Taylor, S.J. (2000) Multi-step organic synthesis using solid-supported reagents and scavengers: a new paradigm in chemical library generation. *Journal of the Chemical Society-Perkin Transactions 1*, 3815–4195.

55 Baxendale, I.R., Lee, A.L. and Ley, S.V. (2005) Integrating microwave-assisted synthesis and solid-supported reagents, in *Microwave Assisted Organic Synthesis* (eds J. Tierney and P. Lidström), Blackwell, Oxford, pp. 133–176.

56 Beller, M., Cornils, B., Frohning, C.D. and Kohlpaintner, C.W. (1995) Progress in hydroformylation and carbonylation. *Journal of Molecular Catalysis A-Chemical*, **104**, 17–85.

57 Skoda-Foldes, R. and Kollar, L. (2002) Synthetic applications of palladium catalyzed carbonylation of organic halides. *Current Organic Chemistry*, **6**, 1097–1119.

58 Morimoto, T. and Kakiuchi, K. (2004) Evolution of carbonylation catalysis: no need for carbon monoxide. *Angewandte Chemie-International Edition*, **43**, 5580–5588.

59 Wannberg, J. and Larhed, M. (2008) Microwave-promoted carbonylations. In *Modern Carbonylation Methods* (ed. L. Kollár), Wiley-VCH Verlag GmbH, Weinheim, pp. 93–114.

60 Lesma, G., Sacchetti, A. and Silvani, A. (2006) Palladium-catalyzed hydroxycarbonylation of aryl and vinyl triflates by in situ generated carbon monoxide under microwave irradiation. *Synthesis*, 594–596.

61 Wu, X. and Larhed, M. (2005) Microwave-enhanced aminocarbonylations in water. *Organic Letters*, **7**, 3327–3329.

62 Wu, X., Ekegren, J.K. and Larhed, M. (2006) Microwave-promoted aminocarbonylation of aryl iodides, aryl bromides and aryl chlorides in water. *Organometallics*, **25**, 1434–1439.

63 Kormos, C. and Leadbeater, N. (2006) Microwave-promoted hydroxycarbonylation in water using gaseous carbon monoxide and pre-pressurized reaction vessels. *Synlett*, 1663–1666.

64 Sonogashira, K. (2002) Development of Pd−Cu catalyzed cross-coupling of terminal acetylenes with sp^2-carbon halides. *Journal of Organic Chemistry*, **653**, 46–49.

65 Leadbeater, N.E., Marco, M. and Tominack, B.J. (2003) First examples of transition-metal free Sonogashira-type couplings. *Organic Letters*, **5**, 3919–3922.

66 Gil-Moltó, J., Karlstrom, S. and Najera, C. (2005) Di(2-pyridyl)methylamine–palladium dichloride complex covalently anchored to a styrene–maleic anhydride co-polymer as recoverable catalyst for C−C cross-coupling reactions in water. *Tetrahedron*, **61**, 12168–12176.

67 Chen, G., Zhu, X., Cai, J., and Wan, Y. (2007) Palladium-free copper-catalyzed coupling reaction of aryl iodides and terminal acetylenes in water. *Synthetic Communications*, **37**, 1355–1361.

68 Hartwig, J.F. (1998) Transition metal catalyzed synthesis of arylamines and aryl ethers from aryl halides and triflates: scope and mechanism. *Angewandte Chemie-International Edition*, **37**, 2046–2067.

69 Yang, B.H. and Buchwald, S.L. (1999) Palladium-catalyzed amination of aryl halides and sulfonates. *Journal of Organometallic Chemistry*, **576**, 125–146.

70 Ley, S.V. and Thomas, A.W. (2003) Modern synthetic methods for copper-mediated C(aryl)–O, C(aryl)–N and C(aryl)–S bond formation. *Angewandte Chemie-International Edition*, **42**, 5400–5449.

71 Yadav, L.D.S., Yadav, B.S. and Rai, V.K. (2006) Active-copper-promoted expeditious *N*-arylations in aqueous media under microwave irradiation. *Synthesis*, 1868–1872.

72 Roettger, S., Sjoeberg, P.J.R. and Larhed, M. (2007) Microwave-enhanced copper-catalyzed *N*-arylation of free and protected amino acids in water. *Journal of Combinatorial Chemistry*, **9**, 204–209.

73 Anderson, K.W., Ikawa, T., Tundel, R.E. and Buchwald, S.L. (2006) The selective reaction of aryl halides with KOH: synthesis of phenols, aromatic ethers and benzofurans. *Journal of the American Chemical Society*, **128**, 10694–10695.

74 Kormos, C.M. and Leadbeater, N.E. (2006) Direct conversion of aryl halides to phenols using high-temperature or near-critical water and microwave heating. *Tetrahedron*, **62**, 4728–4732.

75 Ishibashi, K., Takahashi, M., Yokota, Y., Oshima, K. and Matsubara, S. (2005) Ruthenium-catalyzed isomerization of alkenol into alkanone in water under irradiation of microwaves. *Chemistry Letters*, **34**, 664–665.

76 Shi, L., Tu, Y.Q., Wang, M., Zhang, F.M. and Fan, C.A. (2004) Microwave-promoted three-component coupling of aldehyde, alkyne and amine via C−H activation catalyzed by copper in water. *Organic Letters*, **6**, 1001–1003.

77 Lerebours, R. and Wolf, C. (2007) Palladium(II)-catalyzed conjugate addition of arylsiloxanes in water. *Organic Letters*, **9**, 2737–2740.

78 Lagerlund, O., Odell, L.R., Mowbray, S.L., Nilsson, M.T., Krajcewski, W.W., Nordqvist, A., Karlén, A. and Larhed, M. (2007) Microwave-enhanced alfa-arylation of a protected glycine in water. Evaluation of 3-phenylglycine derivatives as inhibitors of the tuberculosis enzyme, glutamine synthetase. *Combinatorial Chemistry & High Throughput Screening*, **10**, 783–789.

5
Ionic Liquids and Catalysis: the IFP Biphasic Difasol Process

Hélène Olivier-Bourbigou, Frédéric Favre, Alain Forestière, and François Hugues

5.1
Introduction

The driving forces for the introduction of new industrial processes are economic considerations which depend mainly on production costs and on product quality. Increasing demand for pure products requires higher selectivity. Optimal exploitation of raw materials, energy savings and the environmental friendliness of processes nowadays take a major place. All this implies better use of raw materials, less formation of side products and, if possible, simplified separation work-up steps. Stricter environmental requirements will probably lead to the development of milder reaction conditions for operations in the manufacture of products with high atom efficiency or E-factor.

In this economic and environmental context, homogeneous catalysis, which still contributes to the inventory of bulk chemicals and high-value chemical manufacture, offers many advantages and great potential for future challenges [1]. Homogeneous processes are usually easy to scale up for industrial practice. In a continuous process, the ease of mixing and removal of the reaction heat of such systems ensure good temperature control and restricts mass transfer limitations. Flexibility of operations renders homogeneous processes easy to operate. The catalyst rate can be adjusted to the reaction feed rate, taking into account the presence of feed impurities, to maintain both conversion and selectivity.

While the solubility of the organometallic catalysts in common organic solvents appears to be an advantage in terms of site availability and tunability, it becomes a major drawback in terms of catalyst and solvent separation and recycling. The quest for new catalyst immobilization or recovery strategies to facilitate its reuse is still a paramount challenge [2]. There is, of course, no single solution to this issue and the search for innovative approaches continues.

One of the most successful approaches to bridging the gap between homogeneous and heterogeneous catalysis is multiphasic catalysis. In its simplest version, there are

Green Catalysis, Volume 1: Homogeneous Catalysis.
Edited by Robert H. Crabtree

ISBN: 978-3-527-32496-5

only two liquid phases ('biphasic' catalysis or 'two-phase' catalysis). The catalyst is dissolved in one phase (generally a polar phase) while the products and the substrates remain mainly in the second phase. The catalyst can be separated by simple settling and recycled under mild conditions.

During the last 20 years, water has emerged as a new useful reaction medium. Despite its 'green nature', its utilization is still limited because of the low solubility of organic hydrophobic compounds. In addition, water cannot be regarded as an inert solvent. More recently, other media such as supercritical fluids, fluorous phases and organic polymer supports have proven their utility for some organic and catalytic reactions. Ionic liquids have recently emerged as a new class of solvents, offering large opportunities for the development of a biphasic (multiphasic) approach [3].

In this chapter, Ni-catalyzed olefin oligomerization is described. Starting from the original industrial homogeneous Dimersol process, the emergence of the biphasic Difasol system using ionic liquids as the catalyst solvent is detailed. This biphasic process was designed and developed with the aim of reducing catalyst consumption, waste and chemicals, all in an economically feasible manner.

5.2
The Solvent in Catalytic Reactions

Most chemical transformations occur in the liquid phase and the solvent is a strategic parameter on both the laboratory and industrial scales. Solvent effects may be limited to 'physical effects' in just making possible the dissolution of reagents, helping to bring them into contact at suitable concentrations, but with no direct interaction with the catalytic center. However, solvents can also interact through specific forces, such as hydrogen bonds, with reaction intermediates and transition states. The presence of such a solvent can alter the reaction mechanism, modify the reaction rate and influence the selectivity. In homogeneous catalysis involving an unsaturated cationic transition metal center, the solvent should be able to dissolve and stabilize the metal, while maintaining its ionic character through weak and labile metal–solvent bonding. Highly polar organic solvents are mostly used but they are often too strongly coordinating and may deactivate the catalytic center.

From an industrial point of view, choosing a selective solvent for a catalytic reaction is probably one of the trickiest steps in process development. The use of a solvent not only impacts the handling and operation of the catalyst, it also determines the conception and design of work-up procedures and technologies and the recycling and disposal strategies. Within the framework of green chemistry, innovative concepts for the replacement of volatile organic solvents in catalytic processes has become a topic of interdisciplinary research. When possible, industrial processes are performed solventless. This can be an alternative to remove product contamination, solvent separation and recycling, which are often energy consuming.

However, in many cases, particularly in the fine chemistry and pharmaceutical industries, solventless reactions are not always feasible. The selection of the solvent is then influenced not only by considerations focused on practical and economic

benefits, but also on safety issues and environmental concerns, which are becoming more and more stringent. The whole life cycle of the solvent has to be taken into account: manufacture, storage, use, separation, recycling, destruction, disposal, toxicity and biodegradability. Recent years have seen enormous interest in the search for alternative solvents. Promising approaches include catalysis in water, fluorinated phases, thermoregulated systems, supercritical fluids, agro-solvents and non-aqueous ionic liquids [3, 4].

5.2.1 Non-Aqueous Ionic Liquids

In contrast to molecular organic solvents which contain only molecules, ionic liquids are liquids fully composed of ions. For the last 10 years, ionic liquids have attracted growing attention from the scientific and industrial community. This has been demonstrated by the exponential growth of the number of publications and patents in this area [5]. The ionic liquids known today are based on many different combinations of organic cations and inorganic or organic anions (Figure 5.1). Over the years, different generations of ionic liquids have been developed, from water-sensitive chloroaluminates to biodegradable eutectic mixtures based on choline chloride and task-specific ionic liquids. So, why is there such an interest in these media?

Ionic liquids have the advantages over conventional solvents of being liquid over a large range of temperatures and of having a non-volatile character. This latter property has probably been one of the driving forces for their development as an environmentally friendly alternative commonly termed 'green solvents', even if their toxicity and biodegradability are not always proven. In fact, the intense interest in these media really originates from their unique and fascinating wide range of

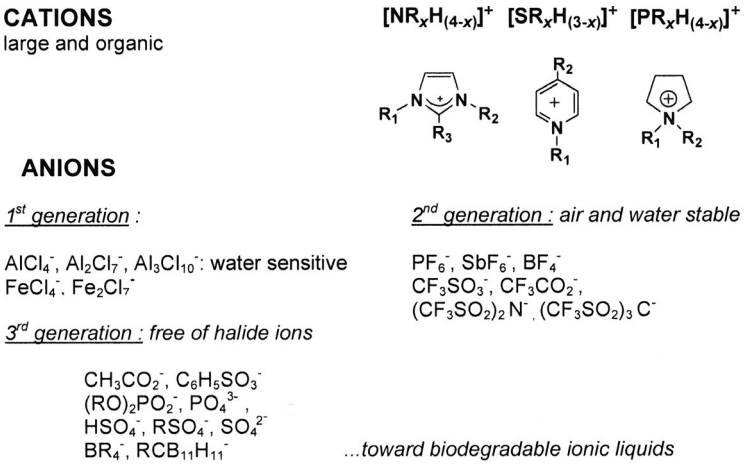

Figure 5.1 Different generations of ionic liquids.

physicochemical properties. Their tunable polarity and hard/soft character, their negligible vapor pressure and their adjustable solvating ability make them completely different from classical organic solvents. As a consequence, the development of novel technologies is possible. By a judicious combination of cations and anions, it is possible to adjust the solvent properties to the requirements of the applications, thus creating an almost indefinite set of 'designer solvents'. Most ionic liquids are now commercially available, which contributes to the development of their applications. The diversity of their properties is demonstrated by their broad range of potential applications, extending from organic drug synthesis to high-capacity batteries, novel specialty chemicals, novel materials and engineering fluids [6]

5.2.2
Applications of Non-Aqueous Ionic Liquids in Catalysis

The main challenge when using ionic liquids in catalysis is probably the selection of the right anion–cation combination from among the huge diversity of possible associations. Even though the physicochemical properties of ionic liquids tend to be well known they remain very complex solvents, leading to different possible kinds of interactions. It is very difficult to classify these media into the different categories of the conventional organic solvents and to anticipate their effect on reactions.

Nevertheless, due to the great versatility of ionic liquids, the range of homogeneous catalytic reactions that has been developed in these media is probably wider than that in supercritical CO_2 and fluorous solvents [7]. Most of these reactions have been performed on the bench scale. In many cases, the focus is made on the possibility of recycling the homogeneous catalyst without loss of activity/selectivity and with a minimum loss of catalyst. Ionic liquids offer the advantages of traditional solvents plus the possibility of simple product separation and catalyst phase recycling. This is all the more important when costly ligands and metals are used. In some cases, specific solvent effects have been observed, such as transfer of chirality [8]. Just a few examples of pilot-scale (or commercial) applications of ionic liquids have been described (Figure 5.2). The selection of ionic liquids for an industrial reaction raises a series of specific problems which have already been reported [9]. The main factors worth mentioning here are probably the possible solubility of ionic liquids in the reaction products, leading to product contamination and ionic liquid loss, and the incomplete immobilization of transition metal catalysts in the ionic liquid phase.

5.3
The Catalytic Oligomerization of Olefins

Refinery cracking processes, such as steam cracking or catalytic cracking, produce significant amounts of light olefin streams as co-products of ethylene/propylene or gasoline.

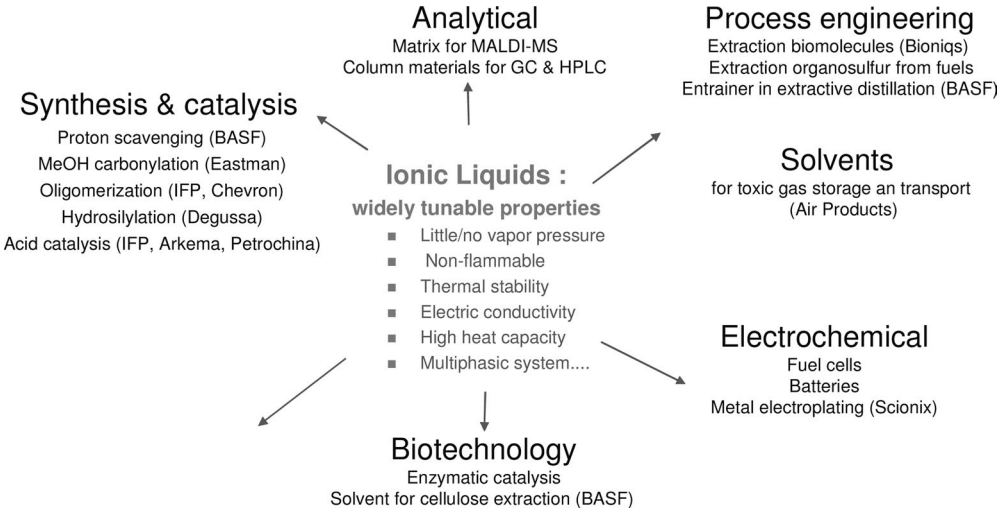

Figure 5.2 Diversity of applications of ionic liquids.

Dimerization and oligomerization reactions are widely used on an industrial scale to upgrade these light olefin streams or olefins coming from hydrocarbon forming processes (e.g. Fischer–Tropsch synthesis) into heavier products that find applications as fuels or as valuable petrochemicals [10].

Several years ago, dimerization was essentially operated by means of acid catalysts (liquids or solids). Organometallics of highly electropositive metals (Al, K) afford better selectivities than acid catalysts, but their specific and poor activity restrict their use to some specific applications. In 1953, Ziegler and Natta initiated a new age when they demonstrated the effectiveness of titanium complexes associated with alkylaluminum compounds to promote ethylene polymerization. The possibility of tailor-made ligands involved in coordination catalysts offers a broader spectrum of reactivities and diversified selectivities. Industrial olefin oligomerization processes catalyzed by coordination complexes (Ti, Zr, Ni or Cr) are generally performed in homogeneous systems with or without solvents (Table 5.1).

When costly catalysts are used, catalyst recycling is advantageous to make industrial processes economically viable. The Shell Higher Olefin Process (SHOP) was the first industrial catalytic process to benefit from two-phase liquid–liquid technology. The P−O chelate Ni complex operates in butanediol in which the α-olefins produced by ethylene oligomerization are only partially soluble. The Ni-containing butanediol polar phase can then be separated from the reaction products by decantation and recycled to the reaction section. It is interesting to highlight here the solvent effect on the reaction selectivity: α-olefins are obtained when the reaction is performed both in toluene (single-phase system) and in butanediol (biphasic system), but polyethylene is produced in biphasic systems when water is the solvent of the Ni catalyst.

Table 5.1 Transition metal-catalyzed oligomerization processes.

Process	Catalytic system	Solvent	Products	Ref.
Alphabutol (IFP)[a]	Ti (ligand)–$AlEt_3$	None	1-Butene	[13b], [13d]
Dimersol (IFP)[a]	Ni–$EtAlCl_2$	None	C_6 or C_8	[13a], [13d]
SHOP (Shell)[a]	Ni (ligand P–O)	Butanediol (biphasic)	α-Olefins: C_4–C_{30}	[14d]
Chevron-Phillips[a]	Cr–(ligand)	Cyclohexane	1-Hexene	[13e]
Idemitsu[a]	$AlEt_xCl_{(3-x)}$–Zr (ligand)	Cyclohexane	α-Olefins: C_6–C_{30}	[13f], [13g]
Alphaselect (IFP)[b]	$AlEt_xCl_{(3-x)}$–Zr (ligand)	Aromatic hydrocarbon	α-Olefins: C_4–C_{10}	[13d]
AlphaSabLin (Sabic)[b]	$AlEt_xCl_{(3-x)}$–Zr (ligand)	Toluene	α-Olefins	[13h]
Linear-1 (UOP)[b]	Ni (ligand)	Polar solvent (biphasic)	α-Olefins: C_4–C_{10}	[13i]

[a]Industrial.
[b]Commercialized.

5.3.1 The Homogeneous Dimersol Process

5.3.1.1 The Reaction

The olefin dimerization reaction catalyzed by Ni complexes activated by an alkylaluminum derivatives was originally described in 1955 [11]. Later, in 1966, Wilke *et al.* showed that the well-defined cationic η^3-allylnickel complex was able to catalyze the reaction [12].

The reaction mechanism was confirmed to be an olefin polyaddition reaction to an Ni−H and an Ni−C bond. The formation of the active cationic Ni−H or Ni−C species results from the transfer of an alkyl group from the aluminum to the Ni^{II} catalyst precursor, followed by a β-H elimination. The successive steps are illustrated in the Scheme 5.1 in the case of propylene, but can be written similarly in the case of butenes. The position of the double bond inside the structure depends mainly on the catalytic system composition and on the olefin conversion.

Olefin dimers predominate in the reaction products due to high rate of β-H elimination. Trimers and tetramers can be formed by either parallel reaction or consecutive reaction of the formed dimers with the monomers. Thus at high monomer conversion, the dimer selectivity decreases. The type of reactor (perfectly mixed batch reactor or plug flow) can influence these consecutive reactions, but has no effect on the parallel reactions. The reactivity of olefins decreases in the order ethylene > propylene > butenes ≫ hexenes, octenes. The kinetics of the reaction can be described by Equation 5.1, where the reaction rate is first order in the catalyst (Ni) and second order in the monomer (C_n, n = number of carbons in the monomer):

$$R = k_2[C_n]^2[Ni] \tag{5.1}$$

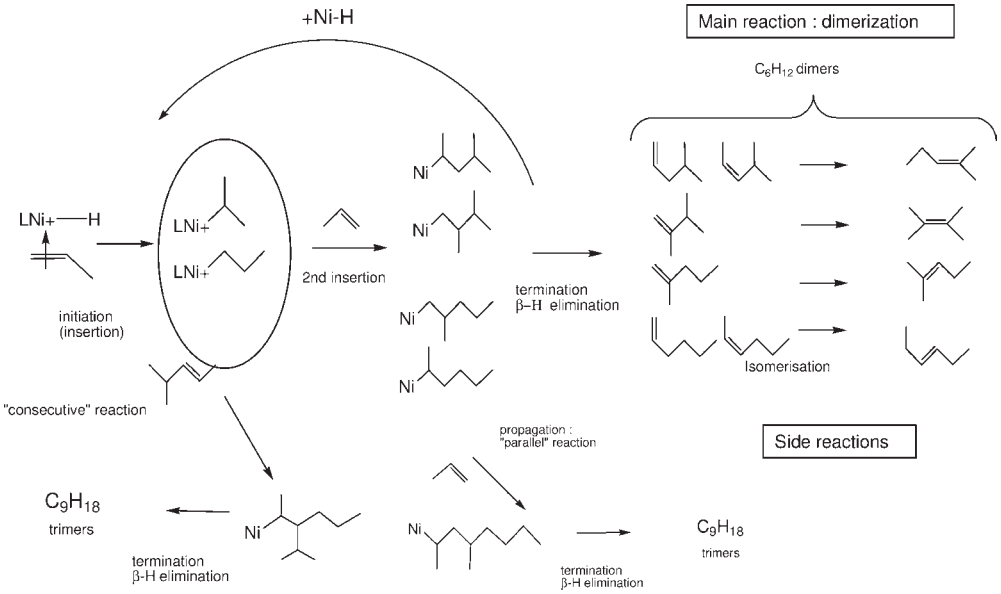

Scheme 5.1 Propylene dimerization scheme.

5.3.1.2 The Process

In the mid-1970s, IFP developed such a process, Dimersol, involving a homogeneous catalyst (Scheme 5.2). The industrial unit can be set out in different manners inside refinery and petrochemical complexes, depending on the available feedstock and desired products [13a–d].

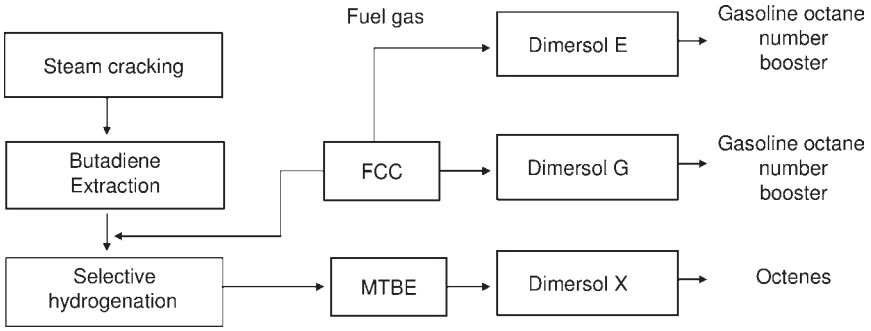

Scheme 5.2 Dimersol units to upgrade light olefin cuts.

- Dimersol G converts a C_3 cut into a gasoline effluent with excellent octane blending properties. In this way, the dimerization reaction increases the yield of high research octane number (RON) gasoline that can be obtained from a cracker. It is interesting that the RONs of olefins are much less sensitive to branching than those of the corresponding alkanes.

- Dimersol E is used to upgrade $C_2 + C_3$ fuel gas. Co-oligomerization of ethylene and propylene leads to a gasoline stream very similar to the Dimersol G product. Mixed butenes are also obtained with Dimersol E (from ethylene dimerization). They can be used in paraffinic alkylation or to make propene through a subsequent cross-metathesis reaction with ethylene.
- The Dimersol X process has been developed to produce octenes as raw material for the manufacture of isononanols through a hydroformylation reaction. In a typical refinery/petrochemical scheme, the crude cracker's C_4 cut is freed from its butadiene and selectively hydrogenated to remove acetylenics. The resulting raffinate-1 C_4 stream obtained is sent to an MTBE (methyl *tert*-butyl ether) unit, removing isobutene by reaction with methanol. The resulting raffinate-2, sometimes after de-isobutanization, is a good feedstock for the Dimersol X unit (Scheme 5.3).

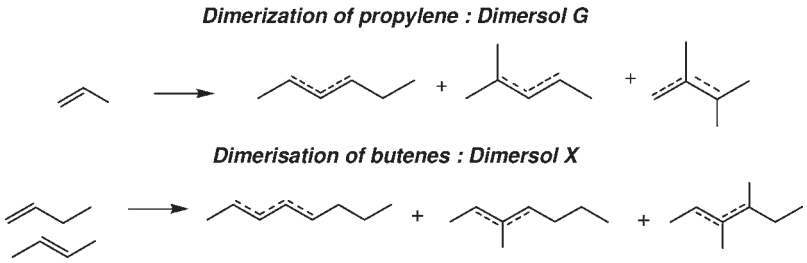

Scheme 5.3 Dimerization of olefins: the Dimersol process.

5.3.1.3 Effect of Some Parameters

Due to the ionic nature of the Ni catalyst, the reaction rate can be increased by using polar solvents such as chlorobenzene. However, the industrial process is operated in one liquid phase without any a solvent. This choice was essentially driven by economic reasons.

The temperature of the reaction section has been optimized in order to satisfy two competitive effects: the normal reaction activation and the deactivation of the catalytic system as the temperature increases. The reaction is operated at 40–60 °C. The pressure is controlled in order to maintain the reactor content in the liquid phase.

The concentration ratio between dimers and monomer in the reactor strongly influences the dimer selectivity. This ratio depends on the monomer conversion. This olefin conversion level is highly dependent on its initial concentration.

Finally, the catalytic system is strongly sensitive to two types of impurities: the polyunsaturated compounds and the polar compounds which can be present in the different feedstocks. Fortunately, a light pretreatment is usually sufficient to remove such impurities. Furthermore, the Dimersol unit operation is fairly flexible: the catalyst rate can be adjusted to the feed rate to maintain both conversion and selectivity if contamination of the feed occurs. This cannot be operated with units using heterogeneous catalysts, where contamination of the feed can be irreversible and where a higher and constant purity of the feed is required.

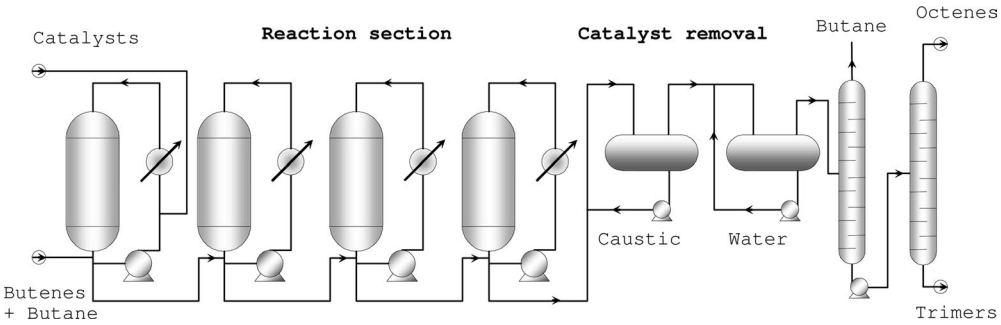

Figure 5.3 Dimersol process scheme.

5.3.1.4 Process Performance: the Case of Dimersol X (Transformation of Butenes)

The typical C_4 cut feeding a Dimersol X plant contains 60–90 wt% olefins, the remaining part being paraffins. The butenes conversion level is related to their initial concentration. With 70 wt% butenes in the feed, commercial Dimersol X technology achieves 80% conversion of butenes with up to 85% octene selectivity. A process flow diagram is depicted in Figure 5.3. The reaction takes place at low temperature in a series (three or four) of well-mixed reactors. The pressure (1.5 MPa) is chosen to maintain all reactants and products in the liquid phase. Mixing and heat removal are ensured by an external recirculation loop over a heat exchanger system. The two components of the catalytic system (Ni and Al) are injected separately into this reaction loop under flow control.

At the outlet of the finishing reactor, the active catalyst is neutralized and the products are washed with caustic soda and water to remove the deactivated catalyst. The product stream is finally distilled to remove the C_4 unreacted olefins and inert paraffins, which can be used as such (LPG) or sent back to the cracker. The octenes produced are finally distilled from the heavier oligomers.

Without any particular ligand introduced into the catalytic system and for an isobutene-free feed, the C_8 isomers produced have the following distribution:

• *n*-octenes	7 wt%
• methylheptenes	58 wt%
• dimethylhexenes	35 wt%.

5.3.1.5 Economics of the Dimersol X Process

Typical economic data are given in Table 5.2.

Thirty-five Dimersol units treating various olefinic C_3 and C_4 cuts have been licensed and 25 are still in operation. Typical dimer capacities range from 20 000 up to 90 000 t per year.

In its present commercial form, Dimersol X produces octenes with low branching index. This product quality allows higher reaction rates in subsequent hydroformylation units engaging octenes. It also leads to less branched isononyl alcohols and better plasticizer quality for PVC production.

Table 5.2 Dimersol X process: economic data.

Feed	Raffinate-2 cut (75 wt% *n*-butenes)	Capacity 50 000 t yr^{-1}
Products	LPG	18,200 t yr^{-1}
	Octenes	27,000 t yr^{-1}
	Dodecenes	3,200 t yr^{-1}
	Fuels	1,600 t yr^{-1}
Battery limit costs[a]		US$6 million
Utilities[b]	Electricity	30 kW h
	Cooling water	50 m^3
	MP steam	0.5 t
Catalyst and chemicals[b]		US$60

[a]IBSL 2002 for a Gulf Coast Basis, excluding licenser fees and detailed engineering.
[b]Per ton of octenes produced.

5.3.1.6 Dimersol Process Limitations

Despite all the advantages of the Dimersol process, some limitations remain:

- No recycling of the catalyst and continuous catalyst carry-over by the products imply extensive loss of nickel and aluminum catalysts and continuous waste disposal.
- The reaction is sensitive to the concentration of monomer in the feed, so it cannot be used with feedstocks that have a low olefin content (typically less than 60%). The selectivity is decreased at higher conversions (above 85%) as a result of sequential reactions to form higher oligomers.
- Large reactor volumes are needed.

In the early 1990s, biphasic liquid catalysis appeared as a highly attractive approach to solve some of these problems, especially active catalyst recovery. However, using such an approach means identifying a solvent that will allow catalyst solubilization to be achieved, with no impact on its activity and with a low solubility with the reaction products. Two of these solvents are now used in industrial liquid–liquid biphasic catalytic processes: butane-1,4-diol in Shell Oil's Shop oligomerization process and water in the Ruhrchemie/Rhône-Poulenc olefin hydroformylation process [14].

Due to moisture sensitiveness and reactivity of the Dimersol alkylaluminum co-catalyst, protic media such as butanediol and water are not suitable at all. Chauvin *et al*. nearly 20 years ago anticipated that chloroaluminate ionic liquids could meet biphasic liquid–liquid solvent requirements [15].

5.3.2 The Biphasic Approach

5.3.2.1 The Choice of the Ionic Liquid

Chloroaluminates (mixtures of $AlCl_3$ and an organic pyridinium or imidazolium chloride) were developed several years before by electrochemists who were seeking liquid electrolytes with large electrochemical windows for batteries [16] (Figure 5.4).

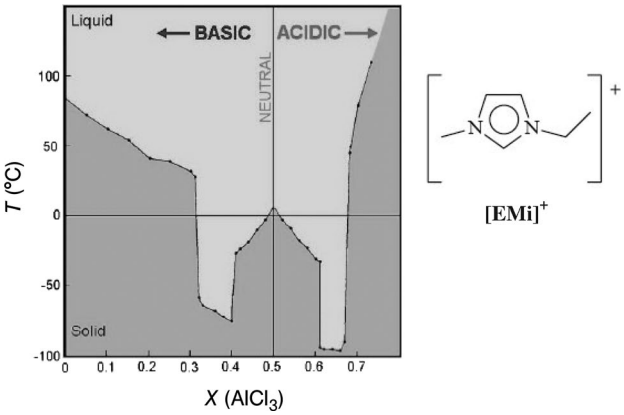

Figure 5.4 EMIC–$AlCl_3$ phase diagram. $X(AlCl_3)$ = molar fraction in $AlCl_3$.

However, it was the first time that chloroaluminates were used as a combination of solvent and co-catalyst for a chemical reaction [15].

Raman spectroscopy showed that at $AlCl_3$: dialkylimidazolium chloride molar ratios > 1, polynuclear $Al_2Cl_7^-$ and $Al_3Cl_{10}^-$ anions appear. They can dissociate into $AlCl_4^-$ and the $AlCl_3$ Lewis acid.

When the molar fraction of aluminum chloride (denoted X) is <0.5, the ionic liquid contains an excess of free Cl^- anions and can be considered as basic material. When X is >0.5, the salt can be considered as an acidic material.

Ionic liquids indeed present several advantages for the Ni-catalyzed oligomerization reaction

- They are non-protic solvents and therefore compatible with the metal–carbon or metal–hydride bond active species.
- They are liquid over a large range of composition (see Figure 5.4).
- They are poorly miscible with hexenes, octenes and longer chain olefins (which, actually, is the first prerequisite to form a biphasic system).
- The solubility of propene and butenes is sufficient to stabilize the nickel active species and ensure high catalytic activity.
- Chloroaluminates can easily be prepared from commercially available *N*-alkylimidazole, alkyl chloride and aluminum chloride.
- The chloroaluminate anions proved to be weakly coordinating towards the nickel complex catalyst involved in our system. Moreover, the nickel active species is efficiently stabilized in the ionic medium, without the need for further modification.
- Chloroaluminate ionic liquids could be extended to chloroalkylaluminum derivatives; the ionic liquids play the role of both solvent and co-catalyst.
- Chloroaluminate ionic liquids can be turned acidic by adjusting the amount of aluminum chloride.

The challenge was to choose the right selection of both cation and anion. In addition to the physicochemical properties described above, the chemical

composition proved to be of the utmost importance. The first observation indicated that the oligomerization reaction did not occur in *basic* chloroaluminates. These ionic liquids contain an excess of coordinating chloride anions that inhibit the Ni catalyst activity by forming stable blue tetrahedral $[NiCl_4]^{2-}$ anions (Equation 5.2).

$$NiX_2 + 2Cl^- \rightarrow NiX_2Cl_2{}^{2-} \qquad \text{(inactive complex)} \qquad (5.2)$$

On the other hand, acidic chloroaluminates seemed particularly suitable. For practical reasons, it is necessary to generate the active Ni catalyst '*in situ*' in the ionic liquid starting from an air-stable commercial Ni^{II} salt (Equation 5.3). This is the reason why attention had been focused on the organochloroaluminates based on a mixture of ethylaluminum dichloride (EADC) and 1-methyl-3-butylimidazolium chloride (BMIC).

$$NiX_2 + EtAlCl_3{}^- \rightarrow [Ni{-}Et]^+ [AlCl_3X_2]^- \qquad \text{(active catalyst)} \qquad (5.3)$$

The nature of the anion associated with the cationic nickel catalyst greatly influences the activity of the system. The more basic the anion, the less active is the catalyst. For example, in [BMIC]–$EtAlCl_2$ ionic liquids (1 : 1.2 molar ratio), dimerization of propylene with $NiCl_2$.2L as the precatalyst is slower than in [BMIC]–$AlCl_3$–$EtAlCl_2$ (1 : 1.2 : 0.11) mixture. In addition, in the organochloroaluminate ionic liquid [BMIC]–$EtAlCl_2$, deactivation of the catalyst is observed. This deactivation is ascribed to a change in the nature of the anion present in the ionic liquid in the presence of a hydrocarbon layer.

However, at that time, these organochloroaluminate ionic liquids were new and their acid–base properties, so important for the catalytic processes, were not known. A new research effort was therefore initiated to determine the species formed in such mixtures as a function of the compositions and then to deduce the acid–base equilibria involved. The major investigations were made at the Analytical Chemistry and Electrochemistry Laboratory of the University of Liège [17].

From this study, it appeared that organochloroaluminate salts based on mixtures of $(Et)_nAlCl_{(3-n)}$ ($n = 1$–3) with 1-methyl-3-butylimidazolium chloride (BMIC) are liquid near room temperature over a very large composition range. The structural properties of all these mixtures have been studied by Raman spectroscopy and compared with those of classical chloroaluminate melts [17] (Table 5.3). The ethylaluminum derivatives mixed with *N,N′*-dialkylimidazolium chloride thus form a new class of ionic mixtures containing both mono- and polynuclear anions. A whole new family of species has been identified. The tendency of these species to form polynuclear anions declines with increase in the number of ethyl groups.

It has also been shown that, for a same global aluminum molar fraction, the global acidity level of BMIC–[$EtAlCl_2$ + $AlCl_3$] mixtures was higher than that of BMIC–$EtAlCl_2$ mixtures [18]. Since the activity of the nickel system is dependent on this Lewis acidity, ionic liquids based on mixtures of $EtAlCl_2$ + $AlCl_3$ emerged as the best solution. An accurate adjustment of the $EtAlCl_2$ to $AlCl_3$ ratio was the key to optimizing the catalytic system efficiency.

Table 5.3 Anionic species identified from the Raman spectra as a function of the molar fraction of $(Et)_nAlCl_{(3-n)}$.[a]

n	Mole fraction of $(Et)_nAlCl_{(3-n)}$ ($n = 0$–3), *N*				
	0	**0.50**	**0.67**	**0.75**	**1.0**
0	Cl^- $AlCl_4^-$	$AlCl_4^-$ $Al_2Cl_7^-$	$Al_2Cl_7^-$ $Al_3Cl_{10}^-$		*Mixed species*
1	Cl^- $(EADC)Cl^-$	$(EADC)Cl^-$ $(EADC)_2Cl^-$	$(EADC)_2Cl^-$ $(EADC)_3Cl^-$	$(EADC)_3Cl^-$	$(AlCl_3)(EADC)Cl^-$
2	Cl^- $(DEAC)Cl^-$	$(DEAC)Cl^-$ $(DEAC)_2Cl^-$	$(DEAC)_2Cl^-$ DEAC	$(DEAC)_2Cl^-$ DEAC	$(EADC)(DEAC)Cl^-$
3	Cl^- $(TEA)Cl^-$	$(TEA)Cl^-$ $(TEA)_2Cl^-$	$(TEA)_2Cl^-$ TEA		(EADC)(DEAC)

[a] EADC = $EtAlCl_2$; DEAC = Et_2AlCl; TEA = Et_3Al.

5.3.2.2 Production of the Ionic Liquid

The chloroaluminate ionic liquid used in the Difasol reaction section can easily be prepared in two steps. The first is the reaction of an alkyl chloride with *N*-alkylimidazole. The second is the direct reaction of the resulting *N*,*N*′-dialkylimidazolium chloride with aluminum chloride (Scheme 5.4). This synthesis has already been scaled up to several tens of kilograms using IFP-Lyon standard pilot plant facilities. The reaction conditions chosen allow easy control of reaction exothermicity. Impurities or excess of volatile starting materials are removed during the reaction. Good-quality ionic liquids are obtained and the production is ready for industrial scale-up. (unpublished results).

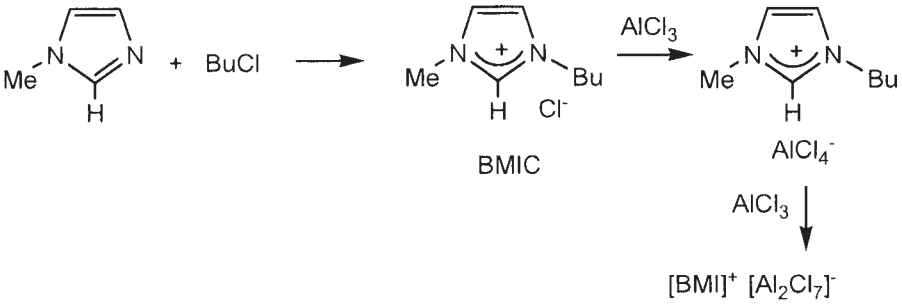

Scheme 5.4 Synthesis of acidic chloroaluminate ionic liquids.

5.4 The Biphasic Difasol Process

The first laboratory experiments [15] were performed with an Ni^{II} salt and the BMIC–$AlCl_3$–$EtAlCl_2$ ionic liquid in a semi-batch manner to evaluate the activity and

selectivity of the system into dimers. These experiments showed that the Ni catalyst is dissolved and remains immobilized in the ionic liquid where the reaction products are poorly soluble. The reactant miscibility remains adequate to ensure reaction. No catalytic activity occurs in the organic phase. Experiments also showed that raising the mixing efficiency increases the reaction rate but does not change the dimer selectivity. Excellent mixing is necessary to ensure good conversion by rapid mass transfer and efficient interaction of the ionic catalyst with the substrate. No co-miscibility between the products and the ionic liquids was observed; product separation could be operated by simple decantation of the two phases.

In order to demonstrate the recyclability and the lifetime of the catalytic system, a continuous flow pilot plant was operated.

5.4.1
The Biphasic Transformation of Butenes (Pilot Development)

The continuous experiments were run with a representative industrial C_4 raffinate-2 cut composed of 70% butenes (27% of which is 1-butene) and 1.5% isobutene (the remainder being *n*-butane and isobutane). These reactants are introduced continuously into a well-stirred reactor operated full of liquid. The effluent (a mixture of the two liquid phases) leaves the reactor via an overflow and is transferred to a phase separator (Figure 5.5). The separation of the ionic liquid (density around 1200 g L^{-1}) and the oligomers occurs rapidly and completely (favored by the difference in densities). The ionic liquid containing the Ni catalyst is recycled to the reactor, while the product stream is recovered and analyzed on-line. The test was conducted continuously over a period of 5500 h, after which it was deliberately stopped. No additional fresh ionic liquid was required during the test. No ionic liquid can be detected in the products (nitrogen analysis). The volume of ionic liquid recovered after the 5500 h was identical with that engaged. Throughout the whole test, the butene conversion was maintained above 70 wt%.

Very small amounts of Al and Ni catalyst components are carried over by the organic stream. It appeared necessary to introduce continuously some nickel catalyst precursor and alkylaluminum co-catalyst at a small rate to counterbalance this

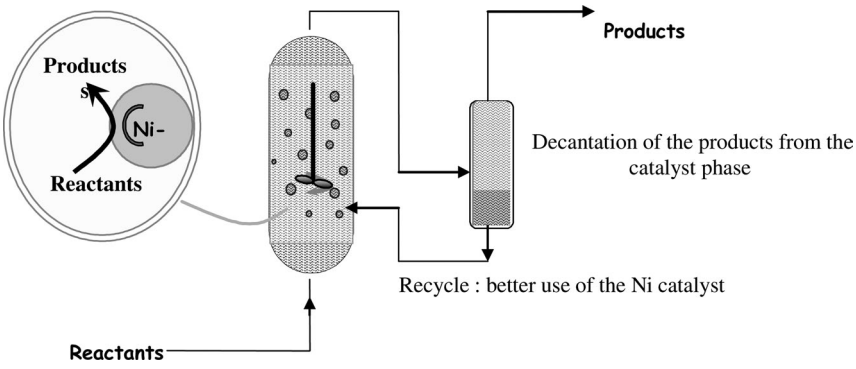

Figure 5.5 Biphasic system.

leaching. The injection flow rates of nickel and alkylaluminum are defined to maintain the butenes conversion constant. It must be emphasized that in this case, the nickel and aluminum consumption is lower than in a Dimersol system.

Butenes are converted into octenes with high selectivity (95 wt% of octenes relative to the total products). In such a system, consecutive side reactions (octenes + butenes) are minimized due to the lower solubility of octenes compared with butenes in the ionic liquid. Moreover, unlike what is observed in the Dimersol process, octene selectivity remains higher than 90%, even at 80% butene conversion, easily obtained by increasing the Ni catalyst concentration.

Whatever the butene conversion, for less than 2 wt% of isobutene in the feed, the C_8 isomer distribution proved to be equivalent to the distribution classically reported for the industrial Dimerol process.

This continuous pilot test definitely demonstrated the stability of chloroaluminates under dimerization conditions. The main advantage of the biphasic Difasol process remains in the easy product separation that can be performed in a subsequent step. The product separation by settling does not require heating and results in energy savings plus reduced catalyst consumption.

Another interesting result is the excellent activity obtained when diluted feedstock is used. With Dimersol X technology, olefin conversion is highly dependent on its concentration in the feed. In contrast, Difasol performances are maintained over a wide range of butene concentration, with the same catalyst consumption (Table 5.4).

5.4.1.1 The Difasol Process: Different Process Schemes and Estimated Performances

Owing to the solubility of the catalyst in the ionic liquid and to the poor miscibility of the products, the unit is essentially reduced to a well-stirred reactor followed by a phase separator.

The Difasol reaction section involves a reactor and two settlers (Figure 5.6). An injection of fresh catalyst components is adjusted to compensate for a slight catalyst carryover by the organic phase. Nickel and alkylaluminum injections are defined so as to maintain the butene conversion constant.

The Difasol catalyst is concentrated and operates in the ionic phase or maybe at the phase boundary. The reaction volume is therefore much lower than in the conventional one-phase Dimersol process, where the catalyst concentration is very low.

Different process schemes including this Difasol reaction section have been envisioned so far.

Table 5.4 Effect of butene feed dilution on Difasol catalytic performance.

Concentration of butenes (wt%)	Conversion (wt%)	Dimer selectivity (wt%)
20	65–70	>92
40	65–70	>92
60	65–70	>92

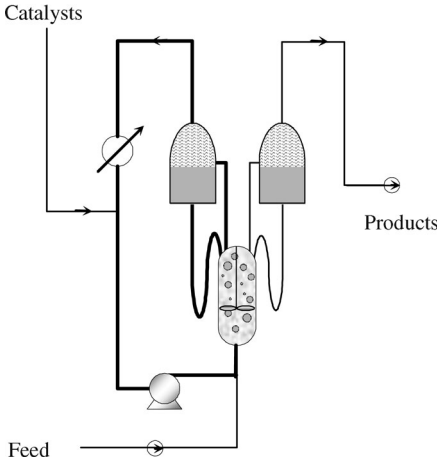

Figure 5.6 Difasol reaction and decantation.

Difasol Integrated Concept: [Dimersol + Difasol] Combination As the biphasic Difasol process can be operated on diluted feedstock, the biphasic reactor can ideally be integrated as a finishing reaction section after a Dimersol reactor.

In this first scheme, the design consists of a first homogeneous Dimersol dimerization step (1), a vaporization–condensation section (2) and a biphasic dimerization section (3) (Figure 5.7). The catalyst injection rate is decreased in the one-phase Dimersol reactor to provide low butene conversion. The effluent from the Dimersol reactor is partly vaporized to separate unconverted C_4s from octenes. Products and catalyst are sent to the neutralization section while the vapor phase is condensed and sent to the Difasol reactor. Butene conversion is achieved with less catalyst and more selectivity thanks to the biphasic system. This [Dimersol + Difasol] combination, which uses the same Dimersol catalytic system, improves the yield of octenes by about 10 wt% with a lower consumption of nickel.

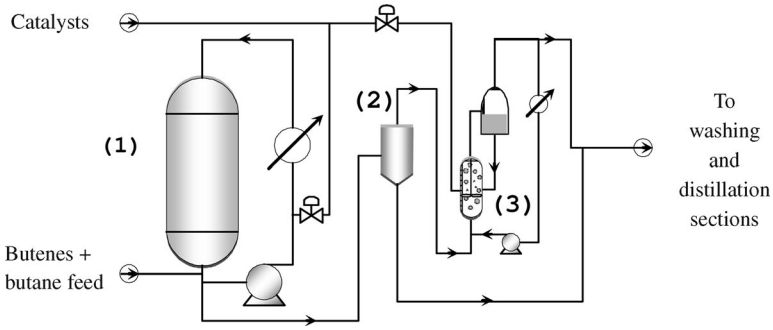

Figure 5.7 Dimersol + Difasol package reaction section scheme. (1) Dimersol reactor; (2) vaporisation–condensation; (3) Difasol reactor.

Table 5.5 Comparison of performances.[a]

	Dimersol (4 reactors)	Dimersol + Difasol integrated concept (1 Dimersol + 1 Difasol reactor)
Yield of octenes	0.66	0.73
Relative nickel consumption	1.0	0.70
Total reactor volume[a]	$4 \times 120\ m^3$	$1 \times 120\ m^3$ (Dimerol) + $30\ m^3$ (Difasol)

[a]On 75 wt% butenes feed, for $20\ t\ h^{-1}$ feed rate.

It should be noted that, in such a combination, the one-phase Dimersol reaction totally purifies the Difasol feed from impurities that could potentially be accumulated in the ionic liquid.

This particular combination of one-phase and two-phase technologies is possible because of the high Difasol efficiency on the diluted feed issued from the Dimersol reactor. This arrangement is suitable either to grassroots units or to upgrading of existing Dimersol X units. It considerably reduces the overall unit volume compared with existing Dimersol X units. It also induces lower catalyst consumption, which means lower catalyst and disposal costs (Table 5.5).

Difasol Standalone Concept: Comparison with [Dimersol + Difasol] Combination *In a second scheme,* there could be only one Difasol reaction section. For such a grassroots unit, Difasol standalone, the main concern is how to protect the chloroaluminate ionic liquid from feedstock impurities. The proper pretreatments are highly dependent on the origin of the feed. Fortunately, the current poisons of chloroaluminates are the same as those of the well-known Dimersol catalyst. The lower the content of these pollutants in standalone Difasol feedstock, the longer is the chloroaluminate ionic liquid lifetime. The best arrangement, to remove these poisons as completely as possible, includes a water wash with condensed or feed boiling water, followed by a water removal device. Currently a simple azeotropic and partial de-isobutane fractionator is recommended. The dry feed is then treated with the proper molecular sieves in order to remove both oxygenates and sulfur compounds. It should be noted that all these feedstock treatments are also recommended to minimize classical Dimersol catalyst consumption, but using the standalone Difasol process leads to more severe treatments and therefore higher investment and chemical expense.

Rather than a purification section, a standalone Difasol plant also requires a larger biphasic reactor than a [Dimersol + Difasol] unit. For instance, a 160 000 t per year C_4 cut unit requires a $50\ m^3$ Difasol reactor when it operates in standalone mode but only a $30\ m^3$ reactor when it works as a finishing reaction conversion after Dimersol.

Table 5.6 shows a simplified mass balance comparison for the Dimersol process, Dimersol-Difasol arrangement and a standalone Difasol unit.

Table 5.6 Comparison of unit performances.[a]

		[Dimersol (1 reactor) + Difasol]			
	Dimersol (4 reactors)	**Dimersol reactor**	**Difasol reactor**	**Global arrangement**	**Difasol standalone**
Conversion (wt%)	80	50	75	82	75
Selectivity (wt%):					
Octenes	82	89	91	90	91
Dodecenes	14	10	8.5	9	8.5
Hexadecenes	4	1	0.5	1	0.5

[a]Feed 160 000 t yr^{-1}; 75 wt% butenes; iso-investment per ton of octenes.

5.4.1.2 Economics of the Difasol Process

Both butene conversion and octene selectivity are clearly improved using the [Dimersol + Difasol] arrangement, whereas the standalone Difasol process appears to be able to achieve the best octenes selectivity with lower butene conversions. Calculations were done for iso-investment on a grassroots unit. The standalone Difasol process can achieve higher butene conversion (more than 85 wt% is feasible) with still 91% octene selectivity. Table 5.7 gives a Capex (capital expenditure) comparison for the three unit arrangements mentioned above, taking into account the same constraint: all units have the same Capex per ton of octenes.

Table 5.8 gives the operating expenditure (unit operating costs or Opex) for the three unit arrangements mentioned above using the same constraint.

In conclusion, clearly, both the [Dimersol + Difasol] and standalone Difasol processes furnish an interesting Opex economy. The standalone Difasol process

Table 5.7 Unit Capex estimation.[a]

	Dimersol (4 reactors)	**Dimersol (1 reactor) + Difasol**	**Difasol standalone**
Feed purification section (%)	10	10	26
Reaction section (%)	47	42	24
Distillation section (%)	20	20	20
Catalyst section (%)	5	5	5
Catalyst removal section (%)	18	18	18
Difasol cooling section (%)		8	11
Total unit investment (%) (*a*)	100	103	104
Butenes conversion (wt%)	80	82	75
Octenes selectivity (wt%)	82	90	91
Octenes yield (wt%) (*b*)	66	73	68
Relative Capex per ton of octenes: (*a*)/(*b*)	1.5	1.4	1.5

[a]Feed 160 000 t yr^{-1}; 75 wt% butenes; iso-investment per ton of octenes.

Table 5.8 Chemicals and utilities consumption.[a]

	Dimersol (4 reactors)	Dimersol (2 reactors) + Difasol	Difasol standalone
Cooling water (%)	2	2	12
Steam MP (distillation) (%)	6.5	10	8
Electricity (%)	0.5	1	1
Difasol cooling (%)		4	11
Total unit (%)	100	91	68
Consumption per ton of octenes	1.5	1.3	1.0

[a]Feed 160 000 t yr^{-1}; 75 wt% butenes; iso-investment per ton of octenes.

allows interesting chemical consumption and flexibility in terms of octene production just by tuning the chemical consumption, in comparison with the classical Dimersol process. The [Dimersol + Difasol] combination gives the best octene yields and fairly low operating costs.

To summarize the advantages of the Difasol process, one can include the following main benefits:

- The overall octene selectivity is higher than that for the homogeneous process.
- The dimer selectivity does not decrease much at high conversion.
- The overall yield of C_8 octenes is higher than in the homogeneous process (by about 10 wt%)
- The system can be run with poorly concentrated alkene feeds (as low as 20 wt% butenes) and hence streams such as raffinate-2 are suitable feeds.
- The nickel loss is much less than the consumption in the homogeneous process.
- Although some loss of [$EtAlCl_2$] occurs, it is much less than in the homogeneous system.
- No ionic liquid can be detected in the products.
- A much smaller reactor can give the same throughput of octenes.
- Dimersol Ni commercial catalyst precursor can be used without modification.
- Substrate preparation and product purification are similar to that used in the Dimersol process (but with much less NaOH consumption and waste generation).

5.4.2 The Biphasic Transformation of Propylene

The dimerization of propylene with a nickel catalyst precursor that does not contain any phosphine ligand usually gives oligomers with uncontrolled regioselectivity (typically a mixture of dimethylbutenes, methylpentenes and hexenes), as described in Schemes 5.1 and 5.3. The addition of bulky and basic phosphine ligands such as triisopropylphosphine or tricyclohexylphosphine can drive the reaction to high selectivity in 2,3-dimethylbutenes (2,3-DMB-1 and 2,3-DMB-2) [19].

2,3-Dimethylbutenes are especially important since they can be used as key starting olefins for fine chemical intermediates. 2,3-DMB-2 is used for the synthesis of Danitol, which is a high-performance pyrethroid insecticide developed by Sumitomo in 1976, and to produce other intermediates (e.g. pinacolone). 2,3-DMB-1 is a key intermediate for the production of musk fragrances (Tonalid) [20].

Numerous studies have been performed on these Ni–phosphine catalytic systems in order to improve the activity and the selectivity, not only by varying the phosphine ligand, but also by varying the additives. The anchorage of Ni complexes on solid supports was also reported [21]. Fluorinated biphasic systems were also applied to try to immobilize nickel β-diketonate complexes modified with a long perfluorinated alkyl chain. However, the polar character of the Ni active species was not favorable to the non-polar fluorinated layer [22].

More promising is the use of ionic liquids. Regioselective propylene dimerization can be performed in acidic chloroaluminates. The phosphine effect can be maintained with the right adjustment of the ionic liquid acidity [23]. The reaction has been carried out in a semi-continuous way in a glass apparatus. The main issue was to maintain constant the 2,3-DMB selectivity with time. The 2,3-DMB selectivity decreases rapidly if no phosphine is added. This has been ascribed to a competition for the basic phosphine between the 'soft' Ni catalyst and the 'hard' aluminum chloride potentially present in the acidic ionic liquid. To prevent this loss of phosphine effect, different organic bases have been added to the ionic liquid to 'buffer' their Lewis acidity. Aromatic hydrocarbons proved to be ideal basic additives. Thanks to their poor basicity, they do not interfere strongly with the Ni active center and do not decrease the catalytic activity. They can be considered as buffers, thus stabilizing the 'phosphine effect'.

The propylene dimerization was then performed semi-continuously in an effective way using acidic chloroaluminate as the catalyst solvent and aromatic hydrocarbons as additives. Propylene is introduced through a valve in the reactor in the vapor phase under pressure control. The reaction consumes the propylene to produce liquid hexenes mixture rich in 2,3-DMB-1. When the reactor is full of liquid, the organic upper phase can be withdrawn without stopping the reaction. The reaction has been performed continuously during more than 50 h without loss of 2,3-DMB-1 selectivity. The hexene selectivity was maintained constant at around 75–80 wt% hexenes/total products and the 2,3-DMB-1 was maintained at 70–75 wt% relative to the total hexene content (Figures 5.8 and 5.9).

A process scheme including a reaction section and an effluent washing section was then designed to produce, in a continuous way, a stream in which 2,3-DMB-1 is the major component (Figure 5.10).

As in the Dimersol process, the heat of the reaction is released thanks to a pump-around. The temperature of the reactor is controlled by a refrigerant flow on the pump-around cooler. The product stream is sent to a hydrocarbon/ionic liquid settler in which the ionic liquid decants and is sent back to the reactor under level control. Part of the unreacted propylene is recycled, under pressure control, to the reactor after vaporization. The products are finally washed in a similar way as in the Dimersol process. A material balance (weight) is given in Table 5.9.

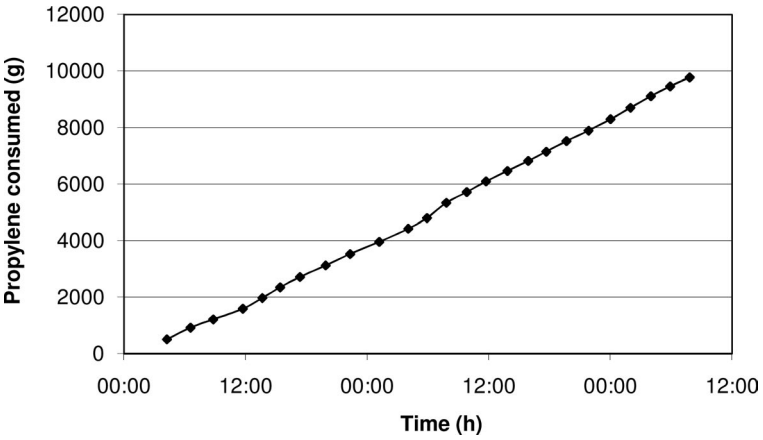

Figure 5.8 Regioselective dimerization of propylene: propylene consumption as a function of time. 15 mL chloroaluminate ionic liquid; $T = -15\,^{\circ}C$; catalytic system: Ni^{II}–PCy_3 (1 : 1 molar ratio).

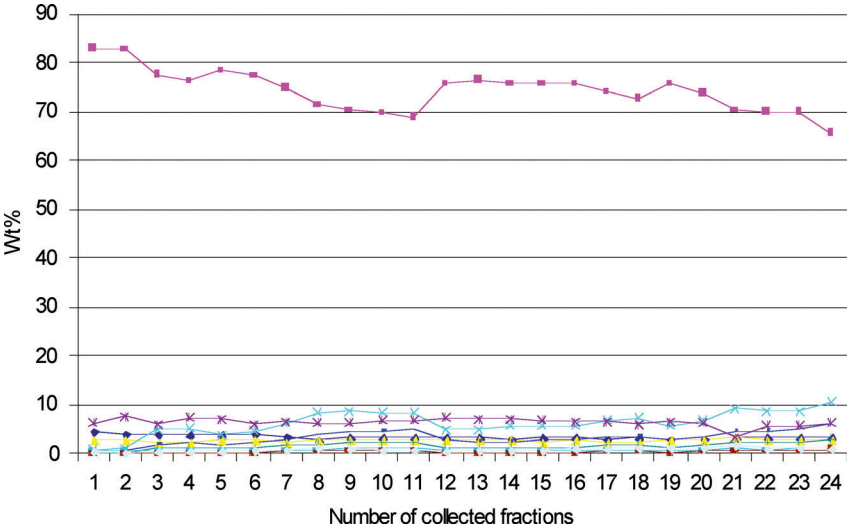

Figure 5.9 Semi-continuous dimerization of propene Ionic liquid: 15 mL, propene: atmospheric pressure, duration: 60 hours (24 fractions of 250 mL each), production: 11 L of products; C6 selectivity: 80–81%/products; 2,3-DMB-1 selectivity: 70–75%/C6.

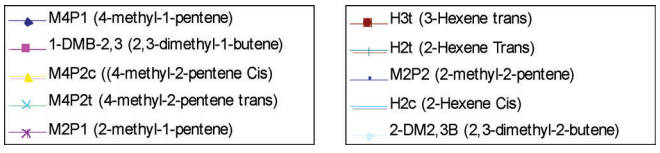

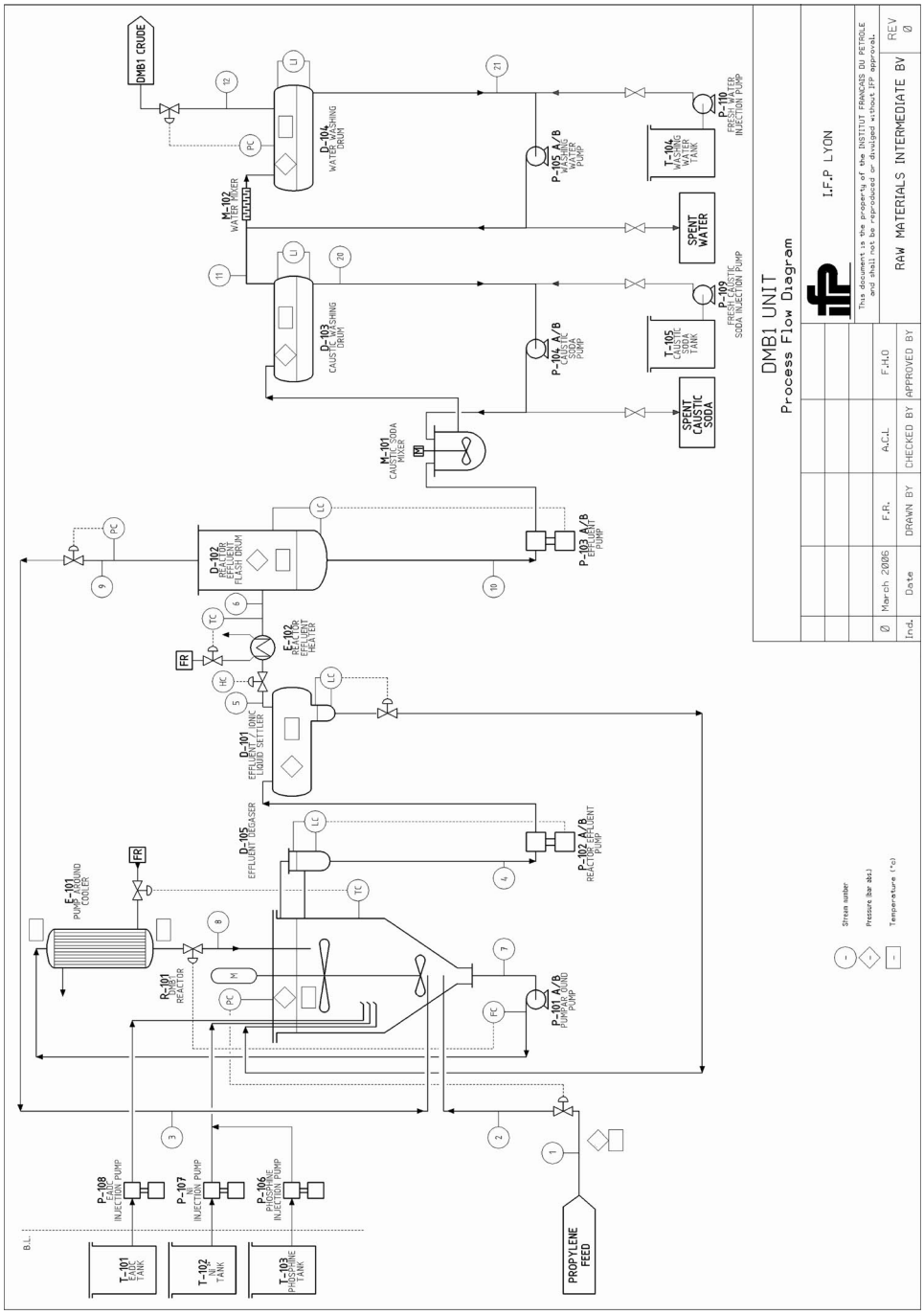

Figure 5.10 Regioselective biphasic propylene dimerization unit scheme.

Table 5.9 Propylene dimerization: mass balance.[a]

Flow rate ($kg\,h^{-1}$)	Propylene feed	Propylene recycle	Reactor outlet	Pump-around inlet	Flash drum vapor	Flash drum liquid	DMB crude
				Line No. (see Fig. 10)			
	1	2	4	7	9	10	12
Incondensables	0.1	0.4	0.5	21.5	0.4	0.1	0.1
Propylene	248.7	32.2	50.6	2 168.1	32.2	18.3	18.3
Propane	1.0	1.6	2.6	111.9	1.6	1.0	1.0
Butane	0.1		0.2	7.4		0.1	0.1
4MP-1		0.4	6.4	274.9	0.4	6.0	6.0
2,3-DMB-1		7.7	145.0	6 215.1	7.7	137.3	137.3
4MP2-*cis*		0.3	5.1	218.5	0.3	4.8	4.8
4MP2-*trans*		0.6	11.1	476.4	0.6	10.5	10.5
2MP-1		0.5	11.7	501.9	0.5	11.2	11.2
H-3-*trans*			0.7	31.7		0.7	0.7
H-2-*trans*		0.1	2.8	119.0	0.1	2.7	2.7
2MP–2		0.2	5.3	228.3	0.2	5.1	5.1
H-2-*cis*			1.6	67.4		1.5	1.5
2,3-DMB-2		0.1	1.7	72.2	0.1	1.6	1.6

[a]Flow numbers refer. to Figure 5.10.

5.5 Conclusion

The Difasol process has been developed to transform the butenes cut into octenes used as raw materials for the manufacture of isononanols. In comparison with the homogeneous industrial Dimersol process, the biphasic Difasol process can be shown to have lower capital investment because of the smaller reactor size required, higher selectivity, higher yield, faster throughput and greater environmental acceptability (lower E-factor) as a result of reduced catalyst waste production.

Another option of the biphasic Difasol process concerns the regioselective dimerization of propylene for the production of hexene effluent rich in 2,3-DMB-1, a high-value intermediate used in fine chemistry. In this option, the biphasic process leads to a high 2,3-DMB-1 yield with reduced catalyst and costly ligand consumption due to catalyst recycling.

List of Abbreviations

BMIC	1-methyl-3-butylimidazolium chloride
EADC	ethylaluminum dichloride
EMIC	1-ethyl-3-methylimidazolium chloride

References

1 (a) Cornils, B. (2002) in *Applied Homogeneous Catalysis with Organometallic Compounds* Vol. 1, 2nd edn (eds B. Cornils and W.A. Herrmann), Wiley-VCH Verlag GmbH, Weinheim, pp. 1–24; (b) Cornils, B. and Herrmann, W.A. (2003) *Journal of Catalysis*, **216**, 23–31.

2 Gladysz, J.A. (2002) *Chemical Reviews*, **102**, 3215–3216.

3 (a) Cornils, B., Herrmann, W.A., Horvath, I.T., Leitner, W., Mecking, S., Olivier-Bourbigou, H. and Vogt, D. (2005) in *Multiphase Homogeneous Catalysis*, Vol. 1 (eds B. Cornils, W.A. Herrmann, I.T. Horvath, W. Leitner, S. Mecking, H. Olivier-Bourbigou and D. Vogt), Wiley-VCH Verlag GmbH, Weinheim, pp. 1–23; (b) Cornils, B. and Kunz, E. (2004) in *Aqueous-phase Organometallic Catalysis: Concept and Applications*, 2nd edn. (eds B. Cornils and A.W. Herrmann), Wiley-VCH Verlag GmbH, Weinheim, pp. 351–364; (c) Kuntz, E.G. (1987) *Chemtech*, 570–575.

4 (a) Reichardt, C. (2003) in *Solvent and Solvent Effects in Organic Chemistry*, 3rd edn. (ed. C. Reichardt), Wiley-VCH Verlag GmbH, Weinheim, pp. 147–329; (b) Cornils, B. (1999) *Topics in Current Chemistry*, **106**, 133–152; (c) Constable, D.J.C., Jimenez-Gonzalez, C. and Henderson, R.K. (2007) *Organic Process Research & Development*, **11**, 133–137.

5 (a) Zhang, S., Sun, N., He, X., Lu, X. and Zhang, X. (2006) *Journal Physical And Chemical Reference Data*, **35**, 1475–1517; (b) Welton, T. (2005) in *Multiphasic Homogeneous Catalysis*, Vol 2 (eds B. Cornils, W.A. Herrmann, I.T. Horvath, W.

Leitner, S. Mecking, H. Olivier-Bourbigou and D. Vogt), Wiley-VCH Verlag GmbH, Weinheim, pp. 431–455; (c) Olivier-Bourbigou, H. and Magna, L. (2002) *J Mol Catal A*, **182–183**, 419–437; (d) Dupont, J., de Souza, R.F. and Suarez, P.A.Z. (2002) *Chemical Reviews*, **102**, 3667–3692; (e) Zhao, D., Wu, M., Kou, Y. and Min, E. (2002) *Catalysis Today*, **74**, 157–189; (f) Gordon, C.M. (2001) *Applied Catalysis A-General*, **222**, 101–117; (g) Wasserscheid, P. and Keim, W. (2000) *Angewandte Chemie-International Edition*, **39**, 3773–3789; (h) Sheldon, R. (2001) *Chemical Communications*, 2399–2407; (i) Chauvin, Y. and Olivier, H. (1995) *Chemtech*, **9** (25), 26–38.

6 (a) Freemantle, M. (2007) *Chemical & Engineering News*, **85** (1), 23–26; (b) Rodgers, R. and Seddon, K. (2003) *Science*, **302**, 792–793; (c) Short, P.L. (2006) *Chemical & Engineering News*, **84** (17), 15–21; (d) Plechklova, N. and Seddon, K. (2008) *Chemical Society Reviews*, in press.

7 (a) Zhang, Z. (2006) *Advances in Catalysis*, **49**, 153–237; (b) Welton, T. (2004) *Coordination Chemistry Reviews*, **248**, 2459–2477; (c) Pârvulescu, V.I. and Hardacre, C. (2007) *Chemical Reviews*, **107**, 2615–2665; (d) Giernoth, R. (2007) *Topics in Current Chemistry*, **276**, 1–23.

8 Durand, J., Teuma, E. and Gomez, M., (2007) *Comptes Rendus Chimie*, **10**, 152–177.

9 (a) Joglekar, H.G., Rahman, I. and Kulkarni, B.D. (2007) *Chemical Engineering & Technology*, **30**, 819–828; (b) Chauvin, Y. (2005) in *Multiphasic Homogeneous Catalysis*, Vol. 2 (eds B. Cornils, W.A. Herrmann, I.T. Horvath, W. Leitner, S. Mecking, H. Olivier-Bourbigou and D. Vogt), Wiley-VCH Verlag GmbH, Weinheim, pp. 407–413.

10 (a) Olivier-Bourbigou, H. and Saussine, L. (2002) in *Applied Homogeneous Catalysis with Organometallic Compounds*, Vol. 1 (eds B. Cornils and W.A. Herrmann), Wiley-VCH Verlag GmbH, Weinheim, pp. 253–264; (b) Vogt, D. (2002) in *Applied Homogeneous Catalysis with Organometallic Compounds*, Vol. 1 (eds B. Cornils and W.A. Herrmann), Wiley-VCH Verlag GmbH, Weinheim, pp. 240–253.

11 Nowlin, G., Burnie, G. and Lyons, H.D. (1955) US Patent 2 969 408 (Phillips Petroleum).

12 Wilke, G., Bogdanovic, B., Hardt, P., Heimbach, O., Kroner, W., Oberkirch, W., Tanaka, K., Steinrucke, E., Walter, D. and Aimmerman, H. (1966) *Angewandte Chemie-International Edition*, **5**, 151–164.

13 (a) Chauvin, Y., Gaillard, J.F., Dang, Vu Quang and Andrews, J.W. (1974) *Chemistry & Industry*, 375–378; (b) Convers, A., Commereuc, D. and Torck, B. (1994) *Revue del'IFP*, **49**, 437–451; (c) Favre, F., Forestière, A., Hugues, F., Olivier-Bourbigou, H. and Chodorge, J.A.(June 2 2005) *Oil Gas-European Magazine*, 83–87; (d) Olivier-Bourbigou, H., Chodorge, J.A. and Travers, P. (1999) *Petroleum Technology Quarterly*, 141–149; (e) Dixon, J.T. Green, M.J. Hess, F.M. and Morgan, D.H. (2004) *Journal of Molecular Catalysis A-Chemical*, **689**, 3641–3668; (f) Kobayashi, R. and Kura, S. (2007) US Patent 7 169 961 (Idemitsu Petroleum); (g) Al-Jarallah, A.M., Anabtawi, J.A., Siddiqui, M.A.B., Aitani, A.M. and Al-Sa'doun, A.W. (1992) *Catalysis Today*, **14**, 1–121; (h) Anon, (2001) *Chemical & Engineering News*, **79** (45), 16; (i) Krawczyk, M.A. and Marinangeli, R.E. (1996) US Patent 5 523 508 (UOP).

14 (a) Cornils, B. (1998) *Organic Process Research & Development*, **2**, 121–127; (b) Freitas, E.R. and Gum, C.R. (1979) *Chemical Engineering Progress*, 73–76.

15 Chauvin, Y., Gilbert, B. and Guibard, I. (1990) *Journal of the Chemical Society. Chemical Communications*, 1715–1716

16 (a) Gale, R.J., Gilbert, B. and Osteryoung, R.A. (1978) *Inorganic Chemistry*, **17**, 2728–2729; (b) Hussey, H.C. (1983) in *Advances in Molten Salt Chemistry* Vol. 5 (ed. G. Mamantov), Elsevier, Amsterdam, pp. 185–230.

17 Gilbert, B., Chauvin, Y. and Guibard, I. (1991) *Vibrational Spectroscopy*, **1**, 299–304.

18 Chauvin, Y., Di Marco-Van Tiggelen, F. and Olivier, H. (1993) *Journal of the Chemical Society-Dalton Transactions*, 1009–1011.

19 Uchino, M., Chauvin, Y. and Lefebvre, G. (1967) *Comptes Rendus de l'Academie des Sciences Paris C*, **265**, 103–106.

20 (a) Sato, H., Tojima, H. and Ikimi, K. (1999) *Journal of Molecular Catalysis A-Chemical*, **144**, 285–293; (b) Sato, H. and Tojima, H. (1993) *Bulletin of the Chemical Society of Japan*, **66**, 3079–3084; (c) Itagaki, M., Suzukalo, G. and Nomura, K. (1998) *Bulletin of the Chemical Society of Japan*, **71**, 79–82.

21 Carlini, C., Marchionna, M., Patrini, R., Galletti, A.M.R. and Sbrana, G. (2001) *Applied Catalysis A-General*, **207**, 387–395.

22 Benvenuti, F., Carlini, C., Marchionna, M., Galletti, A.M.R. and Sbrana, G. (2002) *Journal of Molecular Catalysis A-Chemical*, **178**, 9–20.

23 (a) Chauvin, Y., Einloft, S. and Olivier, H. (1995) *Industrial & Engineering Chemistry Research*, **34**, 114–115; (b) Olivier-Bourbigou, H., Pellier, E. and Forestière, A. (2007) Patent WO2007/080287, (IFP).

6
Immobilization and Compartmentalization of Homogeneous Catalysts

Christian Müller and Dieter Vogt

6.1
Introduction

The contribution of soluble transition metal complexes as selective homogeneous catalysts for a number of chemical transformations under mild reaction conditions has increased significantly in recent decades. A number of important large-scale processes, such as the production of adiponitrile, α-olefins (SHOP process), acetic acid, acetic anhydride and butanal, are nowadays based on homogeneous catalysis [1]. Nevertheless, the separation and recovery of the catalyst from the product mixture remains a crucial feature for the commercialization of a catalytic process. Consequently, there is considerable interest in the development of organometallic catalysts anchored on various supports.

Several concepts for the immobilization of homogeneous catalysts have been developed and investigated, including ionic liquids [2], solid supports [3], supramolecular architectures and applications in supercritical CO_2 [4]. This chapter focuses exclusively on soluble dendritic and polymeric supports for homogeneous catalysts for the purpose of molecular weight enlargement or multiphase catalysis. Examples and highlights of their performance are presented, with emphasis on their application in continuous homogeneous catalysis by membrane filtration and catalyst separation/recovery by means of precipitation/filtration techniques. Recent developments in true heterogenization of homogeneous catalysts on solid supports, Merrifield resins, mesoporous materials, insoluble polymers, grafting on polyvinylpyridines and encapsulation by imprinting in polymers are outwith the scope of this chapter. A number of excellent review articles on recoverable catalysts using recyclable polymer- and dendrimer-based supports have also recently been published [5].

Green Catalysis, Volume 1: Homogeneous Catalysis.
Edited by Robert H. Crabtree

ISBN: 978-3-527-32496-5

6.2
Soluble Dendrimer-bound Homogeneous Catalysts

6.2.1
Covalently Linked Dendrimer-bound Catalysts

Since the pioneering work on dendritic structures by Vögtle and co-workers [6], dendrimers have attracted much attention. The synthesis and investigation of their structural properties became a new field in science. The application of dendrimers as support molecules for homogeneous catalysts was first reported by the groups of van Koten and van Leeuwen in 1994 [7]. In contrast to polymers, dendrimers have the advantage of a perfectly defined molecular structure and their catalytic properties can be investigated by standard high-resolution spectroscopic techniques in solution. However, detailed studies on the macromolecular structure of dendrimers have revealed that they do not always adopt the ideal spherical structures that their drawings suggest; especially amphiphilic dendrimers have structures that are far from spherical [8]. As a disadvantage, their syntheses are usually tedious and expensive and, correspondingly, commercial applications of dendrimers are scarce.

In principle, dendritic catalysts can show the kinetic behavior and thus the activity and selectivity of a conventional homogeneous catalyst. In periphery-functionalized systems the transition metals are located on the outer sphere and are directly accessible for the substrates, which allows for reaction rates that are comparable to those in ordinary homogeneous systems. On the other hand, multiple reaction sites in close proximity to one another result in extremely high local catalyst and ligand concentrations. For example, a second-generation carbosilane dendrimer functionalized with 36 terminal phosphines, results theoretically in local concentrations of 8 *M* of ligand and 4 *M* of catalyst. In reactions where excess ligand is required to stabilize the catalyst, this local concentration effect can indeed result in stable systems. However, several deactivation processes can operate by a bimetallic mechanism. Examples are ruthenium-catalyzed metathesis [9], palladium-catalyzed reductive coupling of benzene and chlorobenzene [10] and reactions that involve radicals [11].

A difficult problem in the use of dendrimers is leaching. Two forms of leaching are known: leaching of the dendritic catalyst through the membrane and metal leaching from the dendrimer into the solution and further leaching of the active metal through the membrane, usually in the form of small homogenized complexes. For industrial applications, the overall retention of the dendritic catalyst must be extremely good to maintain high activity in a continuous reactor for longer reaction times. The required retention obviously depends on the application, since processes for the bulk industry generally require more efficient catalyst recycling – higher turnover numbers (TONs) – than those for fine chemicals. Generally, a retention of at least 99.99% is required to obtain a catalyst system that remains in the reactor for a prolonged period of time, even for fine chemical production processes.

Most commonly, carbosilane, polyphenylene, poly(benzyl ether), DAB, PANAM and PPI dendrimers have been applied for the immobilization of transition metal complexes [12].

6.2.1.1 Carbosilane Dendrimers as Soluble Supports

Soluble dendritic Ni catalysts of the type **1** for the atom-transfer radical addition (ATRA, i.e. polyhalogenated alkane addition to olefins, Kharasch addition) were investigated by van Koten and co-workers. G0 and G1 carbosilane dendrimers, functionalized with NCN pincer-nickel(II) groups, were synthesized and applied as homogeneous catalysts for the addition of organic halides to alkenes (Scheme 6.1) [13].

Pd complexes of soluble *P,O*-functionalized carbosilane dendrimers, such as **2** (Scheme 6.2) were used by Vogt and co-workers for the hydrovinylation reaction (codimerization of ethene and styrene). This C−C coupling reaction is of high interest, because it opens up an easy access to building blocks for fine chemicals and also pharmaceuticals [14].

For the codimerization of ethene and styrene, a pressure membrane reactor was developed and the reaction ran almost without any isomerization to a mixture of the *E* and *Z* isomers of 2-phenyl-2-butenes or formation of any side products, which are usually observed at high conversions. Nevertheless, the space–time yield dropped to zero within 15 residence times and low retention of the dendrimer and precipitation of palladium on the membrane were observed. Larger dendritic catalysts with higher retentions did not show much improvement, indicating that catalyst deactivation was indeed the major problem.

The core-functionalized dendritic dppf analogue **3** (dppf = diphenylphosphinoferrocene) was reported by van Leeuwen and co-workers [15]. While the

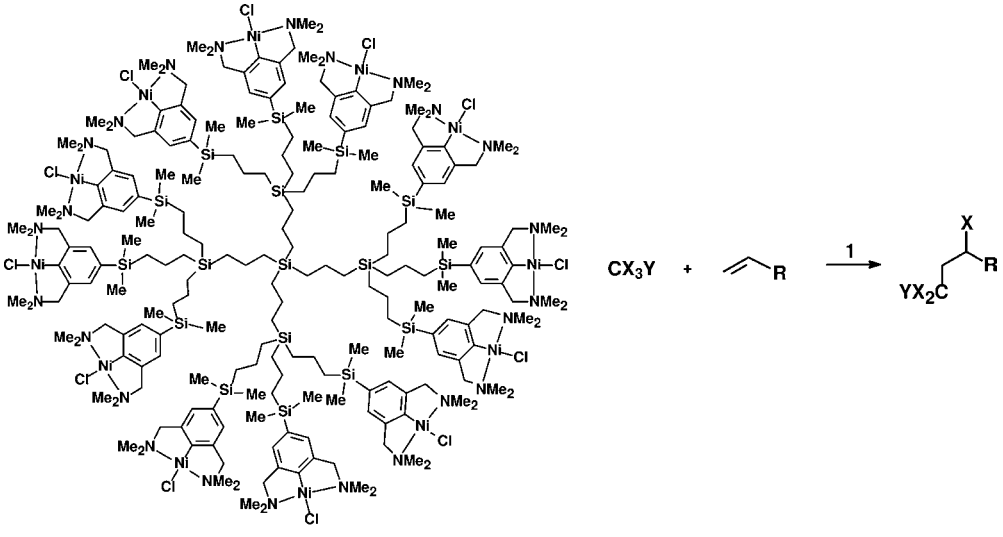

1

Scheme 6.1 Dendritic NCN-pincer-Ni(II) complex for the Kharasch addition reaction.

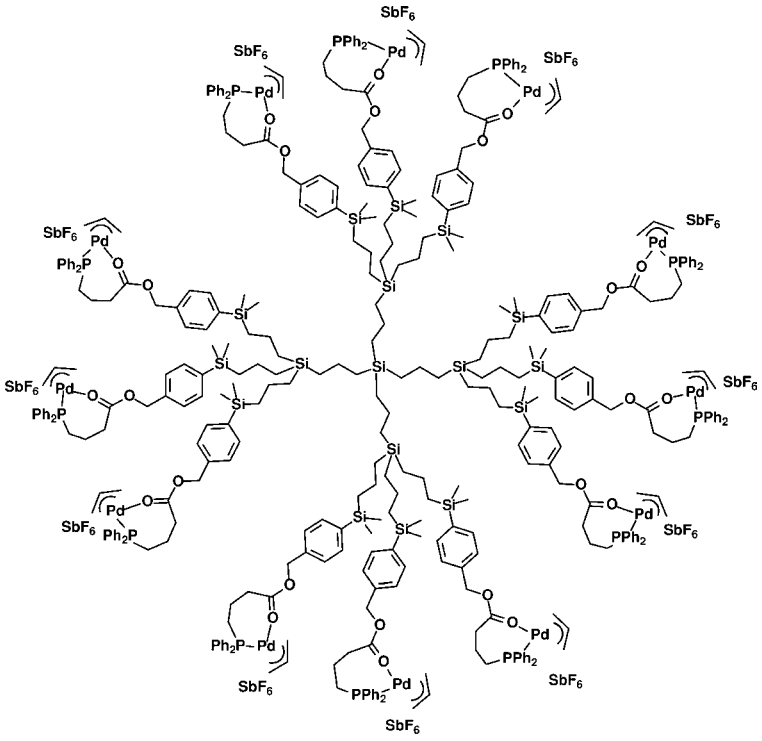

2

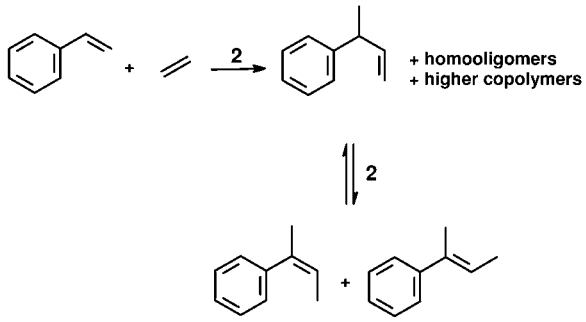

Scheme 6.2 Dendritic Pd–allyl complex for the hydrovinylation reaction.

corresponding rhodium complex could only be applied in a batch-wise hydroformylation reaction [the hydroformylation reaction is typically performed at elevated temperature (40–80 PC) and also under a syngas pressure of 10–20 bar], the hydrogenation of dimethyl itaconate could be performed under continuous reaction conditions (Scheme 6.3). Interestingly, no deactivation of the catalyst occurred during the catalytic experiment, which has often been observed in continuous palladium-catalyzed reactions. The drop in conversion (77% after 35 exchanged reactor volumes) could be fully explained by the retention of the dendritic system (99.8%) [15].

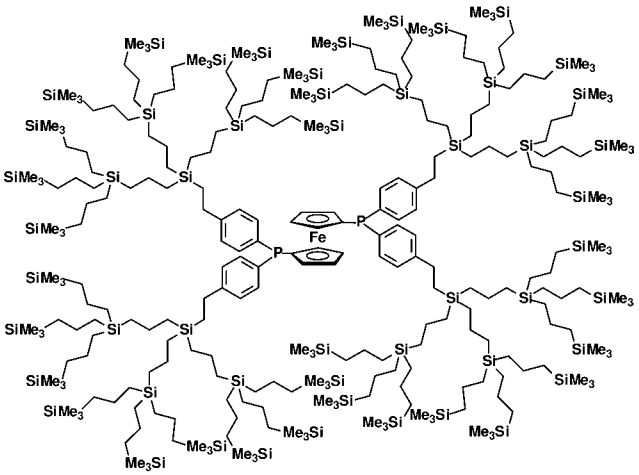

3

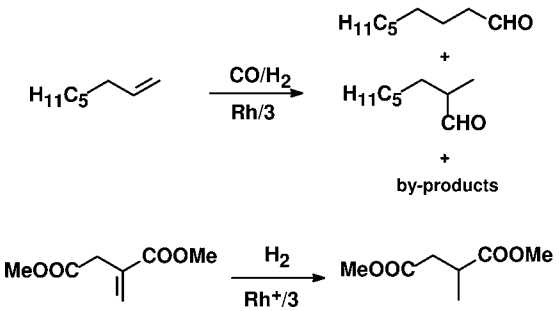

Scheme 6.3 Core-functionalized dendritic dppf analogue for hydroformylation and hydrogenation reactions.

Van Leeuwen and co-workers also investigated the preparation and application of dendrimer-substituted *P,O* ligands in the Ni-catalyzed oligomerization and polymerization of ethene (SHOP-process) [16]. Interestingly, a clear positive dendritic effect was observed: The dendritic system **4** showed a much higher productivity in toluene as the solvent compared with the non-supported *o*-hydroxytriphenylphosphine–Ni catalyst (Figure 6.1). In more polar solvents (methanol, THF), the parent compound was catalytically inactive due to the formation of Ni bischelates, while the molecular enlarged system produced mainly oligoethenes. Interestingly, the presence of primarily monoligated dendritic Ni species and the suppression of bischelates due to the dendrimer substituents under catalytic conditions could be verified by high-pressure NMR spectroscopy.

P,N-type ligands substituted with second-generation carbosilane dendrimers, such as **5**, were reported by Reek and co-workers [17]. These systems ('ClickPhine') were prepared by a Cu(I)-catalyzed azide–alkyne 'click' cycloaddition reaction, a concept previously developed by Sharpless and co-workers. The corresponding

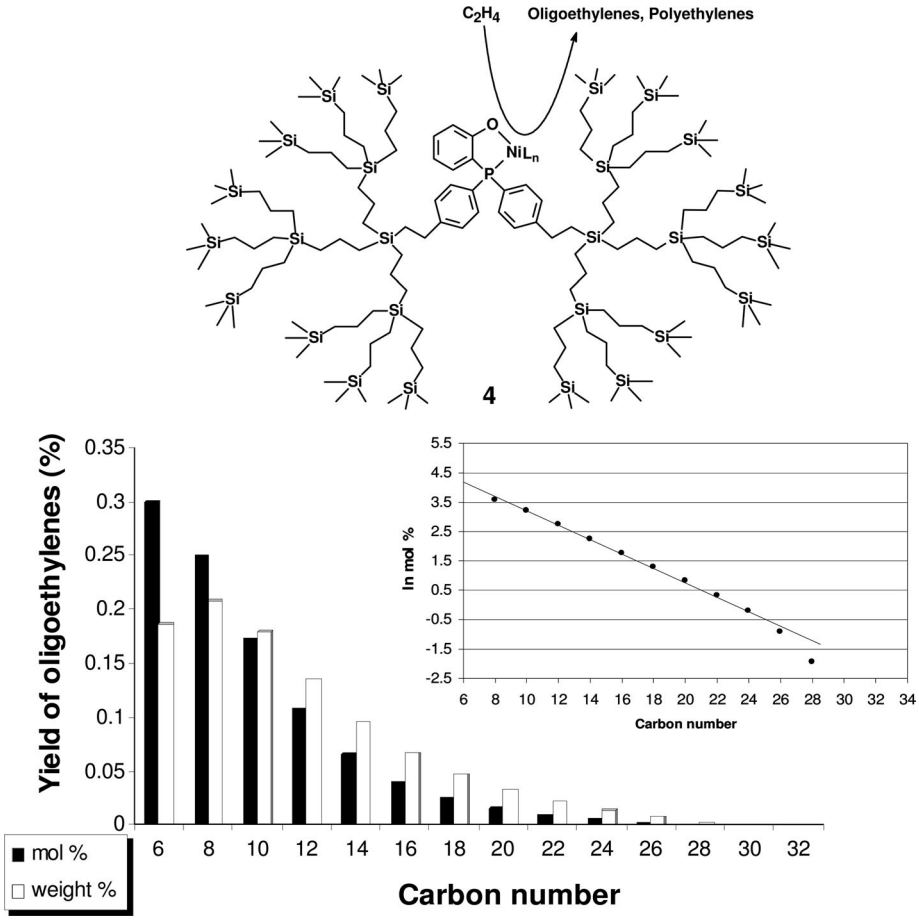

Figure 6.1 Dendritic P,O−Ni complex for the oligomerization and polymerization of ethene.

cationic Pd–allyl complexes were investigated in the allylic alkylation of cinnamyl acetate, showing high conversion (91%) and high selectivity (98%) for the linear *cis*-product (Scheme 6.4).

6.2.1.2 Poly(Benzyl Ether) Dendrimers as Soluble Supports

Bolm and co-workers studied the diethylzinc addition to benzaldehyde with soluble polymeric catalysts [18]. Dendritic chiral catalysts consisting of poly(benzyl ethers) (**6**) and chiral pyridyl alcohols were used as organocatalysts for the asymmetric C−C linkage reaction (Scheme 6.5).

The enantiocontrol by the dendritic systems was slightly lower compared with the parent pyridyl alcohols [2–3% drop in enantiomeric excess (*ee*)], but the conversion towards the chiral secondary alcohol was actually slightly higher for the largest hyperbranched catalyst (84% versus 80% yield after a 3 h reaction time).

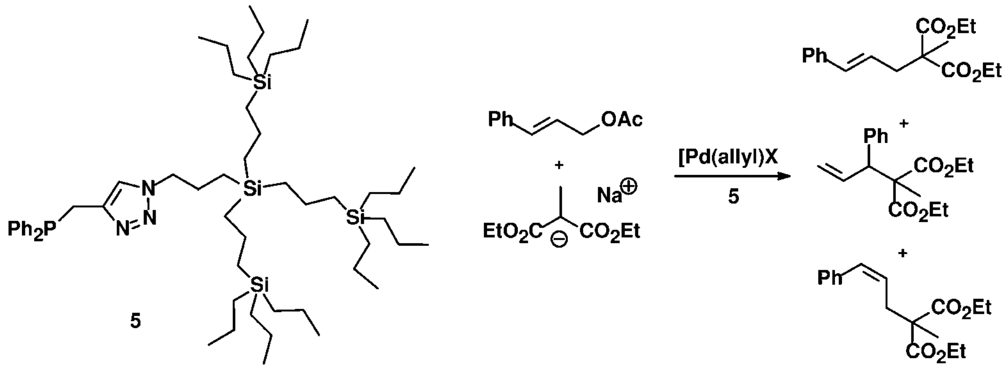

Scheme 6.4 Dendritic 'ClickPhine' ligand for Pd-catalyzed allylic alkylation reactions.

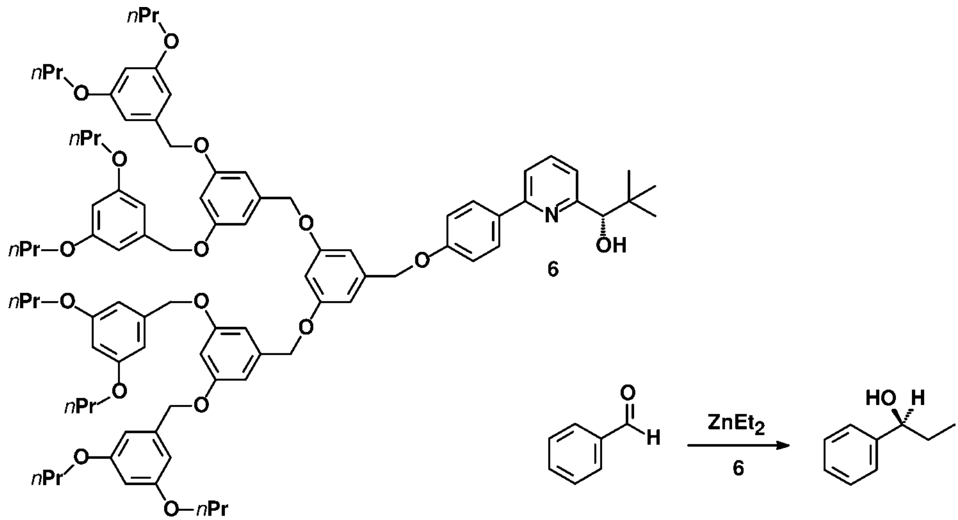

Scheme 6.5 Dendritic poly(benzyl ether) catalyst for the diethylzinc addition to benzaldehyde.

Double Michael addition reactions between methyl vinyl ketone (MVK) and ethyl α-cyanoacetate under continuous conditions (dead-end reactor) were performed with the dodecakis(NCN–Pd^{II}) catalyst **7** by van Koten's group [19] (Scheme 6.6). High productivity and retention (99.5%) of the catalyst for more than 24 h were observed, but slow deactivation of the system occurred after reaching stable conversion.

6.2.1.3 DAB Dendrimers as Soluble Supports

Commercially available DAB dendrimers of the fourth and fifth generation were functionalized with diphenylphosphino groups at the periphery by Reetz and co-workers [20]. The corresponding Pd complexes, such as **8**, were used for the Pd-catalyzed allylic amination between cinnamyl acetate and morpholine to yield *N*-(3-phenyl-2-propenyl)morpholine in a continuous membrane reactor (Scheme 6.7).

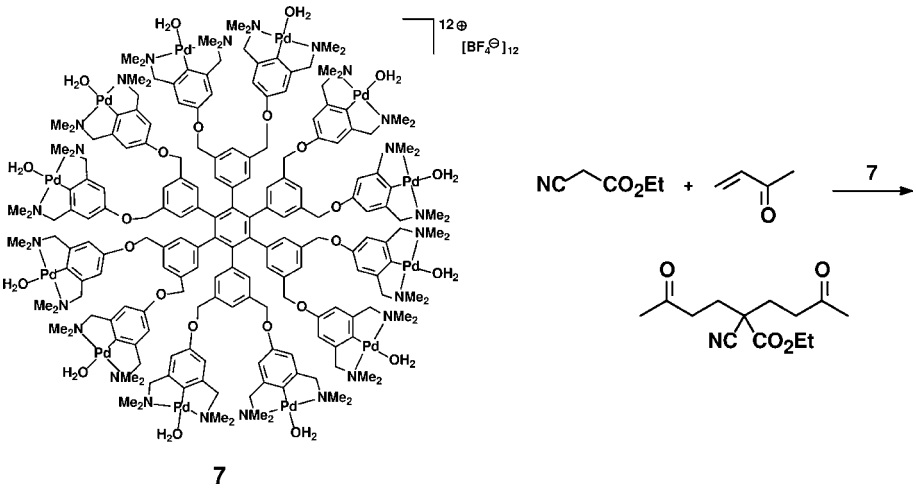

7

Scheme 6.6 Dendritic poly(benzyl ether)-based dodecakis (NCN–Pd^{II}) catalyst for Michael addition reactions.

Fourth- and fifth-generation phosphine-functionalized DAB dendrimers were applied, for which 100% conversion was obtained at the beginning. A 20% decrease was observed after 100 h and also palladium leaching between 0.07 and 0.14% per residence time. The soluble support, on the other hand, was completely retained in the membrane reactor.

6.2.1.4 PAMAM Dendrimers as Soluble Supports

Dendrimer-based organophosphites, organophosphonites and organophosphinites, such as **9**, and also their corresponding metal complexes, were described and patented by Tulchinsky and Miller for the hydroformylation of propene in batch processes [21]. The recovery of the catalysts by means of nanofiltration was described for phosphite-substituted PAMAM dendrimers of generations G0–G4 (Scheme 6.8).

After the hydroformylation run, the reaction mixture was passed through nanofiltration membranes (reverse osmosis) of the MPF-50 type or cross-linked GKSS membranes. The dendrimers were stable under hydroformylation conditions and no detectable amount of dendritic material was found in the permeate solutions. The highest retention for Rh (99.96%) was achieved by using GKSS (10 μm) membranes and the third-generation PAMAM dendrimer. Even higher Rh retentions and flux rates were found for nanofiltration experiments using a 50 Å ultrafiltration membrane and the fourth-generation PAMAM system (99.997%).

6.2.1.5 PPI Dendrimers as Soluble Supports

The first application of dendrimers in a thermomorphic system was described by Kaneda and co-workers [22]. Polypropylenimine (PPI) dendrimer-bound Pd(0) complexes of the type **10** were synthesized by reduction of dendritic Pd(II) systems with hydrazine and used for allylic substitution reactions (Scheme 6.9). The Pd complexes were efficiently recycled by running the reaction in a thermomorphic

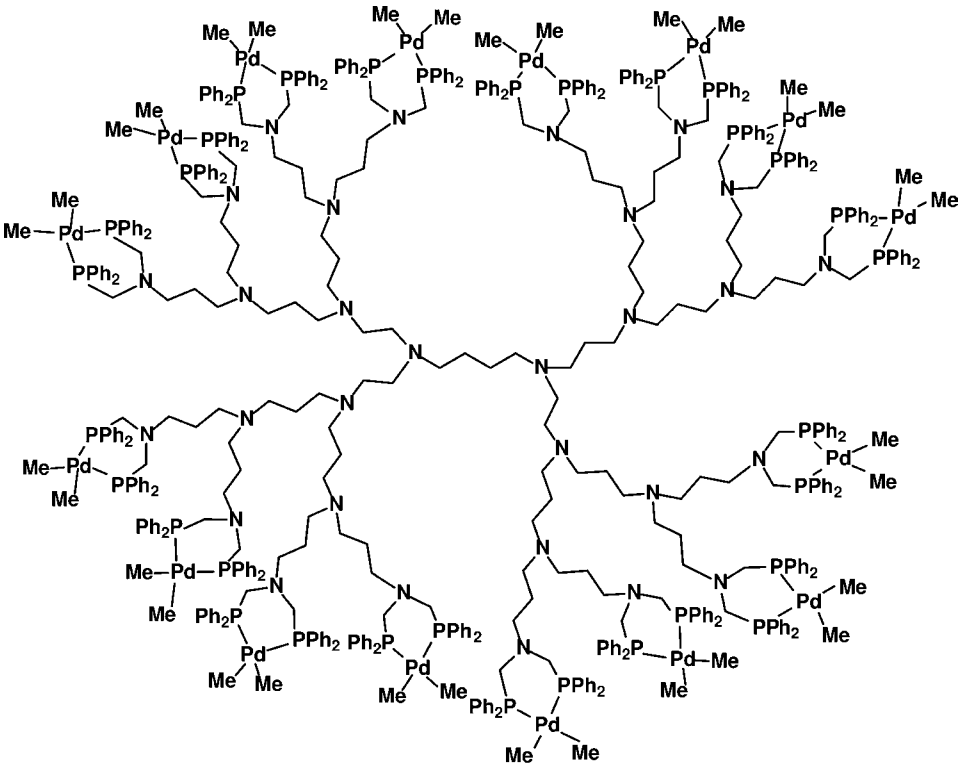

8

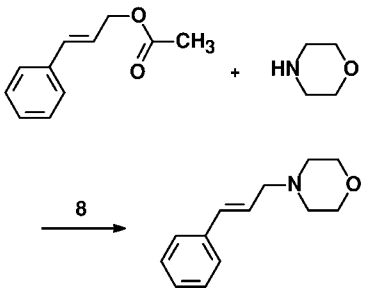

Scheme 6.7 DAB dendrimer-based Pd complexes for allylic amination reactions.

system at 75 °C; under these conditions, a biphasic system consisting of DMF and heptane became homogeneous. Phase separation occurred again by cooling the reaction medium to room temperature. The dendritic catalyst system was almost completely insoluble in heptane and was transferred to the polar DMF phase, while the heptane solution containing the products could easily be decanted. Furthermore, the stereoselectivity for the *cis*-product in the amination of *cis*-3-acetoxy-5-carbomethoxycyclohex-1-ene with morpholine increased with the generation of the

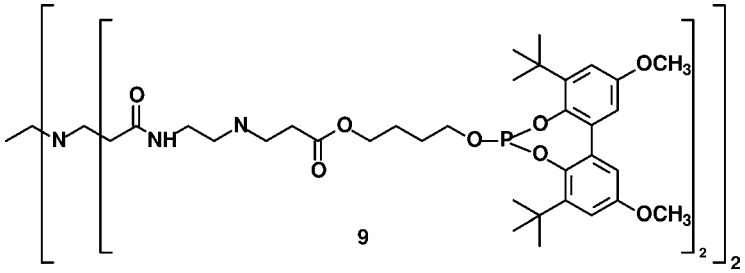

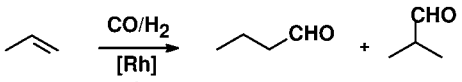

Scheme 6.8 PAMAM-based phosphite ligands for Rh-catalyzed hydroformylations.

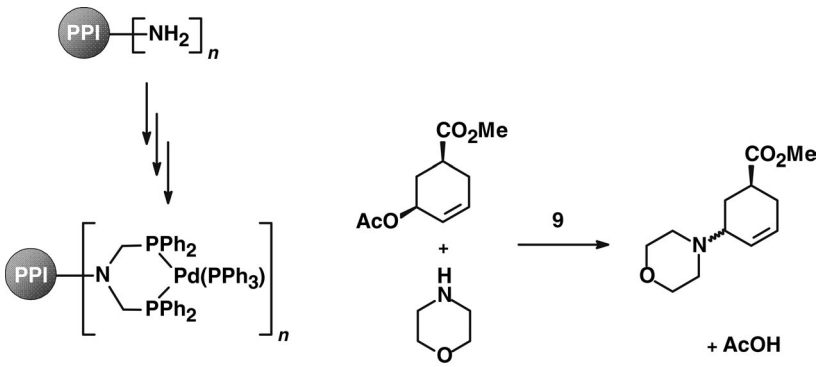

9 **a:** $n = 4$; **b:** $n = 16$; **c:** $n = 32$; **d:** $n = 64$

Scheme 6.9 Polypropylenimine (PPI) based Pd(0) complexes for allylic amination reactions.

dendrimers. Up to 94% *cis* selectivity was observed for the fifth-generation dendrimer, whereas only a slight excess of *cis*-product was observed for the non-supported $Pd(PPh_3)_4$ complex. As an explanation, steric congestion at the periphery of the dendrimer was suggested, which leads to steric steering of the nucleophilic attack to a surface (π-allyl)Pd intermediate and strongly shielding from the *endo* attack of the nucleophile at the active center.

6.2.2
Non-covalently Linked Dendrimer-bound Catalysts

Dendritic host–guest catalysts stabilized by hydrogen bonding and ionic interactions were studied by van Leeuwen and co-workers [23]. The non-covalently functionalized dendrimer **11** containing 32 phosphine ligands was generated by reaction of PPI dendrimers equipped with urea adamantyl groups and phosphorus ligands functionalized with urea acetic groups (Scheme 6.10).

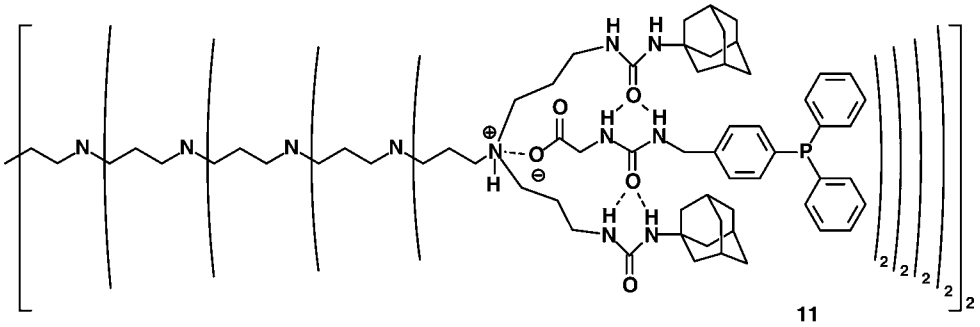

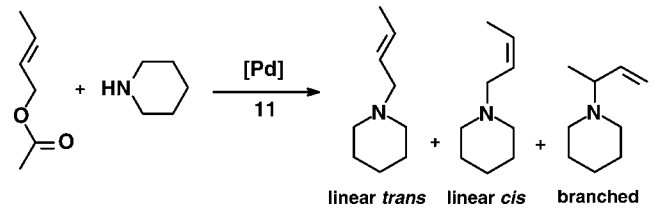

Scheme 6.10 Supramolecular host–guest complexes for Pd-catalyzed allylic amination reactions.

This supramolecular complex was applied in the Pd-catalyzed reaction between crotyl acetate and piperidine, showing a very fast reaction, which indicates that every active site on the dendrimer acts as an independent catalyst. Furthermore, the same selectivities were found compared with the unbound monomeric analogue. Under continuous conditions, a maximum conversion of approximately 80% was reached after 1.5 h and only a slight decrease in conversion was observed during the course of the experiment due to slow catalyst deactivation. Remarkably, a retention of 99.4% for the supramolecular host–guest–Pd complex was found, which demonstrates that the non-covalently assembled systems are indeed suitable soluble supports for continuous flow applications.

The immobilization of the perfluoro-tagged palladium catalyst **12** on a dendritic polyglycerol ester containing a perfluorinated shell was investigated by Haag and co-workers [24]. This supramolecular Pd complex showed good solubility in organic solvents and was applied in a Suzuki coupling reaction (Scheme 6.11). The supported

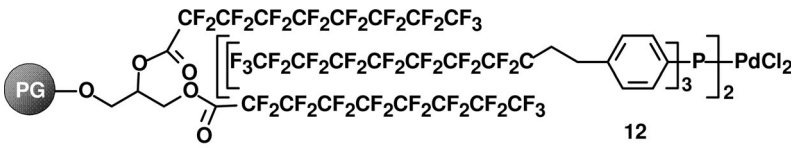

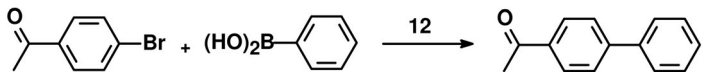

Scheme 6.11 Perfluorinated host–guest complexes for Pd-catalyzed Suzuki reactions.

catalyst could be separated from the product by simple precipitation using a DME–water mixture and recycling and multiple use proved to be straightforward.

6.3 Polymer-bound Homogeneous Catalysts

Because of the often tedious synthesis of dendrimers, many research groups are working on the use of polymers as supports for homogeneous catalysts. Polymers have the advantage of easy and cheap synthesis, while the resulting catalyst still often acts as a true homogeneous system without the problems usually related to heterogeneous systems such as mass transfer limitation and lower activity. First examples on the concept of binding catalytically active metal complexes to soluble supports were reported in the 1970s, when Rh-containing soluble polymers were successfully applied as hydrogenation catalysts [25]. Later, functionalized soluble polystyrenes [26], poly(ethylene glycol)s [27], poly(methyl methacrylate)s [28], polyvinylpyrrolidines [28], polyethene oligomers [28], poly(vinyl chloride)s [28], hyperbranched polymers [29] and polyelectrolytes [30] were applied as soluble polymeric supports for transition metal complexes. In this section, catalytic systems using polymeric supports and possible applications are discussed, with the focus on two concepts: covalently and electrostatically linked homogeneous catalysts. The immobilization of homogeneous catalysts on truly solid supports such as resins, fibers, silica and zeolites is outwith the scope of this chapter and will be mentioned only briefly.

6.3.1 Covalently Linked Polymer-bound Catalysts

6.3.1.1 Molecular Weight Enlargement for Continuous Homogeneous Catalysis

First attempts at the concept of binding catalytically active metal complexes to soluble supports were reported by Manassen in the early 1970s, where Rh-containing polymers were successfully applied as hydrogenation catalysts [25a] Soon afterwards, Bayer and Schurig reported the use of soluble polymers as supports for homogeneous catalysts [25b] They used non-cross-linked linear polystyrene (M_w ca 100 000), which was chloromethylated and converted by treatment with potassium diphenylphosphide into soluble polydiphenyl(styrylmethyl)phosphines. Soluble macromolecular metal complexes were prepared by addition of various metal precursors, e.g. $[Rh(PPh_3)Cl]$ (**13**) and $[RhH(CO)(PPh_3)_3]$ (**14**) (Scheme 6.12). 1-Pentene was hydroformylated to C_6-aldehydes (77% *n*-hexanal and 23% methylpentanal), without any hydrogenation, isomerization or hydrogenation to C_6 alcohols at 22 °C under 1 atm of H_2–CO. After 72 h, the reaction mixture was filtered through a polyamide membrane and the catalysts could be recycled. Instead of membrane filtration, the catalysts could also be separated by precipitation with *n*-hexane. The precipitates retained both their original solubility properties and, after re-dissolution, their catalytic activity. In the hydrogenation of 1-pentene at 22 °C and 1 atm of H_2, the reaction mixture was filtered through a polyamide membrane after 24 h (50% conversion in 3 h) and the

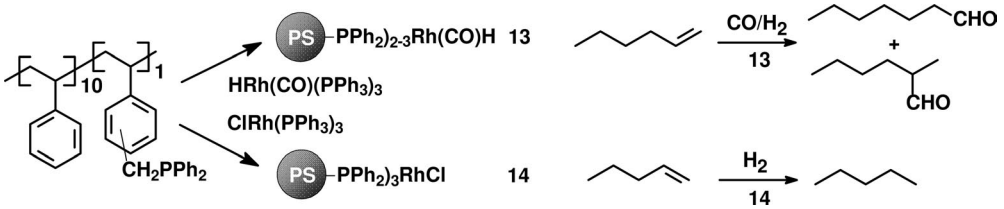

Scheme 6.12 Soluble polystyrene-based ligands for Rh-catalyzed hydroformylation and hydrogenation reactions.

catalyst could be retained quantitatively in the membrane filtration cell and was recycled five times.

Kragl and Dreisbach reported the asymmetric addition of diethylzinc to benzaldehyde using a chiral homogeneous catalyst of the type **15** supported on a soluble polymethacrylate (Scheme 6.13) [31]. α,α-Diphenyl-L-prolinol was bound to a copolymer from 2-hydroxyethyl methacrylate and octadecyl methacrylate forming a soluble catalyst with an M_w of 96 000.

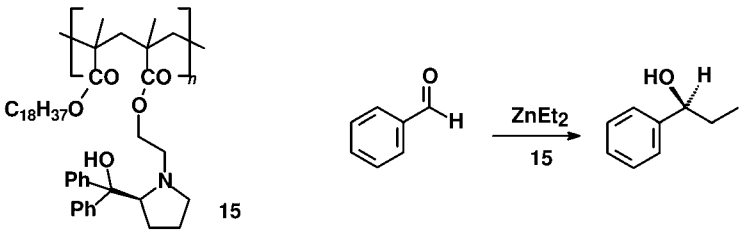

Scheme 6.13 Polymethacrylate-bound prolinol catalysts for diethylzinc addition reactions.

Membrane filtration using a polyaramide membrane showed a retention of more than 99.8%. Application of this catalyst in a continuously operated membrane reactor showed conversion for more than 150 h. The *ee* dropped from 80% at the beginning (non-bonded analogue 97%) to about 20% after 150 h. The average *ee* for the first 80 h was 50%.

Another soluble polymer-enlarged catalyst was synthesized and tested by Wandrey and co-workers [32]. The catalyst **16** was prepared by coupling of an oxazaborolidine via a hydrosilylation reaction to a methylhydrosiloxane–dimethylsiloxane copolymer (Scheme 6.14) and was used in the enantioselective borane reduction of ketones.

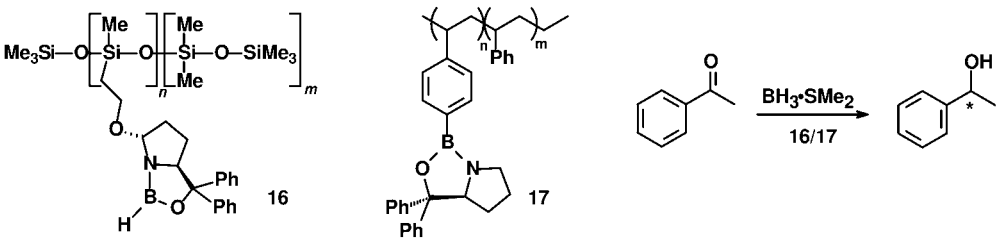

Scheme 6.14 Immobilized oxazaborolidines for borane reduction of ketones.

The reduction of acetophenone was carried out at room temperature, giving an 86% yield with an *ee* of 97%. This is similar to the *ee* obtained with unbound analogues. A limited study was conducted on the retention of the catalyst by nanofiltration. It was found that the compound could be retained in the membrane reactor but no specific details were given about these measurements.

The use of such an oxazaborolidine system in a continuously operated membrane reactor was demonstrated by Kragl and co-workers [33]. Various oxazaborolidine catalysts of the type **17** were prepared with polystyrene-based soluble supports. The catalysts were tested in a dead-end setup for the reduction of ketones (Scheme 6.14). These experiments showed higher *ee*s than batch experiments in which the ketone was added in one portion. The *ee*s vary from 84% for the reduction of propiophenone to up to >99% for the reduction of α-tetralone. The catalyst showed only a slight deactivation under the reaction conditions. The TTON could be increased from 10 for the monomeric system to 560 for the polymer-bound catalyst.

Liese and co-workers attached a transfer-hydrogenation catalyst to a soluble polymer and applied this system (**18**) in a continuously operated membrane reactor [34]. A Gao–Noyori catalyst was bound to a soluble polysiloxane polymer via a hydrosilylation reaction (Scheme 6.15).

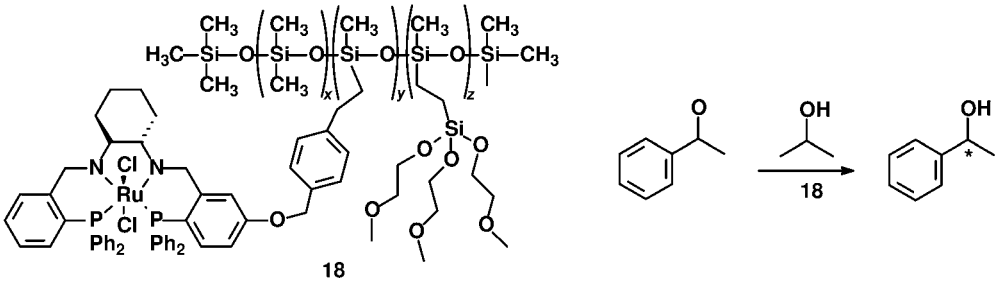

18

Scheme 6.15 Polysiloxane-immobilized Gao–Noyori catalyst for transfer-hydrogenation reactions.

Application of this system in the continuous transfer-hydrogenation reaction of acetophenone gave a stable conversion of about 87%, an *ee* of 94% and a space–time yield of 255 g L^{-1} d^{-1}. A continuous dosage of isopropoxide was necessary in order to compensate for deactivation caused by traces of water in the feed stream. Under these circumstances, a TTON of 2360 was reached. Comparison of this system with an enzymatic process showed that both approaches offer different advantages and are therefore complementary.

Plenio and co-workers tested the soluble polystyrene-bound adamantylphosphine ligand **19** (Scheme 6.16) in various palladium-catalyzed C−C coupling reactions [35]. The retentions of metal complexes of the polymer-bound phosphine ligand were determined to be higher than 99.95%.

A complex prepared from this ligand system and $[Pd(PhCN)_2Cl_2]$ was tested in Sonogashira coupling, showing high yields. After the reaction, the solution was filtered through a hydrophobic membrane composed of a dense polydimethylsiloxane layer cast on a porous sublayer of polyacrylonitrile. The catalyst was recycled

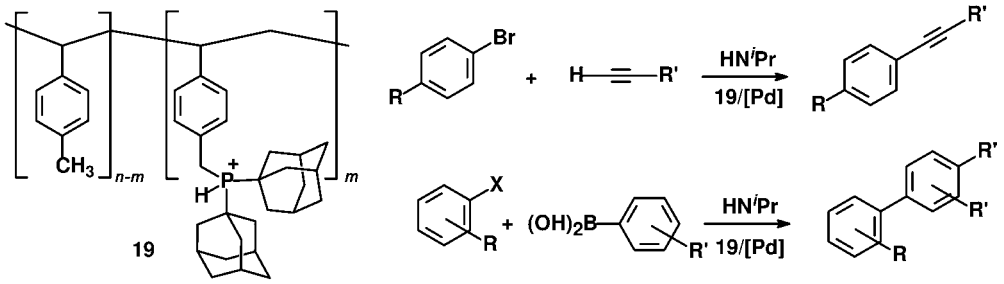

Scheme 6.16 Polystyrene-bound phosphines for Pd-catalyzed C–C coupling reactions.

seven times, resulting in a slight decrease in conversion from 98 to 80% in the last cycle. The $Pd(OAc)_2$ complexes of the same polymeric ligand were tested in Suzuki coupling, also showing high yields with a slowly decreasing conversion over multiple cycles. Using $[Pd(dba)_2]$ as the metal source, the system was tested in the Heck coupling reaction. Yields between 87 and 80% were obtained. However, on attempting the nanofiltration of the NMP solution, the membrane immediately suffered severe damage. No suitable solvent could be found for this system. Nanofiltration experiments were conducted with the NMP solutions diluted with large amounts of cyclohexane. However, low yields and deactivation of the catalyst resulted.

Van Koten and co-workers used a hyperbranched polytriallylsilane as the support for palladium-pincer complexes [36]. The supported palladium-pincer complexes of the type **20** were applied in the catalytic aldol condensation of benzaldehyde and methyl isocyanate (Scheme 6.17). Their activity was similar to that of single-site Pd catalysts. The hyperbranched polymeric systems showed similar properties to

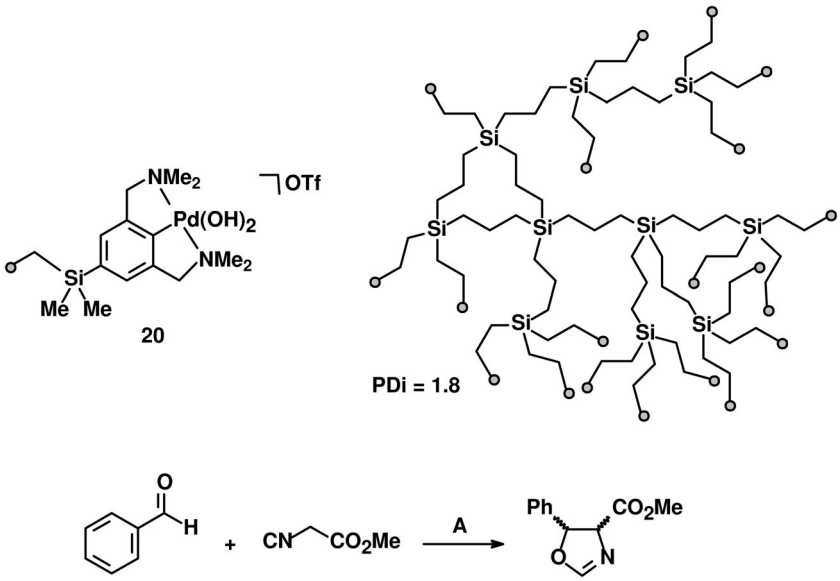

Scheme 6.17 Hyperbranched polysilane support for Pd-catalyzed aldol condensations.

analogous dendritic compounds, indicating that structural perfection is not always required. The polymers were purified by means of dialysis, showing a potential application in continuous flow membrane reactors.

Yao [37] described stable and soluble poly(ethylene glycol)-bound Ru catalysts of the type **21** for the ring-closing metathesis (RCM) of a variety of α,ω-dienes (Scheme 6.18). Bidentate non-phosphine ligands are in fact promising candidates for the recycling of Ru–carbene complexes, since the formation of chelates is entropically favored at the end of the reaction.

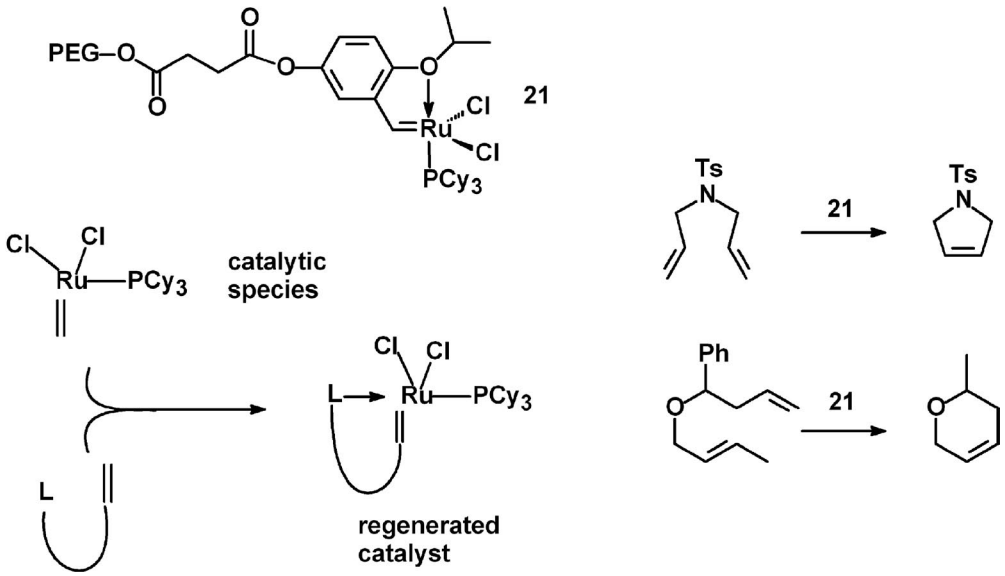

Scheme 6.18 Poly(ethylene glycol)-supported Ru catalyst for ring-closing metathesis reactions.

Indeed, Ru complexes which could be repeatedly reused in the metathesis of various diene substrates could be prepared and showed only a slight decrease in activity during recycle experiments. However, this concept cannot be applied for continuous conditions: the intermediate in the ring-closing metathesis reaction is not necessarily bound to the chelate, because one ligand has to dissociate from the Ru center in order to provide a free coordination site for the incoming alkene. Therefore, a constant stream of substrate would ultimately lead to a loss of catalyst across the membrane.

Similar to this concept is the recycling of polymer-supported organolanthanide hydroamination catalysts, reported by Zhao and Marks [38]. Complexes of the type $Cp'_2SmCH(SiMe_3)_2$, $Cp'_2LaCH(SiMe_3)_2$ ($Cp' = \eta^5$-Me_5C_5) and CGCSmN $(SiMe_3)_2$ {CGC = $Me_2Si[(\eta^5$-$Me_4C_5)(^tBuN)]$} were immobilized on a series of divinylbenzene cross-linked amino-functionalized polystyrene resins such as aminomethylated polystyrenes of varying mesh size and used for the intramolecular hydroamination/cyclization reaction (Scheme 6.19). During the catalytic cycle, the metal complex is released from the support, functioning as a true homogeneous

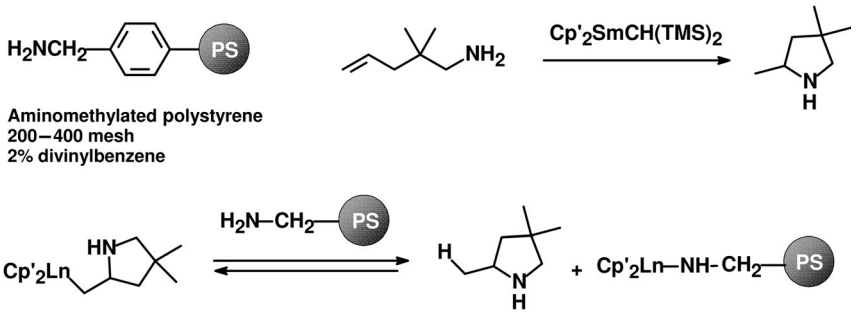

Scheme 6.19 Polymer-supported organolanthanide catalyst for intramolecular hydroamination/cyclization reactions.

catalyst with consequently comparable activities. Upon substrate consumption, the catalysts were readsorbed on the solid supports and could be recycled with only minor to moderate loss of activity.

Soluble, poly(ethylene glycol)-supported bisoxazolines of the type **22** were used as ligands for enantioselective Diels–Alder reactions, and also for cyclopropanation and ene reactions (Scheme 6.20) [39].

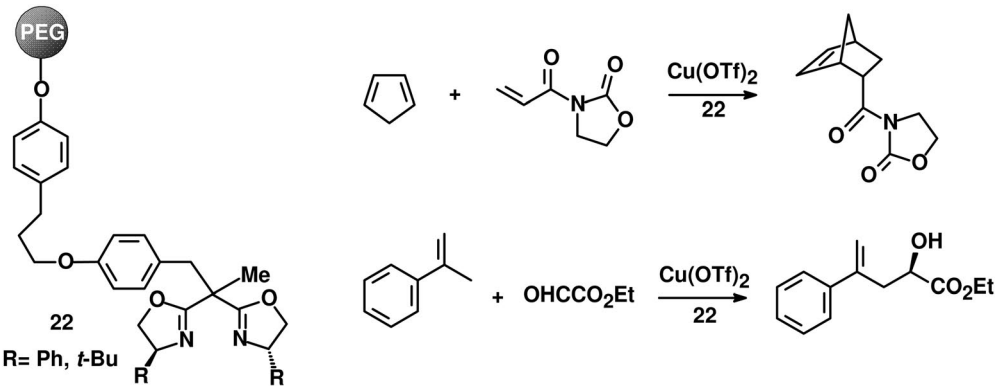

Scheme 6.20 Poly(ethylene glycol)-supported bisoxazolines for Cu-catalyzed cyclopropanation and ene reactions.

In combination with Cu(II) and Cu(I) salts, the polymer-anchored enantiomerically pure bisoxazolines showed only poor enantioselectivity in the Diels–Alder cycloaddition between *N*-acryloyloxazolidinone and cyclopentadiene (up to 45% *ee*). Better stereocontrol was found in the cyclopropanations of styrene and 1,1-diphenylethene with ethyl diazoacetate (up to 93% *ee*) and in the ene reactions between ethyl glyoxalate and α-methylstyrene or methylenecyclohexane (up to 95% *ee*), which was comparable to the structurally related, unsupported ligands. Only a slight decrease in activity and in stereocontrol was observed upon recovery and recycling of the catalyst. The catalytic transformations were as efficient as performed with corresponding catalysts supported on insoluble polymers.

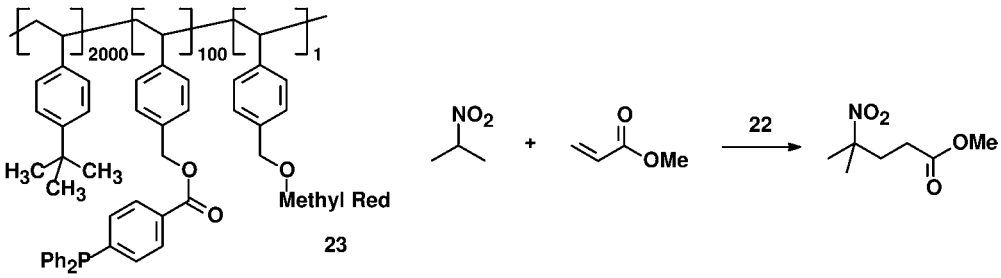

Scheme 6.21 Poly(4-*tert*-butylstyrene) copolymers as nucleophilic catalysts for Michael addition reactions.

Michael additions of 2-nitropropane to methyl acrylate with soluble, triphenylphosphine-functionalized poly(4-*tert*-butylstyrene) copolymers (**23**) as nucleophilic catalysts were investigated by Bergbreiter and Li (Scheme 6.21) [26b].

The catalytic reactions were performed in a monophasic system consisting of a mixture of ethanol and heptane at room temperature. After 24 h, a small amount of water was added and phase separation occurred. With this water-induced liquid–liquid-phase separation, the polymeric catalyst could be recycled and successfully applied again in a catalytic cycle. UV–visible spectroscopy showed that the catalyst was quantitatively dissolved in the apolar, heptane-rich phase.

6.3.1.2 Soluble Polymer-supported Catalysts for Liquid–Liquid Recovery of Catalysts

A very elegant strategy to design recoverable catalysts is the use of polymers that show phase-selective solubility under biphasic conditions. Soluble polymer-supported homogeneous catalysts can be applied under biphasic reaction conditions by making use of, for example, aqueous–organic (see below), fluorous–organic or other biphasic systems [40]. Alternatively, thermomorphic or latent biphasic systems can be used under monophasic reaction conditions if the mixture is heated to the upper critical solution temperature (UCTS), leading to a homogeneous solution. After completion of the reaction, phase separation occurs upon cooling to ambient temperature and the catalyst can be recovered.

Water as perhaps the most environmentally benign solvent has been considered to be an ideal reaction medium for this purpose. Due to the high partition coefficient between water and most organic solvents, ideal separation often occurs under biphasic reaction conditions. Jin and co-workers used thermoregulated phase-transfer catalysts for the hydroformylation of higher olefins in an aqueous–organic biphasic system (Figure 6.2) [41]. Due to a thermoregulated solubility, their solubility in water decreases as the temperature increases. In the presence of an organic solvent, the soluble polymer-supported catalysts moves form the aqueous phase to the organic phase as a function of temperature. This property is very attractive because mass transfer limitations are eliminated since the polymer-supported catalyst is soluble in the same phase as the substrate. Upon cooling, the catalyst moves back into the water phase allowing easy separation of the product from the catalyst.

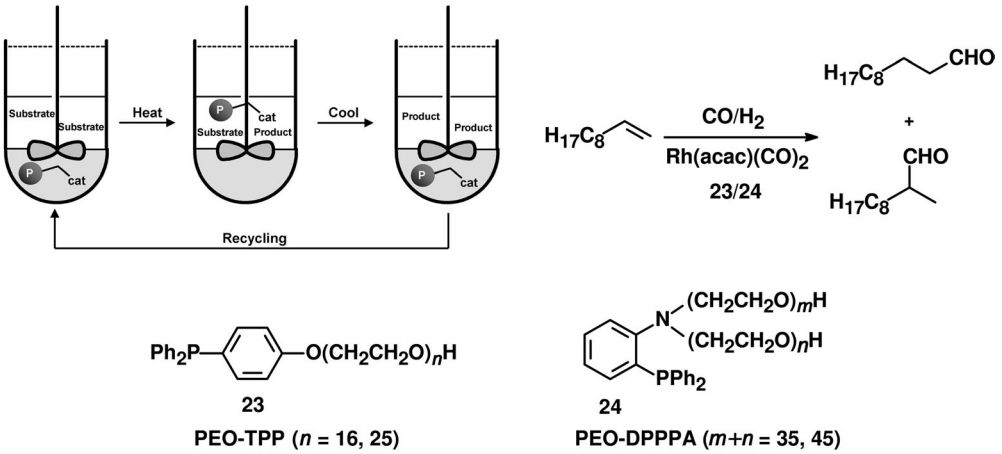

Figure 6.2 Thermoregulated phase-transfer catalysts for the hydroformylation of higher olefins.

Several non-ionic water-soluble triphenylphosphine derivatives have been reported by Jin and co-workers, which are substituted by polyoxyethene moieties as hydrophilic groups (e.g. **23**, **24**; Figure 6.2) [41] These ligands demonstrate inverse temperature-dependent solubility in water, similar to that of non-ionic surfactants. At room temperature, their metal complexes are soluble in water, whereas they become soluble in an organic phase at higher temperature. In the Rh-catalyzed hydroformylation of higher olefins, such as 1-decene, good activities (TOF = 470 h^{-1}, conversion 94.6%, time = 2 h, T = 120 °C, l/b = 0.64) were reached with the system Rh–DPPPA in the solvent mixture H_2O–toluene.

Thermomorphic systems are systems which are miscible at higher temperature, but immiscible at lower temperature. As an example, mixtures of heptane with polar solvents such as *N*,*N*-dimethylformamide, *N*,*N*-dimethylacetamide and 90% aqueous ethanol are biphasic at 25 °C but are monophasic at 70 °C. Using these phenomena in homogeneous catalysis thus allows reactions in a completely homogeneous environment, avoiding at the same time mass-transfer limitations in combination with easy catalyst separation under biphasic conditions. Bergbreiter *et al.* developed this concept by making use of the temperature-dependent solubility of polymeric phosphine ligands. Early work reported on Rh(I) complexes, which were immobilized on poly(*N*-isopropylacrylamide) (PNIPAM) to produce supported versions of Wilkinson's catalysts **25** [42]. These catalysts were applied in the hydrogenation of 1-octadecene or 1-dodecene in a heptane–90% aqueous ethanol thermomorphic system (Figure 6.3). The soluble polymer-bound catalyst had comparable activity to the low molecular weight analogue and the polymeric catalyst could be recycled four times with no decrease in catalytic activity.

This concept has been extended to other catalytic C−C coupling reactions, oxidations and hydrogenation reactions, such as Pd-catalyzed cross-coupling and allylic substitution reactions, Rh-catalyzed hydroformylations and Ru-catalyzed Kharasch reactions, with satisfactory activities, recyclability and little catalyst loss [5a] Nevertheless, it should be kept in mind that the preparation of these catalyst

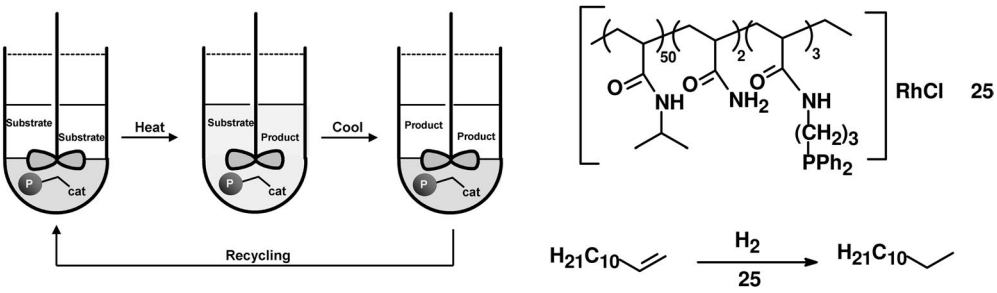

Figure 6.3 Thermomorphic systems for Rh-catalyzed hydrogenation reactions.

systems is generally time consuming and that classical homogeneous catalysts have also been applied in temperature-dependent multicomponent solvent systems with efficient catalyst recycling properties [43].

6.3.2
Electrostatically Bound Catalysts

The immobilization of homogeneous catalysts via electrostatic interactions with a suitable support, rather than covalent tethering, is a very attractive strategy as it circumvents the need for time-consuming and often difficult ligand modification [44]. Anchoring transition metal compounds via non-covalent binding to polymeric supports has attracted relatively little attention to date.

To avoid even the synthetic challenges associated with the introduction of ionic substituents in (phosphine) ligands, Vogt and co-workers investigated the concept of non-covalent binding of a transition metal complex carrying a cationic charge on the metal itself [45]. The catalyst carriers, based on a polymerizable borate anion, were easily obtained as stable and redispersible polystyrene latices **26** (Figure 6.4; see also

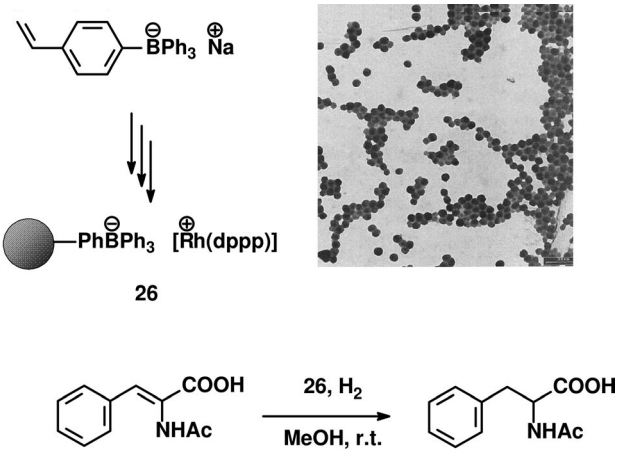

Figure 6.4 Borate-containing polystyrene latices as supports for cationic Rh hydrogenation catalysts.

the TEM image in the inset) by aqueous emulsion polymerization. As a first proof of principle in terms of applicability, the authors showed that a rhodium complex supported on coagulated latex has constant catalytic activity in the hydrogenation of a model substrate during several recycles, with very low metal leaching (Figure 6.4). Future work is focusing on asymmetric hydrogenation, exploring the full scope of this approach and on the use of functionalized latices in continuously operated membrane reactors.

Schwab and Mecking also reported on hydroformylation reactions with Rh (I) complexes electrostatically fixed to soluble polyelectrolytes of the type **27** (Scheme 6.22) [30]. The non-covalently bound catalyst was prepared by reacting poly(diallyldimethylammonium chloride) (PDADMA-Cl) with $NaBAr^F$ to form PDAMA-BAr^F. By reaction with $[HRh(CO)(NaTPPTS)_3]$, multiple BAr^{F-} anions were exchanged and a methanol-soluble polymer with electrostatically bound Rh(I) fragments was thus generated. In the hydroformylation of 1-hexene, an activity in the range $TOF = 160\,mol\,h^{-1}$ was found, which is comparable to a non-supported catalyst. The catalyst was subsequently separated from the products by means of ultrafiltration, using a poly(ether sulfone) membrane supplied by Sartorius with a molecular weight cutoff (MWCO) of 50 kDa. Interestingly, a retention of 99.8% was found and repetitive recycling experiments in which virtually the same catalytic activity was observed showed a 2–7% loss of rhodium, most likely due to partial oxidation of the phosphine ligand.

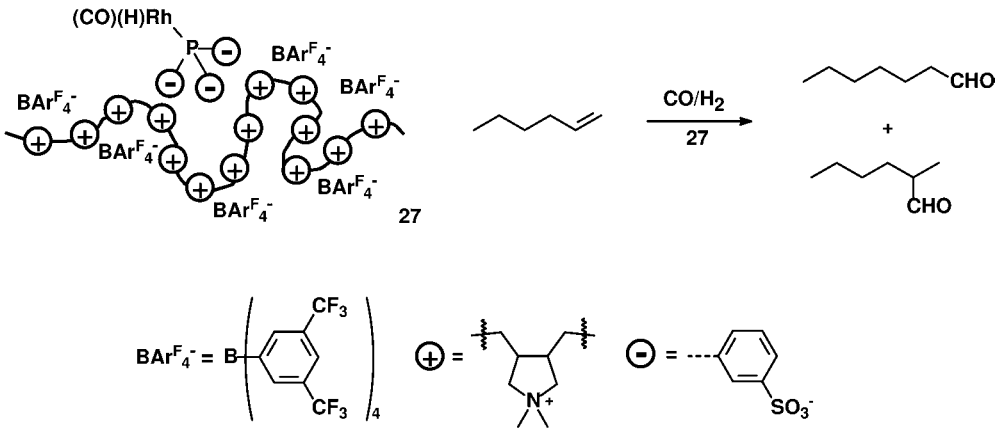

Scheme 6.22 Polyelectrolytes as ionic support for Rh hydroformylation catalysts.

Zr(IV)–Fe(III) catalysts of the type **28** immobilized on *N*-(polystyrylbutyl) pyridinium triflylimides were reported by Ishihara and co-workers [46]. These solid catalysts were used for the esterification of an equimolar mixture of carboxylic acids and alcohols and could be reused repeatedly without any loss of activity. Interestingly, it was found that the Zr(IV)–Fe(III) catalyst was released from the supporting polystyrene polymer in the presence of the carboxylic acid, acting as a homogeneous catalyst. After full consumption of the substrates the catalyst was re-immobilized on its support and could thus be recycled (Scheme 6.23).

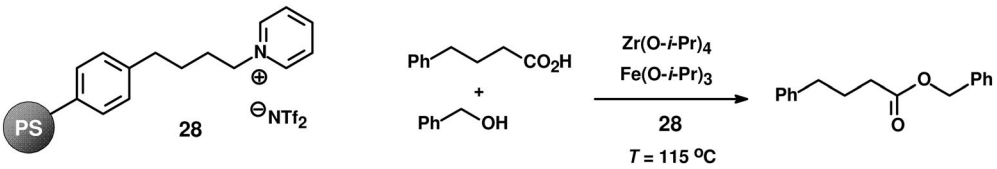

Scheme 6.23 *N*-(Polystyrylbutyl)pyridinium triflylimide-supported Zr(IV)–Fe(III) catalysts for esterification.

The possibility of polystyrene-based latices acting as phase-transfer agents in the aqueous-phase hydroformylation of 1-octene was investigated by Vogt and co-workers [47]. Polystyrene-based latices composed of different styryl salts (**29**) showed a significant influence on the conversion of 1-octene. In the absence of any latex particles, the hydroformylation of 1-octene with $CO-H_2$ (1 : 1) in water using NaTPPTS–[Rh(acac)$(CO)_2$] at 80 °C and 20 bar pressure showed no conversion at all. The addition of **29.1a** to the reaction mixture increased the conversion of 1-octene to 9% during the 140 h reaction time and with **29.1b** to 11%. Interestingly, when the same reaction was carried out using **29.1c** as phase-transfer agent, the conversion of 1-octene increased to 70%. By using a higher amount of phase-transfer agent, the conversion of 1-octene increased to 100% with an observed turnover frequency of 150 h^{-1} (Figure 6.5). The observed strikingly better performance of the styrylammonium-modified latex may be explained by a preferred association of the sulfonated

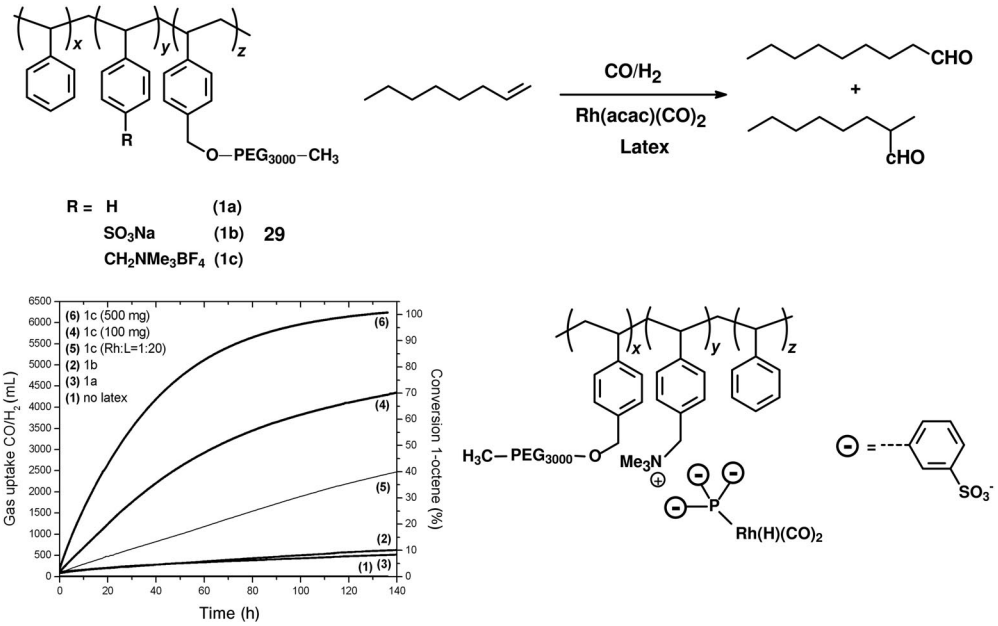

Figure 6.5 Polystyrene-based latices as phase transfer agents in the aqueous-phase hydroformylation of 1-octene.

catalyst complex with these latex particles, thereby associating the catalyst with the phase-transfer agent and thus enhancing the hydroformylation reaction. This association might be described as a combination of electrostatic, van der Waals and hydrophobic interactions. These catalytic systems might provide new options in the field of continuous aqueous organometallic catalysis.

6.4 Conclusion and Outlook

Over recent years, the knowledge about immobilized catalyst systems has increased considerably. Most of the time, this development has been curiosity driven and performed by academic groups. However, with an ever-growing interest in sustainable production methods, making more efficient use of raw materials and reducing waste production, industry has become aware of the economic benefits that process intensification can bring about. Rapidly increasing prices of most metals, not only noble metals, used as catalysts, incidentally contribute to the development and acceptance of new catalysis technologies. Also, the fast development of solvent-resistant membrane materials in recent years has helped to spur this process. For the near future, we foresee the implementation of a number of commercial applications of homogeneous catalyst immobilization and compartmentalization. Recently, Evonik Oxeno has announced a pilot production-scale commercial use of organophilic membranes for the immobilization of Rh catalysts on a large industrial scale [48]. Even with retentions of only slightly more than 90%, this can be feasible at a rhodium price of now more than €120 000 kg^{-1}. A lot more research has to be carried out both in academia and in industrial research laboratories to develop this methodology to its full potential. We should keep in mind that for the problem of homogeneous catalyst recovery and recycling, there is no such thing as the ultimate method. Typically, each process, meaning not only a certain type of conversion, but each substrate and product, might need a different approach. Therefore, a whole range of generic procedures are needed to tackle the demands of new technology because undoubtedly catalysis is the key technology for the future of chemical production.

References

1 (a) Cornils, B. and Herrmann, W.A. (2002) *Applied Homogeneous Catalysis with Organometallic Compounds*, 2nd edn, Wiley-VCH Verlag GmbH; (b) Vogt, D. (2004) in *Aqueous Phase Organometallic Catalysis – Concepts and Application*, 2nd edn (eds Cornils, B. and Herrmann, W.A.), Wiley-VCH Verlag GmbH, pp. 541–547.

2 (a) Hamers, B., Bäuerlein, P., Müller, C. and Vogt, D. (2008) Advanced Synthesis and Catalysis, **350**, 322. (b) Wasserscheid, P. and Keim, W. (2000) *Angewandte Chemie-International Edition*, **39**, 3772; (c) Bronger, R.P.J., Silva, S.M., Kamer, P.C.J. and van Leeuwen, P.W.N.M. (2004) *Dalton Transactions*, **10**, 1590; (d) Silva, S.M., Bronger, R.P.J., Freixa, Z., Dupont, J. and van Leeuwen, P.W.N.M. (2003) *New Journal of Chemistry*, **27**, 1294; (e) Wang, Y.Y., Luo, M.M., Lin, Q., Chen,

H. and Li, X.J. (2006) *Green Chemistry*, **8**, 545; (f) Miao, W. and Chan, T.H. (2006) *Accounts of Chemical Research*, **39**, 897.

3 Corma, A. and Garcia, H. (2006) *Advanced Synthesis and Catalysis*, **348**, 1391.

4 (a) Bektesevic, S., Tack, T., Mason, M.R. and Abraham, M.A. (2005) *Industrial & Engineering Chemistry Research*, **44**, 4973; (b) Stephenson, P., Kondor, B., Licence, P., Scovell, K., Ross, S.K. and Poliakoff, M., (2006) *Advanced Synthesis and Catalysis*, **348**, 1605.

5 (a) Bergbreiter, D.E. (2002) *Chemical Reviews*, **102**, 3345; (b) Bräse, S., Lauterwasser, F. and Ziegert, R.E. (2003) *Advanced Synthesis and Catalysis*, **345**, 869; (c) McNamara, C.A., Dixon, M.J. and Bradley, M. (2002) *Chemical Reviews*, **102**, 3275; (d) Dijkstra, H.P., van Klink, G.P.M. and van Koten, G. (2002) *Accounts of Chemical Research*, **35**, 798; (e) Wöltinger, J., Drauz, K. and Bommarius, A.S. (2001) *Applied Catalysis A-General*, **221**, 171; (f) Cole-Hamilton, D.J. (2003) *Science*, **299**, 1702; (g) Fan, Q.-H., Li, Y.-M. and Chan, A.S.C. (2002) *Chemical Reviews*, **102**, 3385; (h) van Heerbeek, R., Kamer, P.C.J., van Leeuwen, P.W.N.M. and Reek, J.N.H. (2002) *Chemical Reviews*, **102**, 3717; (i) Oosterom, G.E., Reek, J.N.H., Kamer, P.C.J. and van Leeuwen, P.W.N.M. (2001) *Angewandte Chemie-International Edition*, **40**, 1828; (j) Müller, C. and Vogt, D. (2005) *European Journal of Inorganic Chemistry*, 4011; (k) Müller, C. and Vogt, D. (2005) in *Multiphase Homogeneous Catalysis* (eds B. Cornils, W.A. Herrmann, I.T. Horváth, W. Leitner, S.Mecking, H. Olivier-Bourbigou and D. Vogt), Wiley-VCH Verlag GmbH, Weinheim, Chapter 7. 4. 1, pp. 776–793; (l) Ronde, N.J. and Vogt, D. (2005) in *Recovery and Recycling of Homogeneous Catalysts* (eds D. Cole-Hamilton and R.P.Tooze), Springer, Berlin, Chapter 4, pp. 73–104; (m) Dioos, B.M.L., Vankelecom, I.F.J. and Jacobs, P.A. (2006) *Advanced Synthesis and Catalysis*, **348**, 1413.

6 Buhleier, E., Wehner, W. and Vögtle, F. (1978) *Synthesis*, 155.

7 Knapen, J.W.J., van der Made, A.W., de Wilde, J.C., van Leeuwen, P.W.N.M., Wijkens, P. and Grov, D.M. (1994) *Nature*, **372**, 659.

8 Schenning, A.P.H.J., Elissen-Roman, C., Weener, J.-W., Baars, M.W.P.L., van der Gaast, S.J. and Meijer, E.W. (1998) *Journal of the American Chemical Society*, **120**, 8199.

9 Ulman, M. and Grubbs, R.H. (1999) *The Journal of Organic Chemistry*, **64**, 7202.

10 Mukhopadhyah, S., Rothenberg, G., Gitis, D. and Sasson, Y. (2000) *The Journal of Organic Chemistry*, **65**, 3107.

11 van de Kuil, L.A., Grove, D.M., Gossage, R.A., Zwikker, J.W., Jenneskens, L.W., Drenth, W. and van Koten, G. (1997) *Organometallics*, **16**, 4985.

12 (a) Dijkstra, H.P., van Klink, G.P.M. and van Koten, G. (2002) *Accounts of Chemical Research*, **35**, 798; (b) van Heerbeek, R., Kamer, P.C.J., van Leeuwen, P.W.N.M. and Reek, J.N.H. (2002) *Chemical Reviews*, **102**, 3717; (c) Oosterom, G.E., Reek, J.N.H., Kamer, P.C.J. and van Leeuwen, P.W.N.M. (2001) *Angewandte Chemie-International Edition*, **40**, 1828; (d) Frey, H. and Schlenk, C. (2000) *Topics in Current Chemistry*, **210**, 69–129.

13 (a) van Koten, G. and Jastrzebski, J.T.B.H. (1999) *Journal of Molecular Catalysis A-Chemical*, **146**, 317; (b) Kleij, A.W., Gossage, R.A., Jastrzebski, J.T.B.H., Boersma, J. and van Koten, G. (2000) *Angewandte Chemie-International Edition*, **39**, 176; (c) Kleij, A.W., Gossage, R.A., Klein Gebbink, R.J.M., Brinkmann, N., Reijerse, E.J., Kragl, U., Lutz, M., Spek, A.L. and van Koten, G. (2000) *Journal of the American Chemical Society*, **122**, 12112.

14 (a) Hovestad, N.J., Eggeling, E.B., Heidbüchel, H.J., Jastrzebski, J.T.B.H., Kragl, U., Keim, W., Vogt, D. and van Koten, G. (1999) *Angewandte Chemie-International Edition*, **38**, 1655; (b) Eggeling, E.B., Hovestad, N.J., Jastrzebski, J.T.B.H., Vogt, D. and van Koten, G. (2000) *The Journal of Organic Chemistry*, **65**, 8857.

15 Oosterom, G.E., Steffens, S., Reek, J.N.H., Kamer, P.C.J. and van Leeuwen, P.W.N.M. (2002) *Topics in Catalysis*, **19**, 61.

16 Müller, C., Ackerman, L., Reek, J.N.H., Kamer, P.C.J. and van Leeuwen, P.W.N.M. (2004) *Journal of the American Chemical Society*, **126**, 14960.

17 Detz, R.J., Arévalo Heras, S., De Gelder, R., Van Leeuwen, P.W.N.M., Hiemstra, H., Reek, J.N.H. and Van Maarseveen, J.H. (2006) *Organic Letters*, **8**, 3227.

18 (a) Bolm, C., Derrien, N. and Seger, A. (1996) *Synlett*, 387; (b) Bom, C., Dinter, C.L., Seger, A., Höcker, H. and Brozio, J. (1999) *The Journal of Organic Chemistry*, **64**, 5730.

19 Dijkstra, H.P., Ronde, N.J., van Klink, G.P.M., Vogt, D. and van Koten, G. (2003) *Advanced Synthesis and Catalysis*, **345**, 364.

20 Brinkmann, N., Giebel, D., Lohmer, G., Reetz, M.T. and Kragl, U. (1999) *Journal of Catalysis*, **183**, 163.

21 (a) Tulchinsky, M.L. and Miller, D.J. (2002) US Patent 6 350 819; (b) (2002) *Chemical Abstracts*, **136**, 200619.

22 Mizugaki, T., Murata, M., Ooe, M., Ebitani, K. and Kaneda, K. (2002) *Chemical Communications*, 52.

23 de Groot, D., de Waal, B.F.M., Reek, J.N.H., Schenning, A.P.H.J., Kamer, P.C.J., Meijer, E.W. and van Leeuwen, P.W.N.M. (2001) *Journal of the American Chemical Society*, **123**, 8453.

24 Garcia-Bernabe, A., Tzschucke, C.C., Bannwarth, W. and Haag, R. (2005) *Advanced Synthesis and Catalysis*, **347**, 1389.

25 (a) Manassen, J. (1971) *Platinum Metals Review*, **15**, 142; (b) Bayer, E. and Schurig, V. (1975) *Angewandte Chemie-International Edition*, **14**, 493.

26 (a) McNamara, C.A., Dixon, M.J. and Bradley, M. (2002) *Chemical Reviews*, **102**, 3275; (b) Bergbreiter, D.E. and Li, C. (2003) *Organic Letters*, **5**, 2445.

27 (a) Yao, Q. (2000) *Angewandte Chemie-International Edition*, **39**, 3896; (b) Annunziata, R., Benaglia, M., Cinquini, M., Cozzi, F. and Pitillo, M. (2001) *The Journal of Organic Chemistry*, **66**, 3160.

28 Bergbreiter, D.E. (2002) *Chemical Reviews*, **102**, 3345.

29 (a) Bolm, C., Derrien, N. and Seger, A. (1996) *Synlett*, 387; (b) Bolm, C., Dinter, C.L., Seger, A., Höcker, H. and Brozio, J. (1999) *The Journal of Organic Chemistry*, **64**, 5730; (c) Schlenk, C., Kleij, A.W., Frey, H. and van Koten, G. (2000) *Angewandte Chemie-International Edition*, **39**, 3445.

30 Schwab, E. and Mecking, S. (2001) *Organometallics*, **20**, 5504.

31 Kragl, U. and Dreisbach, C. (1996) *Angewandte Chemie-International Edition*, **108**, 684.

32 Felder, M., Giffels, G. and Wandrey, C. (1997) *Tetrahedron: Asymmetry*, **8**. 1975.

33 Giffels, G., Beliczey, J., Felder, M. and Kragl, U. (1998) *Tetrahedron: Asymmetry*, **9**, 691.

34 Laue, S., Greiner, L., Wöltinger, J. and Liese, A. (2001) *Advanced Synthesis and Catalysis*, **343**, 711.

35 Datta, A., Ebert, K. and Plenio, H. (2003) *Organometallics*, **22**, 4685.

36 Schlenk, C., Kleij, A.W., Frey, H. and van Koten G. (2000) *Angewandte Chemie-International Edition*, **39**, 3445.

37 Yao, Q. (2000) *Angewandte Chemie-International Edition*, **39**, 3896.

38 Zhao, J. and Marks, T.J. (2006) *Organometallics*, **25**, 4763.

39 Annunziata, R., Benaglia, M., Cinquini, M., Cozzi, F. and Pitillo, M. (2001) *The Journal of Organic Chemistry*, **66**, 3160.

40 Bergbreiter, D.E. and Sung, S.D. (2006) *Advanced Synthesis and Catalysis*, **348**, 1352.

41 (a) Wang, Y., Jiang, J., Miao, Q., Wu, X. and Jin, Z. (2002) *Catalysis Today*, **74**, 85; (b) Liu, C., Jiang, J., Wang, Y., Cheng, F. and Jin, Z. (2003) *Journal of Molecular Catalysis A-Chemical*, **198**, 23.

42 Bergbreiter, D.E., Liu, Y.S. and Osburn, P.L. (1998) *Journal of the American Chemical Society*, **120**, 4250.

43 Behr, A., Henze, G. and Schomäcker, R. (2006) *Advanced Synthesis and Catalysis*, **348**, 1485.

44 (a) Augustine, R., Tanielyan, S., Anderson, S. and Yang, H. (1999) *Chemical*

Communications, 1257; (b) Simons, C., Hanefeld, U., Arends, I.W.C.E., Sheldon, R.A. and Maschmeyer, T. (2004) *Chemistry - A European Journal*, **10**, 5829.

45 Sablong, R., van der Vlugt, J.I., Thomann, R., Mecking, S. and Vogt, D. (2005) *Advanced Synthesis and Catalysis*, **347**, 633.

46 Nakamura, Y., Maki, T., Wang, X., Ishihara, K. and Yamamoto, H. (2006) *Advanced Synthesis and Catalysis*, **348**, 1505.

47 Kunna, K., Müller, C., Loos, J. and Vogt, D. (2006) *Angewandte Chemie-International Edition*, **45**, 7289.

48 (a) Wiese, K.-D., Baumgarten, G., Kuppinger, F.-F., Möller, O., Ortmann, D., Borgmann, C. and Büschken, W. (Oxeno Olefinchemie GmbH), Patent WO 2007/036424; (2007) *Chemical Abstracts* **146**, 361048; (b) Elements, (2007) *Evonik-ScienceNewsletter*, 18, 30.

7
Industrial Applications of Homogeneous Enantioselective Catalysts

Hans-Ulrich Blaser, Garrett Hoge, Benoît Pugin, and Felix Spindler

7.1
Introduction and Scope

For many applications of chiral compounds, the racemic forms will no longer be accepted. Today, pharmaceuticals and vitamins [1], agrochemicals [2], flavors and fragrances [3] and also functional materials [4a] are increasingly produced as enantiomerically pure compounds. The reason for this development is the often superior performance of the pure enantiomers and/or that regulations demand the evaluation of both enantiomers of a biologically active compound before its approval. This trend has made the economical enantioselective synthesis of chiral performance chemicals a very important topic. Four general approaches for producing enantiopure [enantiomeric excess (*ee*) >99%] or enantioenriched compounds have evolved [5a].

Separation of enantiomers via classical resolution, i.e. crystallization of diastereomeric adducts, probably still accounts for the production of the majority of enantioenriched drugs [6]. An emerging technology is separation by chiral high-performance liquid chromatography (HPLC) using moving simulated bed technology [7]. While crystallization of diastereomeric adducts can be applied on any scale, separation via HPLC is probably most important in the early phase of product development and is restricted to relatively small-scale, high-value products. In both cases, large amounts of solvents have to be handled and, of course, at least 50% of the material with the wrong absolute configuration has to be either recycled or discarded.

The *chiral pool approach* [8] uses chiral building blocks originating from natural products for the construction of the final molecule. This approach is often chosen in the early phases of drug development but, depending on the commercial availability of the starting material, it can also be used for large-scale products. Because natural products very often (but not always!) have high enantiomeric purity, no further enrichment is usually necessary. A recent complication is the fact that products of human or animal origin must be declared for the manufacture of medicinal products in order to minimize the risk of transmitting animal spongiform encephalopathy.

Green Catalysis, Volume 1: Homogeneous Catalysis.
Edited by Robert H. Crabtree

ISBN: 978-3-527-32496-5

Enantioselective syntheses are performed with the help of covalently bound chiral auxiliaries (often from the chiral pool). These are not incorporated in the target molecule but are removed after the stereogenic centers have been established and must be either recycled or discarded.

In many respects, the most elegant approach is *enantioselective catalysis*, where prochiral starting materials are transformed to enantioenriched products with the help of chiral catalysts. Effective catalysts are either synthetic (chemocatalysis) or can be of natural origin (biocatalysis). In this discussion, we will focus on the application of chemical catalysts, but the use of enzymatic and microbial transformations has in many respects similar opportunities and concerns [9, 10a]. An important issue is often the time needed to find and develop an efficient biocatalyst, especially when the starting material is not a very close analogue to the natural substrate and the enzyme has to be genetically engineered [10b, c]. In addition, product isolation can be a serious problem since reactions are often carried out in a dilute aqueous solution. However, as several recent publications convincingly show, these hurdles can be overcome [9, 10].

Over the years, three types of enantioselective chemocatalysts have proven to be synthetically useful. The most versatile ones are *homogeneous metal complexes* containing bidentate ligands with a chiral backbone carrying two coordinating heteroatoms. For noble metals, especially Rh, Pd, Ru, Ir and Os, these are P or N atoms; for metals such as Ti, B, Zn, Co, Mn and Cu, ligands with coordinating O or N atoms are usually preferred. This methodology has recently received its due recognition with the 2001 Nobel Prize to Knowles and Noyori for enantioselective hydrogenation and to Sharpless for enantioselective oxidation catalysis [11]. Also useful for synthetic application are *heterogeneous metallic catalysts*, modified with chiral auxiliaries [12]. *Organocatalysis*, i.e. the use of small organic molecules as catalysts, is at the moment a very hot research topic with some potential for future industrial applications [13]. Chiral polymeric and gel-type materials [14a], phase-transfer catalysts [15] and immobilized complexes [16] are not practically useful for synthetic purposes.

Although most applications described in this overview are *asymmetric syntheses* starting from a prochiral substrate, *kinetic resolution*, i.e. the preferential transformation of one enantiomer of a racemic substrate, is of growing synthetic importance [17]. So far, relatively few enantioselective catalysts are used on an industrial scale [9, 18, 19] and some of the reasons for this fact will be discussed below. A very good overview on the scientific state of the art of enantioselective catalysis can be found in two recent monographs, *Comprehensive Asymmetric Catalysis* edited by Jacobsen, Yamamoto and Pfaltz [14] and *Catalytic Asymmetric Synthesis* edited by Ojima [20]. Progress in enantioselective hydrogenation has been summarized in several recent reviews [21–24] and a comprehensive monograph [19]. For the compilation of industrial applications, we have relied on a monograph on large-scale asymmetric catalysis [9] and several excellent up-to-date overviews [25–30] describing applications of enantioselective technology, mainly in the pharmaceutical industry. Since it is notoriously difficult to obtain precise information on industrial processes, many references relate to rather informal sources such as *Chemical and Engineering News* reports and proceedings of commercial meetings. This chapter is

an amended and updated version of a paper written in 2001 [18]. The industrial application of homogeneous hydrogenation catalysts has been reviewed in 2007 [19]. For this reason, we concentrate on the one hand on established manufacturing processes either with a significant production volume or which are important for historical reasons, and on the other on an update of newer results for pilot- and bench-scale applications.

7.2 Critical Factors for the Technical Application of Homogeneous Enantioselective Catalysts

The application of homogeneous enantioselective catalysts on a technical scale presents some very special challenges and problems [4, 5, 9a, 18, 31]. Some of these problems are due to the special manufacturing situation of the products involved, others are due to the nature of the enantioselective catalytic processes.

7.2.1 Characteristics of the Manufacture of Enantiomerically Enriched Products

The manufacture of chiral fine chemicals and in particular of pharmaceuticals and agrochemicals can be characterized as follows (typical numbers are given in parentheses):

- *Multifunctional molecules* produced via multistep syntheses (10–15 steps for pharmaceuticals and 3–7 steps for agrochemicals) with short product lives (often <20 years).
- *Relatively small scale products* (1–1000 t year^{-1} for pharmaceuticals, 500–10 000 t year^{-1} for agrochemicals), usually produced in multipurpose batch equipment.
- *High purity requirements* (usually >99% and <50 ppm metal residue in pharmaceuticals).
- *High added values* and therefore tolerant to higher process costs (especially for very effective, small-scale products).
- The *development time* can be a hurdle, especially when the optimal catalyst has to yet be developed or no commercial catalyst is available for a particular substrate (substrate specificity) and/or when not much is known about the desired catalytic transformation (technological maturity). When developing a process for a new chemical entity (NCE) in the pharmaceutical or agrochemical industry, time restraints can be severe. In these cases, it is more important to find a competitive process on time than an optimal process too late. So-called second-generation processes, e.g. for chiral switches, generic pharmaceuticals or the manufacture of other fine chemicals, have different requirements; here the time factor is usually not so important but a high-performance process is necessary.

7.2.2
Characteristics of Enantioselective Catalytic Processes

Enantioselective catalysis is a relatively young but rapidly expanding field. Up to 1985, only a few catalysts affording enantioselectivities of more than 90% were known [32]. This has changed dramatically in recent years and there are now a large number of chiral catalysts able to catalyze a variety of transformation with *ee*s >98% [14, 20]. A major challenge still remaining is the transfer of the results obtained for a particular substrate to a close analog due to the low tolerance for structure variation even within a class of substrates (substrate specificity). The industrial application of enantioselective catalysts is also often hampered by a lack of information on their synthetic scope and limitations. In addition, catalyst activities or productivities are often not given for new catalysts (in the literature enantioselectivity is still the dominant criterion) and applications to the synthesis of multifunctional, 'real-world' substrates are rather scarce (usually simple model reaction are studied). Finally, many chiral ligands and metal precursors are still expensive and/or in many cases not easily available in technical quantities.

7.2.3
Critical Factors for the Application of Enantioselective Catalysts

In the final analysis, the choice of a specific catalytic step is usually determined by the answer to two questions:

- Can the costs for the overall manufacturing process compete with alternative routes?
- Can a robust catalytic process be developed in the given time frame?

As a consequence of the peculiarities of enantioselective catalysis described above, the following critical factors often determine the viability of an enantioselective process:

- The *enantioselectivity*, expressed as enantiomeric excess (% *ee*), i.e. % desired – % undesired enantiomer. The *ee* of the catalytic reaction should be >99% for pharmaceuticals if no purification is possible (via recrystallization or at a later stage via separation of diastereomeric intermediates). This case is rare and *ee*s >90% are often acceptable; for agrochemicals *ee*s >80% can be sufficient.
- The *chemoselectivity and/or functional group tolerance* will be very important when multifunctional substrates are involved.
- The *catalyst productivity*, given as turnover number (TON), determines catalyst costs. TONs ought to be >1000 for small-scale, high-value products and >50 000 for large-scale or less expensive products (catalyst re-use increases the productivity).
- The *catalyst activity*, given as turnover frequency for >95% conversion (TOF, h^{-1}), determines the production capacity. For hydrogenations, TOFs ought to be >500 h^{-1} for small-scale and >10 000 h^{-1} for large-scale products.

- *Availability and cost of ligands*. In the majority of cases these are chiral diphosphines that need special synthetic know-how and can be expensive. Typical prices are UIS$200–1000 g^{-1} for laboratory quantities and from $10 000 to >$40 000 kg^{-1} on a larger scale. Chiral ligands such as diamines or amino alcohols used for early transition metals are usually cheaper.
- *Intellectual property*. Many chiral ligands and/or catalysts are patent protected. It is essential to obtain the right to use proprietary catalysts on a commercial basis at reasonable cost and conditions.
- *Availability and cost of starting materials*. Starting materials are often expensive and difficult to manufacture on a large scale with the high purity required for catalytic reactions.
- *Development time*. This can be crucial if an optimal ligand has to be developed for a particular substrate (substrate specificity) and when not much know-how is available on the catalytic process (technological maturity).

Which of these criteria will be critical for the development of a specific process depends on the specific catalyst and transformation. The following factors have to be considered: the field of application and the price of the active compound (added value of the catalytic step); the scale of the process; the technical experience and the production facilities of a company; the maturity of the catalytic process; and the chemist who plans the synthesis must be aware of the catalytic route!

7.2.4 Classification of Enantioselective Transformations

In a recent overview [33], we tried to classify enantioselective catalytic transformations according to their industrial potential and the conclusions are summarized in Table 7.1.

7.3 Industrial Processes: General Comments

In 2001, we collected and tabulated information on processes operated in regular production and also on those in the pilot- and bench-scale state [18]. The following terms were defined and will also be used in this overview: *Production processes* are (or have been) operated on a more or less regular basis, i.e. all relevant problems concerning catalyst performance and separation, supply of materials, product isolation and purification, noble metal recovery, etc., have been solved. *Pilot-scale processes* are technically on a similar level especially concerning catalyst performance, they have been carried out on multi-kilogram to ton scale (depending on the area of application) but have not (yet) been applied on a regular basis. *Bench-scale processes* have an optimized catalyst performance, have been carried out a few times on a small scale but are for some reason not yet ready for production purposes. *Feasibility studies*

Table 7.1 Classification of industrial potential of selected transformations.

Existing applications, broad scope	Hydrogenation of enamides and itaconates
	Hydrogenation of β-functionalized C=O
Existing applications, medium scope	Hydrogenation of C=C–COOR and C=C−CH−OH
	Hydrogenation of α-functionalized and aryl C=O
	Hydrogenation of C=N−Ar
Existing applications, narrow scope, niche applications	Hydrogenation/reduction of other C=C and C=O
	Hydrogenation of and addition to various C=N
	Dihydroxylation and epoxidation of C=C
	Oxidation of aryl sulfides
	Epoxide opening (kinetic resolution)
	Isomerization, cyclopropanation, hydrocyanation of C=C
Broad substrate scope, good chance for selected application	(Hetero) Diels–Alder
	Michael additions, allylic alkylation
	Aldol and ene reactions
	Various addition reactions to C=O and C=N
Narrow substrate scope, niche applications only	Aminohydroxylation of C=C
	Hydrocarbonylation, hydroboration, hydrosilylation of C=C
	Cross-coupling, metathesis and Heck reactions

very often demonstrate proof of principle (acceptable *ee*) without much optimization of the catalytic performance.

An analysis of the processes described in the study showed that hydrogenation of C=C and C=O functions is by far the predominant transformation applied for industrial processes, followed by epoxidation and dihydroxylation reactions. On the one hand, this is due to the broad scope of catalytic hydrogenation and on the other it could be attributed to the early success of Knowles with the L-dopa process, because for many years, most academic and industrial research was focused on this transformation. The success with epoxidation and dihydroxylation can essentially be attributed to the efforts of the groups of Sharpless, Katsuki and Jacobsen. If one analyzes the structures of the starting materials, it is obvious that many of these compounds are complex and multifunctional, i.e. the successful catalytic systems are not only enantioselective but also tolerate many functional groups.

The most often cited *success factor* by industrial developers was ligand design, i.e. the desired transformation was possible because either a new ligand type was found (or claimed to be designed) or because an existing ligand could be optimized by adapting the coordinating groups to the needs of the reaction (electronic and/or steric tuning). However, also the choice of the right metal precursor (especially for Ru-catalyzed reactions) and/or anion together with the addition of promoters were

reported to be decisive for high catalyst activity and productivity. Careful optimization of the reaction conditions (temperature, pressure, solvent, concentrations, etc.) and the ability to crystallize the product directly from the reaction solution with very high *ee* were also mentioned several times to have been important for a successful commercial process.

The following *critical factors* often made process development difficult. The sensitivity of the catalyst towards impurities (by-products in the starting material, oxygen, water, etc.) usually could be controlled with a strict purification protocol, but in some cases a change of the overall synthetic route of the substrate was necessary. Sometimes, the stability of the ligand or catalyst and its productivity (given as TON, moles of product/moles of catalyst) or its activity (given as TOF, moles of product/moles of catalyst per hour) were problematic, but careful optimization was often successful in overcoming these problems. Other critical issues have been mentioned: the need for high pressures or very low temperatures (expensive equipment), lack of commercial availability or difficult preparation of the ligand or catalyst and problems with a patented ligand system. Surprisingly, despite the fact that homogeneous catalysts were used in most applications, catalyst separation was mentioned only once to have been a major obstacle. More of an issue were residual metals in the product, especially for pharmaceutical applications and when the homogeneous catalyst was used late in the synthesis.

7.4 Hydrogenation of C=C Bonds

7.4.1 Hydrogenation of Dehydro-α-amino Acid Derivatives

There is little doubt that the hydrogenation of dehydro α-amino acids is the best studied enantioselective catalytic reaction. This was initiated by the successful development of the L-dopa process by Knowles (see below) and, for many years, acetylated aminocinnamic acid derivatives were the model substrates to test most newly developed ligands. Today, this is the transformation most often used for the stereoselective synthesis of a variety of pharmaceutical and agrochemical targets, even though the difficult and expensive preparation of the dehydroamino acid derivatives precluded the manufacture of large-volume α-amino acids. Because of their importance for the development of industrial asymmetric catalysis, we will discuss several early applications in some detail, but will only summarize the results obtained in other cases.

7.4.1.1 L-Dopa (Monsanto, VEB Isis-Chemie)

According to Knowles [9b, 34], Monsanto has been producing L-dopa, a drug for the relief of Parkinson's disease, on a scale of ca 1 t year^{-1} for many years. The former East German company VEB Isis-Chemie also carried out this process on a similar scale but terminated the production after a few years [35]. The key step in

the synthesis is the enantioselective hydrogenation of an enamide intermediate (Scheme 7.1).

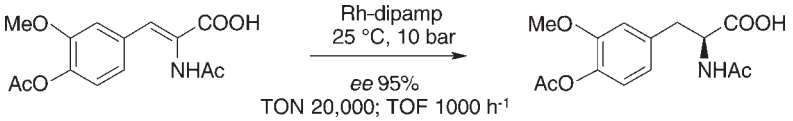

Scheme 7.1 The Monsanto L-dopa process.

Monsanto carried out the reaction in a water–2-propanol mixture at relatively low temperature and pressure. Because the free ligand racemizes slowly, an isolated $[Rh(dipamp)(diene)]^+BF_4^-$ complex was used as the catalyst, showing a very good performance: An *ee* of 95%, TON 10–20 000, TOF 1000 h^{-1}. Today *ee* values of 95% are no longer exceptional for the hydrogenation of enamides, but this was certainly not the case at the time the process was developed. It is therefore not surprising that for many years enamide hydrogenation was *the* standard test reaction for new ligands. One of the key factors for success was, of course, the dipamp ligand developed by Knowles and his team within an amazingly short time. Scheme 7.2 shows the concept of the Monsanto scientists: (i) a stereogenic phosphorous atom with an anisyl groups and (ii) a bidentate structure with C_2 symmetry. The VEB Isis team chose a different approach by starting with a (cheap) chiral pool molecule for the construction of the glup ligand, also with two coordinating P atoms. The Rh–glup sulfate complex worked at 40 °C/1 bar; with *ee*s of 91–92%, TONs of 2000 and TOFs of ~330 h^{-1}; it did not quite reach the performance of Rh–dipamp.

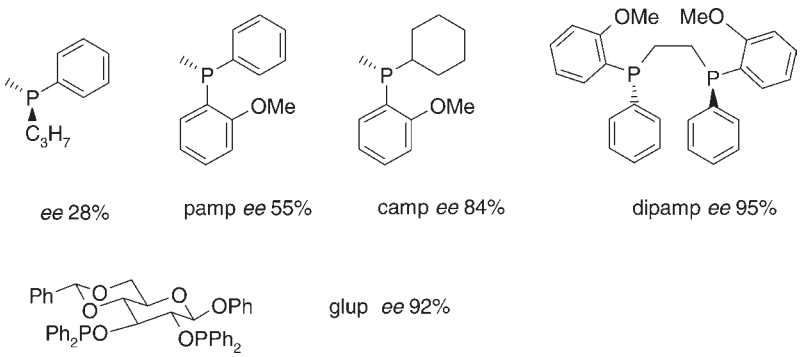

Scheme 7.2 Ligands developed for the manufacture of L-dopa.

A very important feature of the Monsanto process was the fact that the reaction was started with a slurry of reactants and ended with a slurry of the pure product with close to 100% *ee*, allowing the easy separation of both the catalyst and the undesired racemate in one step. Critical issues for both the Monsanto and the VEB Isis process were the quality of the starting material (enamide syntheses are often problematic) and especially the concentration of oxygen and peroxides in the reaction solution.

An Rh–dipamp complex was later applied by NSC Technologies for the production of several unnatural amino acids with good catalyst performances (*ee* 95–98%, TON 5–20 000) [9c] and was also very selective but with low activity (*ee* 98%, TON 20) in a feasibility study for a synthesis of acromelobic acid by Abbott Laboratories [36] (Scheme 7.3).

Ar = (subst)Ph, heteroaryl acromelobic acid

Scheme 7.3 Target structures for Rh–dipamp catalyst.

7.4.1.2 Aspartame (Enichem/Anic, Degussa)

Phenylalanine is an intermediate for the aspartame sweetener and, for a few years, it was produced by Enichem/Anic [37] on a scale of ca 15 t, using a variant of the L-dopa procedure as summarized in Scheme 7.4. The Rh–eniphos catalyst was considerably less selective than Rh–dipamp but easier to prepare and much cheaper. Traces of Rh were removed by treatment with a thiol containing resin and crystallization of the ammonium salt gave product of >99% *ee* [38]. Due to the low stability of the ligand (P–N bond cleavage), the reaction conditions had to be carefully controlled. A few years later, Degussa developed a pilot process with an Rh–deguphos catalyst which operated at 50 °C/15 bar and achieved *ee*s up to 99% (TON 10 000, TOF 3000 h^{-1}) [39].

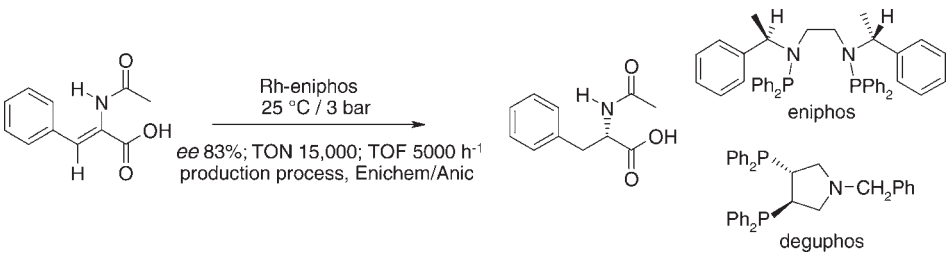

Scheme 7.4 Phenylalanine process.

7.4.1.3 Various Pilot- and Bench-Scale Processes for the Synthesis of α-Amino Acid Derivatives

Processes for several α-amino acid derivatives with a variety of structural elements were developed and carried out on a pilot or bench scale by Dow/Chirotech [40–42]. In addition to the three examples shown in Scheme 7.5, Dow regularly produces multi-hundred kilograms of various α-amino acids using its Rh–DuPhos technology [42, 43]. Interestingly, PhanePhos proved superior to DuPhos for the preparation of diphenyl

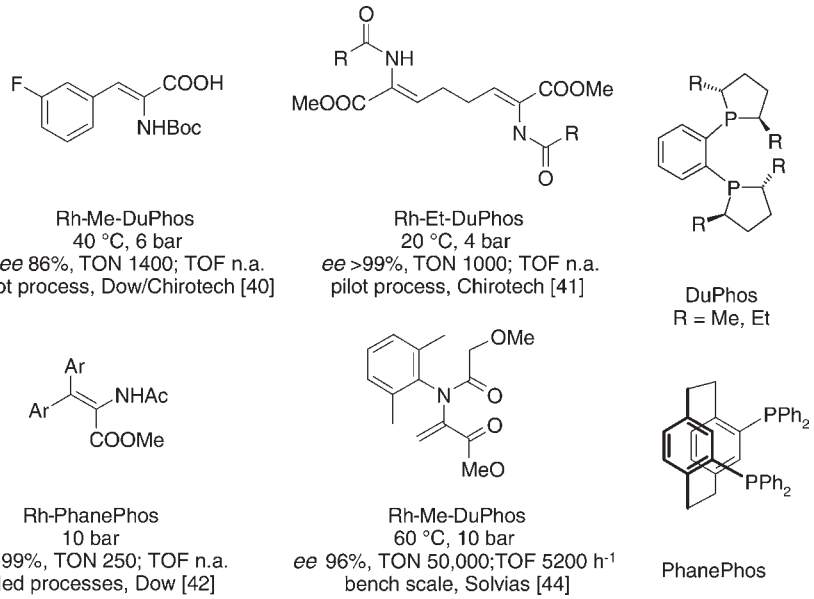

Scheme 7.5 Substrates and ligands for the synthesis of various α-amino acid derivatives.

aniline derivatives. Solvias described the hydrogenation of a relatively hindered enamide on a bench scale [44] also using an Rh–DuPhos catalysts (Scheme 7.5).

Tunable ferrocene-based diphosphines lead to effective catalysts for the production of α-amino acid derivatives with less conventional structural elements. 2-Piperazinecarboxylic acid derivatives are interesting intermediates, e.g. for Crixivan, the well-known HIV protease inhibitor from Merck. The hydrogenation of an unusually substituted cyclic enamide was used by Lonza [45] to produce >200 kg of the piperazine intermediate depicted in Scheme 7.6 using an optimized Rh–Josiphos catalyst. Important for good catalyst performance were the choice of the ligand and the substituents at the tetrahydropyrazine. Surprisingly, the same catalyst was also able to hydrogenate a corresponding pyrazine amide with *ee*s up to 77%, but much lower activity [46].

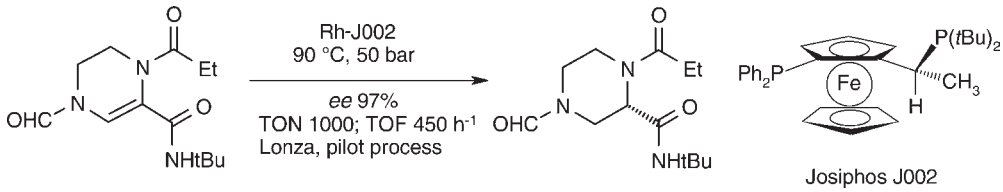

Scheme 7.6 Process for a 2-piperazinecarboxylic acid derivative.

Ru– and Rh–Josiphos complexes were selective for the hydrogenation of tetra-substituted C=C bonds, intermediates of taranabant, a CB-1 R inverse antagonist (Merck [47]) and of an anthrax lethal factor inhibitor (Merck [48]), respectively, as

depicted in Scheme 7.7. In the former case, the nitrile substituent had to be transformed to an amide group since it inhibited the Rh catalyst and the reaction had to be carried out in trifluoroethanol. Rh–Josiphos (Lonza [45]) and Rh–BoPhoz (Eastman [49]) catalysts were effective for the hydrogenation of an exocyclic and a cyclopropyl-substituted C=C bond.

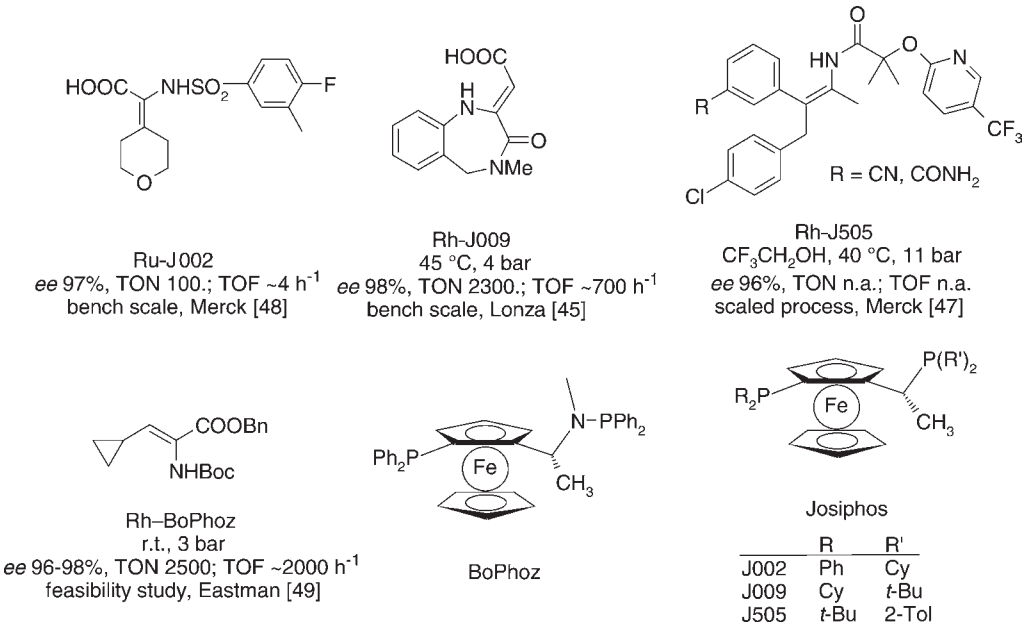

Scheme 7.7 Substrates and ligands for the synthesis of various α-amino acid derivatives.

Earlier examples of pilot- and bench-scale processes are summarized in [18]: several cases with high *ee*s and medium activity using Rh–bppm ligands were reported by Hoechst (now Sanofi Aventis) [50]; Ru–binap and Ru–biphep complexes were also effective catalysts for cyclic and exocyclic dehydroamino acid derivatives.

7.4.2
Hydrogenation of Dehydro-β-amino Acid Derivatives

In contrast to dehydro-α-amino acids, the hydrogenation of acetylated dehydro-β-amino acid derivatives has only recently attracted industrial interest and, accordingly, only a few applications on a larger scale have been reported. Several ligands, mostly of the phospholane type such as DuPhos and analogs, might have industrial potential but up to now have only been tested on model substrates under standard conditions [51]. Chiral Quest's TangPhos and Binapine (Scheme 7.8) have been shown to hydrogenate several acetylated dehydro-β-amino acid derivatives with *ee*s of 98–99% and TONs of 10 000 at room temperature, 1 bar [1, 52], and Pfizer has reported the diastereoselective hydrogenation with 96% *ee* for a drug intermediate using an unusual combination of Binapine (*ee* >98%, but not very active) and TCFP

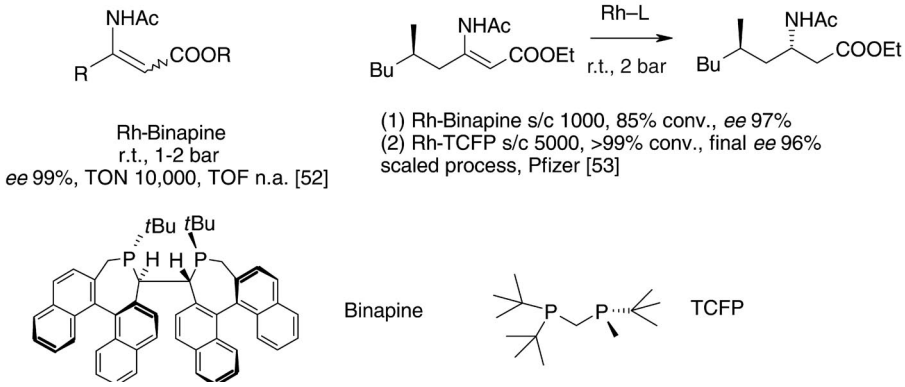

Scheme 7.8 Hydrogenation of *N*-acetyldehydro-β-amino acid derivatives.

(*ee* 94%, but highly active); the TCFP ligand was developed in its own laboratories [53–55].

7.4.2.1 **Sitagliptin (Merck)**

With this background, the finding by Merck chemists [56] that unprotected dehydro-β-amino acids are good substrates for Rh-catalyzed hydrogenations was both very unexpected and very exciting. This discovery, which required the screening of dozens of ligands and additives, led to a new synthesis for sitagliptin, a DPP-IV inhibitor for the treatment of type 2 diabetes, now being marketed by Merck [47, 57]. Of special importance for reproducible manufacture were the choice of the right ligand and the presence of trace amounts of ammonium chloride. Interestingly, deuteration experiments indicate that it is not the enamine C=C bond which is reduced but the tautomeric imine! The resulting optimized reaction is depicted in Scheme 7.9 and over 20 t has been produced to date. Although the enantioselectivities are very good (up to 98% *ee*), TONs and TOFs are relatively low. However, the overall synthesis is superior to two alternative routes with substrate- and auxiliary-controlled asymmetric synthesis of the β-amino acid moiety.

Almost at the same time, Takasago [58, 59] reported that an Ru–segphos catalyst is able to hydrogenate unprotected dehydro-β-amino esters with *ee*s of 94–97%. Of special industrial relevance is the fact that the Ru–segphos catalysts also work very well for the reductive amination of a variety of β-keto esters to give the corresponding β-amino ester in one step with *ee*s up to 99% at a substrate to catalyst ratio (s/c) of 1000 with TOFs of $\sim 60\,h^{-1}$ (Scheme 7.9).

7.4.3 **Hydrogenation of Simple Enamides and Enol Acetates**

The hydrogenation of enamides and enol acetates without an acid function is often more demanding and is not applied widely. In addition to an early bench-scale application by Roche with an Ru–biphep catalyst [60], three examples are of interest, a pilot process for a cyclic enol acetate by Roche [60], a feasibility study by Bristol-Myers

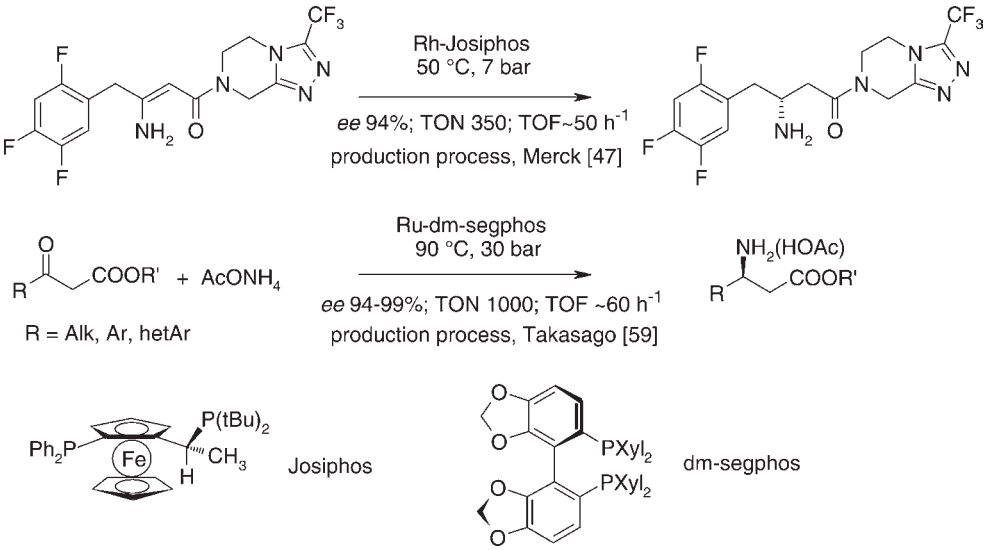

Scheme 7.9 Hydrogenation of dehydro-β-amino acid derivatives.

Squibb [61], both using Rh–DuPhos catalysts, and a pilot process for an intermediate of norsertraline developed by Dow for Sepracor [62], with Rh–norphos giving the best stereoselectivity(Scheme 7.10).

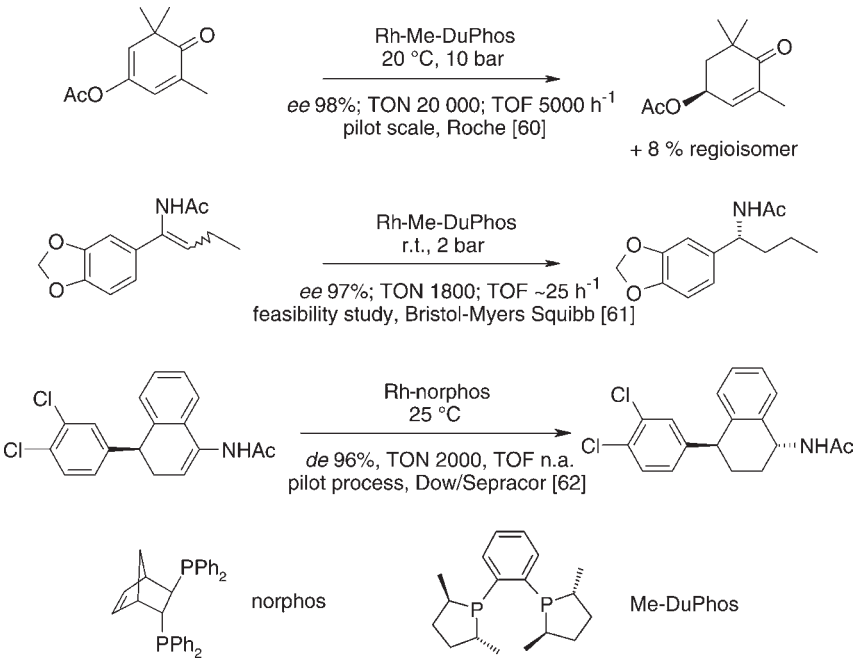

Scheme 7.10 Hydrogenation of enamides and enol acetates.

7.4.4
Hydrogenation of Itaconic Acid Derivatives

Even though it was realized early on that, in analogy with enamides, itaconic acid derivatives are also preferred substrates due to the presence of a second coordinating group, industrial applications are still rare. Just as dehydroamino acids, substituted itaconic derivatives exist as *E* and *Z* isomers, but several phospholane-type ligands are able to accept *E*–*Z* mixtures. Two early examples using an Rh–deguphos and an Rh–bpm catalyst, respectively, were described by Hoechst (now Sanofi Aventis) with good to high *ee*s but low TONs (for details, see [18, 50]).

In the last few years, several applications on the pilot and bench scales have been reported (Scheme 7.11). Rh–DuPhos is among the most effective catalysts. Dow has optimized the hydrogenation of dimethyl itaconate and of succinic acid monoamide with very good catalyst performance [42]. BASF successfully applied its analogous rophos ligands in a pilot process for the unsubstituted monoester of itaconic acid with high *ee*, TON and TOF [63]. Interestingly, in two cases not the otherwise very effective Rh–phospholane complexes as successfully applied by Dow [64] but an Ru–binap catalyst was selected for preparative purposes. As described by GlaxoSmithKline, Rh–DuPhos actually gave higher *ee*s in the ligand screening but the results were not always reproducible and the Ru–binap catalyst was cheaper [65]. Pfizer obtained good results for the Rh–FerroTANE-catalyzed hydrogenation of the free acid (*ee* 94%, TON 1000), but in the end also chose an Ru–binap catalyst for scale-up [66].

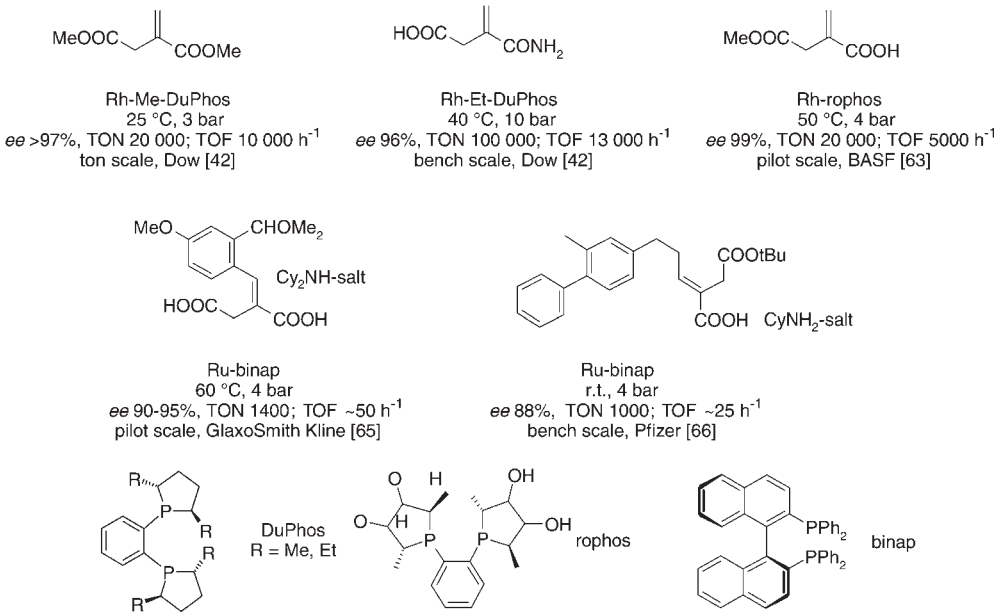

Scheme 7.11 Hydrogenation of itaconic acid derivatives.

7.4.5
Hydrogenation of Allylic Alcohols and α,β-Unsaturated Acids

The hydrogenation of allylic alcohols and α,β-unsaturated acids leads to products with a very high synthetic potential and both transformations were used early on for industrial applications. In both cases, Ru complexes with axially chiral biaryl ligands (binap analogs) are the catalysts of choice. We will discuss two example in some detail and summarize the results for other processes.

7.4.5.1 Hydrogenation of Allylic Alcohols (Scheme 7.12)

Citronellol, a fragrance and also an intermediate for vitamin E, can be prepared starting with geraniol. This transformation requires a specific Ru precursor and is highly chemoselective. It is carried out by Takasago on a 300 t year^{-1} scale [67]. Roche has reported a similar pilot process which works at 20 °C and 60 bar using the same Ru precursor with MeO-biphep as ligand, the *ee* is 99%, TON 30 000 and TOF 1500 h^{-1} [9d, 14b]. Pilot processes with similar catalyst performances were developed by Roche [9d, 14b] and Takasago [68] for the longer chain vitamin E intermediate. Obviously, the existing stereogenic center does not affect the enantioselectivity of the catalysts. Bench-scale processes for the hydrogenation of allylic alcohols using an Ru–binap and an Ru–biphep catalyst, respectively, were reported by Roche earlier (summarized in [18]) and a recent feasibility study showed that heterobiaryl ligands can also be effective ligands for this transformation [69].

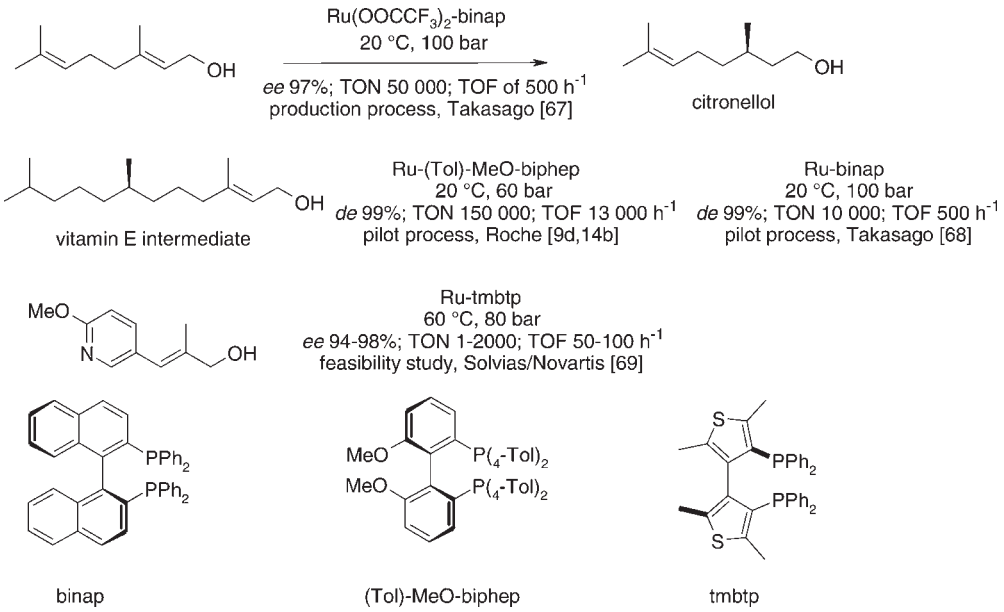

Scheme 7.12 Hydrogenation of various allylic alcohols.

The hydrogenation of a racemic homoallylic alcohol is the key reaction for a new synthetic route for producing paroxetine, recently reported by Ricordati [70] (Scheme 7.13). Best results (>99% *ee* for both *cis* and *trans* product) were obtained with a recrystallized [RuCl(*p*-cymene)(binap)]Cl complex in 2-propanol. The reaction was carried out on a 100 kg batch size.

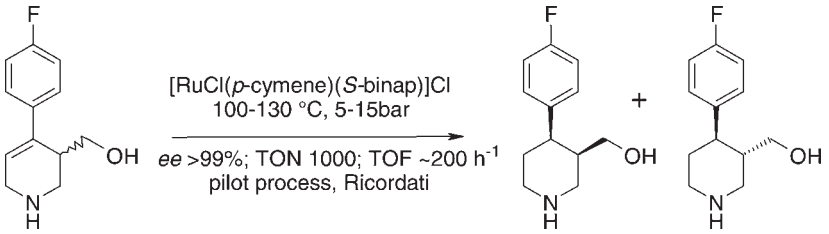

Scheme 7.13 Hydrogenation of a homoallylic alcohol.

7.4.5.2 Hydrogenation of α,β-Unsaturated Acids

One of the first applications of the then newly developed Ru–binap catalysts for α,β-unsaturated acids was for an alternative process for (*S*)-naproxen. (*S*)-Naproxen is a large-scale anti-inflammatory drug and is actually produced via the resolution of a racemate. For some time it was considered to be one of the most attractive goals for asymmetric catalysis. Indeed, several catalytic syntheses have been developed for the synthesis of (*S*)-naproxen intermediates in recent years (for a summary, see [18]). Best results for the hydrogenation route were obtained by Takasago [71] (Scheme 7.14), which recently reported that an Ru–H_8-binap catalyst achieved even higher activities (TON 5000, TOF 600 h^{-1} at 15 °C, 50 bar) [25]. However, despite some fairly good catalytic results, it has become clear that the original resolution variant will be the optimal process for some time since on the one-hand the Syntex resolution process is extraordinarily efficient and on the other the starting materials for most catalytic processes are more expensive and an extra purification step would be necessary [72].

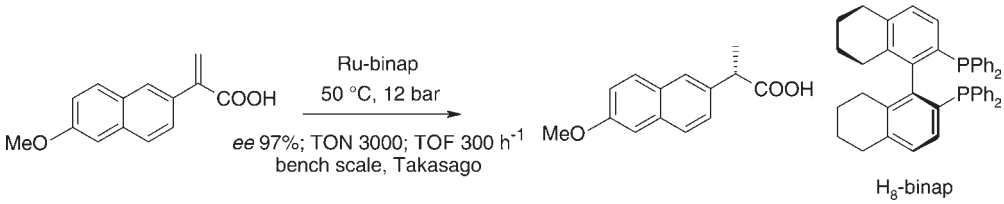

Scheme 7.14 Naproxen via enantioselective hydrogenation.

Ru complexes containing biaryl-type ligands are often the catalysts of choice for α,β-unsaturated acids and some relevant examples are depicted in Scheme 7.15. The substrates range from tetrasubstituted C=C bonds [14b, 73] to substrates with OR substituents [74, 75] to exocyclic C=C bonds [47, 76]. In the last case, it was

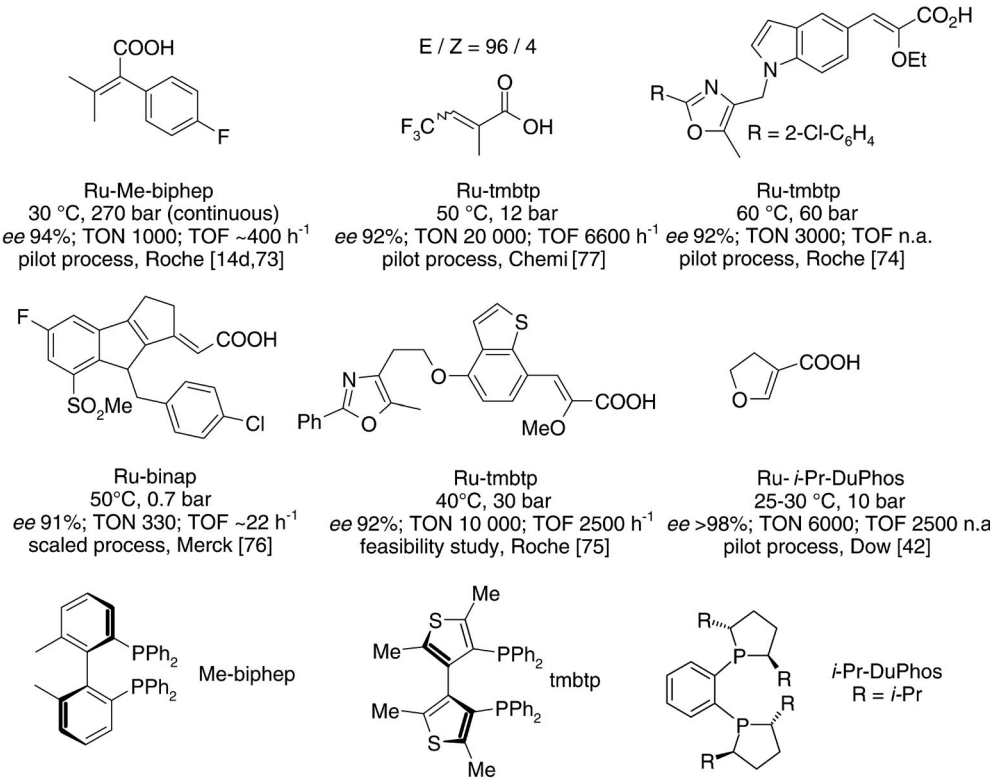

Scheme 7.15 Ru-catalyzed hydrogenation of α,β-unsaturated acids.

found that prior to hydrogenation, the exocyclic C=C bond migrates into the ring. A trifluoromethyl-substituted unsaturated acid (*E–Z* mixture) was hydrogenated by Chemi in a 4000 L reactor on a 340 kg scale with tmbtp, a hetero binap analog [38, 77]. Dow disclosed a pilot process for the Ru-catalyzed hydrogenation of dihydrofuroic acid with bulky DuPhos catalyst [42].

Recently, it was found that Rh complexes can also be used effectively for sterically hindered α.β-unsaturated acids or salts, as evidenced by the processes depicted in Schemes 7.16 and 7.17. Although the enantioselectivities of the catalysts in Scheme 7.16 are adequate, the TON and TOF values are insufficient for a technical synthesis of a PPAR antagonist by Lilly [78], of an endothelin receptor antagonists by SmithKline Beecham [79] or of a neurodegenerative disease agent by Takeda Chemical Industries [80]. Indeed, Takeda has developed an alternative technical process. Interestingly, in some cases the addition of a base or the use of the Na salt gave better results than the free acids.

7.4.5.3 **Hydrogenation for Synthon A of Aliskiren (Speedel/Novartis)**

Few details have been released of various scaled processes developed by Solvias [81], DSM [82] and BASF [83] (Scheme 7.17) for producing a precursor of synthon A of the

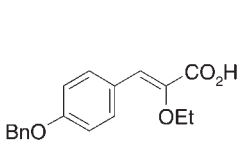

Rh-Walphos
25 °C, 3 bar
ee 92%, TON ~300, TOF ~20 h^{-1}
feasibility study
Lilly [78]

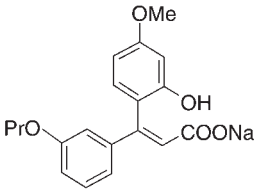

Rh-chiraphos
50 °C, 13 bar
ee 94%; TON 1000; TOF ~50 h^{-1}
bench scale
SmithKline Beecham [79]

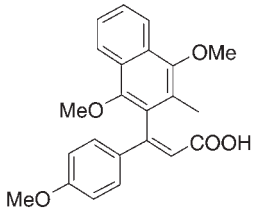

Rh-J002-Et_3N
70 °C, 100 bar
ee 94%; TON 100; TOF ~4 h^{-1}
feasibility study
Takeda Chemical Ind. [80]

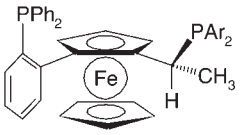

Walphos
Ar = 3,5-$(CF_3)_2$Ph

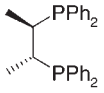

chiraphos

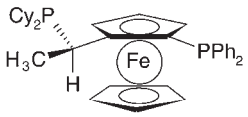

Josiphos J002

Scheme 7.16 Rh-catalyzed hydrogenation of α,β-unsaturated acids.

renin inhibitor aliskiren of Speedel/Novartis, but the transformation is being carried out on a multi-ton scale. Whereas the process developed by Solvias is based on an Rh–ferrocenyl diphosphine complex, DSM has developed a novel Rh–phosphoramidite–$P(3\text{-Tol})_3$ catalyst with somewhat lower enantioselectivity and BASF has patented a process with an Rh–phanephos catalyst using a *E*–*Z* substrate mixture.

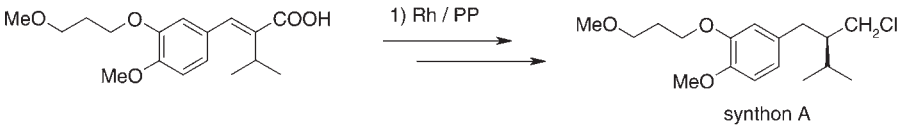

synthon A

Rh-Walphos
50-80 °C, 40-60 bar
ee 95%; TON >5000; TOF >350 h^{-1}
scaled process, Solvias [81]

Rh-phosphoramidite-$P(3\text{-Tol})_3$
55 °C, 80 bar
ee 90%; TON >5000; TOF >500 h^{-1}
scaled process, DSM [82]

Rh-phanephos
75 °C, 200 bar
ee 86%; TON ~23 000; TOF ~1600 h^{-1}
scaled process, BASF [83]

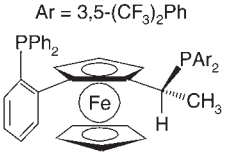

Walphos

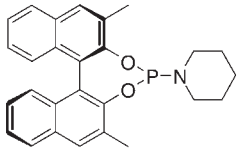

phosphoramidite

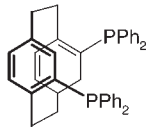

phanephos

Scheme 7.17 Processes for synthon A of aliskiren.

7.4.6
Hydrogenation of Miscellaneous C=C Systems

In addition to olefins with privileged substitution patterns (enamides, allylic alcohols, α,β-unsaturated acids), several complex C=C substrates have been hydrogenated with good to excellent success on a production scale. Here, we describe several processes in some detail and summarize others without much comment.

7.4.6.1 Hydrogenation of a Biotin Intermediate (Lonza)

In the course of the development of a new technical synthesis at Lonza for biotin (a water-soluble vitamin), the Rh–Josiphos-catalyzed diastereoselective hydrogenation of a tetrasubstituted C=C bond turned out to be a key step [45, 84] (Scheme 7.18).

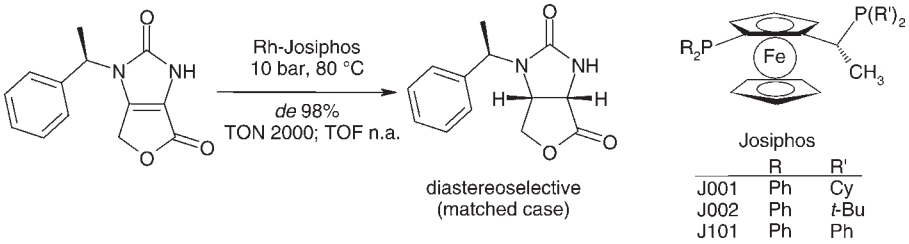

Scheme 7.18 Hydrogenation of a biotin intermediate.

Selected results of the process development are summarized in Table 7.2. It is remarkable that homogeneous catalysts with most ligand classes gave even lower selectivities than the achiral heterogeneous Rh–Al_2O_3 catalyst and Rh–Josiphos complexes with aromatic R′ groups were inactive. The high effectiveness of catalysts with J002 as ligand was therefore even more surprising. While the feasibility study was carried out with s/c ratios of 50–100, optimization of the reaction resulted in TONs of 2000. The enantioselective hydrogenation [*N*-benzyl instead of *N*-(*R*)-phenethyl)] with Rh–J002 afforded the desired enantiomer with up to 90% *ee*. For the production process, the diastereoselective variant was chosen and several tons of biotin were manufactured with this process.

Table 7.2 Selected results for the hydrogenation of the biotin intermediate.

Catalyst	*de* (%)	Comments/ligand structures
Rh–Al_2O_3	40	Heterogeneous
Rh–bdpp	50	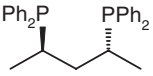 bdpp
Rh–mod-diop	66	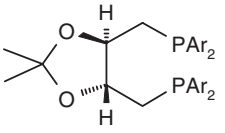 mod-diop Ar = 3,5-Me_2-4-(OMe)Ph
Rh–J101	No reaction	
Rh–J001	88	
Rh–J002	99	

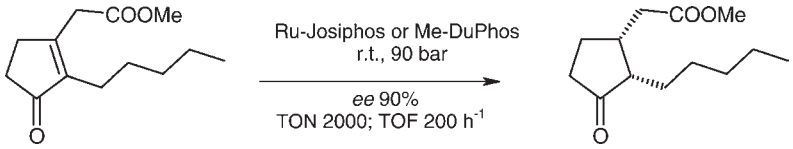

Scheme 7.19 Hydrogenation of a dihydrojasmonate intermediate.

7.4.6.2 Synthesis of (+)-Methyl *cis*-Dihydrojasmonate (Firmenich)

Dihydrojasmonates are ubiquitous cheap perfume ingredients. Firmenich has established that (+)-methyl *cis*-dihydrojasmonate (Scheme 7.19) is the preferred stereoisomer, has developed an enantioselective process and has started production on a multi-tons per year scale [85]. A novel Ru precursor and a new reaction system had to be found because the classical Ru complexes and conditions for the hydrogenation of C=C bonds did not work. In addition to the enantioselectivity, chemo- and *cis*-selectivity and activity problems (tetrasubstituted C=C) were solved on a very good level. As summarized in Table 7.3, the ligand structure and s/c affect both the *cis*/*trans* ratio and the *ee* value.

7.4.6.3 Intermediate for Tipranavir

The diastereoselective process depicted in Scheme 7.20 was developed by Chirotech [26, 40] for Pharmacia & Upjohn [86] and is being carried out on a 'production' scale.

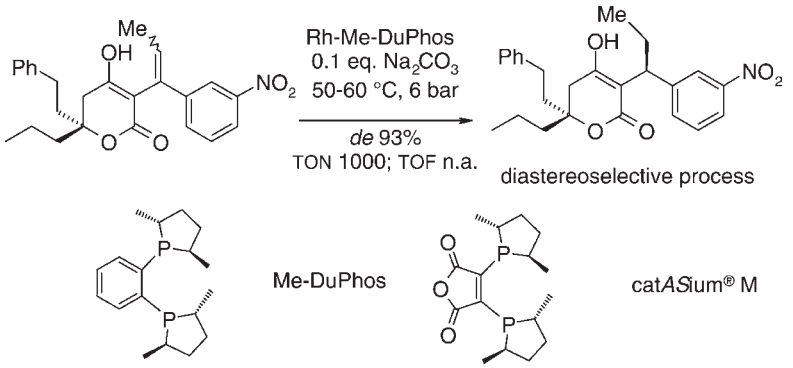

Scheme 7.20 Hydrogenation of a tipranavir intermediate.

Table 7.3 Ligand effect on activity and selectivity.[a]

Ligand	s/c	TOF (h^{-1})	*cis*/*trans*	*ee cis* (%)	
Me-DuPhos	300	5	99/1	69	
Josiphos	500	250	98/2	86	
Me-DuPhos	2000	120	>97/3	60	
Josiphos	2000	200	>97/3	90	

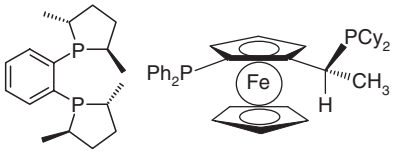

Me-DuPhos Josiphos J001

[a]Catalyst: [Ru(H)(cyclooctatriene)(ligand)]BF_4.

Essential was the addition of Na_2CO_3 as co-catalyst. The catalyst tolerates an *E*–*Z* mixture of substrate and shows high chemoselectivity with respect to reduction of the nitro group, which can be a problem. An alternative pilot process was recently described by Boehringer-Ingelheim using an Rh–cat*A*Sium M catalyst, which achieved selectivities of >98% *de* and a TOF of ca 40 h^{-1} with an s/c ratio of 1000 at 60 °C/10 bar [87].

7.4.6.4 **Intermediate for Candoxatril**

The α,β-unsaturated ester shown in Scheme 7.21 with a rather unusual substitution pattern was hydrogenated successfully for the synthesis of the antihypertensive candoxatril. The hydrogenation was carried out on 12 kg scale for Pfizer by Dow/Chirotech, using a cationic Rh–DuPhos catalyst [88], and on 250 kg scale by PPG-Sipsy with an Ru–biphep complex [89]. Both catalysts achieved very high enantioselectivities and medium activities.

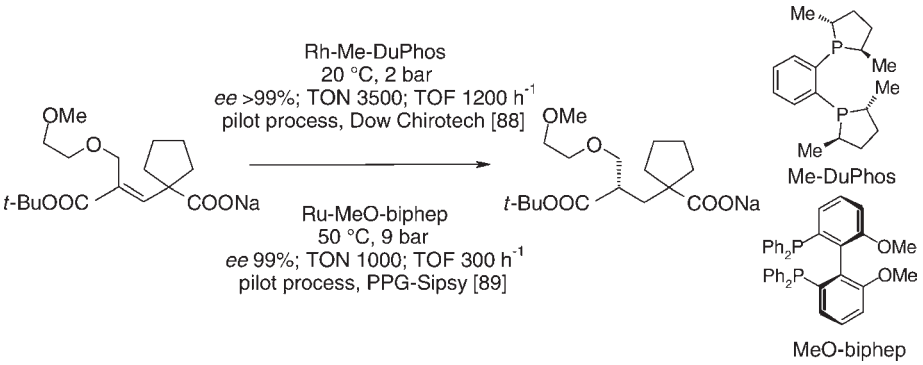

Scheme 7.21 Hydrogenation of a candoxatril intermediate.

7.4.6.5 **Intermediate for Pregabalin**

The hydrogenation of the α,β-unsaturated nitrile (Scheme 7.22), an intermediate for the anticonvulsant pregabalin of Pfizer, was carried out on a bench scale by Dow

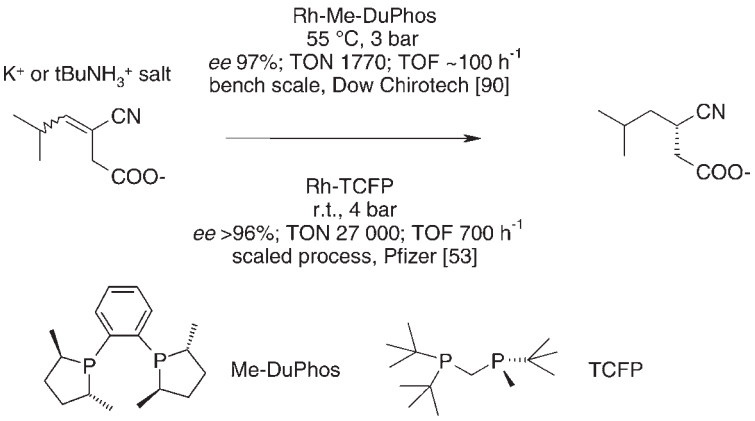

Scheme 7.22 Hydrogenation of pregabalin intermediate.

using an Rh–DuPhos complex [90] and up to production scale with the TCFP ligand developed by Pfizer [53, 55] with very high *ee* values.

Further C=C substrates as depicted in Scheme 7.23 were hydrogenated with acceptable to high enantioselectivities but the TON and TOF of most processes are probably not (yet) sufficient for manufacturing purposes [14b, 91–97]. Indeed, several of the papers explicitly mention that further development was stopped either because another route proved to be superior or because the compound was abandoned. Special mention is due to the rare case of an Ir–diphosphine catalyst, developed by Bristol-Myers Squibb [91], the hydrogenation of an essentially unfunctionalized C=C bond with the asymmetrically substituted MeO-biphep1 [14b, 92] and the high *ee* achieved for a tetrasubstituted C=C bond [97] by Roche.

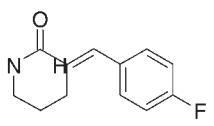

Ir-bdpp
r.t., 4 bar
ee 91%; TON 400; TOF ~35 h^{-1}
pilot process, Bristol-Myers Squibb [91]

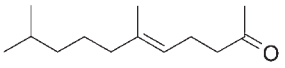

Ru-MeO-biphep1
20 °C, 60 bar
ee 94%; TON 1000; TOF 45 h^{-1}
bench scale, Roche [14b,92]

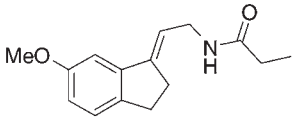

Ru-binap
70 °C, 90 bar
ee 95%; TON 100; TOF 33 h^{-1}
feasibility study, Takeda [93]

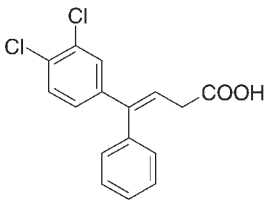

Rh-PhanePhos
222 °C, 9 bar
ee 97-98%; TON 2-3000; TOF 4-700 h^{-1}
feasibility study, Dow Chirotech [94]

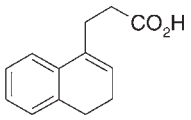

Ru-P-Phos
ee 96%, TON 1000-5000, TOF ~400h^{-1}
50-75°C / 10-20 bar
bench scale, Johnson Matthey [95]

Ru-MeO-biphep
20 °C, 100 bar
ee 94%; TON 100; TOF ~1 h^{-1}
feasibility study, Roche [96]

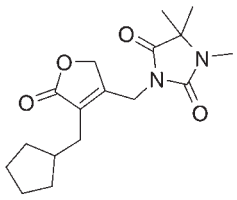

Ru-MeO-biphep
80-90 °C, 100 bar
ee 98%; TON 1000; TOF 130 h^{-1}
feasibility study, Roche [97]

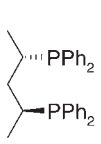

bdpp

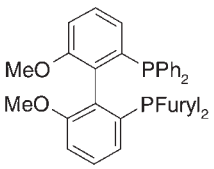

MeO-biphep1

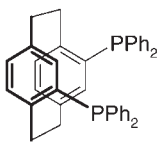

PhanePhos

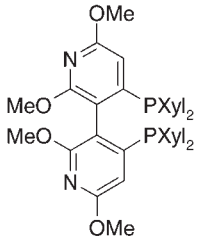

P-Phos

Scheme 7.23 Hydrogenation of various functionalized olefins.

7.5
Hydrogenation of C=O Bonds

Most catalysts originally developed for C=C bonds show a poor performance for the hydrogenation of ketones. This changed dramatically when it was found that selected Ru–binap and later Ru–binap–diamine complexes achieve excellent enantioselectivities and very high TONs and TOFs for a variety of ketones [20a, 98a]. Since then, it has been demonstrated that many α- and β-functionalized and aromatic ketones are suitable substrates for hydrogenation with industrially viable catalytic results. For the reduction of various ketones, biocatalytic methods are an industrially viable alternative to the use of chemocatalysts [9].

7.5.1
Hydrogenation of α-Functionalized Ketones

(*R*)-1,2-propanediol is an intermediate for (*S*)-oxfloxazin, a bactericide sold until recently as the racemate. The (*R*)-diol is now produced by Takasago via hydrogenation of hydroxyacetone as shown in Scheme 7.24 using an Ru–Tol-binap catalyst on a 50 t year^{-1} scale [98b]. Recently it was reported that segphos, a newly developed biaryl diphosphine, shows even better results, achieving >98% *ee* and TON and TOF of 10 000 and ~1400 h^{-1}, respectively [25, 99].

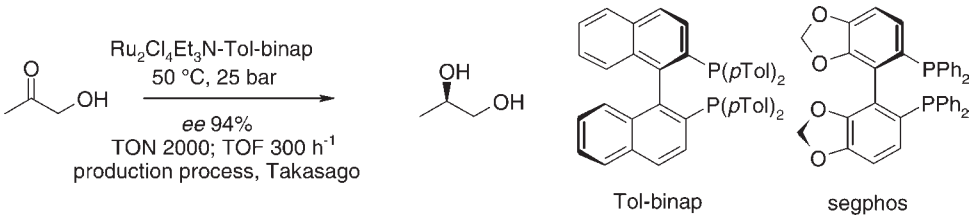

Scheme 7.24 Hydrogenation of hydroxyacetone.

The two production processes using α-amino ketone substrates depicted in Scheme 7.25 were developed by Boehringer-Ingelheim to improve on existing resolution syntheses for adrenaline and phenylephrine [100]. Both processes are carried out with an Rh–mccpm catalyst with very high TONS and TOFs, albeit with medium *ee*s of 88–92%, which increase to >99% after precipitation of the free base.

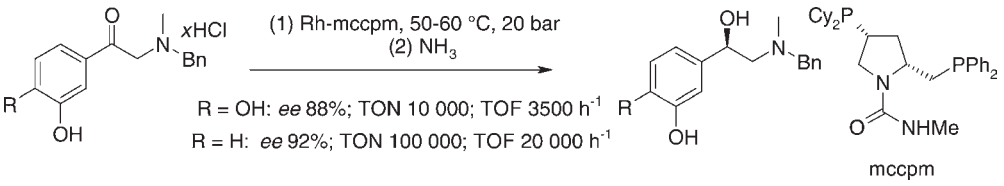

Scheme 7.25 Production processes for adrenaline (R = OH) and phenylephrine (R = H) intermediates.

The hydrogenation of α-amino ketones was also key step for the synthesis of pharma-actives (Scheme 7.26). Roche [101] disclosed a pilot process involving the hydrogenation–dynamic kinetic resolution of a cyclic α-amino ketone using an optimized MeO-biphep ligand. The Ru-catalyzed reaction was carried out on a 9 kg scale with excellent enantio- and diastereoselectivities and very high TON and TOF. A pilot process was reported by Solvias/Ciba-Geigy which was operated on a multi-tens of kilograms scale involving an Rh–bppfoh-catalyzed hydrogenation of an intermediate for the antidepressant levoprotiline [102]. Important for success was the fact that crystallization of the product both enhanced *ee*s and allowed the separation of the catalyst from the product. A pilot process was developed by Solvias for Novartis for the hydrogenation of an α-amino-β′-phosphinate ester with moderate catalyst performance using an Ru–MeO-biphep catalyst [103]. Obviously, this substrate could also be considered to be an analog of a β-keto ester (see below).

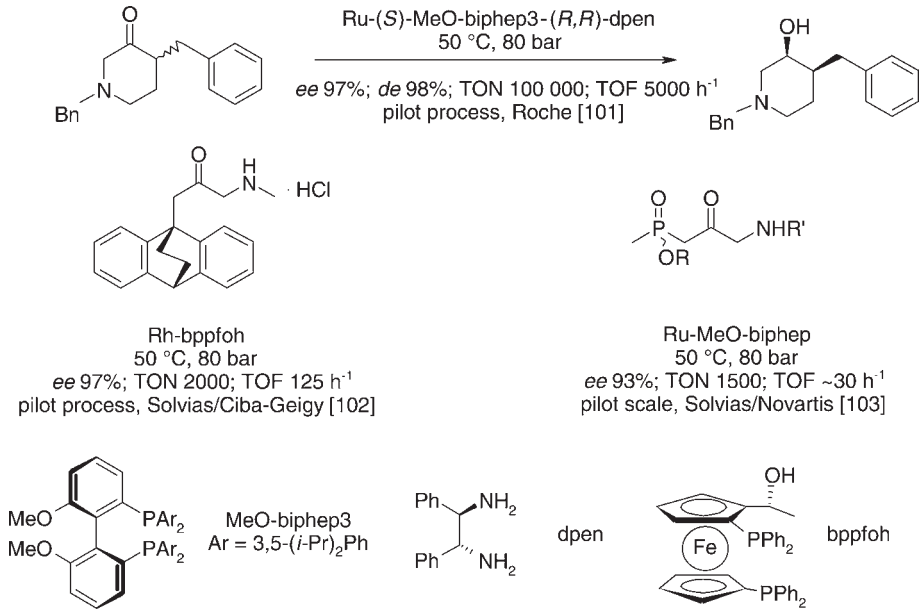

Scheme 7.26 Hydrogenation of various α-amino ketones.

The hydrogenation of α-keto acid derivatives is a promising route to a variety of α-hydroxy and α-amino acids. Up to now, homogeneous catalysts achieved good *ee*s but only insufficient TONs and TOFs and, indeed, heterogeneous cinchona-modified Pt catalysts are a viable alternative [9e, 21]. The hydrogenation of ketopantolactone depicted in Scheme 7.27 was the key step for the enantioselective synthesis of pantothenic acid. A pilot process was developed by Roche [14b] and (*R*)-pantolactone was produced in multi-hundred kilogram quantities. An Rh–bpm catalyst proved to be highly active with satisfactory selectivity. Important were the fine tuning of the ligand and the choice of the anion; critical for the very good catalyst performance were the purity of the substrate, the solvent and hydrogen. For the production of kilogram

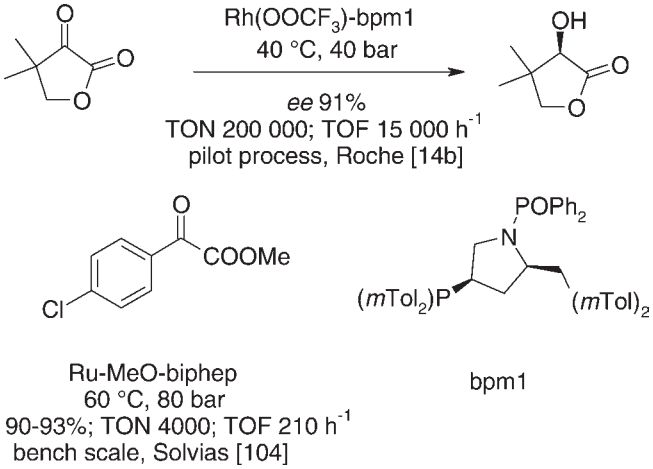

Scheme 7.27 Hydrogenation of α-keto acid derivatives.

amounts of (*S*)-*p*-chloromandelic acid, an Ru–MeO-biphep catalyst achieved 90–93% *ee* with acceptable TONs and TOFs, indicating that this hydrogenation might be feasible for the production of an agrochemical intermediate from both a technical and an economic point of view [104].

7.5.2
Hydrogenation of β-Functionalized Ketones

β-Keto esters are certainly privileged substrates and several industrial processes rely on this transformation. The most important is the hydrogenation–dynamic kinetic resolution shown in Scheme 7.28 for the production of an intermediate for penem antibiotics carried out by Takasago on a scale of 50–120 t year^{-1} [68, 98b, 105]. Similar results (*ee* 98–99%, *de* 94%, TON 200, TOF ~600 h^{-1} at 50 °C/100 bar) were obtained

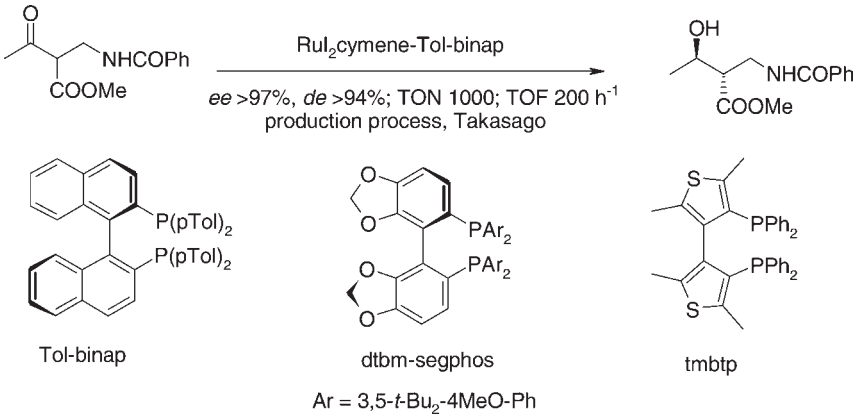

Scheme 7.28 Hydrogenation–dynamic kinetic resolution of a penem intermediate.

by Chemi with an Ru–tmbtp catalyst [38, 106] and recently it was reported that an optimized dtbm–segphos ligand can achieve even higher stereoselectivities with >99% *ee* and 99% de (TON and TOF not specified) [25, 99].

Several processes using simple β-keto ester substrates were developed to various stages. Some early examples of bench scale processes using Ru–binap were described by Takasago and Aventis (for more information, see [18]). Lanxess has developed similar technology for the hydrogenation of several substrates on the basis of its ClMeO-biphep ligand, which is applied on a technical scale [1, 107] (Scheme 7.29). Also depicted in Scheme 7.29 is the hydrogenation of a chlorinated β-keto ester developed to the pilot stage and applied on a multi-hundred kilogram scale by Chemi using its proprietary tmbtp ligand [77]. Roche has described a pilot process for the long-chain β-keto ester, an intermediate for the anti-obesity drug orlistat [108].

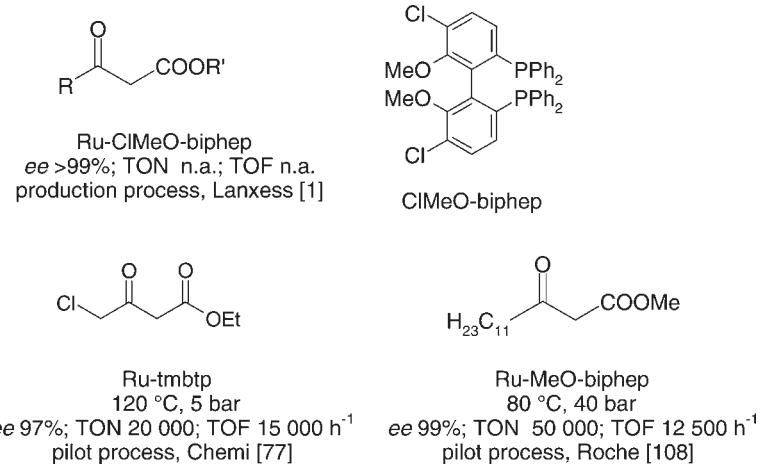

Scheme 7.29 Hydrogenation of β-keto acid derivatives.

7.5.3
Hydrogenation of Aromatic Ketones

The effective hydrogenation of ketones without α- or β-functionality has only recently been developed into an important methodology with Noyori's discovery of the Ru-based transfer hydrogenation catalysts on the one hand and the very active Ru–diphosphine–diamine systems on the other [98a]. Both methodologies rely on the presence of an NH bond allowing an effective outer-sphere reduction mechanism. The technology has been licensed by several companies using various diphosphines, but it is not clear whether it is actually used for concrete manufacturing purposes.

Processes for the hydrogenation of a number of aromatic ketones are shown in Scheme 7.30. Noyori's very effective Ru–diphosphine–diamine technology was developed by several companies. It is not clear on what scale the processes developed by Takasago (dm-binap = 3,5-xylyl-binap) [25] and Dow/Chirotech [27, 109, 110] for the reduction of substituted acetophenones are actually applied, but according to

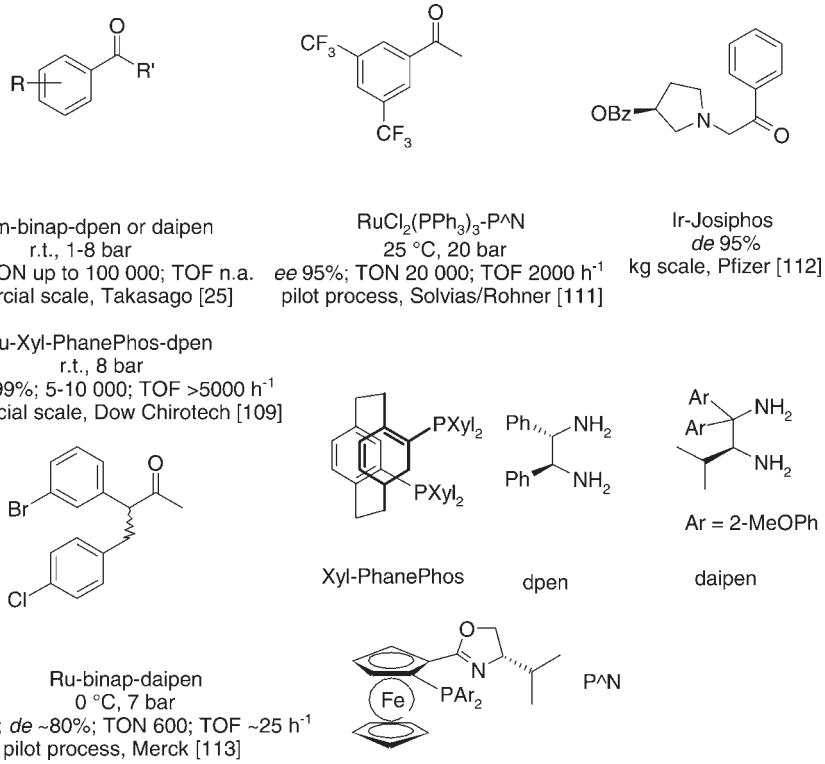

Scheme 7.30 Hydrogenation of aromatic ketones.

Dow, several aromatic ketones have been reduced on a 100–750 kg scale [43]. Using the Xyl-PhanePhos–dpen catalyst, a highly efficient bench scale process was developed for the hydrogenation of *p*-fluoroacetophenone (*ee* 98%, TON 100 000, TOF 50 000 h^{-1} at room temperature, 8 bar) [109]. A pilot process was developed by Solvias and carried out by Rohner for the production of 3,5-bis(trifluoromethyl)phenylethanol using a newly developed Ru–(phosphinoferrocenyl)oxazoline complex [111]. Even though the complex does not contain an NH bond, it shows very high activity for the hydrogenation of a variety of aryl ketones. Pilot-scale processes were reported by Pfizer for the synthesis of the opioid receptor antagonist CJ-15,161 [112] and by Merck for an intermediate of the CB-1R inverse agonist taranabant [113].

Several Ru-catalyzed transfer hydrogenations have been developed and operated on a multi-tens of kilograms scale. Two variants are applied, one based on Ru–amino alcohol complexes with *i*-PrOH and the other based on Ru–Ts-dpen complexes with HCOOH–NEt_3 as reducing system, respectively. As shown in Scheme 7.31, excellent enantioselectivities have been obtained for several aryl ketones but with lower activities than for comparable hydrogenation reactions described above [compare, e.g., the results for bis(trifluoromethyl)acetophenone in Scheme 7.30 with the process developed by Merck [114] in Scheme 7.31]. Avecia (now NPIL Pharma) developed transfer hydrogenation technology under the term CATHy using Me_5cp–Ru catalysts and

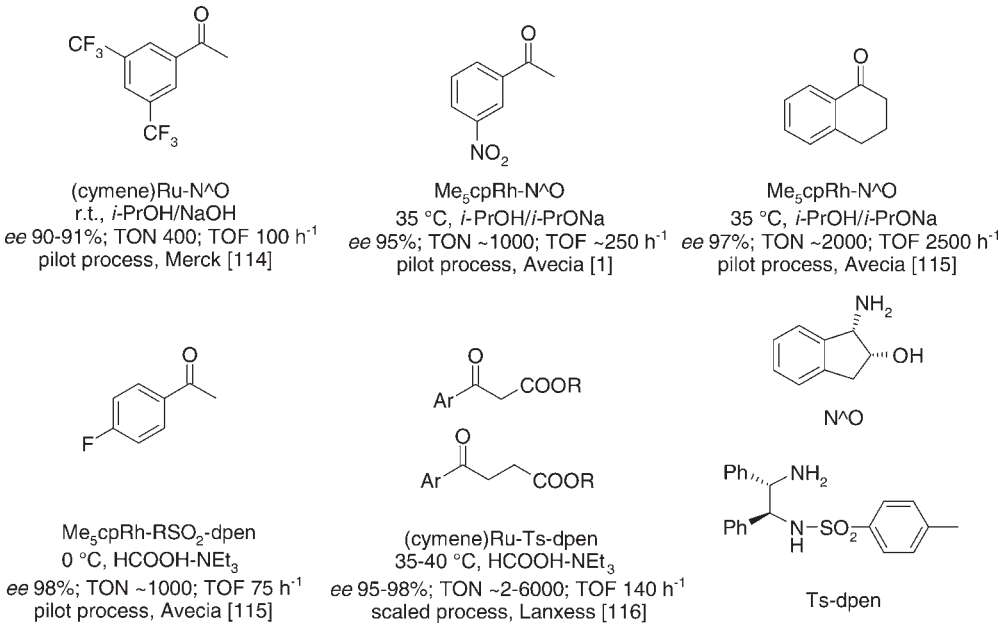

Scheme 7.31 Transfer hydrogenation of aromatic ketones.

claimed several applications on the multi-hundred kilograms scale [1, 115, 117]. Lanxess has applied Noyori's Ru–Ts-dpen system to the reduction of aryl keto esters on a scale of >2 t [107, 116]. Fairly complex molecules are amenable to the catalysts, as illustrated by the feasibility studies by Otsuka for the vasopressin V_2 receptor antagonist OPC-41061 [118] and Merck for a PDE4 inhibitor [119] (Scheme 7.32).

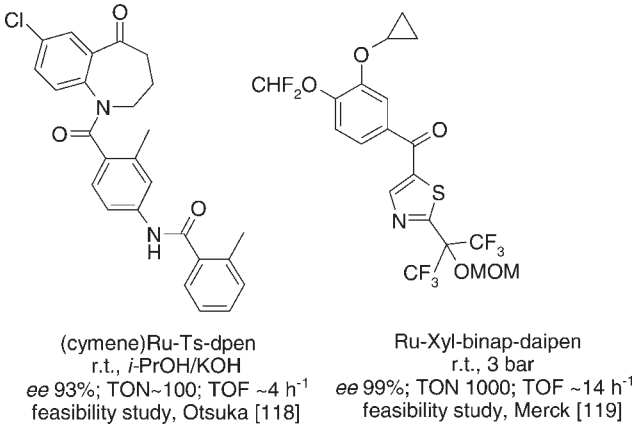

Scheme 7.32 Feasibility studies.

Finally, hydride reduction using BH_3 in the presence of 1,2-amino alcohols (CBS reduction) can be run catalytically, albeit with very low TONs and TOFs. Furthermore, compared with (transfer) hydrogenations, reductions with hydrides require more

complex work-up procedures and produce more waste. Nevertheless, several processes based on this technology have been developed and run on a scale of up to 50 kg (for details, see [18]). Co–salen-catalyzed borohydride reductions are an alternative technology which in special cases can give good results. An example is depicted in Scheme 7.33 for the reduction of a heteroaryl ketone, an intermediate for a serotonin-2 receptor antagonist, albeit with relatively low *ee*s, developed by Mitsui [120].

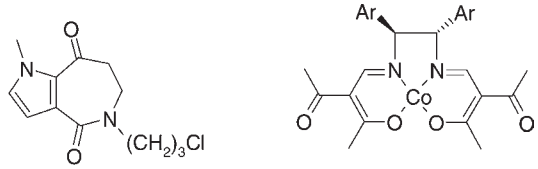

Scheme 7.33 Hydride reduction.

7.6 Hydrogenation of C=N Bonds

The enantioselective hydrogenation of C=N bonds is the least developed hydrogenation reaction, even though many active ingredients contain chiral amine moieties. The main reason for this situation is that effective catalysts, mainly Ir-diphosphine complexes, were developed only in the last 10 years [121]. A major incentive for the development of more active catalysts was the chiral switch of metolachlor made in 1997 by Ciba-Geigy [122, 123].

7.6.1 (S)-Metolachlor Process

Metolachlor is the active ingredient of Dual, one of the most important grass herbicides for use in maize and a number of other crops. In 1997, after years of intensive research, Dual Magnum with a content of approximately 90% (1′*S*)-diastereomers and with the same biological effect at about 65% of the use rate was introduced in the market. This 'chiral switch' was made possible by the new technical process that is briefly described below. The key step of this new synthesis is the enantioselective hydrogenation of the isolated MEA imine depicted in Scheme 7.34.

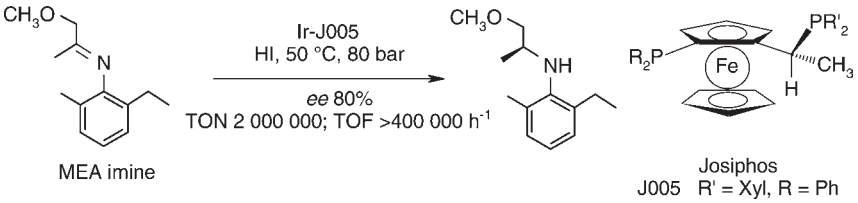

Scheme 7.34 Metolachlor hydrogenation process.

Table 7.4 Most successful ligands for the hydrogenation of MEA imine (for ligand structure, see Scheme 7.34).

R	R′	TON	TOF (h^{-1})	*ee*	Comments
Ph	3,5-Xylyl	2 000 000	>400 000	79	Production process
p-CF_3Ph	3,5-Xylyl	800	400	82	Ligand screening
Ph	4-*t*-Bu-C_6H_4	5000	80	87	Low temperature
Ph	4-(*n*-Pr)$_2$N-3,5-xyl	100 000	28 000	83	Optimized conditions

The search for a commercially viable process took many years [123]. Several approaches with Rh or Ir complexes using commercially available diphosphine ligands were not successful. A critical breakthrough was achieved when Ir complexes with a new class of ferrocenyl-based ligands, now called Solvias Josiphos, were used. Especially in presence of acid and iodide ions, extremely active and productive catalysts were obtained. Different Josiphos ligands were tested and a selection of the best results is given in Table 7.4.

The optimized process operates at 80 bar hydrogen and 50 °C with a catalyst generated *in situ* from [Ir(cod)Cl]$_2$ and the Josiphos ligand J005 (short name Xyliphos) at an s/c of 2 000 000 in the presence of trace amounts of hydrogen iodide. Complete conversion is reached within 3–4 h, initial TOFs exceed 1 800 000 h^{-1} and the *ee* is around 80%. This process is now operated by Syngenta on a scale of >10 000 t $year^{-1}$ [124].

After this success, a number of technical C=N hydrogenation processes were developed, as depicted in Scheme 7.35. Although the enantioselectivities are good to

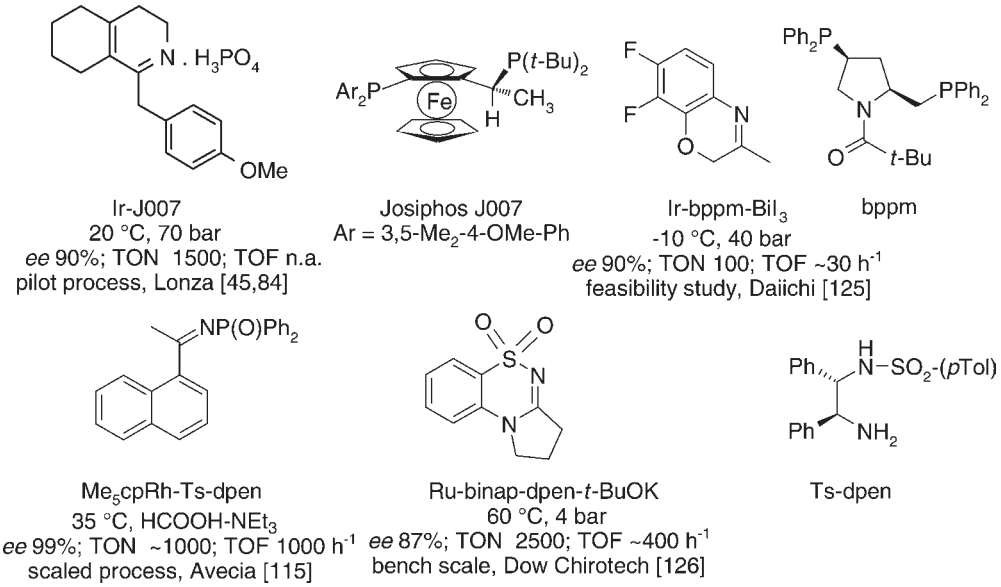

Scheme 7.35 Hydrogenation of a various C=N bonds.

excellent, the catalytic activities and productivities are far behind those for the metolachlor process. An Ir-catalyzed hydrogenation developed by Lonza for an intermediate of dextromethorphan was carried out on the >100 kg scale [45, 84]. Important success factors were fine tuning of the ligand and the use of a biphasic system. Chemoselectivity is high but catalyst productivity rather low for an economic technical application. Satoh *et al*. reported up to 90% *ee* for the hydrogenation of an intermediate of the antibiotic levofloxacin using Ir–diphosphine complexes [125]. Best results were obtained with bppm and modified diop ligands in the presence of bismuth iodide at low temperature.

In addition to Ir–diphosphines, two more catalyst systems showed promise for industrial application. As mentioned above, the Rh–Josiphos-catalyzed hydrogenation of unprotected dehydro-β-amino acid derivatives by Merck actually involves the hydrogenation of a C=N and not a C=C bond (Scheme 7.9) [47, 53]. Noyori's Ru–PP/NN catalyst system also seems suitable for C=N hydrogenation and was successfully applied in a feasibility study by Dow/Chirotech for the hydrogenation of a sulfonylamidine [126]; Avecia showed the viability of its CATHy catalyst also for the transfer hydrogenation of phosphinylimines [115].

7.7
Oxidation Processes

Oxidation reactions are the second most important application of enantioselective catalysts [18]. Important transformations are the oxidation of sulfides with cumyl hydroperoxide (CHP) as oxidant, epoxidation [oxidants *tert*-butyl hydroperoxide (TBHP), CHP or NaOCl] and the Sharpless dihydroxylation reaction of olefins with $K_3Fe(CN)_6$ or *N*-methylmorpholine oxide (NMO) as most common oxidants. In contrast to hydrogenation, the oxidants are often problematic and catalyst activity and productivity are generally much lower. Despite some early successes, the application of the epoxidation and dihydroxylation reactions developed by Sharpless [11], which have been (and still are) used very much for preparative purposes on a laboratory scale, has never really caught on in industry. As a consequence, most transformations described in this sector are probably not being used for manufacturing purposes.

7.7.1
Sulfide Oxidation

7.7.1.1 Esomeprazole (AstraZeneca)

Esomeprazole is the (*S*)-enantiomer of omeprazole, the best selling anti-ulcer compound, and is produced on a multi-tons per year scale. The key step of the new synthesis is the Ti-catalyzed oxidation of the sulfide intermediate (Scheme 7.36) [127]. Although this idea looks straightforward, the development of a successful catalyst system was difficult. Indeed, first attempts with the original Kagan method with quasi-stoichiometric amounts of Ti–tartrate complexes and cumyl hydroperoxide led to almost racemic products. In the course of the investigation, three measures gave

significant improvements: (i) the preparation of the Ti complex from Ti(*i*-PrO)$_4$, diethyl tartrate (DET) and H_2O in the presence of the sulfide, (ii) the equilibration of the catalyst solution and (iii) the presence of a tertiary amine such as EtN(*i*-Pr)$_2$ during the oxidation. Taken together, these changes resulted in a process with *ee*s between 91% (4% catalyst loading) and >94% (with 30 mol% catalyst). The reaction is actually run under the latter conditions (resulting in a more robust process) and the *ee* is enhanced to >99% by crystallization of the Na salt from methyl isobutyl ketone and acetonitrile. Critical issues are over-oxidation to sulfone and substrate purity.

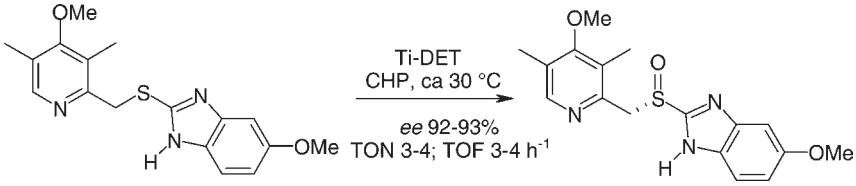

Scheme 7.36 Esomeprazole synthesis.

In addition to this production process, several companies have described sulfide oxidations using cumyl hydroperoxide in the presence of Ti catalysts on a multi-kilogram scale for the synthesis of a variety of drug candidates [128–132] (Scheme 7.37). The range of sulfides amenable to catalytic oxidation and the *ee* values achieved are remarkable, but the TONs are low and in some cases stoichiometric amounts of the Ti complex are needed for satisfactory reaction times and yields.

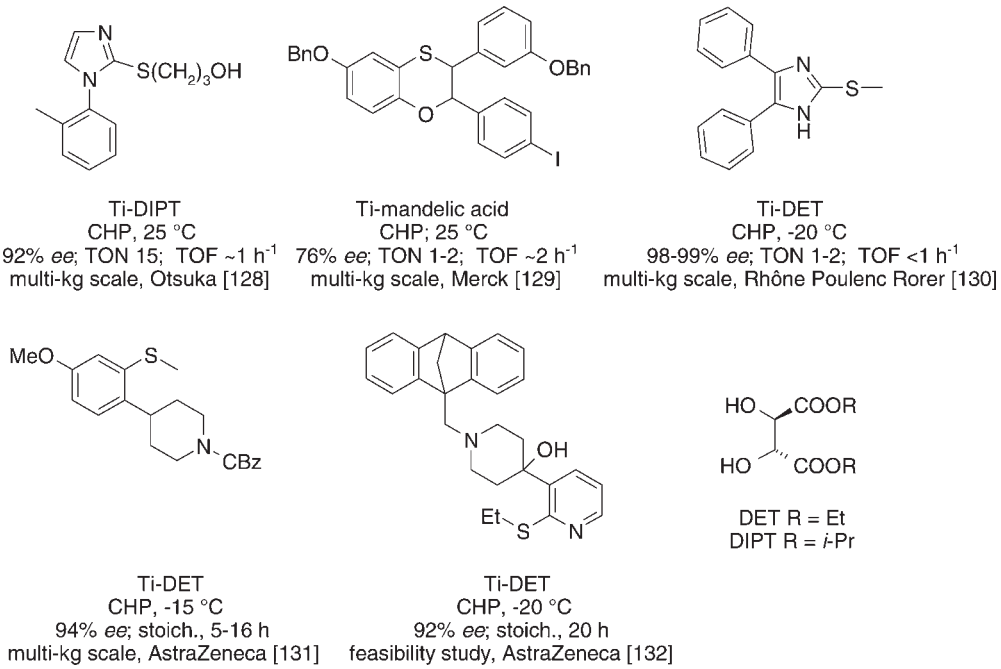

Scheme 7.37 Various sulfide oxidations.

7.7.2 Sharpless Epoxidation

The epoxidation of allylic alcohols using Ti–diisopropyl tartrate (Ti–DIPT) or Ti–diethyl tartrate (Ti–DET) catalysts with either TBHP or CHP as oxidant has been applied in numerous multi-step syntheses of bioactive compounds [14c, 20b]. However, applications on a larger scale are still restricted to the two processes described below. In the presence of molecular sieves, the catalyst is effective for a variety of substituents at the C=C bond and tolerates most functional groups with good to high *ee*s but low activity.

7.7.2.1 Glycidol (PPG-Sipsy)

In the late 1980s, the first large-scale application of the Sharpless epoxidation technology was developed by Arco Chemical for the production of glycidol, a versatile C_3 building block (Scheme 7.38). A detailed account was published by Shum and Cannarsa [4c]. The technology was licensed to PPG-Sipsy, which produced glycidol on a multi-tons per year scale by epoxidation of allylic alcohol using a Ti–diisopropyl tartrate catalyst.

The reaction has been carefully optimized and was run with cumyl hydroperoxide as oxidant in the presence of molecular sieves in order to reach high TONs. After completion of the reaction, the molecular sieves were filtered off and the glycidol was extracted into an aqueous solution and then distilled. The isolation of the glycidol is very difficult and was a challenging aspect of process development. Residual hydroperoxide had to be treated with a reducing agent before disposal. Other epoxy alcohols can be prepared under similar conditions.

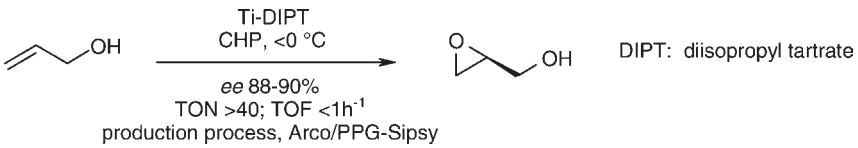

Scheme 7.38 Production process for glycidol.

7.7.2.2 Disparlure (J.T. Baker)

The first commercial application of the very powerful Sharpless epoxidation technology has reportedly been an intermediate for disparlure (an insect pheromone) by J.T. Baker (Scheme 7.39), probably on a very small scale of a few kilograms per year [133]. On this scale, the rather low temperature and relatively high catalyst loading of Ti–diisopropyl tartrate are not problematic.

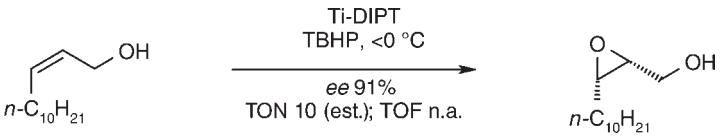

Scheme 7.39 Production process for disparlure.

In addition to these two production processes, Upjohn [134], Aventis [50], Esai [135] and Pfizer [136] described small-scale applications for the epoxidation of simple allylic alcohols depicted in Scheme 7.40. Enantioselectivities ranged from 92 to >98% and in some cases the use of molecular sieves proved beneficial 134].

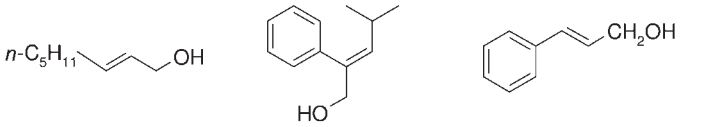

Scheme 7.40 Epoxidation of various allylic alcohols with TBHP.

7.7.3 Jacobsen Epoxidation

The Mn–salen-catalyzed epoxidation originally developed by Jacobsen is able to convert olefins without any functional group to the corresponding epoxide. Mn–salen-type catalysts give good results for terminal and *cis*-substituted olefins with *ee*s up to >97% and moderate to good catalytic activity [14d, 20c], often in high yield and enantioselectivity. In the last few years, the epoxidation of unfunctionalized olefins using cheap NaOCl as oxidizing agent has been developed industrially by Rhodia Chirex in collaboration with Jacobsen [137].

7.7.3.1 Indene Oxide (ChiRex)

The epoxidation of indene (Scheme 7.41) is an attractive route to *cis*-1-amino-2-indanol, an intermediate in the Crixivan synthesis (HIV protease inhibitor, Merck)

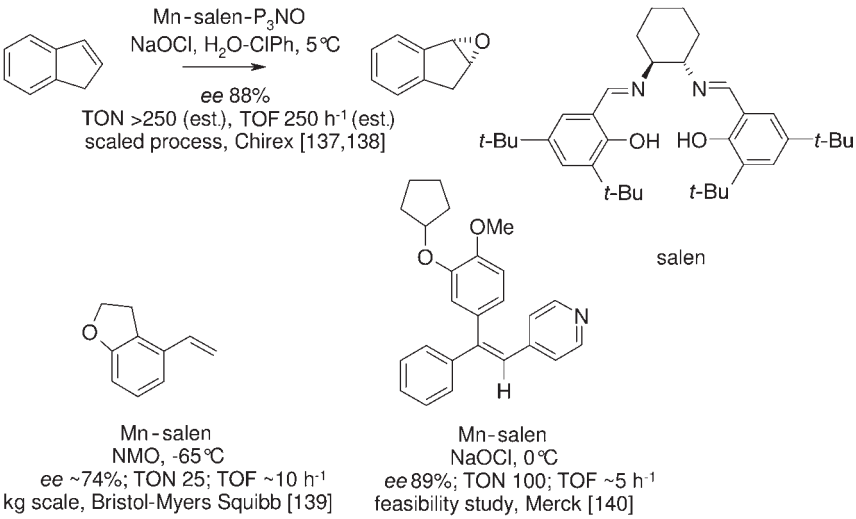

Scheme 7.41 Applications of the Jacobsen epoxidation.

and ligand for BH_3 reductions of ketones. The reaction was optimized in a collaboration between Merck and ChiRex (now part of Rhodia) and is reportedly carried out on a small scale [137, 138]. Decisive for good results of this biphasic (water–ClPh) process was the control of the pH (in order to decrease ligand decomposition) and the addition of 3-phenylpropylpyridine *N*-oxide (P_3NO) to increase catalyst activity and stability.

Two industrial applications have been described by Bristol-Myers Squibb (using NMO as oxidant) [139] and Merck [149] with relatively low *ee*.

7.7.4
Sharpless Dihydroxylation (AD) and Aminohydroxylation

The asymmetric dihydroxylation (AD) of olefins developed by Sharpless [11] leads to *cis*-diols with high to very high *ee*s using Os–cinchona alkaloid complexes (for a representative structure, see Scheme 7.42) [14e, 20d]). This reaction has been applied in numerous laboratory-scale syntheses and a catalyst–oxidant mixture (AD-mix) is available from Strem. However, even though it has been developed by Rhodia Chirex [141], its application on a large scale seems to be challenging and relatively few cases have been published. $K_3Fe(CN)_6$–K_2CO_3, the oxidant used in the commercially available AD-mixes, is problematic on a larger scale. The analogous aminohydroxylation reaction [20e] leading directly from olefins to 1,2-amino alcohols has a similar synthetic potential but the additional problems of chemo- and regioselectivity make synthetic and particularly industrial applications more difficult.

According to Rhodia ChiRex, the asymmetric dihydroxylation represents a robust manufacturing technology, giving good chemical yields and enantioselectivities. Several diols, such as 3-chlorophenylethanediol, have been manufactured on a scale

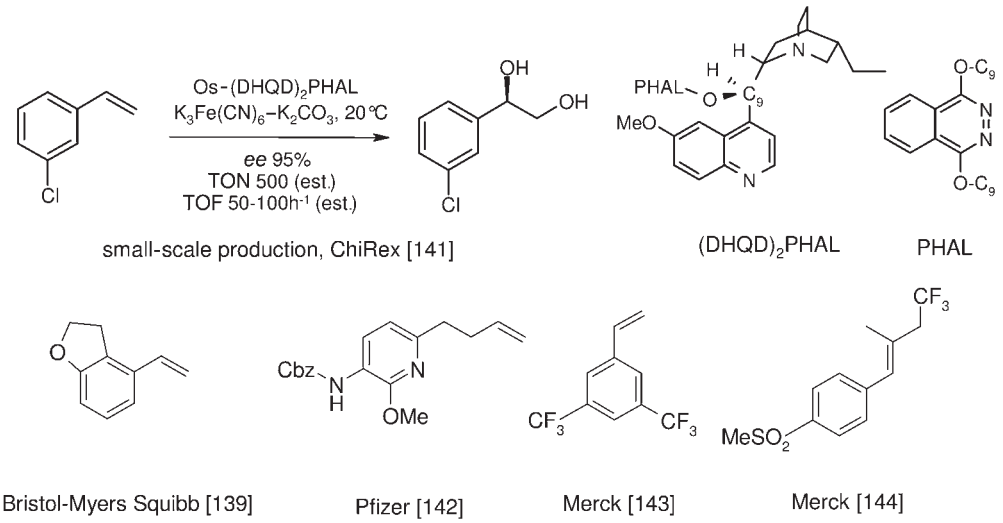

Scheme 7.42 Applications of the Sharpless dihydroxylation.

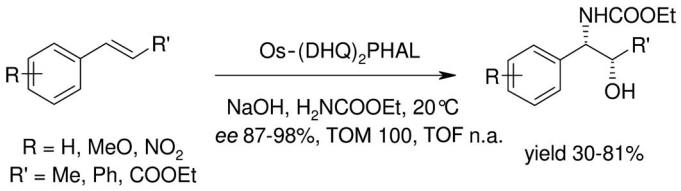

Scheme 7.43 Sharpless aminohydroxylation

of hundreds of kilograms [141] (Scheme 7.42). Furthermore, feasibility studies for the application of the AD reaction to the synthesis of active ingredients have been published by Bristol-Myers Squibb (scaled up to the 10 kg scale) [139], Pfizer [142] and Merck [143, 144]. Enantioselectivities ranged from 79 to >90% and s/c ratios of around 100 were achieved. With the exception of bistrifluorostyrene (NMO), $K_3Fe(CN)_6$ was used as oxidant.

We are aware of only one application of aminohydroxylation for the synthesis of chiral building blocks on a kilogram scale reported by Merck (Scheme 7.43). The original oxidant *t*-BuOCl was replaced by dichlorodimethylhydantoin and both regioselectivities (from 2:1 to 8:1) and enantioselectivity were acceptable [145].

7.8 Miscellaneous Transformations (Isomerization, Addition Reactions to C=C, C=O and C=N Bonds, Opening of Oxacycles)

7.8.1 Isomerization, Allylic Alkylation

Although the isomerization of allylamines, which is operated on a very large scale in the menthol process, has a rather narrow scope, nucleophilic allylic substitution reactions [20f] with C- and N-nucleophiles have been applied not just in model studies but also for the synthesis of many natural products and pharmaceutically relevant molecules [146]. However, even though Dow Chirotech [147] has commercialized two ligands developed by Trost and produces them regularly on a kilogram scale [43], to our knowledge no large-scale application has been reported up to now.

7.8.1.1 (−)-Menthol Process (Takasago)

As described by Akutagawa [67], Takasago produced 28 700 t of (−)-menthol between 1983 and 1996 using only 250 kg of the chiral ligand binap. The key step is the enantioselective isomerization of diethylgeranylamine to the chiral enamine depicted in Scheme 7.44.

The history of the discovery of the Rh–binap catalyst and the first large-scale enantioselective process have been well described in several reviews [5b, 20g, 67]. Decisive for the very high catalyst productivity were the purification of the starting material (distillation and pretreatment with vitride) and the efficient catalyst recycling after distillation. Catalyst loss with each recycle was reported to be ca 2%. In addition

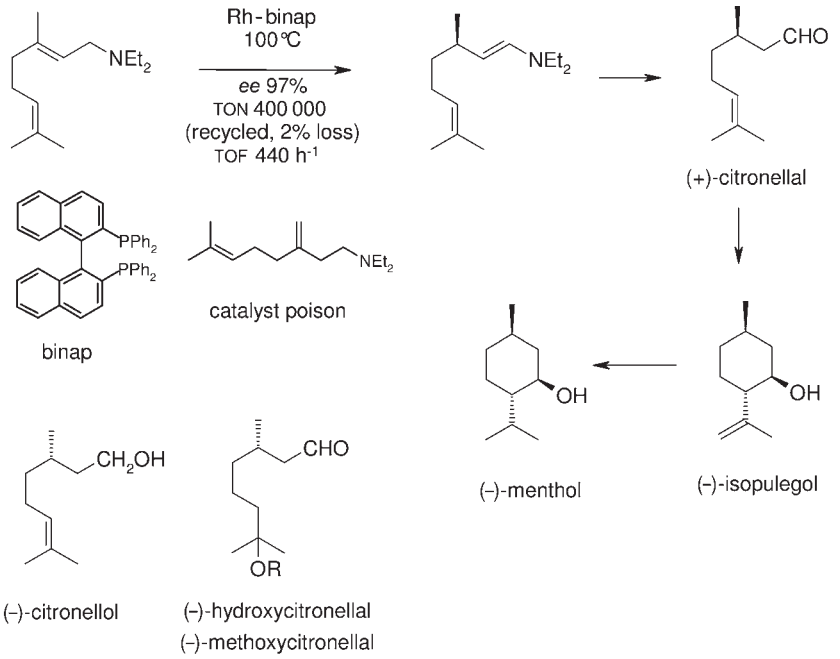

Scheme 7.44 Isomerization of diethylgeranylamine and structure of commercialized products.

to O_2, H_2O and CO_2, the presence of amines in concentrations as low as 0.07% also negatively affects the catalyst performance (Scheme 7.44). The following products are being produced based on the isomerization technology [20g, 68]: L-menthol (>1000 t year^{-1}), 7-hydroxycitronellal (40 t year^{-1}), D- and L- citronellol (20 t year^{-1} each), 7-methoxycitronellal (10–20 t year^{-1}) and 3,7-dimethyloctanal (7 t year^{-1}).

7.8.1.2 Various Alkylation Reactions

The allylic alkylation reaction was used by Merck chemists [148–150] for the gram to multi-kilogram preparation of a variety of intermediates for active compounds (Scheme 7.45). In all cases, the Trost ligand (licensed to Dow, produced on a multi-kilogram scale [43]) was used and very good enantioselectivities but relatively low TON were achieved. The classical Pd-based system was applied for the two reactions with cyclopentenyl acetate whereas the Mo-based catalyst was used for the unsymmetrical linear substrate.

7.8.2 Addition Reactions to C=C Bonds

Addition reactions to olefins can be used both for the construction and the functionalization of molecules. Accordingly, chiral catalysts have been developed for many different types of reactions with often very high enantioselectivity. Despite the early success of Sumitomo with cyclopropanation, most catalysts have either a narrow

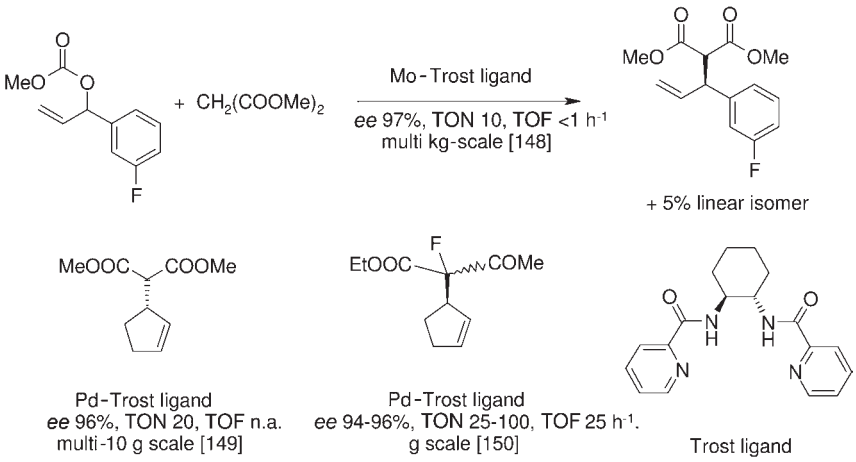

Scheme 7.45 Allylic alkylation reactions.

synthetic scope or are not yet developed for immediate industrial application due to insufficient activities and/or productivities, and most of the ligands are not available on a technical scale and only few industrial applications have been reported [18].

7.8.2.1 Cilastatin (Sumitomo)

Ethyl dimethylcyclopropanecarboxylate is an intermediate for cilastatin, an inhibitor for dehydropeptidase I, which is administered in combination with the carbapenem antibiotic imipenem produced by Sumitomo on a small scale via addition of a carbene to isobutene. Sumitomo introduced this process almost at the same time as the L-dopa process was put on-stream [14f, 151]. However, even though the reaction is really remarkable, its impact on enantioselective catalysis was marginal. This could be due to two reasons: first, cyclopropanes are relatively rare structural motifs, and, second, Sumitomo, with the exception of the ligand design and optimization (see Scheme 7.46), has not given much detail on the process except that preparation and handling of the diazo compound are a critical issue.

In addition to this application, Bristol-Myers Squibb has described an Ru–pybox-catalyzed cyclopropanation on the 500 kg scale to produce an intermediate for melatonin antagonists which also included scale-up of the ligand [152], and Abbot has used an Mg-catalyzed Michael reaction for the preparation of kilogram amounts of an intermediate for a selective endothelin A receptor antagonist [153] (Scheme 7.47). In both cases good *ee* and respectable TONs were achieved.

7.8.3 Addition Reactions to C=O Bonds

Addition reactions to carbonyl groups are very important in synthetic methodology. Even though a wealth of catalysts with high enantioselectivity have been developed in recent years, there are only few industrial applications and some examples are

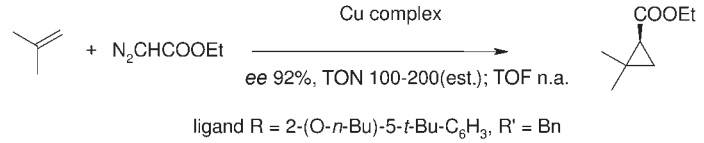

ee (%) for ethyl chrysanthemate

R'	R	OMe	OBu	OBu (Me)	OBu (Ph)	OBu (tBu)	OBu (tBu)	OOct
Me	5	20	50	50	55	65	70
Bn	10	40	45		45	50	50
iBu	20	30	30			30	

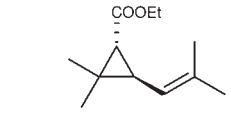

ethyl chrysanthemate

Scheme 7.46 Sumitomo cyclopropanation: optimized process for cilastatin and results of the ligand optimization for ethyl chrysanthemate.

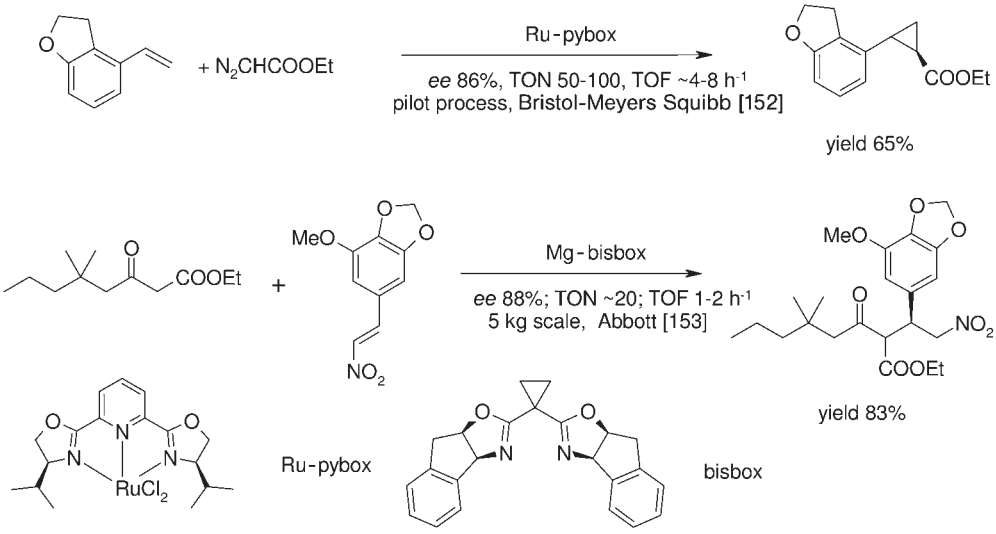

Scheme 7.47 C–C bond-forming applications.

depicted in Schemes 7.48 and 7.49. Most catalysts have low to medium catalytic activity and TONs of 5–100.

The first industrial ene reaction was carried out by Roche [14b, 154] on a multi-hundred kilogram scale to produce an intermediate for the collagenase inhibitor

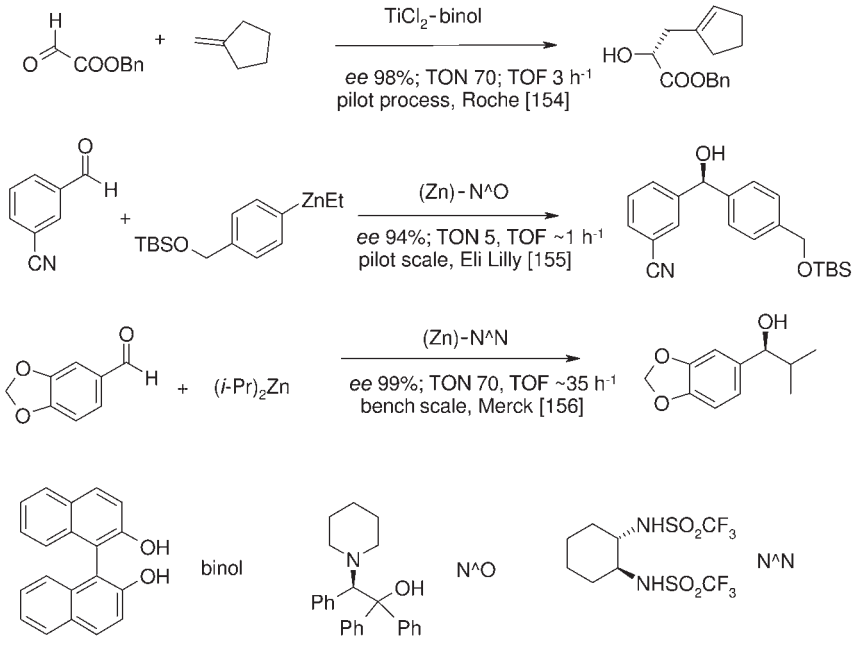

Scheme 7.48 Addition reactions to aldehydes.

Trocade with very high *ee*. Critical for good results was the addition of molecular sieves with a defined water content (6–10%). Eli Lilly [155] carried out the addition of an organozinc species to an aromatic aldehyde on a kilogram scale, and Merck [156] applied a similar reaction on the 500 g scale and, in a feasibility study, Mitsubushi Rayon [157] added TMSCN to *m*-chlorobenzaldehyde (Al–binol, 90% *ee*). Enantioselectivities varied between 90 and 98% and TONs up to 70 were achieved.

Two diastereoselective catalytic asymmetric aldol reactions are depicted in Scheme 7.49. Both have been carried out on a kilogram scale. The so-called gold–aldol reaction developed by Ciba-Geigy is the shortest synthesis of MeBmt, cyclosporin's unusual amino acid [158]. The nitroaldol reaction for the preparation of *erythro*-AHPA, a subunit of the promising HIV-protease inhibitors KNI-227 and KNI-272, has been developed for industrial-scale application using an Al complex with three binol ligands and will be carried out by Kaneka upon request [159].

7.8.4
Addition Reactions to C=N Bonds

The same heterobimetallic catalysts developed by Shibasaki were also applied to the asymmetric hydrophosphonylation used for the preparation of several α-aminophosphonic acids on an industrial scale [160] (Scheme 7.50). This industrial process will be carried out by Hokko Chemical Industry on request.

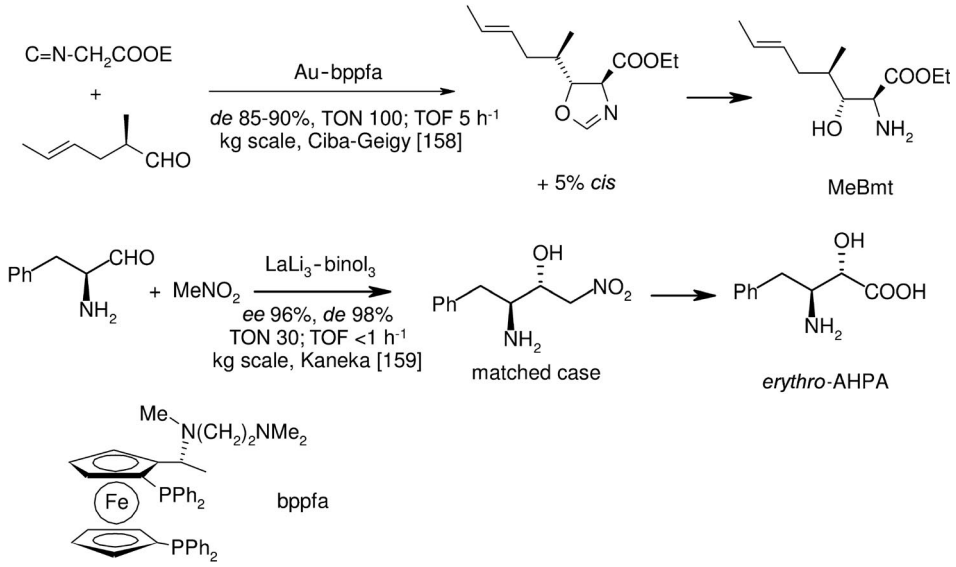

Scheme 7.49 Diastereoselective aldol reactions.

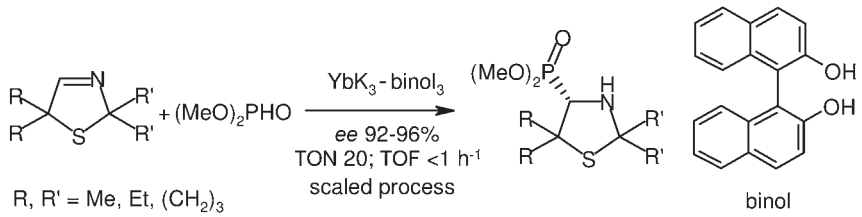

Scheme 7.50 Hydrophosphonylation of C=N bond.

7.8.5
Ring-opening Reactions of Oxacycles

Finally, two ring-opening reaction have interesting potential and have already been applied on a larger scale (Scheme 7.51). The first is the Co–salen-catalyzed hydrolytic kinetic resolution (HKR of epoxides [9f, 161], a reaction which is in many cases more economical for the preparation of enantiopure epoxides than asymmetric epoxidation and often competitive with biocatalytic methods. Rhodia Chirex has developed a catalytic system for resolving propene and styrene oxide and also epichlorohydrin on a multi-hundred kilogram scale [9f]. The catalyst used is the relatively cheap Co–salen complex, which can be recycled. The amount of water and the presence of an acid co-catalyst are critical. The two products can be separated via fractional distillation and both are available with very high *ee*. The reaction is very general for almost all terminal epoxides. The technology was recently licensed to Daiso for epichlorohydrin resolution on a multi-tons per year scale [161b].

The second transformation, the Rh–Josiphos-catalyzed opening of oxabicyclic olefins, has not yet been applied on very large scale but is a very promising method

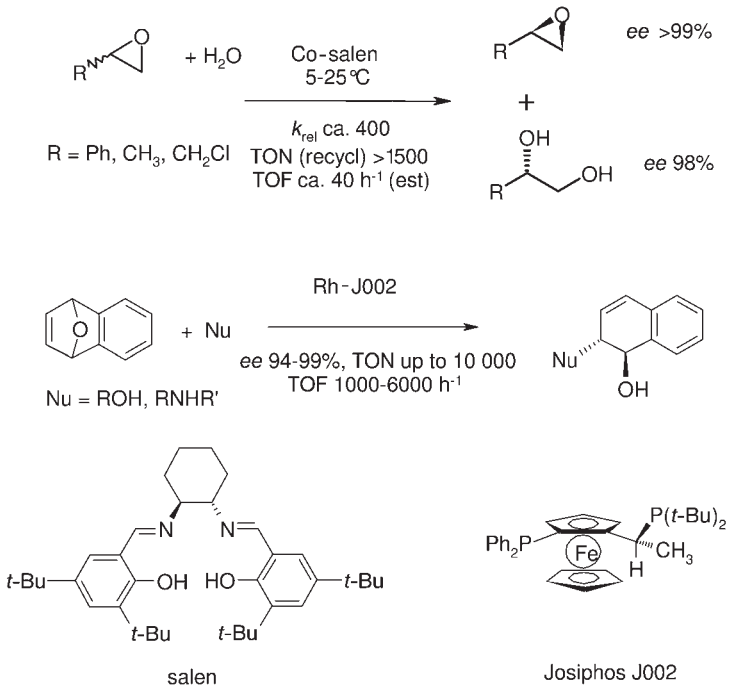

Scheme 7.51 Ring-opening reactions of oxacycles.

for the synthesis of substituted dihydronaphthalenes, important building blocks in medicinal chemistry [162]. The reaction works with various alcohols and *N*-nucleophiles. The s/c ratios were between 50 and 400 and reaction times varied from 6 to >24 h. At 100 °C and without solvent, s/c ratios up to 10 000 are feasible (reaction time 1–8 h) with similar *ee*s. The catalytic system has been developed and scaled to the multikilogram scale by Solvias and several building blocks are available on request [163].

The ring opening of an allylic epoxide (Scheme 7.52) was carried out by Dow Chirotech on a kilogram scale using the Trost technology with good *ee* and TON [164].

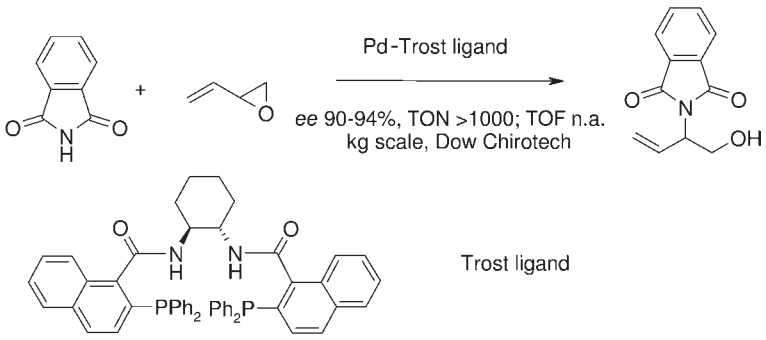

Scheme 7.52 Ring-opening reactions of oxacycles.

7.9
Conclusions and Future Developments

Is homogeneous asymmetric catalysis a mature manufacturing technology? The answer is 'not yet' – with, maybe, the exception of the hydrogenation of a few privileged substrate types. Our definition of a mature manufacturing technology can be summarized as follows:

- Well-defined and widely known scope and limitations (selectivity, activity, productivity, functional group tolerance).
- Many existing technical applications; required equipment widely available.
- Routinely considered in route design during process development.
- Relevant catalysts and auxiliaries are commercially available (including well-defined handling of IP issues), both in large numbers for screening and in technical quantities for production.

The results summarized in the preceding sections show that even for asymmetric hydrogenation, the most advanced catalytic methodology, some of these requirements are 'not quite fulfilled' or 'not yet satisfactory'. However, in the last few years, technical progress has accelerated and one of the most significant signs of this development is the growing number of companies active in this exciting area of chemical technology. The visibility of enantioselective hydrogenation as a superb manufacturing tool for chiral intermediates and active products will certainly be enhanced by their scientific/technical publications but also by their considerable marketing efforts.

Since the first processes were implemented by Monsanto and Sumitomo in the early 1970s, the number of production processes has grown only slowly and today comprises only about 15–20 entries. Of these, 11 are medium to large scale; all others are applied on a scale of $1\,t\,year^{-1}$ or less and several of them are no longer in operation. In addition, many more processes developed to the pilot or bench scale are in principle ready for technical application.

There are several reasons for the rather slow progress. Maybe the most important one is the very high attrition rate for new chemical entities in the pharmaceutical industry, and also the relatively low number of new drugs introduced in the last decade. Another reason is the fact that it takes more time (and money!) to find and develop a catalytic process compared with classical organic transformations. Even though we have shown that many enantioselective catalysts are very tolerant of functional groups, the scope and limitations of valuable enantioselective catalysts are not (yet) well known, making synthesis planning difficult. Further, some chiral ligands have not been readily available in large quantities and are not trivial to prepare.

Despite these hurdles, we are convinced that in the near future the industrial application of enantioselective catalytic technology will accelerate further, and there are several pointers to strengthen this view. There is the usual time lag for any new technology to be used in actual production – we think (or hope!) that we are at the present moment right at the beginning of the steep part of the classical S-shaped

curve. More and more medium and small companies have expertise in developing catalytic syntheses and offer their services to companies who cannot or do not want to develop such processes in-house. In addition, several companies now offer several different chiral ligands or catalysts in quantities required for large-scale processes.

On the chemical side, there is no doubt that new and more selective and active catalysts will be developed for ever more types of transformations. It is hoped that some of them will belong to the small, elite group of privileged catalysts able to tolerate significant structural variations without loss in catalyst performance. In addition, high-throughput experimentation will in many cases allow more tests to be carried out, thereby shortening the time needed for finding the right catalyst.

Acknowledgments

We would like to thank our many colleagues and friends in the industrial catalytic community for their willingness to give advice and share invaluable information cited as personal comments in the references.

References

1 For a recent update on chiral pharmaceuticals, see Rouhi, A.M. (2004) *Chemical & Engineering News*, June 14, 47.

2 Ramos Tombo, G.M. and Blaser, H.U. (1999) in *Pesticide Chemistry and Bioscience* (eds G.T. Brooks and Roberts, T.R.), Royal Society of Chemistry, Cambridge, pp. 33 (and references cited therein).

3 For a recent overview on the application of hydrogenation technology, see Saudan, L.A. (2007) *Accounts of Chemical Research*, **40**, 1309.

4 Collins, A.N., Sheldrake, G.N. and Crosby, J. (eds) (1997) *Chirality in Industry II*, John Wiley & Sons, Ltd, Chichester: (a) Pauluth, D. and Wächter, A.E.F., p. 263; (b) Bruggink, A., p. 81; (c) Shum, W.P. and Cannarsa, M.J., p. 363.

5 Collins, A.N., Sheldrake, G.N. and Crosby, J. (eds) (1992) *Chirality in Industry I*, John Wiley & Sons, Ltd, Chichester: (a) Crosby, J., p. 1; (b) Akutagawa, S., p. 313.

6 Ager, A. (ed.) (2006) *Handbook of Chiral Chemicals*, 2nd edn, Taylor & Francis, Boca Raton, FL: (a) Kaptein, B., de Vries, T.R., Nieuwenhuijzen, J.W., Kellog, R.M., Grimbergen, R.F.P. and Broxterman, Q.B., p. 97; (b) Ager, D. and Bayley, C.R. p. 589.

7 Franco, P., Schaeffer, M., Zhang, T. and Heckmann, D. (2004) *Chimica Oggi-Chemistry Today*, **22** (5), Suppl. Chiral Catal., 28.Bruno, J.R. (2004) *Chimica Oggi-Chemistry Today*, **22** (5), Suppl. Chiral Catal., 32.

8 Taylor, M.S. and Jacobsen, E.N. (2004) *Proceedings of the National Academy of Sciences of the United States of America*, **101**, 5368.

9 Blaser, H.U. and Schmidt, E. (eds) (2003) *Large Scale Asymmetric Catalysis*, Wiley-VCH Verlag GmbH, Weinheim: (a) Blaser, H.U. and Schmidt, E., p. 1; (b) Knowles, W.S., p. 23; (c) Ager, D.J. and Lanemann, S.A., p. 259; (d) Netscher, T. Scalone, M. and Schmid, R., p. 71; (e) Blaser, H.U., Eissen, M., Fauquex, P.F., Hungerbühler, K., Schmidt, E., Sedelmeier, G. and Studer, M., p. 91;

(f) Aouni, L., Hemberger, K.E., Jasmin, S., Kabir, H., Larrow, J.F., Le-Fur, I., Morel, P. and Schlama, T., p. 165.

10 (a) Straathof, A.J.J., Panke, S. and Schmid, A. (2002) *Current Opinion in Biotechnology*, **13**, 548; (b) Sonet, J.-M. (2007) *sp*^{2}, **6** (7), 32; (c) Tao, J. (2007) *sp*^{2}, **6** (7), 34.

11 For details, see Nobel Lectures, *Angewandte Chemie (International Edition in English)*, **41**, (2002) 1998–2022.

12 Studer, M., Blaser, H.U. and Exner, C. (2003) *Advanced Synthesis and Catalysis*, **345**, 45.

13 For a recent account, see Houk, K.N. and List, B., (2004) *Accounts of Chemical Research*, **37**, 487.

14 Jacobsen, E.N., Yamamoto, H. and Pfaltz, A. (eds) (1999) *Comprehensive Asymmetric Catalysis*, Springer, Berlin: (a) Blaser, H.U. and Studer, M., p. 1353; (b) Schmid, R. and Scalone, M., p. 1439; (c) Katsuki, T., p. 621; (d) Jacobsen, E.N. and Wu, M.H., p. 649; (e) Marko, I.E. and Svendsen, J.S., p. 713; (f) Aratani, T., p. 1451; (g) Akutagawa, S. and Tani, S., p. 145.

15 Maruoka, K. and Ooi, T. (2003) *Chemical Reviews*, **103**, 3013.

16 McMorn, P. and Hutchings, G.J. (2004) *Chemical Society Reviews*, **33**, 108.

17 (a) Keith, J.M., Larrow, J.F. and Jacobsen, E.N. (2001) *Advanced Synthesis and Catalysis*, **343**, 5; (b) Robinson, D.E.J.E. and Bull, S.D. (2003) *Tetrahedron: Asymmetry*, **14**, 1407.

18 Blaser, H.U., Spindler, F. and Studer, M. (2001) *Applied Catalysis A-General*, **221**, 119.

19 Blaser, H.U., Spindler, F. and Thommen, M. (2007) in *Handbook of Homogeneous Hydrogenation* (eds J.G. de Vries and C.J. Elsevier), Wiley-VCH Verlag GmbH, Weinheim, pp. 1279.

20 Ojima, I. (ed.) (2000) *Catalytic Asymmetric Synthesis*, 2nd edn, Wiley-VCH Verlag GmbH, Weinheim: (a) Ohkuma, T., Kitamura, M. and Noyori, R., p. 1; (b) Johnson, R.A. and Sharpless, K.B., p. 231; (c) Katsuki, T., p. 287; (d) Johnson, R.A. and Sharpless, K.B., p. 357; (e) Bolm, C., Hildebrand, J.P. and Muniz, K., p. 399; (f) Trost, B.M. and Lee, C., p. 593; (g) Sawamura, M. and Ito, Y., p. 493.

21 Blaser, H.U., Malan, C., Pugin, B., Spindler, F., Steiner, H. and Studer, M. (2003) *Advanced Synthesis and Catalysis*, **345**, 103.

22 Au-Yeung, T.T.-L. and Chan, A.S.C. (2004) *Coordination Chemistry Reviews*, **248**, 2151.

23 Tang, W. and Zhang, X. (2003) *Chemical Reviews*, **103**, 3029.

24 Barbaro, P., Bianchini, C., Giambastiani, G. and Parisel, S.L. (2004) *Coordination Chemistry Reviews*, **248**, 2131.

25 Kumobayashi, H., Miura, T., Sayo, N., Saito, T. and Zhang, X. (2001) *Synlett*, 1055.

26 Lennon, I.C. and Moran, P.H. (2003) Curr. Opin. *Current Opinion in Drug Discovery & Development*, **6**, 855.

27 Lennon, I.C. and Pilkington, C.J. (2003) *Synthesis*, 1639.

28 Iida, T. and Mase, T. (2002) Curr. Opin. *Current Opinion in Drug Discovery & Development*, **5**, 834.

29 Ikunaka, M. (2003) *Chemistry - A European Journal*, **9** 379.

30 Breuer, M., Ditrich, K., Habicher, T., Hauer, B., Kessler, M., Stürmer, R. and Zelinski, T. (2004) *Angewandte Chemie-International Edition*, **43**, 788.

31 Sheldon, R.A. (1993) *Chirotechnology*, Marcel Decker, New York..

32 Morrison J.D. (ed.) (1985) *Asymmetric Synthesis*, Vol. 5, Academic Press, New York.

33 Blaser, H.U., Pugin, B. and Spindler, F. (2005) *Journal of Molecular Catalysis A-Chemical*, **231**, 1.

34 (a) Knowles, W.S. (2002) *Angewandte Chemie-International Edition*, **41**, 1998; (b) earlier publications: Knowles, W.S. *Chem. Ind. (Dekker)* **68**, (1996) 141; Knowles, W.S. (1983) *Accounts of Chemical Research* **16**, 106; Knowles, W.S. (1986) *J Chem Educ*, **63** 222.

35 Selke, R. (2003) in *Large Scale Asymmetric Catalysis* (eds H.U. Blaser and E. Schmidt), Wiley-VCH Verlag GmbH, Weinheim, pp. 39.

36 Adamczyk, M., Akireddy, S.R. and Reddy, R.E. (2000) *Organic Letters*, **2**, 3421.

37 Fiorini, M. Riocci, M. and Giongo, M. (1982) European Patent EP 077099, assigned to Anic SpA; described in Ojima, I., Clos, N. and Bastos, C. (1989) *Tetrahedron*, **45**, 6901.

38 Piccolo, O.personal communication.

39 Andrade, J.G. and Prescher, G. (1989) *Chemistry Industry (Dekker)*, **40**, 33.

40 Cobley, C.J., Johnson, N.B., Lennon, I.C., McCague, R., Ramsden, J.A. and Zenotti-Gerosa, A. (2003) in *Large Scale Asymmetric Catalysis* (eds H.U. Blaser and E. Schmidt), Wiley-VCH Verlag GmbH, Weinheim, pp. 269.

41 Hiebl, J., Kollmann, H., Rovenszky, F. and Winkler, K. (1999) *The Journal of Organic Chemistry*, **64**, 1947.

42 Johnson, N.B., Lennon, I.C., Moran, P.H. and Ramsden, J.A. (2007) *Accounts of Chemical Research*, **40**, 1291.

43 Lennon (Dowpharma), I.C.personal communication.

44 Blaser, H.U. and Spindler, F. (1997) *Topics in Catalysis*, **4**, 275.

45 McGarrity, J.F., Brieden, W., Fuchs, R., Mettler, H.-P., Schmidt, B. and Werbitzky, O. (2003) in *Large Scale Asymmetric Catalysis* (eds H.U. Blaser and E. Schmidt), Wiley-VCH Verlag GmbH, Weinheim, pp. 283.

46 Fuchs, R. (1996) European Patent EP 803502, assigned to Lonza AG.

47 Shultz, C.S. and Krska, S.W. (2007) *Accounts of Chemical Research*, **40**, 1320.

48 Shultz, C.S., Dreher, S.D., Ikemoto, N., Williams, J.M., Grabowski, E.J.J., Krska, S.W., Sun, Y., Dormer, P.G. and DiMichele, L. (2005) *Organic Letters*, **7**, 3405;Sun, Y. (2004) *Proceedings of Chiral USA 2004*, Scientific Update, 2004.

49 Boaz, N.W., Debenham, S.D., Large, S.E. and Moore, M.K. (2003) *Tetrahedron: Asymmetry*, **14**, 3575.

50 Beck, G. (2002) *Synlett*, 837.

51 Drexler, H..-J., You, J., Zhang, S., Fischer, C., Baumann, W., Spanneberg, A. and Heller, D. (2003) *Organic Process Research & Development*, **7**, 355, and references cited therein.

52 Zhang, X. (2004) *Chimica Oggi-Chemistry Today*, **22** (5), Suppl. Chiral Catal., 10.

53 Hoge, G. (2005) *Proceedings Chiral USA Symposium*, Spring Innovation, Stockport.

54 Wu, H.-P. and Hoge, G. (2004) *Organic Letters*, **6**, 3645.

55 Hoge, G., Wu, H..-P., Kissel, W.S., Pflum, D.A., Greene, D.J. and Bao, J. (2004) *Journal of the American Chemical Society*, **126**, 5966.

56 Hsiao, Y., Rivera, N.R., Rosner, T., Krska, S.W., Njolito, E., Wang, F., Sun, Y., Armstrong, J.D., Grabowski, E.J.J., Tillyer, R.D., Spindler, F. and Malan, C. (2004) *Journal of the American Chemical Society*, **126**, 9918.

57 Clausen, A.M., Dziadul, B., Cappuccio, K.L., Kaba, M., Starbuck, C., Hsiao, Y. and Dowling, T.M. (2006) *Organic Process Research & Development*, **10**, 723.

58 Matsumura, K., Zhang, X., Xiaoyong, and Saito, T. (2005) European Patent EP 1386901, assigned to Takasago;.

59 Shimizu, H., Nagasaki, I., Matsumura, K., Sayo, N. and Saito, T. (2007) *Accounts of Chemical Research*, **40**, 1385; Saito, T., personal communication.

60 Scalone, M., Schmid, R., Broger, E.A., Burkart, W., Cereghetti, M., Crameri, Y., Foricher, J., Henning, M., Kienzle, F., Montavon, F., Schoettel, G., Tesauro, D., Wang, S., Zell, R. and Zutter, U. (1997) in *Proceedings of the ChiraTech'97 Symposium*.

61 Storace, L., Anzalone, L., Confalone, P.N., Davies, W.P., Fortunak, J.M., Giangiordano, M., Haley, J.J., Kamholz, K., Li, H..-Y., Ma, P., Nugent, W.A., Parson, R.L., Sheeran, P.J., Silverman, C.E., Waltermire, R.E. and Wood, C.C. (2002) *Organic Process Research & Development*, **6**, 54.

62 Thayer, A.M. (2007) *Chemical & Engineering News*, **85** (32), 11.

63 Hettche, F., Jaekel, C., Friedrich, M. and Paciello, R. (2004) Patent WO, 2006002999, assigned to BASF.

64 Cobley, C.J., Lennon, I.C., Praquin, C., Zenotti-Gerosa, A., Appell, R.B., Goralski, C.T. and Sutterer, A.C. (2003) *Organic Process Research & Development*, **7**, 407; Burk, M.J., Bienewald, F., Harris, M. and Zanotti-Gerosa, A. (1998) *Angewandte Chemie-International Edition*, **37**, 1931.

65 Wallace, M.D., McGuire, M.A., Yu, M.S., Goldfinger, L., Liu, L., Dai, W. and Shilcrat, S. (2004) *Organic Process Research & Development*, **8**, 738.

66 Ashcroft, C.P., Challenger, S., Derrick, A.M., Storey, R. and Thomson, N.M. (2003) *Organic Process Research & Development*, **7**, 362.

67 Akutagawa, S. (1997) *Topics in Catalysis*, **4**, 271; Akutagawa, S. Takasago, personal communication.

68 Akutagawa, S. (1995) *Appl Catal*, **128**, 171.

69 Bänziger, M., Cercus, J., Hirt, H., Laumen, K., Malan, C., Spindler, F., Struber, F. and Troxler, T. (2003) *Tetrahedron: Asymmetry*, **14**, 3496.

70 Bonifacio, F., Macinetti, D., Crescenti, C., De Iasi, G., Donnarumma, M. and Mastrangeli, C. (2003) *PharmaChem*, **2** (11–12), 13.

71 Kumobayashi, H. (1996) *Recueil des Travaux Chimiques des Pays-Bas*, **115**, 201.

72 Harrington, P.J. and Lodewijk, E. (1997) *Organic Process Research & Development*, **1**, 72.

73 Crameri, Y., Foricher, J., Hengartner, U., Jenny, C.J., Kienzle, F., Ramuz, H., Scalone, M., Schlageter, M., Schmid, R. and Wang, S. (1997) *Chimia*, **51**, 303.

74 Scalone, M. (2007) Roche Basel, ISOC Conference Camerino September 8–12; via F. Sannicolo (CAFC8 Verbania).

75 Puentener, K. and Scalone, M. (2004) US Patent Appl. 2005/0070714A1. assigned to Roche.

76 Tellers, D.M., Williams, J.C., Humphrey, G., Journet, M., DiMichele, L., Hinksmon, J., McKeown, A.E., Rosner, T. and Tillyer, R.D. (2006) *Journal of the American Chemical Society*, **128**, 17063.

77 Benincori, T., Rizzo, S., Sannicolo, F. and Piccolo, O. (2000) in *Proceedings of the ChiraSource2000 Symposium*, The Catalyst Group, Spring House, PA.

78 Houpis, I.N., Patterson, L.E., Alt, C.A., Rizzo, J.R., Zhang, T.Y. and Haurez, M. (2005), *Organic Letters*, **7**, 1947.

79 McGuire, M.A., Shilcrat, S.C. and Sorenson, E. (1999) *Tetrahedron Letters*, **40**, 3293.

80 Ikemoto, T., Nagata, T., Yamano, M., Ito, T., Mizuno, Y. and Tomimatsu, K. (2004) *Tetrahedron Letters*, **45** 7757; Yamano, T. Takeda Chemical Industries, personal communication.

81 Sturm, T., Weissensteiner, W. and Spindler, F. (2003) *Advanced Synthesis and Catalysis*, **345**, 160; Spindler, F. Solvias AG, unpublished results.

82 Boogers, J.A.F., Felfer, U., Kotthaus, M., Lefort, L., Steinbauer, G., de Vries, A.H.M. and de Vries, J.G. (2007) *Organic Process Research & Development*, **11**, 585; Lefort, L., Boogers, J.A.F., de Vries, A.H.M. and de Vries, J.G. (2006) *Topics in Catalysis*, **40**, 185; Minnaard, A.J., Freinga, B.L., Lefort, L. and de Vries, J.G. (2007) *Accounts of Chemical Research*, **40**, 1267.

83 Hettche, F., Völkert, M. and Jäckel, C. (2006) Patent WO 2006097314, assigned to BASF.

84 Imwinkelried, R. (1997) *Chimia*, **51**, 300.

85 Rautenstrauch, V. (1999) in *Proceedings of the International Symposium on Chirality*, 5–7 September Cambridge, Spring Innovation, Stockport, pp. 204; Dobbs, D.A., Vanhessche, K.P.M., Brazi, E., Rautenstrauch, V., Lenoir, J.-Y., Genet, J.-P., Wiles, J. and Bergens, S.H. (2000) *Angewandte Chemie-International Edition*, **39**, 1992; Dobbs, D.A., Vanhessche, K.P.M. and Rautenstrauch, V. (1997) PatentWO 98/52687 assigned to Firmenich.

86 Hewitt, B.D. (1999) *Chemical and Engineering News*, **77** (44), 35.

87 Klingler, F.D. and Börner, A.personal communication; Klingler, F.D., Steigerwald, M. and Ehlenz, R. (2003) German Patent DE 103 13 118 A1, assigned to Boehringer-Ingelheim.

88 Burk, M., Bienewald, F., Challenger, S., Derrick, A. and Ramsden, J.A. (1999) *The Journal of Organic Chemistry*, **64**, 3290.

89 Bulliard, M., Laboue, B., Lastennet, J. and Roussiane, S. (2001) *Organic Process Research & Development*, **5**, 438.

90 Burk, M.J., de Koning, P.D., Grote, T.M., Hoekstra, M.S., Hoge, G., Jennings, R.A., Kissel, W.S., Le, T.V., Lennon, I.C., Mulhern, T.A., Ramsden, J.A. and Wade, R.A. (2003) *The Journal of Organic Chemistry*, **68**, 5731.

91 Yue, T.-Y. and Nugent, W.A. (2002) *Journal of the American Chemical Society*, **124**, 13692.

92 Broger, E., Crameri, Y. and Jones, P. (1997) Patent WO 99/01453 assigned to Hoffmann-La Roche.

93 Fukatsu, K., Uchikawa, O., Kawada, M., Yamano, T., Yamashita, M., Kato, K., Hirai, K., Hinuma, S., Miyamoto, M. and Ohkawa, S. (2002) *Journal of Medicinal Chemistry*, **45**, 4212.

94 Boulton, L.T., Lennon, I.C. and McCague, R. (2003) *Organic Biomolecular Chemistry*, **1**. 1094.

95 Zanotti-Gerosa, A. and Hems, W. (2007) *Book of Abstracts, CAFC8*.

96 Wichmann, J., Adam, G., Roever, S., Hennig, M., Scalone, M., Cesura, A.M., Dautzenberg, F.M. and Jenck, F. (2000) *European Journal of Medicinal Chemistry*, **35**, 839.

97 Schmid, R. and Scalone, M. (2007); *Electronic Encyclopedia of Reagents for Organic Synthesis*, eEROS, Scalone, M. and Zutter, J.(2000) European Patent Appl. EP 974590 A1, assigned to F. Hoffmann-La Roche.

98 (a) For a recent account, see Noyori, R., Kitamura, M. and Ohkuma, T. (2004) *Proceedings of the National Academy of Sciences of the United States of America*, **101** 5356; (b) Kumobayashi, H. (1996) *Recueil des Travaux Chimiques des Pays-Bas*, **115**, 201.

99 Saito, M., Yokozawa, T., Ishizaki, T., Moroi, T., Sayo, N., Miura, T. and Kumobayashi, H. (2001) *Advanced Synthesis and Catalysis*, **343**, 264.

100 Klingler, F.D. (2007) *Accounts of Chemical Research*, **40**, 1367; Klingler, F.D., Wolter, L. and Dietrich, W. (1999) European Patent, EP 1147075, assigned to Boehringer-Ingelheim; Klingler, F.D. and Wolter, L. (1999) European Patent, EP 1210318, assigned to Boehringer-Ingelheim.

101 Scalone, M. and Waldmeier, P. (2003) *Organic Process Research & Development*, **7**, 418.

102 Blaser, H.U., Gamboni, R., Rihs, G., Sedelmeier, G., Schaub, E., Schmidt, E., Schmitz, B., Spindler, F. and Wetter, Hj. (1999) in *Process Chemistry in the Pharmaceutical Industry* (ed. K.G. Gadamasetti), Marcel Dekker, New York, pp. 189.

103 Penn (Novartis), G. and Spindler (Solvias), F.unpublished work.

104 Cederbaum, F., Lamberth, C., Malan, C., Naud, F., Spindler, F., Studer, M. and Blaser, H.U. (2004) *Advanced Synthesis and Catalysis*, **346**, 842.

105 Noyori, R., Tokunago, M. and Kitamura, M. (1995) *Bulletin of the Chemical Society of Japan*, **68**, 36.

106 Benincori, T., Cesarotti, E., Piccolo, O. and Sannicolo, A. (2000) *The Journal of Organic Chemistry*, 2043. **65**.

107 Gerlach, A. and Scholz, U. (2004) *Speciality Chemicals Magazine*, **24** (4), 37.

108 Schwindt, M.A., Fleming, M.P., Han, Y.-K., Hodges, L.M., Johnston, D.A., Micheli, R.P., Roberts, C.R., Snyder, R., Topping, R.J., Püntener, K. and Scalone, M. (2007) *Organic Process Research & Development*, **11**, 524.

109 Chaplin, D., Harrington, P., Henschke, J.P., Lennon, I.C., Meck, G., Moran, P., Pilkington, C.J., Ramsden, J.A., Warkins, S. and Zenotti-Gerosa, A. (2003) *Organic Process Research & Development*, **7**, 89.

110 Lennon, I.C. and Moran, P. (2004) *Chimica Oggi-Chemistry Today*, **22** (5), Suppl. Chiral Catal., 37.

111 Naud, F., Malan, C., Spindler, F., Rüggeberg, C., Schmidt, A.T. and Blaser, H.U. (2007) *Organic Process Research & Development*, **11**, 319.

112 Andresen, B.M., Caron, S., Couturier, M., DeVries, K.M., Do, N.M., Dupont, K., Gosh, A., Girardin, M., Hawkins, J.M., Makowski, T.M., Riou, M., Sieser, J.E., Tucker, J.L., Vanderplas, B.C. and Watson, T.J.N. (2006) *Chimia*, **60**, 554.

113 Chen, C., Frey, L.F., Shultz, S., Wallace, D.J., Marcantonio, K., Payack, J.F., Vazquez, E., Springfield, S.A., Zhou, G., Liu, P., Kieczykowski, G.R. and Krska, S.W. (2007) *Organic Process Research & Development*, **11**, 616.

114 Hansen, K.B., Chilenski, J.R., Desmond, R., Devine, P.N., Grabowski, E.J.J., Heid, R., Kubryk, M., Mathre, D.J. and Varsolona, R. (2003) *Tetrahedron: Asymmetry*, **14**, 3581.

115 Blacker, J. and Martin, J. (2003) in *Large Scale Asymmetric Catalysis* (eds H.U. Blaser and E. Schmidt), Wiley-VCH Verlag GmbH, Weinheim, pp, 201.

116 Rampf, F. (2004) in *Proceedings of Chiral USA 2004*, Scientific Update.

117 Ikariya, T. and Blacker, A.J. (2007) *Accounts of Chemical Research*, **40**, 1300.

118 Yamashita, H., Ohtani, T., Morita, S., Otsubo, K., Kan, K., Matsubara, J., Kitano, K., Kawano, Y., Uchida, M. and Tabusa, F. (2002) *Heterocycles*, **56**, 123.

119 O'Shea, P.D., Chen, C.-y., Chen, W., Dagneau, P., Frey, L.F., Grabowski, E.J.J., Marcantonio, K.M., Reamer, R.A., Tan, L., Tillyer, R.D., Roy, A., Wan, X. and Zhao, D. (2005) *The Journal of Organic Chemistry*, **70**, 3021.

120 Nagata, T. (2002) *Speciality Chemicals Magazine*, **22** (6), 34.

121 Spindler, F. and Blaser, H.U. (2004) in *Transition Metals for Organic Synthesis*, 2nd edn (eds C. Bolm and M. Beller), Wiley-VCH Verlag GmbH, Weinheim, Vol. 2, pp. 113.

122 Blaser, H.U., Buser, H.P., Coers, K., Hanreich, R., Jalett, H.P., Jelsch, E., Pugin, B., Schneider, H.D., Spindler, F. and Wegmann, A. (1999) *Chimia*, **53**, 275.

123 Blaser, H.U. (2002) *Advanced Synthesis and Catalysis*, **344**, 17.

124 Hofer, R. (2005) *Chimia*, **59**, 10.

125 Satoh, K., Inenaga, M. and Kanai, K. (1998) *Tetrahedron: Asymmetry*, **9**, 2657.

126 Cobley, C.J., Foucher, E., Lecouve, J..-P., Lennon, I.C., Ramsden, J.A. and Thominot, G. (2003) *Tetrahedron: Asymmetry*, **14**, 3431.

127 Cotton, H., Elebring, T., Larsson, M., Li, L., Sörensen, H. and von Unge, S. (2000) *Tetrahedron: Asymmetry*, **11**, 8319; Federsel, H.J. and Larsson, M. (2003) in *Large Scale Asymmetric Catalysis* (eds H.U. Blaser and E. Schmidt), Wiley-VCH Verlag GmbH, Weinheim, pp. 413.

128 Matsugi, M., Fukuda, N., Muguruma, Y., Yamaguchi, T., Minamikawa, J. and Otsuka, S. (2001) *Tetrahedron*, **57**, 2739.

129 Song, Z.J., King, A.O., Waters, M.S., Lang, F., Zewge, D., Bio, M., Leazer, J.L., Javadi, G., Kassim, A., Tschaen, D.M., Reamer, R.A., Rosner, T., Chilenski, J.R., Mathre, D.J., Volante, R.P. and Tillyer, R. (2004) *Proceedings of the National Academy of Sciences of the United States of America*, **101**, 5776.

130 Pitchen, P., France, C.J., McFarlane, I.M., Newton, C.G. and Thompson, D.M. (1994) *Tetrahedron Letters*, **35**, 485.

131 Bowden, S.A., Burke, J.N., Gray, F., McKown, S., Moseley, J.D., Moss, W.O., Murrray, P.M., Welham, M.J. and Young, M.J. (2004) *Organic Process Research & Development*, **8**, 33.

132 Hogan, P.J., Hopes, P.A., Moss, W.O., Robinson, G.E. and Patel, I. (2002) *Organic Process Research & Development*, **6**, 255.

133 Scott, J.W. (1989) *Top Stereochem*, **19**, 209.

134 Sharpless, B.K. (1988) *Janssen Chimica Acta*, **6**, 3.

135 Kimura, T., Yamamoto, N., Suzuki, Y., Kawano, K., Norimine, Y., Ito, K., Nagato,

S., Iimura, Y. and Yonaga, M. (2002) *The Journal of Organic Chemistry*, **67**, 6228.

136 Henegar, K.E. and Cebula, M. (2007) *Organic Process Research & Development*, **11**, 354.

137 Senanayake, C.H. and Jacobsen, E.N. (1999) in *Process Chemistry in the Pharmaceutical Industry* (ed. K.G. Gadamasetti), Marcel Dekker, New York, pp. 347.

138 Davies, I.W. and Reider, P.J. (1996) *Chemical & Engineering News*, 3 June, 413; Hughes, D.L., Smith, G.B., Liu, J., Dezeny, G.G., Senanayake, C.H., Larsen, R.D., Verhoeven, T.R. and Reider, P.J. (1997) *The Journal of Organic Chemistry*, **62** 2222.

139 Prasad, J.S., Vu, T., Totleben, M.T., Crispino, G.A., Kacsur, D.J., Swaminathan, S., Thornton, J.E., Fritz, A. and Singh, A.K. (2003) *Organic Process Research & Development*, **7**, 821.

140 Lynch, J.E., Choi, W..-B., Churchill, H.R.O., Volante, P.R., Reamer, R.A. and Ball, R.G. (1997) *The Journal of Organic Chemistry*, **62**, 9223.

141 Smith, A.A. (1996) in *Proceedings of the ChiraTech'96 Symposium*, The Catalyst Group, Spring House, PA.

142 Dragovich, P.S., Zhou, R. and Prins, T.J. (2002) *The Journal of Organic Chemistry*, **67**, 741.

143 Pye, P.J., Rossen, K., Weissman, S.A., Maliakal, A., Reamer, R.A., Ball, R., Tsou, N.N., Volante, R.P. and Reider, P.J., (2002) *Chemistry - A European Journal*, **8**, 1372.

144 Tan, L., Chen, C-y., Larson, R.D., Verhoeven, T.R. and Reider, P.J. (1998) *Tetrahedron Letters*, **39**, 3961.

145 Barta, N.S., Sidler, D.R., Somerville, K.B., Weissman, S.A., Larsen, R.D. and Reider, P.J. (2000) *Organic Letters*, **2**, 2821.

146 Trost, B.M. (2004) *The Journal of Organic Chemistry*, **69**, 5813.

147 Chaplin, D., Lennon, I.C., Jackson, M., Ramsden, J.A. and Winter, S. (1998) in *Proceedings of the ChiraTech'98 Symposium*, The Catalyst Group, Spring House, PA.

148 Palucki, M., Um, J.M., Yasuda, N., Conlon, D.A., Tsay, F.-R., Hratner, F.W., Hsiao, Y., Marcune, B., Karady, S., Hughes, D.L., Dormer, P.G., and Reider, P.J. (2002) *The Journal of Organic Chemistry*, **67**, 5508.

149 Campos, K.R., Journet, M., Grabowski, E.J.J. and Tillyer, R.D. (2005) *The Journal of Organic Chemistry*, **70**, 268.

150 Zhang, F., Song, Z.J., Tschaen, D. and Volante, R.P. (2004) *Organic Letters*, **6**, 3775.

151 Aratani, T. (1839) *Pure and Applied Chemistry*, **1985**, **57**.

152 Simpson, J.H., Godfrey, J., Fox, R., Kotnis, A., Kacsur, D., Hamm, J., Totleben, M.J., Rosso, V., Mueller, R., Delaney, E., Deshpande, R.P. and Kodersha, G.A. (2003) *Tetrahedron: Asymmetry*, **14** 3569; Gage, J. and Houser, D. (2007) *Speciality Chemicals Magazine*, **27** (8), 40.

153 Barnes, D.M. (2000) *Current Opinion in Drug Discovery & Development*, **3**, 818.

154 Hilpert, H. (2001) *Tetrahedron*, **57**, 7675.

155 Magnus, N.A., Anzeveno, P.B., Coffey, D.S., Hay, D.A., Laurilla, M.E., Schkeryantz, J.M., Shaw, B.W. and Staszak, M.A. (2007) *Organic Process Research & Development*, **11**, 560.

156 Cvetovich, R.J., Chartrain, M., Hartner, F.W., Roberge, C., Amato, J.S. and Grabowski, E.J.J. (1996) *The Journal of Organic Chemistry*, **61**, 6675.

157 Nogami, H., Kanai, M. and Shibasaki, M. (2003) *Chemical Pharmaceutical Bulletin*, **51**, 702.

158 Togni, A., Pastor, S.D. and Rihs, G. (1989) *Helvetica Chimica Acta*, **72**, 1471.

159 Sasai, H., Kim, W.-S., Suzuki, T. and Shibasaki, M. (1994) *Tetrahedron Letters*, **35**, 6123; Shibasaki, M. (University of Tokyo), personal communication.

160 Gröger, H., Saida, Y., Sasai, H., Yamaguchi, K., Martens, J. and Shibasaki, M. (1998) *Journal of the American Chemical Society*, **120**, 3089.

161 (a) Keith, J.M., Larrow, J.F. and Jacobsen, E.N. (2001) *Advanced Synthesis*

and Catalysis, **343**, 5; (b) Stinson, S.C. (2000) *Chemical & Engineering News*, 4 December, 35.

162 For recent reviews, see Lautens, M., Fagnou, K., Hiebert, S., (2003) *Accounts of Chemical Research*, **36**, 48; Lautens, M. and Fagnou, K. (2004) *Proceedings of the National Academy of Sciences of the United States of America*, **101**, 5455.

163 Spielvogel, D. (Solvias) unpublished results.

164 Harris, M.C.J., Jackson, M., Lennon, I.C., Ramsden, J.A. and Samuel, H. (2000) *Tetrahedron Letters*, **41**, 3187.

8
Hydrogenation for C–C Bond Formation

John F. Bower and Michael J. Krische

8.1
By-product-free C–C Coupling and the Departure from Preformed Organometallic Reagents

The formation of chemical bonds between carbon atoms is of fundamental significance. A major goal in the emerging field of green chemistry involves the design of by-product-free chemical processes, especially C–C bond-forming processes applicable to renewable feedstocks [1]. This objective is aligned with longstanding economic and aesthetic forces that have shaped the field of chemical synthesis and which have given rise to such concepts as atom-economy [2], step-economy and the 'ideal synthesis' [3]. As revealed by the 'E-factor' (kilogram of waste generated per kilograms of product) [4], it is not surprising that an inverse correlation between process volume and waste generation exists in the chemical industry. For large-volume processes, where minute improvements in efficiency confer significant economic return, by-product-free chemical processes are desirable as they mitigate costs associated with waste disposal and product isolation. Here, 'fiscal natural selection' mandates the practice of green chemistry. In contrast, the fine chemical and pharmaceutical industrial segments often engage in multi-step syntheses where the value of late-stage intermediates can easily exceed the cost of waste stream disposal or product separation, undermining motivation to develop by-product-free protocols (Table 8.1).

Must waste production generally increase with increasing molecular complexity? What transformations would be practiced on a vast scale if only efficient by-product-free variants were developed? In the specific case of C–C bond-forming processes, especially those involving non-stabilized carbanions and their equivalents, a significant cause of waste production resides in the use of stoichiometrically preformed organometallic reagents, which give rise to equimolar quantities of chemical by-products in the form of metal salts. For example, the vinylation and allylation of carbonyl compounds and imines, which are core reactions in synthetic organic chemistry, uniformly employ preformed vinylmetal and allylmetal reagents. The

Green Catalysis, Volume 1: Homogeneous Catalysis.
Edited by Robert H. Crabtree

ISBN: 978-3-527-32496-5

Table 8.1 Consideration of the 'E-factor' (kilogram of waste per kilogram of product) for various segments of the chemical industry.

Industry segment	Product tonnage	E-factor
Oil refining	10[6]–10[8]	<0.1
Commodity chemicals	10[4]–10[6]	<1–5
Fine chemicals	10[2]–10[4]	5–50
Pharmaceuticals	10–10[3]	25–100

same is true for cross aldol and Mannich additions, which generally employ preformed alkali metal enolates or enol derivatives. A hidden cost associated with the use of such preformed organometallics is that they are often prepared via transmetallation, hydrometallation or acid–base chemistry, where a series of metallated precursors is used. For example, enol silane generation typically involves the use of butyllithium to prepare lithium diisopropylamide, which then serves as a base to generate the lithium enolate, which, finally, upon exposure to a chlorosilane, generates the enol silane. Here, three preformed organometallic reagents are used stoichiometrically. Similarly, vinylmetal reagents and organoboron reagents, which are now indispensable building blocks in pharmaceutical process chemistry [5], also are typically prepared using multiple preformed organometallic reagents, resulting in the generation of multiple stoichiometric by-products and the handling of multiple air- and moisture-sensitive materials. Notably, catalytic hydrogenations of enones, alkynes and aryl halides are all postulated to proceed through analogous organometallic intermediates, raising the question of whether catalytic intermediates of this type can be intercepted and rerouted to products of C–C bond formation (Scheme 8.1).

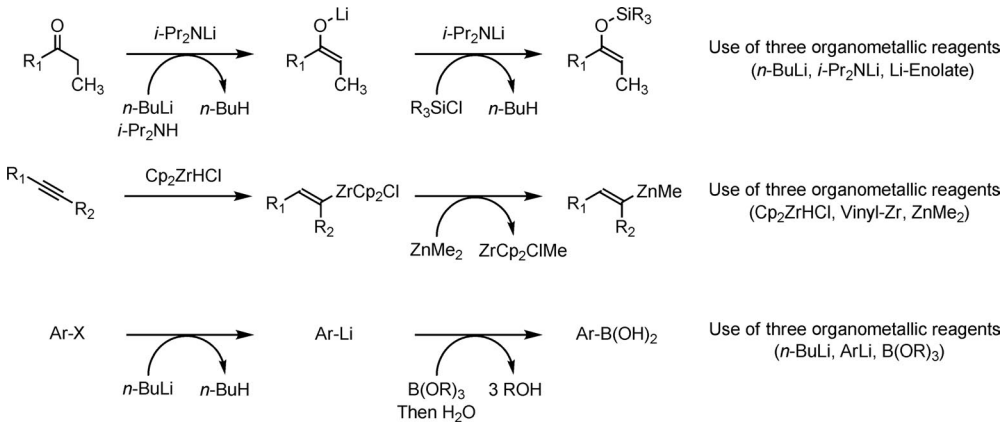

Scheme 8.1 The generation of preformed organometallics often requires successive use of multiple organometallic reagents, contributing to excessive waste generation.

Indeed, the recognition that the addition of non-stabilized carbanions to C=X (X=O, NR) π-bonds represent reductions of the carbonyl or imine moiety evokes the possibility of corresponding catalytic reductive processes, and for catalytic reductive coupling to proceed with complete atom economy, elemental hydrogen should be used as the terminal reductant. In other words, organometallics arising transiently in the course of catalytic hydrogenation may provide an alternative to stoichiometrically preformed organometallic reagents employed routinely in C=X addition processes. Because organic molecules, by their very definition, contain both carbon and hydrogen, a broad new family of *hydrogenative C–C couplings* may be envisioned wherein exposure of two or more molecules to gaseous hydrogen in the presence of a metallic catalyst produces a single, more complex, product in a completely by-product-free fashion. In this way, one may achieve by-product-free variants of classical carbanionic transformations such as carbonyl vinylation, allylation and aldol addition (Scheme 8.2).

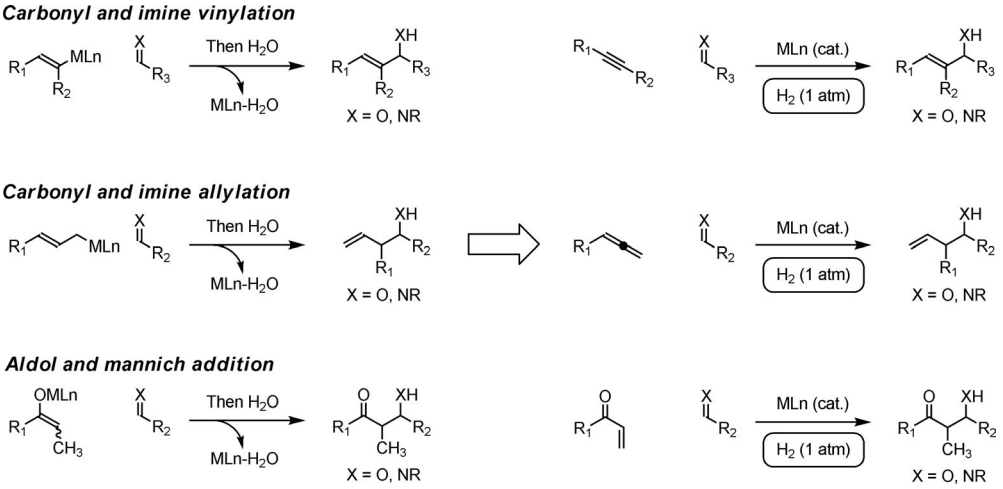

Scheme 8.2 Hydrogenative variants of classical carbonyl additions employing preformed organometallic reagents are by-product-free processes.

Given the long history of catalytic hydrogenation and its enormous transformative impact on society, the use of catalytic hydrogenation for reductive C–C bond formation is remarkably underdeveloped. Catalytic hydrogenation has been known for nearly 200 years and ranks among the first reported examples of metal catalysis. Sir Humphrey Davy, in an 1817 lecture to the Royal Society of London, revealed that mixtures of coal gas and air over platinum wire cause the wire to glow. This heterogeneous catalytic oxidation led to the invention of a safety lamp for miners. In 1822, Johann Wolfgang Döbereiner disclosed a method for the production of acetic acid and water, involving the air oxidation of alcohol in the presence of platinum. This innovation formed the basis of the 'Schtitzenbach quick vinegar process'. One year later, Döbereiner reported that mixtures of hydrogen and air ignite in the presence of

platinum sponge [6, 7]. In 1823, Döbereiner devised a household lighter based upon the platinum catalyzed hydrogenation of atmospheric oxygen [6, 7]. Discovered at a time when fire was still created with flint and tinder, Döbereiner's household lighter captured worldwide attention and served as a prototype for legion devices used for the self-ignition of coal-gas burners. Interestingly, Döbereiner's innovation preceded the phenomenological recognition of catalysis [8]. Recognition that certain chemical reactions will only take place in the presence of specific substances was articulated by Eilhard Mitscherlich [8a]. However, it was the Swedish chemist Berzelius who first recognized that certain substances, termed 'catalysts', will alter reaction rate and yet remain unchanged themselves [8b]. Interestingly, Berzelius also coined the term 'organic' to define chemical substances characteristic of living organisms, and it was his student Wöhler who contributed to the genesis of organic chemistry and demise of vitalism by preparing synthetic urea in 1828. From their origins, catalysis and organic chemistry were closely linked – a bond that persists today! The catalytic hydrogenation of atmospheric nitrogen to produce ammonia, was reported by Haber in 1905 [9]. Currently, over 10^8 tons of ammonia are produced annually through the Haber–Bosch process, providing cost-effective routes to nitrogenous fertilizers and increasing worldwide food production to unprecedented levels [10]. The hydrogenation of C=X (X=C, N, O) π-bonds was first described by Paul Sabatier at the University of Toulouse in the late 1890s [11]. Sabatier's work led to the broad use of heterogeneous hydrogenation in organic synthesis. However, it was not until the 1960s that the first catalysts for homogeneous hydrogenation were developed (prior to the work of Halpern and Wilkinson, the first transformations recognized as homogeneous hydrogenations involved the reduction of benzoquinone to the corresponding hydroquinone [12]), largely driven by the work of Jack Halpern [13] and Geoffrey Wilkinson [14]. Soon thereafter, enantioselective hydrogenations were developed by Knowles [15], Kagan [16] and Noyori [17]. Clean, cost-effective and powerful, asymmetric hydrogenation is currently the most broadly utilized catalytic enantioselective process employed industrially (Scheme 8.3) [18].

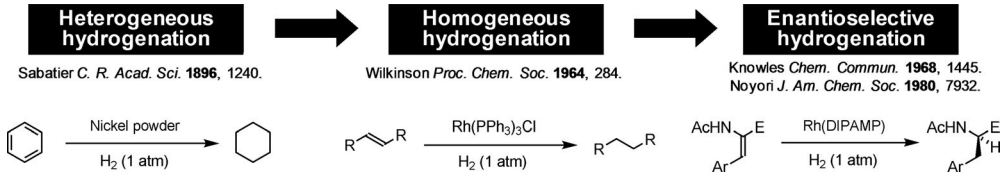

Scheme 8.3 Selected milestones in the catalytic hydrogenation of organic substrates.

It was not until 1923 that the formation of C–C bonds under hydrogenation conditions was first observed by Fischer and Tropsch, who discovered that, under the conditions of catalytic hydrogenation, carbon monoxide (coal gas) is subject to reductive polymerization to deliver hydrocarbons [19]. The 'Fischer–Tropsch process' was broadly implemented by Germany in World War II, which in 1944 used this process to produce over 6.5 million tons of synthetic petroleum [20]. With the rising cost of crude oil, interest in Fischer–Tropsch chemistry has been rekindled, leading to

the development of improved catalytic systems [21]. In 1938, in the course of studies on the Fischer–Tropsch reaction, Otto Roelen discovered another hydrogen-mediated C−C coupling: alkene hydroformylation or the 'oxo synthesis' [22]. Hydroformylation employs basic feedstocks as reactants (α-alkenes, carbon monoxide and hydrogen), combining them with perfect atom economy – true green chemistry. The utility of hydroformylation is borne out by the production of over 7 million metric tons of aldehyde annually, making hydroformylation the largest volume application of homogeneous metal catalysis [23].

The Fischer–Tropsch reaction and alkene hydroformylation may be viewed as the prototypical C−C bond-forming hydrogenations. Subsequent to their discovery, systematic efforts toward the development of related hydrogen-mediated C−C couplings were absent for nearly 70 years. In 2001, the present author embarked upon the first systematic investigation into the development of C−C bond-forming hydrogenations beyond the Fischer–Tropsch reaction and hydroformylation. With the exception of two isolated reports [24, 25], along with the infrequent detection of reductive coupling side-products in catalytic hydrogenation (side-products of reductive C−C bond formation have been observed in catalytic hydrogenation on rare occasions [26]), the field of hydrogenative C−C bond formation lay fallow. The fact that hydroformylation is equivalent to a carbonylative hydrogenation, which suggests that related insertion processes may accompany hydrogenation, was not appreciated. It is now known that diverse π-unsaturated partners engage in C−C coupling upon exposure to hydrogenation or transfer hydrogenation conditions, offering a by-product-free alternative to stoichiometrically preformed organometallic reagents in an ever-increasing range of C=X (X=O, NR) addition processes (Scheme 8.4) [27].

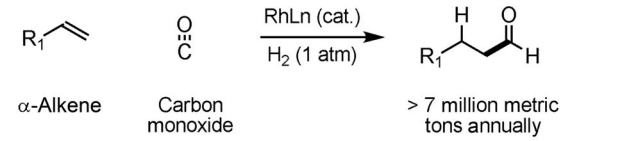

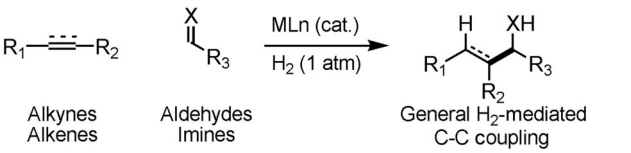

Scheme 8.4 Hydroformylation, which is equivalent to a carbonylative hydrogenation, suggests that other insertion processes may accompany hydrogenation.

In this chapter, the first systematic efforts toward hydrogen-mediated C−C coupling beyond the Fischer–Tropsch reaction and alkene hydroformylation are

described. Whereas classical methods for the addition of *C*-nucleophiles to carbonyl compounds and imines generally require stoichiometric use of potentially hazardous air- and moisture-sensitive organometallic reagents, hydrogenative C–C coupling combines π-unsaturated reactants under neutral conditions and with complete atom economy. In this way, waste production is prevented at its source. In this emerging field, only a small fraction of hydrogenation's potential to serve as a method of C–C bond formation has been realized. General methods for hydrogenative coupling promise to add a broad, new dimension to catalytic hydrogenation, one of chemistry's oldest and most widely utilized processes.

8.2
Hydrogenative Vinylation of Carbonyl Compounds and Imines

The utility of allylic alcohols and allylic amines as building blocks in fine chemical and pharmaceutical synthesis has inspired the development of methods for their preparation in optically enriched form [28, 29]. For example, metal-catalyzed allylic substitution using *O*- and *N*-nucleophiles is a highly effective and versatile protocol for the synthesis of chiral non-racemic allylic alcohols and allylic amines [30]. Another potentially powerful approach, although far less developed, involves the enantioselective catalytic vinylation of aldehydes and imines. The majority of work in this area stems from the seminal studies of the groups of Oguni in 1984 [31a] and Noyori in 1986 [31b] on the enantioselective addition of dialkylzinc reagents to aldehydes [32]. The first asymmetric aldehyde vinylations of this type were reported in 1992 by Oppolzer and co-workers [33a,34] and involve the generation of vinylzinc reagents via alkyne hydroboration, followed by transmetallation of the resulting vinylboron reagent to zinc using $ZnMe_2$. A related strategy for asymmetric aldehyde vinylation was reported by Wipf and Xu in 1994 and involves alkyne hydrozirconation–transmetallation *en route* to vinylzinc reagents [33d]. Following catalytic enantioselective additions of alkylzinc and arylzinc reagents to ketones [32b–d] described by Ramón and Yus in 1998 [35a,b] and Dosa and Fu in 1998 [35c], respectively, catalytic asymmetric ketone vinylations were devised by Walsh and co-workers in 2004 [36]. Most recently, rhodium-catalyzed additions of vinylboronic acids have shown promise as a method for aldehyde vinylation [37].

Corresponding efforts to develop enantioselective imine additions using preformed metallic reagents reveal an additional set of challenges [38]. Pursuant to Soai *et al.*'s seminal report in 1992 [39a], several organocatalysts for the enantioselective addition of organozinc reagents to imines emerged [39]. Because conventional imines are generally less reactive than aldehydes with respect to organocatalyzed organozinc addition, for example using amino alcohol-based catalysts, these studies employ *N*-acyl and *N*-(diphenylphosphinoyl)imines. To address further the issue of reactivity, metal-catalyzed enantioselective organozinc additions to imines were developed [40], as first described by Tomioka and coworkers in 2000, using a copper-based catalyst [40a]. Early transition metal catalysts (Ti, Zr, Hf) [41] and late transition metal catalysts (Rh) [42] also have

been found to promote highly enantioselective organozinc additions to imines. Beyond organozinc reagents, the enantioselective addition of organolithium reagents to imines catalyzed by chiral Lewis basic chelating agents has been described [43]. Additionally, using rhodium catalysts, organotin [44a,b], organotitanium [44c] and organoboron [44d–k] reagents participate in catalytic asymmetric imine additions. Despite considerable effort, highly enantioselective vinyl transfer to imines employing preformed organometallic reagents has not been achieved. Catalyzed addition of vinylzirconocenes to imines is known, but enantioselective variants have not been developed [45]. Enantioselective Ni-catalyzed alkyne, imine, triethylborane three-component coupling has been reported, but modest selectivities [51–89% enantiomeric excess (*ee*)] are observed. For this method, vinylation is accompanied by ethyl transfer [46].

Direct metal-catalyzed alkyne-C=X (X = O, NR) reductive coupling circumvents the use of preformed organometallics [47, 48]. The first catalytic process of this type, a rhodium-catalyzed reductive cyclization of acetylenic aldehydes mediated by silane, was reported in 1994 by Ojima *et al.* [49]. In 1995, Crowe and Rachita disclosed related silane-mediated titanocene catalyzed cyclizations [50]. Corresponding nickel-catalyzed cyclizations were reported by Montgomery and coworkers in 1997 [51a–c,e]. Finally, based on Montgomery and co-workers' finding, intermolecular reductive alkyne–aldehyde coupling was achieved under the conditions of nickel catalysis by Jamison and co-workers in 2000 [52]. Improved nickel catalysts later were developed by Takai *et al.* [53] and Montgomery and co-workers [51d]. While reductive couplings of this type signal a departure from the use of preformed organometallic reagents, the aforementioned methods employ terminal reductants such as hydrosilanes, hydrostannanes, organozinc reagents, organoboron reagents or chromium(II) chloride, which ultimately produce molar equivalents of chemical by-products.

Under the conditions of catalytic hydrogenation, alkynes participate in completely by-product-free reductive couplings to both carbonyl compounds and imines. The first-generation catalytic systems developed for this purpose employ cationic rhodium complexes and require the use of conjugated alkynes as nucleophilic partners and activated aldehydes and ketones in the form of vicinal dicarbonyl compounds as electrophilic partners [54a–c]. Brønsted acid co-catalysts are required to enforce high rates and conversions. In all cases, high levels of asymmetric induction are achieved using catalysts modified by chiral chelating phosphine ligands, thus permitting access to optically enriched α-hydroxy esters. Under related conditions, coupling to heterocyclic aromatic aldehydes and ketones is observed, providing access to heteroaryl-substituted carbinols [54d]. Notably, hydrogenative coupling allows access to fully substituted carbinol stereocenters in highly optically enriched form through asymmetric ketone additions. Further, although highly unsaturated diene- and enyne-containing products are generated, over-reduction of the products under the conditions of hydrogenative coupling is not observed. Presumably, upon consumption of the electrophile, which is the limiting reagent, excess alkyne nonproductively coordinates the catalyst and so retards the rate of further conventional hydrogenation (Scheme 8.5).

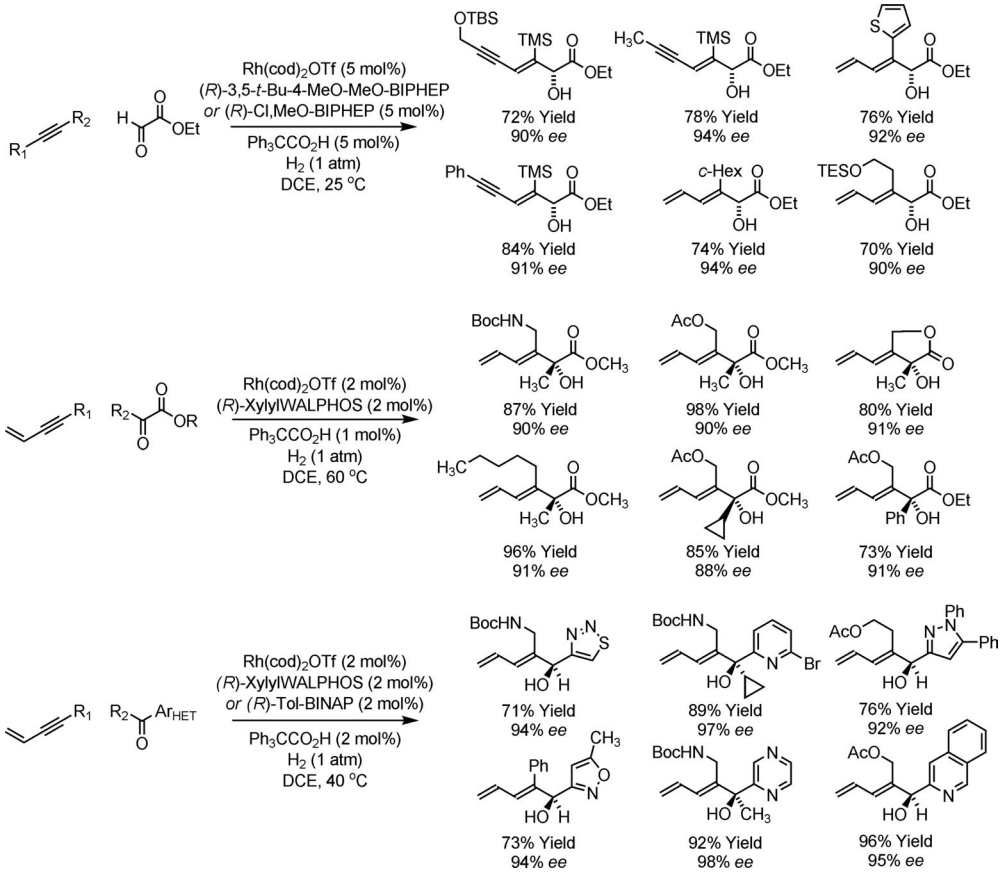

Scheme 8.5 First-generation catalysts for hydrogenative C–C couplings based on rhodium allow direct, by-product-free coupling of conjugated alkynes and activated carbonyl compounds and imines.

The collective data are consistent with a general mechanism involving alkyne-C=X (X=O, NR) oxidative coupling followed by direct or Brønsted acid co-catalyzed hydrogenolysis of the resulting metallacycle. Cationic complexes of rhodium (or iridium) are required. Unlike related neutral complexes, hydrogen activation is slower for cationic rhodium precatalysts [55, 56], providing a greater kinetic window for entry into alkyne-C=X (X=O, NR) oxidative coupling manifolds. Oxidative coupling is promoted further by the coordinative unsaturation of cationic rhodium complexes. As supported by theoretical studies [57], Brønsted acid co-catalysts likely circumvent highly energetic four-centered transition structures **A** for σ-bond metathesis, as required for direct hydrogenolysis of metallacyclic intermediates, as follows. Metallacycle protonolysis, which may itself occur through the six-centered transition structure **B**, delivers a rhodium carboxylate, which then engages in hydrogenolysis through the six-centered transition structure **C** (Scheme 8.6).

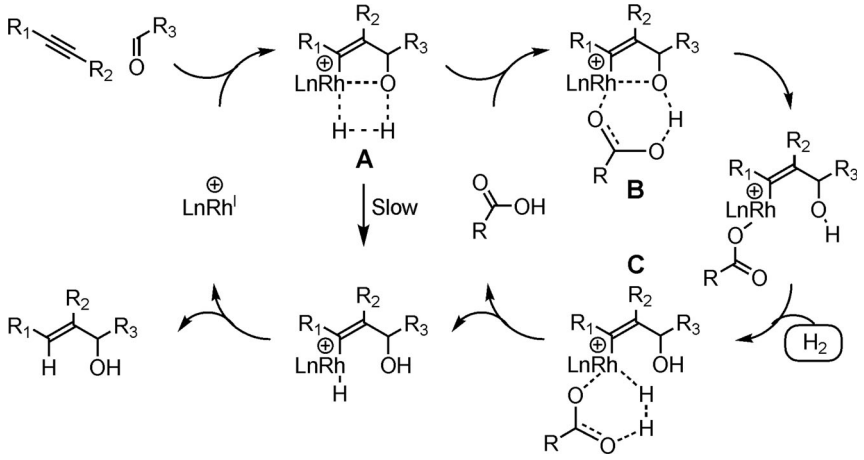

Scheme 8.6 Plausible catalytic mechanism for hydrogenative alkyne–carbonyl coupling accounting for the effect of Brønsted acid co-catalysts.

This interpretation of the catalytic mechanism is consistent with the results of deuterium labeling. For example, reductive coupling of the indicated phenyl-substituted enyne to ethyl pyruvate under a deuterium atmosphere results in >95% deuterium incorporation. Even when using 50 mol% loadings of Brønsted acid under otherwise standard conditions that involve 2 mol% loadings of the rhodium catalyst, clean monodeuteration persists. This result excludes mechanisms involving protonolytic cleavage of the rhodium–carbon bond of the oxametallacycle, but is consistent with protonolytic cleavage of the rhodium–oxygen bond. Oxidative coupling is suggested further by ESI-MS analysis of reaction mixtures, where the most abundant ion observed is consistent with the mass calculated for Rh(BIPHEP) (metallacycle). Reductive coupling of 1-phenylbut-3-en-1-yne to 2-pyridinecarboxaldehyde performed using an achiral rhodium catalyst in the presence of a chiral phosphoric acid derived from BINOL [58] leads to substantial levels of optical enrichment (82% *ee*). This result requires intervention of the chiral Brønsted acid co-catalyst during the enantiodetermining C−C coupling event. Notably, the chiral Brønsted acid co-catalyst does not induce asymmetry in the coupling of enynes to pyruvates or glyoxalates. These data suggest that protonation of 2-pyridinecarboxaldehyde, a more basic substrate, occurs in advance of oxidative coupling. Additionally, substrate protonation or hydrogen-bond formation appears to accelerate oxidative coupling by lowering the substrate LUMO, accounting for a noncompetitive racemic background reaction (Scheme 8.7).

Couplings to ethyl (*N*-sulfinyl)iminoacetates, although studied prior to the discovery of the Brønsted acid co-catalyst effect, are nevertheless fairly efficient [59]. By simply hydrogenating conjugated enynes or diynes in the presence of appropriately substituted (*N*-sulfinyl)iminoacetates, one generates the corresponding β, γ-unsaturated α-amino acid esters as single diastereomers. Exhaustive hydrogenation of the

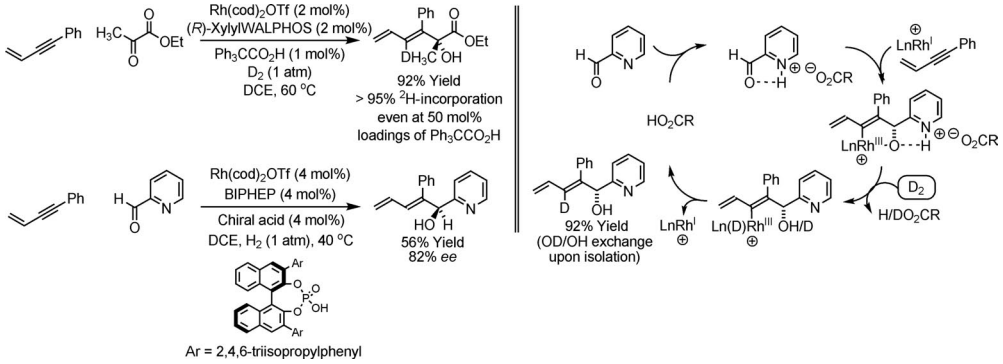

Scheme 8.7 The results of isotopic labeling and the observance of asymmetric induction in connection with the use of a chiral Brønsted acid co-catalyst.

unsaturated side-chain permits access to β-substituted α-amino acids. Reductive coupling under an atmosphere of deuterium provides the indicated monodeuterated adduct. This result is again consistent with a catalytic mechanism involving alkyne–imine oxidative coupling followed by hydrogenolysis of the resulting metallacycle (Scheme 8.8).

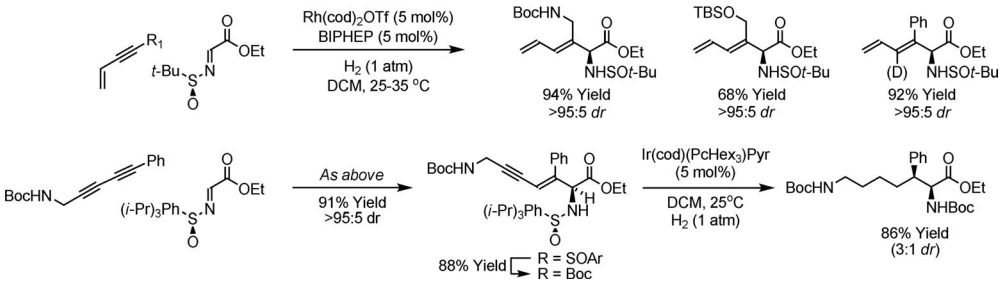

Scheme 8.8 Unnatural α-amino acids via C–C bond-forming hydrogenation.

Gaseous acetylene couples to aldehydes under hydrogenation conditions to furnish products of (*Z*)-butadienylation [60]. Isotopic labeling and ESI-MS analysis are consistent with a catalytic mechanism involving carbonyl insertion into a cationic rhodacyclopentadiene [61] followed by Brønsted acid-assisted hydrogenolysis of the resulting oxarhodacycloheptadiene. Using chirally modified catalysts, allylic alcohols are formed with high levels of optical enrichment. Similarly, *N*-arylsulfonyl aldimines are converted to the corresponding (*Z*)-butadienyl allylic amines upon rhodium-catalyzed hydrogenation in the presence of acetylene. Again, using chirally modified catalysts, highly enantioselective coupling is observed [62]. Consistent with the goals of green chemistry, these by-product-free couplings combine acetylene, an abundant feedstock [63], with carbonyl compounds or imines to furnish chiral adducts in the absence of any preformed organometallic reagents (Scheme 8.9).

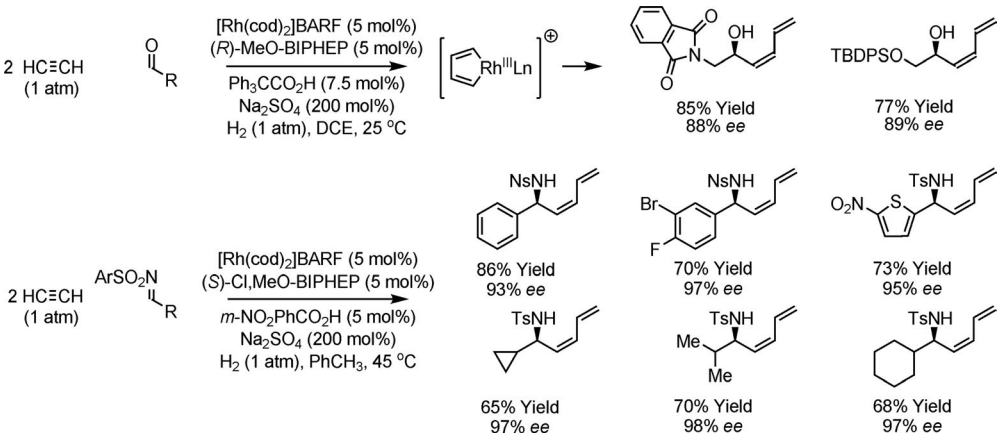

Scheme 8.9 Asymmetric carbonyl and imine (*Z*)-butadienylation via hydrogenative coupling of acetylene (Ns = *p*-nitrobenzenesulfonyl).

The coupling of unactivated 1,2-dialkyl-substituted alkynes is promoted by second-generation catalysts based on iridium. Specifically, upon hydrogenation of 1,2-dialkyl-substituted alkynes in the presence of *N*-arylsulfonylimines, trisubstituted allylic amines are formed with complete levels of *E*:*Z* selectivity (≥95:5) and, using catalysts modified by (*R*)-Cl,MeO-BIPHEP, exceptional levels of asymmetric induction are observed [64]. With the use of non-symmetric alkynes, excellent regiocontrol is observed. This by-product-free coupling provides trisubstituted allylic amines that are not accessible via metal-catalyzed asymmetric allylic alkylation (Scheme 8.10).

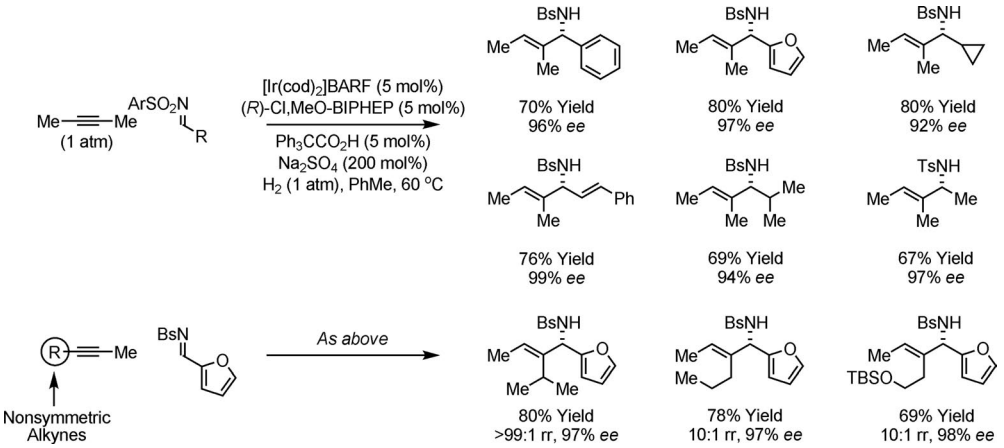

Scheme 8.10 Iridium-catalyzed asymmetric imine vinylation employing non-conjugated alkynes.

A plausible stereochemical model accounting for the observed sense of absolute stereoinduction and regioselectivity involves complexation of the alkyne and imine at adjacent coordination sites of square planar iridium(I). Complexation of the

N-arylsulfonylimine is expected to occur in a bidentate fashion, wherein one of the sulfoxide oxygens is bound at the apical coordination site of iridium. The bidentate κ2-mode of binding has been observed by single-crystal X-ray diffraction analysis for a related palladium *N*-arylsulfonamidate complex [65]. As explained by the Dewar–Chatt–Duncanson model [66], and as borne out by single-crystal X-ray diffraction analysis of iridium(I)–alkyne complexes [alkyne complexation by iridium(I) results in substantial deviation from linearity, as revealed by single-crystal X-ray diffraction analysis] [67], coordination of the alkyne should confer iridacyclopropene character. Enantiodetermining insertion of the imine into the iridium–carbon bond of the iridacyclopropene delivers the indicated aza-iridacyclopentene, which upon Brønsted acid-assisted hydrogenolysis delivers the allylic amine. Whereas non-bonded interactions of the arylsulfonyl moiety with the phenyl groups of (*R*)-Cl,MeO-BIPHEP disfavor insertion on the *pro*-(*R*) imine π-face, such interactions are absent in the alternative mode of approach involving insertion into the *pro*-(*S*) imine π-face. Regioselective coupling requires the larger propargylic position of the alkyne to reside distal to the metal center at the stage of the alkyne complex and incipient metallacycle (Scheme 8.11).

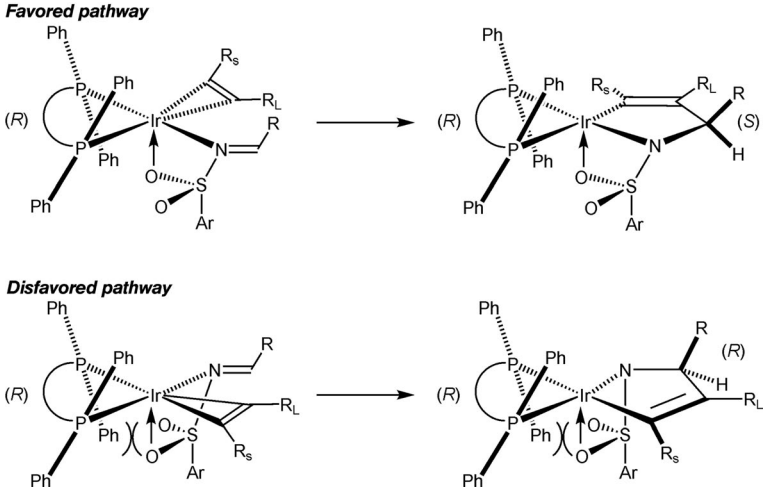

Scheme 8.11 Stereochemical models accounting for the observed sense of absolute stereoinduction and regioselectivity.

The ability of iridium-based catalysts to activate non-conjugated alkynes may be due to the fact that iridium is a stronger π-donor than rhodium, as a consequence of relativistic effects [68]. The energy of infrared radiation absorbed by isostructural carbonyl complexes of iridium and rhodium are consistent with this assertion: $(Ph_3P)_2M(Cl)(CO)$, M = Ir, $\nu_{co} = 1965\ cm^{-1}$; M = Rh, $\nu_{co} = 1980\ cm^{-1}$ [69]. π-Backbonding in the metal–alkyne complex, as described by the Dewar–Chatt–Duncanson model [66], may facilitate alkyne-C=X (X = O, NR) oxidative coupling by conferring nucleophilic character to the bound alkyne. Hence iridium, a stronger π-donor than

rhodium, is capable of activating non-conjugated alkynes, which embody higher lying LUMOs.

8.3
Hydrogenative Allylation of Carbonyl Compounds

Carbonyl allylation is of enormous importance to the field of synthetic organic chemistry [70]. The first carbonyl allylation, employing an isolable preformed allyl metal reagent, triallylborane, was reported by Mikhailov and Bubnov in 1964 [71a]. Hosomi and Sakurai reported that carbonyl compounds are subject to allylation upon exposure to allylsilanes in the presence of Lewis acids in 1976 [71b]. The first chirally modified allyl metal reagent, reported by Hoffmann and Herold in 1978 [72a,b], was an allylborane derived from camphor. Subsequently, a host of chirally modified allyl metal reagents for asymmetric carbonyl allylation were disclosed. These include reagents developed by the groups of Kumada (1982) [30c], Brown (1983) [30d], Roush (1985) [30e], Reetz (1988) [30f], Masamune (1989) [30g], Corey (1989) [30h], Seebach (1987) [30i], Duthaler (1989) [30j], Panek (1991) [30k] and Leighton (2002) [30l,m]. Despite exceptional enantioselectivities, the effort required to prepare such preformed allyl metal reagents detracts from their utility. Further, such chirally modified allyl metal reagents give rise to stoichiometric quantities of chemical by-products (Scheme 8.12).

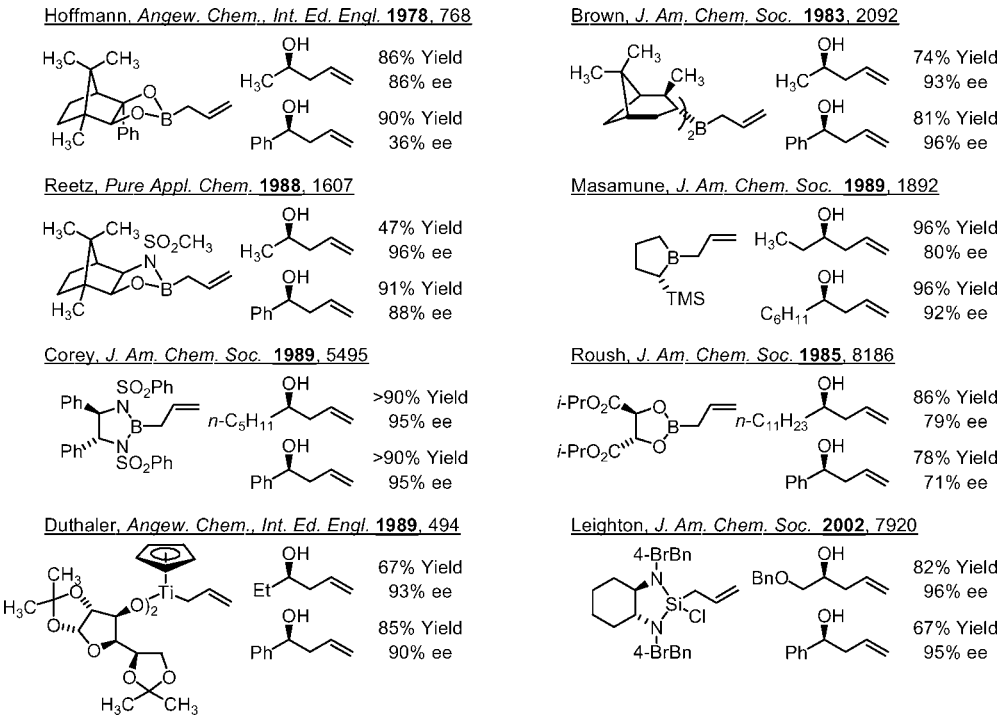

Scheme 8.12 Chirally modified allyl metal reagents for enantioselective carbonyl allylation.

Catalytic enantioselective carbonyl allylation has been achieved using chiral Lewis acid catalysts, as first described by Umani-Ronchi and co-workers [73a] and Keck *et al.* [73b] in 1993. Chiral Lewis bases also catalyze enantioselective carbonyl allylation, as reported by Denmark and co-workers in 1994 [73c,d]. However, allylstannanes employed in the former process generate stoichiometric quantities of tin by-products and trichlorosilanes used in the latter process are highly moisture sensitive and generate hydrochloric acid upon hydrolysis. Other methods for catalytic carbonyl allylation include the reduction of metallo-π-allyls derived from allylic alcohols and allylic carboxylates [74]. Here, stoichiometric quantities of metal-based terminal reductants, for example SmI_2, $SnCl_2$ and Et_2Zn, are required for catalytic turnover [75]. Finally, carbonyl–ene processes form products of carbonyl allylation [76, 77]. Although the development of general by-product-free methods for catalytic enantioselective carbonyl allylation remains a significant challenge, one potential solution resides in the generation of transient allyl metal species via allene or 1,3-diene hydrogenation and their capture by exogenous carbonyl electrophiles (Scheme 8.13).

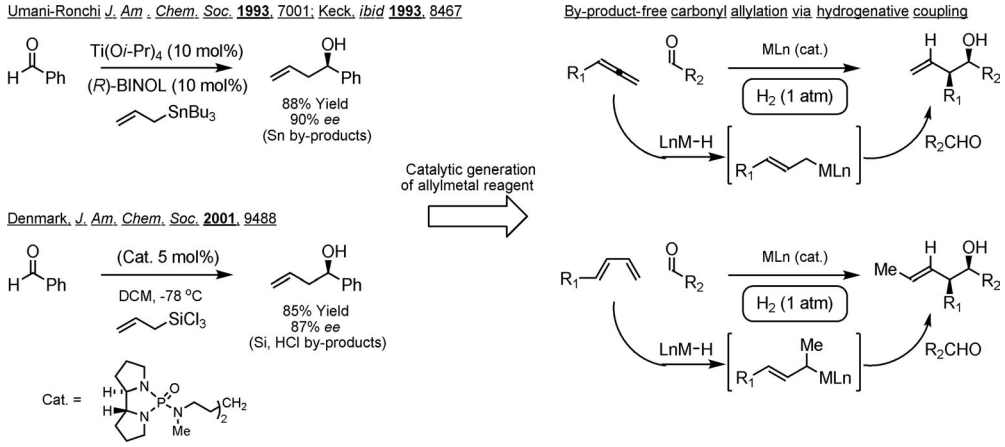

Scheme 8.13 Towards by-product-free catalytic enantioselective carbonyl allylation.

The feasibility of hydrogenative carbonyl allylation is borne out by results recently obtained by the present author, who reported that iridium-catalyzed hydrogenation of commercially available dimethylallene in the presence of carbonyl electrophiles delivers products of reverse prenylation [78]. Additionally, functional groups typically considered to be 'hydrogen labile', such as benzylic ethers, nitroarenes and aryl halides, are not subject to over-reduction under the conditions of hydrogenative allylation. The basic additive Li_2CO_3 is found to suppress over-reduction of the olefinic reverse prenyl side-chain. Alternative bases, KOAc, LiOH, Cs_2CO_3 and *i*-Pr_2NEt, were only slightly less effective at suppressing over-reduction. Most importantly, unlike established methods for carbonyl allylation, preformed allyl metal reagents are avoided, thus circumventing the stoichiometric generation of metallic by-products (Scheme 8.14).

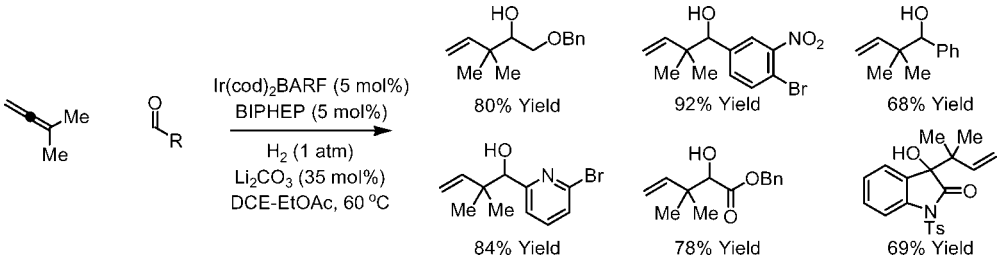

Scheme 8.14 Catalytic carbonyl addition via iridium-catalyzed hydrogenative coupling of dimethylallene.

A plausible catalytic mechanism involves allene hydrometallation to deliver the primary σ-allyliridium complex **I**, which engages the carbonyl partner in a closed six-centered transition structure **II**. Carbonyl addition with allylic inversion, followed by hydrogenolytic cleavage of the resulting iridium alkoxide **III**, accounts for the formation of the reverse prenylated adducts. Under a deuterium atmosphere, 80% deuterium incorporation is observed at the vinylic position, consistent with the proposed hydrometallative mechanism. However, mechanisms involving allene–aldehyde oxidative coupling are potentially operative and cannot be excluded on the basis of available data (Scheme 8.15).

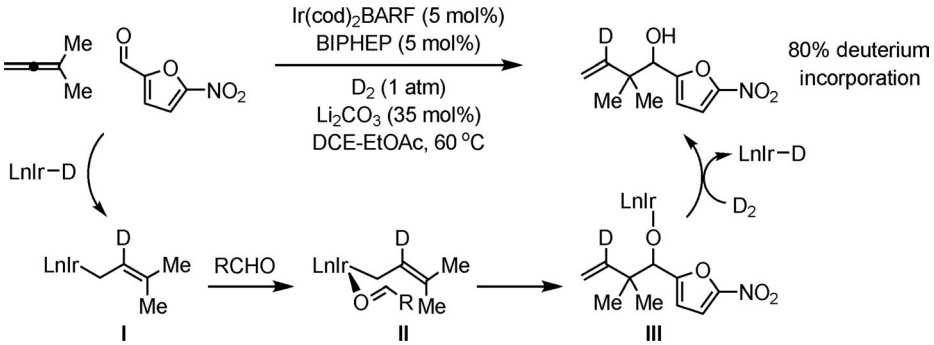

Scheme 8.15 A plausible catalytic mechanism for iridium-catalyzed hydrogenative allylation, as corroborated by deuterium labeling.

The use of alcohols as hydrogen donors in transfer hydrogenation suggests the feasibility of *alcohol-mediated* C−C couplings. The use of alcohols as hydrogen donors in reductive coupling, in turn, supports the feasibility of developing processes in which an alcohol serves both as the reductant and as the electrophile precursor. That is, direct allene–alcohol coupling is potentially achieved by simply shuffling hydrogen between reactants to generate nucleophile–electrophile pairs that engage in by-product-free C−C coupling. Beyond the atom economy of this process, carbonyl addition directly from the alcohol oxidation level circumvents the redox

manipulations typically required to convert alcohols to aldehydes. The use of alcohols as electrophiles in such 'hydrogen auto-transfer processes' [79] was first demonstrated by Guerbet in 1908 [80, 81]. Subsequently, it has been shown that diverse nucleophiles (ketones [82], nitriles [81], activated methylene compounds [82] and stabilized Wittig reagents [85]) may be alkylated by alcohols via hydrogen auto-transfer in accordance with the following three fundamental steps: (a) alcohol dehydrogenation to provide an aldehyde, which (b) undergoes condensation or olefination to furnish an unsaturated adduct, which (c) re-accepts hydrogen to deliver the saturated product. However, carbonyl addition under the conditions of hydrogen auto-transfer has not been described (Scheme 8.16).

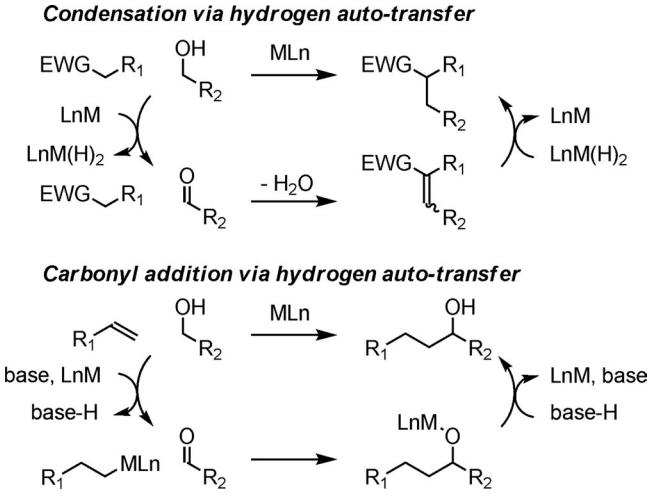

Scheme 8.16 Condensation via hydrogen auto-transfer supports the feasibility of related by-product-free carbonyl additions including carbonyl allylation.

Remarkably, under transfer hydrogenation conditions employing 2-propanol as the terminal reductant, iridium-catalyzed reductive coupling of 1,1-dimethylallene to aldehydes occurs efficiently to deliver the products of reverse prenylation [86]. Even more surprising, under identical conditions but in the absence of 2-propanol, 1,1-dimethylallene engages in direct coupling to alcohols to furnish the very same set of reverse prenylated adducts [86]. Whereas attempted allene–aldehyde reductive coupling to furnish products of allylation and crotylation suffers from over-reduction of the olefinic adduct under conditions that employ gaseous hydrogen as the terminal reductant, under the conditions of transfer hydrogenation and hydrogen auto-transfer over-reduction is not observed (Scheme 8.17).

Insight into the catalytic mechanism is provided by the following experiments [86]. Coupling of dimethylallene to benzyl alcohol that is fully deuterated at the methylene position under hydrogen auto-transfer conditions provides an adduct that incorporates deuterium primarily at the internal vinylic position (85%). A similar result is obtained for the analogous reaction performed under

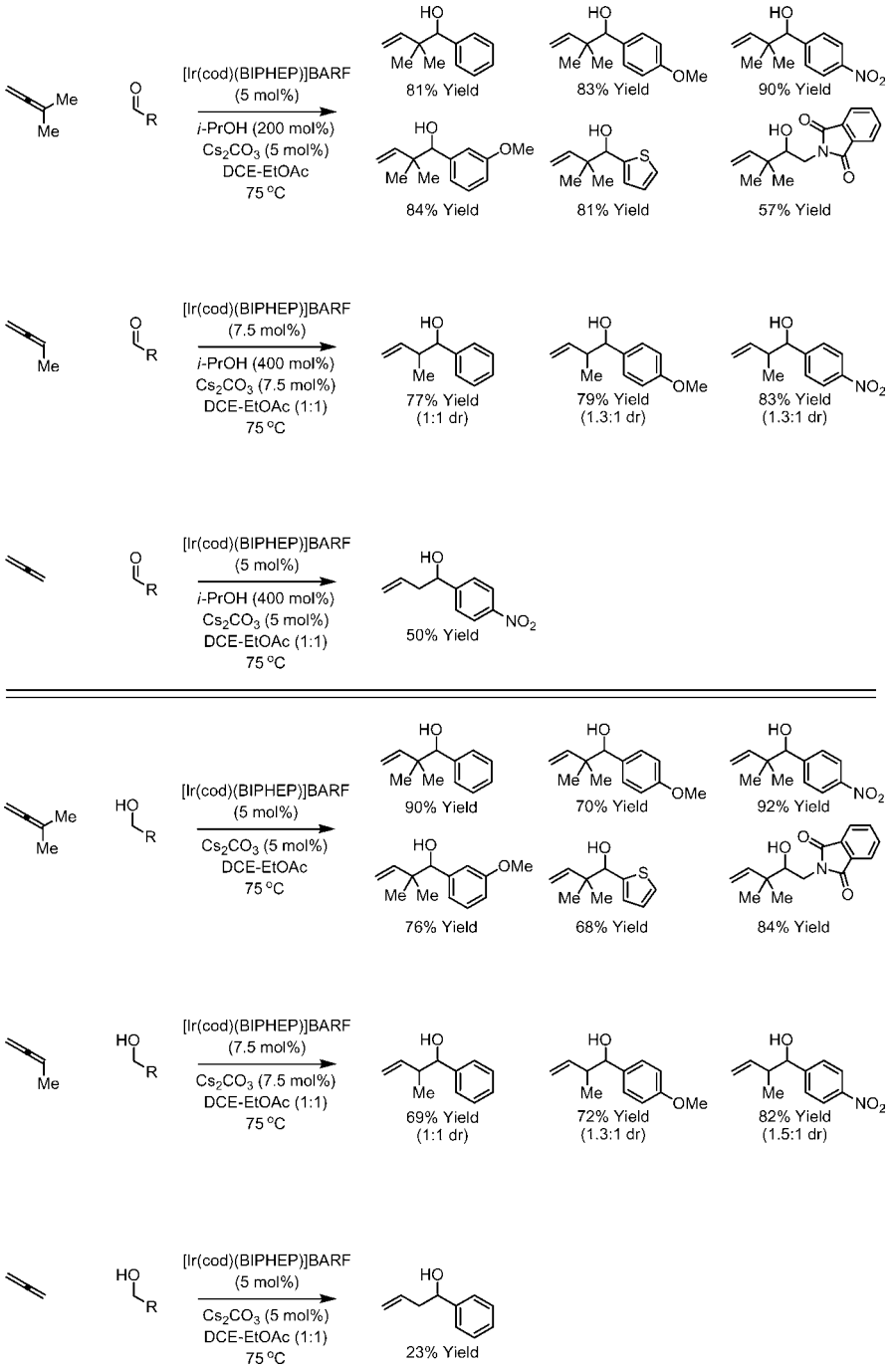

Scheme 8.17 (a) Catalytic carbonyl allylation from the aldehyde oxidation level via transfer hydrogenation. (b) Catalytic carbonyl allylation from the alcohol oxidation level via hydrogen autotransfer.

transfer hydrogenation conditions using 2-propanol-*d*8 as terminal reductant. These data are consistent with a mechanism involving hydrogen donation from the alcoholic reactant or sacrificial alcohol (*i*-PrOH). Related competition experiments involving exposure of dimethylallene to equimolar quantities of *p*-nitrobenzyl alcohol and benzaldehyde provide the indicated products of reverse prenylation in a 4:1 ratio. An identical product distribution is observed upon exposure of dimethylallene to equimolar quantities of *p*-nitrobenzaldehyde and benzyl alcohol, suggesting rapid alcohol–aldehyde redox equilibration in advance of C–C coupling. Indeed, on exposure of equimolar quantities of *p*-nitrobenzyl alcohol and benzaldehyde or *p*-nitrobenzaldehyde and benzyl alcohol to standard conditions, but in the absence of allene, an identical 4 : 1 : 1 : 4 *p*-nitrobenzyl alcohol–*p*-nitrobenzaldehyde–benzyl alcohol–benzaldehyde mixture is observed (Scheme 8.18).

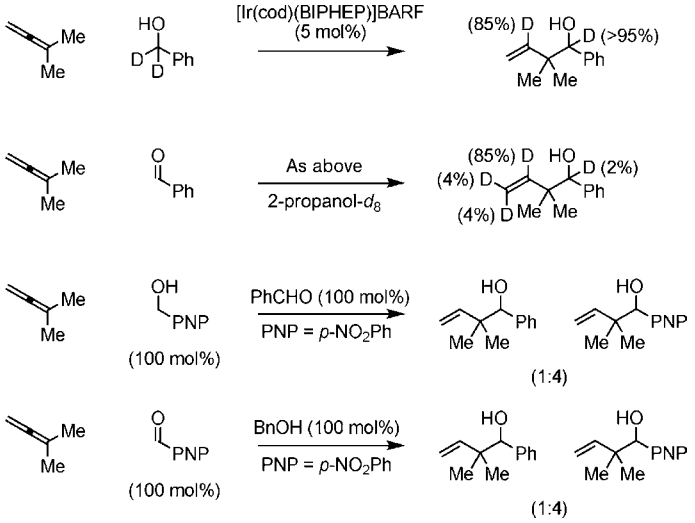

Scheme 8.18 Mechanistic studies on carbonyl allylation under the conditions of transfer hydrogenation and hydrogen auto-transfer.

Through transfer hydrogenation and hydrogen auto-transfer, there exists the potential to develop a broad new family of catalytic C–C bond formations wherein alcohols or aldehydes couple to diverse π-unsaturated reactants. Initial studies aimed at exploring the scope of such processes auger well for the generality of this novel approach to catalytic C–C coupling [87]. For example, upon exposure to the neutral iridium precatalyst derived from $[Ir(cod)Cl]_2$ and BIPHEP, 1,3-cyclohexadiene couples readily to aldehydes under the conditions of transfer hydrogenation employing 2-propanol as terminal reductant. Under similar conditions, the identical set of carbonyl adducts may be prepared from the corresponding alcohols by way of hydrogen auto-transfer. Hence, carbonyl addition is again achieved from the aldehyde or alcohol oxidation level and, in the latter case, completely by-product-free coupling is achieved (Scheme 8.19).

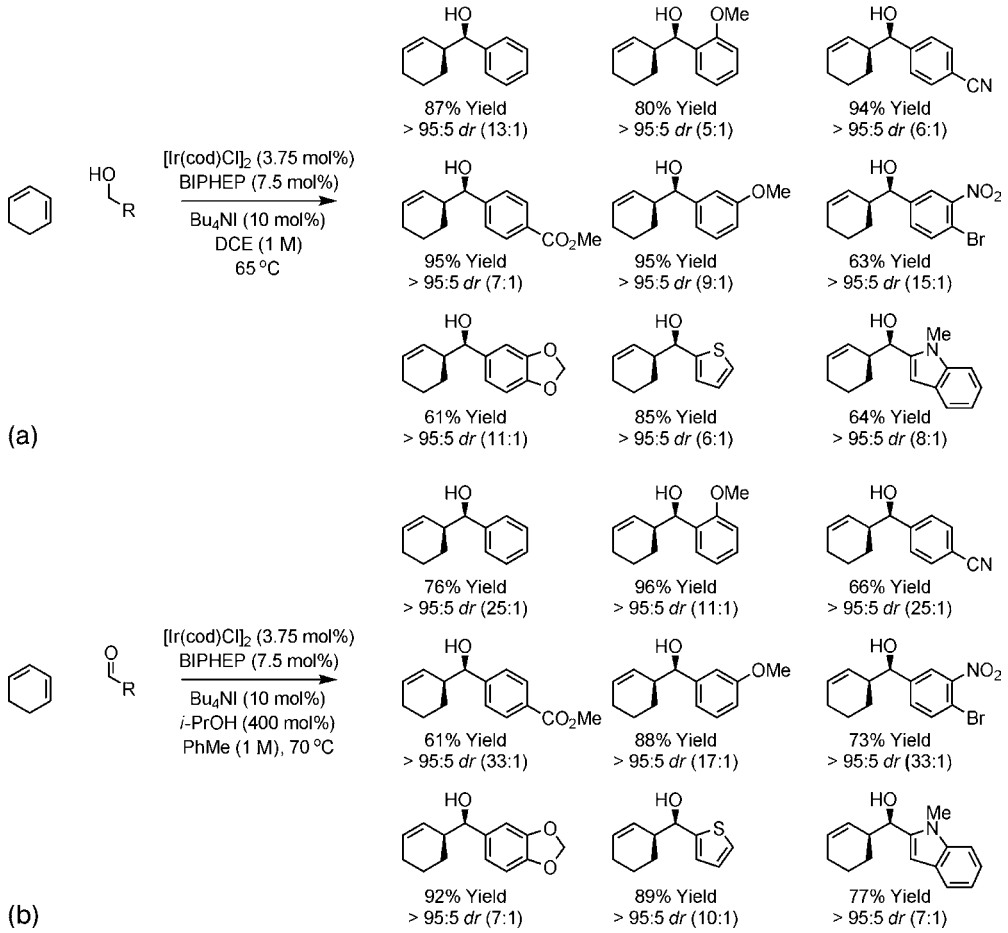

Scheme 8.19 (a) Catalytic coupling of 1,3-cyclohexadiene to alcohols via iridium-catalyzed hydrogen auto-transfer. (b) Catalytic coupling of 1,3-cyclohexadiene to aldehydes under the conditions of iridium-catalyzed transfer hydrogenation. The ratio of the indicated 1,4-olefinic alcohol and the isomeric 1,5-olefinic alcohol is given in parentheses.

More recently, ruthenium complexes have been found to catalyze transfer hydrogenative C−C coupling and related auto-transfer processes [88]. For example, isoprene couples to *p*-nitrobenzaldehyde in 73% isolated yield upon exposure to $RuHCl(CO)(PPh_3)_3$ in the presence of 2-propanol, which again serves as terminal reductant. The same complex promotes C−C coupling under hydrogen auto-transfer conditions employing *p*-nitrobenzyl alcohol as both the reductant and electrophile precursor. These collective data support the feasibility of developing a broad new family of C−C couplings predicated on transfer hydrogenative C−C coupling and related hydrogen auto-transfer processes (Scheme 8.20).

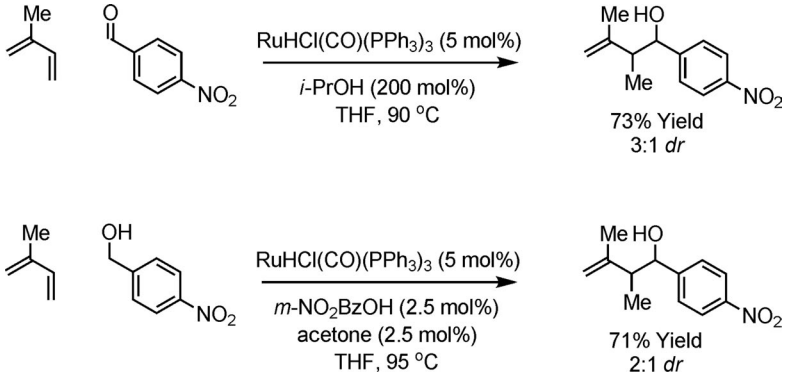

Scheme 8.20 Ruthenium-catalyzed C–C couplings of isoprene under the conditions of transfer hydrogenation and hydrogen auto-transfer.

8.4 Hydrogenative Aldol and Mannich Additions

Discovered over a century ago, the aldol reaction continues to challenge chemists, inspiring increasingly selective protocols for aldol addition [89] (although largely attributed to Würtz, the aldol reaction was reported first by Borodin [90]; Borodin's earliest results are cited in [90]); The advent of metallic [91] and organic catalysts [92] for 'direct' asymmetric aldol addition of unmodified ketones represents an especially significant milestone, as these by-product-free processes herald a departure from the use of chiral auxiliaries and preformed enol(ate) derivatives. Nevertheless, for direct asymmetric aldol additions, the challenge of regioselective enolization remains largely unresolved. Direct enantioselective aldol additions of non-symmetric ketones generally favor activation of the less substituted enolizable position. For example, direct aldol couplings of 2-butanone catalyzed by L-proline [93] (using amides of L-proline, direct catalyzed aldol coupling of 2-butanone to *p*-nitrobenzaldehyde affords mixtures of regioisomeric products [94]) or the heterobimetallic catalyst $LaLi_3$-tris (binaphthoxide) (LLB) furnish linear aldol adducts [95]. For construction of poly-propionate motifs, methods for the stereoselective formation of the corresponding branched aldol adducts would be highly desirable (Scheme 8.21).

For non-symmetric ketones possessing different degrees of substitution at the α-positions, e.g. methylcyclohexanone, regioselective deprotonation may be achieved by exploiting kinetic or thermodynamic control [96]. However, for non-symmetric ketones that possess identical degrees of α-substitution, regioselective enolization is problematic. A classic example involves the deprotonation of cholesterane-3-one. The Δ_3-enolate is thermodynamically preferred. The Δ_2-enolate cannot be formed cleanly via deprotonation under kinetic or thermodynamic conditions. Introduction of 7,8-unsaturation inverts the thermodynamic preference. Now the Δ_3-enolate cannot be formed selectivity under kinetic or thermodynamic conditions (Scheme 8.22) [97, 98].

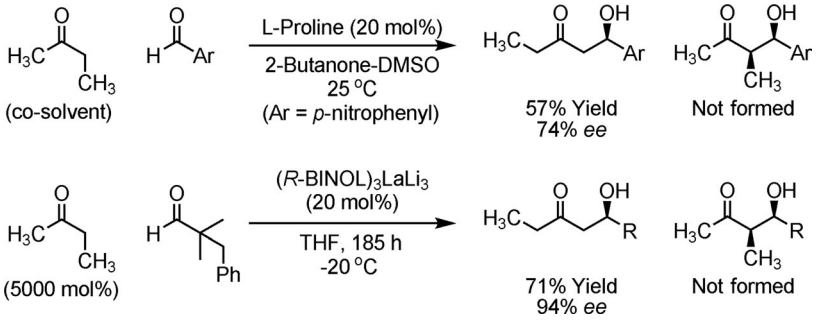

Scheme 8.21 Direct methods for asymmetric aldol couplings of 2-butanone do not provide the branched regioisomers necessary for the construction of polypropionate motifs.

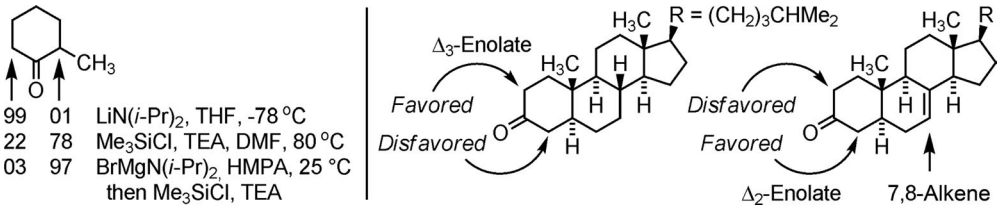

Scheme 8.22 Regioselective enolization of non-symmetric ketones via deprotonation.

As first reported by Stork *et al.* [99], regiospecific enolate generation may be achieved via enone reduction. Specifically, dissolving metal reduction (Li–NH_3) of conjugated enones was found to promote regiospecific enolate formation, enabling access to enolate isomers and adducts thereof, that cannot be formed by way of base-mediated deprotonation (Scheme 8.23).

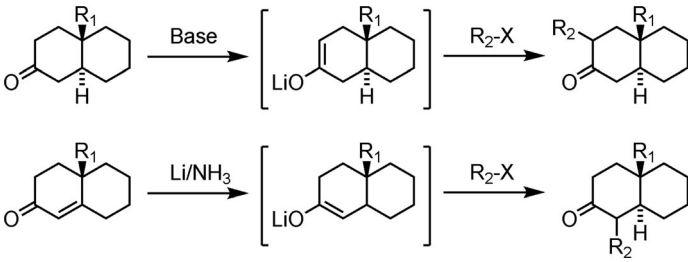

Scheme 8.23 Regiospecific enolization via dissolving metal reduction represents the first use of enones as latent enolates.

Subsequent to Stork *et al.*'s work, direct metal-catalyzed reductive couplings of enones to aldehydes were devised, termed 'reductive aldol reactions' [100]. To date, numerous catalysts for reductive aldol coupling have been reported, including those based on rhodium [101], cobalt [102], iridium [103], ruthenium [104], palladium [105], copper [106, 107], nickel [108] and indium [109, 110]. Such transformations generally

employ silanes or stannanes as the terminal reductant, resulting in the generation of stoichiometric by-products. The use of elemental hydrogen as a terminal reductant would allow completely by-product-free aldol coupling.

Reductive aldol coupling under hydrogenation conditions was first demonstrated via cyclization of enone–aldehydes [111a]. Whereas catalytic hydrogenation of the indicated enone–aldehyde using the neutral complex $Rh(PPh_3)_3Cl$ primarily delivers the product of conventional conjugate reduction, rhodium salts that embody increased cationic character, such as $Rh(cod)_2OTf$, provide nearly equal proportions of aldol and 1,4-reduction products. When $Rh(cod)_2OTf$ is used in conjunction with substoichiometric quantities of a basic additive, potassium acetate, the aldol adduct is formed as the major reaction product, with nearly complete suppression of the competitive 1,4-reduction manifold. Under these conditions, a range of enone–aldehydes engage in cycloreduction to form five- and six-membered ring products (Scheme 8.24).

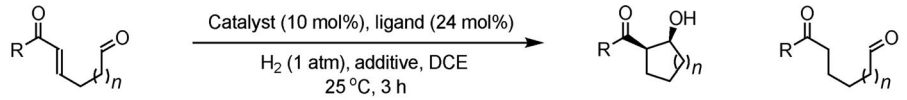

Substrate	Catalyst	Ligand	Additive (mol%)	Yield aldol (%) (*syn*:*anti*)	Yield 1,4-reduction (%)
n = 2, R = Ph	$Rh(PPh_3)_3Cl$	---	---	1 (99:1)	95
n = 2, R = Ph	$Rh(cod)_2OTf$	Ph_3P	---	21 (99:1)	25
n = 2, R = Ph	$Rh(cod)_2OTf$	Ph_3P	KOAc (30%)	59 (58:1)	21
n = 2, R = Ph	$Rh(cod)_2OTf$	$(p\text{-}CF_3Ph)_3P$	---	57 (14:1)	22
n = 2, R = Ph	**$Rh(cod)_2OTf$**	**$(p\text{-}CF_3Ph)_3P$**	**KOAc (30%)**	**89 (10:1)**	**0.1**
n = 2, R = *p*-MeOPh	"	"	"	74 (5:1)	3
n = 2, R = 2-naphthyl	"	"	"	90 (10:1)	1
n = 2, R = 2-thiophenyl	"	"	"	76 (19:1)	2
n = 2, R = 2-furyl	"	"	"	70 (6:1)	10
n = 1, R = Ph	"	"	"	71 (24:1)	1
n = 2, R = CH_3	"	"	"	65 (1:5)	---

Scheme 8.24 Reductive aldol cyclization of aldo-enones via catalytic hydrogenation.

Basic additives may partition aldol addition and conjugate reduction pathways by disabling enolate–hydrogen reductive elimination pathways through deprotonation of (hydrido)rhodium intermediates, thus promoting entry into monohydride-based catalytic cycles where the formation of such intermediates is circumvented. The observance of *syn*-aldol adducts is consistent with the intervention of a (*Z*)-enolate and a closed Zimmerman–Traxler-type transition structure [112]. Re-exposure of the 1,4-reduction product to the reaction conditions does not result in aldolization, nor does re-exposure of the aldol product to the reaction conditions result in retro-aldol addition. Finally, exposure of the substrate to standard reaction conditions in the *absence* of hydrogen does not provide products of Morita–Baylis–Hillman cyclization (Scheme 8.25).

Although pathways involving enone–aldehyde oxidative coupling cannot be excluded on the basis of available data, the aforementioned mechanistic interpretation finds support in studies of alkene hydrogenation using cationic rhodium precatalysts.

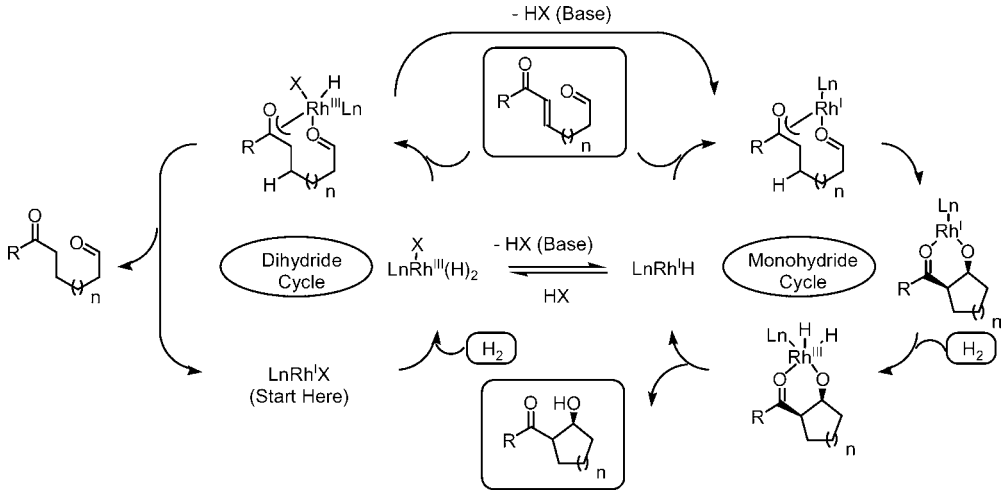

Scheme 8.25 Bifurcated catalytic mechanism accounting for the effect of basic additives on partitioning of conjugate reduction and aldol addition pathways.

Monohydride catalytic cycles initiated via deprotonation of cationic rhodium dihydrides have been postulated [113]. Here, basic additives are found to increase alkene isomerization in advance of reduction. A bifurcated catalytic mechanism that partitions dihydride and monohydride cycles by virtue of an acid–base equilibrium between a cationic rhodium(III) dihydride and a neutral rhodium(I) monohydride was postulated. The stoichiometric reaction of a cationic rhodium(I) complex with elemental hydrogen to furnish a neutral rhodium(I) monohydride provides further support for the indicated equilibrium and represents a formal *heterolytic* activation of elemental hydrogen ($H_2 + M-X \rightarrow M-H + HX$) [114]. Cationic rhodium hydrides, unlike their neutral counterparts, are especially acidic and, hence, are particularly prone to heterolytic hydrogen activation (Scheme 8.26) [115].

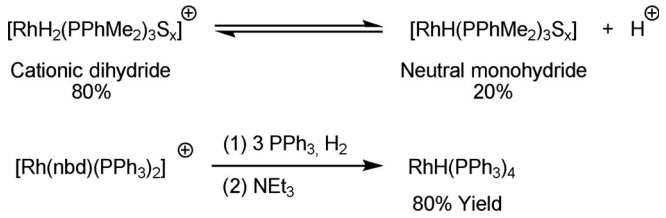

Scheme 8.26 Equilibration between cationic rhodium dihydrides and neutral rhodium monohydrides and the stoichiometric formation of the latter through heterolytic hydrogen activation in the presence of base.

Keto-enones engage in reductive aldol cyclization upon exposure to nearly identical hydrogenation conditions [111b]. Both five- and six-membered ring *syn*-aldol adducts

are formed as single diastereomers, accompanied by substantial quantities of conjugate reduction product. While aldolization proceeds readily at ambient temperature, more reproducible ratios of aldol and 1,4-reduction product are observed at 80 °C. Again, retro-aldol products are not observed upon resubmission of the aldol products to the reaction conditions. Aldol cyclization under an atmosphere of deuterium results in deuterium incorporation exclusively at the former enone β-position, but as a distribution of deuterated products, suggesting reversible enone hydrometallation in the case of ketone acceptors, where reversible carbonyl addition is expected (Scheme 8.27).

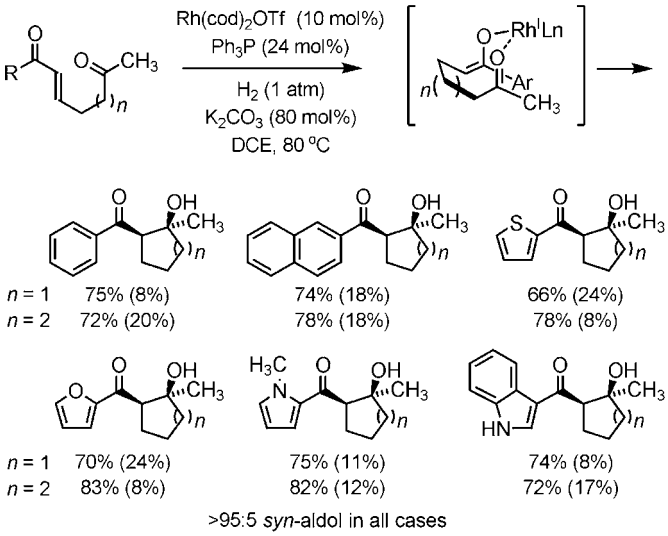

Scheme 8.27 Reductive aldol cyclization of keto-enones via catalytic hydrogenation. The yield of conjugate reduction product is given in parentheses.

The preceding results suggest that ketones are only marginally less electrophilic than required to suppress competitive 1,4-reduction manifolds fully. 1,3-Diones are more electrophilic due to inductive effects and the relief of dipole–dipole interactions. Exposure of enone-diones to standard hydrogenation conditions at ambient temperature and pressure provides the corresponding aldol adducts as single diastereomers. Only when forming a strained *cis*-decalone is competitive 1,4-reduction observed (Scheme 8.28) [111b].

A particularly challenging variant of the aldol reaction involves the addition of aldehyde enolates to ketones. A single stoichiometric variant of this transformation is known [116]. As aldolization is driven by chelation, intramolecular addition to afford a robust transition metal aldolate may bias the enolate–aldolate equilibria toward the latter [117]. The failure of tris(dialkylamino)sulfonium enolates to react with aldehydes is attributed to unfavorable enolate–aldolate equilibria [118]. Indeed, upon exposure to basic hydrogenation conditions, keto-enal substrates provide the

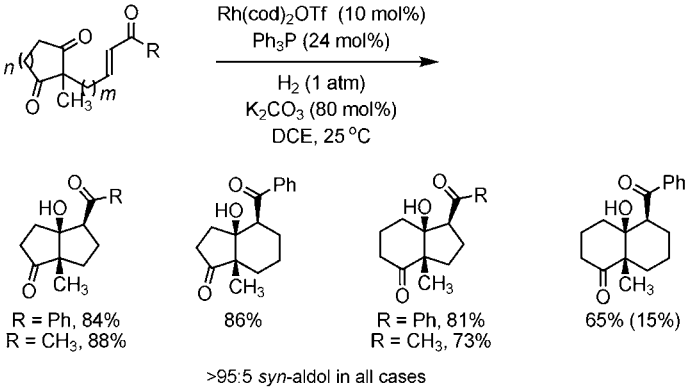

Scheme 8.28 Reductive aldol cyclization of enone-diones via catalytic hydrogenation. The yield of conjugate reduction product is given in parentheses.

corresponding cycloaldol products, though competitive 1,4-reduction is observed (Scheme 8.29) [111c].

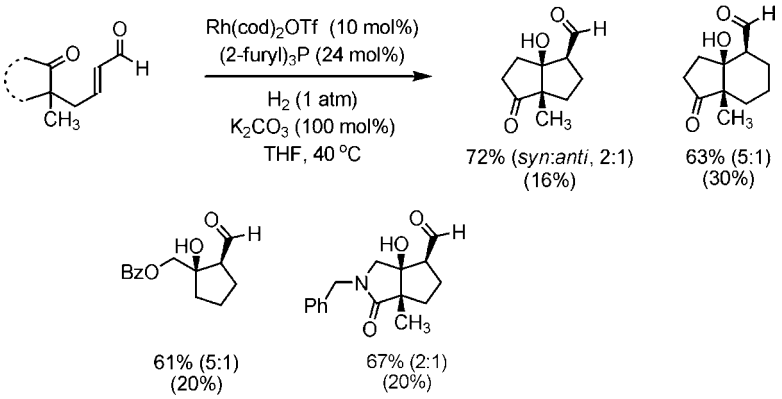

Scheme 8.29 Reductive aldol cyclization of enal-ketones via catalytic hydrogenation. The yield of conjugate reduction product is given in parentheses.

Intermolecular reductive aldol coupling of vinyl ketones under hydrogenation conditions was first reported in 2002 [111a]. The catalyst initially employed, which is derived from $Rh(cod)_2OTf$ and triphenylphosphine, provides good yields of the aldol adducts as mixtures of diastereomers. As revealed through a ligand assay, π-acidic ligands such as tri-2-furylphosphine [119] promote exceptional *syn*-diastereoselectivity [111e]. Stereospecific (*Z*)-(*O*)-enolate formation by way of internal hydride delivery to the enone *s-cis* conformer through a six-centered transition structure is postulated. Consistent with internal hydride delivery to the enone *s-cis* conformer through a six-centered transition structure, enones constrained in the *s-trans*

configuration, such as cyclohexenone, do not participate in hydrogen-mediated reductive aldol coupling. Addition of the (*Z*)-(*O*)-enolate to the aldehyde through a Zimmerman–Traxler-type transition structure delivers the *syn*-aldol product. High levels of *syn*-diastereoselectivity require kinetically controlled enolization and aldolization. The *anti*-aldol diastereomers are thermodynamically preferred. Hence, high *syn*-diastereoselectivity suggests kinetic control at the stages of both enolization and aldol addition; for a review, see [120]. Notably, reduction of 'hydrogen-labile' functional groups (alkynes, alkenes, benzylic ethers and nitroarenes) is not observed, permitting chemoselective coupling of unsaturated reactants, including divinyl ketones [111f]. As the hydrogenative coupling occurs under essentially neutral conditions in low-dielectric media, sensitive *N*-Boc-α-aminoaldehydes undergo aldol addition through hydrogen-bonded chelates without racemization to deliver aldol adducts that embody exceptional levels of *syn*-aldol diastereoselectivity and *anti*-Felkin–Anh control (Scheme 8.30) [111g].

Diastereoselective reductive coupling of methyl vinyl ketone (MVK) and *p*-nitrobenzaldehyde performed under an atmosphere of deuterium provides an aldol adduct incorporating a single deuterium atom at the former enone β-position [29e]. Deuterium incorporation at the α-carbon is not observed, excluding Morita–Baylis–Hillman pathways *en route* to product. Incorporation of a single deuterium atom suggests irreversible enone hydrometallation (Scheme 8.31).

Enantioselective reductive aldol couplings of vinyl ketones, such as MVK, would permit access to branched aldol adducts, providing a regiochemical complement to direct organocatalytic and metal-catalyzed aldol couplings of non-symmetric ketones, such as 2-butanone, which furnish linear aldol adducts [93–95]. Enantioselective variants of the hydrogenative aldol couplings are especially challenging for the following reasons: (a) only trace amounts of product are obtained using chelating phosphine ligands, (b) π-acidic ligands such as Fur_3P are required to enforce high levels of diastereoselection, yet (c) commercially available π-acidic chiral monodentate ligands, for example, BINOL-derived phosphites and phosphoramidites, are presumably too π-acidic and provide only trace quantities of product. Consequently, the design of an effective chiral monodentate *P*-based ligand was required.

TADDOL-like phosphonites offer a versatile template amenable to systematic structural variation, allowing key structure–selectivity trends to be defined. For the indicated TADDOL template, the ketal moiety, the carbinol substituents and *P*-aryl group were independently optimized. This led to an effective TADDOL-like phosphonite ligand that combines the optimal diethyl ketal, dimethylcarbinol and *P*-2-benzothienyl substructures (Scheme 8.32). Using the optimal TADDOL-like phosphonite ligand, methyl vinyl ketone and ethyl vinyl ketone reductively couple to diverse aldehydes with high levels of relative and absolute stereocontrol and, by virtue of using elemental hydrogen as terminal reductant, with complete atom economy (Scheme 8.33) [111h].

α,β-Unsaturated carbonyl compounds are known to participate in reductive Mannich couplings mediated by silane [121, 122] and the Hantzsch ester [123]. Completely by-product-free reductive Mannich couplings are potentially achieved using elemental hydrogen as the terminal reductant. In the event, hydrogenation of

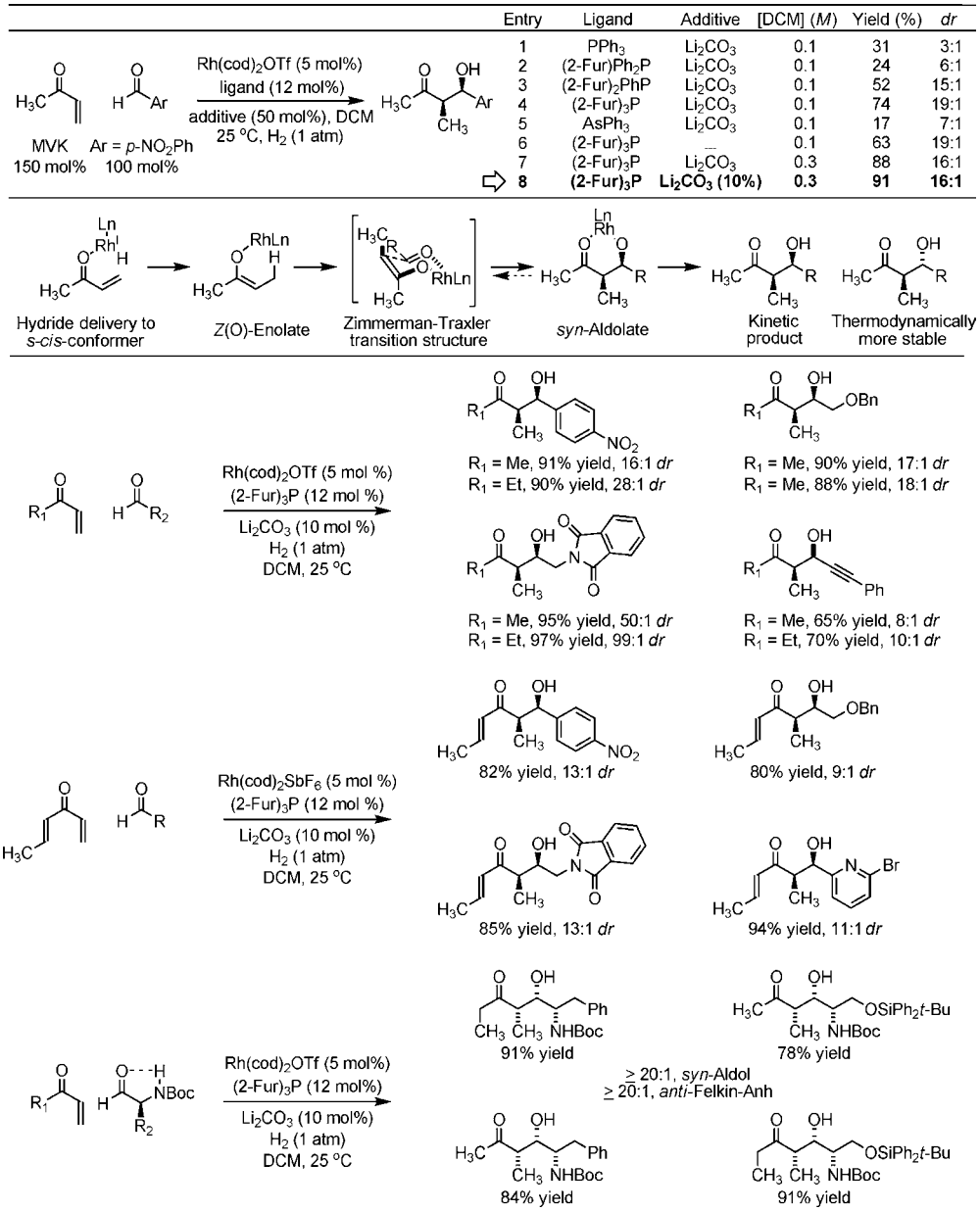

Scheme 8.30 *syn*-Diastereoselective hydrogen-mediated aldol coupling employing cationic rhodium catalysts ligated by tri-2-furylphosphine.

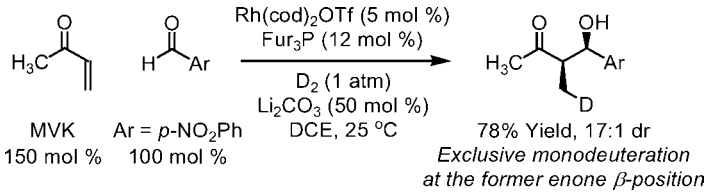

Scheme 8.31 Diastereoselective Rh-catalyzed hydrogenative aldol coupling under an atmosphere of deuterium.

vinyl ketones in the presence of *N*-(*o*-nitrophenyl)sulfonyl aldimines using a tri-2-furylphosphine-ligated rhodium catalyst provides the desired Mannich addition products with good levels of *syn*-diastereoselectivity [124]. These studies set the stage for the development of enantioselective variants (Scheme 8.34).

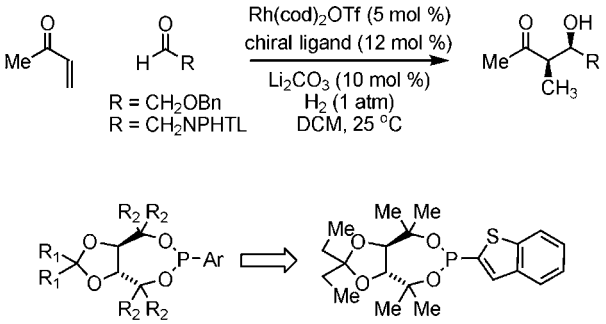

Phosphonite ligand	RCHO	Yield (%) (*dr*)	*ee* (%)
$R_1 = R_2 = Me$, Ar = 2-Fur	CH_2OBn	76 (12:1)	+35
$R_1 = R_2 = Me$, Ar = 2-Fur	CH_2NPHTL	90 (>30:1)	+59
$R_1 = R_2 = Me$, Ar = Ph	CH_2NPHTL	20 (>30:1)	+80
$R_1 = R_2 = Me$, Ar = 1-[3,5-$(CF_3)_2$Ph]	CH_2NPHTL	30 (>30:1)	+45
$R_1 = R_2 = Me$, Ar = 2-[5-Me-Fur]	CH_2NPHTL	52 (>30:1)	+50
$R_1 = R_2 = Me$, Ar = 2-benzofuryl	CH_2NPHTL	64 (>30:1)	+66
$R_1 = R_2 = Me$, Ar = 2-benzothienyl	CH_2NPHTL	65 (>30:1)	+86
$R_1 = Me$, $R_2 = Et$, Ar = 2-benzofuryl	CH_2NPHTL	32 (>30:1)	+76
$R_1 = Me$, $R_2 = Ph$, Ar = 2-benzofuryl	CH_2NPHTL	15 (>30:1)	+30
$R_1 = Et$, $R_2 = Me$, Ar = 2-benzofuryl	CH_2NPHTL	75 (>30:1)	+75
$R_1 = (CH_2)_5$, $R_2 = Me$, Ar = 2-benzofuryl	CH_2NPHTL	90 (>30:1)	+56
$R_1 = i$-Pr, $R_2 = Me$, Ar = 2-benzofuryl	CH_2NPHTL	76 (>30:1)	+69
R_1 = Et, R_2 = Me, Ar = 2-benzothienyl	CH_2NPHTL	**90 (>30:1)**	**+92**
R_1 = Et, R_2 = Me, Ar = 2-benzothienyl	CH_2NPHTL	**94 (>30:1)**	**+94[a]**
R_1 = Et, R_2 = Me, Ar = 2-benzothienyl	CH_2OBn	**91 (11:1)**	**+84**
R_1 = Et, R_2 = Me, Ar = 2-benzothienyl	CH_2OBn	**85 (25:1)**	**+91[a]**

[a]Reaction was conducted at 0 °C.

Scheme 8.32 Optimization of a TADDOL-like phosphonite ligand for enantioselective hydrogenative aldol coupling (NPHTL = phthalimido).

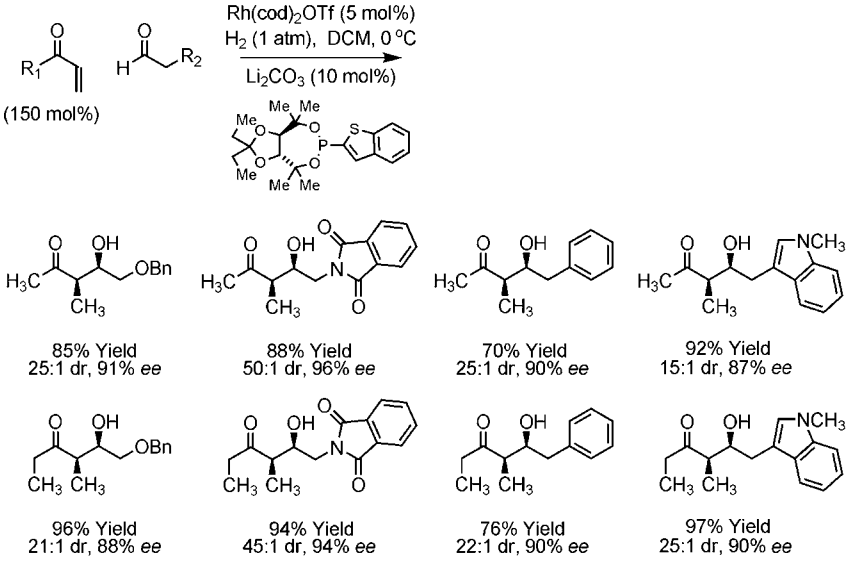

Scheme 8.33 *syn*-Diastereoselective and enantioselective hydrogen-mediated aldol coupling employing cationic rhodium catalysts ligated by a novel TADDOL-like phosphonite ligand.

8.5
Hydrogenative Acyl Substitution (Reductive Hydroacylation)

The coupling of *C*-nucleophiles to anhydrides has been achieved using palladium-[125], rhodium- [126] and nickel-based [127] catalysts. Recently, chirally modified catalysts have been applied to the desymmetrization of *meso*-anhydrides [125f, 126b,c]. Virtually all catalytic *C*-nucleophile–anhydride couplings involve the use of preformed organometallics, e.g. organozincs or organoboronic acids. Notwithstanding studies in our laboratory, the reductive coupling of aryl iodides and anhydrides represents an exception to the use of preformed organometallic reagents in *C*-nucleophile–anhydride

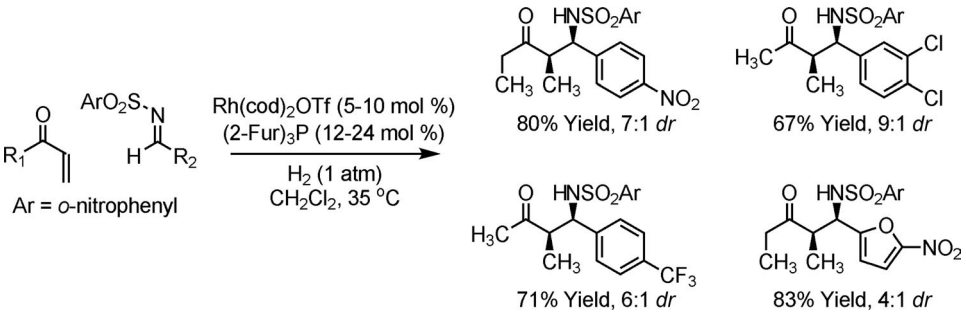

Scheme 8.34 *syn*-Diastereoselective intermolecular Mannich coupling under hydrogenation conditions.

coupling chemistry [128]. The hydrogenation of alkenes in the presence of anhydrides potentially allows the capture of transient organometallic species to provide products of formal acyl substitution, thus circumventing the use of preformed organometallic reagents, which are generally sensitive to air and moisture (Scheme 8.35).

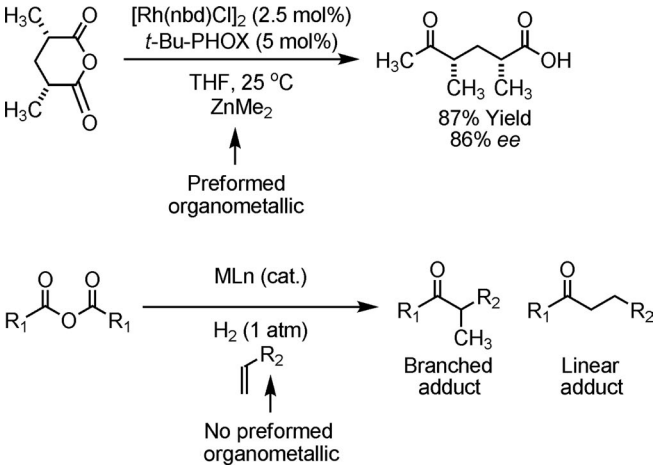

Scheme 8.35 Catalytic coupling of anhydrides to *C*-nucleophiles.

Hydrogenative alkene–anhydride coupling is equivalent to reductive hydroacylation. The significance of this is that whereas conventional rhodium-catalyzed *intramolecular* hydroacylation using aldehydes as acyl donors is well developed [129], intermolecular variants are foiled by competitive decarbonylation of acylrhodium intermediates to furnish catalytically inactive carbonyl complexes [130]. Conventional *intermolecular* hydroacylation has only been achieved using β-chelating aldehydes, e.g. salicylaldehydes, β-sulfidoaldehydes and (*N*-2-pyridyl)aldimines. To suppress decarbonylation in intermolecular rhodium-catalyzed hydroacylation, aldehyde donors that possess an adjacent site of coordination are required (for example, salicyladehydes and β-sulfidoaldehydes). Alternatively, conventional aldehyde donors may be converted to the corresponding (*N*-2-pyridyl)aldimines, which are then used as aldehyde equivalents [131]. Intermolecular ruthenium-catalyzed hydroacylation has been described, but generally requires exceptionally high reaction temperatures and provides mixtures of linear and branched coupling products [132]. Intermolecular cobalt-catalyzed hydroacylation has been described, but is restricted to the use of vinylsilanes as coupling partners [133]. This limitation is, in part, overcome through the use of acrylamides as coupling partners in intermolecular hydroacylation [134].

In the event, hydrogenative coupling of vinylarenes to aromatic or α,β-unsaturated carboxylic anhydrides using cationic rhodium catalysts proceeds efficiently [135] (see also [25]). Furthermore, under optimum conditions using triphenylarsine as ligand, complete levels of branch regioselectivity are enforced. It is again noteworthy that olefinic functionality remains intact under the conditions of hydrogenative coupling (Scheme 8.36).

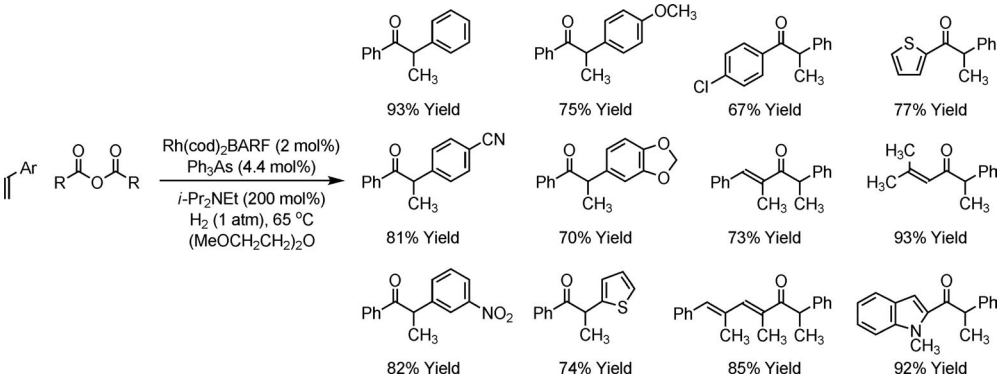

Scheme 8.36 Branch-selective hydroacylation via hydrogen-mediated coupling of vinylarenes to carboxylic anhydrides.

As these reductive hydroacylations transfer only one acyl residue of the anhydride, selective *C*-acylation employing mixed anhydrides derived from pivalic acid was explored. Applying standard conditions used for the symmetrical anhydrides to mixed anhydrides results in the selective transfer of the aryl or α,β-unsaturated acyl moiety. Efficiencies are comparable to that of the parent process and complete branched regioselectivities are observed (Scheme 8.37).

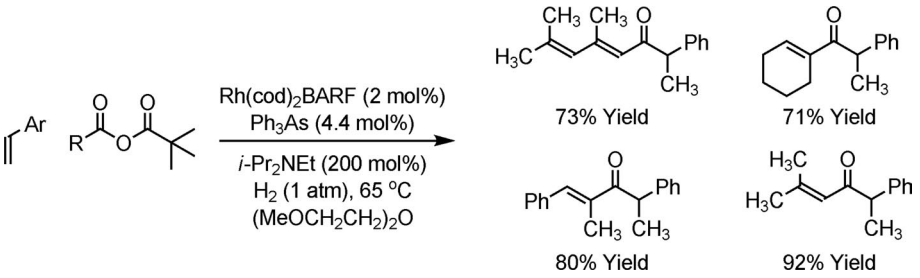

Scheme 8.37 Selective acyl transfer in reductive hydroacylations involving mixed carboxylic anhydrides derived from pivalic acid.

Whereas simple α-alkenes and aliphatic anhydrides remain challenging substrates (under optimum conditions employing cationic rhodium catalysts ligated by triphenylarsine, 4-phenyl-1-butene couples to benzoic acid in 34% yield with a 1 : 2.5 ratio of branched to linear regioisomers, and acetic anhydride couples to styrene in 27% yield with a 9 : 1 ratio of branched to linear regioisomers), activated alkenes such as norbornene couple efficiently to aromatic and α,β-unsaturated anhydrides, including mixed anhydrides derived from pivalic acid. Additionally, hydrogenation of ethylene in the presence of carboxylic anhydrides provides the corresponding ethyl ketones. For example, using a balloon containing roughly equal volumes of hydrogen and ethylene gas, 2-carboxyindole anhydride (chosen due to the low volatility of the product) is converted to the corresponding ethyl ketone in an unoptimized 44% isolated yield (Scheme 8.38).

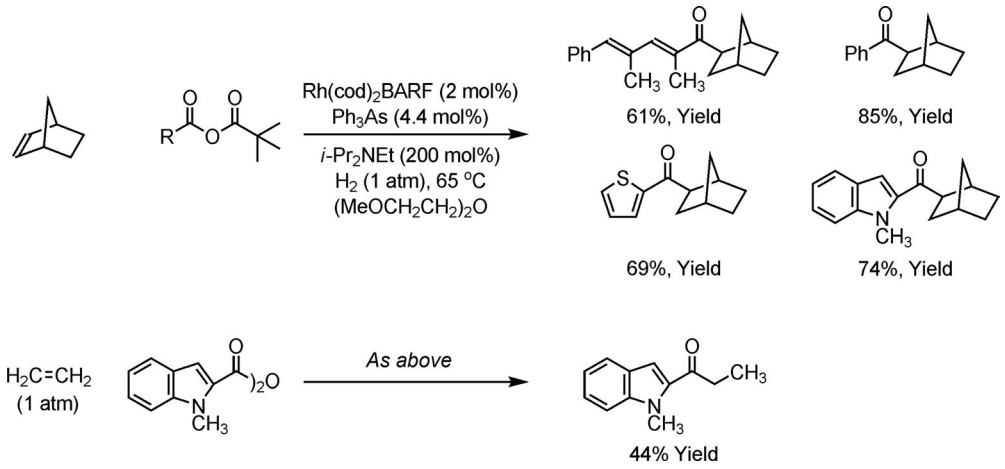

Scheme 8.38 Reductive hydroacylation via hydrogen-mediated coupling of activated non-conjugated alkenes to carboxylic anhydrides.

The results of isotopic labeling suggest two possible catalytic cycles. In catalytic mechanism **A**, heterolytic hydrogen activation is followed by insertion of styrene to furnish an organorhodium intermediate that engages in formal acyl substitution to provide the product of hydroacylation. In mechanism **B**, anhydride oxidative addition (related acyl–rhodium complexes have been prepared independently through reaction of $(Ph_3P)_3RhCl$ with anhydrides [136]) is followed by insertion of styrene and hydrogenolysis of the resulting alkylrhodium intermediate. Under an atmosphere of deuterium, deuterium incorporation occurs primarily at the β-position, but the extent of deuterium incorporation is base dependent. Using *i*-Pr_2NEt or Li_2CO_3 as base, 0.4 and 0.8 deuterium atoms are incorporated, respectively, suggesting incomplete deuteration may stem from dehydrogenation of *i*-Pr_2NEt. Reversible hydrometallation of styrene through mechanism **A** also may account for incomplete deuterium incorporation. Finally, it is interesting that the ratio of branched to linear product is influenced by the leaving group, suggesting intervention of the anhydride in advance of the regiodetermining step, as in mechanism **B** (Scheme 8.39).

8.6 Hydrogenative Carbocyclization

Metal-catalyzed reductive carbocyclization represents a major class of C–C bond-forming reactions [137]. Recently, it was demonstrated that a range of different reductive carbocyclizations are promoted under hydrogenation conditions. For example, catalytic hydrogenation of 1,6-diynes using cationic rhodium precatalysts at ambient temperature and pressure allows reductive carbocyclization to afford 1,2-dialkylidenecyclopentanes as single alkene stereoisomers [138]. Nearly identical

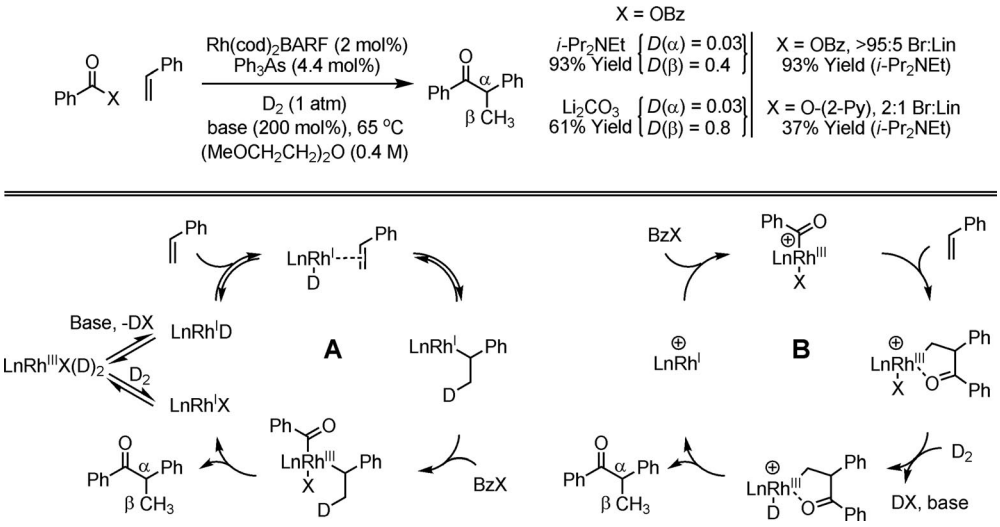

Scheme 8.39 Plausible catalytic mechanisms for hydrogen-mediated coupling of styrene to carboxylic anhydrides as corroborated by deuterium labeling and the influence of the acyl leaving group (Br = branched; Lin = linear).

hydrogenation conditions are effective for the reductive cyclization of 1,6-enynes. Substrate preorganization via the Thorpe–Ingold effect is not required for cyclization and olefinic products are not subject to further over-hydrogenation (Scheme 8.40).

Asymmetric hydrogenation of 1,6-enynes using chirally modified cationic rhodium precatalysts permits enantioselective reductive cyclization to afford alkylidene-substituted carbocycles and heterocycles [139]. Good to excellent yields and exceptional levels of asymmetric induction are observed across a structurally diverse set of substrates. For systems that incorporate 1,2-disubstituted alkenes ($R_2 \neq H$), competitive β-hydride elimination *en route* to products of cycloisomerization is observed. Related enone-containing substrates cannot engage in β-hydride elimination and participate in efficient reductive cyclization (Scheme 8.41).

Reductive cyclization of the indicated 1,6-diyne under an atmosphere of deuterium provides the 1,2-dialkylidenecyclopentane with complete incorporation of deuterium at both vinylic positions. This result is consistent with a catalytic mechanism involving oxidative coupling of the diyne to form a rhodacyclopentadiene, followed by deuteriolytic cleavage of the metallacycle. Consistent with the oxidative coupling mechanism, the indicated 1,6-enyne incorporating a terminal alkene moiety participates in reductive cyclization under a hydrogen deuteride atmosphere to furnish a monodeuterated product. Under identical conditions employing elemental deuterium as the reductant, the related 1,6-enyne possessing a 1,2-disubstituted alkene provides the corresponding cycloisomerization product without deuterium incorporation [140]. Presumably, β-hydride insertion from the intermediate metallacycle followed by C−H reductive elimination is faster than hydrogenolysis of the metallacycle (Scheme 8.42).

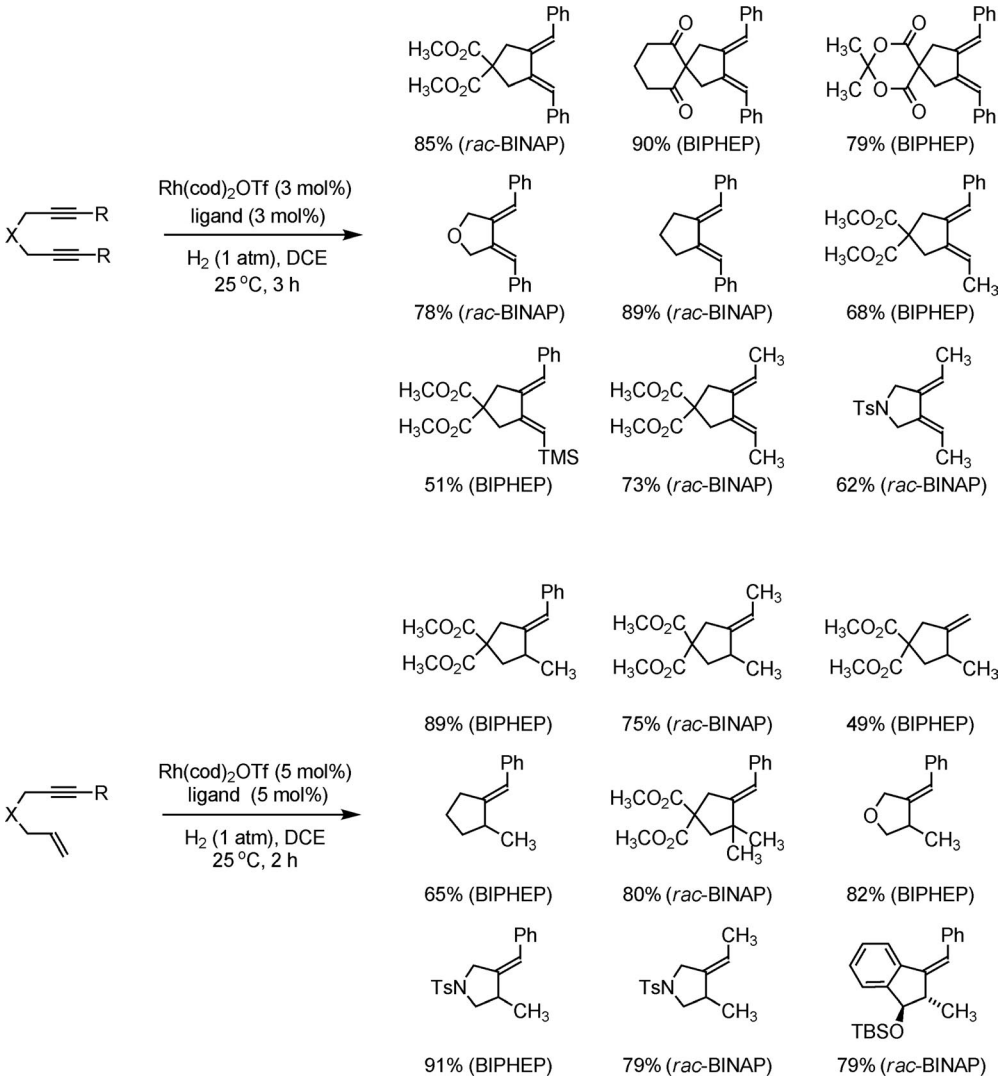

Scheme 8.40 Reductive carbocyclization of 1,6-diynes and 1,6-enynes via catalytic hydrogenation.

Catalytic hydrogenation of acetylenic aldehydes using chirally modified rhodium catalysts delivers the desired products of reductive carbocyclization with uniformly high levels of optical enrichment [141]. Brønsted acid co-catalysts were found to enhance reaction rate and conversion. Reductive cyclization under a deuterium atmosphere results in monodeuteration at the vinylic position, consistent with a catalytic mechanism involving alkyne–carbonyl oxidative coupling followed by hydrogenolytic cleavage of the resulting oxametallacycle. These hydrogen-mediated transformations represent the first examples of the enantioselective reductive cyclization of acetylenic aldehydes. Using an achiral hydrogenation catalyst, chiral

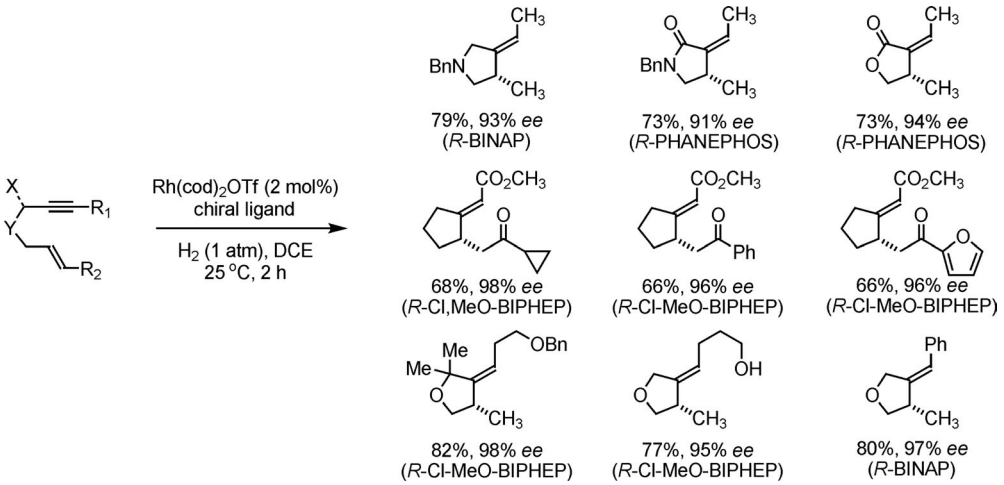

Scheme 8.41 Enantioselective carbocyclization of 1,6-enynes via asymmetric hydrogenation.

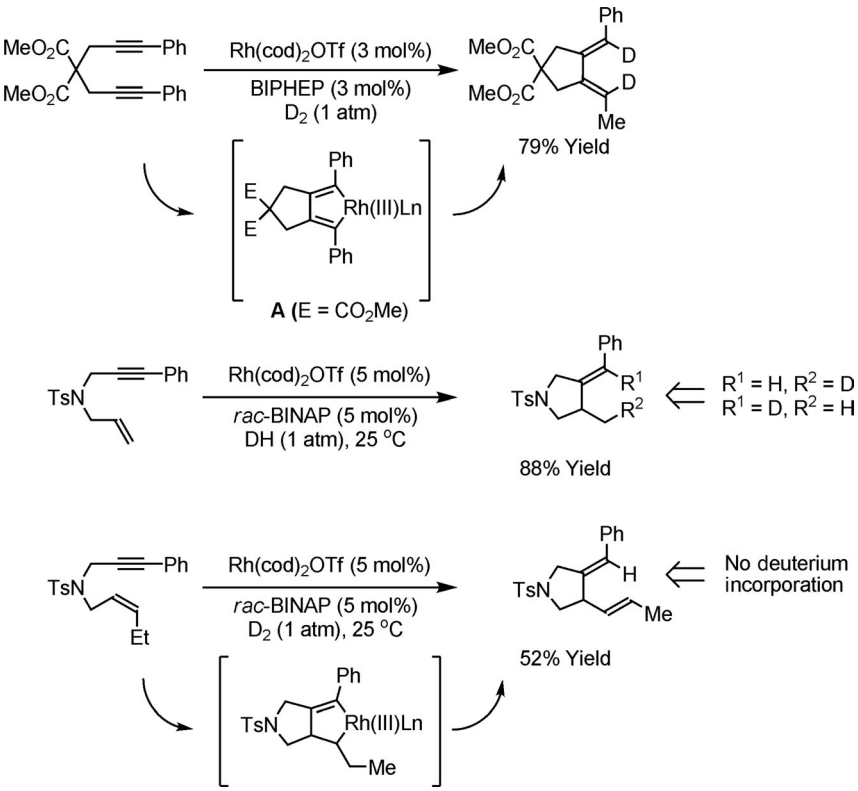

Scheme 8.42 Isotopic labeling studies corroborate a mechanism involving oxidative coupling in advance of hydrogen activation.

racemic acetylenic aldehydes engage in highly *syn*-diastereoselective reductive cyclizations to afford cyclic allylic alcohols (Scheme 8.43).

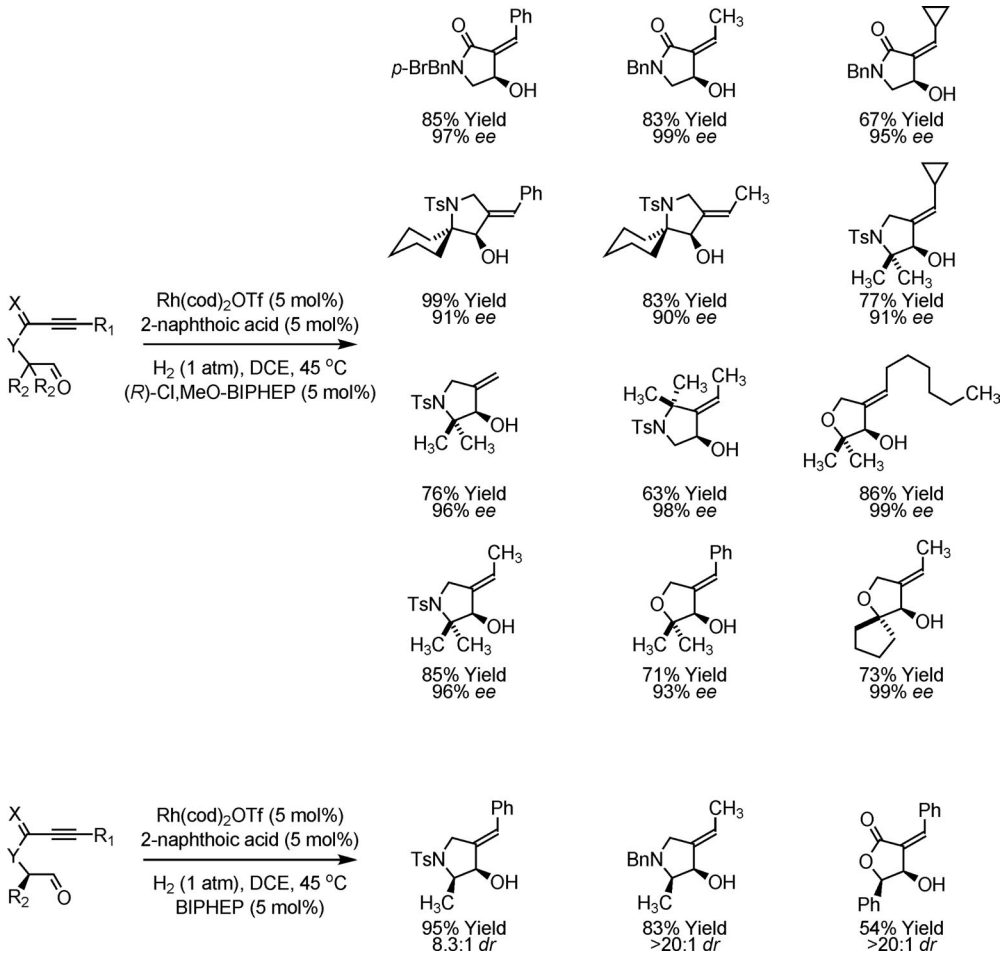

Scheme 8.43 Enantioselective carbocyclization of acetylenic aldehydes via asymmetric hydrogenation.

8.7 Future Directions

Through hydrogenative C–C bond formation there resides the potential to develop a broad range of by-product-free processes. Clearly, we have only just begun to tap the true potential of this novel reactivity mode, yet one must already question whether processes that have traditionally employed one or more stoichiometric metallic reagents can now be conducted catalytically under hydrogenative conditions.

Sustainable production of chemical commodities that does not compromise human health, the environment or the economy requires an increasing focus of the pharmaceutical and industrial sectors on green chemistry, especially the development and implementation of processes that are by-product free and employ inexpensive renewable feedstocks. Given the enormous socioeconomic impact of the Fischer–Tropsch reaction and alkene hydroformylation (prototypical C−C bond-forming hydrogenations), it is likely that hydrogenative C−C bond formation will emerge as a core method for green chemical synthesis.

Acknowledgments

Acknowledgment is made to the Robert A. Welch Foundation, Johnson & Johnson, Eli Lilly, Merck, the NIH-NIGMS (RO1-GM69445) and the ACS-GCI for partial support of the research described in this chapter. Dr Oliver Briel of Umicore and Dr John Chan of Aldrich are thanked for the generous donation of rhodium and iridium salts.

References

1 Board on Chemical Sciences, Technology, National Research Council of the National Academies (2005) *Sustainability in the Chemical Industry: Grand Challenges and Research Needs*, National Academies Press, Washington, DC.

2 For reviews, see: (a) Trost, B.M. (1991) *Science*, **254**, 1471–1477; (b) Trost, B.M. (1995) *Angewandte Chemie – International Edition*, **34**, 259–281.

3 (a) Wender, P.A. and Miller, B.L. (1993) *Organic Synthesis: Theory and Applications*, **2**, 27–66; (b) Wender, P.A., Handy, S. and Wright, D.L. (1997) *Chemistry & Industry*, 767–769.

4 (a) Sheldon, R.A. (1997) *Chemistry & Industry*, 12–15; (b) Sheldon, R.A. (2007) *Green Chemistry*, **9**, 1273–1283.

5 Rouhi, A.M. (2004) *Chemical & Engineering NEWS*, **82** (36), 49–58.

6 Hoffmann, R. (1998) *American Scientist*, **86**, 326–329.

7 Williams, W.D. (1999) *Bulletin for the History of Chemistry*, **24**, 66–68.

8 (a) Mitscherlich, E. (1834) *Annalen der Physik und Chemie*, **31**, 273–282; (b) Berzelius, J.-J. (1836) *Annales de Chimie et de Physique (Paris)*, **61**, 146–151.

9 Nobel Foundation (1966) *Nobel Lectures, Chemistry, 1901–1921*, Elsevier, Amsterdam.

10 Smil, V. (2004) *Enriching the Earth: Fritz Haber, Carl Bosch and the Transformation of World Food Production*, MIT Press, Cambridge, MA.

11 (a) Sabatier, P. and Senderens, J.-B. (1897) *Comptes Rendus Hebdomadaires des Seances de l'Académie des Sciences*, **124**, 1358–1361; (b) Sabatier, P. and Senderens, J.-B. (1899) *Comptes Rendus Hebdomadaires des Seances de l Academie des Sciences*, **128**, 1173–1176; (c) Sabatier, P. and Senderens, J.-B. (1901) *Comptes Rendus Hebdomadaires des Seances de l Academie des Sciences*, **132**, 210. For a biographical sketch of Paul Sabatier, see: Lattes, A. (2000) *Comptes Rendus de l'Académie des Sciences - Series IIC - Chemistry*, **3**, 705–709.

12 (a) Calvin, M. (1938) *Transactions of the Faraday Society*, **34**, 1181–1191; (b) Calvin, M. (1939) *Journal of the*

American Chemical Society, **61**, 2230–2234.

13 (a) Halpern, J., Harrod, J.F. and James, B.R. (1961) *Journal of the American Chemical Society*, **83**, 753–754; (b) Halpern, J., Harrod, J.F. and James, B.R. (1966) *Journal of the American Chemical Society*, **88**, 5150–5155.

14 (a) Gillard, R.D., Osborn, J.A., Stockwell, P.B. and Wilkinson, G. (1964) *Proceedings of the Chemical Society*, 284–285; (b) Jardine, F.H., Osborn, J.A., Wilkinson, G. and Young, J.F. (1965) *Chemistry & Industry*, 560; (c) Young, J.F., Osborn, J.A., Jardine, F.H. and Wilkinson, G. (1965) *Chemical Communications*, 131–132.

15 Knowles, W.S. and Sabacky, M.J., *Chemical Communications*, 1968, 1445–1446. See also: Horner, L., Siegel, H. and Buethe, H. (1968) *Angewandte Chemie – International Edition*, **7**, 942.

16 Dang, T.P. and Kagan, H.B. (1971) *Chemical Communications*, 481

17 Miyashita, A., Yasuda, A., Takaya, H., Toriumi, K., Ito, T., Souchi, T. and Noyori, R. (1980) *Journal of the American Chemical Society*, **102**, 7932–7934.

18 (a) Thommen, M. (2005) *Speciality Chemicals Magazine*, **25** (4), 26–28; (b) Thayer, A. (2005) *Chemical & Engineering NEWS*, **83** (36), 40–48; (c) Jäkel, C. and Paciello, R. (2006) *Chemical Reviews*, **106**, 2912–2942.

19 (a) Fischer, F. and Tropsch, H. (1923) *Brennst-Chem*, **4**, 276–285; (b) Fischer, F. and Tropsch, H. (1923) *Chemische Berichte*, **56 B**, 2428–2443.

20 (a) Storch, H.H., Anderson, R.B., Hofer, L.J.E., Hawk, C.O., Anderson, H.C. and Golumbic, N. (1948) *Synthetic Liquid Fuels From Hydrogenation of Carbon Monoxide. Part 1. Review of Literature*, Technical Paper 709, US Department of the Interior, Washington, DC. (b) US Department of Energy, http://www. fossil.energy.gov/aboutus/history/syntheticfuels_history.html (11 January (2008))

21 Jacoby, M. (2006) *Chemical & Engineering NEWS*, **84** (23), 57–61.

22 Roelen, O., (1938) (Chemische Verwertungsgesellschaft mbH), German Patent DE 849 548; *Chemical Abstracts*, **38**, (1944) 5501.

23 (a) Frohning, C.D. and Kohlpaintner, C.W. (1996) in *Applied Homogeneous Catalysis with Organometallic Compounds, Vol. 1* (eds B. Cornils and W.A. Herrmann), Wiley-VCH, Weinheim, pp. 29–104; (b) van Leeuwen, P.W.N.M. (2004) *Homogeneous Catalysis, Understanding the Art*, Kluwer, Dordrecht.

24 Molander, G.A. and Hoberg, J.O. (1992) *Journal of the American Chemical Society*, **114**, 3123–3125.

25 Kokube, K., Miura, M. and Nomura, M. (1995) *Organometallics*, **14**, 4521–4524.

26 (a) Moyes, R.B., Walker, D.W., Wells, P.B., Whan, D.A. and Irvine, E.A. (1992) *Spec Publ Chem Soc*, **114**, pp. 207–212; (b) Bianchini, C., Meli, A., Peruzzini, M., Vizzi, F., Zanobini, F. and Frediani, P. (1989) *Organometallics*, **8**, 2080–2082.

27 For recent reviews on hydrogen-mediated C–C coupling, see: (a) Ngai, M.-Y. and Krische, M.J. (2006) *Chimica Oggi-Chemistry Today*, **24** (4) (Chiral Technol. Suppl.) 12–14; (b) Iida, H. and Krische, M.J. (2007) *Topics in Current Chemistry*, **279**, 77–104; (c) Ngai, M.-Y., Kong, J.-R. and Krische, M.J. (2007) *The Journal of Organic Chemistry*, **72**, 1063–1072.

28 For reviews encompassing the synthesis of allylic alcohols, see: (a) Allyl alcohol and monoallyl derivatives, in Seidel, A. (ed.), *Kirk-Othmer's Encyclopedia of Chemical Technology*, 5th edn, Vol. 2, John Wiley & Sons, Inc., Hoboken, NJ, (2004) pp. 234–249; (b) Banerjee, A.K., Poon, P.S., Laya, M.S. and Vera, W.J. (2004) *Russian Chemical Reviews*, **73**, 621–636.

29 For reviews encompassing the synthesis of allylic amines, see: (a) Cheikh, R.B., Chaabouni, R., Laurent, A., Mison, P. and Nafti, A. (1983) *Synthesis*, 685–700; (b) Laurent, A., Mison, P., Nafti, A., Cheikh, R.B. and Chaabouni, R. (1984) *Journal of*

Chemical Research-S, 354–355; (c) Johannsen, M. and Jørgensen, K.A. (1998) *Chemical Reviews*, **98**, 1689–1708.

30 For reviews on metal-catalyzed allylic amination and alkoxylation, see: (a) Acemoglu, L. and Williams, J.M.J. (2002) in *Handbook of Organopalladium Chemistry for Organic Synthesis*, Vol. 2 (eds E.-i. Negishi and A. de Meijere), John Wiley & Sons, Inc, New York, pp. 1689–1705. (b) Trost, B.M. and Crawley, M.L. (2003) *Chemical Reviews*, **103**, 2921–2943; (c) Trost, B.M. (2004) *The Journal of Organic Chemistry*, **69**, 5813–5837; (d) Miyabe, H. and Takemoto, Y. (2005) *Synlett*, 1641–1655; (e) Takeuchi, R. and Kezuka, S. (2006) *Synthesis*, 3349–3366.

31 (a) Oguni, N. and Omi, T. (1984) *Tetrahedron Letters*, **25**, 2823–2824; (b) Kitamura, M., Suga, S., Kawai, K. and Noyori, R. (1986) *Journal of the American Chemical Society*, **108**, 6071–6072.

32 For reviews encompassing catalytic enantioselective addition of organozinc reagents to carbonyl compounds, see: (a) Pu, L. and Yu, H.-B. (2001) *Chemical Reviews*, **101**, 757–824; (b) Betancort, J.M., García, C. and Walsh, P.J. (2004) *Synlett* 749–760; (c) Ramón, D.J. and Yus, M. (2004) *Angewandte Chemie – International Edition*, **43**, 284–287; (d) García, C. and Martín, V.S. (2006) *Current Organic Chemistry*, **10**, 1849–1889; (e) Ramón, D.J. and Yus, M. (2006) *Chemical Reviews*, **106**, 2126–2208.

33 For enantioselective catalytic addition of vinylzinc reagents to aldehydes, see: (a) Oppolzer, W. and Radinov, R.N. (1992) *Helvetica Chimica Acta*, **75**, 170–173; (b) Oppolzer, W. and Radinov, R.N. (1993) *Journal of the American Chemical Society*, **115**, 1593–1594; (c) Soai, K. and Takahashi, K. (1994) *Journal of the Chemical Socity, Perkin Transaction 1*, 1257–1258; (d) Wipf, P. and Xu, W. (1994) *Tetrahedron Letters*, **35**, 5197–5200; (e) Oppolzer, W., Radinov, R.N. and De Brabander, J. (1995) *Tetrahedron Letters*, **36**, 2607–2610; (f) Wipf, P. and Ribe, S. (1998) *The Journal of Organic Chemistry*, **63**, 6454–6455; (g) Oppolzer, W., Radinov, R.N. and El-Sayed, E. (2001) *The Journal of Organic Chemistry*, **66**, 4766–4770; (h) Dahmen, S. and Bräse, S. (2001) *Organic Letters*, **3**, 4119–4122; (i) Chen, Y.K., Lurain, A.E. and Walsh, P.J. (2002) *Journal of the American Chemical Society*, **124**, 12225–12231; (j) Ji, J.-X., Qiu, L.-Q., Yip, C.W. and Chan, A.S.C. (2003) *The Journal of Organic Chemistry*, **68**, 1589–1590; (k) Lurain, A.E. and Walsh, P.J. (2003) *Journal of the American Chemical Society*, **125**, 10677–10683; (l) Ko, D.-H., Kang, S.-W., Kim, K.H., Chung, Y. and Ha, D.-C. (2004) *Bulletin of the Korean Chemical Society*, **25**, 35–36; (m) Sprout, C.M., Richmond, M.L. and Seto, C.T. (2004) *The Journal of Organic Chemistry*, **69**, 6666–6673; (n) Jeon, S.-J., Chen, Y.K. and Walsh, P.J. (2005) *Organic Letters*, **7**, 1729–1732; (o) Lauterwasser, F., Gall, J., Höfener, S. and Bräse, S. (2006), *Advanced Synthesis and Catalysis*, **348**, 2068–2074; (p) Jeon, S.-J., Fisher, E.L., Carroll, P.J. and Walsh, P.J. (2006) *Journal of the American Chemical Society*, **128**, 9618–9619; (q) Salvi, L., Jeon, S.-J., Fisher, E.L., Carroll, P.J. and Walsh, P.J. (2007) *Journal of the American Chemical Society*, **129**, 16119–16125; (r) Wu, H.-L., Wu, P.-Y. and Uang, B.-J. (2007) *The Journal of Organic Chemistry*, **72**, 5935–5937.

34 For reviews encompassing catalytic enantioselective aldehyde vinylation using organozinc reagents, see: (a) Wipf, P. and Kendall, C. (2002) *Chemistry - A European Journal*, **8**, 1778–1784; (b) Wipf, P. and Nunes, R.L. (2004) *Tetrahedron*, **60**, 1269–1279.

35 (a) Ramón, D.J. and Yus, M. (1998) *Tetrahedron Letters*, **39**, 1239–1242; (b) Ramón, D.J. and Yus, M. (1998) *Tetrahedron*, **54**, 5651–5666; (c) Dosa, P.I. and Fu, G.C. (1998) *Journal of the American Chemical Society*, **120**, 445–446.

36 For catalytic enantioselective ketone vinylation using organozinc reagents, see:

(a) Li, H. and Walsh, P.J. (2004) *Journal of the American Chemical Society*, **126**, 6538–6539; (b) Li, H. and Walsh, P.J. (2005) *Journal of the American Chemical Society*, **127**, 8355–8361; (c) Jeon, S.-J., Li, H., García, C., LaRochelle, L.K. and Walsh, P.J. (2005) *The Journal of Organic Chemistry*, **70**, 448–455.

37 Schmidt, F., Rudolph, J. and Bolm, C. (2006) *Synthesis*, 3625–3630.

38 For reviews encompassing the catalytic enantioselective addition of organozinc reagents to imines, see: (a) Bloch, R. (1998) *Chemical Reviews*, **98**, 1407–1438; (b) Kobayashi, S. and Ishitani, H. (1999) *Chemical Reviews*, **99**, 1069–1094; (c) Vilaivan, T., Bhanthumnavin, W. and Sritana-Anant, Y. (2005) *Current Organic Chemistry*, **9**, 1315–1392; (d) Schmidt, F., Stemmler, R.T., Rudolph, J. and Bolm, C. (2006) *Chemical Society Reviews*, **35**, 454–470.

39 For enantioselective organocatalytic addition of organozinc reagents to imines, see: (a) Soai, K., Hatanaka, T. and Miyazawa, T. (1992) *Journal of the Chemical Society. Chemical Communications*, 1097–1098; (b) Katritzky, A.R. and Harris, P.A. (1992) *Tetrahedron: Asymmetry*, **3**, 437–442; (c) Andersson, P.G., Guijarro, D. and Tanner, D. (1996) *Synlett*, 727–728; (d) Andersson, P.G., Guijarro, D. and Tanner, D. (1997) *The Journal of Organic Chemistry*, **62**, 7364–7375; (e) Guijarro, D., Pinho, P. and Andersson, P.G. (1998) *The Journal of Organic Chemistry*, **63**, 2530–2535; (f) Brandt, P., Hedberg, C., Lawonn, K., Pinho, P. and Andersson, P.G. (1999) *Chemistry - A European Journal*, **5**, 1692–1699; (g) Jimeno, C., Reddy, K.S., Solà, L., Moyano, A., Pericàs, M.A. and Riera, A. (2000) *Organic Letters*, **2**, 3157–3159.

40 For enantioselective copper-catalyzed addition of organozinc reagents to imines, see: (a) Fujihara, H., Nagai, K. and Tomioka, K. (2000) *Journal of the American Chemical Society*, **122**, 12055–12056; (b) Nagai, K., Fujihara, H., Kuriyama, M., Yamada, K.-i. and Tomioka, K. (2002) *Chem Lett*, 8–9; (c) Wang, C.-J. and Shi, M. (2003) *The Journal of Organic Chemistry*, **68**, 6229–6237; (d) Soeta, T., Nagai, K., Fujihara, H., Kuriyama, M. and Tomioka, K. (2003) *The Journal of Organic Chemistry*, **68**, 9723–9727; (e) Shi, M. and Zhang, W. (2003) *Tetrahedron: Asymmetry*, **14**, 3407–3414; (f) Shi, M. and Wang, C.-J. (2003) *Advanced Synthesis and Catalysis*, **345**, 971–973; (g) Boezio, A.A. and Charette, A.B. (2003) *Journal of the American Chemical Society*, **125**, 1692–1693; (h) Boezio, A.A., Pytkowicz, J., Côté, A. and Charette, A.B. (2003) *Journal of the American Chemical Society*, **125**, 14260–14261; (i) Côté, A., Boezio, A.A. and Charette, A.B. (2004) *Proceedings of the National Academy of Sciences of the United States of America*, **101**, 5405–5410; (j) Côté, A., Boezio, A.A. and Charette, A.B. (2004) *Angewandte Chemie – International Edition*, **43**, 6525–6528; (k) Wang, M.-C., Xu, C.-L., Zou, Y.-X., Liu, H.-M. and Wang, D.-K. (2005) *Tetrahedron Letters*, **46**, 5413–5416; (l) Desrosiers, J.-N., Côté, A. and Charette, A.B. (2005) *Tetrahedron*, **61**, 6186–6192; (m) Wang, M.-C., Liu, L.-T., Hua, Y.-Z., Zhang, J.-S., Shi, Y.-Y. and Wang, D.-K. (2005) *Tetrahedron: Asymmetry*, **16**, 2531–2534; (n) Kim, B.-S., Kang, S.-W., Kim, K.H., Ko, D.-H., Chung, Y. and Ha, D.C. (2005) *Bulletin of the Korean Chemical Society*, **26**, 1501–1502; (o) Lauzon, C. and Charette, A.B. (2006) *Organic Letters*, **8**, 2743–2745; (p) Wang, M.-C., Xu, C.-L., Cheng, F. and Ding, X. (2006) *Tetrahedron*, **62**, 12220–12226; (q) Shi, M., Lei, Z.-Y. and Xu, Q. (2006) *Advanced Synthesis and Catalysis*, **348**, 2237–2242.

41 For enantioselective zirconium-, titanium- and hafnium-catalyzed addition of organozinc reagents to imines, see: (a) Porter, J.R., Traverse, J.F., Hoveyda, A.H. and Snapper, M.L. (2001) *Journal of the American Chemical Society*, **123**, 984–985; (b) Porter, J.R., Traverse, J.F., Hoveyda, A.H. and Snapper, M.L. (2001) *Journal of*

the American Chemical Society, **123**, 10409–10410; (c) Akullian, L.C., Snapper, M.L. and Hoveyda, A.H. (2003) *Angewandte Chemie – International Edition*, **42**, 4244–4247; (d) Akullian, L.C., Porter, J.R., Traverse, J.F., Snapper, M.L. and Hoveyda, A.H. (2005) *Advanced Synthesis and Catalysis*, **347**, 417–425; (e) Basra, S., Fennie, M.W. and Kozlowski, M.C. (2006) *Organic Letters*, **8**, 2659–2662.

42 For enantioselective rhodium-catalyzed addition of organozinc reagents to imines, see: Nishimura, T., Yasuhara, Y. and Hayashi, T. (2006) *Organic Letters*, **8**, 979–981.

43 For reviews encompassing catalytic enantioselective addition of organolithium reagents to carbonyl compounds and imines, see: (a) Tomioka, K. (1990) *Synthesis*, 541–549; (b) Berrisford, D.J. (1995) *Angewandte Chemie – International Edition*, **34**, 178–180; (c) Denmark, S.E. and Nicaise, O.J.-C. (1996) *Chemical Communications*, 999–1004. (d) Enders, D. and Reinhold, U. (1997) *Tetrahedron: Asymmetry*, **8**, 1895–1946.

44 For enantioselective rhodium-catalyzed addition of organometallic reagents to imines, see: (a) Organotin reagents: (a) Hayashi, T. and Ishigedani, M. (2000) *Journal of the American Chemical Society*, **122**, 976–977; (b) Hayashi, T. and Ishigedani, M. (2001) *Tetrahedron*, **57**, 2589–2595. Organotitanium reagents: (c) Hayashi, T., Kawai, M. and Tokunaga, N. (2004) *Angewandte Chemie–International Edition*, **43**, 6125–6128. Organoboron reagents: (d) Kuriyama, M., Soeta, T., Hao, X., Chen, Q. and Tomioka, K. (2004) *Journal of the American Chemical Society*, **126**, 8128–8129; (e) Tokunaga, N., Otomaru, Y., Okamoto, K., Ueyama, K., Shintani, R. and Hayashi, T. (2004) *Journal of the American Chemical Society*, **126**, 13584–13585; (f) Weix, D.J., Shi, Y. and Ellman, J.A. (2005) *Journal of the American Chemical Society*, **127**, 1092–1093; (g) Otomaru, Y., Tokunaga, N., Shintani, R. and Hayashi, T. (2005) *Organic Letters*, **7**, 307–310; (h) Duan, H.-F., Jia, Y.-X., Wang, L.-X. and Zhou, Q.-L. (2006) *Organic Letters*, **8**, 2567–2569; (i) Wang, Z.-Q., Feng, C.-G., Xu, M.-H. and Lin, G.-Q. (2007) *Journal of the American Chemical Society*, **129**, 5336–5337; (j) Marelli, C., Monti, C., Gennari, C. and Piarulli, U. (2007) *Synlett*, 2213–2216; (k) Nakagawa, H., Rech, J.C., Sindelar, R.W. and Ellman, J.A. (2007) *Organic Letters*, **9**, 5155–5157.

45 (a) Kakuuchi, A., Taguchi, T. and Hanzawa, Y. (2003) *Tetrahedron Letters*, **44**, 923–926; (b) Wipf, P., Kendall, C. and Stephenson, C.R.J. (2003) *Journal of the American Chemical Society*, **125**, 761–768.

46 Patel, S.J. and Jamison, T.F. (2004) *Angewandte Chemie – International Edition*, **43**, 3941–3944.

47 For a compilation of reviews on the subject of metal-catalyzed reductive C–C coupling, see: (2007) *Topics in Current Chemistry* **279**, 1–248.

48 For selected reviews encompassing intra- and intermolecular direct reductive coupling of alkynes to carbonyl partners, see: (a) Ojima, I., Tzamarioudaki, M., Li, Z. and Donovan, R.J. (1996) *Chemical Reviews*, **96**, 635–662; (b) Montgomery, J. (2000) *Accounts of Chemical Research*, **33**, 467–473; (c) Montgomery, J., Amarasinghe, K.K.D., Chowdhury, S.K., Oblinger, E., Seo, J. and Savchenko, A.V. (2002) *Pure and Applied Chemistry*, **74**, 129–133; (d) Ikeda, S.-i. (2003) *Angewandte Chemie – International Edition*, **42**, 5120–5122; (e) Miller, K.M., Molinaro, C. and Jamison, T.F. (2003) *Tetrahedron: Asymmetry*, **14**, 3619–3625; (f) Montgomery, J. (2004) *Angewandte Chemie – International Edition*, **43**, 3890–3908; (g) Montgomery, J. and Sormunen, G.J. (2007) *Topics in Current Chemistry*, **279**, 1–23; (h) Moslin, R.M., Miller-Moslin, K. and Jamison, T.F. (2007) *Chemical Communications*, 4441–4449.

49 Ojima, I., Tzamarioudaki, M. and Tsai, C.-Y. (1994) *Journal of the American Chemical Society*, **116**, 3643–3644.

50 (a) Crowe, W.E. and Rachita, M.J. (1995) *Journal of the American Chemical Society*, **117**, 6787–6788. For an aligned study, see: (b) Kablaoui, N.M. and Buchwald, S.L. (1995) *Journal of the American Chemical Society*, **117**, 6785–6786.

51 (a) Oblinger, E. and Montgomery, J. (1997) *Journal of the American Chemical Society*, **119**, 9065–9066; (b) Tang, X.-Q. and Montgomery, J. (1999) *Journal of the American Chemical Society*, **121**, 6098–6099; (c) Tang, X.-Q. and Montgomery, J. (2000) *Journal of the American Chemical Society*, **122**, 6950–6954; (d) Mahandru, G.M., Liu, G. and Montgomery, J. (2004) *Journal of the American Chemical Society*, **126**, 3698–3699; (e) Knapp-Reed, B., Mahandru, G.M. and Montgomery, J. (2005) *Journal of the American Chemical Society*, **127**, 13156–13157.

52 (a) Huang, W.-S., Chan, J. and Jamison, T.F. (2000) *Organic Letters*, **2**, 4221–4223; (b) Miller, K.M., Huang, W.-S. and Jamison, T.F. (2003) *Journal of the American Chemical Society*, **125**, 3442–3443; (c) Miller, K.M. and Jamison, T.F. (2005) *Organic Letters*, **7**, 3077–3080.

53 Takai, K., Sakamoto, S. and Isshiki, T. (2003) *Organic Letters*, **5**, 653–655.

54 (a) Kong, J.-R., Ngai, M.-Y. and Krische, M.J. (2006) *Journal of the American Chemical Society*, **128**, 718–719; (b) Cho, C.-W. and Krische, M.J. (2006) *Organic Letters*, **8**, 3873–3876; (c) Hong, Y.-T., Cho, C.-W., Skucas, E. and Krische, M.J. (2007) *Organic Letters*, **9**, 3745–3748; (d) Komanduri, V. and Krische, M.J. (2006) *Journal of the American Chemical Society*, **128**, 16448–16449.

55 For mechanistic studies of alkene hydrogenation catalyzed by neutral Rh(I) complexes, see: (a) Tolman, C.A., Meakin, P.Z., Lindner, D.L. and Jesson, J.P. (1974) *Journal of the American Chemical Society*, **96**, 2762–2774; (b) Halpern, J. and Wong, C.S. (1973) *Journal of the Chemical Society. Chemical Communications*, 629–630; (c) Halpern, J., Okamoto, T. and Zakhariev, A. (1977) *Journal of Molecular Catalysis*, **2**, 65–68.

56 For reviews encompassing the mechanism of asymmetric hydrogenation catalyzed by cationic rhodium complexes, see: (a) Halpern, J. (1985) *Asymm Synth*, **5**, 41–69; (b) Landis, C.R. and Brauch, T.W. (1998) *Inorganica Chimica Acta*, **270**, 285–297.

57 Musashi, Y. and Sakaki, S. (2002) *Journal of the American Chemical Society*, **124**, 7588–7603.

58 (a) Akiyama, T., Itoh, J., Yokota, K. and Fuchiba, K. (2004) *Angewandte Chemie–International Edition*, **43**, 1566–1568; (b) Uraguchi, D. and Terada, M. (2004) *Journal of the American Chemical Society*, **126**, 5356–5357; (c) Hoffmann, S., Seayad, A.M. and List, B. (2005) *Angewandte Chemie – International Edition*, **44**, 7424–7427.

59 Kong, J.-R., Cho, C.-W. and Krische, M.J. (2005) *Journal of the American Chemical Society*, **127**, 11269–11276.

60 Kong, J.-R. and Krische, M.J. (2006) *Journal of the American Chemical Society*, **128**, 16040–16041.

61 Bianchini, C., Caulton, K.G., Chardon, C., Eisenstein, O., Folting, K., Johnson, T.J., Meli, A., Peruzzini, M., Rauscher, D.J., Streib, W.E. and Vizza, F. (1991) *Journal of the American Chemical Society*, **113**, 5127–5129, and references cited therein.

62 Skucas, E., Kong, J.-R. and Krische, M.J. (2007) *Journal of the American Chemical Society*, **129**, 7242–7243.

63 Acetylene, in Seidel, A. (ed.), (2004) *Kirk-Othmer's Encyclopedia of Chemical Technology*, 5th edn, Vol. 1, John Wiley & Sons, Inc., Hoboken, NJ, pp. 216–217.

64 (a) Barchuk, A., Ngai, M.-Y. and Krische, M.J. (2007) *Journal of the American Chemical Society*, **129**, 8432–8433; (b) Ngai, M.-Y., Barchuk, A. and Krische, M.J. (2007) *Journal of the American Chemical Society*, **129**, 12644–12645.

65 Fujita, K.-i., Yamashita, M., Puschmann, F., Alvarez-Flacon, M.M., Incarvito, C.D. and Hartwig, J.F. (2006) *Journal of the American Chemical Society*, **128**, 9044–9045.

66 (a) Dewar, M.J.S. (1951) *Bulletin de la Societe Chimique de France*, C71–C79 (b) Chatt, J. and Duncanson, L.A. (1953) *Journal of the Chemical Society*, 2939–2947; (c) Dewar, M.J.S. and Ford, G.P. (1979) *Journal of the American Chemical Society*, **101**, 783–791.

67 (a) Kirchner, R.M. and Ibers, J.A. (1973) *Journal of the American Chemical Society*, **95**, 1095–1101; (b) Calabrese, J.C., Roe, D.C., Thorn, D.L. and Tulip, T.H. (1984) *Organometallics*, **3**, 1223–1230; (c) Rappoli, B.J., Churchill, M.R., Janik, T.S., Rees, W.M. and Atwood, J.D. (1987) *Journal of the American Chemical Society*, **109**, 5145–5149; (d) Rees, W.M., Churchill, M.R., Fettinger, J.C. and Atwood, J.D. (1987) *Journal of Organometallic Chemistry*, **319**, 411–422; (e) Marinelli, G., Streib, W.E., Huffman, J.C., Caulton, K.G., Gagné, M.R., Takats, J., Dartiguenave, M., Chardon, C., Jackson, S.A. and Eisenstein, O. (1990) *Polyhedron*, **9**, 1867–1881.

68 Li, J., Schreckenbach, G. and Ziegler, T. (1995) *Journal of the American Chemical Society*, **117**, 486–494.

69 (a) Vaska, L. and Peone, J., Jr. (1971) *Chemical Communications*, 418–419; (b) Haynes, A., McNish, J. and Pearson, J.M. (1998) *Journal of Organometallic Chemistry*, **551**, 339–347; (c) Grotjahn, D.B., Collins, L.S.B., Wolpert, M., Bikzhanova, G.A., Lo, H.C., Combs, D. and Hubbard, J.L. (2001) *Journal of the American Chemical Society*, **123**, 8260–8270.

70 For reviews on enantioselective carbonyl allylation, see: (a) Ramachandran, P.V. (2002) *Aldrichimica Acta*, **35**, 23–35; (b) Kennedy, J.W.J. and Hall, D.G. (2003) *Angewandte Chemie – International Edition*, **42**, 4732–4739; (c) Denmark, S.E. and Fu, J. (2003) *Chemical Reviews* **103**, 2763–2793; (d) Yu, C.-M., Youn, J. and Jung, H.-K. (2006) *Bulletin of the Korean Chemical Society*, **27**, 463–472; (e) Marek, I. and Sklute, G. (2007) *Chemical Communications*, 1683–1691; (f) Hall, D.G. (2007) *Synlett*, 1644–1655.

71 (a) Mikhailov, B.M. and Bubnov, Y.N. (1964) *Izv Akad Nauk SSSR, Ser Khim* 1874–1876; (b) Hosomi, A. and Sakurai, H. (1976) *Tetrahedron Letters*, **17**, 1295–1298.

72 Chirally modified allyl metal reagents: (a) Herold, T. and Hoffmann, R.W. (1978) *Angewandte Chemie – International Edition*, **17**, 768–769; (b) Hoffmann, R.W. and Herold, T. (1981) *Chemische Berichte*, **114**, 375–383; (c) Hayashi, T., Konishi, M. and Kumada, M. (1982) *Journal of the American Chemical Society*, **104**, 4963–4965; (d) Brown, H.C. and Jadhav, P.K. (1983) *Journal of the American Chemical Society*, **105**, 2092–2093; (e) Roush, W.R., Walts, A.E. and Hoong, L.K. (1985) *Journal of the American Chemical Society*, **107**, 8186–8190; (f) Reetz, M. (1988) *Pure and Applied Chemistry*, **60**, 1607–1614; (g) Short, R.P. and Masamune, S. (1989) *Journal of the American Chemical Society*, **111**, 1892–1894; (h) Corey, E.J., Yu, C.-M. and Kim, S.S. (1989) *Journal of the American Chemical Society*, **111**, 5495–5496; (i) Seebach, D., Beck, A.K., Imwinkelried, R., Roggo, S. and Wonnacott, A. (1987) *Helvetica Chimica Acta*, **70**, 954–974; (j) Riediker, M. and Duthaler, R.O. (1989) *Angewandte Chemie – International Edition*, **28**, 494–495; (k) Panek, J.S. and Yang, M. (1991) *Journal of the American Chemical Society*, **113**, 6594–6600; (l) Kinnaird, J.W.A., Ng, P.Y., Kubota, K., Wang, X. and Leighton, J.L. (2002) *Journal of the American Chemical Society*, **124**, 7920–7921.

73 Catalytic asymmetric carbonyl allylation: (a) Costa, A.L., Piazza, M.G., Tagliavini, E., Trombini, C. and Umani-Ronchi, A. (1993) *Journal of the American Chemical Society*, **115**, 7001–7002; (b) Keck, G.E., Tarbet, K.H. and Geraci, L.S. (1993)

Journal of the American Chemical Society, **115**, 8467–8468; (c) Denmark, S.E., Coe, D.M., Pratt, N.E. and Griedel, B.D. (1994) *The Journal of Organic Chemistry*, **59**, 6161–6163; (d) Denmark, S.E. and Fu, J. (2001) *Journal of the American Chemical Society*, **123**, 9488–9489; Nakajima, M., Saito, M., Shiro, M. and Hashimoto, S.-i. (1998) *Journal of the American Chemical Society*, **120**, 6419–6420.

74 For selected examples of reactions involving nucleophilic π-allyls, see: (a) Palladium: Tabuchi, T., Inanaga, J. and Yamaguchi, M. (1986) *Tetrahedron Letters*, **27**, 1195–1196; (b) Takahara, J.P., Masuyama, Y. and Kurusu, Y. (1992) *Journal of the American Chemical Society*, **114**, 2577–2586; (c) Kimura, M., Ogawa, Y., Shimizu, M., Sueishi, M., Tanaka, S. and Tamaru, Y. (1998) *Tetrahedron Letters*, **39**, 6903–6906; (d) Kimura, M., Shimizu, M., Shibata, K., Tazoe, M. and Tamaru, Y. (2003) *Angewandte Chemie – International Edition*, **42**, 3392–3395; (e) Zanoni, G., Gladiali, S., Marchetti, A., Piccinini, P., Tredici, I. and Vidari, G. (2004) *Angewandte Chemie – International Edition*, **43**, 846–849. Rhodium: (f) Masuyama, Y., Kaneko, Y. and Kurusu, Y. (2004) *Tetrahedron Letters*, **45**, 8969–8971. Ruthenium: (g) Tsuji, Y., Mukai, T., Kondo, T. and Watanabe, Y. (1989) *Journal of Organometallic Chemistry*, **369**, C51–C53 (h) Kondo, T., Ono, H., Satake, N., Mitsudo, T.-a. and Watanabe, Y. (1995) *Organometallics*, **14**, 1945–1953.

75 For selected reviews covering carbonyl allylation via umpolung of π-allyls, see: (a) Tamaru, Y. (2002) in *Handbook of Organopalladium Chemistry for Organic Synthesis*, Vol. 2 (eds E.-i. Negishi, and A. de Meijere), John Wiley & Sons, Inc, New York, pp. 1917–1943. (b) Tamaru, Y. (1999) in *Perspectives in Organopalladium Chemistry for the XXI Century* (ed. J. Tsuji), Elsevier, Amsterdam, pp. 215–231. (c) Kondo, T. and Mitsudo, T.-a. (2002) *Current Organic Chemistry*, **6**, 1163–1179.

76 For reviews on carbonyl-ene reactions, see: (a) Mikami, K. and Shimizu, M. (1992) *Chemical Reviews*, **92**, 1021–1050; (b) Berrisford, D.J. and Bolm, C. (1995) *Angewandte Chemie – International Edition*, **34**, 1717–1719; (c) Johnson, J.S. and Evans, D.A. (2000) *Accounts of Chemical Research*, **33**, 325–335.

77 For nickel-catalyzed carbonyl-ene reactions, see: (a) Ho, C.-Y., Ng, S.-S. and Jamison, T.F. (2006) *Journal of the American Chemical Society*, **128**, 5362–5363; (b) Ng, S.-S., Ho, C.-Y. and Jamison, T.F. (2006) *Journal of the American Chemical Society*, **128**, 11513–11528.

78 Skucas, E., Bower, J.F. and Krische, M.J. (2007) *Journal of the American Chemical Society*, **129**, 12678–12679.

79 For recent reviews on hydrogen auto-transfer processes, see: (a) Guillena, G., Ramón, D.J. and Yus, M. (2007) *Angewandte Chemie – International Edition*, **46**, 2358–2364; (b) Hamid, M.H.S.A., Slatford, P.A. and Williams, J.M.J. (2007) *Advanced Synthesis and Catalysis*, **349**, 1555–1575.

80 (a) Guerbet, M.C.R. (1908) *Comptes Rendus Chimie*, **146**, 298–300; (b) Machemer, H. (1952) *Angewandte Chemie – International Edition*, **64**, 213–220; (c) Pratt, E.F. and Kubler, D.G. (1954) *Journal of the American Chemical Society*, **76**, 52–56; (d) Ndou, A.S., Plint, N. and Coville, N.J. (2003) *Applied Catalysis A-General*, **251**, 337–345.

81 (a) Gregorio, G., Pregaglia, G.F. and Ugo, R. (1972) *Journal of Organometallic Chemistry*, **37**, 385–387; (b) Burk, P.L., Pruett, R.L. and Campo, K.S. (1985) *Journal of Molecular Catalysis*, **33**, 1–14; (c) Cho, C.S., Kim, B.T., Kim, H.-S., Kim, T.-J. and Shim, S.C. (2003) *Organometallics*, **22**, 3608–3610; (d) Carlini, C., Macinai, A., Galletti, A.M.R. and Sbrana, G. (2004) *Journal of Molecular Catalysis A-Chemical*, **212**, 65–70; (e) Fujita, K.-i., Asai, C., Yamaguchi, T., Hanasaka, F. and Yamaguchi, R. (2005) *Organic Letters*, **7**,

4017–4019; (f) Cho, C.S., Ren, W.X. and Shim, S.C. (2005) *Bulletin of the Korean Chemical Society*, **26**, 1611–1613; (g) Carlini, C., Marchionna, M., Noviello, M., Galletti, A.M.R., Sbrana, G., Basile, F. and Vaccari, A. (2005) *Journal of Molecular Catalysis A-Chemical*, **232**, 13–20; (h) Matsu-ura, T., Sakaguchi, S., Obora, Y. and Ishii, Y. (2006) *The Journal of Organic Chemistry*, **71**, 8306–8308; (i) Martínez, R., Ramón, D.J. and Yus, M. (2006) *Tetrahedron*, **62**, 8982–8987.

82 (a) Chabardes, P. and Querou, Y. (1969) (Rhône-Poulenc), French Patent 1 582 621; (1970) *Chemical Abstracts*, **73**, 61760; (b) Cho, C.S., Kim, B.T., Kim, T.-J. and Shim, S.C. (2001) *The Journal of Organic Chemistry*, **66**, 9020–9022; (c) Cho, C.S., Kim, B.T., Lee, M.J., Kim, T.-J. and Shim, S.C. (2001) *Angewandte Chemie – International Edition*, **40**, 958–960; (d) Cho, C.S., Kim, B.T., Kim, T.-J. and Shim, S.C. (2002) *Tetrahedron Letters*, **43**, 7987–7989; (e) Martínez, R., Brand, G.J., Ramón, D.J. and Yus, M. (2005) *Tetrahedron Letters*, **46**, 3683–3686; (f) Cho, C.S. (2005) *Journal of Molecular Catalysis A-Chemical*, **240**, 55–60; (g) Kwon, M.S., Kim, N., Seo, S.H., Park, I.S., Cheeddrala, R.K. and Park, J. (2005) *Angewandte Chemie – International Edition*, **44**, 6913–6915; (h) Cho, C.S. and Shim, S.C. (2006) *Journal of Organometallic Chemistry*, **691**, 4329–4332; (i) Onodera, G., Nishibayashi, Y. and Uemura, S. (2006) *Angewandte Chemie – International Edition*, **45**, 3819–3822; (j) Martínez, R., Ramón, D.J. and Yus, M. (2006) *Tetrahedron*, **62**, 8988–9001; (k) Yamada, Y.M.A. and Uozumi, Y. (2006) *Organic Letters*, **8**, 1375–1378.

83 (a) Miyano, S. and Abe, N. (1971) *The Journal of Organic Chemistry*, **36**, 2948–2951; (b) Grigg, R., Mitchell, T.R.B., Sutthivaiyakit, S. and Tongpenyai, N. (1981) *Tetrahedron Letters*, **22**, 4107–4110; (c) Motokura, K., Nishimura, D., Mori, K., Mizugaki, T., Ebitani, K. and Kaneda, K. (2004) *Journal of the American Chemical Society*, **126**, 5662–5663; (d) Löfberg, C., Grigg, R., Whittaker, M.A., Keep, A. and Derrick, A. (2006) *The Journal of Organic Chemistry*, **71**, 8023–8027; (e) Motokura, K., Fujita, N., Mori, K., Mizugaki, T., Ebitani, K., Jitsukawa, K. and Kaneda, K. (2006) *Chemistry - A European Journal*, **12**, 8228–8239.

84 (a) Löfberg, C., Grigg, R., Keep, A., Derrick, A., Sridharan, V. and Kilner, C. (2006) *Chemical Communications*, 5000–5002; (b) Slatford, P.A., Whittlesey, M.K. and Williams, J.M.J. (2006) *Tetrahedron Letters*, **47**, 6787–6789.

85 (a) Edwards, M.G. and Williams, J.M.J. (2002) *Angewandte Chemie – International Edition*, **41**, 4740–4743; (b) Edwards, M.G., Jazzar, R.F.R., Paine, B.M., Shermer, D.J., Whittlesey, M.K., Williams, J.M.J. and Edney, D.D. (2004) *Chemical Communications*, 90–91; (c) Black, P.J., Cami-Kobeci, G., Edwards, M.G., Slatford, P.A., Whittlesey, M.K. and Williams, J.M.J. (2006) *Organic and Biomolecular Chemistry*, **4**, 116–125; (d) Black, P.J., Edwards, M.G. and Williams, J.M.J. (2006) *European Journal of Organic Chemistry*, 4367–4378.

86 Bower, J.F., Skucas, E., Patman, R.L. and Krische, M.J. (2007) *Journal of the American Chemical Society*, **129**, 15134–15135.

87 Bower, J.F., Patman, R.L. and Krische, M.J. (2008) *Organic Letters*, **10**, 1033–1035.

88 Shibahara, F., Bower, J.F. and Krische, M.J. (2008) *Journal of the American Chemical Society*, **130**, 6338–6339.

89 For selected reviews on stereoselective aldol additions, see: (a) Heathcock, C.H. (1981) *Science*, **214**, 395–400; (b) Heathcock, C.H. (1982) *ACS Symposium Series*, **185**, 55–72; (c) Evans, D.A., Nelson, J.V. and Taber, T.R. (1982) *Topics in Stereochemistry*, **13**, 1–115; (d) Machajewski, T.D. and Wong, C.-H. (2000) *Angewandte Chemie – International Edition*, **39**, 1352–1374; (e) Palomo, C., Oiarbide, M. and García, J.M. (2004) *Chemical Society Reviews*, **33**, 65–75.

90 (a) von Richter, V. (1869) *Berichte der Deutschen Chemischen Gesellschaft*, **2**, 552–554; (b) Würtz, A. (1872) *Bulletin de la Societe Chimique de France*, **17**, 436–442; (c) Borodin, A. (1873), *Berichte der Deutschen Chemischen Gesellschaft*, **6**, 982–985; see also Kane, R. (1838) *Ann. Phys. Chem., Ser. 2* **44**, 475.

91 For a recent review on the use of metallic catalysts for direct enantioselective aldol additions, see: Shibasaki, M., Matsunaga, S. and Kumagai, N. (2004) in *Modern Aldol Reactions*, Vol. 2 (ed. R. Mahrwald), Wiley-VCH Verlag GmbH, Weinheim, pp. 197–227.

92 For recent reviews on the use of organic catalysts for direct enantioselective aldol addition, see: (a) List, B. (2004) in *Modern Aldol Reactions, Vol. 1* (ed. R. Mahrwald), Wiley-VCH Verlag GmbH, Weinheim, pp. 161–200. (b) Notz, W., Tanaka, F. and Barbas, C.F., III, (2004) *Accounts of Chemical Research*, **37**, 580–591.

93 Sakthivel, K., Notz, W., Bui, T. and Barbas, C.F., III (2001) *Journal of the American Chemical Society*, **123**, 5260–5267.

94 Tang, Z., Yang, Z.-H., Chen, X.-H., Cun, L.-F., Mi, A.-Q., Jiang, Y.-Z. and Gong, L.-Z. (2005) *Journal of the American Chemical Society*, **127**, 9285–9289.

95 Yoshikawa, N., Yamada, Y.M.A., Das, J., Sasai, H. and Shibasaki, M. (1999) *Journal of the American Chemical Society*, **121**, 4168–4178.

96 (a) House, H.O., Czuba, L.J., Gall, M. and Olmstead, H.D. (1969) *The Journal of Organic Chemistry*, **34**, 2324–2336; (b) Kraft, M.E. and Holton, R.A. (1983) *Tetrahedron Letters*, **24**, 1345–1348.

97 For a review, see: Velluz, L., Valls, J. and Nominé, G. (1965) *Angewandte Chemie – International Edition*, **4**, 181–200.

98 (a) Corey, E.J. and Sneen, R.A. (1955) *Journal of the American Chemical Society*, **77**, 2505–2509; (1955) (b) Berkoz, B., Chavez, E.P. and Djerassi, C. (1962) *Journal of the Chemical Society*, 1323–1329; (c) Mazur, Y. and Sondheimer, F. (1958) *Journal of the American Chemical Society*, **80**, 6296–6299.

99 (a) Stork, G., Rosen, P. and Goldman, N.L. (1961) *Journal of the American Chemical Society*, **83**, 2965–2966; (b) Stork, G., Rosen, P., Goldman, N., Coombs, R.V. and Tsuji, J. (1965) *Journal of the American Chemical Society*, **87**, 275–286.

100 For recent reviews on the reductive aldol reaction, see: (a) Nishiyama, H. and Shiomi, T. (2007) *Topics in Current Chemistry*, **279**, 105–137; (b) Garner, S., Han, S.B. and Krische, M.J. (2007) in *Modern Reductions* (eds P. Andersson and I. Munslow), Wiley-VCH Verlag GmbH, Weinheim, in press.

101 For rhodium-catalyzed reductive aldol reactions mediated by silane, see: (a) Revis, A. and Hilty, T.K. (1987) *Tetrahedron Letters*, **28**, 4809–4812; (b) Matsuda, I., Takahashi, K. and Sato, S. (1990) *Tetrahedron Letters*, **31**, 5331–5334; (c) Taylor, S.J. and Morken, J.P. (1999) *Journal of the American Chemical Society*, **121**, 12202–12203; (d) Taylor, S.J., Duffey, M.O. and Morken, J.P. (2000) *Journal of the American Chemical Society*, **122**, 4528–4529; (e) Zhao, C.-X., Bass, J. and Morken, J.P. (2001) *Organic Letters*, **3**, 2839–2842; (f) Emiabata-Smith, D., McKillop, A., Mills, C., Motherwell, W.B. and Whitehead, A.J. (2001) *Synlett*, 1302–1304; (g) Freiría, M., Whitehead, A.J., Tocher, D.A. and Motherwell, W.B. (2004) *Tetrahedron*, **60**, 2673–2692; (h) Nishiyama, H., Shiomi, T., Tsuchiya, Y. and Matsuda, I. (2005) *Journal of the American Chemical Society*, **127**, 6972–6973; (i) Willis, M.C. and Woodward, R.L. (2005) *Journal of the American Chemical Society*, **127**, 18012–18013; (j) Fuller, N.O. and Morken, J.P. (2005) *Synlett*, 1459–1461; (k) Ito, J.i., Shiomi, T. and Nishiyama, H. (2006) *Advanced Synthesis and Catalysis*, **348**, 1235–1240; (l) Shiomi, T., Ito, J.-i., Yamamoto, Y. and Nishiyama, H. (2006) *European Journal of Organic Chemistry*, 5594–5600; (m) Shiomi, T. and

Nishiyama, H. (2007) *Organic Letters*, **9**, 1651–1654.

102 For cobalt-catalyzed reductive aldol reactions, see: (a) Isayama, S. and Mukaiyama, T. (1989) *Chemistry of Materials*, 2005–2008; (b) Baik, T.G., Luis, A.L., Wang, L.C. and Krische, M.J. (2001) *Journal of the American Chemical Society*, **123**, 5112–5113; (c) Wang, L.C., Jang, H.-Y., Roh, Y., Lynch, V., Schultz, A.J., Wang, X. and Krische, M.J. (2002) *Journal of the American Chemical Society*, **124**, 9448–9453; (d) Lam, H.W., Joensuu, P.M., Murray, G.J., Fordyce, E.A.F., Prieto, O. and Luebbers, T. (2006) *Organic Letters*, **8**, 3729–3732; (e) Lumby, R.J.R., Joensuu, P.M. and Lam, H.W. (2007) *Organic Letters*, **9**, 4367–4370.

103 For iridium-catalyzed reductive aldol reaction, see: Zhao, C.X., Duffey, M.O., Taylor, S.J. and Morken, J.P. (2001) *Organic Letters*, **3**, 1829–1831.

104 For ruthenium-catalyzed reductive aldol reaction, see: Doi, T., Fukuyama, T., Minamino, S. and Ryu, I. (2006) *Synlett*, 3013–3016.

105 For palladium-catalyzed reductive aldol reaction, see: Kiyooka, S.i., Shimizu, A. and Torii, S. (1998) *Tetrahedron Letters*, **39**, 5237–5238.

106 For copper-promoted reductive aldol reaction, see: (a) Chiu, P., Chen, B. and Cheng, K.F. (1998) *Tetrahedron Letters*, **39**, 9229–9232; (b) Chiu, P. (2004) *Synthesis*, **13**, 2210–2215. For copper-promoted reductive intramolecular Henry reaction, see: (c) Chung, W.K. and Chiu, P. (2005) *Synlett*, 55–58. For copper-promoted and -catalyzed reductive cyclizations of α, β-acetylenic ketones tethered to ketones, see: (d) Chiu, P. and Leung, S.K. (2004) *Chemical Communications*, 2308–2309.

107 For copper-catalyzed reductive aldol reaction, see: (a) Ooi, T., Doda, K., Sakai, D. and Maruoka, K. (1999) *Tetrahedron Letters*, **40**, 2133–2136; (b) Lam, H.W. and Joensuu, P.M.A. (2005) *Organic Letters*, **7**, 4225–4228; (c) Lam, H.W., Murray, G.J. and Firth, J.D. (2005) *Organic Letters*, **7**, 5743–5746; (d) Deschamp, J., Chuzel, O., Hannedouche, J. and Riant, O. (2006) *Angewandte Chemie – International Edition*, **45**, 1292–1297; (e) Chuzel, O., Deschamp, J., Chauster, C. and Riant, O. (2006) *Organic Letters*, **8**, 5943–5946; (f) Zhao, D., Oisaki, K., Kanai, M. and Shibasaki, M. (2006) *Tetrahedron Letters*, **47**, 1403–1407; (g) Zhao, D., Oisaki, K., Kanai, M. and Shibasaki, M. (2006) *Journal of the American Chemical Society*, **128**, 14440–14441; (h) Welle, A., Diez-González, S., Tinant, B., Nolan, S.P. and Riant, O. (2006) *Organic Letters*, **8**, 6059–6062.

108 For nickel-catalyzed reductive aldol reaction, see: Chrovian, C.C. and Montgomery, J. (2007) *Organic Letters*, **9**, 537–540.

109 For a reductive aldol coupling employing stoichiometric quantities of indium reagent, see: Inoue, K., Ishida, T., Shibata, I. and Baba, A. (2002) *Advanced Synthesis and Catalysis*, **344**, 283–287.

110 For indium-catalyzed reductive aldol reaction, see: (a) Shibata, I., Kato, H., Ishida, T., Yasuda, M. and Baba, A. (2004) *Angewandte Chemie – International Edition*, **43**, 711–714; (b) Miura, K., Yamada, Y., Tomita, M. and Hosomi, A. (2004) *Synlett*, 1985–1989.

111 For rhodium-catalyzed reductive aldol reactions mediated by hydrogen, see: (a) Jang, H.Y., Huddleston, R.R. and Krische, M.J. (2002) *Journal of the American Chemical Society*, **124**, 15156–15157; (b) Huddleston, R.R. and Krische, M.J. (2003) *Organic Letters*, **5**, 1143–1146; (c) Koech, P.K. and Krische, M.J. (2004) *Organic Letters*, **6**, 691–694; (d) Marriner, G.A., Garner, S.A., Jang, H.Y. and Krische, M.J. (2004) *The Journal of Organic Chemistry*, **69**, 1380–1382; (e) Jung, C.K., Garner, S.A. and Krische, M.J. (2006) *Organic Letters*, **8**, 519–522; (f) Han, S.B. and Krische, M.J. (2006) *Organic Letters*, **8**, 5657–5660; (g) Jung,

C.K. and Krische, M.J. (2006) *Journal of the American Chemical Society*, **128**, 17051–17056; (h) Bee, C., Iida, H., Han, S.B., Hassan, A. and Krische, M.J. (2008) *Journal of the American Chemical Society*, **130**, 2746–2747.

112 Zimmerman, H.E. and Traxler, M.D. (1957) *Journal of the American Chemical Society*, **79**, 1920–1923.

113 (a) Schrock, R.R. and Osborn, J.A. (1976) *Journal of the American Chemical Society*, **98**, 2134–2143; (b) Schrock, R.R. and Osborn, J.A. (1976) *Journal of the American Chemical Society*, **98**, 2143–2147; (c) Schrock, R.R. and Osborn, J.A. (1976) *Journal of the American Chemical Society*, **98**, 4450–4455.

114 (a) For reviews on the heterolytic activation of elemental hydrogen, see: Brothers, P.J. (1981) *Progress in Inorganic Chemistry*, **28**, 1–61. (b) See also, Jeske, G., Lauke, H., Mauermann, H., Schumann, H. and Marks, T.J. (1985) *Journal of the American Chemical Society*, **107**, 8111–8118.

115 For a review of the acidity of metal hydrides, see: Kristjansdottir, S.S. and Norton, J.R. (1992) in *Transition Metal Hydrides* (ed. A. Dedieu), VCH, New York, pp. 309–359.

116 Yachi, K., Shinokubo, H. and Oshima, K. (1999) *Journal of the American Chemical Society*, **121**, 9465–9466.

117 Arnett, E.M., Fisher, F.J., Nichols, M.A. and Ribeiro, A.A. (1989) *Journal of the American Chemical Society*, **111**, 748–749.

118 (a) Noyori, R., Nishida, I., Sakata, J. and Nishizawa, M. (1980) *Journal of the American Chemical Society*, **102**, 1223–1225; (b) Noyori, R., Nishida, I. and Sakata, J. (1981) *Journal of the American Chemical Society*, **103**, 2106–2108; (c) Noyori, R., Nishida, I. and Sakata, J. (1983) *Journal of the American Chemical Society*, **105**, 1598–1608.

119 For tri-2-furylphosphine and triphenylarsine effects in metal-catalyzed reactions, see: (a) Farina, V. and Krishnan, B. (1991) *Journal of the American Chemical Society*, **113**, 9585–9595; (b) Farina, V. (1996) *Pure and Applied Chemistry*, **68**, 73–78; (c) Anderson, N.G. and Keay, B.A. (2001) *Chemical Reviews*, **101**, 997–1030.

120 Evans, D.A., Nelson, J.V. and Taber, T.R. (1982) *Topics in Stereochemistry*, **13**, 1–115.

121 Muraoka, T., Kamiya, S.-i., Matsuda, I. and Itoh, K. (2002) *Chemical Communications*, 1284–1285.

122 Townes, J.A., Evans, M.A., Queffelec, J., Taylor, S.J. and Morken, J.P. (2002) *Organic Letters*, **4**, 2537–2540.

123 For secondary amine-catalyzed reductive Mannich coupling of enal to imines mediated by Hantzsch ester, see: Zhao, G.-L. and Córdova, A. (2006) *Tetrahedron Letters*, **47**, 7417–7421.

124 Garner, S.A. and Krische, M.J. (2007) *The Journal of Organic Chemistry*, **72**, 5843–5846.

125 For palladium-catalyzed couplings of *C*-nucleophiles to anhydrides, see: (a) Gooßen, L.J. and Ghosh, K. (2001) *Angewandte Chemie – International Edition*, **40**, 3458–3460; (b) Kakino, R., Yasumi, S., Shimizu, I. and Yamamoto, A. (2002) *Bulletin of the Chemical Society of Japan*, **75**, 137–148; (c) Gooßen, L.J. and Ghosh, K. (2002) *European Journal of Organic Chemistry*, 3254–3267; (d) Gooßen, L.J., Winkel, L., Döhring, A., Ghosh, K. and Paetzold, J. (2002) *Synlett*, 1237–1240; (e) Wang, D. and Zhang, Z. (2003) *Organic Letters*, **5**, 4645–4648; (f) Bercot, E.A. and Rovis, T. (2004) *Journal of the American Chemical Society*, **126**, 10248–10249.

126 For rhodium-catalyzed couplings of *C*-nucleophiles to anhydrides, see: (a) Frost, C.G. and Wadsworth, K.J. (2001) *Chemical Communications*, 2316–2317; (b) Johnson, J.B., Bercot, E.A., Williams, C.M. and Rovis, T. (2007) *Angewandte Chemie – International Edition*, **46**, 4514–4518; (c) Cook, M.J. and Rovis, T. (2007) *Journal of*

the American Chemical Society, **129**, 9302–9303.

127 For nickel-catalyzed couplings of *C*-nucleophiles to anhydrides, see: (a) Bercot, E.A. and Rovis, T. (2002) *Journal of the American Chemical Society*, **124**, 174–175; (b) Zhang, Y. and Rovis, T. (2004) *Journal of the American Chemical Society*, **126**, 15964–15965; (c) Bercot, E.A. and Rovis, T. (2005) *Journal of the American Chemical Society*, **127**, 247–254; (d) Johnson, J.B., Yu, R.T., Fink, P., Bercot, E.A. and Rovis, T. (2006) *Organic Letters*, **8**, 4307–4310; (e) Johnson, J.B., Bercot, E.A., Rowley, J.M., Coates, G.W. and Rovis, T. (2007) *Journal of the American Chemical Society*, **129**, 2718–2725.

128 Cacchi, S., Fabrizi, G., Gavazza, F. and Goggiamani, A. (2003) *Organic Letters*, **5**, 289–291.

129 For reviews of rhodium-catalyzed hydroacylation involving aldehyde donors, see: (a) Bosnich, B. (1998) *Accounts of Chemical Research*, **31**, 667–674; (b) Tanaka, M., Sakai, K. and Suemune, H. (2003) *Current Organic Chemistry*, **7**, 353–367;(c) Fu, G.C. (2005) in *Modern Rhodium-catalyzed Organic Reactions* (ed. P.A. Evans), Wiley-VCH, Weinheim, pp. 79–91; (d) Jun, C.-H., Jo, E.A. and Park, J.-W. (2007) *European Journal of Organic Chemistry*, 1869–1881.

130 For rhodium-catalyzed decarbonylation of aldehydes, see: (a) Doughty, D.H. and Pignolet, L.H. (1978) *Journal of the American Chemical Society*, **100**, 7083–7085; (b) O'Connor, J.M. and Ma, J. (1992) *The Journal of Organic Chemistry*, **57**, 5075–5077; (c) Beck, C.M., Rathmill, S.E., Park, Y.J., Chen, J. Crabtree, R.H., Liable-Sands, L.M. and Rheingold, A.L. (1999) *Organometallics*, **18**, 5311–5317.

131 (a) Vora, K.P., Lochow, C.F. and Miller, R.G. (1980) *Journal of Organometallic Chemistry*, **192**, 257–264; (b) Rode, E., Davis, M.E. and Hanson, B.E. (1985) *Journal of the Chemical Society. Chemical Communications*, 716–717; (c) Marder, T.B., Roe, D.C. and Milstein, D. (1988) *Organometallics*, **7**, 1451–1453; (d) Jun, C.-H., Lee, H. and Hong, J.-B. (1997) *The Journal of Organic Chemistry*, **62**, 1200–1201; (e) Jun, C.-H., Lee, D.-Y., Lee, H. and Hong, J.-B. (2000) *Angewandte Chemie – International Edition*, **39**, 3070–3072; (f) Jun, C.-H., Chung, J.-W., Lee, D.-Y., Loupy, A. and Chatti, S. (2001) *Tetrahedron Letters*, **42**, 4803–4805; (g) Willis, M.C. and Sapmaz, S. (2001) *Chemical Communications*, 2558–2559; (h) Tanaka, M., Imai, M., Yamamoto, Y., Tanaka, K., Shimowatari, M., Nagumo, S., Kawahara, N. and Suemune, H. (2003) *Organic Letters*, **5**, 1365–1367; (i) Imai, M., Tanaka, M., Tanaka, K., Yamamoto, Y., Imai-Ogata, N., Shimowatari, M., Nagumo, S., Kawahara, N. and Suemune, H. (2004) *The Journal of Organic Chemistry*, **69**, 1144–1150; (j) Willis, M.C., McNally, S.J. and Beswick, P.J. (2004) *Angewandte Chemie – International Edition*, **43**, 340–343; (k) Tanaka, K., Tanaka, M. and Suemune, H. (2005) *Tetrahedron Letters*, **46**, 6053–6056; (l) Willis, M.C., Randell-Sly, H.E., Woodward, R.L. and Currie, G.S. (2005) *Organic Letters*, **7**, 2249–2251.

132 (a) Isnard, P., Denise, B., Sneeden, R.P.A., Cognion, J.M. and Durual, P. (1982) *Journal of Organometallic Chemistry*, **240**, 285–288; (b) Isnard, P., Denise, B., Sneeden, R.P.A., Cognion, J.M. and Durual, P. (1983) *Journal of Organometallic Chemistry*, **256**, 135–139; (c) Kondo, T., Tsuji, Y. and Watanabe, Y. (1987) *Tetrahedron Letters*, **28**, 6229–6230; (d) Kondo, T., Akazome, M., Tsuji, Y. and Watanabe, Y. (1990) *The Journal of Organic Chemistry*, **55**, 1286–1291; (e) Kondo, T., Hiraishi, N., Morisaki, Y., Wada, K., Watanabe, Y. and Mitsudo, T.-a. (1998) *Organometallics*, **17**, 2131–2134.

133 (a) Lenges, C.P. and Brookhart, M. (1997) *Journal of the American Chemical Society*, **119**, 3165–3166; (b) Lenges, C.P., White,

P.S. and Brookhart, M. (1998) *Journal of the American Chemical Society*, **120**, 6965–6979.

134 Tanaka, K., Shibata, Y., Suda, T., Hagiwara, Y. and Hirano, M. (2007) *Organic Letters*, **9**, 1215–1218.

135 Hong, Y.-T., Barchuk, A. and Krische, M.J. (2006) *Angewandte Chemie – International Edition*, **45**, 6885–6888.

136 Miller, J.A. and Nelson, J.A. (1991) *Organometallics*, **10**, 2958–2961.

137 For a recent comprehensive review of metal-catalyzed reductive carbocyclization, see: Krische, M.J. and Jang, H.-Y. (2006) in *Comprehensive Organometallic Chemistry III, Vol. 10* (eds M. Mingoe and R. Crabtree), Elsevier, Oxford, pp. 493–536.

138 Jang, H.-Y. and Krische, M.J. (2004) *Journal of the American Chemical Society*, **126**, 7875–7880.

139 Jang, H.-Y., Hughes, F.W., Gong, H., Zhang, J., Brodbelt, J.S. and Krische, M.J. (2005) *Journal of the American Chemical Society*, **127**, 6174–6175.

140 For a review of metal-catalyzed cycloisomerization, see: Trost, B. and Krische, M.J. (1998) *Synlett*, 1–16.

141 Rhee, J.-U. and Krische, M.J. (2006) *Journal of the American Chemical Society*, **128**, 10674–10675.

9
Organocatalysis

Isabelle McCort-Tranchepain, Morgane Petit, and Peter I. Dalko

9.1
Introduction

Organocatalysis is a way of accelerating chemical reactions with a catalytic amount of an organic compound without the presence of a metal, metal salt or other metal derivatives. The development of organocatalytic methods of wide synthetic scope is of real scientific, economic and environmental interest [1–3]. Organocatalytic reactions can be performed usually under (very) simple experimental conditions, under an aerobic atmosphere and in wet solvents; Catalysts are inexpensive and also they are more stable than metal-based or bioorganic analogs; recovery is simpler than with metal-based or bioorganic catalysts; they can be anchored to a solid support and reused; and there are fewer toxicity and environmental problems associated than with metal catalysts (this only applies when dealing with the more notorious metals; it should be pointed out that little is known about the toxicity of many of the organic catalysts).

Despite the steadily growing number of catalysts and more and more selective transformations that are appearing, applications to more complex systems in multistep synthesis seem to be following these spectacular advances reluctantly. Are organocatalytic systems suitable for a broad range of transformations with high levels of reliability and generality? Organocatalytic reactions are often characterized by narrow substrate scope and low reactivity. An often encountered difficulty also arises from the almost complete lack of a mechanism-based predictive power of the underlying mechanistic pathway compared with most metal-mediated reactions. As an example, the variation of the enantioselectivity in the venerable Hajos–Wiecher reaction, using L-proline and L-homoproline [(pyrrolidin-2-yl)acetic acid], can be cited (Scheme 9.1). While the fact is well precedented from the early days of proline catalysis, this puzzling observation has not responded to rationalization attempts in the literature until very recently [4, 5].

This chapter attempts to highlight asymmetric organocatalytic transformations of general synthetic scope illustrating the generality of the transformation in multistep synthesis [6]. The selection that will treat additions to C=O, C=N and C=C bonds and also discusses domino and cascade reactions is not intended to be exhaustive as it is limited by space restrictions: more specialized reviews may complete the reading.

Green Catalysis, Volume 1: Homogeneous Catalysis.
Edited by Robert H. Crabtree

ISBN: 978-3-527-32496-5

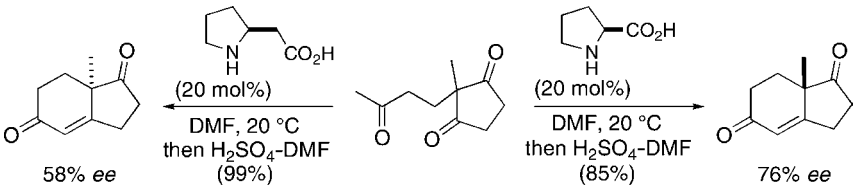

Scheme 9.1 The Hajos–Wiecher reaction, using L-proline and L-homoproline ((pyrrolidin-2-yl)acetic acid).

9.2 Catalysts

Most currently used efficient organocatalyst are bi- or multifunctional catalysts, commonly having Brønsted acid and Lewis base centers. Hence their structures incorporate known hydrogen bond donor motifs such as thiourea, 2,2′-dihydroxy-1,1′-binaphthyl (BINOL) or phosphoric acid and different nucleophile-activating groups. According to the common organocatalytic concept, these functions may be able to activate one or both of the reagents in the same transition state (TS). Such cooperative activation gives rise to well-organized TSs and results in a considerable rate acceleration. Interactions between the catalyst and the substrates are assured by passive and/or dynamic binding and also via hydrogen bonding. The passive binding includes hydrophobic, van der Waals and electrostatic interactions whereas dynamic binding refers to interactions between catalyst and substrate at the reaction center. Hydrogen bond interactions constitute a major driving force in the formation of specific molecular and complex geometries. Thus, protein and nucleic acid secondary and tertiary structural elements and also many natural and artificial host–guest complexes are partly based on the directive power of intra- and intermolecular hydrogen bond formation.

The molecular events in organocatalytic reactions can be remarkably complex, as has been demonstrated in a very limited number of mechanistic studies [5, 7, 14]. Structural variations of any of the reacting partners may fine tune interconnecting mechanistic pathways that are dependent on the plethora of experimental parameters and, not least, on whether the reactions are run under homogeneous or heterogeneous conditions.

9.2.1 Catalyst Functions

9.2.1.1 **Brønsted Acids** [8]

Proton is the most abundant Lewis acid existing in Nature. In solutions, there are countless variations in hydrogen bond strengths and geometric orientations and they may change even within the same bond partners. Formation of a hydrogen bond to the electrophile (typically a carbonyl or imine) occurs through either a one-point or two-point interaction. Some of the principal modes of coordination are depicted in

Scheme 9.2: (a) single H bond; (b) single H-bond assisted by an intramolecular H-bonding increasing Brønsted acidity of the hydroxyl proton which coordinates to the electrophile; (c) double H-bond, with one (c-1) or two (c-2, c-3) heteroatoms. The bonding results in lowering of the LUMO energy of the electrophile, increasing the electrophilicity, thereby making it more reactive to the second reactant, such as a nucleophile or a diene.

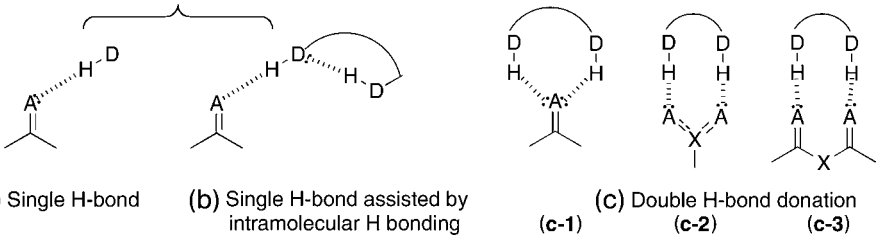

Scheme 9.2 Different modes of activation by H-bonding.

Mild *and* moderately strong Brønsted acid catalysts having single or multiple H-donor ability have been extensively tested for organocatalytic reactions. Among the protic functions, carboxylic and phosphoric acids, tertiary alcohols, phenols, activated amides including thioureas and sulfonamides were developed. Protonated tertiary amines are also efficient H donors. The match between the Brønsted acidity of the catalyst and the substrate is a determinant factor both in the selectivity and in the reactivity of the system.

In hydrogen bonding activation, the solvent participates directly or indirectly in the structure of the TS complex and thus influences substantially the enantioselectivity. Non-polar solvents avoid hydrogen bond competition with the electrophile that could be formed in polar or protic solvents.

Proton can be provided not only by the catalyst but also by achiral protic additives such as water or other Brønsted acid co-catalysts used generally in stoichiometric amounts with respect to the catalyst. Beyond the fact that electrophilic assistance may activate the reagent(s) by LUMO lowering and also help to organize the TS via extensive H-bonding, the protic additive may play further key roles, e.g. (i) it increases the ligand instability of covalently bonded catalysts, resulting in overall rate acceleration and in increased conversion; (ii) it allows efficient asymmetric proton transfer to the substrate; (iii) it avoids base-catalyzed undesired secondary reactions; and (iv) it avoids catalyst deactivation by hydrolyzing inactive dead-end complexes. Although reaction conditions compatible with water as solvent were devised [9], the presence of large amounts of water and in particular water as solvent usually results in a lower reaction rate or complete suppression of the reactivity of the catalyst.

9.2.1.2 **Lewis acids**

Typical Lewis acid (LA) functions can be emulated by covalently linked functions such as iminium (see below) or by forming donor–acceptor complexes with metalloids such as boron and silicon derivatives. Iminium activation is chemically equivalent to the electrophile activation of the parent carbonyl compound resulting in LUMO

lowering. Also, among the typical Lewis acids, chiral oxazaborolidines and hypervalent boron and silica derivatives have found wide application in enantioselective organocatalytic transformations.

9.2.1.3 **Brønsted Bases**

Asymmetric organocatalytic reactions can be mediated by general-base catalysts, provided that experimental conditions for the formation of a tight ion pair between the achiral anion (substrate) and the chiral cation can be found. The most frequently used organic bases are chiral quinuclidines derived from cinchona alkaloids. General-base-mediated reactions can be conduced under homogeneous conditions or under phase-transfer (PT) conditions.

9.2.1.4 **Lewis Bases**

As metals form Lewis acids easily, non-metallic elements are more prone to form Lewis bases. Among the various organic Lewis bases, the most common are amines, but also P-, O- and, less frequently, S-compounds that proceed through diverse mechanisms to convert the substrates in either activated nucleophiles or electrophiles. Nucleophilic carbenes (NHC) are a recent addition to the synthetic arsenal and represent a dynamic area of current research [10]. The reactive intermediate species involved in catalysis are typically enamines/imines, ammonium enolates, acylammonium ions, carbenes and ylides.

Amine catalysts, due to their natural abundance, are more readily available than phosphorus catalysts. There is no natural P-containing chiral substrate for catalytic use. The particular advantage of phosphorus-based catalysts is their ability to act as both a nucleophilic *and* a stereogenic reaction center. Furthermore, the diminished Brønsted basicity of the phosphorus atom compared with the amine function may be advantageous in avoiding base-mediated secondary reactions.

9.2.2
Catalyst Structures

The great majority of organic catalyst are derived either from 'privileged' catalyst structures (privileged catalysts may promote high enantioselectivity in mechanistically distinct reactions) or are assembled by sequential manner from chiral organic building blocks such as peptides, peptide analogs or more recently nucleotides as well as other accessible chiral organic units.

9.2.2.1 **Privileged Catalysts**

The Pyrrolidine Class [11–13)

L-Proline (**1**) (Scheme 9.3) is probably the best known organocatalyst that mediates essentially enamine- or iminium-type asymmetric reactions: many of the derivatives have also proven to be very useful catalysts [15]. The high, often exceptional, enantioselectivity of proline-mediated reactions has been subject to considerable mechanistic interest [5, 14], and will be discussed briefly later. Although proline

continues to play a central role in aminocatalysis, synthetic analogs may offer better reactivity and selectivity in a number of reactions [15]. In particular, diarylprolinol ether derivatives **2–4** emerged as potentially general enamine/iminium organocatalysts [16]. The parent alcohol **2** that was developed earlier as a chiral ligand, although generally inefficient in organocatalytic reactions, trimethylsilyl (TMS) ethers **3** and methyl ether **4** derivatives were seen as generally more efficient [17].

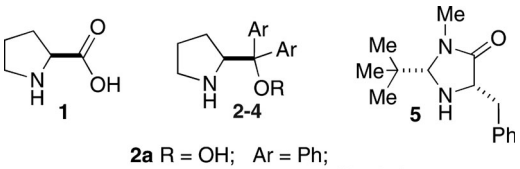

2a R = OH; Ar = Ph;
2b R = OH; Ar = 3,5-$(CF_3)_2C_6H_3$;
3a R = TMS, Ar = Ph;
3b R = TMS, Ar = 3,5-$(CF_3)_2C_6H_3$;
4 R = Me; Ar = Ph.

Scheme 9.3 L-Proline, diarylprolinol and imidazolidinone derivatives as organic catalysts.

The pyrrolidine ring can be replaced advantageously in a number of transformations by other five-membered nitrogen-containing chiral saturated heterocycles. The structurally related MacMillan's imidazolidinone catalysts are highly selective in a number of enamine- or iminium-type transformations: salts of **5** was identified as one the most reactive and versatile amine catalysts, acting preferentially via iminium formation [18].

Amino Catalysis with Pyrrolidine Derivatives [19]

The condensation of amine catalysts with ketones or aldehydes gives rise to enamines and/or iminium intermediates. The former structure results in increased electron density at the reaction center(s); the latter corresponds to a decreased electron density of the reaction center(s) (Scheme 9.4). A feature of this type of chemistry is the facile

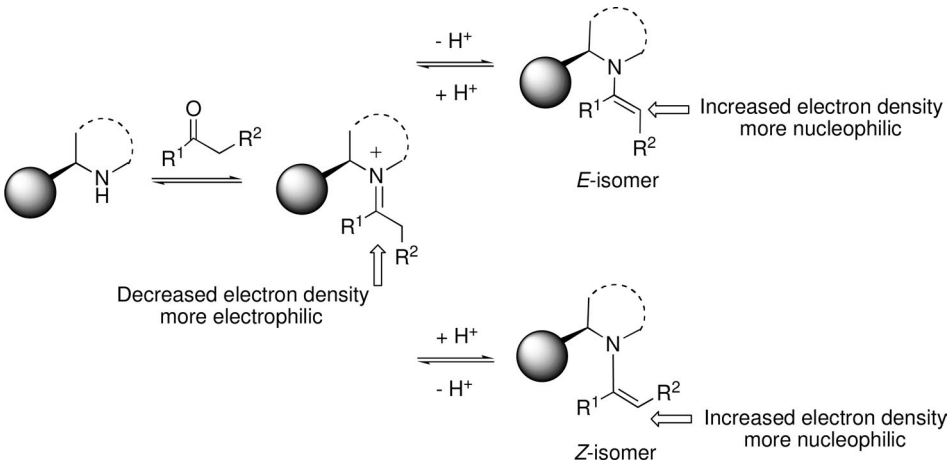

Scheme 9.4 The interconversion of the *Z*/*E* geometry of enamines.

equilibrium between these two, electron-rich and electron-deficient, states (i.e. the acid–base form) of the same center. Like protonation–deprotonation, this may activate the reagent and contribute to the kinetic lability of the ligand. The notable feature of this activation is the fact, that due to this equilibrium process, the same center may act as a Lewis acid or a Lewis base, depending on the reaction conditions. More importantly, the same catalyst may promote the complementary nucleophile–electrophile activation (i.e. promoting reactions via enamine and iminium intermediates, respectively) in the same reaction pot in a domino sequence [20].

Catalysis by Enamine Formation

The partial steps of the aminocatalytic reactions are in dynamic equilibrium, hence products are formed under thermodynamic control. This is also reflected in the geometry of the enamine intermediates, which can be either *E* or *Z* (Scheme 9.4), leading to the product. The geometry of the enamine depends essentially on the catalyst structure and to a lesser extent on the substrate. Whereas proline-catalyzed reactions with α-alkyl-substituted ketones preferentially form the *E*-isomer, enamines derived from pipecolic acid afford an approximately 1 : 1 mixture of *E*- and *Z*-isomers [21].

Noteworthily, the relative stability and the reactivity of the rotamers such as **A** and **B** (Scheme 9.5) have a determinant role in the facial selectivity of the addition.

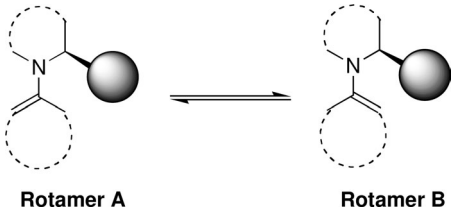

Scheme 9.5 Enamine rotamers as factors in stereocontrol of catalysts.

Finally, the acceptor (electrophile) may approach the enamine by two different routes, as depicted in Scheme 9.6. Stabilizing interactions such as hydrogen bonding

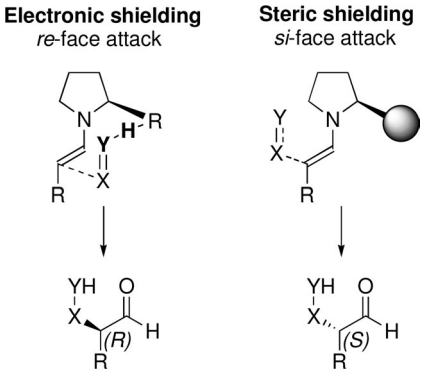

Scheme 9.6 The guiding and shielding TSs.

or electrostatic interactions between the catalyst and the alkene may offset repulsive (steric) interactions. In the latter (shielding) scenario, it is considered that the acceptor approaches the enamine via an acyclic synclinal TS, as suggested by Seebach and Golinski [22].

Catalysis via Iminium Activation

A great number of secondary amine catalysts provide rate acceleration via iminium formation. In the case of the imidazoline catalyst **5**, according to the computational model, the π-facial differentiation of enamine–iminium intermediates can be rationalized by the concerted shielding of the *re* face of the benzyl and *tert*-butyl groups. The selective formation of the (*E*)-iminium isomer in the TS, and also the preferred *E* geometry of the enamine, can be attributed to the minimized non-bonding interactions with the bulky *tert*-butyl group (Scheme 9.7).

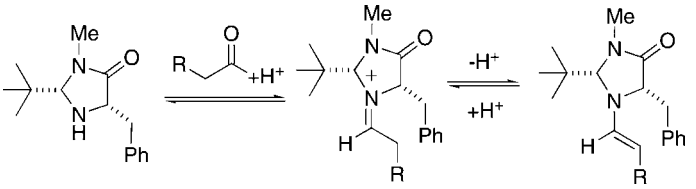

Scheme 9.7

The analysis of these simplified conditions reveals that in aminocatalytic reactions there are a number of viable alternative reaction paths leading to different TSs and rendering possible the formation of a number regio- and stereoisomers. It is astonishing and difficult to understand thus the often very high regio- and stereoselectivity of many of the pyrrolidine-class mediated reactions.

Cinchona Alkaloids [23]

The readily available and inexpensive cinchona alkaloids having pseudoenantiomeric forms, such as quinine and quinidine or cinchonine and cinchonidine, are among the most efficient catalysts (Scheme 9.8). The range of reaction types over which the cinchona alkaloids impart high enantioselectivity is astonishing. The key structural feature responsible for their synthetic utility is the presence of the tertiary quinuclidine nitrogen, which complements the proximal polar hydroxyl function of the natural compound that may be easily transformed into a variety of chemical functions. The modification of the cinchona backbone resulted notoriously in the past in a decrease in or loss of selectivity and such derivatives were disregarded as catalysts. The major event that pushed cinchona alkaloids to the center of interest was the development of dimeric cinchona alkaloid ligands for asymmetric dihydroxylation of simple alkenes [24]. The presence of the Brønsted acidic (H-bonding) and Lewis basic (quinuclidine nitrogen) sites in the natural compounds makes them bifunctional catalysts.

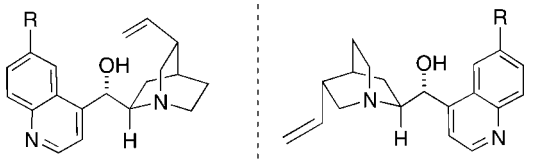

6: R = OMe, (+)-quinidine
7: R = H (+)-cinchonine
8: R = OMe, (–)-quinine
9: R = H (–)-cinchonidine

Scheme 9.8 Cinchona alkaloids.

Moreover, the Brønsted basicity of the quinuclidine moiety makes cinchona alkaloids one of the strongest organic bases. Deprotonation of relatively acidic substrates forming a chiral ion pair is an efficient way to promote asymmetric reactions (Scheme 9.9).

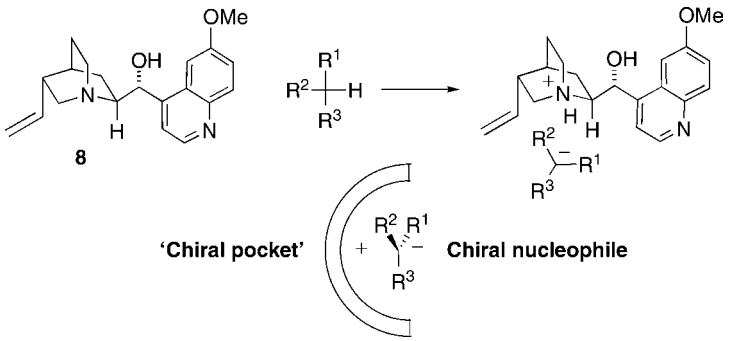

Scheme 9.9 Cinchona alkaloids allowing the formation of chiral ion pairs.

Noteworthily, the same principle operates in phase-transfer catalysis (PTC), where the chiral cinchonium forms tight ion pairs with one of the charged substrates, ensuring asymmetric induction [25].

Axially Chiral Diols and Diamines

TADDOL and Derivatives [26]

TADDOL (**10**) is one of the oldest and most extraordinarily versatile chiral auxiliary catalysts (Scheme 9.10). The design of TADDOL was driven by practical considerations, because it is derived from tartaric acid, the least expensive chiral starting material with two-fold symmetry available from natural sources. The genuine molecule has two conveniently oriented hydroxyl functions that can act as a double hydrogen bond donor catalyst and also gives a wide scope for further derivatizations.

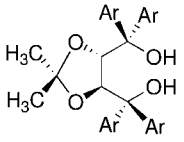

10a: Ar = Ph, TADDOL

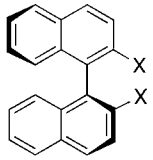

11: X = OH : BINOL
12: X = PPh_2 : BINAP

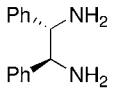

13

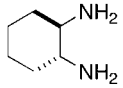

14

Scheme 9.10 Axially chiral catalysts.

Binaphthol Derivatives [27]
The enantiomeric atropoisomers of 1,1′-binaphthyl-2,2′-diol (**11**) (BINOL) and bis-diphenylphosphonate derivatives **12** (BINAP) are completely synthetic molecules developed to exploit the axial dissymmetry induced by the restricted rotation of the biaryl bond (Scheme 9.10). These compounds are among the most widely used ligands in catalytic asymmetric transformations. A great number of analogs and derivatives have been developed in the last decade.

Chiral C_2-Symmetric 1,2-Diamines [28]
Chiral vicinal diamines such as 1,2-diaminocyclohexane (**13**) and *threo*-diphenylethylenediamines (**14**) (Scheme 9.10) have proven valuable tools as ligands in asymmetric metal-mediated reactions and have found rich applications as building blocks for the construction of chiral organocatalysts.

9.2.2.2 **Synthetic Oligopeptides and Peptide Analogs** [29]
Synthetic oligopeptides and peptide analogs are highly modular catalyst platforms. While some oligopeptide sequences may be considered as 'privileged' catalyst structures, the main advantage of the 'oligopeptide approach' is that the catalyst can be improved by varying the nature of the amino acids using combinatorial synthetic methods. Combinatorial synthesis and screening have made it possible to test the large structural and functional diversity of peptides to select the best candidates. The flexibility of the method is of great use since it is possible to prepare a peptide sequence that can eventually produce the opposite enantiomer or its diastereoisomer, a hardly amenable process with enzymes. Moreover, this oligopeptide approach may provide a solution to the reactivity versus selectivity problem, in particular when the steric hindrance of the chiral appendage compromises the reactivity of the catalyst. The strategy consists of building a simplified version of a complex chiral environment around the catalytic site, in a similar way to enzymes, where the chiral handle is thus distant from the active site. Such artificial enzymes may comprise a short oligopeptide sequence including an active site (such as imidazole) and a basic secondary structure: α/β turn or α/β hairpin, for example.

It is interesting to contemplate that, with the spectacular increase in the molecular weight and complexity of many catalyst structures, not only the selectivity but also the kinetic profile of the catalyst is sharply ameliorated.

9.3 Reactions

9.3.1 Nucleophilic Additions to C=O

9.3.1.1 Aldol- and Knoevenagel-type Additions

Cross-aldol Reactions of Unmodified Aldehydes and Ketones [19]

Aminocatalytic aldol reactions have matured into synthetically useful tools in organic chemistry. Intermolecular cross-aldol reactions allowing the preparation of both *syn* and *anti* isomers have been developed for aromatic and aliphatic substrates.

The design of a cross-aldol reaction is far to be trivial. The success of the reaction relies on the difference in reactivity of the reagents with regard to the catalyst forming an enamine (donor) selectively and the acceptor (Scheme 9.11). Such a difference can be found between ketone and aldehyde reagents, enolizable and non-enolizable carbonyls, and alkyl and heteroatom-substituted alkyl (oxyketone) donors. In cross-aldol reactions, it is often required that the donor aldehyde be added slowly to the acceptor and catalyst or one of the reagents be used in large (5–10-fold) excess. Although this transformation has probably attracted the largest amount of synthetic and mechanistic interest in organocatalytic transformations, many facets of the reaction remains puzzling [5, 14].

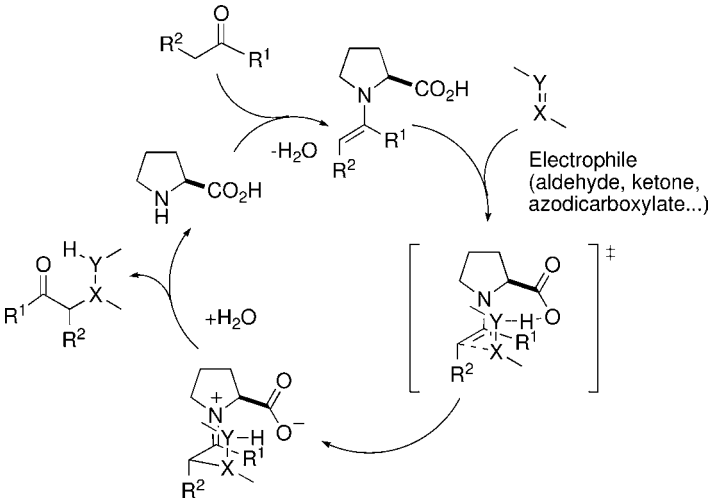

Scheme 9.11 The generalized enamine cycle

Using (*S*)-proline (**1**) as catalyst, the reaction proceeds preferentially via the (*E*)-enamine intermediate. The predominant structural factor that determines stereoselectivity is assumed to be the activation of the electrophilic reactant by an intramolecular H-bond between the proline COOH group and the carbonyl O-atom of an aldehyde in a nine-membered H-bonded ring. A second determinant is the s-*trans* arrangement of the enamine and carbonyl double bonds relative to the position of the COOH group. It is noteworthy that unsymmetrical ketones, in the simplest case 2-butanone, are reported to give regioselectively β-hydroxy ketones on the higher substituted α-C-atom (Scheme 9.12).

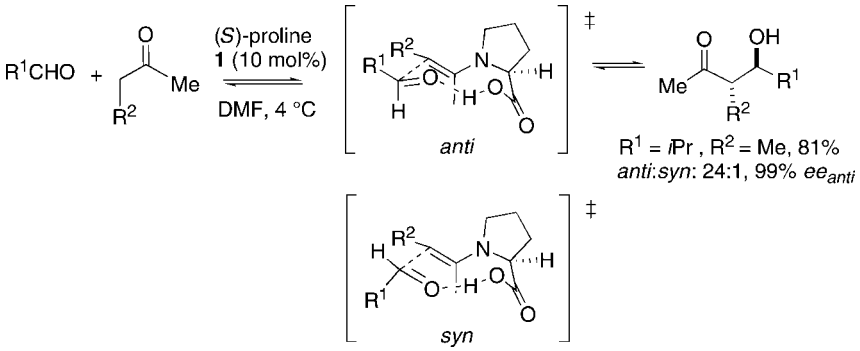

Scheme 9.12 Cross-aldol reaction of unmodified aldehydes and ketones.

The reaction affords satisfactory results for α-branched aliphatic aldehydes, whereas the enantiomeric excess (*ee*) decreases with aromatic aldehydes to the range 60–70%. The range of donors can be extended to butanone, 2-pentanone, cycloalkanones and α-hydroxy ketones, whereas simple ketones such as acetophenone and 3-pentanone are inert and acetaldehyde affords a mixture using proline as catalyst. This last transformation can be best mediated by diarylprolinol as catalyst (Scheme 9.13) [30].

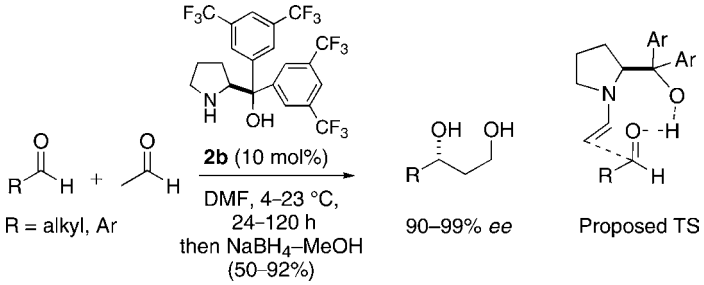

Scheme 9.13 Cross-aldol reaction of acetaldehydes with aldehyde acceptors.

An elegant application of the proline-mediated cross-aldol reaction is the synthesis of the tetrahydropyran fragment of callipeltoside C (Scheme 9.14) [31].

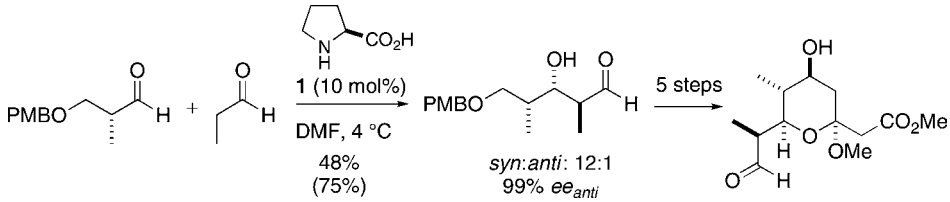

Scheme 9.14 Application of the cross-aldol reaction in the synthesis of the tetrahydropyran fragment of callipeltoside C.

Usually proline-mediated aldol reactions are tolerant to small amounts of tertiary amine bases. Weak acids or water as an *additive* were beneficial for the overall selectivity and efficiency of the transformation, whereas the reaction was inhibited by the presence of a strong acid [32].

Noteworthily, the usually long reaction time can be shortened by applying microwave irradiation without loss of selectivity [33]. Polymer-supported catalysts were also prepared and tested [11, 12, 34]. Poly(ethylene glycol)-supported proline derivatives [34] allowed the convenient reuse of the catalyst (10 runs).

Although proline derivatives dominate the organocatalytic field, primary amino acids [35], short oligopeptide catalysts and axially chiral bisaryl derivatives are emerging as alternatives, allowing usually complementary stereoselectivity and affording preferentially the *syn*-aldol products (in addition to *anti*-Mannich reactions; see below). The preference for *syn* selectivity can be attributed to the preferred formation of the (*Z*)-enamine that generates the *syn* product via the TS similar to that discussed above and also to the cooperativity between the catalyst and the acceptor resulting in a more organized TS. Amide catalysts having an amino alcohol such as **15** (Scheme 9.15) activate the electrophilic aldehyde of the aldol reaction by forming two hydrogen bonds, from both the amide and the hydroxy functionalities, with the carbonyl (Scheme 9.2c-1) [36, 37].

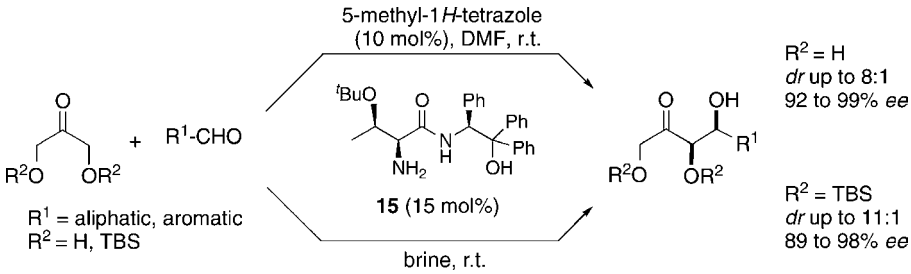

Scheme 9.15 *Syn*-selective cross-aldol reaction of unmodified aldehydes and ketones.

Noteworthily, other basic nitrogen compounds such as pyridine and tertiary amines, may also promote cross-aldol additions [38], some of them with high *syn*-selective internal stereocontrol [38b].

Aldol- and Knoevenagel-type Reactions with Preformed Enolates

Brønsted Acid Activation

Mukaiyama-type asymmetric aldol and Knoevenagel-type reactions can be mediated by asymmetric proton catalysts such as TADDOL and cinchona-derived chiral salts that promote selective addition of *N,O*-silyl ketene acetal with various aromatic and heteroaromatic aldehydes (Scheme 9.16). According to Rawal's selectivity model [39], the aldehyde carbonyl is activated by a single-point intermolecular hydrogen bond to the internally hydrogen-bonded TADDOL (Scheme 9.2b) and is further organized through electrostatic interactions with an aryl (naphthyl) ring of TADDOL.

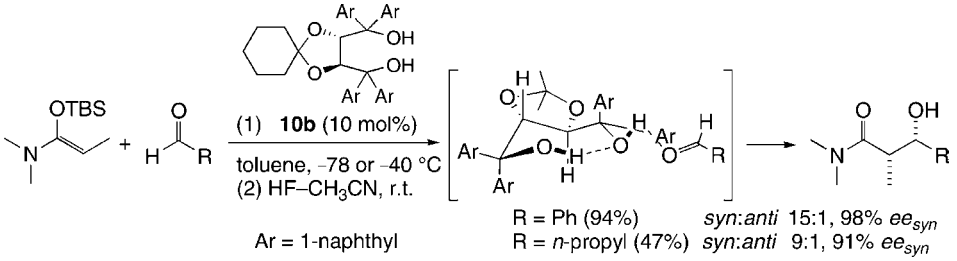

Scheme 9.16 Chiral Brønsted-acid-catalyzed Mukaiyama-type asymmetric Knoevenagel-type reactions

Lewis Acid Activation with Lewis Bases in Aldol-type Additions [40]

Lewis bases typically activate silicon atoms in electron donors such as silyl enolates or allylsilanes, as conventional Lewis acid catalysts activate heteroatoms in electron acceptors such as carbonyl groups. In these reactions, the asymmetric activation relies on the formation of a tightly binding chiral complex between the Lewis base catalyst such as alkoxides, HMPA, *N*-oxides or its asymmetric analogs and the silicon compounds, effecting rate acceleration. The enantio- and diastereoselectivity (*syn*: *anti* ratio) depends strongly on the structure of the chiral phosphoramide that affects the coordination state of the silicon atom of the silyl enol ether in the TS, as was demonstrated in the aldol reaction of cyclohexanone trichlorosilyl enol ether and benzaldehyde [40]. The more selective path with hexacoordinated silicate requires two sterically less demanding phosphoramide ligands (R = Me), leading to a chair-like TS with hexacoordinate silicate and affording the *anti* adduct. In contrast, the sterically demanding phosphoramide (R = Ph) forms a pentacoordinate silicate, which leads to a boat-like TS and affords the *syn* adduct (Scheme 9.17). The enantioselectivity of the reaction is sensitive to the enolate structure, with larger groups providing lower enantioselectivities. A marked effect of the aldehyde structure on the rate of the addition was noted since aliphatic and hindered aldehydes were less reactive.

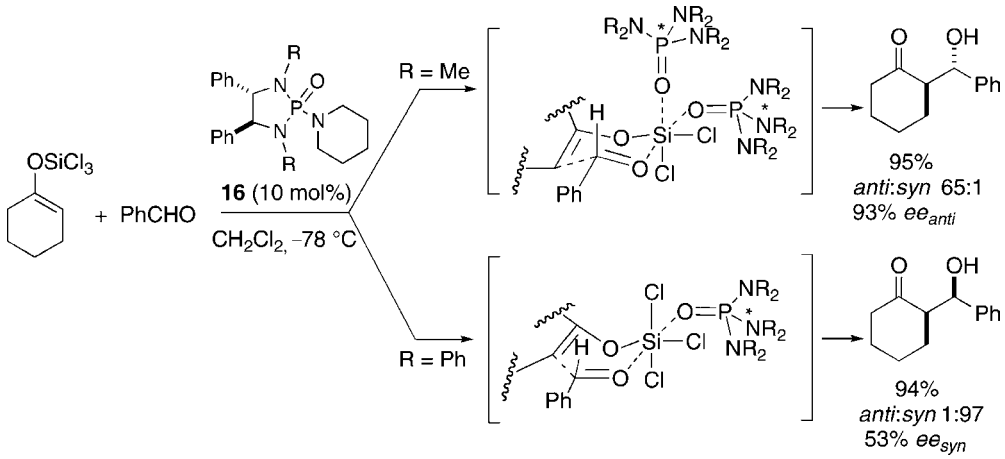

Scheme 9.17 Different stereochemical courses of the mono- and bis-coordinated hypervalent silica in the chiral HMPA-activated addition of cyclohexanone trichlorosilyl enol ether to benzaldehyde.

The bis-coordinated path was optimized in preparing dimeric phosphoramide catalysts. These catalysts were also effective in mediating the cross-aldol reaction of various silyl ether enolates and in the Mukaiyama-reaction of various *exo*-TMS-enolates to aromatic aldehydes [41]. Moreover, a general and selective addition of glycolate-derived silyl ketene acetals to a wide range of aryl- and alkylaldehydes has been developed using silicon tetrachloride and the chiral Lewis basic bisphosphoramide catalyst [42]. The sense of diastereoselectivity can be modulated by changing the size of the R substituents on the silyl ketene acetals (Scheme 9.18). In general, the trimethylsilyl ketene acetals derived from methyl glycolates with a large protecting group on the oxygen provide enantiomerically enriched (*R*)-α,β-dihydroxy esters with high *syn* diastereoselectivity, whereas the *tert*-butyldimethylsilyl ketene acetals

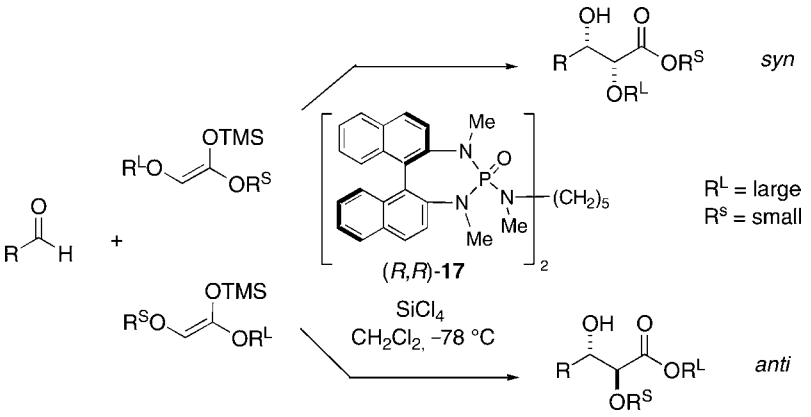

Scheme 9.18 Substrate control in the dimeric chiral HMPA-mediated addition of trimethylsilyl ketene acetals to aldehydes.

derived from bulky esters of methoxyacetic acid provide enantiomerically enriched (*R*)-α,β-dihydroxy esters with high *anti* diastereoselectivity.

9.3.1.2 **Allylation Reactions**

Tethered bis-phosphoramides catalyze the addition of either allyltrichlorosilane (*E*)- or (*Z*)-2-butenyltrichlorosilane to unsaturated aldehydes (Scheme 9.19) [43]. Noteworthily, chiral bidentate imidodiphosphoric tetramides and pyridine-*N*-oxides were also efficient in the allylation of aromatic aldehydes [44].

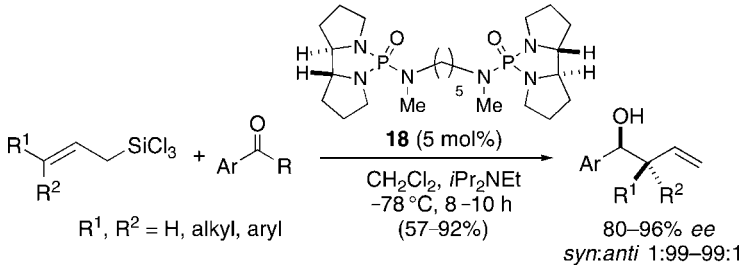

Scheme 9.19

This method has also been applied to the synthesis of chiral quaternary centers (R^1, R^2 = alkyl and/or aryl) and to the synthesis of the serotonin antagonist LY426965 [45].

9.3.1.3 **Nitroaldol (Henry) Reactions** [46]

Direct Nitroaldol Reactions

Nitroaldol (Henry) Reactions via General-base Catalysis and Contact Ion-pair Formation Under Homogeneous Conditions

Chiral bases such as benzoylcupreidine (**19**) and benzoylcupreine (**20**) mediate the reaction of α-keto esters with nitromethane and provide easy access to functionalized compounds (Scheme 9.20) that feature a quaternary stereocenter such as aziridines, β-lactams and α-alkylcysteines [47].

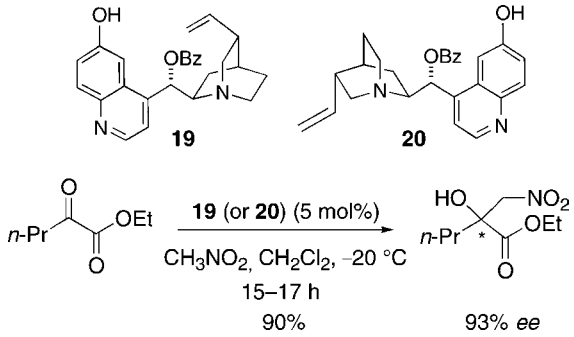

Scheme 9.20 Benzoylcupreidine (**19**) and benzoylcupreine (**20**)-mediated addition of nitromethane to α-keto esters.

Nitroaldol (Henry) Reactions via General-base Catalysis and Contact Ion-pair Formation Under Phase-transfer Conditions [48]

The face-selective nitroaldol reaction of nitromethane with protected (*S*)-phenylalaninal was effected under PT conditions using the functionalized 9-anthracenylmethyl cinchona catalyst **21**. The reaction afforded the key intermediate of the second-generation HIV protease inhibitor amprenavir in good yield and with remarkable stereoselectivity (Scheme 9.21) [49].

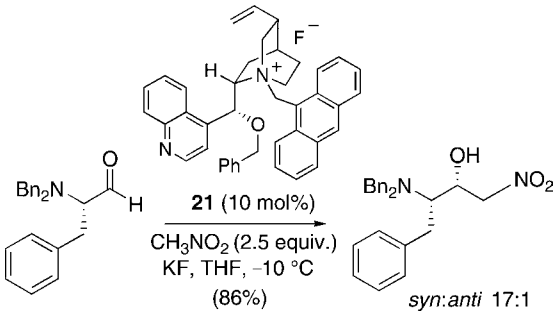

Scheme 9.21 9-Anthracenylmethyl cinchona (**21**)-catalyzed addition of nitromethane to aldehyde under PT conditions in the synthesis of amprenavir.

Nitroaldol (Henry) Reaction of Silyl Nitronates

Chiral ammonium fluoride salt **22** was engineered for the asymmetric nitroaldol reaction of silyl nitronates with aromatic aldehydes (Scheme 9.22) [50]. High enantio- and *anti* diastereoselectivity were observed when a radially extended 3,3′-aryl-substituted catalyst was used.

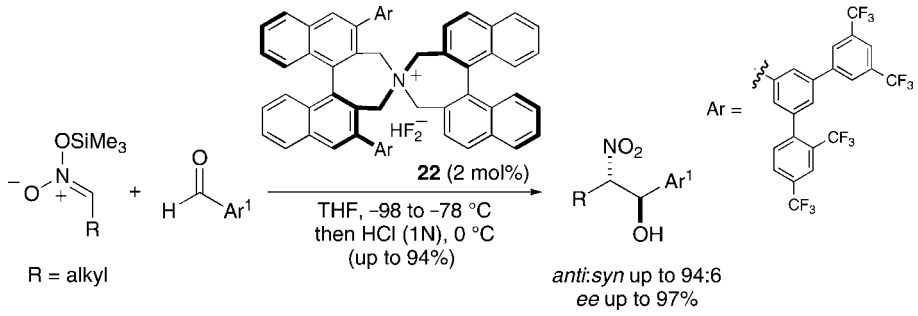

Scheme 9.22 Chiral quaternary ammonium-catalyzed addition of silyl nitronates to aryl aldehydes.

9.3.1.4 Hydrocyanation

Most of the organocatalysts developed to date for hydrocyanation are limited in substrate scope [51]. Chiral diketopiperazine-imidazoles and diaminocyclohexane-derived salem catalysts are efficient in the asymmetric hydrocyanation of aromatic

aldehydes, whereas dihydroquinyl (DHQ) and dihydroquinidyl (DHQD) derivatives can be used for the hydrocyanation of ketones [52]. Tertiary aminothiourea catalysts have, however, remarkably broad substrate compatibility as they can be used for both aldehydes and ketones bearing one sp^2-hydridized substituent. The HCN is generated *in situ*, from TMSCN and trifluoroethanol, affording the addition products in high yields and *ee* (Scheme 9.23) [53]. In the **23**-mediated hydrocyanation, both the thiourea and the tertiary amine of the catalyst are involved productively in the rate-limiting cyanide addition step, as depicted in Scheme 9.23 [54]. According to this cooperative mechanism, the enantioselectivity arises from direct interactions between the ketone substrate and the amino-acid derived portion of the catalyst (Scheme 9.2c-1).

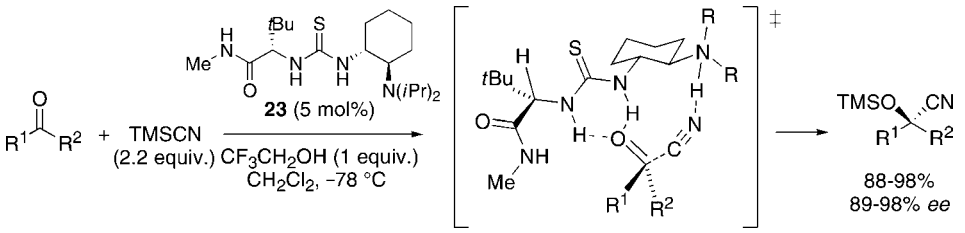

Scheme 9.23 Enantioselective cyanosilylation of ketones catalyzed by tertiary aminothiourea catalysts **23**.

9.3.1.5 **The Morita–Baylis–Hillman (MBH) Reaction** [55]

The addition of aldehydes to enones or α,β-unsaturated esters, the so-called Morita–Baylis–Hillman (MBH) reaction, requires both nucleophile and proton catalysts either in the same structure or in separate catalysts. The action of the Brønsted co-catalyst is at least two-fold: (i) it promotes the conjugate addition by binding to the zwitterionic enolate and stabilizes these intermediates; and (ii) it ensures efficient proton transfer in the rate- and stereo-determining proton abstraction step [7]. Among the number of catalysts that have been developed for the MBH reaction, β-isocupreidine, chiral thiourea and phosphine–BINOL-type catalysts have shown high selectivity and a relatively wide substrate range.

The quinidine-derived β-isocupreidine catalyst (β-ICD) (**24**) mediated the addition of the acrylate to a variety of aromatic and aliphatic aldehydes even at −55 °C in DMF (up to 99% *ee*). The 1,1,1,3,3,3-hexafluoroisopropyl acryl ester (HFIPA) displayed an almost 200-fold rate acceleration compared with methyl acrylate under identical reaction conditions. Limitations were observed with bulky aldehydes such as butyraldehyde, where dimerization of the acrylate was observed. The β-ICD catalyst **24** was used in the synthesis of epopromycin B, a plant cell wall synthesis inhibitor [56], and in the synthesis of mycestericin E, a potent immunosuppressor (Scheme 9.24) [57].

Enones usually provide less selective additions and the scope of the MBH reaction with this class of substrates remains narrow. Chiral (thio)urea–amine catalysts **25** [58]

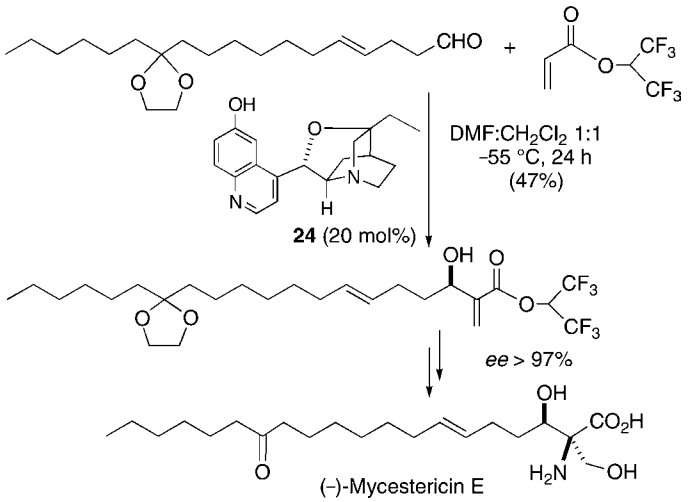

Scheme 9.24 The asymmetric MBH reaction in the synthesis of (−)-mycestericin E.

and the combination of PPh_3 with partially saturated BINOL derivatives such as **26** offered high chemical yield and enantioselectivity in the addition of cyclohexenone with hindered aliphatic aldehydes (Scheme 9.25) [59]. Conjugated and aromatic aldehydes resulted in low yields and enantioselectivities.

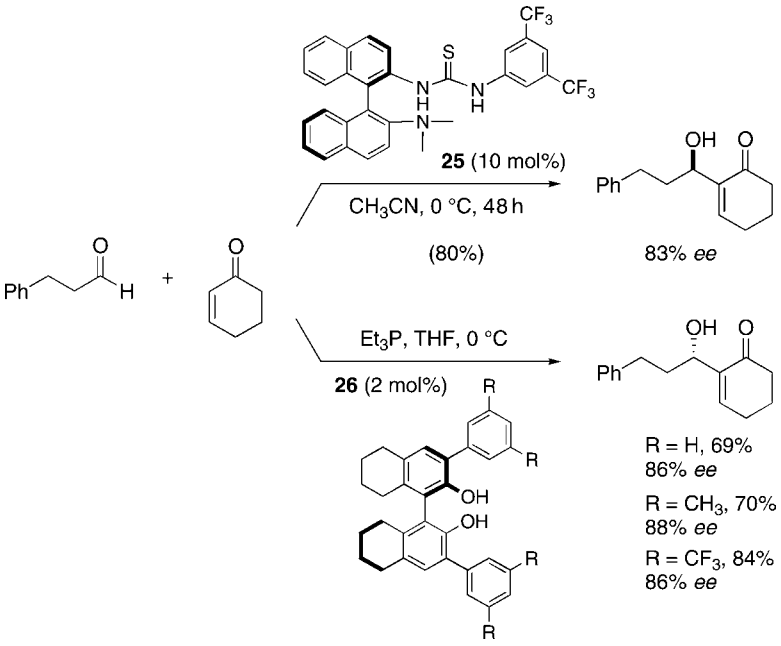

Scheme 9.25 Bifunctional thiourea–amine and achiral phosphine–chiral binaphthol-derived Brønsted acid-catalyzed MBH reactions of cyclohexenone and dihydrocinnamaldehyde.

9.3.1.6 **Asymmetric Acyl Transfer Reactions** [60]

Kinetic Resolution of Secondary Alcohols

Among the great number and variety of DMAP-derived acyl transfer agents, the planar chiral ferrocenyl DMAPs proved to be highly versatile and efficient catalysts for many acyl transfer processes (Scheme 9.26) [60b, e, f]. In particular, the catalyst **27** was found to be efficient in the kinetic resolution of aryl, alkyl and allyl *sec*-alcohols and was the only organocatalyst that has been shown to be generally effective for the kinetic resolution of propargylic *sec*-alcohols [60b, e, f]. The synthetic utility of this catalyst was demonstrated in multistep synthesis; the following example is taken from the kinetic resolution protocol of a racemic aldol intermediate in the Sinha–Lerner synthesis of epothilone A (Scheme 9.26) [61]. It is considered that a π–π stacking interaction between the catalyst and the substrate in the TS is crucial to the observed enantioselectivity [62].

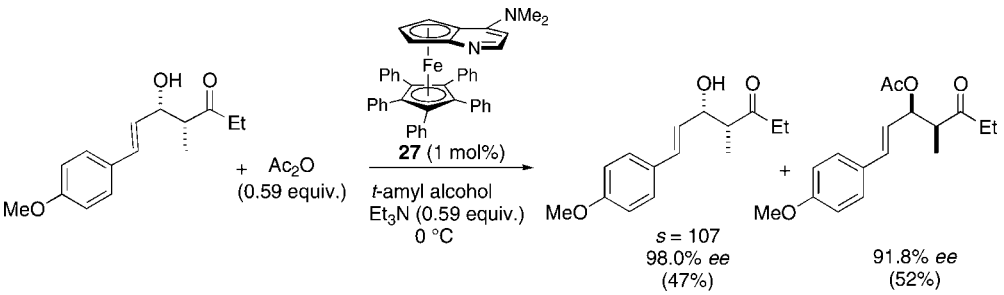

Scheme 9.26 Preparation of an epothilone A intermediate using the planar chiral DMAP **27**.

Among the phosphine-derived catalysts, chiral *P*-aryl-2-phosphabicyclo[3.3.0]octanes (PBO) [63] were shown to be remarkably selective in acylation for a broad range of arylalkyl *sec*-alcohols (Scheme 9.27) [65].

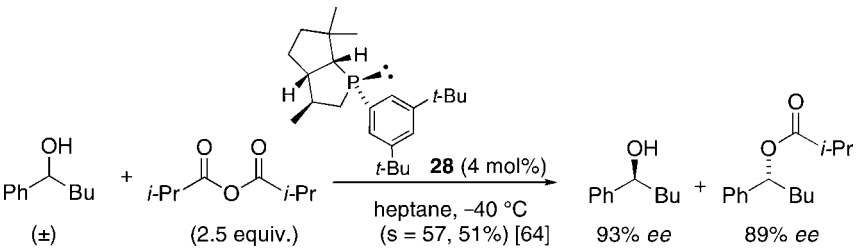

Scheme 9.27 The kinetic resolution of arylalkyl *sec*-alcohols using chiral PBO catalyst.

Engineered oligopeptides such as **29** are efficient for the acylative kinetic resolution of *sec*-alcohols [29, 66]. The substrate scope includes not only arylalkyl

sec-alcohols but also alkyl *sec*-alcohols with which lipases and other organocatalysts invariably perform poorly (Scheme 9.28) [67].

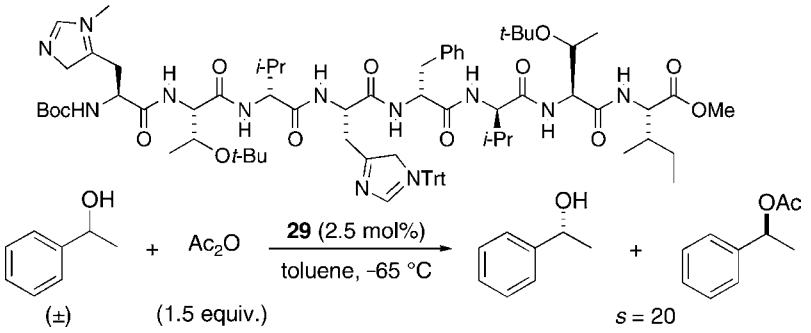

Scheme 9.28 Miller's octapeptide **29**-catalyzed kinetic resolution of *sec*-alcohols.

The kinetic resolution of arylalkyl *sec*-alcohols using various chiral nucleophilic *N*-heterocyclic carbenes (NHCs) has also recently been achieved by the groups of Suzuki [68] and Maruoka [69] (Scheme 9.29). These studies build on an emerging body of work showing that achiral NHCs are extremely efficient nucleophilic organocatalysts for transesterification.

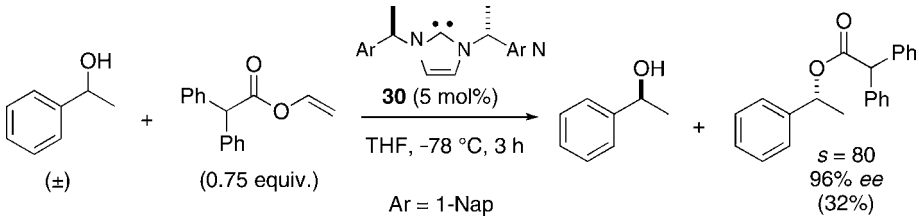

Scheme 9.29 Maruoka's chiral NHC-catalyzed kinetic resolution of *sec*-alcohols.

Asymmetric Desymmetrization of Achiral/*meso* cyclic Anhydrides [23a, 60d, 70]
Asymmetric desymmetrization (ASD) of achiral and *meso* cyclic anhydrides by nucleophilic ring opening with alcohols or thiols can be catalyzed by either chiral Lewis acids or bases. One of the most selective classes of catalyst in this type of transformation is Sharpless ligands. Reaction of a variety of mono-, bi- and tricyclic succinic anhydrides with methanol in diethyl ether and a catalytic amount of the biscinchona alkaloid $(DHQD)_2AQN$ (**31**) provided the corresponding hemiesters with excellent enantioselectivities (91–98%) and good to excellent yields (72–99%) [71, 72]. The synthetic utility of this approach has been demonstrated in a formal total synthesis of (+)-biotin (Scheme 9.30) [73].

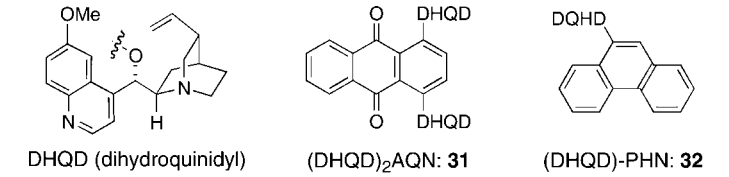

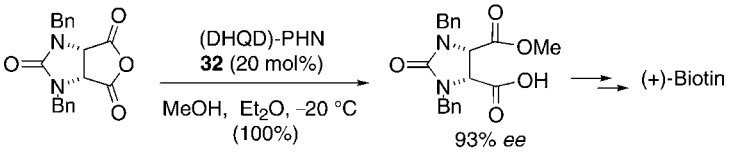

Scheme 9.30 Cinchona-derived (DHQD)–PHN catalyst-mediated asymmetric desymmetrization of a *meso* anhydride in the synthesis of (+)-biotin.

Cinchona-derived catalysts are not the only efficient systems for the ASD of *meso* anhydrides; the bifunctional chiral sulfonamide–amine organocatalyst **33** can also be used for the highly enantioselective catalytic thiolysis of prochiral cyclic anhydrides (Scheme 9.31) [74].

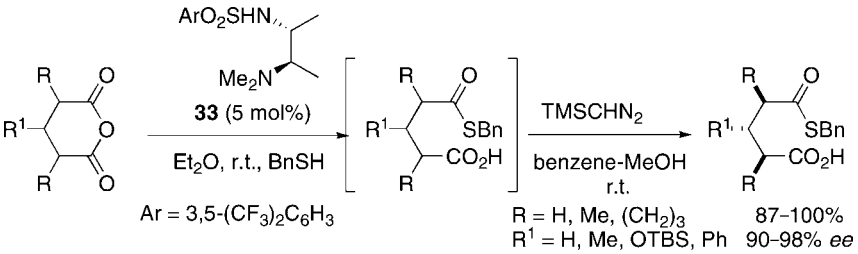

Scheme 9.31 Chiral sulfonamide–amine organocatalyst **33**-mediated asymmetric desymmetrization of achiral and *meso*-anhydrides.

Alcoholative Kinetic Resolution of Racemic Anhydrides

Further application of $(DHQD)_2AQN$-catalyzed asymmetric alcoholysis can be illustrated by the kinetic resolution of monosubstituted succinic anhydrides [75]. A variety of 2-alkyl- and 2-arylsuccinic anhydrides were resolved via this process with good to excellent enantioselectivities (Scheme 9.32).

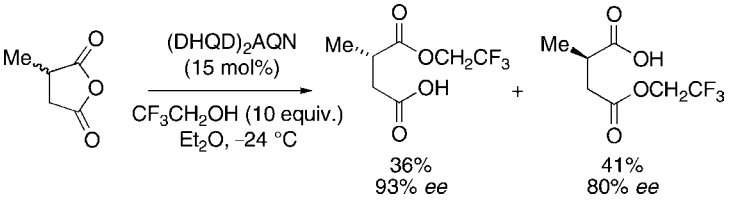

Scheme 9.32 Deng's $(DHQD)_2AQN$-catalyzed ASD of *meso* anhydrides.

9.3.2
Nucleophilic Additions to C=N

9.3.2.1 Mannich-type Reactions [76]

The Organocatalytic Direct Mannich Reaction

Organocatalytic Mannich reactions have been described either under three-component (one-pot) reaction conditions or involving preformed (protected) imines and aldol donors. Proline was found to catalyze both versions, usually in good yields and in high selectivity. Using L-proline (**1**) as catalyst, the stereochemistry of the reaction is catalyst controlled and independent of the chiral centers present in the substrate. The original Mannich reaction provided the highest selectivities with aromatic aldehydes.

Historically, the one-pot, three-component Mannich reaction between a ketone, aldehyde and anisidine was developed first, which also provided practical access to a number of enantiomerically enriched β-aminocarbonyls. The use of preformed imines, such as *N*-PMP-protected α-iminoethyl glyoxylates, is more recent (Scheme 9.33). The advantage of this modification is that under these conditions the potential side-reactions are minimized and both ketones and aldehydes can be used as aldol donors.

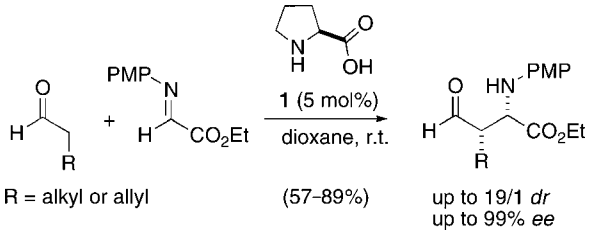

Scheme 9.33 Two-component Mannich reaction between *N*-PMP-protected α-iminoethyl glyoxylates and aldehydes.

Intriguingly, the cross-Mannich reaction using 'unmodified' aldehydes proceeds faster than the competing cross-aldol reaction (Scheme 9.34). The three-component cross-Mannich reaction at temperatures below 0 °C exhibits both higher stereo- and chemo-selectivity ($k_{cross\text{-}Mannich} > k_{cross\text{-}aldol}$). With electron-rich aromatic acceptor aldehydes, the use of a syringe pump was not necessary and the catalyst loading could be reduced. The example in Scheme 9.34 is taken from the formal synthesis of nikkomycin [77].

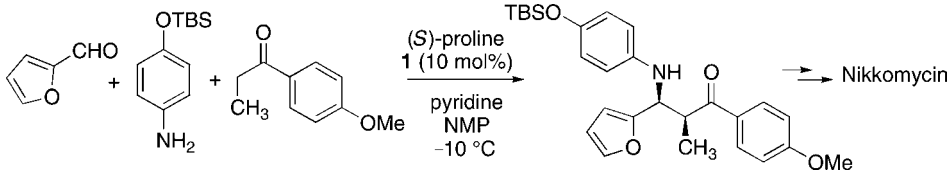

Scheme 9.34 The application of the three-component cross-Mannich reaction in the synthesis of nikkomycin.

The direct Mannich reaction can also be mediated by proline analogs [78]. In particular, TMS-diphenylprolinol derivatives **3a** were seen efficient for the aminomethylations of various aldehydes (Scheme 9.35) [79].

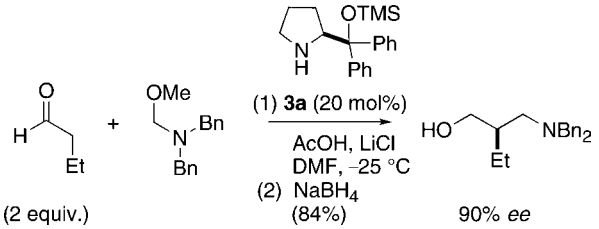

Scheme 9.35 Aminomethylations of aldehydes via direct Mannich reaction.

As proline and proline analogs provide preferentially the *syn* isomer, the *anti*-selective Mannich reactions between unmodified α-hydroxy ketones, arylamines and aldehydes can be realized by L-threonine or L-tryptophan-derived amino acids [80].

The lengthy reaction times, which characterize both the proline and other chiral amine-catalyzed Mannich reactions, can be considerably shortened (up to 4–50 times) by replacing standard organic solvents by ionic liquids such as [bmim].BF_4 or [bmim].PF_6 [81]. This modification may also permit the use of as little as 1 mol% of catalyst while retaining reasonable reaction times (~2 h). The reaction usually affords higher yields than in organic solvents and provides similar enantioselectivity. The enhanced rates may result from ionic liquid-based activation of the imine electrophile.

The proline-catalyzed Mannich reaction shows opposite diastereo- and enantioselectivity to those of the related aldol reactions as the *syn* adducts being obtained as major isomers. In contrast, *anti* addition between *N*-PMP-protected α-iminoethyl

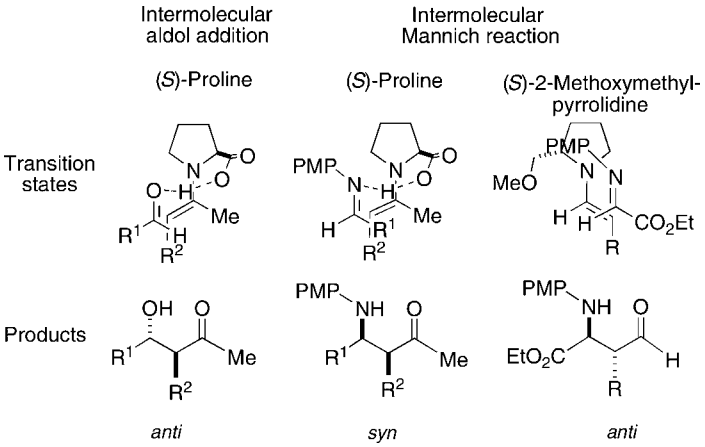

Scheme 9.36 The rationale of the observed difference in the stereoselectivity of (*S*)-proline- and (*S*)-2-methoxymethylpyrrolidine-mediated aldol and Mannich reactions.

glyoxylate and aldehydes was observed using a bulky pyrrolidine catalyst where the acid function was suppressed, such as (*S*)-2-methoxymethylpyrrolidine (SMP). The differences in the reversal of selectivity of the proline-catalyzed Mannich reaction can be explained by the differences in the preferred conformations in the TS of the substrates. As the aldehyde substituents assume a pseudoequatorial conformation in the aldol reaction, the substituents are forced into a pseudoaxial arrangement in the Mannich reaction since the (*E*)-imine is more stable than the (*Z*)-imine (Scheme 9.36).

Mannich-type Reactions with Preformed Enolates and Enolate Equivalents

Brønsted Acid Catalysis

Highly enantioselective Mannich reactions were developed with chiral thiourea-derived Brønsted acid catalysts by Jacobsen's group (Scheme 9.37) [82]. Likewise, bifunctional thiourea catalysts mediated the direct asymmetric vinylogous Mannich reaction of α,α-dicyanoalkenes and *tert*-butyloxycarbonyl (Boc)-protected imines with complete γ-regioselectivity and excellent enantioselectivities [83].

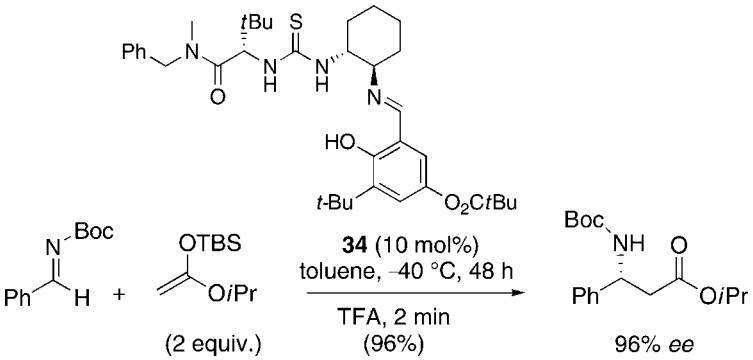

Scheme 9.37 Chiral thiourea catalyst-mediated Mannich reaction of ketenesilyl acetals and arylimines.

One of the more promising classes of catalysts for a broad range of highly enantioselective imine addition reactions is the 2,2′-dihydroxy-1,1′-binaphthyl (BINOL)-based phosphoric acid catalysts that involve chiral contact ion pairs generated *in situ* [8f]. Such a chiral phosphoric acid diester catalyst was developed for the asymmetric Mannich-type addition of silylketene acetals to arylaldimines. The catalyst mediated the addition in favor of the *syn* isomer [84, 85]. In this transformation, the *N*-2-hydroxyphenyl group of aldimine was found to be essential for the high selectivity as the reaction proceeds via a dicoordination pathway through the zwitterionic and nine-membered cyclic TS consisting of the aldimine and the phosphoric acid (Scheme 9.38). The *re*-facial selectivity was rationalized by the aromatic stacking interaction between the 4-nitrophenyl group and the *N*-aryl group that fix the geometry of aldimine in the TS, where the *si*-facial attacking TS is less favored by the steric hindrance of the 3,3′-aryl substituents. Noteworthily, the BINOL-based phosphoric acid catalyst was also efficient in the vinylogous Mukaiyama–Mannich reaction of

acyclic silyl dienolates and imines. The reaction proceeds also with complete regioselectivity in favor of the δ-product [86].

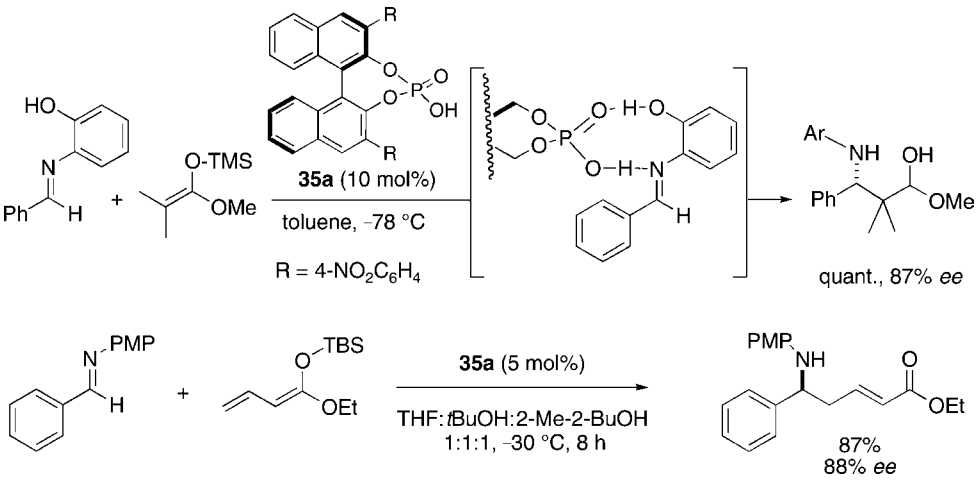

Scheme 9.38 The BINOL-based phosphoric acid-mediated Mukaiyama–Mannich and vinylogous Mukaiyama–Mannich reactions of silylketene acetals and arylimines.

General-base Catalysis and Contact Ion-pair Formation Under Phase-transfer Conditions
Similar transformations can be successfully conducted under phase-transfer conditions with a chiral pyrrolidinium salt in up to 95% *ee* [87].

9.3.2.2 The Nitro-Mannich (Aza-Henry) Reaction

A highly effective thiourea-based catalyst was developed for the nitro-Mannich (aza-Henry) reaction that mediated the *syn*-selective addition of a range of nitroalkanes to aromatic *N*-Boc-imines [88]. The sense of imine enantioface selectivity is the same as that observed in thiourea-catalyzed Strecker, Mannich and hydrophosphonylation reactions, suggesting a common mechanism of imine activation. However, thiourea derivatives are also known to bind and modulate the reactivity of nitronate anions; therefore, the role of the catalyst in this transformation could be either activation of the nitroalkane component or dual activation of both reaction partners. The scope of the transformation can be illustrated by the synthesis of the potent neurokinin-1 receptor antagonists (−)-CP-99,994 (Scheme 9.39).

General-base Catalysis and Contact Ion-pair Formation Under Phase-transfer Conditions [89]
A remarkably general cinchona-derived ammonium catalyst-mediated nitroaldol reaction was developed between nitroalkanes and α-amidosulfones by using $CsOH.H_2O$ as base under phase-transfer conditions. The reaction that generates the reactive imine component *in situ* can be applied to either non-enolizable or enolizable aldehyde-derived azomethines and to nitroalkanes, other than nitromethane, for the production of β-nitroamines (Scheme 9.40).

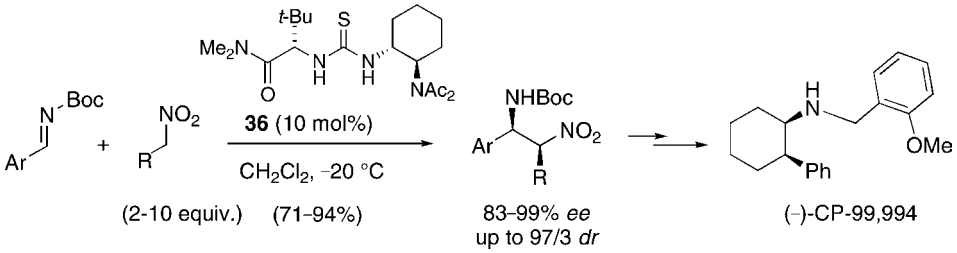

Scheme 9.39 Chiral thiourea-mediated *syn*-selective nitro-Mannich (aza-Henry) reaction in the synthesis of the (−)-CP-99,994.

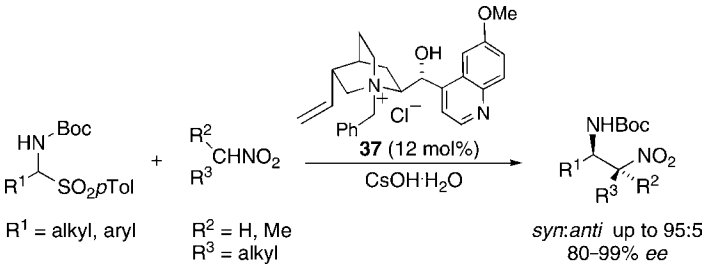

Scheme 9.40 Cinchona-derived ammonium catalyst-mediated nitroaldol reaction between azomethines and to nitroalkanes under PT conditions.

9.3.2.3 **The Asymmetric Strecker Reaction** [90]

Chiral peptide-like urea catalysts have been the subject of considerable study [91]. Surprisingly, the same class of catalyst can be used in asymmetric cyanation reactions of aldimines and methylketimines and in asymmetric Mannich reaction of *N*-Boc-aldimines with silylketene acetals (Scheme 9.41). The thiourea **38** mediated hydrocyanation reactions with a remarkably broad generality: the same catalyst affords >95% *ee* for all aldimines examined, ranging from aromatic to bulky aliphatic such as *tert*-butyl, to small aliphatic such as *n*-pentyl. It is worth noting that ketimines can be used likewise. This level of generality is still unusual in asymmetric catalysis [82b].

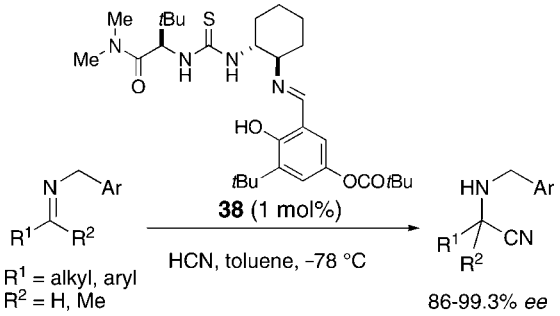

Scheme 9.41 Chiral thiourea-mediated asymmetric Strecker reaction of aldimines and ketimines.

The imine–catalyst complex forms reversibly a hydrogen bond between the imine nitrogen having a *Z* configuration and the acidic proton of the urea. Factors which account for the high enantioselectivity of the reactions are as follows: the steric demand of the substituents flanking the imine group should be markedly different; the *N*-substituent should favor the formation of the *Z* isomer of the imine; and the HCN addition takes place from the diaminocyclohexane side of the catalyst. The reaction was used for the preparation of optically enriched isoquinoline alkaloids, precursors of natural compounds (*R*)-(−)-calycotomine ($R^1 = H$, $R^2 = OH$), (*S*)-(−)-salsolidine ($R^1 = R^2 = H$) and (*S*)-(−)-carnegine ($R^1 = Me$, $R^2 = H$) (Scheme 9.42) [2].

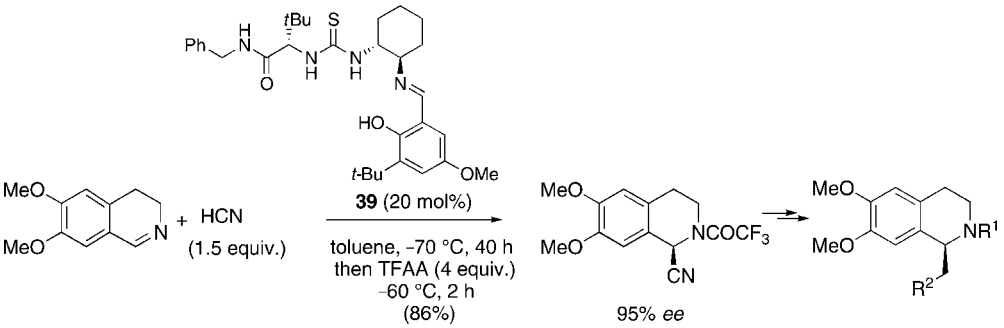

Scheme 9.42 The asymmetric Strecker reaction in the synthesis of isoquinoline alkaloids.

Other Brønsted acid catalysts such as chiral BINOL phosphate-derived catalysts [3] and Lewis base catalysts such as the axially chiral biquinoline *N,N′*-dioxide catalysts used in the presence of trimethylsilyl cyanides showed less general substrate scope.

Strecker Reactions Under Phase-transfer Conditions

Under heterogeneous conditions, the chiral binaphthol-derived quaternary ammonium salts efficiently promotes the Strecker reaction of aldimines when aqueous potassium cyanide is used (Scheme 9.43) [4].

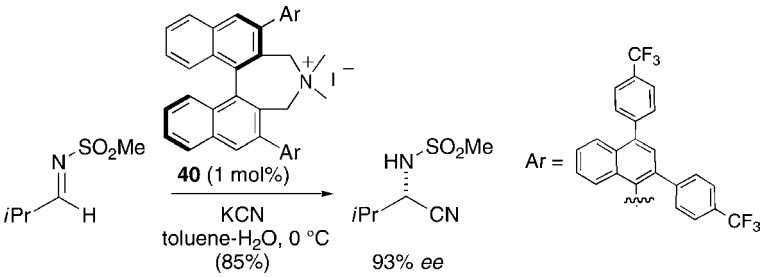

Scheme 9.43 The Strecker reaction of aldimines under PT conditions.

9.3.2.4 **Pictet–Spengler-type Cyclizations**

Brønsted acid catalysts and in particular chiral thiourea catalysts may promote enantioselective Pictet–Spengler reactions (Scheme 9.44) [5]. In the following

example the iminium ions were generated from tryptamine-derived hydroxylactams using TMSCl [5]. Substituent and counterion effect studies pointed to rate-limiting anion abstraction and binding by the thiourea by hydrogen bonding to the putative iminium ion intermediate.

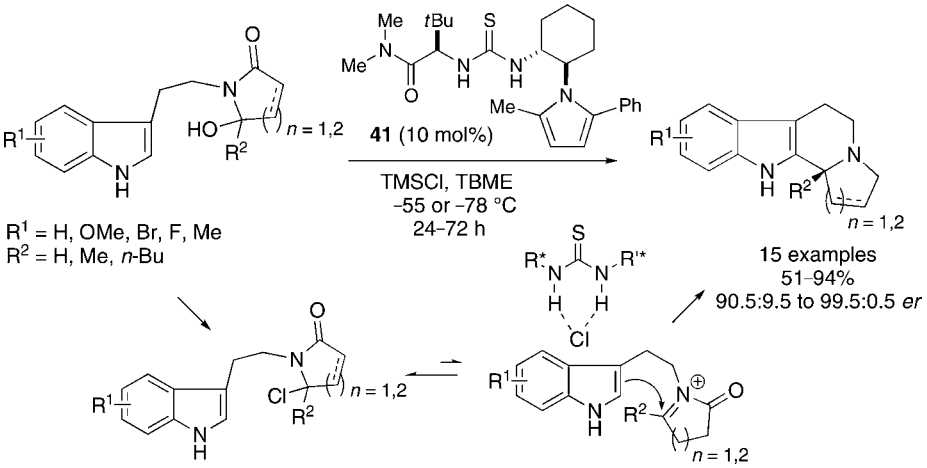

Scheme 9.44 The preparation of enantioenriched indolizinone and quinolizinone products by chiral thiourea-promoted Pictet–Spengler reaction.

9.3.2.5 **Reduction of Ketimines** [6]

Chiral formamides have been developed for the enantioselective reduction of *N*-aryl- and *N*-cycloalkylketimines with trichlorosilane [7]. Among the catalysts developed, pipecolic acid derivative **42** was shown to be comparable with both alkyl- and arylketimines, whereas the valine-derived *N*-methyl-substituted formamide **43** was active in the reduction of arylketimines (Scheme 9.45) [98].

A conceptually different approach for the reduction of ketimines is the use of Hantzsch esters **I** as hydrogen donors that can be used in the presence of a chiral phosphoric acid catalyst (Scheme 9.46). This method can be used for the reduction of both alkyl- and arylketimines [99].

9.3.3 Additions to Alkenes

9.3.3.1 **Michael Addition** [19e, 100]

Aminocatalytic Direct Addition of Aldehydes and Ketones to Nitroalkenes

Enamine Activation

Pyrrolidine-derived catalysts promote *syn*-selective additions of nitroalkenes with aldehydes and also with ketones [1, 101]. While high levels of diastereo- and enantios-

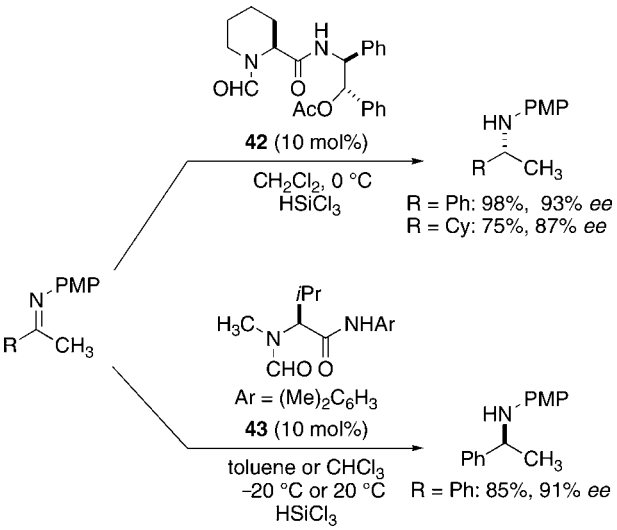

Scheme 9.45 Asymmetric reduction of *N*-aryl- and *N*-cycloalkylketimines by trichlorosilane and chiral formamide catalysts.

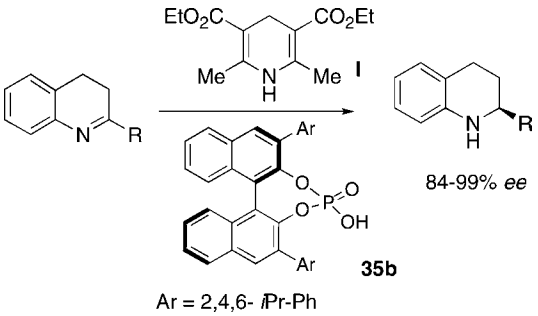

Scheme 9.46 Chiral phosphoric acid catalyst-mediated asymmetric reduction of ketimines in the presence of Hantzsch esters.

electivity can be obtained in selected cases and in particular with cyclohexanone, the reactions are usually substrate dependent. The diphenylprolinol silyl ether catalyst **3a** is remarkably efficient for the addition of α-unbranched aldehydes to aryl- and alkyl-substituted nitroalkenes [17a] and also to nitroethylene in the presence of a carefully selected acidic co-catalyst [102]. The diphenylprolinol silyl ether catalyst **3a** and the perfluoroalkyl derivative **3c** [103] afford high yields, excellent diastereoselectivity and nearly perfect enantioselectivity with a broad range of aldehydes. Moreover, the perfluoroalkyl catalyst **3c** can also be used in aqueous media [104]. The bulky diphenylsilyloxymethyl group probably plays a dual role in promoting the selective formation of the (*E*)-enamine and in providing efficient shielding of the *re*-face of the enamine (Scheme 9.47).

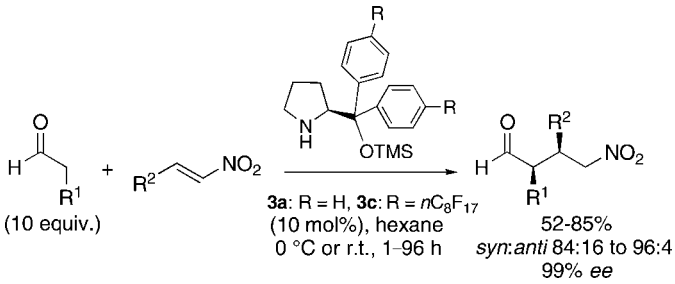

Scheme 9.47 The diphenylprolinol silyl ether-catalyzed Michael addition of aldehydes to nitroalkenes.

α-Substituted nitroalkenes can be used as substrates in bispyrrolidine-catalyzed additions. The efficiency of the catalyst **44** was demonstrated in the synthesis of (−)-botryodiplodin (Scheme 9.48). The addition of propionaldehyde to nitroalkene led to a roughly 2 : 3 mixture of *anti* and *syn* isomers in high yield and *ee* (92 and 93%, respectively) [105].

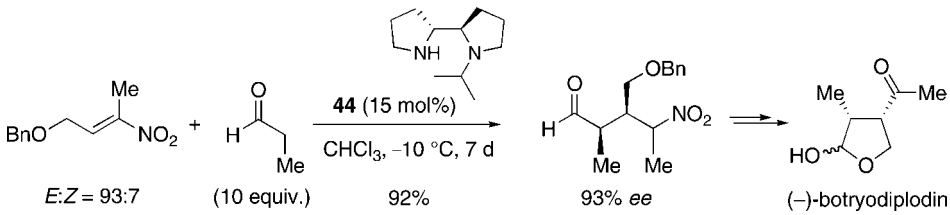

Scheme 9.48 Alexakis's (−)-botryodiplodin synthesis.

Interestingly, the same catalyst induces opposite selectivity with aldehydes compared with ketones. This can be rationalized by the difference in the steric demand of the enamine forms in the TS. As depicted in Scheme 9.49, the equilibrating conformers give rise to product via the less congested TS, forming the thermodynamic product.

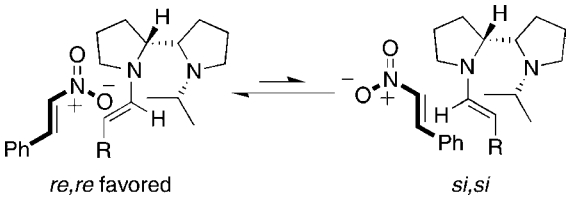

Scheme 9.49 Rationale of enantioselectivity of the pyrrolidine catalyst-mediated additions of aldehydes to nitroalkenes.

Alkylation of asymmetric acyclic ketones takes place regioselectively on the most substituted carbon, affording the *syn* isomers as the major products. α-Hydroxy ketones showed *anti*-selective additions similar to that observed in related aldol-type

additions, but the mechanistic rationale is different (Scheme 9.50). The selectivity is due to the preferred formation of the (*Z*)-enamine intermediate, stabilized by intramolecular hydrogen bonding between the hydroxy group and the tertiary amine of the catalyst [106].

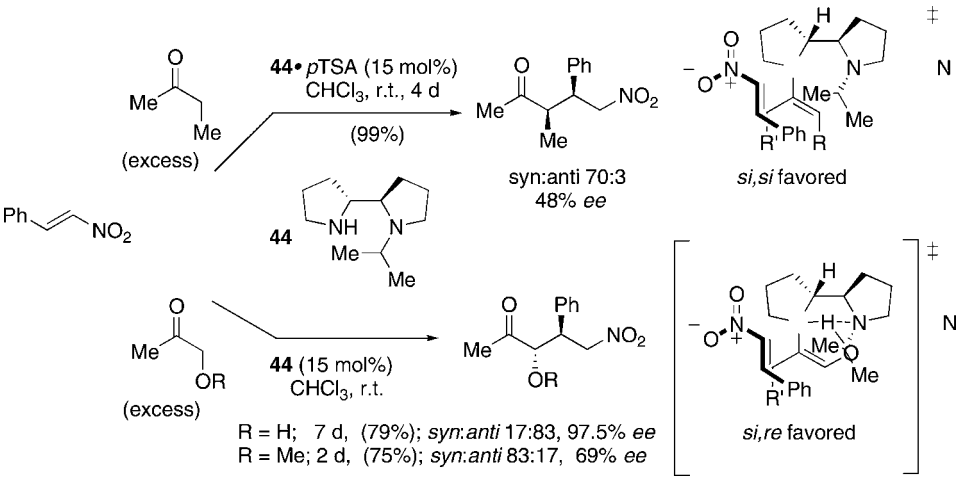

Scheme 9.50 Variation of the *syn*/*anti* diastereoselectivity of the conjugate addition as a function of the substrate.

Short oligopeptides such as H-D-Pro-Pro-Asp-NH_2 and the homologous and more soluble H-D-Pro-Pro-Glu-NH_2 catalyst bearing an additional methylene group also showed remarkable selectivity in the addition of nitroethylene to a great variety of aldehydes [107, 108]. Notably, the product of a homoaldol reaction of the aldehyde that is often observed with other amine-based organocatalysts was not detected.

Amine–Thiourea Catalysts

The bifunctional thiourea catalyst combined with a nucleophilic amine mediates the addition of ketones to nitroalkenes at room temperature in the presence of a weak acid co-catalyst, such as benzoic acid, *n*-butyric acid or acetic acid (Scheme 9.51) [109]. The acid additive allows double alkylation to be avoided and also increases the reaction rate. The *anti* selectivity of the addition is attributed to the preferred (*Z*)-enamine geometry in the TS. The catalyst also activates the acceptor and orientates in space. The regioselectively of the alkylation of non-symmetric ketones is the consequence of this orientation.

General-base Activation: Addition of Esters, Amides and Nitriles to Nitroalkenes

A number of tertiary amine–thiourea catalyst combinations have been developed for the conjugate addition to nitroalkenes with malonates and with various 1,3-dicarbonyl compounds such as diesters and chiral keto esters. Among them, cinchona-derived bifunctional catalysts, where the hydroxy group at C-9 was replaced by an arylthiourea [110, 111], and thiourea derived from binaphthyl [112] are noteworthy.

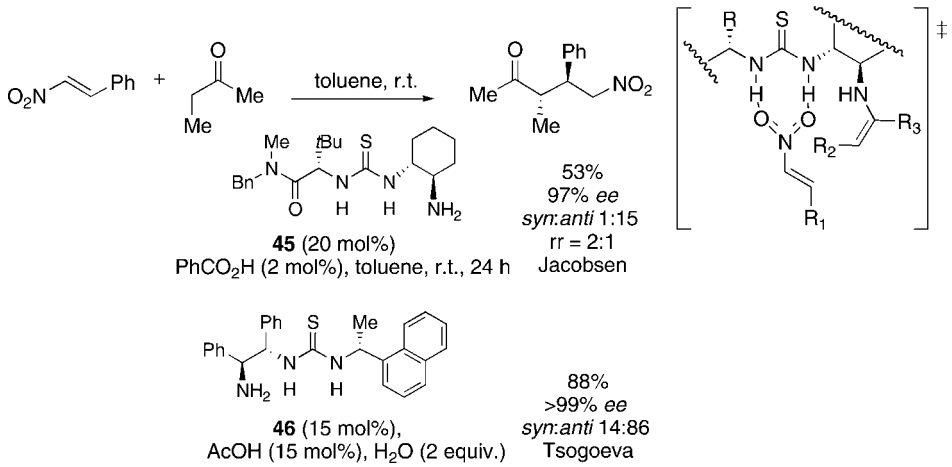

Scheme 9.51 Thiourea–amine catalysts mediated addition of acyclic ketones to nitrostyrenes.

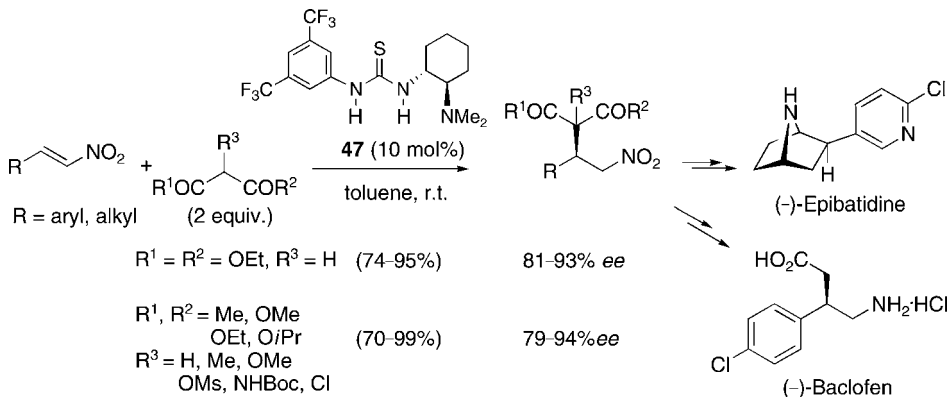

Scheme 9.52 Synthesis of (−)-baclofen and (−)-epibatidine by chiral 1,2-diaminocyclohexane-derived thiourea-mediated conjugate addition to nitroalkenes.

Chiral 1,2-diaminocyclohexane-derived thioureas are also efficient catalysts and were used in the synthesis of (−)-baclofen [113], an analog of GABA used as an antispastic agent, and (−)-epibatidine (Scheme 9.52) [114].

Aminocatalytic Addition of Aldehydes and Ketones to Enones

Enamine Activation

Among the pyrrolidine-derived catalysts, (*S*)-2-[bis(phenyl)methyl]pyrrolidine derivatives such as **4a** allowed good conversion and enantioselectivity in the addition of linear aldehydes to MVK (up to 85 % *ee*) (Scheme 9.53) [115]. Cyclic enones and β-substituted enones afforded no or poor results.

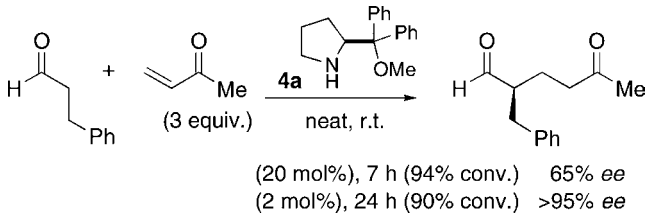

Scheme 9.53 **4a**-catalyzed addition of dihydrocinnamaldehyde to MVK.

The observed small negative non-linear effect suggested the participation of more than one catalyst molecule in the enantiodifferentiating step. This may be a consequence of the simultaneous activation of the nucleophile (enamine formation) and the electrophile partners (iminium formation) [116].

MacMillan's organocatalyst **48a**, which is used typically for electrophilic activation, was also found to be efficient in promoting conjugate addition via enamine formation (Scheme 9.54) [117]. The proof of the enamine pathway was furnished by NMR studies.

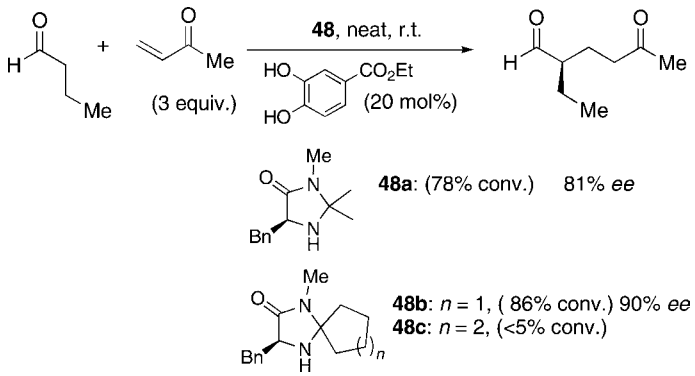

Scheme 9.54 Organocatalyzed asymmetric addition of butyraldehyde to MVK.

Intramolecular Conjugate Additions

The intramolecular addition of aldehydes to enones could also be promoted with iminium catalysts (Scheme 9.25). The cyclization is highly *trans* selective, with the imidazolidinone catalyst forming 1,2-disubstitued cyclopentanes [118]. The reaction tolerates aryl and alkyl substituents on the enone and can be carried out with enals, and also in the presence of heteroatoms (Scheme 9.55). Inverse (*cis*) diastereoselectivity was obtained in the intramolecular Michael addition with the cysteine-derived prolinamide analog **49** (Scheme 9.55) [119].

Activation of Enones via Iminium Formation

Chiral pyrrolidine and imidazolidinone catalysts have been successfully employed in inter- and intramolecular Michael reactions including conjugate reduction, Friedel–Crafts alkylations and cycloadditions (Scheme 9.56). In 1,4-addition, central to these

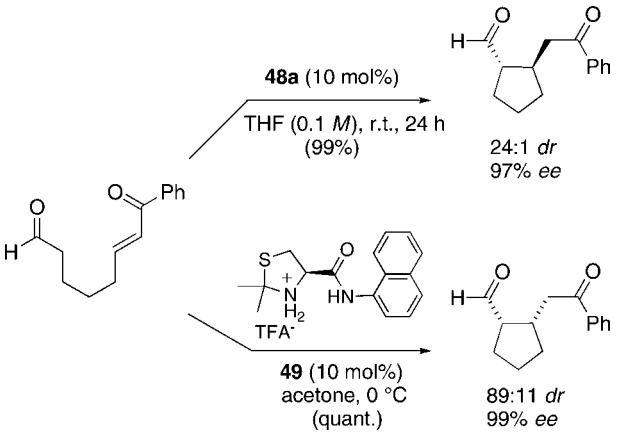

Scheme 9.55 Intramolecular addition of aldehydes to enones.

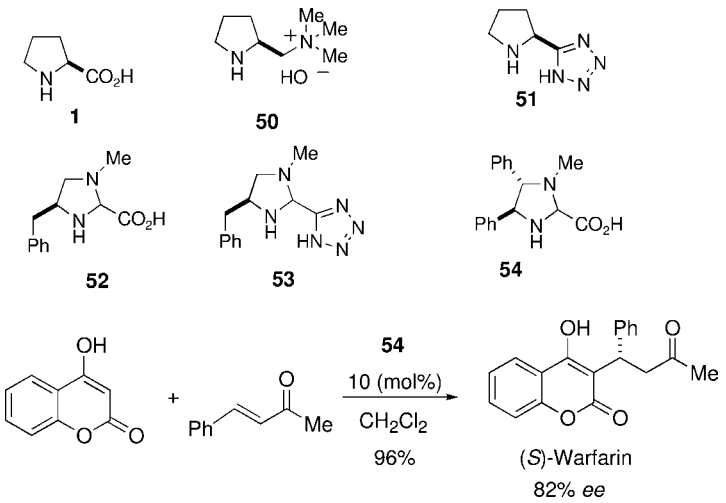

Scheme 9.56 Chiral pyrrolidine and imidazolidinone catalysts and the one-step preparation of warfarin.

reactions is the activation of an α,β unsaturated carbonyl compound by forming an iminium ion, which is activated to nucleophilic attack at the γ-carbon. Iminium activation is chemically equivalent to the electrophilic activation of the parent carbonyl compound resulting in LUMO lowering. The effectiveness of this approach is illustrated by the elegant enantioselective one-step preparation of one of the most widely used anticoagulants, warfarin (Scheme 9.56) [120].

Friedel–Crafts Alkylations

1,4-Additions of electron-rich aromatics and heteroaromatics to α,β-unsaturated aldehydes were developed with iminium catalysts. In particular, pyrrole, indole and

aniline derivatives were used as donors. The reaction is general with respect to the pyrrole architecture as far as incorporation of substituents at the C-2- or C-3-pyrrole positions provide regioselective alkylations at the C-5 and C-2 positions, respectively. The utility of this approach has been highlighted by the short and straightforward preparation of (−)-ketorolac (Scheme 9.57) [121].

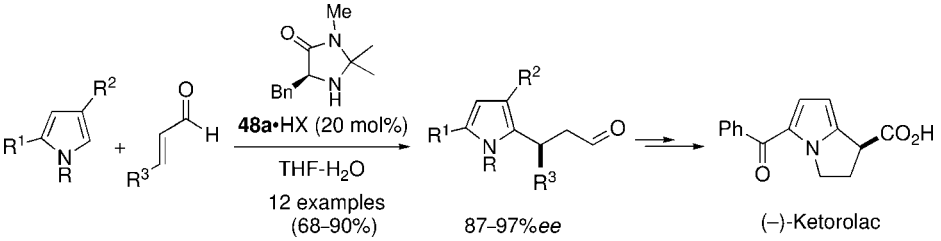

Scheme 9.57 Friedel–Crafts alkylations via iminium activation: synthesis of (−)-ketorolac.

Mukaiyama–Michael Reactions

Chiral imidazolidinone catalyst **5** can also catalyze the addition of silyloxyfurans to α,β-unsaturated aldehydes to provide γ-butenolides [122]. Remarkably, whereas similar Lewis acid-catalyzed transformations give almost exclusively 1,2-addition products (Mukaiyama–aldol reaction), the organocatalyzed variant affords only 1,4-adducts (Mukaiyama–Michael reaction), thus providing a new strategy for the catalytic preparation of enantiomerically enriched butenolides [123]. Treatment of 2-silyloxyfurans with a variety of α,β-unsaturated aldehydes afforded the desired products in good enantiomeric purity with predominantly *syn* selectivity. Significantly, the use of different reaction conditions, namely changing the co-catalyst and solvent, provided butenolide adducts of opposite sense of diastereoinduction, while retaining high levels of enantiocontrol. In a demonstration of the utility of this protocol, a four-step synthesis of spiculisporic acid, a *Penicillium spiculisporum* fermentation adduct which has found commercial application as a bio-surfactant for metal decontamination processes and fine polymer production, and its 5-*epi*-diastereomer has been accomplished (Scheme 9.58) [123].

9.3.3.2 **Cyclopropanation**

Ylide reactions have been developed as one of the powerful approaches for the synthesis of small-ring compounds. Among the vast array of asymmetric methods for the preparation of enantiomerically enriched cyclopropanes, few examples concern organocatalysis; worth mentioning are the pioneering work by the groups of Aggarwal, Gaunt and MacMillan.

Sulfur ylide-mediated cyclopropanation was developed by Aggarwal's group [124]. A sulfur ylide is generated *in situ* from a chiral sulfide catalyst and phenyldiazomethane in the presence of a transition metal catalyst (Scheme 9.59). A modified procedure was introduced by Aggarwal and co-workers which utilized the generation of the diazo compounds *in situ* from tosyl hydrazone salts at 40 °C in the presence of a phase-transfer catalyst.

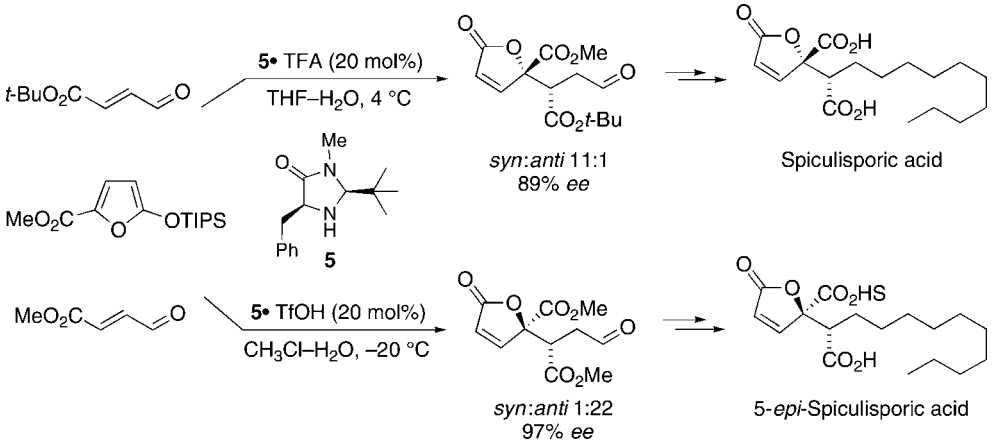

Scheme 9.58 Enantioselective addition of 2-silyloxyfurans to α,β-unsaturated aldehydes via iminium activation.

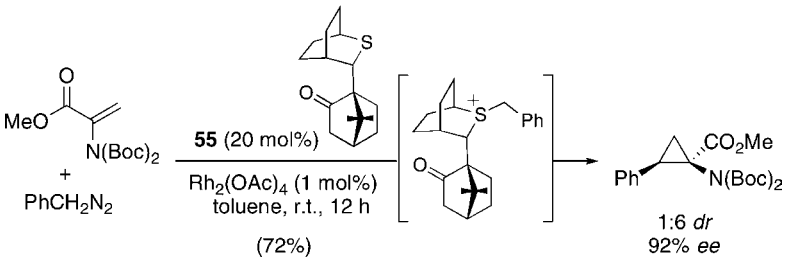

Scheme 9.59 Sulfur ylide-mediated enantiocatalytic cyclopropanation.

Ammonium ylides were generated using cinchona alkaloids by Gaunt and co-workers [125]. Mechanistically, the nucleophilic catalyst forms an ammonium salt with an α-bromocarbonyl species. The pK_a lowering effect of the salt readily effects deprotonation with a mild base to form the ylide, which subsequently undergoes conjugate addition and ring closure to form the cyclopropane as a single diastereomer. The reaction also works in an intermolecular fashion, forming bicycloalkanes in excellent yields and *ee*s (Scheme 9.60).

Another way of directing the stereoselectivity of the cyclopropanation reaction was described by Kunz and MacMillan, who applied the iminium catalysis concept effectively to activate alkene substrates [126]. α,β-Unsaturated aldehydes were converted in the presence of stabilized ylides and dihydroindole-2-carboxylic acid catalyst (**57**) to enantioenriched cyclopropanes (Scheme 9.61). The atypical reactivity and the stereocontrol were rationalized by a mechanistic postulate in which the chiral carboxylic acid catalyst allows the control of the iminium geometry and also by a direct electrostatic effect that activates the approaching sulfonium ylides.

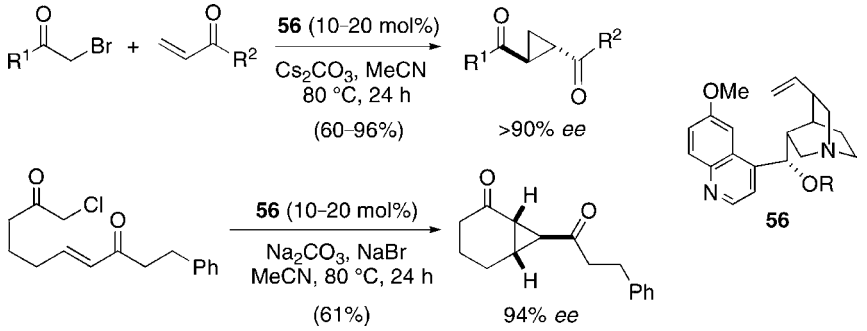

Scheme 9.60 Cinchona alkaloid-catalyzed cyclopropanation of activated alkenes.

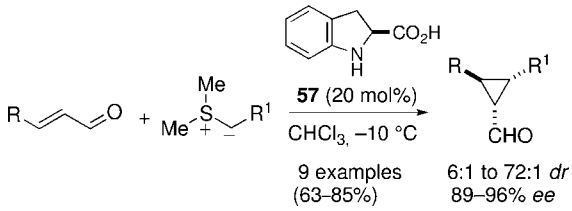

Scheme 9.61 Asymmetric cyclopropanation of activated alkenes via iminium catalysis.

9.3.3.3 Epoxidation of Alkenes

Although the greatest part of current methodology for the catalytic asymmetric epoxidation of alkenes relies on the use of chiral metal complexes [127], organocatalytic methods are taking a more and more important place [128]. Here a brief summary is given of the preparation of enantiomerically enriched epoxides from alkenes and alternative organocatalytic methods including the addition of chiral sulfur ylides to aldehydes [129].

Epoxidation of Electron-deficient Alkenes with Hydrogen Peroxide

Jørgensen and co-workers developed an asymmetric approach allowing the conversion of enals to epoxides. The best catalyst in this transformation was the chiral pyrrolidine **3b** and H_2O_2 as oxidant. The reaction follows the concept of iminium catalysis as depicted in Scheme 9.62 [130]. Importantly, the reaction conditions are

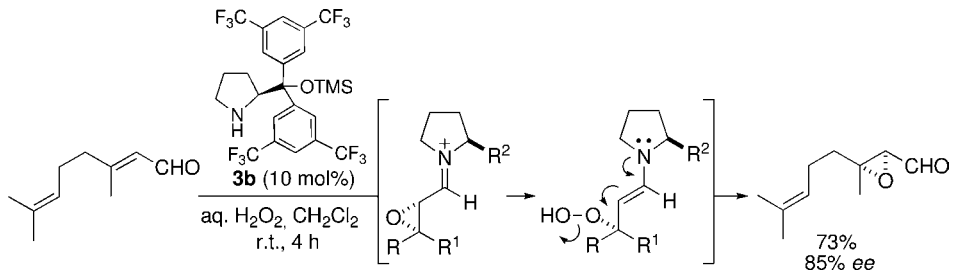

Scheme 9.62 Asymmetric epoxidation of enals by H_2O_2.

tolerant to a variety of functionalities and this chemical transformation proceeds in different solvents with no loss of enantioselectivity.

Cyclic enones can be oxidized likewise using hydrogen peroxide as oxidant and chiral diamine catalysts such as 1,2-diphenylethane-1,2-diamine (DPEN) TFA salt or with a chiral phosphate co-catalyst (TRIP) [131]. The DPEN salts proved to be both active and highly enantioselective catalysts for the oxidation of unsubstituted cyclohexanones when the diamine catalyst was obtained with DPEN mono-TRIP salt, although the TFA salt gave a high yield and enantioselectivity. As in the preceding transformation, the reaction is believed to proceed via an iminium ion intermediate. The second basic amine site of the catalyst may organize the TS by directing the attack of hydrogen peroxide towards one enantioface of the double bond.

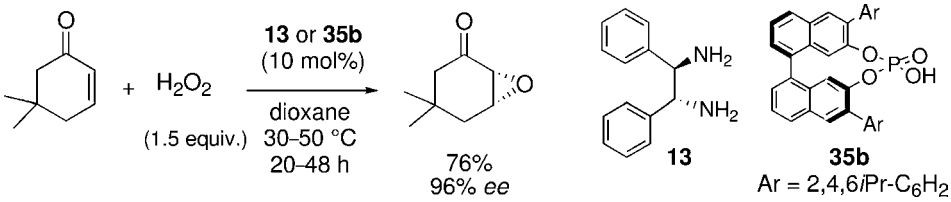

Scheme 9.63 Asymmetric epoxidation of cyclic enones.

The polyleucine-mediated epoxidation, the so-called Julia–Colonna reaction, includes biphasic reaction systems (e.g. use of DBU in THF along with urea–H_2O_2 as oxygen source), which can give shorter reaction times and improved scope [132, 133]. Most of the enones used in this chemistry have aryl, heteroaryl or alkenyl substituents in the β-position, but alkyl substituents can be tolerated in the α′-position. α-Substituted enones are generally unreactive, with the exception of some examples where the alkene is exocyclic to a cyclic ketone, which is suggested to be due to the need for an s-*cis*-enone conformation for the reaction to occur. Most of the enantioselectivities obtained are excellent (>90% *ee*). The synthetic utility of the products has been demonstrated by application to target synthesis; the preparation of the blood pressure-lowering agent diltiazem (Scheme 9.64) illustrates a common tactic since epoxidation of enone is followed by Baeyer–Villiger reaction to give the desired epoxy ester [134].

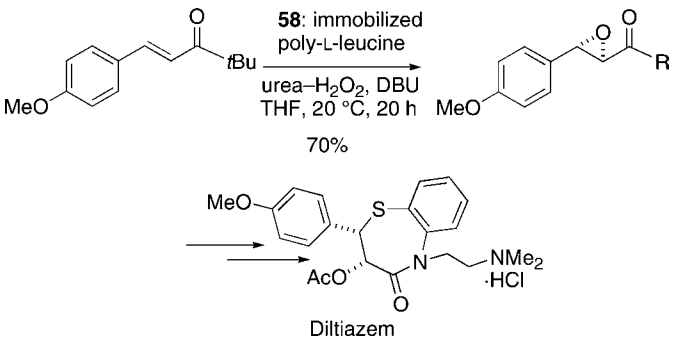

Scheme 9.64 Polyleucine-mediated epoxidation in the synthesis of diltiazem.

Epoxidation of Alkenes via Chiral Dioxirane Intermediates [128b–d]
Isolated alkenes can be oxidized by the triple salt Oxone ($2KHSO_5.KHSO_4.K_2SO_4$), of which the active constituent is $KHSO_5$. Interaction of Oxone with the ketone precursor produces the reactive dioxirane that transfers oxygen to alkenes in a concerted (although possibly asynchronous) manner, resulting in stereospecific epoxidation (i.e. retention of the alkene geometry of the starting alkene). Importantly, the starting ketone or iminium salt is regenerated and so in principle can be used in sub-stoichiometric quantities (Scheme 9.65).

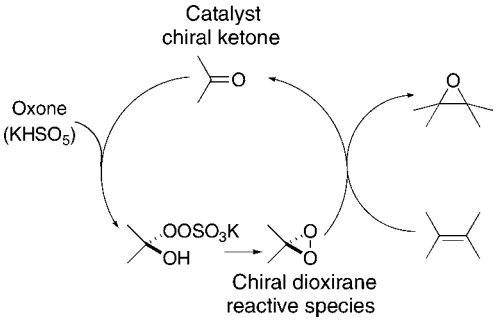

Scheme 9.65 General mechanism of the ketone-catalyzed alkene epoxidation.

Among the chiral ketones developed for asymmetric oxidation, the fructose-derived Shi catalyst and also the binaphthol-derived Yang catalysts have attracted particular attention (Scheme 9.66).

Both oxidation systems have found applications in total synthesis [128b, c] [135]. Particularly attractive are examples in which it has been used to establish the stereochemistry of polyepoxides that can undergo cascade cyclizations to polyether products, mimicking possible biosynthetic pathways. An example is the construction of the tetrahydrofuran rings of the natural product glabrescol via highly stereoselective formation of the tetraepoxide from the polyene (Scheme 9.67). [136].

The replacement of the acetonide function in **59** by a diacetate slows the Baeyer–Villiger decomposition of the catalyst and enables **62** to convert *trans*- and trisubstituted α,β-unsaturated esters to the corresponding epoxides (Scheme 9.68) [137]. In contrast, the catalyst **62** does not allow high *ee* to be obtained for *trans*-aliphatic α,β-unsaturated esters and *cis*-cinammates.

Epoxidation of Alkenes via Acyl Peroxide Intermediates
Oligopeptide catalysts were engineered for the transformation of allylic carbamates to chiral epoxides. The peracid, generated catalytically by H_2O_2 or by the use of hydrogen peroxide–urea clathrate (UHP) from the γ-carboxylic acid function of L-aspartate incorporated into a tripeptide, provided the chiral environment necessary for asymmetric transformation (Scheme 9.69) [138, 139].

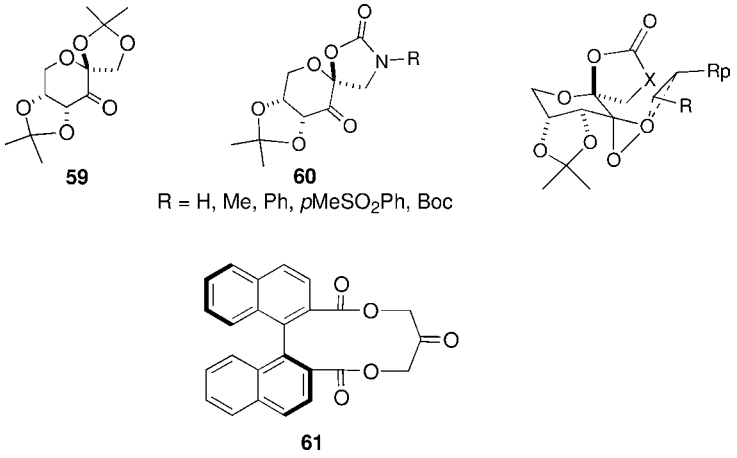

Scheme 9.66 The first- (**59**) and second-generation (**60**) Shi catalysts with the proposed selectivity model and the Yang catalyst (**61**).

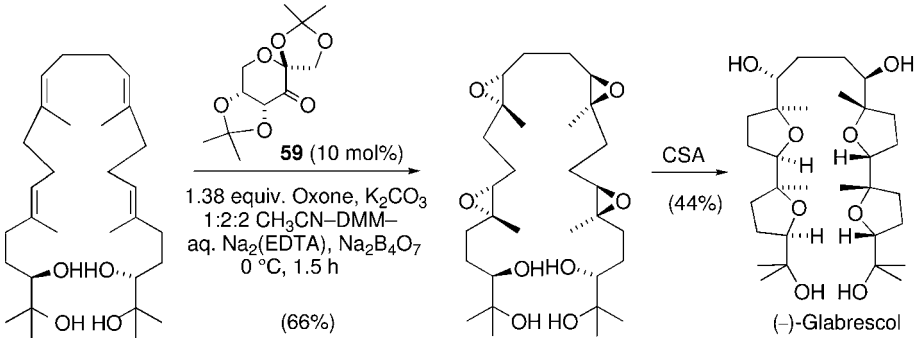

Scheme 9.67 Shi epoxidation in the total synthesis of (−)-glabrescol.

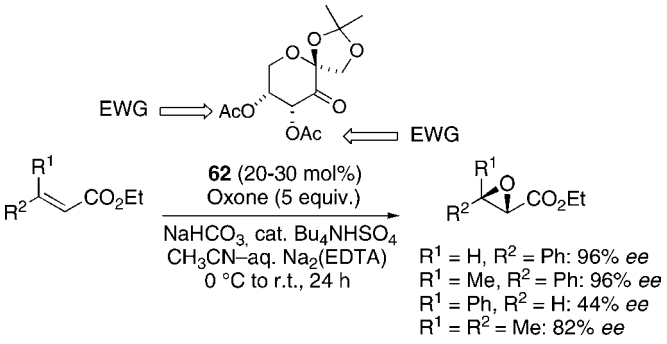

Scheme 9.68 Asymmetric oxidation of electron-poor olefins using modified Shi catalyst.

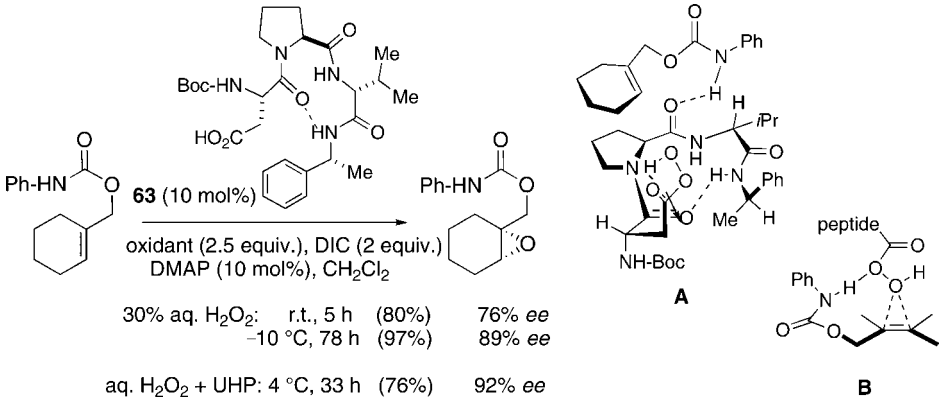

Scheme 9.69 Oligopeptide catalyst-mediated epoxidation of allylic carbamates.

9.3.3.4 Cycloaddition reactions

[4 + 2] Additions

[4 + 2] Additions via Iminium Activation

A MacMillan's iminium catalyst such as **5** was used for the addition of a range of α,β-unsaturated aldehydes (dienophiles) to a variety of symmetrical and unsymmetrical dienes (Scheme 9.70). This chemistry has been highlighted in a number of excellent reviews [18].

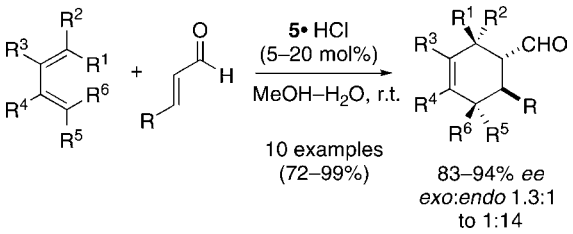

Scheme 9.70 MacMillan's imidazolidinone-mediated [4 + 2] reaction between dienes and α,β-unsaturated aldehydes.

The reaction probably takes place via an asynchronous mechanism where the attack of the diene on the β-carbon atom of the iminium ion is the rate-limiting step and the π–π interaction between the phenyl ring of the catalyst benzyl group and the alkeneic π-system of the iminium ion accounts for the selectivity of the reaction. The reaction was used in the synthesis of (+)-hapalindole Q, a tricyclic alkaloid natural product containing four contiguous stereocenters (Scheme 9.71).

MacMillan's imidazoline catalysts are inefficient for the activation of α-substituted enones. The scope of this formal [4 + 2] cycloaddition was extended to α-substituted α,β-unsaturated aldehydes as dienophiles by using a primary amine organocatalyst, **64** [140] (Scheme 9.72).

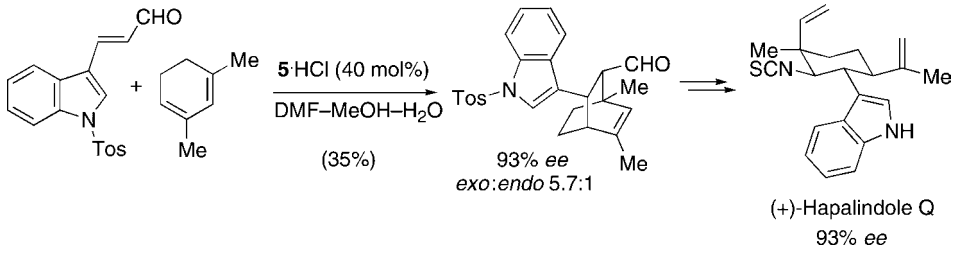

Scheme 9.71 Synthesis of (+)-hapalindole Q via iminium-mediated formal [4 + 2] cycloaddition.

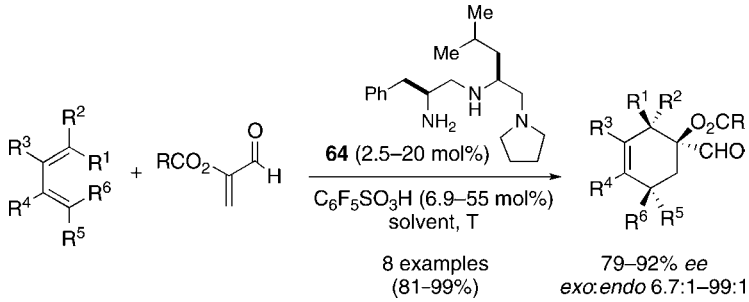

Scheme 9.72 The formal [4 + 2] cycloaddition of α-substituted α,β-unsaturated aldehydes.

The iminium activation strategy was applied in an intramolecular Diels–Alder reaction [141]. This LUMO-lowering iminium activation strategy allowed the preparation of various cycloadducts incorporating ether and quaternary carbon functionalities (Scheme 9.73). The synthetic potential of this methodology was demonstrated by the total synthesis of the marine metabolite solanapyrone D.

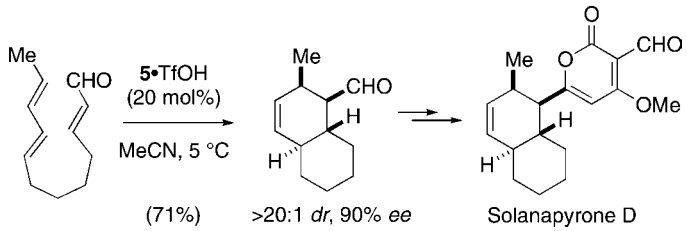

Scheme 9.73 The asymmetric intramolecular Diels–Alder reaction in the synthesis of solanapyrone D.

A similar strategy was used by Selkälä and Koskinen to prepare other bicyclo[4.3.0] nonanes and was applied to the synthesis of amaminol A, a cytotoxic agent against murine leukemia cells (Scheme 9.74) [142].

Imidazolidinone catalyst **65** was identified for Diels–Alder transformations using simple ketone dienophiles (Scheme 9.75) [143]. This reaction is fairly general with respect to diene structure, allowing enantioselective access to a broad range of alkyl-, alkoxy-, amino- and aryl-substituted cyclohexenyl ketones.

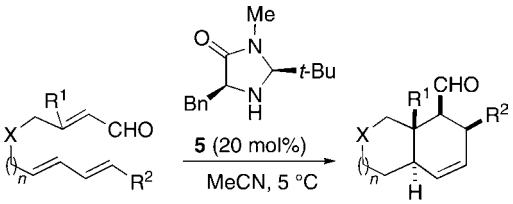

n = 1, X = CH_2, O
R^1 = H, CH_3 (75–99%) >90% *de*
R^2 = Ph, CH_2 = CH, OBn 93–94% *ee*

n = 2, X = CH_2 >90% *de*
R^1 = H, R^2 = Ph (70%) 92% *ee*

Scheme 9.74 The asymmetric intramolecular Diels–Alder reaction in the synthesis of amaminol A.

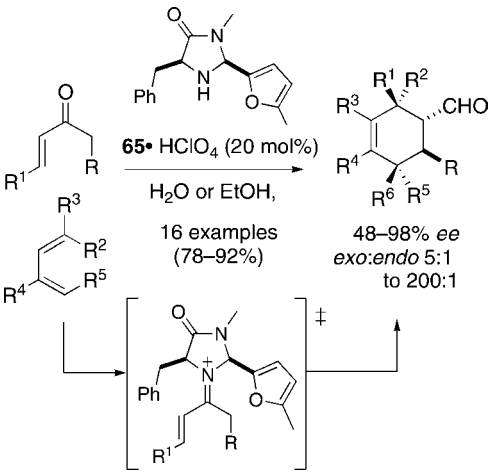

Scheme 9.75 Formal Diels–Alder reaction of simple ketone dienophiles via iminium activation.

Hetero-Diels–Alder Reactions via Brønsted Acid Catalysis

Since the discovery by Huang and Rawal that hetero-Diels–Alder (HDA) reactions between 1-amino-3-silyloxybutadiene and unactivated aldehydes and ketones are considerably accelerated in protic solvents [144], chiral alcohol **3b** has been investigated, in addition to new hydrogen-bonding catalysts derived from TADDOL and binaphthyl (BAMOL) (**5e**) [145] (Scheme 9.76). The acceleration of the reactions is promoted by hydrogen bonding interaction between the diol catalyst and the carbonyl group, as depicted in Scheme 9.2b.

Organocatalyzed aza-Diels–Alder reactions using arylaldimines were also developed in the presence of chiral phosphoric acids as catalysts [146, 147]. These transformations usually provided less selective additions.

Hetero-Diels–Alder Reactions via Enamine Activation

Enamine activation can be used for mediating inverse electron demand [4 + 2] reactions. Chiral secondary amines such as depicted in Scheme 9.77 generate the

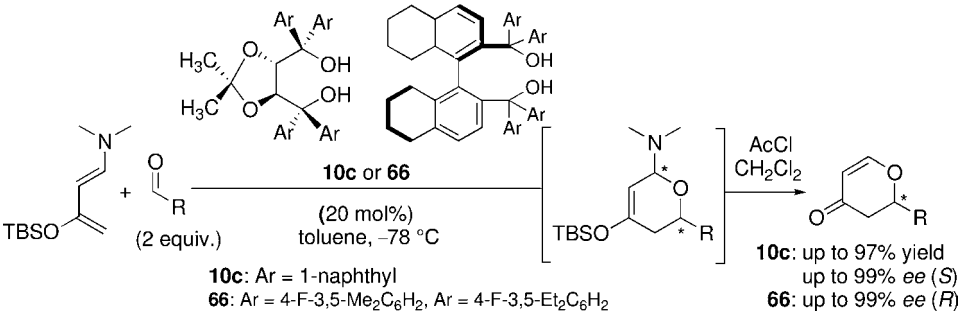

Scheme 9.76 Chiral Brønsted acid-catalyzed hetero-Diels–Alder reaction.

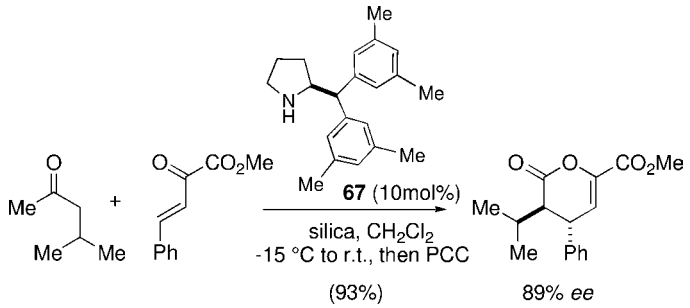

Scheme 9.77 Chiral pyrrolidine-mediated formal [4 + 2] inverse electron demand cycloaddition.

electron-rich enamines from aldehydes, which react subsequently with the enone [148].

[3 + 2] Cycloadditions

[3 + 2] Cycloadditions via Brønsted Acid Activation

N-Protected aryl- and heteroarylaldimines add to electron-deficient allene in the presence of phosphinthiourea catalysts and provide 2-aryl-2,5-hydropyrroles via a [3 + 2] cycloaddition (Scheme 9.78) [149]. The presence of both H_2O and Et_3N as additives was found to be important for achieving optimal rates. Dual activation of both nucleophile and electrophile by the bifunctional catalyst is invoked to account for the observed high reactivity and enantioselectivity. According to the rationale, the thiourea binds and activates the imine by association with the oxygen atom of the phosphinoyl group (Scheme 9.2c-1) and the delivery of the phosphonium ion enolate takes place from the imine *re* face with the thiourea catalyst.

The three-component asymmetric 1,3-dipolar addition reaction between aldehydes, amino esters and dipolarophiles can be promoted by BINOL-derived chiral phosphoric or bisphosphoric acid [150]. As in the former example, the stereoselectivity is controlled by a chiral Brønsted acid bonded to the azomethyne complex (Scheme 9.79). This procedure allows a rapid diversity-oriented synthesis of polyfunctionalized chiral pyrrolidine derivatives.

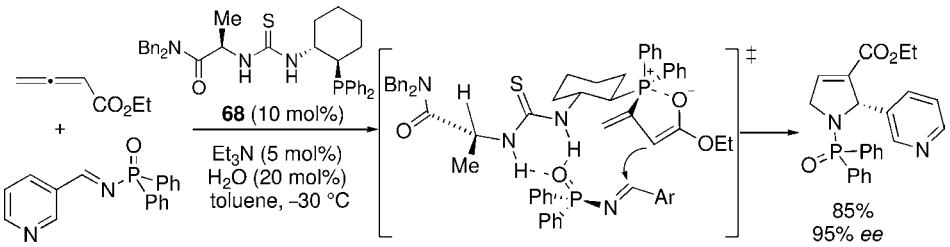

Scheme 9.78 Phosphinthiourea-mediated addition of aldimines to electron-deficient allenes.

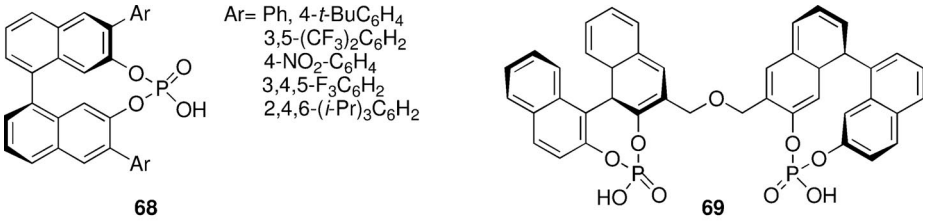

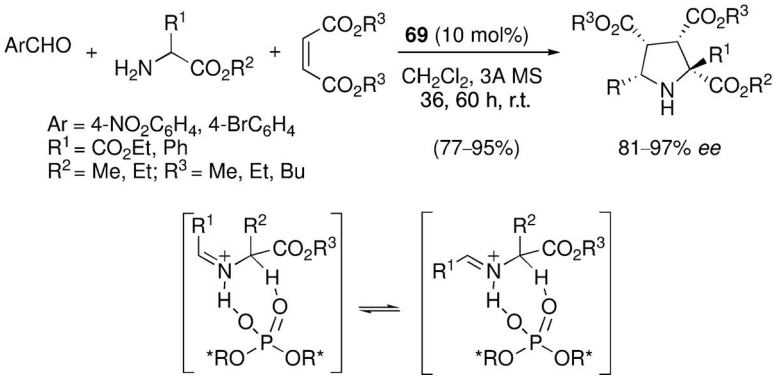

Scheme 9.79 Chiral phosphoric acid-catalyzed three-component asymmetric 1,3-dipolar addition reaction between aldehydes, amino esters and dipolarophiles.

Lewis Acid (Iminium) Activation in [3 + 2] Addition

The addition of several α,β-unsaturated aldehydes to a variety of *N*-alkylated nitrones in the presence of catalytic amounts of imidazolidinone **5** afforded the corresponding isoxazolidines (Scheme 9.80). While the reaction tolerates relatively large functionalization on the nitrone, only limited variation of the dipolarophile can be achieved: crotonaldehyde ($R^2 = Me$) and acrolein ($R^2 = H$) generate cycloadducts in good yields and selectivities, but other β-substituted enals are largely unsuccessful due to the sluggish nature of these reactions.

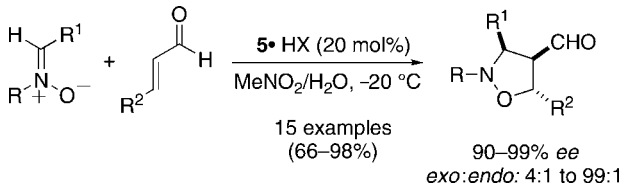

Scheme 9.80 The MacMillan imidazolidinone-catalyzed addition of α,β-unsaturated aldehydes to *N*-alkylated nitrones.

The scope of the reaction was expanded to the 1,3-dipolar cycloaddition of nitrones to cyclic α,β-unsaturated aldehydes, allowing the formation of fused bicyclic isoxazolidines (Scheme 9.81). Noteworthily, the use of catalyst **5** resulted in almost no reaction, whereas a proline-based diamine (**70**) afforded high levels of enantio- and diastereoselectivity [151].

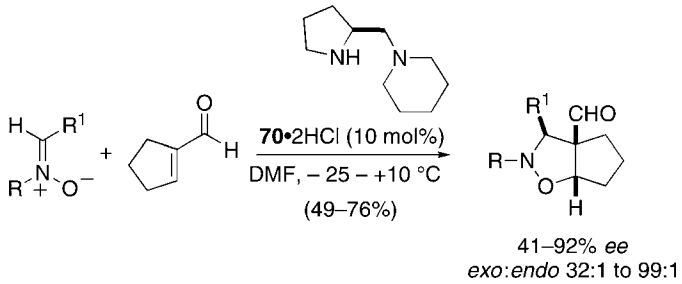

Scheme 9.81 Prolinamide salt-catalyzed asymmetric 1,3-dipolar cycloaddition of nitrones to cyclic α,β-unsaturated aldehydes.

[2 + 2] Cycloadditions

The β-Lactam Synthesis

The best-performing chiral catalysts to date in the dimerization of ketenes, and also in related cycloadditions between ketenes and C=O or C=N compounds, are cinchona alkaloids. Ketenes can be formed from acyl chlorides under homogeneous conditions by using proton-sponge or phosphazine as base (BEMP), but also under heterogeneous conditions using K_2CO_3, NaH, $NaHCO_3$ or a resin-bound variant of BEMP. The cycloaddition reaction can be performed without epimerization of the formed stereocenters when non-pyrolytic methods are used for the preparation of the ketene reagents and also when *O*-functionalized quinine or quinidine derivatives such as *O*-Bz (**39**), *O*-*n*-Pr or *O*-TMS analogs are used [152]. Aldehydes form β-lactones with ketenes in high selectivity and chemical yield [76c]. This reaction was also extended to the addition of ketenes to imines affording β-lactams. A short application of this reaction was described in the preparation of β-substituted aspartic acid derivatives via a cinchona-catalyzed [2 + 2] enantioselective cycloaddition one-pot synthesis (Scheme 9.82).

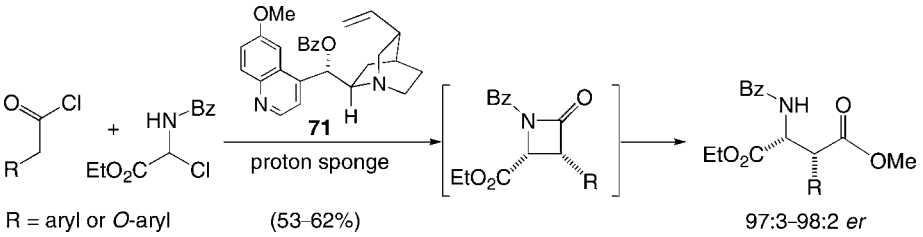

Scheme 9.82 Cinchona alkaloid-catalyzed [2 + 2] enantioselective cycloaddition of *in situ*-generated ketenes to imines.

Although the reaction depicted in Scheme 9.82 proceeds without a Lewis acid co-catalyst, the reaction is far more efficient in its presence. For example, Nelson and co-workers reported that lithium perchlorate assisted the cinchona alkaloid-catalyzed addition of ketenes (generated *in situ* from acid chlorides) to aldehydes to form β-lactones in excellent yields, *dr*s and *ee*s [153]. Lectka and co-workers also reported that the indium(III) complex of a salicylquinine derivative effectively forms the corresponding β-lactam structure from the reaction of ketenes and imines also with excellent stereoselectivities [154].

9.3.3.5 Transfer Hydrogenation of Alkenes

Organocatalytic transfer hydrogenation relies on a similar mechanism to NADH or $FADH_2$ reduction of substrates in combination with enzymes. MacMillan's imidazolidinone catalyst permits LUMO-lowering activation in combination with dihydropyridine (Hantzsch ester I) analogs. The method was used for the selective reduction of various α,β-unsaturated aldehydes [155], and also of β-aryl-β-methyl α,β-unsaturated aldehydes [156]. Importantly, in the latter case an enantioconvergent process was observed when the mixtures of (*E*)- and (*Z*)-alkene substrates could be hydrogenated with comparable enantioselectivities, providing identical enantiomers as the major product (Scheme 9.83).

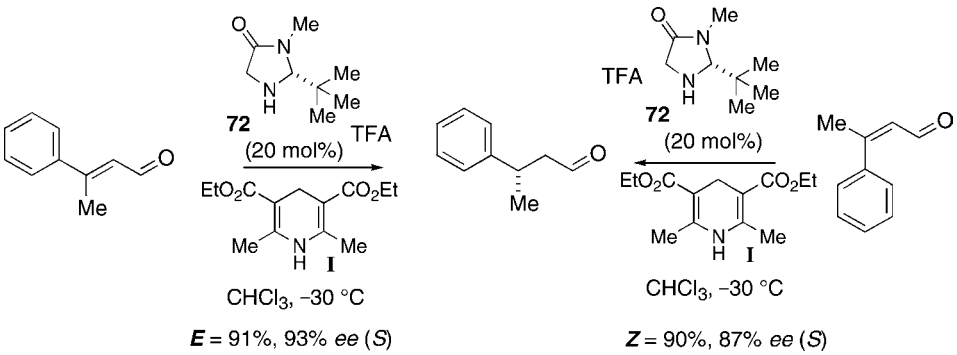

Scheme 9.83 Enantioconvergent reduction of β-aryl-β-methyl α,β-unsaturated aldehydes in the presence of MacMillan's imidazolidine **72** and Hantzsch ester **I**.

9.3.4
Organocatalytic Multicomponent and Cascade Reactions [157]

Organocatalytic reactions are particularly well suited for sequential transformations, providing easy access to structurally complex skeletons from simple starting materials.

9.3.4.1 Single Catalyst-mediated Domino Reactions

The Addition–Cyclization Strategy

Probably the simplest way to generate multiple bonds in a single reaction is to take advantage of the difference in reactivity between inter- and intramolecular reactions. Such a sequence can be realized by an (*S*)-proline-catalyzed asymmetric Mannich-type addition of methyl ketones to form β-carbolines [158]. The reaction was used in the synthesis of the tetracyclic precursor of yohimbine and deserpidine (Scheme 9.84).

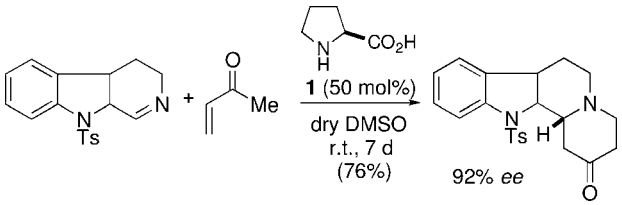

Scheme 9.84 (*S*)-Proline-catalyzed asymmetric synthesis of β-carbolines.

Another example is drawn from the synthesis of (+)-fawcettimine involving a catalytic 1,4-addition–intramolecular aldolization as a key step to prevent heteroatom-substituted hydrianones from participating in the cross-coupling reaction (Scheme 9.85) [159]. Using an organocatalytic Robinson annulation, reaction between a keto ester and crotonaldehyde gave 2-allylcyclohexanone in 88% *ee* and 72% yield.

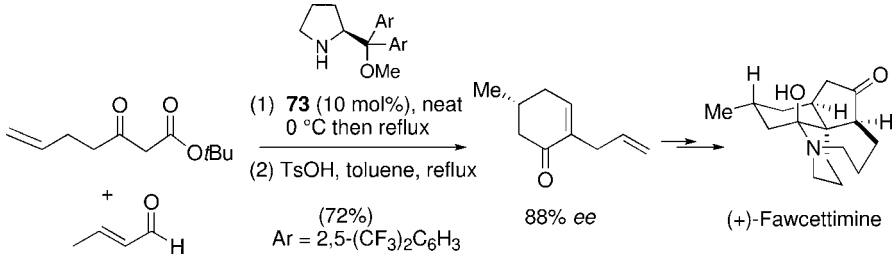

Scheme 9.85 Asymmetric 1,4-addition–Robinson annulation sequence in the synthesis of (+)-fawcettimine.

A one-pot Michael addition Darzens-type domino reaction of α,β-unsaturated aldehydes and γ-chloro-β-keto esters was realized in preparing highly functionalized cyclohexanone oxides (Scheme 9.86) [160]. After decarboxylation, the products were isolated as a single diastereoisomer.

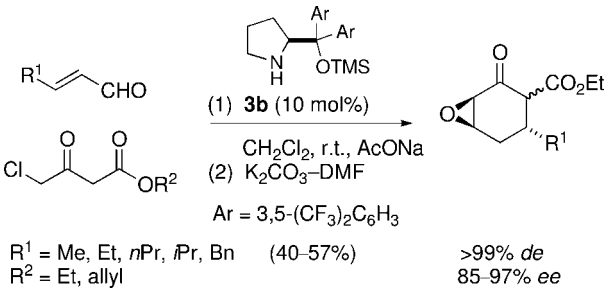

Scheme 9.86 One-pot Michael addition Darzens-type domino reaction of α,β-unsaturated aldehydes and γ-chloro-β-keto esters.

A similar Michael addition–aldol condensation sequence has been devised for the synthesis of chiral tetrahydrothiophenes containing three stereocenters starting from various enals and 2-mercapto-1-phenylethanone and employing a TMS-protected proline derivative (**3b**) as catalyst (Scheme 9.87). It is possible to control the regioselectivity of this domino reaction by varying the pH; indeed, diastereomerically pure (tetrahydrothiophen-2-yl)phenylmethanones were obtained on adding $NaHCO_3$, whereas the same reaction performed with benzoic acid led to tetrahydrothiophene carbaldehydes having one quaternary center [161].

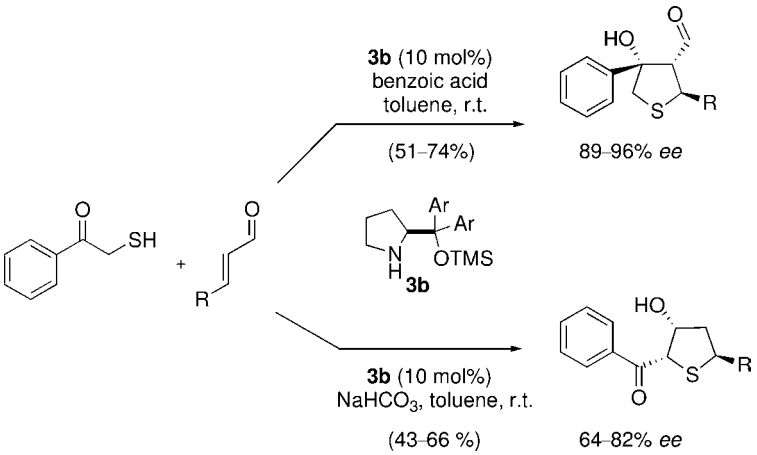

Scheme 9.87 Michael reaction–aldol condensation sequence in the synthesis of chiral tetrahydrothiophenes.

The power of the iminium activation protocol was demonstrated by the synthesis of (−)-flustramine B (Scheme 9.88) [162]. In this sequence, the intermediate iminium is intercepted by intramolecular addition forming the tetrahydropyrroloindoline backbone.

An imidazolidine catalyst can promote the tandem Michael reaction–aldol sequence between α,β-unsaturated ketones and a variety of aromatic and heteroaromatic β-keto esters to provide cyclohexanones containing three or four contiguous

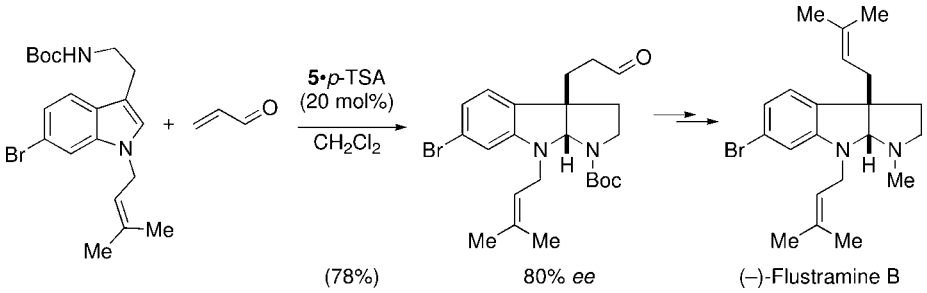

Scheme 9.88 Synthesis of (−)-flustramine B via an addition–cyclization protocol.

stereogenic centers with excellent enantio- and diastereoselectivity (Scheme 9.89) [163]. The first step consists in an intermolecular Michael addition, followed by an intramolecular aldol condensation forming the elaborated cyclohexanone. The whole reaction takes place thanks to a triple role of the catalyst, which first activates the Michael acceptor by formation of an iminium ion, then generates the active Michael donor deprotonating the β-keto ester and finally acts as a base in the intramolecular aldol reaction.

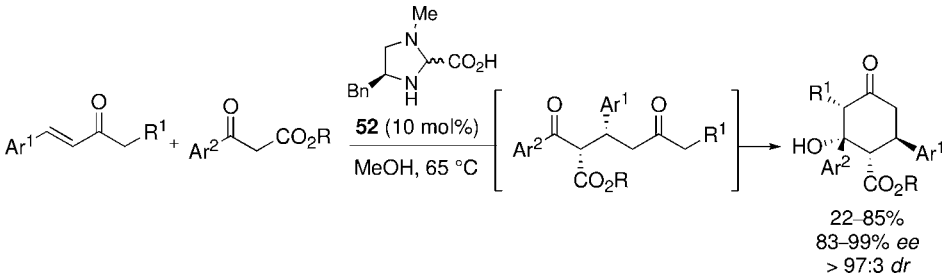

Scheme 9.89 Chiral cyclohexanone synthesis by tandem Michael reaction–aldol sequence between α,β-unsaturated ketones and aromatic and heteroaromatic β-keto esters.

The two-fold domino Michael addition of γ,δ-unsaturated β-keto esters to nitroalkenes catalyzed by a bifunctional thiourea gives rise to highly functionalized cyclohexanones (Scheme 9.90) [164]. The three contiguous stereogenic centers of the

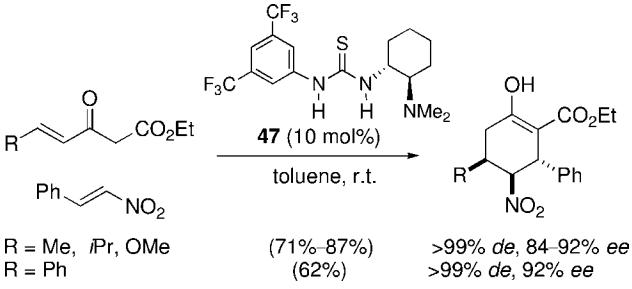

Scheme 9.90 Two-fold domino Michael addition sequence in the synthesis of functionalized cyclohexanes.

products were constructed with high diastereo- and enantioselectivity. This sequence was further applied to the total synthesis of (−)-epibatidine.

A chiral carbene derived from aminoindanol triazolium salts mediated the addition of α,β-unsaturated aldimines to electron-deficient alkenes in azadiene Diels–Alder reactions (Scheme 9.91) [165]. This strategy, mediated by an *N*-heterocyclic carbene, involved the generation of a highly reactive dienophile that participated in LUMO diene-controlled Diels–Alder cyclizations with α,β-unsaturated imines.

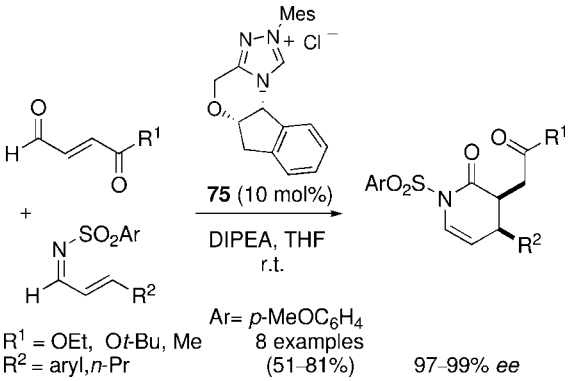

Scheme 9.91 Michael reaction–aldol condensation sequence in the synthesis of chiral tetrahydrothiophenes.

Multicomponent Reactions

Catalysts may promote the assembly of different organic elements. The acid-catalyzed three-component one-pot condensation of an aldehyde, a β-keto ester and (thio) urea, the so-called Biginelli reaction, was realized with a chiral phosphoric acid catalyst (**74**) [166]. The partial steps of the transformation involve a condensation of the urea with the aldehyde, yielding an iminium intermediate that undergoes aldol-type reaction with the keto ester followed by cyclization under the reaction conditions and affords chiral DHMP (Scheme 9.92).

The interconversion of enamines and iminium intermediates was also exploited synthetically in sequential transformations. As the 1,4-addition to iminium-activated enones gives rise to enamines and, in turn, the reaction of enamines gives rise to iminium intermediates, these intermediates can be intercepted with suitable reagents. In seminal work, Enders *et al.*'s three-component domino reaction between excess of aldehyde, nitroalkene and a nearly stoichiometric amount of α,β-unsaturated aldehyde afforded tetrasubstituted cyclohexene carbaldehydes in good yields, high diastereoselectivity and in almost complete enantioselectivity (Scheme 9.93) [167]. The first step of the catalytic cycle involves the conjugate addition via enamine formation of aldehyde and the nitroalkene followed by a Michael addition between the nitroalkane and the α,β-unsaturated aldehyde via an iminium intermediate. The third step of the domino sequence is an intramolecular aldol reaction of the enamine and a subsequent dehydration gives rise to the polyfunctional cyclohexene. The

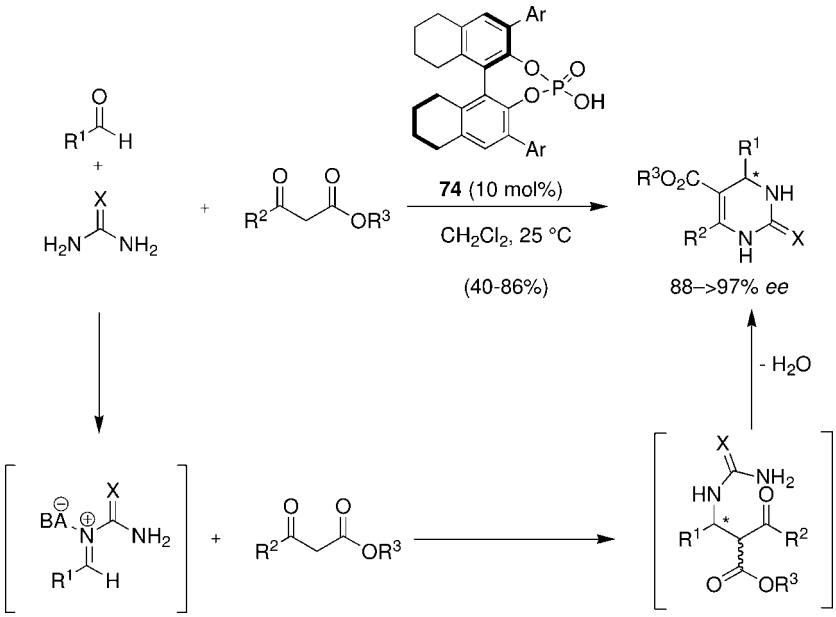

Scheme 9.92 Chiral phosphoric acid-catalyzed Biginelli reaction.

overall high stereoselectivity of the transformation is the consequence of the high selectivity of the first Michael addition; the resulting intermediate presumably dictates the stereochemistry of the reaction.

A catalytic enantioselective strategy was developed in which substituted phenols are directly converted to complex non-racemic molecular architectures (Scheme 9.94) [168]. The process involves oxidative dearomatization of substituted phenols followed by a desymmetrizing secondary amine-catalyzed asymmetric intramolecular Michael addition and forms a range of highly functionalized polycyclic molecules with excellent selectivity.

A domino Mannich–Wittig olefination reaction was devised allowing easy entry to functionalized α,β-unsaturated esters (Scheme 9.95) [169]. A subsequent diastereoselective dihydroxylation of the products allowed the corresponding amino- and iminosugar derivatives to be obtained stereoselectively in two steps (Scheme 9.95).

MacMillan's catalyst **5** allowed the combination of the domino 1,4-hydride addition followed by intramolecular Michael addition (Scheme 9.96) [20a]. The reaction is chemoselective, as the hydride addition takes place first on the iminium-activated enal. The enamine product of the reaction is trapped in a rapid intramolecular reaction by the enone, as depicted in Scheme 9.96. The intramolecular trapping is efficient and no formation of the saturated aldehyde can be observed. The best results were obtained with MacMillan's imidazolidinium salt **5** and Hantzsch ester **I** as hydride source. As was the case in the cyclization reaction, the reaction affords the thermodynamic *trans* product in high selectivity. Interestingly, an opposite sense of asymmetric induction was noted compared with the transformation discussed in Scheme 9.80.

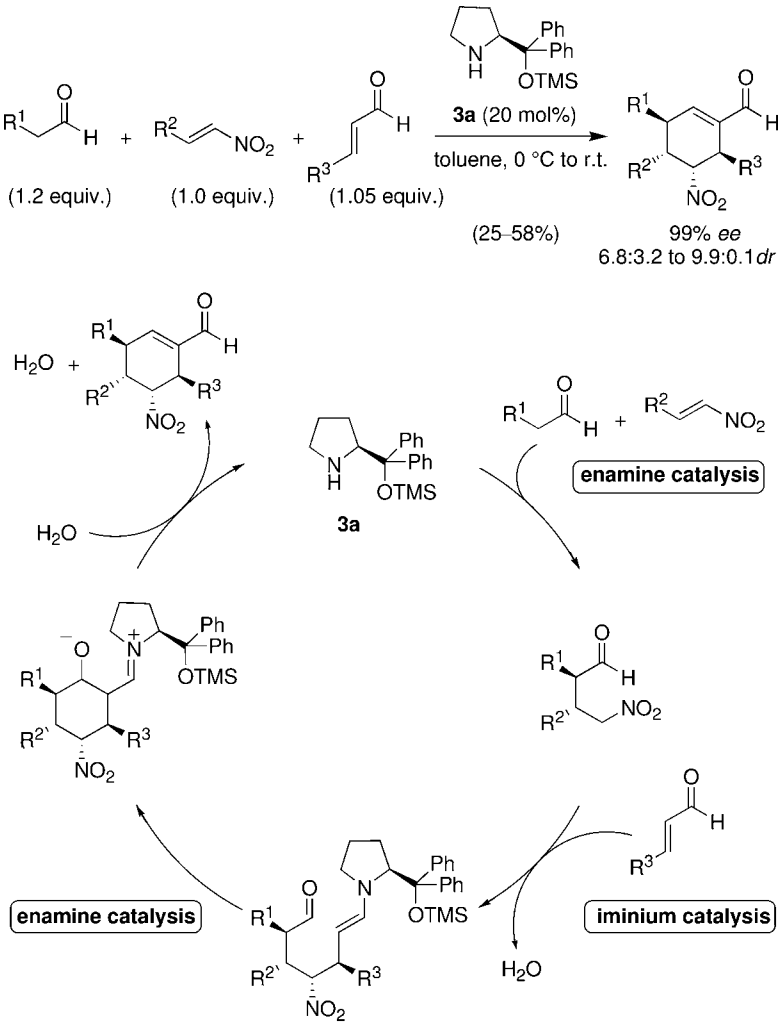

Scheme 9.93 Enders *et al.*'s three-component catalytic asymmetric domino reaction.

9.3.4.2 **Multicatalyst Cascade Reactions**

Polyfunctionalized tricyclic carbon frameworks containing up to eight stereogenic centers were realized in a single pot by relaying Enders *et al.*'s cyclohexenal synthesis with an intramolecular Diels–Alder (IMDA) strategy (Scheme 9.97) [170]. In this case the cyclohexene carbaldehyde product bears a diene moiety able to undergo subsequent cycloaddition. The one-pot synthesis was performed by dilution of the mixture with dichloromethane after complete consumption of the starting materials and adding an excess of dimethylaluminum chloride at −78 °C. In this new Michael–Michael–aldol condensation– IMDA process, five new C−C bonds and eight

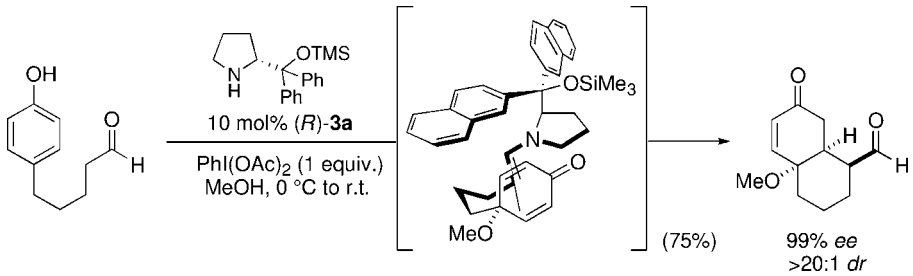

Scheme 9.94 The oxidative dearomatization–intramolecular Michael addition strategy in the synthesis of functionalized polycyclic molecules.

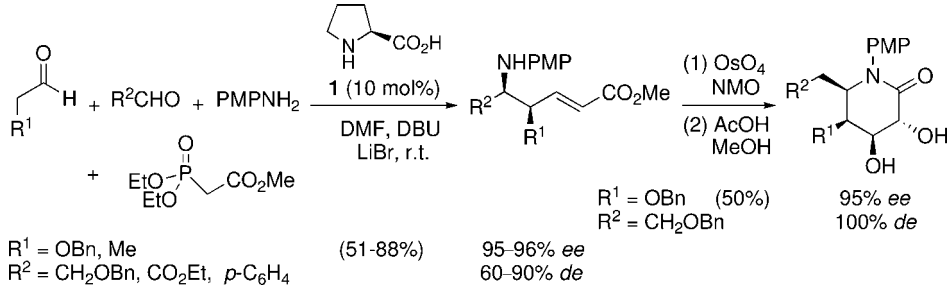

Scheme 9.95 The domino Mannich–Wittig olefination sequence.

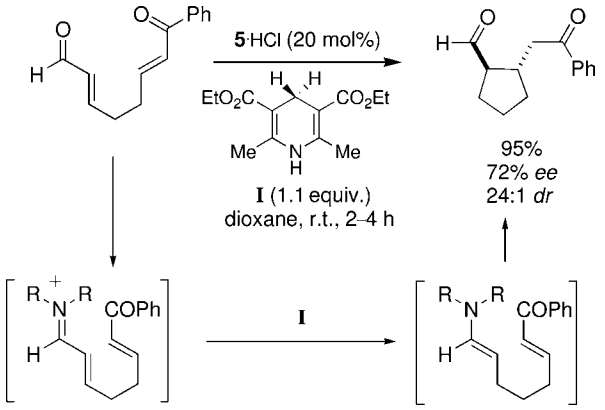

Scheme 9.96 Domino 1,4-hydride addition followed by intramolecular Michael addition.

stereogenic centers were formed with complete enantioselectivity in four steps (>99%). The *endo* approach is favored due to kinetic control and steric interactions in the TS. In this way, decahydroacenaphthylene and decahydrophenalene cores are obtained, which are advanced precursors of biologically active natural products.

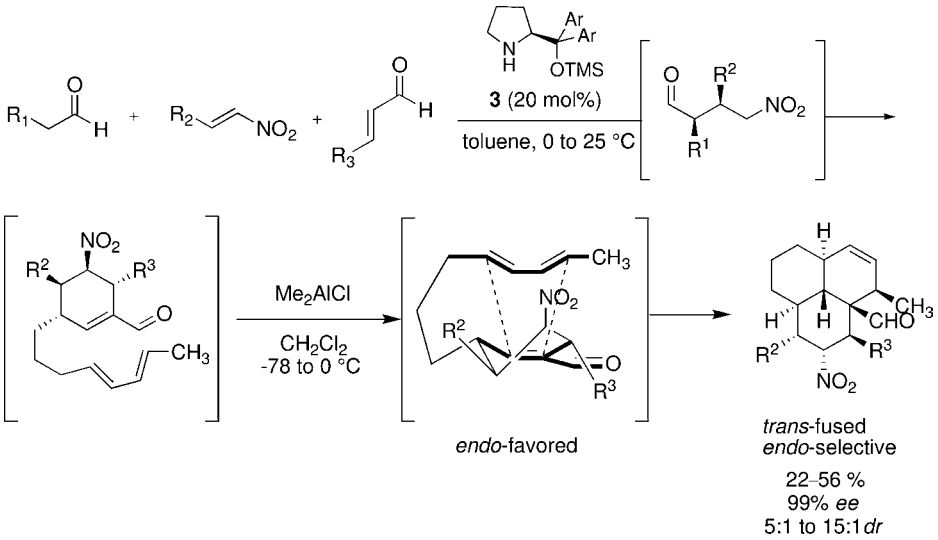

Scheme 9.97 Michael–Michael–aldol condensation–intramolecular Diels–Alder strategy in the synthesis of polycyclic compounds.

9.4 Conclusion

Asymmetric organocatalytic reactions offer synthetically viable alternatives to metal complex-mediated reactions. Most of the major enantiocatalytic transformations have found organocatalytic alternatives, but reaction scopes usually remain below those of metal complex-mediated reactions. Bifunctional cooperative chiral catalysts having both nucleophilic Lewis base and Brønsted acid sites were found to be the most efficient. While many important factors that govern reactions have been uncovered, our understanding of the basic factors controlling reactivity and selectivity remains only partial. Although substrate dependence remains an important issue, there are more and more transformations that are reach the standards of current asymmetric reactions.

References

1 (a) Berkessel, A. and Gröger, H. (2005) *Asymmetric Organocatalysis, from Biomimetic Concepts to Applications in Asymmetric Synthesis*, Wiley-VCH Verlag GmbH, Weinheim; (b) Dalko, P.I. (ed.) (2007) *Enantioselective Organocatalysis: Reactions and Experimental Procedures*, Wiley-VCH Verlag GmbH, Weinheim.

2 For general reviews on asymmetric organocatalysis, see: (a) Dalko, P.I. and Moisan, L. (2001) *Angewandte Chemie-International Edition*, **40**, 3726–3748; (b) Dalko, P.I. and Moisan, L. (2004) *Angewandte Chemie-International Edition*, **43**, 5138–5175; (c) Hayashi, Y. (2005) *Journal of Synthetic Organic Chemistry, Japan*, **63**, 464–477; (d) Jiang, H.F., Wang, Y.G., Liu, H.L. and Liu, P. (2004) *Chinese Journal of Organic Chemistry*, **24**, 1513–1531; (e) Dalko, P.I.

(2003) *The McGraw-Hill 2003 Yearbook*, McGraw-Hill, New York, pp. 312–315; (f) Gaunt, M.J., Johansson, C.C.C., McNally, A. and Vo, N.T. (2006) *Drug Discovery Today*, **12**, 8–27; (g) Pellissier, H. (2007) *Tetrahedron*, **63**, 9267–9331; (h) Dondoni, A. and Massi, A. (2008) *Angewandte Chemie-International Edition*, **47**, 4638–4660.

3 For Special Issues on asymmetric organocatalysis, see: (a) List, B. and Bolm, C. (eds), (2004) Advanced Synthesis and Catalysis, *346*, 1007–1249; (b) Houk, K.N. and List, B. (eds), 2004 Accounts of Chemical Research, **37**, 8; (c) Alexakis, A. (2007) Chimia, *5*, 212–281; (d) List, B.(ed.) (2007) Chemical Reviews, **107**, 12. Halpern, J. and Trost, B.M.(eds) (2004) Proceedings of the National Academy of Sciences of the United States of America, **101** (15 and 16).

4 (a) Buchschacher, P., Cassal, J.-M., Fuerst, A. and Meier, W. (1977) *Helvetica Chimica Acta*, **60**, 2747–2755; (b) Wakabayashi, T., Watanabe, K. and Kato, Y. (1977) *Synthetic Communications*, **7**, 239; (c) Limbach, M. (2006) *Tetrahedron Letters*, **47**, 3843–3847.

5 Seebach, D., Beck, A.K., Badine, D.M., Limbach, M., Eschenmoser, A., Treasurywala, A.M. and Hobi, R. (2007) *Helvetica Chimica Acta*, **90**, 425–471.

6 For organocatalytic synthesis of drugs and bioactive natural products, see: de Figueiredo, R.M. and Christmann, M. (2007) *European Journal of Organic Chemistry*, 2575–2600.

7 Robiette, R., Aggarwal, V.K. and Harvey, T.N. (2007) *Journal of the American Chemical Society*, **129**, 15513–15525.

8 For reviews on Brønsted acid catalysis, see: (a) Schreiner, P.R. (2003) *Chemical Society Reviews*, **32**, 289–296; (b) Pihko, P.M. (2004) *Angewandte Chemie-International Edition*, **43**, 2062–2064; (c) Bolm, C., Rantanen, T., Schiffers, I. and Zani, L. (2005) *Angewandte Chemie-International Edition*, **44**, 1758–1763; (d) Pihko, P.M. (2005) *Letters in Organic Chemistry*, **2**, 398–403; (e) Akiyama, T., Itoh, J. and Fuchibe, K. (2006) *Advanced Synthesis and Catalysis*, **348**, 999–1010; (f) Akiyama, T. (2007) *Chemical Reviews*, **107**, 5744–5788. (g) Doyle, A.D. and Jacobsen, E.N. (2007) *Chemical Reviews*, **107**, 5713–5743; (h) Takemoto, Y. (2005) *Organic and Biomolecular Chemistry*, **3**, 4299–4306; (i) Taylor, M.S. and Jacobsen, E.N. (2006) *Angewandte Chemie-International Edition*, **45**, 1520–1543; (j) Connon, S.J. (2006) *Chemistry – A European Journal*, **12**, 5418–5427; (k) Connon, S.J. (2006) *Angewandte Chemie-International Edition*, **45**, 3909–3912; (l) Connon, S.J. (2006) *Letters in Organic Chemistry*, **3**, 333–338; (m) McGilvra, J.D., Gondi, V.B. and Rawal, V.H. (2007) *Enantioselective Organocatalysis: Reactions and Experimental Procedures* (ed. P.I. Dalko), Chapter 6, Wiley-VCH Verlag GmbH, Weinheim, pp. 189–254; (n) Doyle, A.G. and Jacobsen, E.N. (2007) *Chemical Reviews*, **107**, 5713–5743.

9 (a) Aratake, S., Itoh, T., Okano, T., Usui, T., Shoji, M. and Hayashi, Y. (2007) *Chemical Communications*, 2524–2526; (b) Pan, C. and Wang, Z. (2008) *Coordination Chemistry Reviews*, **252**, 736–750.

10 For reviews, see: (a) Enders, D. and Balensiefer, T. (2004) *Accounts of Chemical Research*, **37**, 534–541; (b) Zeitler, K. (2005) *Angewandte Chemie-International Edition*, **44**, 7506–7510; (c) Enders, D., Balensiefer, T., Niemeier, O. and Christmann, M. (2007) *Enantioselective Organocatalysis: Reactions and Experimental Procedures* (ed. P.I. Dalko), Chapter 9, Wiley-VCH Verlag GmbH, Weinheim, pp. 331–355; (d) Marion, N., Díez-González, S. and Nolan, S.P. (2007) *Angewandte Chemie-International Edition*, **46**, 2988–3000; (e) Enders, D., Niemeier, O. and Henseler, A. (2007) *Chemical Reviews*, **107**, 5606–5655.

11 Kotsuki, H., Ikishima, H. and Okuyama, A. (2008) *Heterocycles*, **75**, 493–529.

12 Kotsuki, H., Ikishima, H. and Okuyama, A. (2008) *Heterocycles*, **75**, 757–797.

13 Allen, W.D., Czinki, E. and Csaszar, A.G. (2004) *Chemistry – A European Journal*, **10**, 4512–4517.

14 (a) Bahmanyar, S. and Houk, K.N. (2003) *Organic Letters*, **5**, 1249–1251; (b) Bahmanyar, S., Houk, K.N., Martin, H.J. and List, B. (2003) *Journal of the American Chemical Society*, **125**, 2475–2479; (c) Hoang, L., Bahmanyar, S., Houk, K.N. and List, B. (2003) *Journal of the American Chemical Society*, **125**, 16–17; (d) Bahmanyar, S. and Houk, K.N. (2001) *Journal of the American Chemical Society*, **123**, 12911–12912; (e) Bahmanyar, S. and Houk, K.N. (2001) *Journal of the American Chemical Society*, **123**, 11273–11283.

15 For a compilation of proline derivatives used in asymmetric organocatalytic reactions, see: Dalko, P.I. (ed.) (2007) in *Enantioselective Organocatalysis: Reactions and Experimental Procedures*, Wiley-VCH Verlag GmbH, Weinheim, Chapter 15, pp. 513–529 (see also [19d]).

16 Palomo, C. and Mielgo, A. (2006) *Angewandte Chemie-International Edition*, **45**, 7876–7880.

17 For selected examples, see: (a) Hayashi, Y., Gotoh, H., Hayasi, T. and Shoji, M. (2005) *Angewandte Chemie-International Edition*, **44**, 4212–4215; (b) Marigo, M., Wabnitz, T.C., Fielenbach, D. and Jørgensen, K.A. (2005) *Angewandte Chemie-International Edition*, **44**, 794–797.

18 (a) Lelais, G. and MacMillan, D.W.C. (2006) *Aldrichim Acta*, **39**, 79–87; (b) Lelais, G. and MacMillan, D.W.C. (2007) in *Frontiers in Asymmetric Catalysis* (eds K. Mikami and M. Lautens), John Wiley & Sons, Inc, Hoboken, NJ; (c) Lelais, G. and MacMillan, D.W.C. (2007) in *Enantioselective Organocatalysis: Reactions and Experimental Procedures* (ed. P.I. Dalko), Chapter 3, Wiley-VCH Verlag GmbH, Weinheim, pp. 95–120; (d) Erkkilä, A., Majander, I. and Pihko, P.M. (2007) *Chemical Reviews*, **107**, 5416–5470.

19 For reviews on aminocatalytic reactions, see: (a) List, B. (2002) *Tetrahedron*, **58**, 5573–5590; (b) List, B. (2004) *Accounts of Chemical Research*, **37**, 548–557; (c) Seayad, J. and List, B. (2005) *Organic and Biomolecular Chemistry*, **3**, 719–724; (d) List, B. (2006) *Chemical Communications*, 819–824; (e) Mukherjee, S., Yang, J.W., Hoffmann, S. and List, B. (2007) *Chemical Reviews*, **107**, 5471–5569; (f) Tanaka, F. and Barbas, C.F., III (2007) *Enantioselective Organocatalysis: Reactions and Experimental Procedures* (ed. P.I. Dalko), Chapter 2, Wiley-VCH Verlag GmbH, Weinheim, pp. 19–55; (g) Melchiorre, P., Marigo, M., Carlone, A. and Bartoli, G. (2008) *Angewandte Chemie-International Edition*, **47**, 6138–6171.

20 (a) Yang, J.W., Hechavarria Fonseca, M.T. and List, B. (2005) *Journal of the American Chemical Society*, **127**, 15036–15037; (b) Huang, Y., Walji, A., Larsen, C.H. and MacMillan, D.W.C. (2005) *Journal of the American Chemical Society*, **127**, 15051–15053.

21 For preferred enamine geometry in related transformations, see: Cheong, P.H.-Y., Zhang, H., Thayumanavan, R., Tanaka, F., Houk, K.N. and Barbas, C.F., III (2006) *Organic Letters*, **8**, 811–814.

22 Seebach, D. and Golinski, J. (1981) *Helvetica Chimica Acta*, **64**, 1413–1423.

23 (a) Tian, S.-K., Chen, Y., Hang, J., Tang, L., McDaid, P. and Deng, L. (2004) *Accounts of Chemical Research*, **37**, 621–631; (b) Ó Dálaigh, C. (2005) *Synlett*, 875–876; (c) Connon, S.J. (2008) *Chemical Communications*, 2499–2510.

24 (a) Kolb, H.C., VanNieuwenhze, M.S. and Sharpless, K.B. (1994) *Chemical Reviews*, **94**, 2483–2547; (b) Marko, I.E. and Svendsen, J.S. (1999) *Comprehensive Asymmetric Catalysis*, Vol II (eds E.N. Jacobsen, A. Pfaltz and H. Yamamoto), Springer, New York, Chapter 20.

25 For reviews on phase-transfer catalysis, see: (a) Ooi, T. and Maruoka, K. (2007) in *Angewandte Chemie-International Edition*, **46**, 4222–4266; (b) Ooi, T. and Maruoka, K. (2007) *Enantioselective Organocatalysis: Reactions and Experimental Procedures* (ed. P.I. Dalko), Chapter 4, Wiley-VCH Verlag

GmbH, Weinheim, pp. 95–150; (c) Ooi, T. and Maruoka, K. (2007) *Aldrichim Acta*, **40**, 77; (d) Hashimoto, T. and Maruoka, K. (2007) *Chemical Reviews*, **107**, 5656–5682.

26 Seebach, D., Beck, A.K. and Heckel, A. (2001) *Angewandte Chemie-International Edition*, **40**, 92–138.

27 (a) Shibasaki, M. and Matsunaga, S. (2006) *Chemical Society Reviews*, **35**, 269–279; (b) Brunel, J.M. (2005) *Chemical Reviews*, **105**, 857–898.

28 (a) Bennani, Y.L. and Hanessian, S. (1997) *Chemical Reviews*, **97**, 3161–3195; (b) Lucet, D., Le Gall, T. and Mioskowski, C. (1998) *Angewandte Chemie-International Edition*, **37**, 2580–2627.

29 For reviews on peptides as asymmetric catalysts, see: (a) Davie, E.A.C., Mennen, S.M., Xu, Y. and Miller, S.J. (2007) *Chemical Reviews*, **107** 5759–5812; (b) Jarvo, E.R. and Miller, S.J. (2002) *Tetrahedron*, **58**, 2481–2495; (c) Miller, S.J. (2004) *Accounts of Chemical Research*, **37**, 601–610; (d) Revell, J.D. and Wennemers, H. (2007) *Current Opinion in Chemical Biology*, **11**, 269–278.

30 Hayashi, Y., Itoh, T., Aratake, S. and Ishikawa, H. (2008) *Angewandte Chemie-International Edition*, **47**, 2082–2084.

31 Carpenter, J., Northrup, A.B., Chung, deM., Wiener, J.J.M., Kim, S.-G. and MacMillan, D.W.C. (2008) *Angewandte Chemie-International Edition*, **47**, 3568–3572.

32 Pihko, P.M., Laurikainen, K.M., Usano, A., Nyberg, A.I. and Kaavi, J.A. (2006) *Tetrahedron*, **62**, 317–328.

33 Mossé, S. and Alexakis, A. (2006) *Organic Letters*, **8**, 3577–3580.

34 (a) Selkälä, S.A., Tois, J., Pihko, P.M. and Koskinen, A.M.P. (2002) *Advanced Synthesis and Catalysis*, **344**, 941–945; (b) Bengalia, M., Puglisi, A. and Cozzi, F. (2003) *Chemical Reviews*, **103**, 3401–3430; (c) Chandrasekhar, S., Reddy, N.R., Sultana, S.S., Narsihmulu, Ch. and Reddy, K.V. (2006) *Tetrahedron*, **62**, 338–345.

35 Xu, L.-W. and Lu, Y. (2008) *Organic and Biomolecular Chemistry*, **6**, 2047–2075.

36 Ramasastry, S.S.V., Albertshofer, K., Utsumi, N. and Barbas, C.F., III (2008) *Organic Letters*, **10**, 1621–1624.

37 For related activation, see: (a) Tang, Z. Yang, Z.-H. Chen, X.-H. Cun, L.-F. Mi, A.-Q. Jiang, Y.-Z. and Gong, L.-Z. (2005) *Journal of the American Chemical Society*, **127**, 9285–9289, and references cited therein. See also (b) Raj, M., Vishnumaya, Ginotra, S.K. and Singh, V.K. (2006) *Organic Letters*, **8**, 4097–4099.

38 (a) Shi, M. and Zhang, W. (2005) *Tetrahedron*, **61**, 11887–11894; (b) Markert, M., Mulzer, M., Schetter, B. and Mahrwald, R. (2007) *Journal of the American Chemical Society*, **129**, 7258–7259.

39 McGilvra, J.D., Unni, A.K., Modi, K. and Rawal, V.H. (2006) *Angewandte Chemie-International Edition*, **45**, 6130–6133.

40 For reviews, see: (a) Denmark, S.E. and Fu, J. (2003) *Chemical Reviews*, **103**, 2763–2794; (b) Denmark, S.E. and Fu, J. (2003) *Chemical Communications*, 167–170; (c) Denmark, S.E. and Fujimori, S. (2004) *Modern Aldol Reactions* (ed. R. Mahrwald), Chapter 7, Wiley-VCH Verlag GmbH, Weinheim, 255–286; (d) Kocovsky, P. and Malkov, A.V. (2007) in *Enantioselective Organocatalysis: Reactions and Experimental Procedures* (ed. P.I. Dalko), Wiley-VCH Verlag GmbH, Weinheim; (e) Denmark, S.E. and Beutner, G.L. (2008) *Angewandte Chemie-International Edition*, **47**, 1560–1638.

41 Denmark, S.E. and Heemstra, J.R. (2003) *Organic Letters*, **5**, 2303–2306.

42 (a) Denmark, S.E. and Chung, W.-J. (2008) *The Journal of Organic Chemistry*, **73**, 4582–4595; (b) Denmark, S.E. and Chung, W.-J. (2008) *Angewandte Chemie-International Edition*, **47**, 1890–1892.

43 Denmark, S.E. and Fu, J. (2001) *Journal of the American Chemical Society*, **123**, 9488–9489.

44 Hellwig, J., Belser, T. and Miller, J.F.K. (2001) *Tetrahedron Letters*, **42**, 5417–5419.

45 Denmark, S.E. and Fu, J. (2002) *Organic Letters*, **4**, 1951–1953.

46 For a review of catalytic asymmetric nitroaldol reactions, see: Palomo, C., Oiarbide, M. and Mielgo, A., (2004) *Angewandte Chemie-International Edition*, **43**, 5442–5444.

47 Li, H., Wang, B. and Deng, L. (2006) *Journal of the American Chemical Society*, **128**, 732–733.

48 For selected references, see: (a) Sasai, H. Suzuki, T. Arai, S. and Shibasaki, M. (1992) *Journal of the American Chemical Society*, **114**, 4418–4420; (b) Shibasaki, M. and Yoshikawa, N. (2002) *Chemical Reviews*, **102**, 2187–2209; (c) Trost, B. and Yeh, V.S.C. (2002) *Angewandte Chemie-International Edition*, **41**, 861–863; (d) Trost, B., Yeh, V.S.C., Ito, H. and Bremeyer, N. (2002) *Organic Letters*, **4**, 2621–2623; (e) Evans, D.A., Seidel, D., Rueping, M., Lam, H.W., Shaw, J.T. and Downey, C.W. (2003) *Journal of the American Chemical Society*, **125**, 12692–12693; (f) Palomo, C., Oiarbide, M. and Laso, A. (2005) *Angewandte Chemie-International Edition*, **44**, 3881–3884.

49 Corey, E.J. and Zhang, F.-Y. (1999) *Angewandte Chemie-International Edition*, **38**, 1931–1934.

50 Ooi, T., Doda, K. and Maruoka, K. (2003) *Journal of the American Chemical Society*, **125**, 2054–2055.

51 Brunel, J.-M. and Holmes, I.P. (2004) *Angewandte Chemie-International Edition*, **43**, 2752–2778.

52 (a) Tian, S.-K. and Deng, L. (2001) *Journal of the American Chemical Society*, **123**, 6195–6196; (b) Tian, S.-K. Hong, R. and Deng, L. (2003) *Journal of the American Chemical Society*, **125**, 9900–9901.

53 Fuerst, D.E. and Jacobsen, E.N. (2005) *Journal of the American Chemical Society*, **127**, 8964–8964.

54 Zuend, S.J. and Jacobsen, E.N. (2007) *Journal of the American Chemical Society*, **129**, 15872–15883.

55 For reviews on MBH reactions, see: (a) Masson, G., Houseman, C. and Zhu, J. (2007) *Angewandte Chemie-International Edition*, **46**, 4614–4628; (b) Menozzi, C. and Dalko, P.I. (2007) *Enantioselective Organocatalysis: Reactions and Experimental Procedures* (ed. P.I. Dalko), Chapter 5, Wiley-VCH Verlag GmbH, Weinheim, pp. 151–187.

56 Iwabuchi, Y., Sugihara, T., Esumi, T. and Hatakeyama, S. (2001) *Tetrahedron Letters*, **42**, 7867–7871.

57 Iwabuchi, Y., Furukawa, M., Esumi, T. and Hatakeyama, S. (2001) *Chemical Communications*, 2030–2031.

58 Wang, J., Li, H., Yu, X., Zu, L. and Wang, W. (2005) *Organic Letters*, **7**, 4293–4296.

59 (a) McDougal, N.T. and Schaus, S.E. (2003) *Journal of the American Chemical Society*, **125**, 12094–12095; (b) McDougal, N.T., Trevellini, W.L., Rodgen, S.A., Kliman, L.T. and Schaus, S.E. (2004) *Advanced Synthesis and Catalysis*, **346**, 1231–1240.

60 (a) Vedejs, E. and Jure, M. (2005) *Angewandte Chemie-International Edition*, **44**, 3974–4001; (b) Fu, G.C. (2004) *Accounts of Chemical Research*, **37**, 542–547; (c) France, S., Guerin, D.J., Miller, S.J. and Lectka, T. (2003) *Chemical Reviews*, **103**, 2985–3012; (d) Spivey, A.C. and Andrews, B.I. (2001) *Angewandte Chemie-International Edition*, **40**, 3131–3134; (e) Spivey, A.C. and McDaid, P. (2007) *Enantioselective Organocatalysis: Reactions and Experimental Procedures* (ed. P.I. Dalko), Chapter 8, Wiley-VCH Verlag GmbH, Weinheim, pp. 287–329; (f) Wurz, Ryan P. (2007) *Chemical Reviews*, **107**, 5570–5595.

61 Bellemin-Laponnaz, S., Tweddell, J., Ruble, J.C., Breitling, F.M. and Fu, G.C. (2000) *Chemical Communications*, 1009–1010.

62 (a) Birman, V.B. and Jiang, H. (2005) *Organic Letters*, **7**, 3445–3447; (b) Birman, V.B., Li, X., Jiang, H. and Uffman, E.W. (2006) *Tetrahedron*, **62**, 285–294.

63 Vedejs, E., Daugulis, O., MacKay, J.A. and Rozners, E. (2001) *Synlett*, 1499–1505.

64 For the definition of the selectivity value(s) see in: Kagan, H.B. and Fiaud,

J.C. (1988) *Topics in Stereochemistry*, **18**, 249–330.

65 Vedejs, E. and Daugulis, O. (2003) *Journal of the American Chemical Society*, **125**, 4166–4173, and references cited therein.

66 For a review, see: Evans, C.A. and Miller, S.J., (2002) *Current Opinion in Chemical Biology*, **6**, 333–338.

67 Copeland, G.T. and Miller, S.J. (2001) *Journal of the American Chemical Society*, **123**, 6496–6502.

68 (a) Suzuki, Y., Yamauchi, K., Muramatsu, K. and Sato, M. (2004) *Chemical Communications*, 2770–2771 (b) Suzuki, Y., Muramatsu, K., Yamauchi, K., Morie, Y. and Sato, M. (2006) *Tetrahedron*, **62**, 302–310.

69 Kano, T., Sasaki, K. and Maruoka, K. (2005) *Organic Letters*, **7**, 1347–1349.

70 (a) Chen, Y., McDaid, P. and Deng, L. (2003) *Chemical Reviews*, **103**, 2965–2983; (b) Tian, S.-K., Chen, Y., Hang, J., Tang, L., McDaid, P. and Deng, L. (2004) *Accounts of Chemical Research*, **37**, 621–631; (c) Atodiresei, I., Schiffers, I. and Bolm, C. (2007) *Chemical Reviews*, **107**, 5683–5712.

71 Chen, Y.G., Tian, S.-K. and Deng, L. (2000) *Journal of the American Chemical Society*, **122**, 9542–9543.

72 For a silica-supported heterogeneous analog of $(DHQD)_2AQN$, see: (a) Song, Y.-M., Choi, J.S., Yang, J.W. and Han, H. (2004) *Tetrahedron Letters*, **45**, 3301–3304; (b) Kim, H.S., Song, Y.-M., Choi, J.S., Yang, J.W. and Han, H. (2004) *Tetrahedron*, **60**, 12051–12057.

73 Choi, C., Tian, S.-K. and Deng, L. (2001) *Synthesis*, 1737–1741.

74 Honjo, T., Sano, S., Shiro, M. and Nagao, Y. (2005) *Angewandte Chemie-International Edition*, **44**, 5838–5841.

75 Chen, Y.G. and Deng, L. (2001) *Journal of the American Chemical Society*, **123**, 11302–11303.

76 (a) Kobayashi, S. and Ishitani, H. (1999) *Chemical Reviews*, **99**, 1069–1094; (b) Liu, M. and Sibi, M.P. (2002) *Tetrahedron*, **58**, 7991–8035; (c) Taggi, A.E., Hafez, A.M. and Lectka, T. (2003) *Accounts of Chemical Research*, **36**, 10–19; (d) Marques, M.M.B. (2006) *Angewandte Chemie-International Edition*, **45**, 348–352; (e) Friestad, G.K. and Mathies, A.K. (2007) *Tetrahedron*, **63**, 2541–2569; (f) Ting, A. and Schaus, S.E. (2007) *European Journal of Organic Chemistry*, 5797–5815; (g) Verkade, J.M.M., van Hemert, L.J.C., Quaedflieg, P.J.L.M. and Rutjes, F.P.J.T. (2008) *Chemical Society Reviews*, **37**, 29–41; (h) de Figueiredo, R.M., Fröhlich, R. and Christmann, M. (2006) *The Journal of Organic Chemistry*, **71**, 4147–4154; (i) Córdova, A. (2004) *Accounts of Chemical Research*, **37**, 102–112.

77 Hayashi, Y., Urushima, T., Shin, N. and Shoji, M. (2005) *Tetrahedron*, **61**, 11393–11404.

78 Selected examples: Cobb, A.J.A., Shaw, D.M., Longbottom, D.A., Gold, J.B. and Ley, S.V., (2005) *Organic and Biomolecular Chemistry*, **3**, 84–96.

79 Chi, Y. and Gellman, S.H. (2006) *Journal of the American Chemical Society*, **128**, 6804–6805.

80 Ramasastry, S.S.V., Zhang, H., Tanaka, F. and Barbas, C.F., III (2007) *Journal of the American Chemical Society*, **129**, 288–289.

81 (a) Chowdari, N.S., Ramachary, D.B. and Barbas, C.F., III (2003) *Synlett*, 1906–1909; (b) Jorapur, Y.R. (2004) *Synlett*, 746–747.

82 (a) Wenzel, A.G. and Jacobsen, E.N. (2002) *Journal of the American Chemical Society*, **124**, 12964–12965; (b) Wenzel, A.G., Lalonde, M.P. and Jacobsen, E.N. (2003) *Synlett*, 1919–1922.

83 Liu, T.-Y., Cui, H.-L., Long, J., Li, B.-J., Wu, Y., Ding, L.-S. and Chen, Y.-C. (2007) *Journal of the American Chemical Society*, **129**, 1878–1879.

84 Akiyama, T., Itoh, J., Yokota, K. and Fuchibe, K. (2004) *Angewandte Chemie-International Edition*, **43**, 1566–1568.

85 Yamanaka, M., Itoh, J., Fuchibe, K. and Akiyama, T. (2007) *Journal of the American Chemical Society*, **129**, 6756–6764.

86 Sickert, M. and Schneider, C. (2008) *Angewandte Chemie-International Edition*, **47**, 3631–3634.

87 Niess, B. and Jørgensen, K.A. (2007) *Chemical Communications*, 1620–1622.

88 (a) Yoon, T.P. and Jacobsen, E.N. (2005) *Angewandte Chemie-International Edition*, **44**, 466–468; (b) Xu, X., Furukawa, T., Okino, T., Miyabe, H. and Takemoto, Y. (2006) *Chemistry – A European Journal*, **12**, 466–476.

89 Gomez-Bengoa, E., Linden, A., López, R., Múgica-Mendiola, I., Oiarbide, M. and Palomo, C. (2008) *Journal of the American Chemical Society*, **130**, 7955–7966.

90 (a) Gröger, H. (2003) *Chemical Reviews*, **103**, 2795–2827; (b) Vilaivan, T., Bhanthumnavin, W. and Sritana-Anant, Y. (2005) *Current Organic Chemistry*, **9**, 1315–1392; (c) Ohfune, Y. and Shinada, T. (2005) *European Journal of Organic Chemistry*, 5127–5143.

91 Becker, C., Hoben, C. and Kunz, H. (2007) *Advanced Synthesis and Catalysis*, **349**, 417–424.

92 Kanemitsu, T., Yamashita, Y., Nagata, K. and Itoh, T. (2006) *Synlett*, 1595–1597.

93 Rueping, M., Sugiono, E. and Azap, C. (2006) *Angewandte Chemie-International Edition*, **45**, 2617–2619.

94 Ooi, T., Uematsu, Y. and Maruoka, K. (2006) *Journal of the American Chemical Society*, **128**, 2548–2549.

95 (a) Seayad, J., Majeed Seayad, A. and List, B. (2006) *Journal of the American Chemical Society*, **128**, 1086–1087; (b) Raheem, I.T., Thiara, P.S., Peterson, E.A. and Jacobsen, E.N. (2007) *Journal of the American Chemical Society*, **129**, 13404–13405.

96 Kagan, H.B. (2007) *Enantioselective Organocatalysis: Reactions and Experimental Procedures* (ed. P.I. Dalko), Chapter 11, Wiley-VCH Verlag GmbH, Weinheim, pp. 391–401.

97 Wang, Z., Ye, X., Wei, S., Wu, P., Zhang, A. and Sun, J. (2006) *Organic Letters*, **8**, 999–1001.

98 Malkov, A.V., Stoncius, S., MacDougall, K.N., Mariani, A., McGeoch, G.D. and Kocovsky, P. (2006) *Tetrahedron*, **62**, 264–284.

99 Metallinos, C., Barrett, F.B. and Xu, S. (2008) *Synlett*, 720–724.

100 For recent reviews, see: (a) Tsogoeva, S.B. (2007) *European Journal of Organic Chemistry*, 1701–1716; (b) Sulzer-Mossé, S. and Alexakis, A. (2007) *Chemical Communications*, 3123–3135; (c) Vicario, J.L., Badía, D. and Carrillo, L. (2007) *Synthesis*, 2065–2092; (d) Almasi, D., Alonso, D.A. and Nájera, C. (2007) *Tetrahedron: Asymmetry*, **18**, 299–365; (e) Bressy, C. and Dalko, P.I. (2007) *Enantioselective Organocatalysis: Reactions and Experimental Procedures* (ed. P.I. Dalko), Chapter 2, Wiley-VCH Verlag GmbH. Weinheim, pp. 77–94.

101 For selected examples, see: (a) Zhu, S., Yu, S. and Ma, D. (2008) *Angewandte Chemie-International Edition*, **47**, 545–548; (b) McCooey, S.H. and Connon, S.J. (2007) *Organic Letters*, **9**, 599–602; (c) Lalonde, M.P., Chen, Y. and Jacobsen, E.N. (2006) *Angewandte Chemie-International Edition*, **45**, 6366–6370; (d) Palomo, C., Vera, S., Mielgo, A. and Gómez-Bengoa, E. (2006) *Angewandte Chemie-International Edition*, **45**, 5984–5987; (e) Mossé, S., Laars, M., Kriis, K., Kanger, T. and Alexakis, A. (2006) *Organic Letters*, **8**, 2559–2562; (f) Mase, N., Watanabe, K., Yoda, H., Takabe, K., Tanaka, F. and Barbas, C.F., III (2006) *Journal of the American Chemical Society*, **128**, 4966–4967; (g) Wang, J., Li, J., Lou, B., Zu, L., Guo, H. and Wang, W. (2006) *Chemistry – A European Journal*, **12**, 4321–4332; (h) Wang, W., Wang, J., and Li, H. (2005) *Angewandte Chemie-International Edition*, **44**, 1369–1371; (i) Andrey, O., Alexakis, A., Tomassini, A. and Bernardinelli, G. (2004) *Advanced Synthesis and Catalysis*, **346**, 1147–1168; (j) Mase, N., Thayumanavan, R., Tanaka, F. and Barbas, C.F., III (2004) *Organic Letters*, **6**, 2527–2530; (k) Betancort, J.M. and Barbas, C.F., III (2001) *Organic Letters*, **3**, 3737–3740; (l) Alexakis, A. and Andrey, O. (2002) *Organic Letters*, **4**, 3611–3614; (m) Alexakis, A., Tomassini, A.,

Chouillet, C., Roland, S., Mangeney, P. and Bernardinelli, G. (2000) *Angewandte Chemie-International Edition*, **39**, 4093–4095; (n) Betancort, J.M., Sakthivel, K., Thayumanavan, R., Tanaka, F. and Barbas, C.F., III (2004) *Synthesis*, 1509–1521; (o) Sakthivel, K., Notz, W., Bui, T. and Barbas, C.F., III (2001) *Journal of the American Chemical Society*, 5260–5267; (p) Ishii, T., Fujioka, S., Sekiguchi, Y. and Kotsuki, H. (2004) *Journal of the American Chemical Society*, **126**, 9558–9559; (q) Pansare, S.V. and Pandya, K. (2006) *Journal of the American Chemical Society*, **128**, 9624–9625; (r) Luo, S., Mi, X., Zhang, L., Liu, S., Xu, H. and Cheng, J.-P. (2006) *Angewandte Chemie-International Edition*, **45**, 3093–3097; (s) Cobb, A.J.A., Longbottom, D.A., Shaw, D.M. and Ley, S.V. (2004) *Chemical Communications*, 1808–1809; (t) Mitchell, C.E.T., Cobb, A.J.A. and Ley, S.V. (2005) *Synlett*, 611–614.

102 Chi, Y., Guo, L., Kopf, N.A. and Gellman, S.H. (2008) *Journal of the American Chemical Society*, **130**, 5608–5609.

103 Zu, L., Li, H., Wang, J., Yu, X. and Wang, W. (2006) *Tetrahedron Letters*, **47**, 5131–5134.

104 Zu, L., Wang, J., Li, H. and Wang, W. (2006) *Organic Letters*, **8**, 3077–3079.

105 Andrey, O., Vidonne, A. and Alexakis, A. (2003) *Tetrahedron Letters*, **44**, 7901–7904.

106 Andrey, O., Alexakis, A. and Bernardinelli, G. (2003) *Organic Letters*, **5**, 2559–2561.

107 Wiesner, M., Revell, J.D. and Wennemers, H. (2008) *Angewandte Chemie-International Edition*, **47**, 1871–1874.

108 Wiesner, M., Revell, J.D., Tonazzi, S. and Wennemers, H. (2008) *Journal of the American Chemical Society*, **130**, 5610–5611; for selected examples of peptidic catalysts for 1,4-additions, see: (a) Tsogoeva, S.B., Jagtap, S.B. and Ardemasova, Z.A. (2006) *Tetrahedron: Asymmetry*, **17**, 989–992; (b) Xu, Y., Zou, W., Sundén, H., Ibrahem, I. and Córdova, A. (2006) *Advanced Synthesis and Catalysis*, **348**, 418–424; (c) Martin, H.J. and List, B. (2003) *Synlett*, 1901–1902; (d) Guerin, D.J. and Miller, S.J. (2002) *Journal of the American Chemical Society*, **124**, 2134–2136.

109 Huang, H. and Jacobsen, E.N. (2006) *Journal of the American Chemical Society*, **128**, 7170–7171.

110 Ye, J., Dixon, D.J. and Hynes, P.S. (2005) *Chemical Communications*, 4481–4483.

111 Connon, S.H. and McCooey, S.J. (2005) *Angewandte Chemie-International Edition*, **44**, 6367–6370.

112 Wang, J., Li, H., Duan, W., Zu, L. and Wang, W. (2005) *Organic Letters*, **7**, 4713–4716.

113 (a) Okino, T., Hoashi, Y. and Takemoto, Y. (2003) *Journal of the American Chemical Society*, **125**, 12672–12673; (b) Okino, T., Hoashi, Y., Furukawa, T., Xu, X. and Takemoto, Y. (2005) *Journal of the American Chemical Society*, **127**, 119–125.

114 Hoashi, Y., Yabuta, T., Yan, P., Miyabe, H. and Takemoto, Y. (2006) *Tetrahedron*, **62**, 365–374.

115 Melchiorre, P. and Jørgensen, K.A. (2003) *The Journal of Organic Chemistry*, **68**, 4151–4157.

116 Chi, Y. and Gellman, S.H. (2005) *Organic Letters*, **7**, 4253–4256.

117 Peelen, T.J., Chi, Y. and Gellman, S.H. (2005) *Journal of the American Chemical Society*, **127**, 11598–11599.

118 Hechavarria Fonseca, M.T. and List, B. (2004) *Angewandte Chemie-International Edition*, **43**, 3958–3960.

119 Hayashi, Y., Gotoh, H., Tamura, T., Yamaguchi, H., Masui, R. and Shoji, M. (2005) *Journal of the American Chemical Society*, **127**, 16028–16029.

120 Halland, N., Hansen, T. and Jørgensen, K.A. (2003) *Angewandte Chemie-International Edition*, **42**, 4955–4957.

121 Pederson, R.L., Fellows, I.M., Ung, T.A., Ishihara, H. and Hajela, S.P. (2002) *Advanced Synthesis and Catalysis*, **344**, 728–735.

122 Brown, S.P., Goodwin, N.C. and MacMillan, D.W.C. (2003) *Journal of the American Chemical Society*, **125**, 1192–1194.

123 Wang, W., Li, H. and Wang, J. (2005) *Organic Letters*, **7**, 1637–1639.

124 (a) McGarrigle, E.M. and Aggarwal, V.K. (2007) *Enantioselective Organocatalysis: Reactions and Experimental Procedures* (ed. P.I. Dalko), Chapter 10, Wiley-VCH Verlag GmbH, Weinheim, pp. 357–389; (b) McGarrigle, E.M., Myers, E.L., Illa, O., Shaw, M.A., Riches, S.L. and Aggarwal, V.K. (2007) *Chemical Reviews*, **107**, 5841–5883.

125 (a) Johansson, C.C.C., Bremeyer, N., Ley, S.V., Owen, D.R., Smith, S.C. and Gaunt, M.J. (2006) *Angewandte Chemie-International Edition*, **45**, 6024–6028; (b) Gaunt, M.J. and Johansson, C.C.C. (2007) *Chemical Reviews*, **107**, 5596–5605.

126 Kunz, R.K. and MacMillan, D.W.C. (2005) *Journal of the American Chemical Society*, **127**, 3240–3241.

127 For reviews of catalytic asymmetric epoxidation, see: (a) Xia, Q.H., Ge, H.Q., Ye, C.P., Liu, Z.M. and Su, K.X. *Chemical Reviews*, (2005) **105**, 1603–1662; (b) McGarrigle, E. and Gilheany, D.G. (2005) *Chemical Reviews*, **105**, 1563–1602.

128 For reviews of organocatalyzed oxidations, see: (a) Adam, W., Saha-Moller, C.R. and Ganeshpure, P.A. (2001) *Chemical Reviews*, **101**, 3499–3548; (b) Shi, Y. (2004) *Accounts of Chemical Research*, **37**, 488–496; (c) Yang, D. (2004) *Accounts of Chemical Research*, **37**, 497–505; (d) Armstrong, A. (2007) in *Enantioselective Organocatalysis: Reactions and Experimental Procedures* (ed. P.I. Dalko), Chapter 12, Wiley-VCH Verlag GmbH, Weinheim, pp. 403–424.

129 Aggarwal, V.K. and Winn, C.L. (2004) *Accounts of Chemical Research*, **37**, 611–620.

130 Marigo, M., Franzen, J., Poulsen, T.B., Zhuang, W. and Jørgensen, K.A. (2005) *Journal of the American Chemical Society*, **127**, 6964–6965.

131 Wang, X., Reisinger, C.M. and List, B. (2008) *Journal of the American Chemical Society*, **130**, 6070–6071.

132 For the use of oligopeptides as catalysts for the enantioselective epoxidation of electron-deficient alkenes, see: Kelly, D.R. and Roberts, S.M., (2006) *Biopolymers*, **84**, 74–89.

133 Adger, B.M., Barkley, J.V., Bergeron, S., Cappi, M.W., Flowerdew, B.E., Jackson, M.P., McCague, R., Nugent, T.C. and Roberts, S.M. (1997) *Journal of the Chemical Society-Perkin Transactions 1*, 3501–3507.

134 Itsuno, S., Sakakura, M. and Ito, K. (1990) *The Journal of Organic Chemistry*, **55**, 6047–6049.

135 (a) Imashiro, R. and Seki, M. (2004) *The Journal of Organic Chemistry*, **69**, 4216–4226; (b) Seki, M. (2008) *Synlett*, 164–176.

136 (a) Xiong, Z. and Corey, E.J. (2000) *Journal of the American Chemical Society*, **122**, 4831–4832; (b) Xiong, Z. and Corey, E.J. (2000) *Journal of the American Chemical Society*, **122**, 9328–9329.

137 (a) Wu, X.Y., She, X.G. and Shi, Y.A. (2002) *Journal of the American Chemical Society*, **124**, 8792–8793; (b) Nieto, N., Molas, P., Benet-Buchholz, J. and Vidal-Ferran, A. (2005) *The Journal of Organic Chemistry*, **70**, 10143–10146.

138 Peris, G., Jakobsche, C.E. and Miller, S.J. (2007) *Journal of the American Chemical Society*, **129**, 8710–8711.

139 For a highlight on this chemistry, see: Berkessel, A. (2008) *Angewandte Chemie-International Edition*, **47**, 3677–3679.

140 Ishihara, K. and Nakano, K. (2005) *Journal of the American Chemical Society*, **127**, 10504–10505.

141 Wilson, R.M., Jen, W.S. and MacMillan, D.W.C. (2005) *Journal of the American Chemical Society*, **127**, 11616–11617.

142 Selkälä, S.A. and Koskinen, A.M.P. (2005) *European Journal of Organic Chemistry*, 1620–1624.

143 Northrup, A.B. and MacMillan, D.W.C. (2002) *Journal of the American Chemical Society*, **124**, 2458–2460.

144 Huang, Y. and Rawal, V.H. (2002) *Journal of the American Chemical Society*, **124**, 9662–9663.

145 Unni, A.K., Takenaka, N., Yamamoto, H. and Rawal, V.H. (2005) *Journal of the American Chemical Society*, **127**, 1336–1337.

146 Liu, H., Cun, L.-F., Mi, A.-Q., Jiang, Y.-Z. and Gong, L.-Z. (2006) *Organic Letters*, **8**, 6023–6026.

147 Akiyama, T., Tamura, Y., Itoh, J., Morita, H. and Fuchibe, K. (2006) *Synlett*, 141–143.

148 Jørgensen, K.A. (2004) *European Journal of Organic Chemistry*, 2093–2102.

149 (a) Fang, Y.-Q. and Jacobsen, E.N. (2008) *Journal of the American Chemical Society*, **130**, 5660–5661; (b) Cowen, B.J. and Miller, S.J. (2007) *Journal of the American Chemical Society*, **129**, 10988–10989.

150 (a) Chen, X.-H., Zhang, W.-Q. and Gong, L.-Z. (2008) *Journal of the American Chemical Society*, **130**, 5652–5653; (b) Jiao, P., Nakashima, D. and Yamamoto, H. (2008) *Angewandte Chemie-International Edition*, **47**, 2411–2413.

151 (a) Karlsson, S. and Högberg, H.-E. (2002) *Tetrahedron: Asymmetry*, **13**, 923; (b) Karlsson, S. and Högberg, H.-E. (2003) *European Journal of Organic Chemistry*, 2782–2791.

152 (a) Calter, M.A. and Liao, W. (2002) *Journal of the American Chemical Society*, **124**, 13127–13129; (b) Calter, M.A., Orr, R.K. and Song, W. (2003) *Organic Letters*, **5**, 4745–4748.

153 Paull, D.H., Abraham, C.J., Scerba, M.T., Alden-Danforth, E. and Lectka, T. (2008) *Accounts of Chemical Research*, **41**, 655–663.

154 Ouellet, S.G., Tuttle, J.B. and MacMillan, D.W.C. (2005) *Journal of the American Chemical Society*, **127**, 32–33.

155 (a) Yang, J.W., Hechavarria Fonseca, M.T. and List, B. (2004) *Angewandte Chemie-International Edition*, **43**, 6660; (b) Yang, J.W., Hechavarria Fonseca, M.T., Vignola, N. and List, B. (2005) *Angewandte Chemie-International Edition*, **44**, 108–110.

156 (a) Seayad, J. and List, B. (2004) Catalytic asymmetric multi-component reactions, in *Multi-component Reactions* (eds J. Zhu, and H. Bienayme), Wiley-VCH Verlag GmbH, Weinhein; (b) Ramachary, D.B., Kishor, M. and Reddy, G.B. (2006) *Organic and Biomolecular Chemistry*, **4**, 1641–1646; (c) Guo, H.-C. and Ma, J.-A. (2006) *Angewandte Chemie-International Edition*, **45**, 354–366.

157 Itoh, T., Yokoya, M., Miyauchi, K., Nagata, K. and Ohsawa, A. (2003) *Organic Letters*, **5**, 4301–4304.

158 Linghu, X., Kennedy-Smith, J.J. and Toste, F.D. (2007) *Angewandte Chemie-International Edition*, **46**, 7671–7673.

159 Gryko, D. (2005) *Tetrahedron: Asymmetry*, **16**, 1377–1383.

160 Zhao, G.-L., Vesely, J., Rios, R., Ibrahem, I., Sundén, H. and Córdova, A. (2008) *Advanced Synthesis and Catalysis*, **350**, 237–242, and references cited therein.

161 Austin, J.F., Kim, S.-G., Sinz, C.J., Xiao, W.-J. and MacMillan, D.W.C. (2004) *Proceedings of the National Academy of Sciences of the United States of America*, **101**, 5482–5487.

162 For tandem Michael–aldol reactions, see: (a) Halland, N., Aburel, P.S. and Jørgensen, K.A. (2004) *Angewandte Chemie-International Edition*, **43**, 1272–1277; (b) Pulkkinen, J., Aburel, P.S., Halland, N. and Jørgensen, K.A. (2004) *Advanced Synthesis and Catalysis*, **346**, 1077–1080.

163 Hoashi, Y., Yabuta, T., Yuan, P., Miyabe, H. and Takemoto, Y. (2006) *Tetrahedron*, **62**, 365–374.

164 He, M., Struble, J.R. and Bode, J.W. (2006) *Journal of the American Chemical Society*, **128**, 8418–8420.

165 Chen, X.-H., Xu, X.-Y., Liu, H., Cun, L.-F. and Gong, L.-Z. (2006) *Journal of the American Chemical Society*, **128**, 14802–14803.

166 Enders, D., Hüttl, M.R.M., Grondal, C. and Raabe, G., (2006) *Nature*, **441**, 861–863.

167 Vo, N.T., Pace, R.D.M., O'Hara, F. and Gaunt, M.J. (2008) *Journal of the American Chemical Society*, **130**, 404–405.

168 Steele, R.M., Monti, C., Gennari, C., Piarulli, U., Andreoli, F., Vanthuyne, N. and Roussel, C. (2006) *Tetrahedron: Asymmetry*, **17**, 999–1006.

169 Enders, D., Hüttl, M.R.M., Raabe, G. and Bats, J.W. (2008) *Advanced Synthesis and Catalysis*, **350**, 267–279.

10
Palladacycles in Catalysis

Jairton Dupont and Fabricio R. Flores

10.1
Introduction

Palladacycles or cyclopalladated compounds are heterocycles in which at least one heteroatom is palladium [1]. However, most of these compounds are composed of a Pd–carbon bond stabilized intramolecularly by coordination of at least one two-electron donor group such as those containing nitrogen, sulfur, phosphorus atoms, etc. The most common palladacycles possess anionic four-electron donor or six-electron donor moieties (Scheme 10.1) [2–16].

Most of the interest in these compounds centers on their facile synthesis and easily handling. Moreover, the possibility of modulating their electronic and steric properties renders them an interesting and varied family of organometallic compounds.

Palladacycle chemistry is a fascinating area and this interesting class of compounds represents a challenge to chemists not only in terms of their synthesis but also in terms of their structures, design and types of ligands metalated. They have applications in domains as diverse as biological chemistry, material science, synthesis, ligand resolution and catalysis. However, the most important application of palladacycles is no doubt in catalysis. The applications of palladacycles as catalyst precursors are fairly recent, with the first use being reported in the 1980s with the hydrogenation of alkenes by a cyclopalladated triphenyl phosphite [17]. This was shortly followed by the use of cyclopalladated azobenzene, hydrazobenzene and *N,N*-dimethylbenzylamine in the selective reduction of nitroaromatic compounds, nitroalkenes, nitriles, alkynes, alkenes and aromatic carbonyl compounds [18, 19]. However, it was not until the first report on the synthesis and applications in catalytic C–C coupling reactions of the palladacycle derived from the cyclopalladation of tris-*o*-tolylphosphine [20, 21] and the use of nitrogen-containing palladacycles as catalyst precursors for the telomerization of 1,3-dienes with alcohols [22] that the rich chemistry of these organopalladium compounds received renewed interest, which still continues to flourish.

Green Catalysis, Volume 1: Homogeneous Catalysis.
Edited by Robert H. Crabtree

ISBN: 978-3-527-32496-5

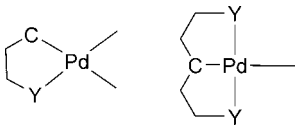

Scheme 10.1 Examples of classical four electron-donor CY and six-electron donor pincer-type palladacycles (Y = NR_2, SR, PR_2, etc.).

This chapter will concentrate on isolated and well-defined compounds that containing a Pd–C bond stabilized by the intramolecular coordination of one or two neutral donor atoms (N, P, As, O, Se or S), i.e. the organic moiety acts as a *C*-anionic four-electron donor ligand or as a *C*-anionic six-electron donor ligand (Scheme 10.1).

This chapter does not attempt to be comprehensive on the catalytic properties of palladacycles, but it summarizes their main applications as catalyst precursors. Various aspects of the applications of palladacycles in catalysis have been the subject of interesting specialized reviews that have catalogued and summarized the main reactions promoted by these organometallic catalyst precursors [3, 23–27]. In this chapter, we will critically present the main achievements, potential and limitations of palladacycles in catalytic C–C and C–heteroatom bond-forming reactions.

10.2
Catalyst Precursors for C–C and C–X (Heteroatom) Coupling Reactions

There have been hundreds of reports over recent years on the use of known and new palladacycles as catalyst precursors for C–C coupling reactions, in particular of the Heck and Suzuki type. Palladacycles have been shown to be very active in a number of important C–C and C–X (heteroatom) bond-forming reactions with very high turnover numbers (TONs), but these reactions proceed in most cases with a variety of simple 'archetypal' substrates. However, most of these catalytic systems are not transposable to more challenging coupling partners where much higher palladacycle loadings are needed.

Although the involvement of Pd(II)/Pd(IV) reaction paths in catalytic reactions promoted by palladacycles has been suggested several times, only recently have Pd(IV) species been isolated and fully characterized (Scheme 10.2) [28]. However, it is the facile redox interchange between the two stable Pd(II)/Pd(0) oxidation states that is mainly responsible for the rich chemistry enjoyed by these compounds. Moreover,

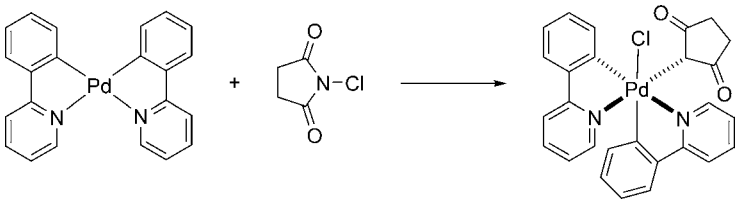

Scheme 10.2

their compatibility with most functional groups also differentiates them from many other transition metal complexes.

In most cases, the palladacycles serve as a reservoir of catalytically active Pd(0) species [29, 30]. In fact, almost any palladacycle can promote the coupling of iodo- and bromoarenes with alkenes, boronic acids and alkynes at relatively elevated temperatures, often combined with a base and an additive salt such as a quaternary ammonium salt [31, 32]. Turnover numbers are usually on the order of 10^4–10^6 cycles, under homogeneous, supported or two- phase conditions and are usually achieved with palladacycles halogen- or acetate- bridged dimers (**1–4**), monomers (**5**) and pincers (**6**) (Scheme 10.3). For example, imine derivatives such as **2** were the first *C,N*-palladacycles reported to promote *de* Heck and Suzuki coupling [33, 34] after the introduction of the *C,P*-palladacycle **1**.

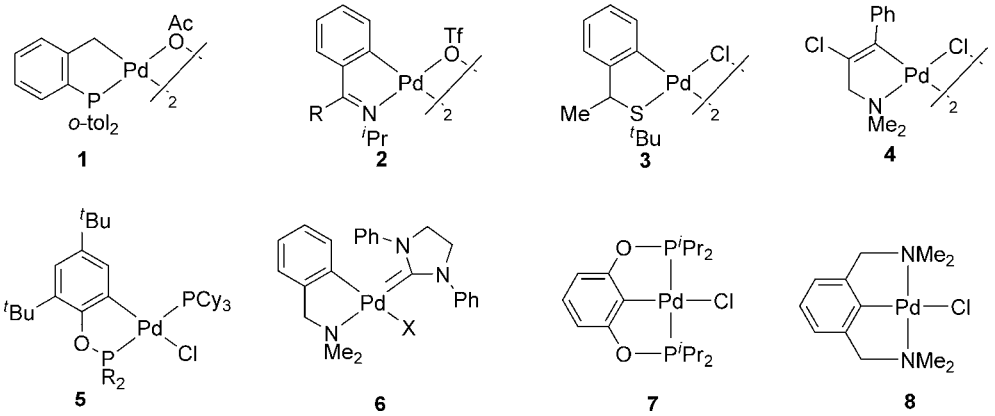

Scheme 10.3 Examples of palladacycles employed as catalyst precursors for C–C and C–heteroatom coupling reactions.

10.2.1
Heck–Mirozoki Coupling

It is well known that under the reaction conditions usually employed (temperatures above 100 °C), even ultra-traces of palladium in reaction vessels promote the coupling of iodo- and bromoarenes with alkenes [31]. In this respect, palladacycles are most likely to serve as a reservoir of catalytically active Pd(0) species that are similar to those formed in the denominated phosphine-free catalytic systems [35, 36], and the reaction most probably follows the classical Pd(0)/Pd(II) catalytic cycle (Scheme 10.4).

The catalytic activity differences observed with these different palladacycle precursors have been rationalized in terms of catalyst preactivation [27]. It has been proposed that the key step in these cases is the slow release of a low-ligated active Pd(0) species. Therefore, the most efficient palladacycles will be those where the release of active Pd is neither too fast (typical of poorly thermally stable palladacycles that preferentially result in the formation of inactive metallic palladium) nor too slow

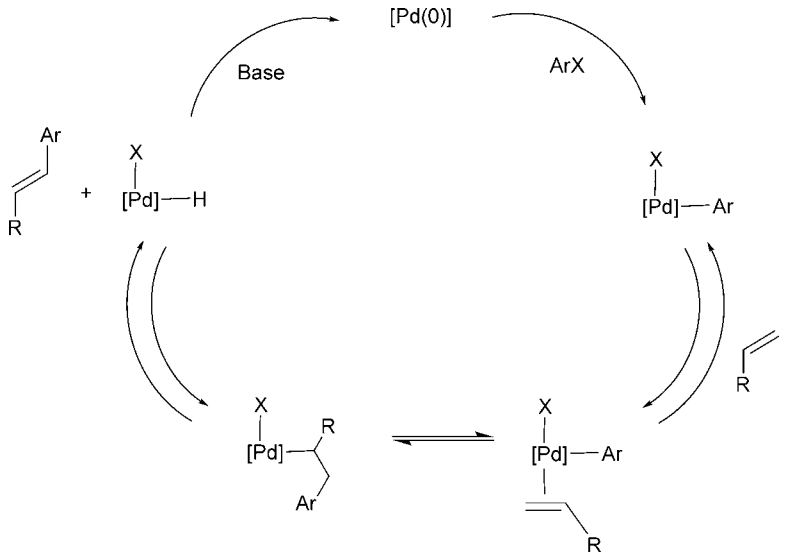

Scheme 10.4

(typical of thermally robust palladacycles, which would require higher temperatures to start the reaction in order to maintain a reasonable reaction rate). The formation of the Pd(0) catalytic active species in the Heck reactions from palladacycles most probably results from an alkene insertion into the Pd−C bond of the palladacycle followed by a β-hydride elimination and reductive elimination (Scheme 10.5) [37–39].

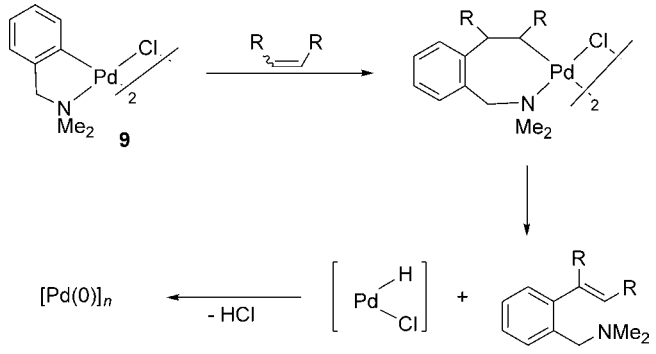

Scheme 10.5

In these systems, the stabilization of the thus formed Pd(0) soluble species is essential to maintain the catalytic activity [29]. This stabilization of soluble Pd(0) species can be achieved either by high dilution of the catalyst or by the addition of extra -stabilizer such as quaternary ammonium salts (Jeffery conditions) [40] and/or ligands. Thus, many of the high TONs observed with palladacycles in the coupling of more easily activated aryl halides are probably a consequence of their low dilution leading to retardation of palladium precipitation.

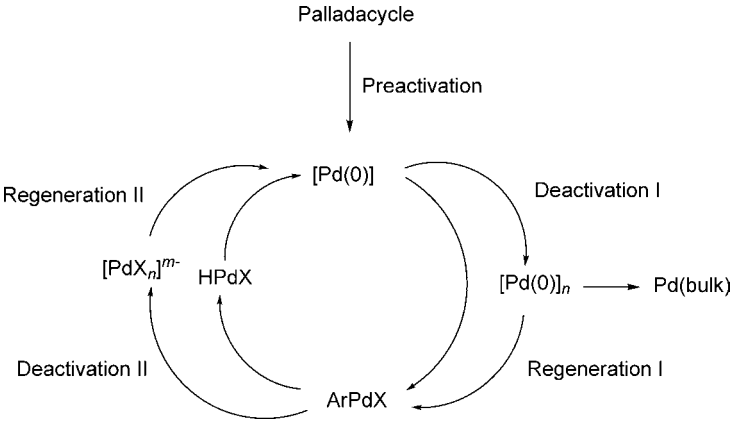

Scheme 10.6 Possible deactivation/regeneration of the Pd species involved in the Heck catalytic process promoted by palladacycles. Adapted from [43].

The role of NBu_4Br additive or ligands such as phosphines and carbenes in the reaction media associated with the palladacycles is as Pd(0)-stabilizing agents which hinder its agglomeration to metallic palladium. In most cases the reactions performed in the absence of the additive NBu_4Br [40, 41] or phosphines or carbenes occur with sedimentation of metallic palladium. Moreover, it is common that deposition of palladium black occurs in reactions performed with a deficiency of aryl halides and reaction deactivation occurs by formation of $[PdX_n]^{m-}$ salts via reductive coupling of the oxidative addition product in reactions performed with an excess of aryl halides. The possible deactivation–regeneration pathways involved in the catalytic process are summarized in Scheme 10.6 [42]. The first decomposition pathway (deactivation I) is the formation of Pd nanoparticles and eventually Pd metal through agglomeration of Pd(0). The agglomeration process is autocatalytic and thermodynamically downhill. In cases where ligands and/or stabilizing agents are present (exerting kinetic control on the nucleation step), the regeneration process occurs through oxidative addition of the haloarene to form soluble Pd(II) species (regeneration I). This regeneration process is dependent on the halide concentration, and the Pd nucleation rate increases with decrease in halide concentration [43].

The second decomposition pathway consists in the formation of Pd(II) halide species [43–45] (such as PdX_2, PdX_3^-, PdX_4^{2-} and $Pd_2X_6^{2-}$) together with the formation of biaryls and haloarene reduction products (deactivation II). These Pd(II) salts and homocoupling and hydrogenolysis products are generated from the oxidative addition intermediate, probably through a bimolecular process [43]. The regeneration (regeneration II) of the catalytically active species occurs through the reduction of Pd (II) halides promoted by the base. The most effective bases are tertiary amines for lower temperatures and acetates for higher temperatures. The use of acetates at lower temperatures promotes the complete deactivation of the system, since the palladium halide species formed during the reaction are not reduced by acetate at temperatures below 130 °C. In contrast, the use of tertiary amines as base induces the formation of

metallic palladium due to their strong and faster reducing properties towards palladium halide species compared with other bases, such as acetate [46].

Not surprisingly, the most efficient and active palladacycles for C–C coupling reactions involving the less reactive aryl chloride substrates are those associated with phosphines and carbenes. There are only a few examples of Heck reactions involving chloroarenes [47] promoted by palladacycles and in most cases the reaction conditions use temperatures above 150 °C in molten salts and give similar results to those for a simple $PdCl_2$ salt in terms of yields and TONs [48]. Of note is the remarkable catalytic activity observed in the high-temperature (>130 °C) Heck coupling of aryl chlorides with styrene with a pincer phosphinito palladacycle (**7**) [49], a cyclopalladated oxime (**10**) [50] and CN-palladacycles associated with carbenes (**11**) [51] or bulky and electron-rich phosphines (**12**) [52] (Schemes 10.7 and 10.8). Other examples of palladacycles that promote the Heck reaction of aryl chlorides with alkyl-acrylates and/or styrenes are dimeric sulfur derivatives (**3**) and 1,2,4-triazole-based palladium (II) pincer complexes (**13**) (Schemes 10.7 and 10.8).

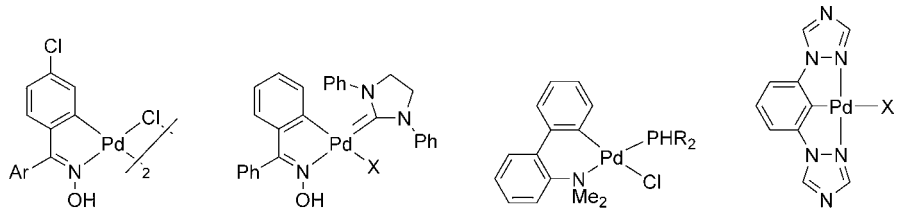

10 **11** **12** **13**

Scheme 10.7 Examples of palladacycles successfully employed for Heck coupling involving aryl chlorides.

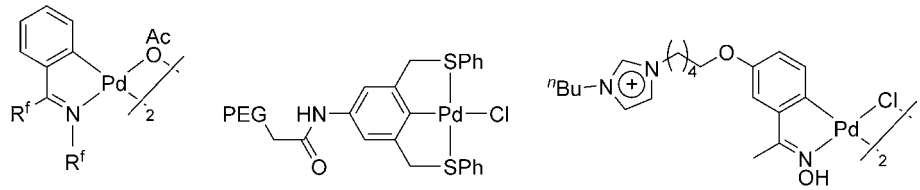

$R^f = (CH_2)_2C_8F_{17}$

Scheme 10.8 Examples of modified palladacycles with perfluoro chains, polyethylene glycol and imidazolium nucleus.

Moreover, there is only one example of a palladacycle that catalyzes the Heck coupling at room temperature [30] (palladacycle **4**, Scheme 10.3), and in this case the chloropalladated propargylamine acts as a reservoir of catalytically active Pd(0) species. Some attempts have been made to support and transform highly active catalysts (Scheme 10.8) into multiphasic systems where the catalyst can be easily separated and reused:

- palladacycles immobilized in ionic liquids [53, 54] or water [55]
- SCS pincer palladacycles covalently bound to a PEG polymer [56–58]

- temperature-dependent miscibility of palladacycles containing perfluoro chains in organic solvents [59, 60]
- immobilization of the palladacycle in polymers [61, 62], such as a polystyrene-immobilized imine–palladacycle system [63]
- MCM-41 mesoporous materials [64–67] and silica [68].

However, leaching of palladium from the solid or liquid supports to solution was observed and a significant amount of catalytic activity was assigned to palladium dissolved in the reaction solution [62, 69–71]. It is now almost a consensus – from detailed mechanistic studies – that in these cases the palladacycles are actually reservoirs of highly catalytically active Pd(0) species [72, 73]. The situation is more complicated because some researchers are, unfortunately, still using electron-poor (activated) aryl bromides, such as 4-bromonitrobenzene, to test the effectiveness of palladacycles [74]. At the very least, an electron-rich aryl halide such as 4-bromoanisole should be used as a benchmark substrate in the Heck reaction [31].

However, Heck-type reactions employing palladacycles are gratifyingly not limited to simple substrates and some recent examples are given below in order to illustrate their expanding synthetic scope. For example, Herrmann–Beller palladacycle **1** has been used for the generation of functionalized arylphosphine ligands starting from bromo-substituted phenylphosphine oxides, for the attachment to solid surfaces [75] or for use as 'ponytails' and 'split pony tails' in fluorinated solvents [76], for the synthesis of an imidazole derivatives [77], for double Heck reactions, one intermolecular process followed by an intramolecular process, along with 2,2′-dibromoaryls and ethyl acrylate (Scheme 10.9) [78]. Heterocycles can be also formed by intramolecular or domino Heck coupling reactions (Scheme 10.9).

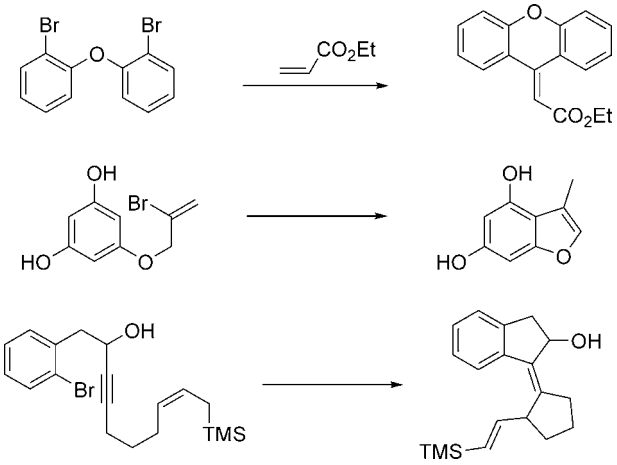

Scheme 10.9 Examples of intramolecular Heck reactions promoted by Herrmann–Beller palladacycle **1**.

10.2.2
Suzuki Coupling

It should be noted once again that highly electronically activated substrates, such as 4-bromoacetophenone, do not provide a particularly useful yardstick for C–C coupling reactions [79]. Indeed, any palladium catalyst precursors, such as palladium acetate in the absence of added ligands, promote the coupling of these substrates with arylboronic acids even at room temperature [32]. Much of the success enjoyed by palladacycles in the Suzuki reaction can be traced to the fact that they act as well-defined, easily handled, stable precursors to highly active Pd(0) catalysts. In this respect, it has been demonstrated in Suzuki and related cross-coupling reactions catalyzed by several distinct types of palladacycles that the generation of the Pd(0) catalytically active species occurs by the activation pathway outlined in Scheme 10.5. The arylboronic acid attacks the palladium center – usually substitution of a halide or other anionic ligand – to generate a palladacycle with an additional aryl ligand. This aryl group and the *ortho*-metalated moiety function then undergo reductive elimination to yield a Pd(0) complex.

In the case of Suzuki coupling, the Pd(0) catalytically active species are formed through a reductive elimination process between the palladated ligand and the arylboronic acid (Scheme 10.10) [80–82].

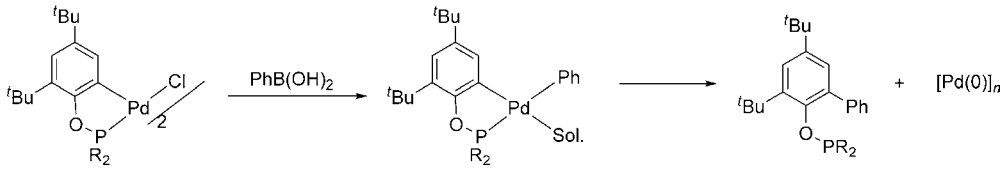

Scheme 10.10

Thus CN, CP, CS, pincer (SCS, NCN and PCP) types associated or not with extra-stabilizing ligands such as phosphines of NC carbenes (Schemes 10.3 and 10.7) have been successfully used in the coupling of simple arylboronic acids and aryl iodides and bromides under different reaction conditions. Thus the coupling of phenylboronic acid with 4-bromoacetophenone, 4-bromoanisole and 4-chloroacetophenone gave TONs (moles product/moles catalyst) of 74 000, 7600 and 2100, respectively, using the Herrmann–Beller CP palladacycle **1** [21]. Other palladacycles under optimized reaction conditions, such as the *ortho*-metalated triaryl phosphites **14** (Scheme 10.11), is considerably more active in the coupling of phenylboronic acid with 4-bromoacetophenone – TONs of up to 1 000 000 [83] – and with the more electronically challenging substrate 4-bromoanisole, a TON of 30 000 was attained. It is worth mentioning the extensive studies on the use of oxime-based palladacycles of the type **10** in a range of Suzuki coupling reactions and TONs of up to 500 000 are seen with the electronically activated substrate 4-bromoacetophenone [84]. Usefully, the catalysis can be performed under aqueous conditions [85, 86] and these complexes are also capable of catalyzing the coupling of aryl halides with alkylboronic

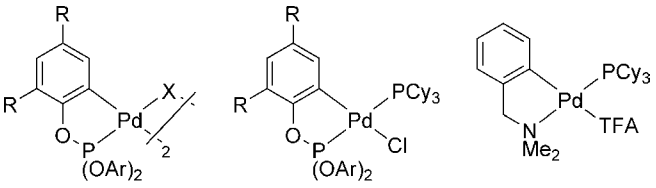

Scheme 10.11 Examples of palladacycles that are highly active catalyst precursors for the Suzuki coupling of aryl chlorides.

acids and anhydrides. Furthermore, they can be employed in the coupling of arylboronic acids with allylic chlorides and acetates and also benzylic chlorides in organic or aqueous media [86, 87]. However, the main challenges in Suzuki coupling are related to the use of less reactive aryl halides such as aryl chlorides and aryl bromides substituted with electron-donating groups, at room temperature and using low Pd loadings (>0.1%), and/or couplings of two sterically hindered substrates. However, with these conditions and substrates, only a few palladacycles have shown some catalytic activity [52, 80, 84, 88–93]. Not surprisingly, the best results on the coupling of arylboronic acids with aryl chlorides were obtained with phosphapalladacycles or with palladacycles modified with carbenes or phosphorus-containing ligands, in particular the CN [94] and CP [92] palladacycles (Scheme 10.11) associated with PCy_3 that catalyzed the coupling of 4-chlorotoluene and 4-mehoxychlorobenzene with phenylboronic acid with TONs up to 96 000 and 8000, respectively.

This might be rationalized by the extra stability provided by these ligands for the stabilization of the low-ligated catalytically active Pd(0) species involved in the main catalytic cycle. In particular, the CNP pincer palladacycle (Scheme 10.12) [95] is a highly efficient catalyst precursor for the coupling of arylboronic acids and electron-rich and -poor aryl chlorides. The corresponding cross-coupled products were isolated in excellent yields and a wide variety of functional groups are tolerated in both aryl chloride and arylboronic acid. The experimental protocol has also been extended to the coupling of iodo- and bromoarenes with arylboronic acids for the generation of hindered biphenyls such as those containing two *ortho* substituents. Steric hindrance is more sensitive for *ortho* substituents in the

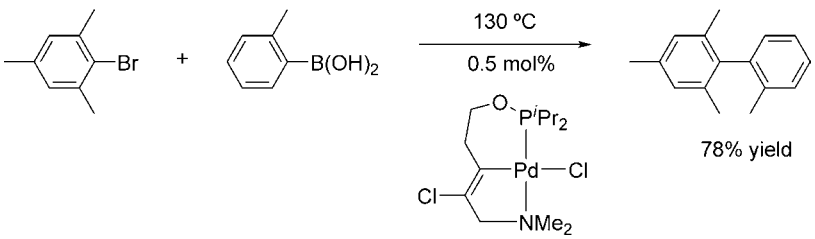

Scheme 10.12

arylboronic acid and is more pronounced when the coupling reaction involves three *ortho* substituents [96].

Moreover, a salicylaldehyde-based phosphite ligand in the palladacycle derivative **17** (Scheme 10.13) gives very high TONs in the coupling of aryl chlorides, up to 128 000 and 2 000 000 with 4-chloroanisole and 4-chloronitrobenzene, respectively [97]. The ferrocene-based palladacycle **18** (Scheme 10.13) is able to couple both electronically deactivated and sterically hindered aryl chlorides such as 4-chloroanisole and 2-chloro-*m*-xylene with phenylboronic acid, even at room temperature. At 60 °C the coupling of the non-activated substrate 4-chlorotoluene proceeds with TONs of over 9500 [93].

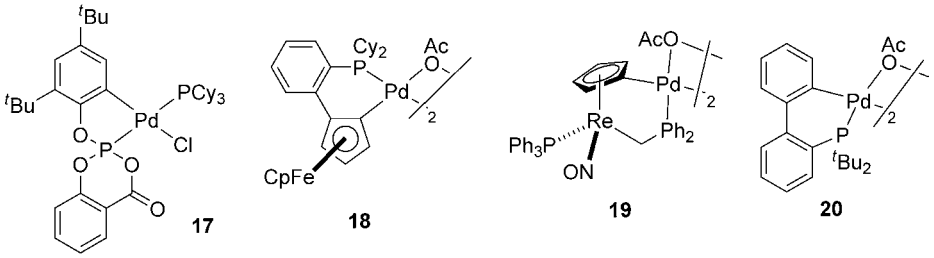

Scheme 10.13 Palladacycles used in C—C and/or C—N coupling reactions.

Palladacycles are being evaluated in more elaborate synthetic challenges, as for example the Suzuki-type cross-couplings involving 2-bromo-*N*,*N*-dimethylacetamide [98] and the six-fold vinylation of a very hindered substrate hexabromobenzene [99] catalyzed by palladacycle **1**. A series of 5,8-π-extended quinoxaline derivatives and 4,7-π-extended 2,1,3-benzothiadiazole derivatives [100, 101] were obtained by Suzuki coupling between 5,8-dibromoquinoxaline derivatives and boronic acids with the employment of an NCP-pincer palladacycle [95, 96] (Scheme 10.12) as a catalyst precursor. Note that the classical Suzuki cross-coupling protocol [102] which employs $Pd(PPh_3)_4$ results in almost no product in this specific coupling [103].

10.2.3
Stille, Kumada and Negishi Coupling

Palladacycles have been exploited in a range of other biaryl coupling reactions, namely the Stille, Kumada and Negishi couplings (Scheme 10.14) of aryl bromide substrates, in particular palladacycle **1** [23, 104].

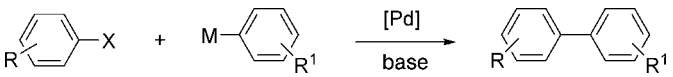

Scheme 10.14 M = SnR_3, MgX, Li, etc.

The Suzuki coupling of aryl bromides has been extensively investigated using oxime-based palladacycles **10** [105] and ferrocenyl derivative **19** (Scheme 10.13) [106],

while the tricyclohexylphosphine adduct palladacycle **5** can be used with aryl chlorides [107].

The formation of the catalytically active species for these coupling reactions is similar to that observed for the Suzuki coupling. It involves the attack of the aryl group on the Pd center followed by reductive elimination of the palladated unit with the aryl ligand (Scheme 10.15) [23]. Indeed, the by-product resulting from the coupling of the metalated ligand and the aryl group has been observed in various cases involving CP [108], CN [81, 109] and CS [110] palladacycles.

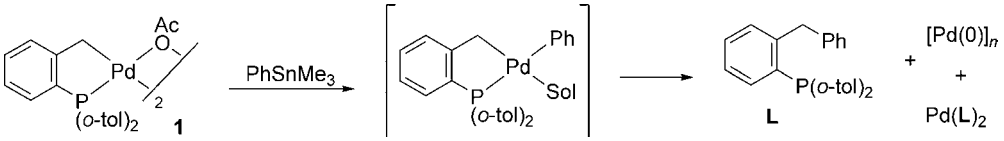

Scheme 10.15

Solid-phase Stille couplings yield biaryls employing a resin-bound stannane [111] and biphenyl analogue precursors to biphenomycin antibiotics [112] were synthesized in excellent yield via a Stille coupling using palladacycle **1**.

10.2.4
Buchwald–Hartwig Amination

The Buchwald–Hartwig amination (Scheme 10.16) of aryl bromide [104] and activated aryl chloride [113] substrates is also catalyzed by palladacycle **1** under relatively mild reaction conditions and the use of potassium *tert*-butoxide as base is crucial for the success of this C–N bond-forming reaction. TONs up to 900 and yields up to 80% have been obtained. The palladacycle **20** (Scheme 10.13) is a single source of air-stable, easily handled and commercially available catalyst for the amination of aryl chlorides [114, 115].

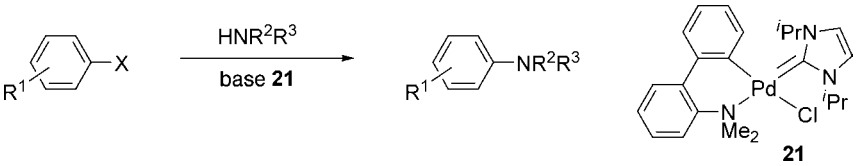

Scheme 10.16 Buchwald–Hartwig amination of aryl halides promoted by palladacycles.

As observed in the Heck and Suzuki reactions, alkylphosphine, in particular tri-*tert*-butylphosphine, adducts of *N,C*- [80, 109] and *P,C*-palladacycles [116] show substantially enhanced activity in the Buchwald–Hartwig amination of aryl chlorides and can be used in the coupling of electronically deactivated aryl chlorides. In particular, those formed *in situ* with P^tBu_3 gives a TON of 920 in the coupling of 4-chloroanisole with morpholine [109]. Carbene adducts of palladacycles also show excellent activity; the complex **21** (Scheme 10.16) can be used for the amination of both aryl chlorides and aryl triflates under mild conditions. In particular, interesting

selectivity was obtained for monoarylated products when monosubstituted amines were used as substrates [117].

It has been demonstrated that Pd(0) is the catalytically active species and in particular that the dimeric palladacycle **1** reacts with diethylamine to give the amine monomer, which is deprotonated in the presence of a base (NaO^tBu) to give the Pd(0) complex via β-elimination of the amide ligand (Scheme 10.17) [104].

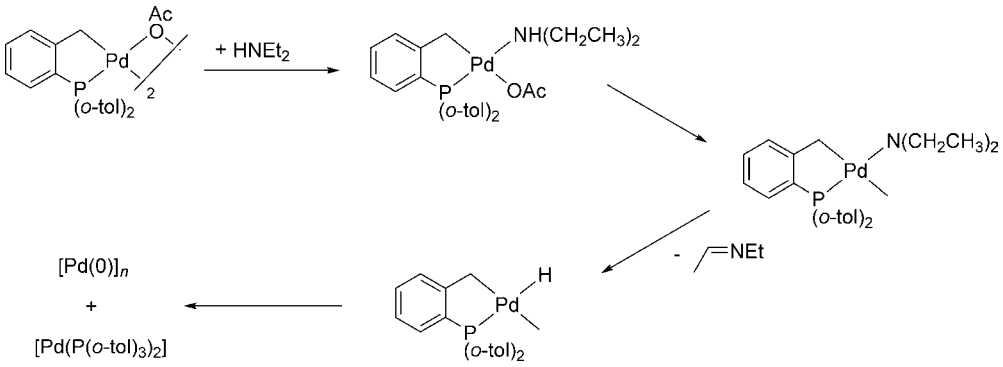

Scheme 10.17

10.2.5
Sonogashira Coupling

Palladacycles have proven also to be useful and versatile catalytic precursors for Sonogashira coupling reactions (Scheme 10.18) and again the first report was on the use of phosphapalladacycle **1** that performs the copper-free coupling of activated and non-activated aryl bromides with phenylacetylene in triethylamine at 90 °C [118]. However, neither aryl chlorides nor alkylacetylenes give satisfactory results.

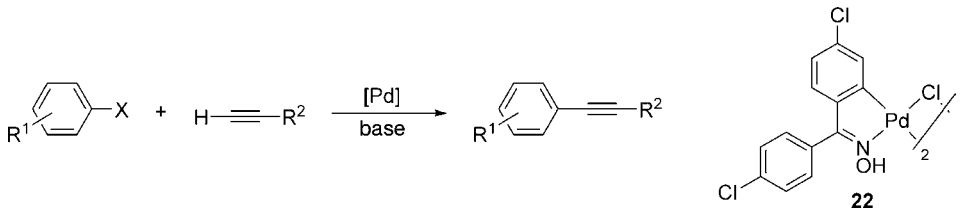

Scheme 10.18

Several nitrogen-derived palladacycles have been presented showing good activity in the Sonogashira reaction under different reaction conditions. The use of oxime-derived palladacycles [119] is an active approach for the conventional copper co-catalyzed Sonogashira coupling of iodobenzene and phenylacetylene in pyrrolidine at 90 °C [105]. However, the use of tetrabutylammonium acetate as base with NMP as solvent at 110–130 °C has allowed the use of these palladacycles for the copper- and

amine-free coupling of aryl iodides, aryl bromides and vinyl bromides with various alkynes [120, 121].

These oxime palladacycles can be used in several other Sonogashira-type couplings such as the dichlorobenzophenone oxime palladacycle **22** (Scheme 10.18) that has been employed as a copper-free promoter for the acylation of terminal alkynes with different carboxylic acid chlorides in toluene in the presence of TEA as base, giving the corresponding ynones or for the sila-Sonogashira coupling between alkynylsilanes and aryl iodides and bromides in the presence of CuI or TBAB as co-catalysts.

Other palladacycles are also effective active catalyst precursors for Sonogashira coupling involving aryl iodides and bromides such as the sulfinimine palladacycle **23** [122], the triphenylphosphine adduct palladacycle **24** derived from benzo[*b*] quinoline [123] and the *N*-heterocyclic NCN-pincer palladium complex **25** (Scheme 10.19) [124].

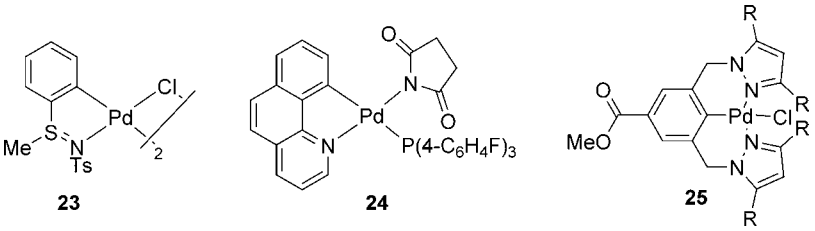

23 24 25

Scheme 10.19 Palladacycles successfully used as catalyst precursors for Sonogashira coupling reactions.

In this respect, the phosphine adduct palladacycles **26** [125] and **27** [126] (Scheme 10.20) are of special interest since they efficiently perform the Sonogashira cross-coupling reaction of aryl iodides, aryl bromides and activated aryl chlorides

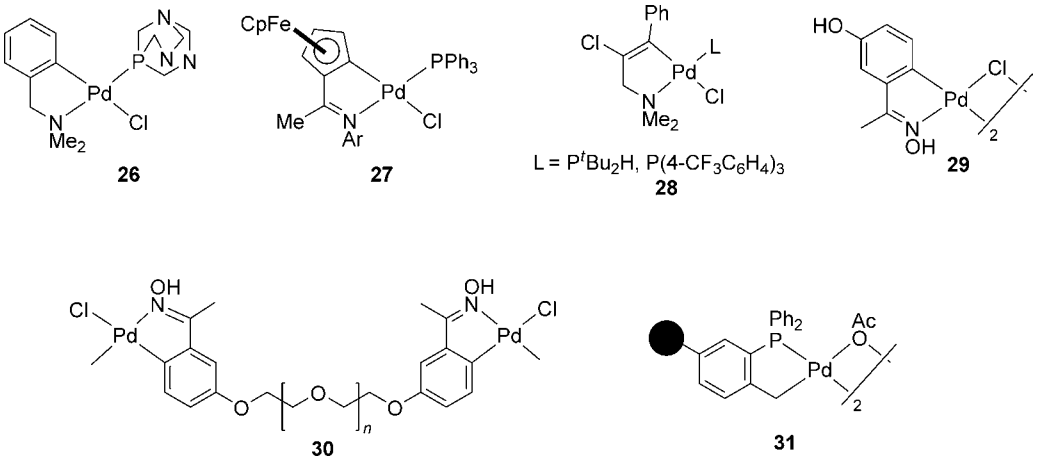

26 27 28 29 30 31

Scheme 10.20 Palladacycles used in Sonogashira coupling reactions.

with aliphatic and aromatic terminal alkynes under amine- and copper-free conditions. Pincer palladacycles such as the PCP **7** were also used to cross-couple a wide range of activated and non-activated aryl chlorides with phenylacetylene using $ZnCl_2$ as additive and the reaction was performed at 160 °C [127].

However, monomeric palladacycles such as **28** promote the alkynylation of bromo- and iodoarenes with terminal alkynes at room temperature and TONs up to 10^5 have been achieved with iodoarenes. Selective poisoning experiments (Hg, Collman and Crabtree tests) suggest that soluble Pd(0) species are the most probable catalytically active species involved in this coupling reaction [128].

Reusable palladacycle catalytic systems for the Sonogashira reaction have been attempted using palladacycle **29** (Scheme 10.20) immobilized in ionic liquids or PEG [129]. However, under copper-free conditions and heating in ionic liquids at 120 °C, palladacycle **29** decomposes, whereas this problem does not occur upon prolonged heating in PEG where decomposition instead generates PEG-stabilized active nanoparticles in a 'homogeneous' recyclable system. In addition, the anchored and soluble PEG palladacycle **30** has been used as a catalyst for a copper-free Sonogashira reaction using cesium acetate as base at 150 °C, forming recyclable catalytically active palladium nanoparticles stabilized by PEG [130].

On the other hand, the soluble linear polystyrene-supported phosphapalladacycle **31** has been used in a copper-free Sonogashira coupling of 4-bromoacetophenone and phenylacetylene and this polymeric catalyst was reused up to four times, maintaining conversions of more than 90%, but no palladium leaching studies were performed [62, 131].

Herrmann's palladacycle **1** in the presence of CuI as co-catalyst has been efficiently employed in a catalytic traceless solid-phase approach to the synthesis of 2,6,9-trisubstituted purines from resin-bound 6-thiopurines [132].

10.2.6
Other Cross-coupling Reactions

Only a few examples of Ullmann homocoupling reaction (Scheme 10.21) promoted by palladacycles such as **3** [133], **23** [122], **29** [84] and others [134] have been reported so far and in those cases only marginal catalytic activities were obtained with less reactive chloroarenes.

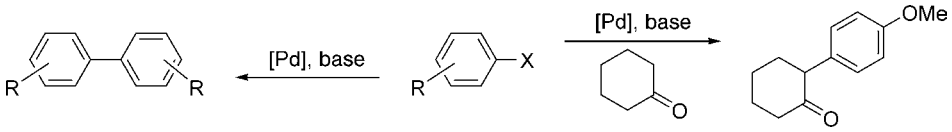

Scheme 10.21

Monomeric phosphine or NCN carbene palladacycle derivatives such as **12** and **21** have been successfully employed for the coupling of ketones (cyclohexanone and ethyl phenyl ketone) with deactivated 4-methoxychorobenzene using sodium *tert*-butoxide as a base and TONs up to 200 were achieved (Scheme 10.21) [52, 117].

10.3
Other Catalytic Reactions Catalyzed by Palladacycles

10.3.1
Asymmetric Rearrangements

When using a non-racemic palladacycle for asymmetric synthesis, two distinct outcomes can be observed depending on whether the palladacycle maintains its oxidation state, where highly enantioselective reactions are often observed, such as in allylic rearrangements or aldol condensations. If there is a prior change in Pd oxidation state as in reactions employing Pd(II) containing precatalysts and precursors to Pd(0), racemic product is usually obtained since the generated Pd(0) is no longer attached to the chiral ligand. Hence Heck reactions [135], hydroarylations [136] and cyclopropanations [137, 138] catalyzed by non-racemic palladacycles yield racemic products. Oxazoline-containing palladacycles, such as **32** (Scheme 10.22), were excellent catalysts for intramolecular asymmetric aminopalladations, achieving *ee*s of 91% (Scheme 10.23) [139].

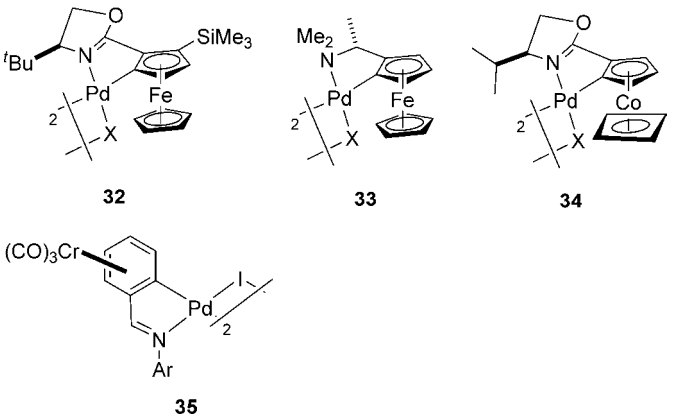

32 **33** **34** **35**

Scheme 10.22 Chiral palladacycles employed as asymmetric catalyst precursors for rearrangement processes.

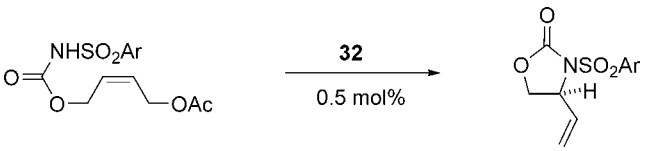

Scheme 10.23

Planar chiral palladacycles (Scheme 10.22) have been used as very successful catalysts for asymmetric allylic rearrangements leading to a high degree of stereodifferentiation. The allylamine (Scheme 10.25, $R^1 = {}^n\text{Pr}$, $R^2 = \text{Ph}$, $\text{Ar} = C_6H_4CF_3$) was obtained in 97% *ee* employing the oxazoline derivative **32**, whereas it is formed with 80% *ee* when the chromium-containing complex **35** was used

(Scheme 10.22) [140]. This process is assumed to be via an associative mechanism with an axial approach of the olefin to the square-planar palladium environment [141]. Indeed, butadiene–cobalt-containing analogues **34** conferred high enantioselectivities in allylic rearrangements leading to protected allylic amines [142–144]. Analogous asymmetric allylic imidate rearrangements and by palladacycle **34** afford chiral allylic esters in nearly quantitative yield and excellent *ee*s (up to 99%) [145].

However, complexes such as **36** (Scheme 10.24) were found to afford relatively poor *ee*s, e.g. 10% *ee* for the allylic rearrangement (Scheme 10.25, $R^1 = Me$, $R^2 = H$, $Ar = Ph$), although **37** (10 mol%) led to a respectable 79% *ee* [146].

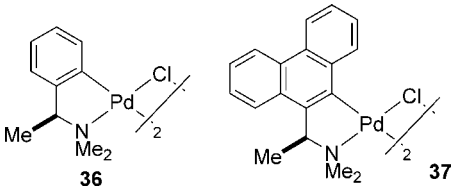

36 **37**

Scheme 10.24 Non-racemic palladacycles tested in allylic rearrangements.

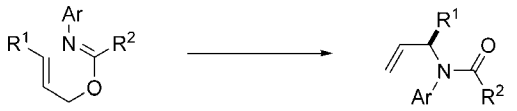

R^1 = Me, Et, ^{n}Pr; R^2 = H, Ph, CF_3; Ar = Ph, $MeOC_6H_4$, $CF_3C_6H_4$

Scheme 10.25

10.3.2
Aldol Condensations and Related Reactions

PCP pincer complexes **38** and **39** (Scheme 10.26) catalyze the addition of allylstannanes or allyl borates to aldehydes, imines and tosylamides (Scheme 10.27). The robust nature of the pincer system ensures that the allylic intermediate is nucleophilic, i.e. η^1-bound to the metal center [147–149].

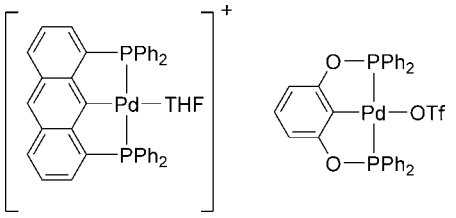

38 **39**

Scheme 10.26 Pincer palladacycles used in aldol condensations.

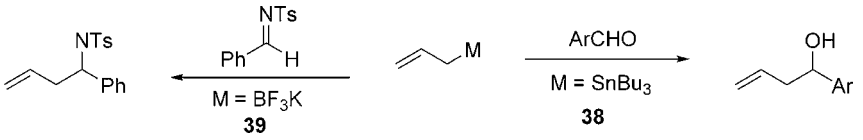

Scheme 10.27

The asymmetric version of this nucleophilic allylic addition chemistry has been disclosed with acceptable *ee*s when employing the BINOL-substituted palladacycle **40** (Scheme 10.28) [150]. This processes is thought to involve a monomeric Pd(II) complex as opposed to (achiral) Pd(0).

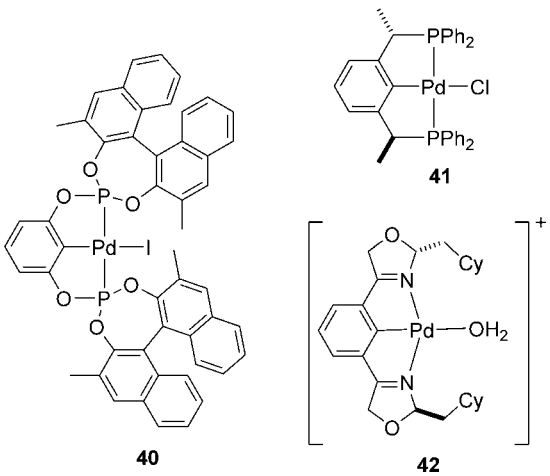

Scheme 10.28 Non-racemic pincer palladacycles used in asymmetric aldol condensations and related reactions.

Pincer-type palladacycles have also been employed as chiral Lewis acids for aldol and Michael-type chemistry in the formation of heterocyclic and acyclic compounds. Moderate to good degrees of success in terms of asymmetric induction were observed, up to 34% *ee* for the formation of the acyclic Michael product (Scheme 10.29) [151–154].

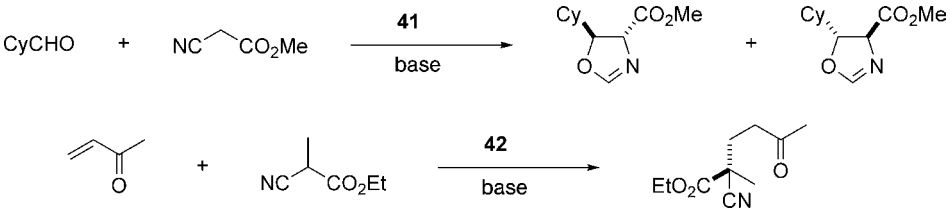

Scheme 10.29

A related Michael addition employed the elaborate pincer complex **42** as catalyst and was used for the formation of the quaternary carbon center with excellent enantioselectivities of up to 83% (Scheme 10.29) [155].

10.3.3
Oxidation, Telomerization and Substitution Reactions

Acetate-bridged palladacycles derived from N(sp^2)-containing ligands such as oxazole **43** and pyridine **44** (Scheme 10.30) are effective catalysts for the oxidation of primary and secondary alcohols to the corresponding aldehydes and ketones under an atmospheric pressure of air without the addition of any other re-oxidants [156–158].

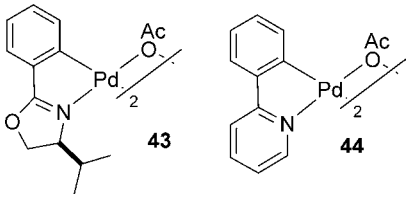

Scheme 10.30 Palladacycles employed as catalyst precursors for aerobic oxidation of alcohols.

The telomerization of 1,3-dienes with alcohols can be performed by palladacycles (Scheme 10.31). Cationic derivatives such as those derived from the cyclopalladation of 8-methylquinoline and *N*,*N*-dimethylbenzylamine promote the telomerization of 1,3-butadiene with methanol, affording the telomers $C_{16}OMe$ as the major products (Scheme 10.32) [22]. These palladacycles associated with phosphine enolate derivatives are effective for the coupling of two 1,3-butadiene units with carbon dioxide, affording the lactone 2-ethylidene-6-hepten-5-olide with selectivity up to 93% (Scheme 10.32) [159].

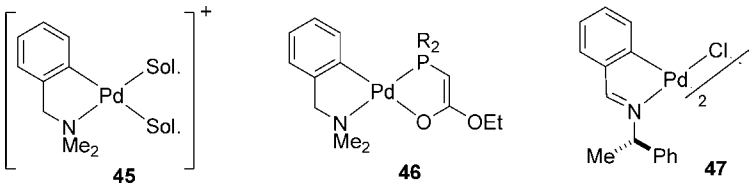

Scheme 10.31 Palladacycles employed as catalyst precursors for the telomerization of 1,3-dienes with alcohols or carbon dioxide.

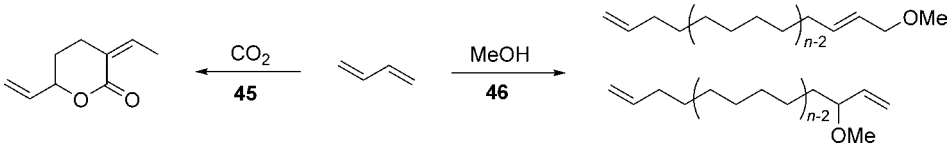

Scheme 10.32

The telomerization of isoprene with methanol was also performed using non-racemic cyclopalladated imines but without any asymmetric induction [160].

Palladium pincer complex **47** (Scheme 10.33) efficiently catalyzes the regioselective transfer of stannyl or silyl groups to propargyl chlorides or epoxides [161, 162].

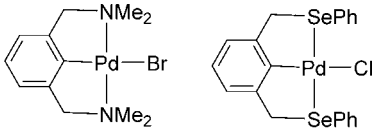

47 48

Scheme 10.33 NCN and SeCSe palladacycles used in nucleophilic substitution reactions.

The proposed reaction mechanism involves a transmetalation step in which the trialkylstannyl or trialkylsilyl groups are transferred to the palladium center followed by the transfer of the organometallic fragment to the propargylic substrate.

Similarly, a hydroxy to boronate substitution process could be achieved under mild conditions using a wide variety of allyl alcohols and diboronic acid with 5 mol% pincer complex **48** (Scheme 10.33) in a mixture of DMSO and MeOH. This reaction can be employed for the regio- and stereoselective synthesis of allyl boronic acids that are not sufficiently stable under solvent-free conditions and were immediately converted to their trifluoro(allyl)borate derivatives (Scheme 10.34) [163].

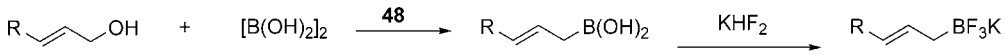

Scheme 10.34

10.4 Conclusion

Palladacycles have numerous applications beyond the usual scope of C–C cross-coupling reactions and related chemistries. Palladacycle precatalysts can show very high activity in Heck and Suzuki coupling, Buchwald–Hartwig amination and related coupling reactions under mild conditions, for instance at room temperature or in water. Their ease of handling, high thermal stability and low air sensitivity add to their general appeal. It is clear, however, that the palladacycles that serve as precursors to highly active palladium(0) species consist of soluble clusters or colloids, often stabilized by quaternary ammonium salts in highly dilute solutions or highly active, low-coordinate complexes of electron-rich phosphines or carbenes. Moreover, there is a fine balance to play between the relative rates of active catalyst production and decomposition and it seems likely that in the many examples palladacycle precursors outperform more than classical palladium sources. Moreover, a greater understanding of the mechanisms involved in palladacycle-mediated reactions has led to the development of reactions that have wide applications in organic synthesis. In particular, chiral palladacycles are very important catalysts for enantioselective allylic rearrangements, allylic additions and aldol chemistry, since they act as Pd(II) Lewis acids and no redox process occurs. Palladacycles will no doubt continue to have a huge impact in atom economical synthesis, in particular in the area of CH activation chemistry that will continue to flourish.

References

1 Cope, A.C. and E.C., Friedric (1968) *Journal of the American Chemical Society*, **90**, 909.
2 Dehand, J. and Pfeffer, M. (1976) *Coordination Chemistry Reviews*, **18**, 327.
3 Dupont, J., Consorti, C.S. and Spencer, J. (2005) *Chemical Reviews*, **105**, 2527.
4 Omae, I. (1979) *Coordination Chemistry Reviews*, **28**, 97.
5 Omae, I. (1979) *Chemical Reviews*, **79**, 287.
6 Omae, I. (1980) *Coordination Chemistry Reviews*, **32**, 235.
7 Omae, I. (1982) *Coordination Chemistry Reviews*, **42**, 245.
8 Omae, I. (1982) *Journal of Synthetic Organic Chemistry, Japan*, **40**, 147.
9 Omae, I. (2004) *Coordination Chemistry Reviews*, **248**, 995.
10 Pfeffer, M. (1990) *Recueil des Travaux Chimiques des Pays-Bas Journal of the Royal Netherlands Chemical Society*, **109**, 567.
11 Pfeffer, M. (1992) *Pure and Applied Chemistry*, **64**, 335.
12 Singleton, J.T. (2003) *Tetrahedron*, **59**, 1837.
13 Albrecht, M. and van Koten, G. (2001) *Angewandte Chemie-International Edition*, **40**, 3750.
14 Steenwinkel, P., Gossage, R.A. and van Koten, G. (1998) *Chemistry – A European Journal*, **4**, 759.
15 van der Boom, M.E. and Milstein, D. (2003) *Chemical Reviews*, **103**, 1759.
16 Bruce, M.I. (1977) *Angewandte Chemie-International Edition*, **16**, 73.
17 Lewis, L.N. (1986) *Journal of the American Chemical Society*, **108**, 743.
18 Bose, A. and Saha, C.R. (1989) *Journal of Molecular Catalysis*, **49**, 271.
19 Santra, P.K. and Saha, C.R. (1987) *Journal of Molecular Catalysis*, **39**, 279.
20 Herrmann, W.A., Brossmer, C., Ofele, K., Reisinger, C.P., Priermeier, T., Beller, M. and Fischer, H. (1995) *Angewandte Chemie-International Edition*, **34**, 1844.
21 Beller, M., Fischer, H., Herrmann, W.A., Ofele, K. and Brossmer, C. (1995) *Angewandte Chemie-International Edition*, **34**, 1848.
22 Camargo, M., Dani, P., Dupont, J., deSouza, R.F., Pfeffer, M. and Tkatchenko, I. (1996) *Journal of Molecular Catalysis A-Chemical*, **109**, 127.
23 Herrmann, W.A., Bohm, V.P.W. and Reisinger, C.P. (1999) *Journal of Organometallic Chemistry*, **576**, 23.
24 Dupont, J., Pfeffer, M. and Spencer, J. (2001) *European Journal of Inorganic Chemistry*, 1917.
25 Bedford, R.B. (2003) *Chemical Communications*, 1787.
26 Bellina, F., Carpita, A. and Rossi, R. (2004) *Synthesis*, 2419.
27 Beletskaya, I.P. and Cheprakov, A.V. (2004) *Journal of Organometallic Chemistry*, **689**, 4055.
28 Whitfield, S.R. and Sanford, M.S. (2007) *Journal of the American Chemical Society*, **129**, 15142.
29 Consorti, C.S., Flores, F.R. and Dupont, J. (2005) *Journal of the American Chemical Society*, **127**, 12054.
30 Consorti, C.S., Zanini, M.L., Leal, S., Ebeling, G. and Dupont, J. (2003) *Organic Letters*, **5**, 983.
31 Gruber, A.S., Pozebon, D., Monteiro, A.L. and Dupont, J. (2001) *Tetrahedron Letters*, **42**, 7345.
32 Zim, D., Monteiro, A.L. and Dupont, J. (2000) *Tetrahedron Letters*, **41**, 8199.
33 Ohff, M., Ohff, A. and Milstein, D. (1999) *Chemical Communications*, 357.
34 Weissman, H. and Milstein, D. (1999) *Chemical Communications*, 1901.
35 Alimardanov, A., de Vondervoort, L.S.V., de Vries, A.H.M. and de Vries, J.G. (2004) *Advanced Synthesis and Catalysis*, **346**, 1812.
36 Reetz, M.T. and de Vries, J.G. (2004) *Chemical Communications*, 1559.

37 Beletskaya, I.P. and Cheprakov, A.V. (2000) *Chemical Reviews*, **100**, 3009.

38 Moritani, I. and Fujiwara, Y. (1973) *Synthesis*, 524.

39 Tsuji, J. (1969) *Accounts of Chemical Research*, **2**, 144.

40 Jeffery, T. (1984) *Journal of the Chemical Society. Chemical Communications*, 1287.

41 Jeffery, T. (1985) *Tetrahedron Letters*, **26**, 2667.

42 Schmidt, A.F., Al Halaiqa, A. and Smirnov, V.V. (2006) *Synlett*, 2861.

43 Shmidt, A.F. and Khalaika, A. (1998) *Kinetics and Catalysis*, **39**, 803.

44 de Vries, A.H.M., Mulders, J.M.C.A., Mommers, J.H.M., Henderickx, H.J.W. and de Vries, J.G. (2003) *Organic Letters*, **5**, 3285.

45 de Vries, A.H.M., Parlevliet, F.J., Schmieder-van de Vondervoort, L., Mommers, J.H.M., Henderickx, H.J.W., Walet, M.A.M. and de Vries, J.G. (2002) *Advanced Synthesis and Catalysis*, **344**, 996.

46 Shmidt, A.F., Khalaika, A. and Bylkova, V.G. (1998) *Kinetics and Catalysis*, **39**, 194.

47 Littke, A.F. and Fu, G.C. (2002) *Angewandte Chemie-International Edition*, **41**, 4176.

48 Bohm, V.P.W. and Herrmann, W.A. (2000) *Chemistry – A European Journal*, **6**, 1017.

49 Morales-Morales, D., Redon, R., Yung, C. and Jensen, C.M. (2000) *Chemical Communications*, 1619.

50 Alonso, D.A., Najera, C. and Pacheco, M.C. (2002) *Advanced Synthesis and Catalysis*, **344**, 172.

51 Iyer, S. and Jayanthi, A. (2003) *Synlett*, 1125.

52 Schnyder, A., Indolese, A.F., Studer, M. and Blaser, H.U. (2002) *Angewandte Chemie-International Edition*, **41**, 3668.

53 Corma, A., Garcia, H. and Leyva, A. (2004) *Tetrahedron*, **60**, 8553.

Q1 **54** Zheng, R., Yang, F., Zou, G., Tang, J. and He, M.-Y. (2003) *Chin J Chem*, **21**, 1111.

55 Botella, L. and Najera, C. (2004) *Tetrahedron Letters*, **45**, 1833.

56 Bergbreiter, D.E., Osburn, P.L. and Liu, Y.S. (1999) *Journal of the American Chemical Society*, **121**, 9531.

57 Bergbreiter, D.E., Osburn, P.L., Wilson, A. and Sink, E.M. (2000) *Journal of the American Chemical Society*, **122**, 9058.

58 Bergbreiter, D.E. and Furyk, S. (2004) *Green Chemistry*, **6**, 280.

59 Rocaboy, C. and Gladysz, J.A. (2003) *New Journal of Chemistry*, **27**, 39.

60 Rocaboy, C. and Gladysz, J.A. (2002) *Organic Letters*, **4**, 1993.

61 McNamara, C.A., King, F. and Bradley, M. (2004) *Tetrahedron Letters*, **45**, 8239.

62 Lin, C.A. and Luo, F.T. (2003) *Tetrahedron Letters*, **44**, 7565.

63 Nowotny, M., Hanefeld, U., van Koningsveld, H. and Maschmeyer, T. (2000) *Chemical Communications*, 1877.

64 Venkatesan, C. and Singh, A.P. (2003) *Catalysis Letters*, **88**, 193.

65 Gholap, A.R., Venkatesan, K., Daniel, T., Lahoti, R.J. and Srinivasan, K.V. (2003) *Green Chemistry*, **5**, 693.

66 Venkatesan, C. and Singh, A.P. (2004) *Journal of Catalysis*, **227**, 148.

67 Venkatesan, C. and Singh, A.P. (2004) *Recent Advances in the Science and Technology of Zeolites and Related Materials, Parts A–C*, **154**, 2795.

68 Yu, K.Q., Sommer, W., Weck, M. and Jones, C.W. (2004) *Journal of Catalysis*, **226**, 101.

69 Bergbreiter, D.E., Osburn, P.L. and Frels, J.D. (2005) *Advanced Synthesis and Catalysis*, **347**, 172.

70 Yu, K.Q., Sommer, W., Richardson, J.M., Weck, M. and Jones, C.W. (2005) *Advanced Synthesis and Catalysis*, **347**, 161.

71 Sommer, W.J., Yu, K.Q., Sears, J.S., Ji, Y.Y., Zheng, X.L., Davis, R.J., Sherrill, C.D., Jones, C.W. and Weck, M. (2005) *Organometallics*, **24**, 4351.

72 Xiong, Z.C., Wang, N.D., Dai, M.J., Li, A., Chen, J.H. and Yang, Z. (2004) *Organic Letters*, **6**, 3337.

73 Takenaka, K. and Uozumi, Y. (2004) *Advanced Synthesis and Catalysis*, **346**, 1693.

74 Chen, C.T., Chan, Y.S., Tzeng, Y.R. and Chen, M.T. (2004) *Dalton Transactions*, 2691.

75 Xu, L.J., Mo, J., Baillie, C. and Xiao, J.L. (2003) *Journal of Organometallic Chemistry*, **687**, 301.

76 Chen, W.P., Xu, L.J. and Xiao, J.L. (2001) *Tetrahedron Letters*, **42**, 4275.

77 Panday, N., Canac, Y. and Vasella, A. (2000) *Helvetica Chimica Acta*, **83**, 58.

78 Prashad, M., Liu, Y.G., Mak, X.Y., Har, D., Repic, J. and Blacklock, T.J. (2002) *Tetrahedron Letters*, **43**, 8559.

79 Old, D.W., Wolfe, J.P. and Buchwald, S.L. (1998) *Journal of the American Chemical Society*, **120**, 9722.

80 Bedford, R.B. and Cazin, C.S.J. (2001) *Chemical Communications*, 1540.

81 Bedford, R.B., Cazin, C.S.J., Hursthouse, M.B., Light, M.E., Pike, K.J. and Wimperis, S. (2001) *Journal of Organometallic Chemistry*, **633**, 173.

82 Monteiro, A.L. and Davis, W.M. (2004) *Journal of the Brazilian Chemical Society*, **15**, 83.

83 Albisson, D.A., Bedford, R.B., Lawrence, S.E. and Scully, P.N. (1998) *Chemical Communications*, 2095.

84 Alonso, D.A., Najera, C. and Pacheco, M.C. (2002) *The Journal of Organic Chemistry*, **67**, 5588.

85 Botella, L. and Najera, C. (2002) *Angewandte Chemie-International Edition*, **41**, 179.

86 Botella, L. and Najera, C. (2002) *Journal of Organometallic Chemistry*, **663**, 46.

87 Costa, A., Najera, C. and Sansano, J.M. (2002) *The Journal of Organic Chemistry*, **67**, 5216.

88 Mino, T., Shirae, Y., Sakamoto, M. and Fujita, T. (2003) *Synlett*, 882.

89 Zim, D., Gruber, A.S., Ebeling, G., Dupont, J. and Monteiro, A.L. (2000) *Organic Letters*, **2**, 2881.

90 Gibson, S., Foster, D.F., Eastham, G.R., Tooze, R.P. and Cole-Hamilton, D.J. (2001) *Chemical Communications*, 779.

91 Navarro, O., Kelly, R.A. and Nolan, S.P. (2003) *Journal of the American Chemical Society*, **125**, 16194.

92 Bedford, R.B., Hazlewood, S.L., Limmert, M.E., Albisson, D.A., Draper, S.M., Scully, P.N., Coles, S.J. and Hursthouse, M.B. (2003) *Chemistry – A European Journal*, **9**, 3216.

93 Roca, F.X. and Richards, C.J. (2003) *Chemical Communications*, 3002.

94 Bedford, R.B. and Welch, S.L. (2001) *Chemical Communications*, 129.

95 Rosa, G.R., Ebeling, G., Dupont, J. and Monteiro, A.L. (2003) *Synthesis*, 2894.

96 Rosa, G.R., Rosa, C.H., Rominger, F., Dupont, J. and Monteiro, A.L. (2006) *Inorganica Chimica Acta*, **359**, 1947.

97 Bedford, R.B., Hazelwood, S.L. and Limmert, M.E. (2002) *Chemical Communications*, 2610.

98 Lu, T.Y., Xue, C.H. and Luo, F.T. (2003) *Tetrahedron Letters*, **44**, 1587.

99 Prinz, P., Lansky, A., Haumann, T., Boese, R., Noltemeyer, M., Knieriem, B. and deMeijere, A. (1997) *Angewandte Chemie-International Edition*, **36**, 1289.

100 Neto, B.A.D., Lapis, A.A.M., Mancilha, F.S., Vasconcelos, I.B., Thum, C., Basso, L.A., Santos, D.S. and Dupont, J. (2007) *Organic Letters*, **9**, 4001.

101 Neto, B.A.D., Lopes, A.S.A., Ebeling, G., Goncalves, R.S., Costa, V.E.U., Quina, F.H. and Dupont, J. (2005) *Tetrahedron*, **61**, 10975.

102 Miyaura, N., Yanagi, T. and Suzuki, A. (1981) *Synthetic Communications*, **11**, 513.

103 Mancilha, F.S., Neto, B.A.D., Lopes, A.S., Moreira, P.F., Quina, F.H., Goncalves, R.S. and Dupont, J. (2006) *European Journal of Organic Chemistry*, 4924.

104 Louie, J. and Hartwig, J.F. (1996) *Angewandte Chemie-International Edition*, **35**, 2359.

105 Alonso, D.A., Najera, C. and Pacheco, M.C. (2000) *Organic Letters*, **2**, 1823.

106 Friedlein, F.K., Kromm, K., Hampel, F. and Gladysz, J.A. (2006) *Chemistry – A European Journal*, **12**, 5267.

107 Bedford, R.B., Cazin, C.S.J. and Hazelwood, S.L. (2002) *Chemical Communications*, 2608.

108 Bedford, R.B., Hazelwood, S.L., Horton, P.N. and Hursthouse, M.B. (2003) *Dalton Transactions*, 4164.

109 Bedford, R.B., Cazin, C.S.J., Coles, S.J., Gelbrich, T., Horton, P.N., Hursthouse, M.B. and Light, M.E. (2003) *Organometallics*, **22**, 987.

110 Bedford, R.B., Cazin, C.S.J. and Hazelwood, S.L. (2002) *Angewandte Chemie-International Edition*, **41**, 4120.

111 Paintner, F.F., Gorler, K. and Voelter, W. (2003) *Synlett*, 522.

112 Brody, M.S. and Finn, M.G. (1999) *Tetrahedron Letters*, **40**, 415.

113 Beller, M., Riermeier, T.H., Reisinger, C.P. and Herrmann, W.A. (1997) *Tetrahedron Letters*, **38**, 2073.

114 Strieter, E.R. and Buchwald, S.L. (2006) *Angewandte Chemie-International Edition*, **45**, 925.

115 Zim, D. and Buchwald, S.L. (2003) *Organic Letters*, **5**, 2413.

116 Bedford, R.B. and Blake, M.E. (2003) *Advanced Synthesis and Catalysis*, **345**, 1107.

117 Viciu, M.S., Kelly, R.A., Stevens, E.D., Naud, F., Studer, M. and Nolan, S.P. (2003) *Organic Letters*, **5**, 1479.

118 Herrmann, W.A., Reisinger, C.P., Ofele, K., Brossmer, C., Beller, M. and Fischer, H. (1996) *Journal of Molecular Catalysis A-Chemical*, **108**, 51.

119 Alonso, D.A., Botella, L., Najera, C. and Pacheco, C. (2004) *Synthesis* 1713.

120 Alonso, D.A., Najera, C. and Pacheco, M.C. (2002) *Tetrahedron Letters*, **43**, 9365.

121 Alonso, D.A., Najera, C. and Pacheco, M.C. (2003) *Advanced Synthesis and Catalysis*, **345**, 1146.

122 Thakur, V.V., Kumar, N.S.C.R. and Sudalai, A. (2004) *Tetrahedron Letters*, **45**, 2915.

123 Fairlamb, I.J.S., Kapdi, A.R., Lee, A.F., Sanchez, G., Lopez, G., Serrano, J.L., Garcia, L., Perez, J. and Perez, E. (2004) *Dalton Transactions*, 3970.

124 Churruca, F., SanMartin, R., Tellitu, I. and Dominguez, E. (2005) *Synlett*, 3116.

125 Ruiz, J., Cutillas, N., Lopez, F., Lopez, G. and Bautista, D. (2006) *Organometallics*, **25**, 5768.

126 Yang, F., Cui, X.L., Li, Y.N., Zhang, J.L., Ren, G.R.R. and Wu, Y.J. (2007) *Tetrahedron*, **63**, 1963.

127 Eberhard, M.R., Wang, Z.H. and Jensen, C.M. (2002) *Chemical Communications*, 818.

128 Consorti, C.S., Flores, F.R., Rominger, F. and Dupont, J. (2006) *Advanced Synthesis and Catalysis*, **348**, 133.

129 Corma, A., Garcia, H. and Leyva, A. (2005) *Tetrahedron*, **61**, 9848.

130 Alacid, E. and Najera, C. (2006) *Synlett*, 2959.

131 Luo, F.T., Xue, C.H., Ko, S.L., Shao, Y.D., Wu, C.J. and Kuo, Y.M. (2005) *Tetrahedron*, **61**, 6040.

132 Brun, V., Legraverend, M. and Grierson, D.S. (2002) *Tetrahedron*, **58**, 7911.

133 Silveira, P.B., Lando, V.R., Dupont, J. and Monteiro, A.L. (2002) *Tetrahedron Letters*, **43**, 2327.

134 Li, Q., Nie, J., Yang, F., Zheng, R., Zou, G. and Tang, J. (2004) *Chinese Journal of Chemistry*, **22**, 419.

135 Dupont, J., Gruber, A.S., Fonseca, G.S., Monteiro, A.L., Ebeling, G. and Burrow, R.A. (2001) *Organometallics*, **20**, 171.

136 Bravo, J., Cativiela, C., Navarro, R. and Urriolabeitia, E.P. (2002) *Journal of Organometallic Chemistry*, **650**, 157.

137 Denmark, S.E., Stavenger, R.A., Faucher, A.M. and Edwards, J.P. (1997) *The Journal of Organic Chemistry*, **62**, 3375.

138 Navarro, R., Urriolabeitia, E.P., Cativiela, C., DiazdeVillegas, M.D., Lopez, M.P. and Alonso, E. (1996) *Journal of Molecular Catalysis A-Chemical*, **105**, 111.

139 Overman, L.E. and Remarchuk, T.P. (2002) *Journal of the American Chemical Society*, **124**, 12.

140 Hollis, T.K. and Overman, L.E. (1997) *Tetrahedron Letters*, **38**, 8837.

141 Watson, M.P., Overman, L.E. and Bergman, R.G. (2007) *Journal of the American Chemical Society*, **129**, 5031.

142 Kirsch, S.F., Overman, L.E. and Watson, M.P. (2004) *The Journal of Organic Chemistry*, **69**, 8101.
143 Overman, L.E., Owen, C.E., Pavan, M.M. and Richards, C.J. (2003) *Organic Letters*, **5**, 1809.
144 Prasad, R.S., Anderson, C.E., Richards, C.J. and Overman, L.E. (2005) *Organometallics*, **24**, 77.
145 Kirsch, S.F. and Overman, L.E. (2005) *Journal of the American Chemical Society*, **127**, 2866.
146 Leung, P.H., Ng, K.H., Li, Y.X., White, A.J.P. and Williams, D.J. (1999) *Chemical Communications*, 2435.
147 Solin, N., Kjellgren, J. and Szabo, K.J. (2004) *Journal of the American Chemical Society*, **126**, 7026.
148 Solin, N., Wallner, O.A. and Szabo, K.J. (2005) *Organic Letters*, **7**, 689.
149 Szabo, K.J. (2006) *Synlett*, 811.
150 Wallner, O.A., Olsson, V.J., Eriksson, L. and Szabo, K.J. (2006) *Inorganica Chimica Acta*, **359**, 1767.
151 Longmire, J.M., Zhang, X.M. and Shang, M.Y. (1998) *Organometallics*, **17**, 4374.
152 Albrecht, M., Kocks, B.M., Spek, A.L. and van Koten, G. (2001) *Journal of Organometallic Chemistry*, **624**, 271.
153 Stark, M.A., Jones, G. and Richards, C.J. (2000) *Organometallics*, **19**, 1282.
154 Stark, M.A. and Richards, C.J. (1997) *Tetrahedron Letters*, **38**, 5881.
155 Takenaka, K. and Uozumi, Y. (2004) *Organic Letters*, **6**, 1833.
156 Hallman, K. and Moberg, C. (2001) *Advanced Synthesis and Catalysis*, **343**, 260.
157 Paavola, S., Zetterberg, K., Privalov, T., Csoregh, I. and Moberg, C. (2004) *Advanced Synthesis and Catalysis*, **346**, 237.
158 Privalov, T., Linde, C., Zetterberg, K. and Moberg, C. (2005) *Organometallics*, **24**, 885.
159 Braunstein, P., Matt, D. and Nobel, D. (1988) *Journal of the American Chemical Society*, **110**, 3207.
160 Dani, P., Dupont, J. and Monteiro, A.L. (1996) *Journal of the Brazilian Chemical Society*, **7**, 15.
161 Kjellgren, J., Sunden, H. and Szabo, K.J. (2004) *Journal of the American Chemical Society*, **126**, 474.
162 Kjellgren, J., Sunden, H. and Szabo, K.J. (2005) *Journal of the American Chemical Society*, **127**, 1787.
163 Olsson, V.J., Sebelius, S., Selander, N. and Szabo, K.J. (2006) *Journal of the American Chemical Society*, **128**, 4588.

11
Homogeneous Catalyst Design for the Synthesis of Aliphatic Polycarbonates and Polyesters

Geoffrey W. Coates and Ryan C. Jeske

11.1
Introduction

Synthetic polymers are more important now than at any other time in history. Although polymeric materials are indispensable in a diverse array of applications, ranging from commodity packaging and structural materials to technologically complex biomedical and electronic devices, their synthesis and proper disposal pose important environmental challenges. Two ways to achieve new polymers with reduced environmental impact are (1) the development of synthetic procedures that reduce energy consumption, the use of non-renewable resources (fossil fuels) or the generation of chemical waste; and (2) the synthesis of polymers that are easily recycled and/or biodegraded [1]. At the present time, fossil fuels are the predominant source of carbon for raw materials used in the chemical industry, with synthetic plastics accounting for approximately 7% of worldwide oil and gas consumption [2]. Because these resources have an uncertain future [3], there is significant interest in finding new routes from biorenewable resources to important chemicals, especially polymers. In addition, the current worldwide production of plastics is approximately 150 million tons per year [2]. Since 30 million tons of this material end up in landfills or are incinerated in the USA alone, there is growing interest in biodegradable and recyclable polymers. Biodegradable materials are especially valuable in applications where unwanted dispersal in the environment leads to disastrous ecological problems. One example of note is the North Pacific Subtropical Gyre, an area of ocean the size of Texas between California and Hawaii, where 6 billion pounds of floating plastic have accumulated over the last half-century [4]. The Technology Vision 2020 Report sponsored by the American Chemical Society proposed that the development of sustainable routes to polymeric materials will be a major challenge for the US chemical industry in the 21st century [5], and a 2005 workshop by the National Research Council of the National Academies [6] concluded that the development of environmentally benign materials should be a major goal of future research.

Green Catalysis, Volume 1: Homogeneous Catalysis.
Edited by Robert H. Crabtree

ISBN: 978-3-527-32496-5

It is therefore timely to summarize some recent progress in the development of biodegradable polymers, especially those from renewable resources. The focus of this chapter is the development and application of homogeneous catalysts for the synthesis of biodegradable, aliphatic polycarbonates and polyesters (Scheme 11.1). Due to limitations of space, this review will not be comprehensive and will focus on select examples of homogeneous catalysts for the synthesis of aliphatic polyesters and polycarbonates, with emphasis on catalysts that exhibit high activities, control of polymer stereochemistry, composition and/or molecular weight, especially those that are used for the polymerization of commodity monomers.

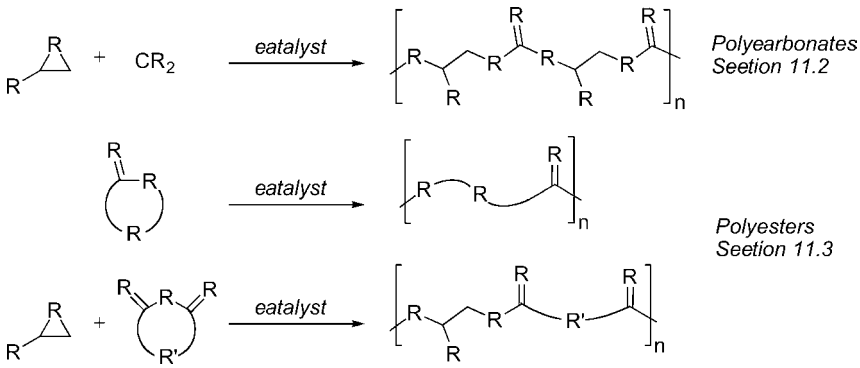

Scheme 11.1 Overview of the focus of this chapter: homogeneous catalysts for the synthesis of aliphatic polyesters and polycarbonates.

11.2
Synthesis of Aliphatic Polycarbonates from Epoxides and Carbon Dioxide

Since petroleum resources are predicted to be exhausted within the next century at the current rate of consumption [7], there is a growing effort to develop new chemical processes using biorenewable resources [8]. One such resource of particular interest is CO_2, a non-toxic, non-flammable, naturally abundant C_1 feedstock [9]. The reaction of CO_2 with metal complexes has been extensively studied, revealing potential pathways for catalytic reactions. However, the thermodynamic stability of CO_2 has hampered its utility as a reagent for chemical synthesis; in fact, its high stability makes it an ideal medium for many chemical processes [10]. To overcome this limitation, reactions employing CO_2 with highly reactive reagents have been explored. In particular, the catalytic coupling of CO_2 with heterocycles has received a considerable amount of attention over the past 35 years [11, 12]. A majority of these publications involve the reaction of CO_2 with epoxides to generate polycarbonates (Scheme 11.2).

The high cost ($\sim$\$100 lb^{-1}) of aliphatic polycarbonates is one of the main barriers to their widespread use as bulk polymeric materials. More economically viable processes and the synthesis of new types of improved aliphatic polycarbonates would

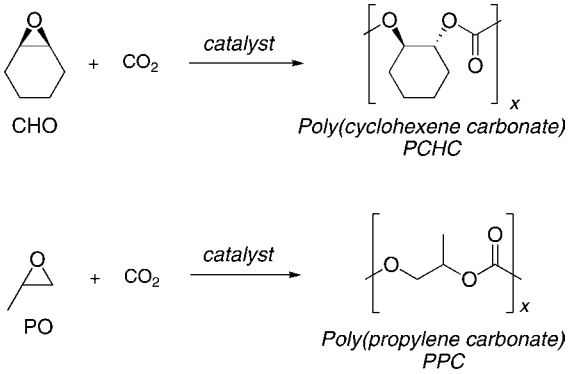

Scheme 11.2 Alternating copolymerization of cyclohexene oxide (CHO) and propylene oxide (PO) with CO_2.

clearly increase the number of applications for these polymers, and also lower their cost. A significant contributor to the cost of these materials is the low activity of the industrial zinc–dicarboxylic acid catalysts used to copolymerize epoxides and CO_2. As a result, a significant amount of recent research has been focused on the discovery and development of new catalysts for this process.

There are many parallels between the development of alkene polymerization catalysts and those for CO_2–epoxide polymerization. In each field, the catalysts initially discovered were heterogeneous in nature; subsequent work was focused on the empirical optimization to provide higher activity and selectivity for the polymerizations. Eventually, discrete, homogeneous metal complexes were explored in academic laboratories as a way to probe reaction mechanisms. By gaining a detailed understanding of the polymerizations at the molecular level, it was hoped that the lessons learned could then be applied to the design of improved catalytic systems. In some cases, these new homogeneous catalysts have significant advantages over their heterogeneous counterparts.

Heterogeneous catalysts are the workhorse of many industrial processes. Although they have many processing advantages over their soluble counterparts, heterogeneous catalysts often contain multiple active sites that result in polymers with broad polydispersity indices (PDIs) and composition distributions. In many cases, only a small percentage of the metal sites are active and residual catalyst remains in the polymeric product. As a result of these drawbacks, a significant amount of research has been directed towards the development of well-defined, single-site homogeneous catalysts. Homogeneous catalysts are typically of the form L_nMR, where L_n is a set of permanently bound ligands, M is a metal center and R is an efficient initiation group. These homogeneous catalysts are discrete species, rendering them amenable to precise modification and detailed mechanistic studies. Most of the major advances in metal-catalyzed polymerization, including stereoselective and living alkene polymerization, lactide and lactone polymerization, alkene metathesis and alkene–CO copolymerization, are the result of progress in homogeneous catalyst design. Homogeneous catalysts are being used to develop unique polymer architectures that lead to new,

industrially relevant materials, although it should be noted that most industrial polymerization catalysts are still of the heterogeneous variety.

The purpose of this section is to give a thorough account of the CO_2–epoxide polymerization literature, with strong emphasis on single-site homogeneous catalysts and their mechanisms of operation. This section is largely based on a review written in part by one of the authors in 2004 [11], and is updated with select papers referencing the original article. The review is organized according to the active metal center of the catalyst and, although polymerization is the focus, the production of cyclic carbonates will be discussed when appropriate.

11.2.1 Background

In 1969, Inoue and co-workers made the remarkable discovery that a mixture of $ZnEt_2$ and H_2O was active for catalyzing the alternating copolymerization of propylene oxide (PO) and CO_2, marking the advent of epoxide–CO_2 coupling chemistry [13]. Following their discoveries, Kuran and co-workers developed a copolymerization system using $ZnEt_2$ and trihydric phenols, including pyrogallol and 4-bromopyrogallol, that produced poly(propylene carbonate) (PPC) with turnover frequencies (TOFs) up to $0.3\ h^{-1}$ at 35 °C and 60 atm CO_2 [14]. In an effort to develop more active catalysts, Hattori and co-workers synthesized a heterogeneous catalyst from $Zn(OH)_2$ and glutaric acid. Under 30 atm CO_2 and at 60 °C, the $Zn(OH)_2$–glutaric acid mixture yielded PPC with a TOF of $1.1\ h^{-1}$ ($M_n = 12\,000\ g\ mol^{-1}$) [15].

While the discoveries of $ZnEt_2$–$R(OH)_x$ and $Zn(OH)_2$–glutaric acid catalysts for epoxide–CO_2 coupling marked salient scientific findings, the active species responsible for polymer and cyclic formation remain unknown. Nevertheless, epoxide–CO_2 copolymerization is generally accepted to proceed via a coordination–insertion mechanism (Scheme 11.3).

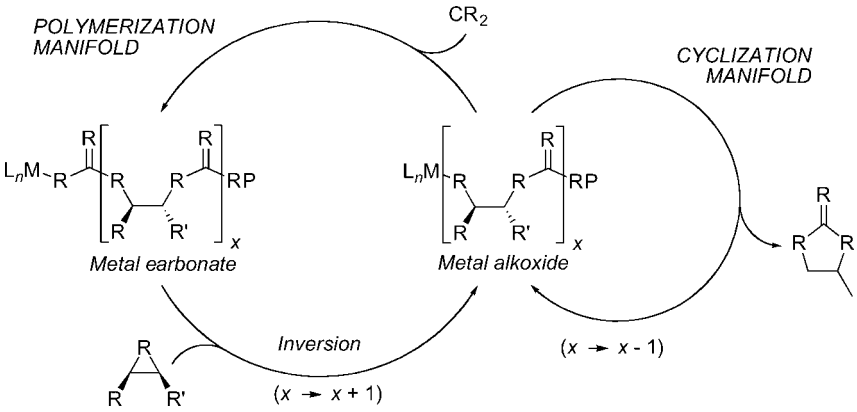

Scheme 11.3 The basic mechanism of epoxide–CO_2 copolymerization and the formation of cyclic carbonates (L_n = ligand set; M = metal; P = polymer chain).

The mechanism includes several prevailing principles:

1. *Mechanism*. The alternating copolymerization of epoxides and CO_2 is a two-step process; the insertion of CO_2 into a metal alkoxide is followed by insertion of epoxide into a metal carbonate. Hence most catalysts (polymerization initiators) are metal alkoxide or metal carboxylate species that are similar to the putative catalytic intermediates.

2. *Regiochemistry*. In the copolymerization of CO_2 and aliphatic epoxides (propylene oxide, etc.), epoxide ring opening is typically favored at the least-hindered C−O bond, although cleavage is normally observed at both C−O bonds, giving regioirregular polymers.

3. *Stereochemistry*. In the copolymerization of CO_2 and alicyclic epoxides, such as cyclohexene oxide (CHO), C−O bond cleavage typically occurs with inversion of configuration at the site of attack (S_N2-type mechanism) to give the *trans* ring-opened product. In general, tactic polycarbonates are not formed by chain-end control mechanisms, presumably due to the distance between the stereogenic center of the chain end and the active metal center. There are examples of stereocontrol by site-control mechanisms using chiral metal catalysts (see below).

4. *Polymer–cyclic selectivity*. Cyclics are a common by-product of the copolymerization of CO_2 and aliphatic epoxides. Many systems produce predominantly cyclics, which are thermodynamically more stable than polycarbonates. The percentage of polymer typically increases at lower reaction temperatures. Systems can be tuned to favor cyclics or polymer formation, depending on the catalyst, additives, CO_2 pressure, epoxide concentration and temperature. Cyclic formation results from degradation of the growing polycarbonate chain by depolymerization or backbiting. In most cases, cyclic carbonate is thought to form via backbiting of a metal-alkoxide into an adjacent carbonate linkage (Scheme 11.3).

5. *Ether and dicarbonate linkages*. The presence of ether linkages due to consecutive epoxide enchainment can be observed in some aliphatic polycarbonates. Most systems can be tuned to favor CO_2 incorporation by catalyst selection, CO_2 pressure, epoxide concentration and polymerization temperature. The enthalpically disfavored consecutive insertion of two molecules of CO_2 to give dicarbonate linkages has not been reported.

These prevailing principles are depicted in a qualitative free energy profile for the copolymerization of epoxides and CO_2 in Figure 11.1.

As observed in early studies, only a few metals have been found to be active for the coupling of epoxides and CO_2, including Al, Cr, Co, Mg, Mn, Li, Zn, Cu and Cd. Studies have shown large differences in catalytic efficacy resulting from the organic frameworks surrounding these metals, especially in the case of zinc. Accordingly, subsequent studies have largely been focused on the empirical modification of ligands to generate improved catalysts. This section will focus on complexes of three metals for epoxide–CO_2 copolymerization: chromium, cobalt and zinc.

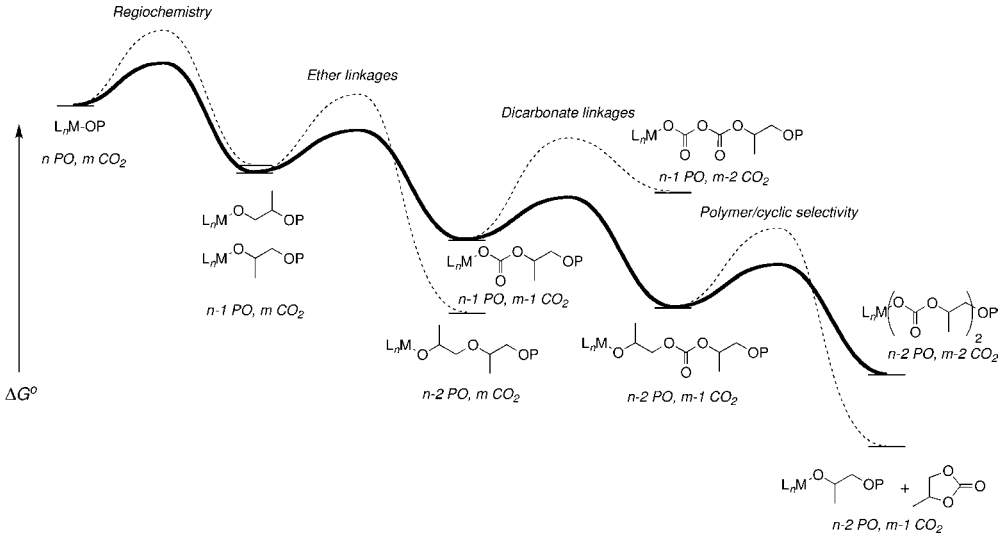

Figure 11.1 Qualitative, ideal free-energy profile depicting alternating copolymerization of epoxides and CO_2, and also potential side-reactions.

11.2.2
Chromium Catalysts

Following a lead by Kruper and Dellar [16], who reported that chromium porphyrins catalyzed the synthesis of cyclic carbonates from epoxides and CO_2, Holmes and co-workers developed (TFPP)CrCl (Scheme 11.4), which showed activities of up to $173\,h^{-1}$ for the alternating copolymerization of CHO and CO_2 at 225 atm CO_2 (supercritical CO_2) and 95 °C [17]. The copolymerization only yielded polycarbonate when (TFPP)CrCl was combined with a co-catalyst such as DMAP. The fluorinated aromatic moieties improved catalyst solubility in supercritical CO_2 and consequently increased the yields of PCHC. Similar to aluminum porphyrin catalysts for epoxide–CO_2 copolymerization, these chromium analogs yielded

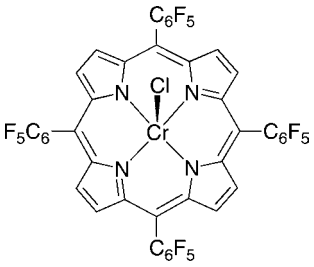

(TFPP)CrCl

Scheme 11.4 A chromium–porphyrin complex for epoxide and CO_2 copolymerization.

polycarbonates with narrow PDIs ($M_w/M_n = 1.08-1.50$) and low molecular weights ($M_n = 1500–9400\ g\ mol^{-1}$). Furthermore, the resultant PCHC contained high percentages of carbonate linkages (97%). More recently, polymer-supported chromium porphyrins have been found to be active for PCHC production [18].

Darensbourg and Yarbrough reported that the air-stable complex (salcy-*t*Bu)CrCl (Scheme 11.5) was an effective catalyst for the alternating copolymerization of CHO and CO_2 [19]. At 80 °C and 60 atm CO_2, (salcy-*t*Bu)CrCl converted CHO to PCHC with a moderate TOF of $10.4\ h^{-1}$. Analysis of the polycarbonate showed nearly 100% carbonate linkages, a M_n of $8900\ g\ mol^{-1}$ and an M_w/M_n of 1.2. Based on the turnover number (TON) and lack of cyclic by-product, the PCHC should exhibit a theoretical molecular weight of approximately $35\,000\ g\ mol^{-1}$. Like the chromium porphyrin systems, activities increased upon addition of *N*-methylimidazole (MeIm), such that 5 equiv. MeIm tripled the copolymerization rates to $32.2\ h^{-1}$. Although the complex (salcy-*t*Bu)CrCl is chiral, the resultant polymer was completely atactic, as determined by ^{13}C NMR spectroscopy. Additionally, (salcy-*t*Bu)CrCl catalyzed the coupling of PO and CO_2 to PC and PPC, although activities were not specified. At 80 °C, cyclic PC is the predominant product, but as the temperature is reduced to 40 °C, PPC production becomes a competitive pathway. Finally, silylated aliphatic epoxides, such as 2-(3,4-epoxycyclohexyl)ethyltrimethoxysilane, and CO_2 can also be copolymerized by salen–chromium complexes and MeIm co-catalyst [20].

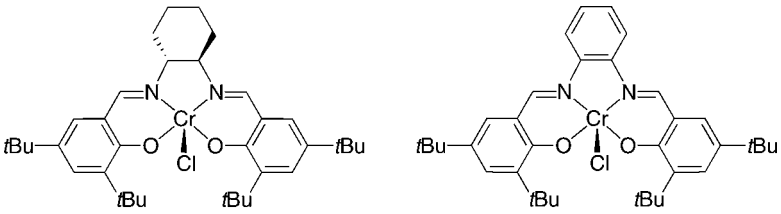

Scheme 11.5 Chromium–salen complexes for epoxide and CO_2 copolymerization.

Subsequent work detailed the intricate energetics of polymer versus cyclic formation using (salcy-*t*Bu)CrCl [23]. In CHO−CO_2 coupling, the activation energies (E_a) for CHC and PCHC were 31.8 and 11.2 kcal mol^{-1}, respectively, which illustrate higher activation barriers for cyclic formation. The activation barriers for PC and PPC in PO−CO_2 coupling were determined to be 24.0 and 16.2 kcal mol^{-1}, respectively. The significantly larger E_a for CHC versus PCHC is consistent with the exclusive formation of PCHC, whereas the slightly larger E_a for PC versus PPC is consistent with the formation of PC during PO−CO_2 copolymerization. A detailed study on the nature of the co-catalyst on catalytic behavior has also been performed [21].

Rieger and co-workers found that the slightly modified complex (salph-*t*Bu)CrCl and DMAP co-catalyst rapidly copolymerized PO and CO_2 (TOFs approaching $226\ h^{-1}$) at 75 °C and only 13 atm CO_2 [22]. Analysis of the PPC revealed molecular weights up to $16\,700\ g\ mol^{-1}$ (lower than predicted assuming the lack of chain transfer reactions), PDIs as low a 1.36 and carbonate linkages as high as 98%. The

DMAP-to-(salph-*t*Bu)CrCl ratio drastically affected the ratio of products in the coupling process. Without DMAP, no conversion to PC or PPC was observed. Interestingly, co-catalyst was not essential for copolymerization using (salcy-*t*Bu)CrCl. At 0.5 equiv. DMAP, the maximum ratio of PPC to PC formation ($154:34\,h^{-1}$) was observed. Higher DMAP-to-(salph-*t*Bu)CrCl ratios decreased the proportion of PPC to PC until only PC was observed. For example, when 2 equiv. DMAP were added, only PC was observed with a TOF of $602\,h^{-1}$.

The proposed CO_2–epoxide copolymerization mechanisms using seemingly similar catalysts, (salcy-*t*Bu)CrCl–MeIm and (salph-*t*Bu)CrCl–DMAP, differ considerably. At the current time, there is a lack of agreement regarding the mode of operation of these catalysts. Darensbourg *et al.* offered a dual CHO−CO_2 copolymerization mechanism for the (salcy-*t*Bu)CrCl –MeIm system, where initiation occurs by a bimetallic process and propagation operates via monometallic enchainment of epoxide [23]. Initiation is accelerated by MeIm, which aids in chloride attack on a CHO monomer bound to a second salen–chromium complex (Scheme 11.6). Subsequent CO_2 insertion into the newly generated chromium alkoxide generates a chromium carbonate. Because rate studies showed a first-order dependence on both CHO and catalyst, chain propagation was proposed to occur by a concerted epoxide ring opening that proceeds through a four-membered transition state.

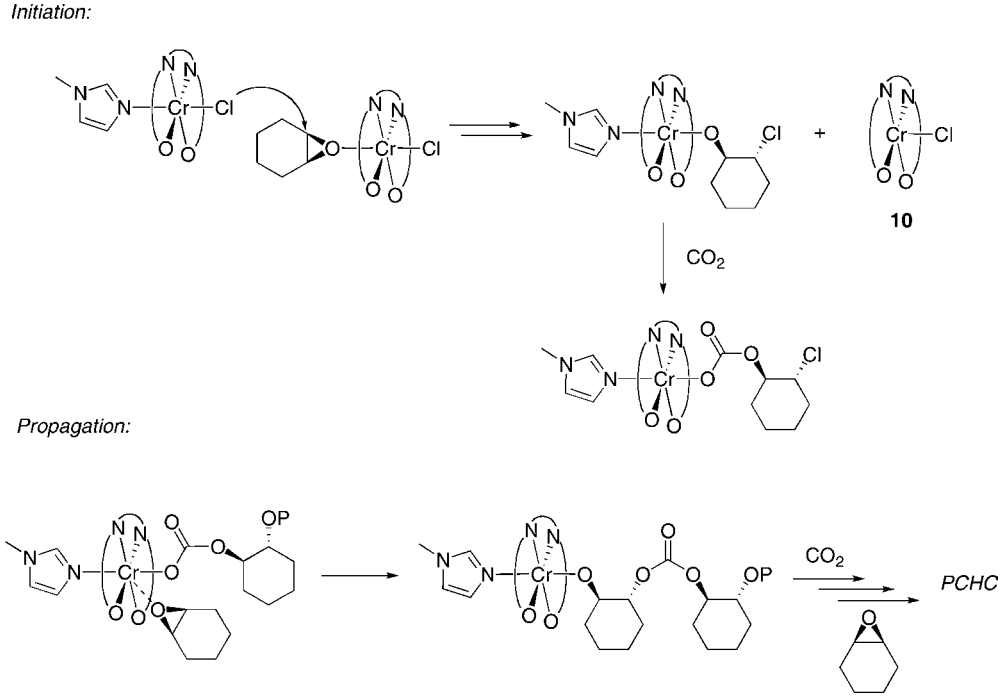

Scheme 11.6 Proposed CO_2−CHO copolymerization mechanism using (salcy-*t*Bu)CrCl–MeIm (P = polymer chain).

Alternatively, in PO–CO_2 copolymerization using (salph-*t*Bu)CrCl–DMAP, Rieger and co-workers proposed that DMAP coordinates strongly to Cr and facilitates dissociation of the polymer chain alcoholate and carbonate (Scheme 11.7) [22]. Under sufficient pressures of CO_2, the dissociated carbonate attacks PO-bound (salph-*t*Bu)CrCl–DMAP in a monometallic fashion. Subsequent CO_2 insertion into the newly formed chromium alkoxide propagates the polycarbonate chain. The anionic nature of the chain-end promotes degradative backbiting to cyclic propylene carbonate. Therefore, increased amounts of DMAP enhance cyclic formation and eventually exterminate copolymer formation.

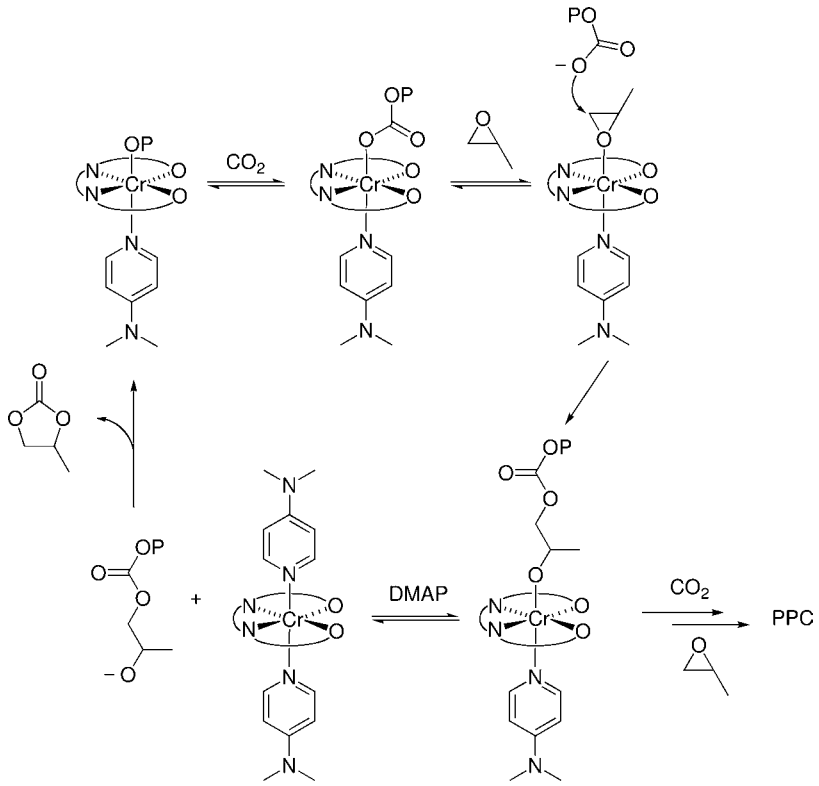

Scheme 11.7 Proposed PO–CO_2 copolymerization mechanism for (salph-*t*Bu)CrCl–DMAP catalyst system.

Owing to similar catalysts and coupling processes, it is unlikely that all of the epoxide ring-opening steps discussed above are occurring simultaneously. Furthermore, no mechanism has accounted for the retention of stereochemistry as reported by Kruper and Dellar or the low polymer molecular weights that are indicative of chain transfer or the formation of macrocycles. All studies do agree that CO_2 reacts with a metal alkoxide and cyclic formation occurs through backbiting of a metal alkoxide into an adjacent carbonate linkage. Detailed mechanistic studies must be

performed to delineate the various intermediates and epoxide ring-opening steps involved in these highly active salen-type chromium catalysts.

11.2.3
Cobalt Catalysts for Epoxide–CO_2 Copolymerization

In 1979, $Co(OAc)_2$ was reported to copolymerize PO and CO_2 with an extremely low TOF ($0.06\,h^{-1}$) [24]. Since that report, few examples of cobalt-catalyzed coupling of epoxides and CO_2 have been reported. He and co-workers reported the synthesis of ethylene carbonate using (salen)Co–co-catalyst mixtures [25]. More recently, Coates and co-workers found that (salcy)CoOAc complexes (Scheme 11.8) exhibited moderate activities (up to $81\,h^{-1}$ with R = Br) for the copolymerization of PO and CO_2 [26]. At 25 °C and 55 atm CO_2, (salcy-Br)CoOAc catalyzed the copolymerization to yield PPC with no observable cyclic by-products, 95% carbonate linkages, an M_n of 15 300 g mol^{-1} and a PDI of 1.22. Pressures of 55 atm were essential for polymerization activity as lower pressures (40 atm) significantly hindered the copolymerization. In contrast to the related salen chromium catalysts, no heterocyclic additives were necessary to effect the copolymerization. In addition, all (salcy-R)CoOAc showed unprecedented selectivities for PPC formation (>99% PPC versus PC). (*S*)-PO−CO_2 copolymerization using enantiomerically-pure (salcy-*t*Bu)CoOAc yielded isotactic (*S*)-PPC (TOF = $71\,h^{-1}$; >99% PPC:PC; 99% carbonate linkages; $M_n = 6900\,g\,mol^{-1}$; $M_w/M_n = 1.58$) with the highest reported level of head-to-tail linkages (93%). Finally, complex (salcy-*t*Bu)CoOAc exhibited a modest level of selectivity ($k_{rel} = 2.8$) in the kinetic resolution of PO.

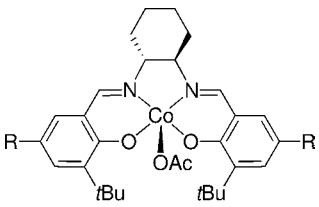

(salcy-R)CoOAc

Scheme 11.8 Cobalt–salen complexes (R = Br, H, *t*Bu) for epoxide and CO_2 copolymerization.

Although it was originally thought that ammonium salt co-catalysts limited the (*R*,*R*)-(salcy)CoX-catalyzed reaction of PO−CO_2 to the production of PC [27], PPC was recently achieved through the careful choice of the complex and co-catalyst [28]. Specifically, (salcy-*t*Bu)CoOAr (OAr = 4-nitrophenoxy, 2,4-dinitrophenoxy or 2,4,6-trinitrophenoxy) derivatives with [nBu$_4$N]Y (Y = Cl, OAc) co-catalysts were described by Lu and Wang to afford PPC with impressively enhanced rates and selectivity [28]. Coates and co-workers have also furthered catalyst optimization, which also led to the use of organic salt co-catalysts (Scheme 11.9) [29]. Specifically, (salcy-*t*Bu)CoOBzF_5 (OBzF_5 = pentafluorobenzoate), in combination with [$Ph_3P{=}N{=}PPh_3$]Cl ([PPN]Cl), was found to produce a highly active catalyst for the living, alternating copolymerization of PO and CO_2, yielding PPC with no detectable by-products. The PPC generated using these catalyst systems is highly regioregular and has up to 99%

carbonate linkages with a narrow molecular weight distribution (MWD). In the case of [PPN]Cl with (*R,R*)-(salcy)CoOBzF$_5$, an unprecedented catalytic activity of 520 turnovers per hour was achieved for the copolymerization of *rac*-PO and CO_2, yielding iso-enriched PPC with 93% head-to-tail connectivity.

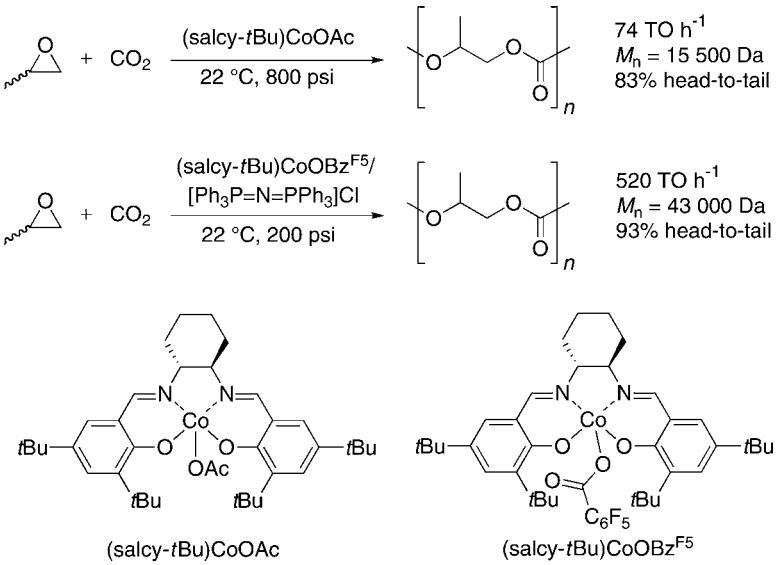

Scheme 11.9 Propylene oxide and CO_2 copolymerization by cobalt–salen complexes.

Two recent studies have extended the co-catalyzed cobalt–salen system by cleverly designing systems with covalent linkages between the metal complex and co-catalyst [30]. These systems claim higher conversions to polymer without undesirable backbiting reactions, and also higher thermal stability of the catalysts.

Coates and co-workers recently reported the first syndioselective copolymerization of cyclohexene oxide and CO_2 (Scheme 11.10) [31]. Using the complex (salpr-*t*Bu)

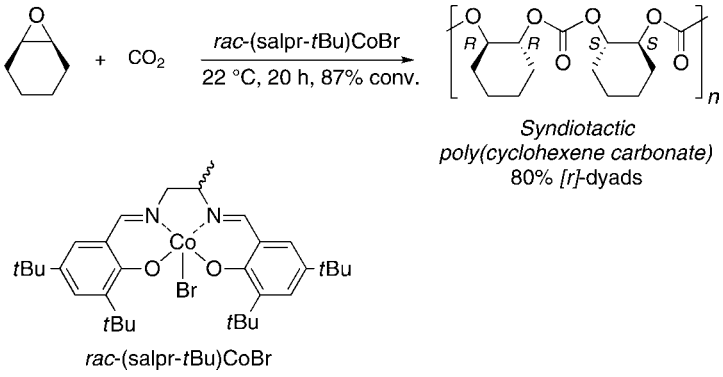

Scheme 11.10 Syndiospecific cyclohexene oxide and CO_2 copolymerization by a cobalt–salen complex.

CoBr, poly(cyclohexene carbonate) was formed with 80% *[r]*-centered tetrads, as determined by ^{13}C NMR spectroscopy. The carbonyl and methylene regions were best simulated using Bernoullian statistical methods, supporting a chain-end stereochemical control mechanism.

11.2.4
Zinc Catalysts for Epoxide–CO_2 Copolymerization

A variety of metal-based catalysts have shown activity for the coupling of epoxides and CO_2; however, few have exhibited the success associated with zinc-based complexes. Therefore, the majority of the work reported in this field has been performed using complexes with zinc as the active metal center. These catalysts have undergone a renaissance over the past 10 years, shifting the focus from heterogeneous mixtures to discrete and single-site catalysts which exhibit unprecedented reaction rates and selectivities.

11.2.4.1 Zinc Phenoxides for Epoxide–CO_2 Copolymerization

Heterogeneous systems are often marred by poor reproducibility and the production of non-uniform polymers, caused by the presence of many different types of active sites that produce polymers with different activities and selectivities. To address these issues, Darensbourg and Holtcamp reported in 1995 the first discrete zinc complexes for the alternating copolymerization of epoxides and CO_2 (Scheme 11.11) [32]. This discovery marked an important step in the development of catalysts for the copolymerization of CO_2 and epoxides. The compound $(Ph_2Ph)_2Zn(Et_2O)_2$, which was synthesized from 2,6-diphenylphenol and $Zn[N(SiMe_3)_2]_2$, crystallized as a bis[(2,6-diphenyl)phenoxy]zinc complex containing two diethyl ether solvent molecules coordinated to a tetrahedral zinc center. Under 55 atm CO_2 and at 80 °C, PCHC (91% carbonate linkages; $M_n = 38\,000\ g\ mol^{-1}$; $M_w/M_n = 4.5$) was produced with a TOF of $2.4\ h^{-1}$. Additionally, $(Ph_2Ph)_2Zn(Et_2O)_2$ catalyzed the random terpolymerization of CHO, PO and CO_2, yielding polycarbonate with approximately 20% propylene carbonate linkages, 70% cyclohexene carbonate linkages and 10% ether linkages. Approximately the same ratios of PO and CHO incorporation were observed regardless of the feedstock composition.

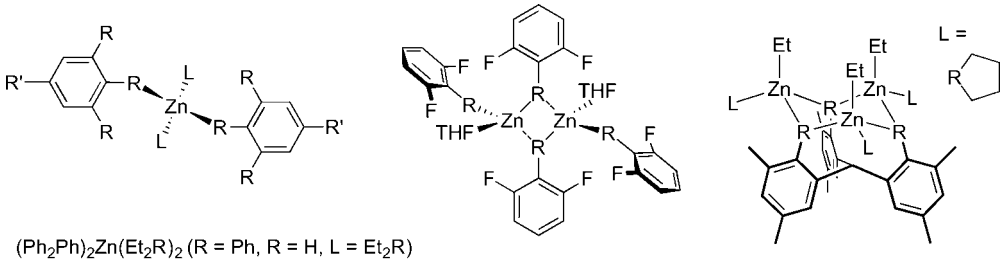

$(Ph_2Ph)_2Zn(Et_2R)_2$ (R = Ph, R = H, L = Et_2R)
$(Me_3Ph)_2Zn(py)_2$ (R, R' = Me, L = pyridine)

$[(F_2Ph)_2Zn(THF)]_2$

$(ArR_3)(ZnEt)_3$

Scheme 11.11 Zinc phenoxide compounds for alternating epoxide–CO_2 copolymerization.

Subsequent work investigated the steric influences of *N*-aryl substituents, including compounds such as $(Me_2Ph)_2Zn(py)_2$, on CHO−CO_2 copolymerization (Scheme 11.11) [33]. Complex $(Me_2Ph)_2Zn(py)_2$ displayed the highest activities (TOF = 9.6 h^{-1}), thus illustrating that bulky *ortho* substituents were not essential for high copolymerization rates. Electronic perturbations of the *N*-aryl *ortho* substituents revealed that electron-withdrawing groups resulted in higher activities for CHO−CO_2 copolymerization: F > Cl > Br [34]. Addition of 2,6-dihalophenols to $Zn[N(SiMe_3)_2]_2$ gave four-coordinate, dimeric zinc phenoxides with bound THF solvent molecules. The compound $[(F_2Ph)_2Zn(THF)]_2$ demonstrated a moderate TOF of 7.6 h^{-1}. Analysis of the PCHC revealed PDIs of over 42, molecular weights of 42 000 g mol^{-1}, a T_g of 115 °C and >99% carbonate linkages [35]. In general, zinc bisphenoxide compounds catalyzed PO−CO_2 copolymerization at 40 °C and PO−CO_2 cyclization at 80 °C in unspecified yields. Finally, zinc bisphenoxide catalysts were active for CHO homopolymerization, CHO−CO_2 copolymerization and CHO−PO−CO_2 terpolymerization, but did not readily react with bulky alicyclic epoxides such as α-pinene and *exo*-2,3-epoxynorbornane.

In a related study, Dinger and Scott reported that zinc phenoxide cluster compounds showed activity for the alternating copolymerization of CHO and CO_2 [36]. A variety of solvent-dependent tri-, tetra-, penta- and hexanuclear compounds were synthesized from tris(3,5-dialkyl-2-hydroxyphenyl)methanes and $ZnEt_2$. For example, $(ArO_3)(ZnEt)_3$ (Scheme 11.11) catalyzed the copolymerization of CHO and CO_2 to give PCHC with 81% carbonate linkages and a TOF of 1.3 h^{-1}.

Although the discrete catalysts above represent an important advance in catalyst design, the active species for the copolymerization remain unclear. Regarding these phenoxide–zinc complexes, one or more ligands are likely to act as polymerization initiators and thus become the chain-end of the growing polymer chain.

11.2.4.2 **Single-site β-Diiminate Zinc Catalysts for Epoxide–CO_2 Coupling**

Coates and co-workers discovered a highly active, living epoxide–CO_2 copolymerization system using bulky β-diiminate (BDI) zinc catalysts at low pressures (7 atm CO_2) and temperatures (50 °C) (Scheme 11.12) [37].

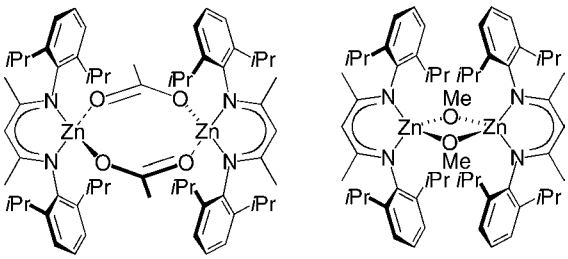

[(BDI-*i*Pr)ZnOAc]$_2$ [(BDI-*i*Pr)ZnOMe]$_2$

Scheme 11.12 β-Diiminate (BDI) zinc catalysts for epoxide–CO_2 copolymerization.

Several key design features, including initiating groups, sterics and electronics drastically altered the efficacy of the catalysts. To model the growing polycarbonate chain, zinc acetate [(BDI-*i*Pr)ZnOAc]$_2$ and methoxide [(BDI-*i*Pr)ZnOMe]$_2$ complexes were synthesized as mimics for zinc carbonates and zinc alkoxides (Scheme 11.12). BDI zinc acetate, methoxide, isopropoxide and bis(trimethylsilyl)amido complexes were all active for the alternating copolymerization of CHO and CO_2. The combination of the unsymmetrical ligand geometries and the electron withdrawing cyano substituent yielded the most active catalysts reported to date [38]. At 50 °C and in only 10 min, [(NC-BDI-*i*Pr,Me)ZnOMe]$_2$ catalyzed the copolymerization of 1000 equiv. CHO at 7 atm CO_2 to give high-MW polymers ($M_n \approx 22\,000\ g\ mol^{-1}$), narrow PDIs ($M_w/M_n = 1.1$) and an extremely high TOF of $2290\ h^{-1}$ (Scheme 11.13).

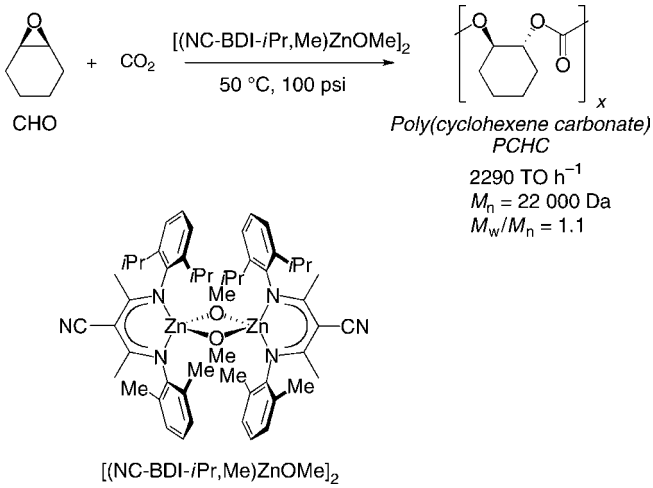

Scheme 11.13 A highly active β-diiminate (BDI) zinc catalyst for cyclohexene oxide–CO_2 copolymerization.

In an attempt to isolate monomeric β-diiminate complexes, Chisholm and co-workers investigated bulky initiators including *t*BuOH and Ph_3SiOH [39]. As expected, the monomeric compounds (BDI-*i*Pr)Zn(THF)OSiPh_3 and (BDI-*i*Pr)ZnO*t*Bu were active for CHO–CO_2 alternating copolymerization. Unexpectedly, their (BDI*i*Pr)ZnN*i*Pr_2, an analog of Coates and co-workers' compound (BDI-*i*Pr)ZnN(SiMe_3)$_2$, was not active for the copolymerization, although it readily reacted with CO_2 to generate (BDI-*i*Pr)ZnOC(=O)N*i*Pr_2. Rieger and co-workers have shown that an ethyl sulfinate is a viable initiator for the copolymerization [40]. The compound [(BDI-*i*Pr)ZnOS(=O)Et]$_2$ was synthesized by bubbling SO_2 through a (BDI)ZnEt solution and was also active for CHO−CO_2 copolymerization. Catalytic activities were comparable to that of [(BDI-*i*Pr)ZnOAc]$_2$, due to similar active species. As a result of bimodal GPC traces, monomeric and dimeric BDI zinc species were believed to be active, although no mechanistic studies were conducted. Oligomeric BDI ligands have been made from 4,4′-methylenedianiline and 2,4-pentanedione. These zinc complexes have shown modest activity for CHO−CO_2 copolymerization (TOF = $11.3\ h^{-1}$) [41].

Subtle electronic and steric perturbations to (BDI)ZnOR (R = alkyl or acyl) complexes resulted in dramatic enhancements of activity for CHO–CO_2 copolymerization. During the course of these studies, catalysts for PO–CO_2 coupling were also discovered by Coates and co-workers [42]. Further modifications of the ligand architecture generated the most potent catalyst reported at that time for PO–CO_2 copolymerization, [(F_3C-BDI-*i*Pr,Et)ZnOAc]$_2$ (Scheme 11.14). The complex copolymerized PO and CO_2 at 25 °C and 7 atm CO_2 to give PPC (>99% carbonate linkages; $M_n = 36\,700\ g\ mol^{-1}$; $M_w/M_n = 1.13$) with a TOF of $235\ h^{-1}$. However, the selectivity for polymer was only 75%. Increasing the CO_2 pressure to 35 atm favored polymer formation with a selectivity of 93%, while only moderately attenuating the catalytic activity (TOF = $138\ h^{-1}$).

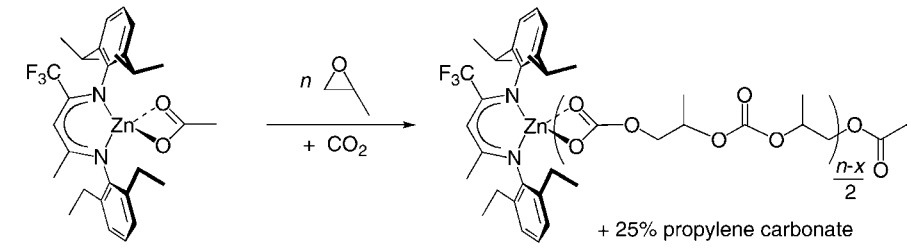

Scheme 11.14 A highly active β-diiminate (BDI) zinc catalyst for propylene oxide–CO_2 copolymerization.

More recently, Coates and co-workers performed mechanistic studies on the (BDI)ZnOR-catalyzed copolymerization of CHO and CO_2 [43]. Stoichiometric reactions of the copolymerization initiation steps showed that zinc alkoxides insert CO_2, whereas zinc acetates react with CHO. For example, (BDI)ZnO*i*Pr complexes were found to react with CO_2 and (BDI)ZnOAc complexes were found to react with cyclohexene oxide (Scheme 11.15). The resultant compounds were characterized by single-crystal X-ray analysis and served as model compounds for presumed intermediates in the copolymerization. Due to the expeditious reaction of CO_2 with (BDI-*i*Pr)ZnO*i*Pr, CHO insertion was predicted to be the rate-determining step. To monitor propagation, rate studies were performed on (BDI)ZnOAc complexes using *in situ* FTIR spectroscopy. The rate studies revealed a zeroth-order dependence in CO_2 and a first-order dependence in CHO. Hence insertion of CHO into a zinc carbonate was indeed the rate-determining step.

The copolymerization of CHO (1.98 *M* in toluene) in 20 atm CO_2 at 50 °C using sterically unhindered, dimeric complexes resulted in an order in [(BDI)ZnOR], where R = alkyl, acyl or polymer chain, of ~1. However, under the same conditions, an order in [(BDI)ZnOR] approaching 2 was determined for bulky complexes. On the basis of [(BDI)ZnOR] solution studies (R = alkyl or acyl), stoichiometric insertion reactions and rate studies, a bimetallic mechanism was proposed (Scheme 11.16). Sterically encumbered BDI zinc complexes ring open CHO in a bimetallic transition state with a

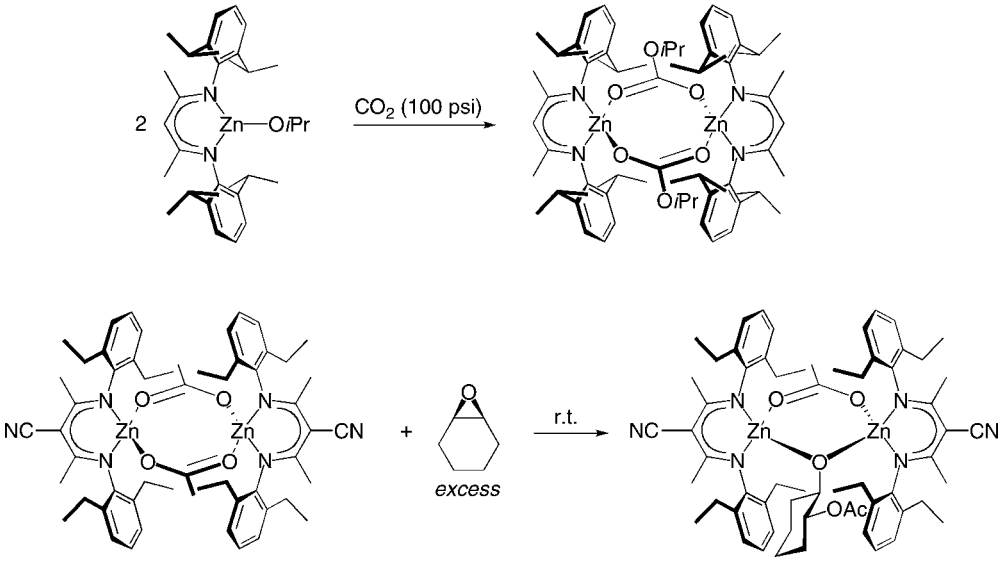

Scheme 11.15 Insertion reaction of (BDI)ZnOR complexes with CO_2 and CHO.

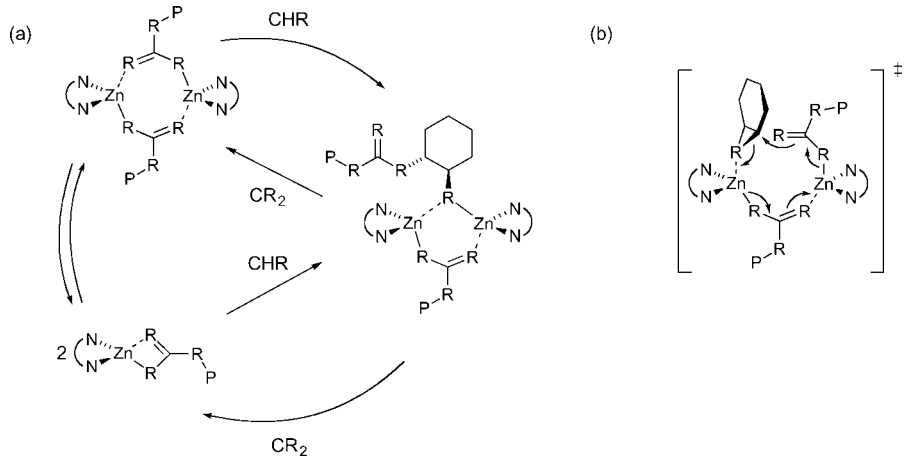

Scheme 11.16 Proposed (a) copolymerization mechanism and (b) epoxide ring-opening transition state using BDI zinc complexes (CHO = cyclohexene oxide; P = polymer chain).

predominantly monomeric ground state. Conversely, sterically unhindered BDI zinc complexes insert CHO in a bimetallic transition state with a completely dimeric ground state. A clever application of this finding was reported by Lee *et al.*, who synthesized bimetallic zinc species in order to take advantage of the bimetallic

transition state for epoxide enchainment [44]. The resulting compounds exhibited excellent TONs at very low catalyst loadings and produced high molecular weight polymers (>200 000 g mol^{-1}).

11.2.4.3 Zinc Catalysts for Asymmetric CHO–CO_2 Copolymerization

There is significant interest in controlling the absolute stereochemistry of ring opening in epoxide–CO_2 copolymerization for several reasons. First, microstructure directly affects polymer properties [45]. Second, the kinetic resolution of racemic epoxides or desymmetrization of *meso*-epoxides by copolymerization is a potential route to valuable chiral building blocks. CHO, a *meso* molecule, is an ideal substrate for desymmetrization using chiral catalysts. In 1999, Nozaki *et al.* reported that a 1 : 1 mixture of $ZnEt_2$ and (*S*)-α,α-diphenylpyrrolidine-2-ylmethanol (DPM)H was active for stereoselective CHO–CO_2 copolymerization at 40 °C and 30 atm CO_2 (Scheme 11.17) [46]. The polycarbonate contained 100% carbonate linkages, an M_n of 8400 g mol^{-1} and a PDI of 2.2. Hydrolysis of PCHC with base produced the corresponding *trans*-cyclohexane-1,2-diol with 73% enantiomeric excess. ^{13}C NMR

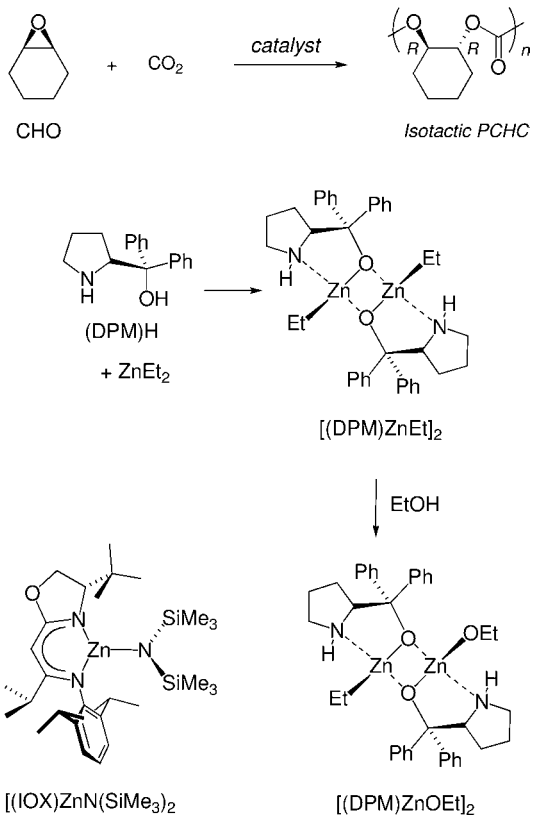

Scheme 11.17 Chiral zinc catalysts for the asymmetric, alternating copolymerization of CHO and CO_2.

spectroscopic studies of model polycarbonate oligomers afforded spectral assignments for isotactic dyads (153.7 ppm) and syndiotactic dyads (153.3–153.1 ppm) [47]. Finally, ring opening proceeded by complete inversion of configuration (S_N2 mechanism), hence no *cis*-cyclohexane-1,2-diol was observed.

In a more recent study, Nozaki and co-workers isolated presumed intermediates in the asymmetric alternating copolymerization [48]. Reaction of $ZnEt_2$ and (*S*)-α,α-diphenylpyrrolidine-2-ylmethanol yielded dimeric $[(DPM)ZnEt]_2$, which was structurally characterized by X-ray diffraction studies (Scheme 11.17). At 40 °C and 30 atm CO_2, $[(DPM)ZnEt]_2$ catalyzed the formation of isotactic PCHC ($M_n = 11\,800\ g\,mol^{-1}$; $M_w/M_n = 15.7$; $TOF = 0.6\ h^{-1}$) with a slightly lower enantiomeric excess (*ee*) of 49%. When the copolymerization was attempted with $[(DPM)ZnOEt]_2$ and 0.2–1.0 equiv. EtOH, enantioselectivities increased up to 80% *ee* and better control of molecular weights and PDIs resulted. The compound [(DPM)ZnOEt]2 was proposed to be the active initiating species. End-group analysis by MALDI-TOF mass spectrometry revealed that in the absence of EtOH, signals assignable to the amino alcohol-initiated polymerization were identified. However, as EtOH addition was increased from 0.2 to 1.0 equiv., signals corresponding to the amino alcohol-derived polycarbonate disappeared as peaks for the EtOH-initiated PCHC emerged. This was further confirmed by end-group analysis using ^1H *NMR* spectroscopy. Finally, mechanistic studies suggested that the dimeric form of the catalyst is, in fact, the active species.

In 2000, Coates and co-workers developed C_1-symmetric imine–oxazoline (IOX) ligated zinc bis(trimethylsilyl)amido compounds for the stereoselective, alternating copolymerization of CHO and CO_2 (Scheme 11.17) [49]. Through multiple electronic and steric manipulations, the compound $(IOX)ZnN(SiMe_3)_2$ was found to exhibit the highest enantioselectivity (*RR*:*SS* ratio = 86 : 14; 72% *ee*). The resultant PCHC possessed 100% carbonate linkages, an M_n of $14\,700\ g\,mol^{-1}$, a PDI of 1.35 and a T_g and T_m of 120 and 220 °C, respectively. Furthermore, stereocontrol was also achieved in the alternating copolymerization of cyclopentene oxide (CPO) and CO_2, producing poly(cyclopentene carbonate) with an *RR* : *SS* ratio of 88 : 12 (76% *ee*). As revealed by ^{13}C NMR spectroscopy, the experimental carbonyl tetrad concentrations matched the predicted tetrad concentrations for an enantiomorphic-site control mechanism. The contributions described above represent an important step forward in the production of well-defined, tactic polycarbonates.

11.3 Synthesis of Aliphatic Polyesters

Aliphatic polyesters constitute an important class of polymers due to their biodegradability [50, 51] and biocompatibility [51, 52], which allows their use in drug delivery systems [51], artificial tissues [52] and commodity materials [53]. As only 6% of plastics in the USA are currently recycled [54], the production of economically competitive biodegradable polymers has recently become of great interest to the scientific community [53a, 55]. Although the polycondensation of a diol and a diacid is the

most common method for aliphatic polyester synthesis, the coordination–insertion method, which employs a well-defined single-site catalyst to effect the ring-opening polymerization (ROP) of cyclic esters, has become increasingly important over the past few decades [50–56]. One reason for this growing attention is that condensation polymerization is energy intensive, requiring high temperature and removal of the alcohol or water by-product to achieve high molecular weight (M_n) polymers; also, very precise stoichiometry between the diacid and diol is required to achieve a high M_n [51, 57]. Conversely, ROP by the coordination insertion mechanism is much more energy efficient; this technique typically uses mild reaction conditions and avoids the formation of small-molecule by-products (Scheme 11.18).

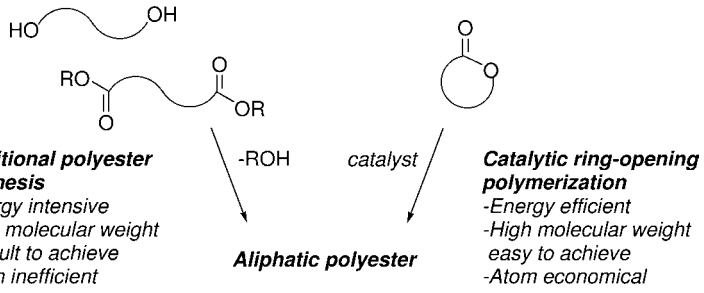

Scheme 11.18 Comparison of methods for aliphatic polyester synthesis.

Many extensive reviews have recently been published on the subject of the ROP of cyclic esters [50b,c, 51, 56]. We will avoid duplicating these and focus our discussion on the ROP of lactide (LA) with high stereocontrol, butyrolactone (BL), ε-caprolactone (CL) and its derivatives and the copolymerization of epoxides and cyclic anhydrides. We will refrain from discussing catalysts not bearing ancillary ligands [$M(OR)_x$], which are among the most common catalysts for the ROP of cyclic esters, and instead refer the reader to the aforementioned reviews for discussion of these compounds. Instead, we will focus on the use of biorenewable starting materials and also discuss some examples of ROP using organocatalysts, of interest in applications requiring ultra-pure (metal-free) materials. Although this topic has recently been reviewed [58], we feel that it deserves mention here as well.

11.3.1 Synthesis of Poly(lactic Acid)

11.3.1.1 Background

Poly(lactic acid) (PLA) is a biodegradable aliphatic polyester synthesized from lactide, a biorenewable monomer derived from corn. One of the most common and useful polyesters [50b,c, 56], PLA is used in a wide range of applications, including food packaging and textiles, and has been commercialized by many companies such as

Cargill and Teijin under the trade name Natureworks [53a, 59]. As the LA dimer contains two stereocenters, there are a number of different PLA stereoarchitectures available (Scheme 11.19) and each possesses different physical properties. A great deal of research has been focused on stereochemical control in PLA synthesis; we will provide a summary of these efforts here.

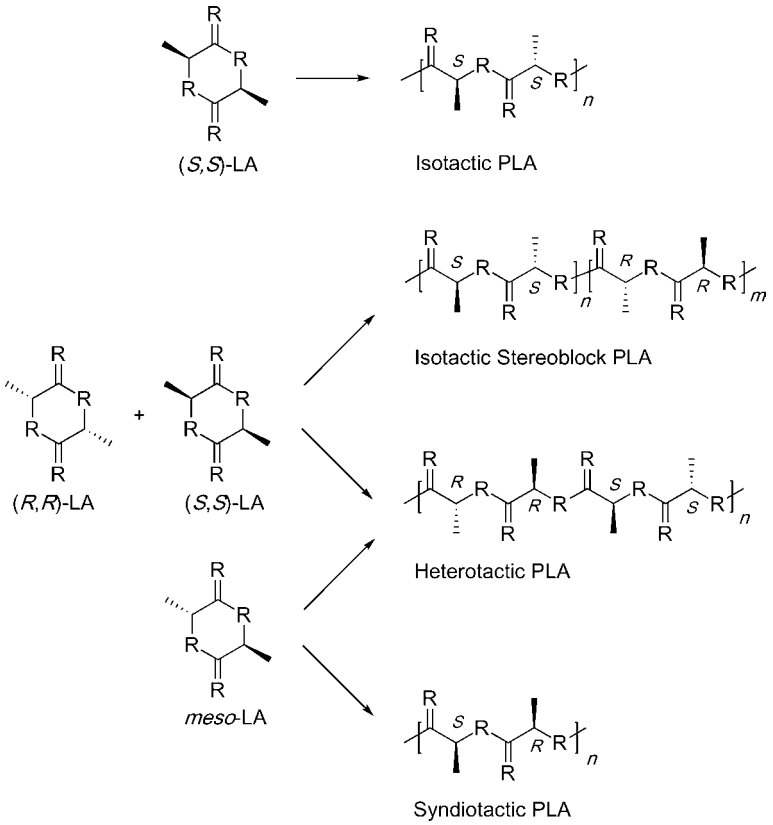

Scheme 11.19 Tacticities of poly(lactic acid) (PLA) and synthetic routes to their formation (LA = lactide).

11.3.1.2 **Aluminum Catalysts for the Synthesis of PLA**

In 1996, Spassky *et al.* reported the kinetic resolution polymerization of *rac*-LA in which the chiral aluminum alkoxide complex (*R*,*R*)-(salbin)AlOMe showed a preference for (*R*,*R*)-LA over the *S*,*S*-enantiomer by a factor of 20 (Scheme 11.20) [60]. This reaction produced predominantly isotactic PLA when the polymerization was run to less than 50% conversion. However, it only slowly approached 100% conversion because of the inactivity of the *S*,*S*-enantiomer. When polymerizations of *rac*-lactide were allowed to proceed to full conversion, a stereoblock copolymer resulted with a

small amount of tapering. This catalyst system exhibited excellent molecular weight control and the polymers produced possessed narrow PDIs.

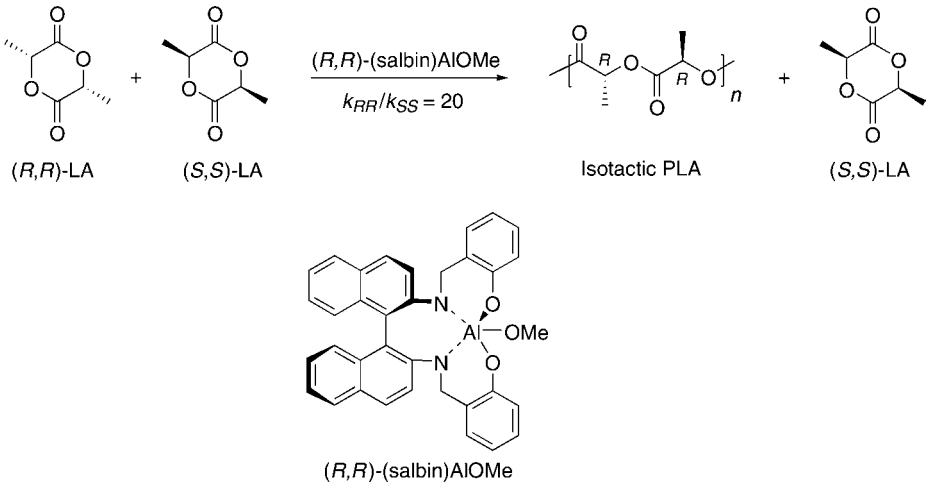

Scheme 11.20 Kinetic resolution ring-opening polymerization of *rac*-LA using (*R*,*R*)-(salbin)AlOMe.

Ovitt and Coates reported the synthesis of syndiotactic PLA from *meso*-LA using (*R*,*R*)-(salbin)AlO*i*Pr (Scheme 11.21) [61a]. PLA with an M_n of 12 000 g mol^{-1} and a PDI of 1.05 was produced in 14 h at 70 °C. Notably, this PLA was highly syndiotactic, with an enantiotopic selectivity of 96%. The ROP of *meso*-LA by *rac*-(salbin)AlO*i*Pr in toluene at 70 °C produced heterotactic PLA after 40 h, with an M_n of 13 600 g mol^{-1} and a PDI of 1.07. Control experiments were used to show that the formation of heterotactic PLA was a result of polymer exchange between (*R*,*R*)-(salbin)AlO*i*Pr and

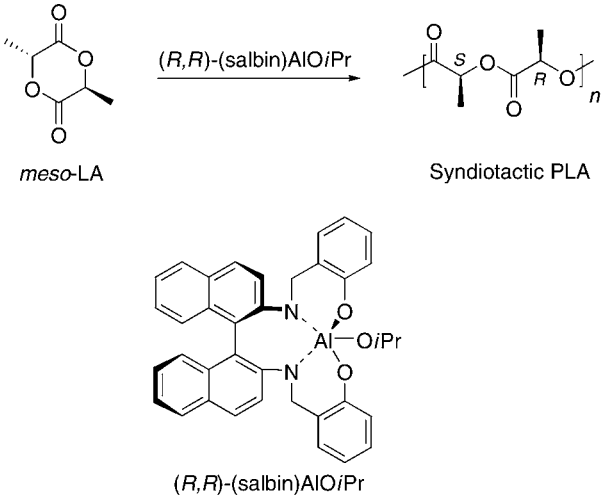

Scheme 11.21 Syndiospecific ring-opening polymerization of *meso*-LA using (*R*,*R*)-(salbin)AlO*i*Pr.

(*S,S*)-(salbin)AlO*i*Pr. Interestingly, stereoblock PLA could also be produced in a living fashion through the ROP of *rac*-LA using *rac*-(salbin)AlO*i*Pr for initiation [62]. This result further supported the proposed polymer exchange mechanism, in which sequences of the preferred LA enantiomer are formed by each enantiomer of (salbin) AlO*i*Pr, followed by chain exchange, which resulted in a stereoblock formation possessing –*RRRRRRSSSSSS*– sequences in the polymer chain.

Feijen and co-workers employed the aluminum alkoxide complex *rac*-(salcy)AlO*i*Pr in their synthesis of isotactic stereoblock PLA from *rac*-LA (Scheme 11.22) [63]. Also, it was discovered that at higher temperatures (130 °C instead of 70 °C), PLA could be polymerized without the use of solvent. Under these harsher conditions, they produced isotactic PLA with a higher M_n (24 000 g mol^{-1}), while retaining the narrow PDI associated with well-controlled, living polymerizations. In addition, the groups of Chen, Nomura and Gibson have all made recent seminal contributions in this area [64].

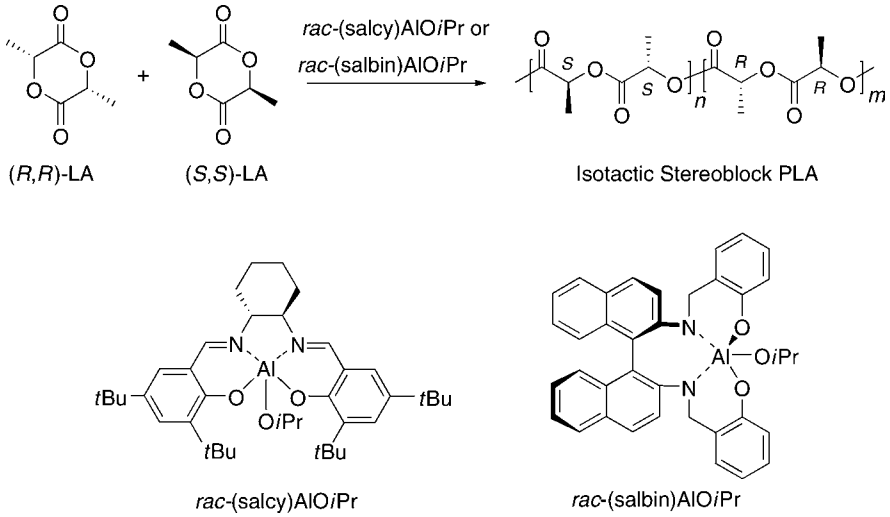

Scheme 11.22 Isospecific ring-opening polymerization of *rac*-LA using racemic, chiral aluminum alkoxides to produce isotactic stereoblock PLA.

11.3.1.3 Zinc Catalysts for the Synthesis of PLA

Coates and co-workers have reported that the β-diiminate zinc compound (BDI-*i*Pr) ZnO*i*Pr is an effective catalyst for the stereoselective ROP of LA (Scheme 11.23) [65]. Highly heterotactic PLA (M_n 38 000 g mol^{-1}, PDI 1.10) was produced via chain-end control from 200 equiv. of *rac*-LA in 20 min at 20 °C. A heterotactic linkage probability of 94% was achieved by performing the polymerization at 0 °C for 2 h. Using (BDI-*i*Pr)ZnO*i*Pr, *meso*-LA was polymerized to afford syndiotactic PLA through the same chain-end control mechanism. Although it is not able to produce isotactic PLA from *rac*-LA like the chiral aluminum catalysts (Scheme 11.22), (BDI-*i*Pr)ZnO*i*Pr exhibited much higher activity while maintaining excellent molecular weight control.

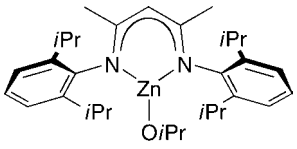

(BDI-*i*Pr)ZnO*i*Pr

Scheme 11.23 β-Diiminate zinc alkoxide (BDI-*i*Pr)ZnO*i*Pr used for the synthesis of heterotactic and syndiotactic PLA.

11.3.1.4 **Germanium Catalysts for the Synthesis of PLA**

The first germanium catalyst for the ROP of LA was reported by Davidson and co-workers [66]. They used a mixed germanium alkoxide–aryloxide [$(ArO_3)GeOiPr$, Scheme 11.24] to produce predominantly heterotactic PLA from the ROP of *rac*-LA in the absence of solvent. Molecular weights as high as 52 000 g mol^{-1} were obtained, with a PDI of 1.19. This was the first example of heterotactic PLA synthesis under solvent-free conditions.

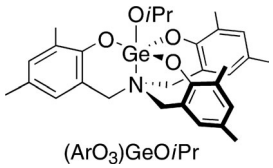

$(ArO_3)GeOiPr$

Scheme 11.24 Germanium catalyst $(ArO_3)GeOiPr$ for the synthesis of heterotactic PLA.

11.3.1.5 **Metal-free Catalysts for the Synthesis of PLA**

Hedrick and co-workers reported the use of an *N*-heterocyclic carbene (NHC, Scheme 11.25) as an organocatalyst for the ROP of cyclic esters through a monomer activation pathway in which the nucleophilic NHC ring opens the cyclic ester and activates it towards attack by the alcohol initiator or the propagating alcoholic polymer chain end [67]. This novel method is of great environmental interest as typical ROPs

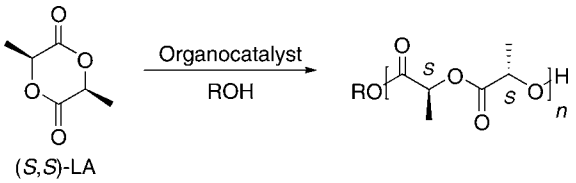

(*S*,*S*)-LA

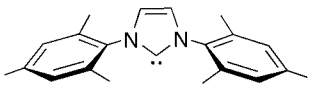

NHC

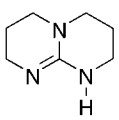

Guanidinium base

Scheme 11.25 Ring-opening polymerization of LA using organocatalysts.

require the removal of the residual catalyst (metal) from the polymer during purification. With an organocatalyst, metal removal is unnecessary and this eliminates the need for expensive purification steps and large volumes of solvent waste. In 2 h, the authors were able to polymerize 120 equiv. of (*S*,*S*)-LA using benzyl alcohol as the initiator, with a PDI of 1.12.

Recently, Waymouth and co-workers reported the ROP of LA in which they used a commercially available guanidinium base (Scheme 11.25) with 4-pyrenebutanol as an initiator for the ROP of (*S*,*S*)-LA [68]. This organocatalyst system exhibited activity that is faster than with many metal catalysts as it polymerized 500 equiv. of LA in 1 min at 20 °C to afford an M_n of 63 000 g mol^{-1} and a PDI of 1.11. They proposed a bifunctional nucleophilic mechanism in which a nitrogen atom on the guanidine base ring opens the cyclic ester while the adjacent nitrogen atom, through a hydrogen bond, activates the alcohol initiator or polymer chain end for nucleophilic attack at the nearby *N*-acyl bond. They hypothesized that this process is responsible for the exceptionally high LA ROP activities that were observed.

11.3.2
Synthesis of Poly(hydroxyalkanoate)s

Poly(hydroxyalkanoate)s (PHAs) are naturally occurring biodegradable and biocompatible polymers that are produced by bacteria and other organisms [50a,d, 52]. Because of the high cost of PHA synthesis via bacterial fermentation, a number of synthetic efforts have been developed for the synthesis of these aliphatic polyesters. We will present just a brief overview of PHA synthesis as a more extensive review has already been published [50b].

Schreck and Hillmyer have reported a synthesis of poly(α-methyl-β-pentyl-β-propiolactone) [69] (PMPP) from the corresponding lactone using a zinc complex (Scheme 11.26), previously shown to be highly active for the ROP of LA [70]. However, the ROP of MPP proceeded significantly more slowly than that of LA. This reaction required 75 h to achieve 89% conversion and an M_n of 40 000. Lactone MPP is readily synthesized from propionic acid and hexanal, two compounds that can be produced

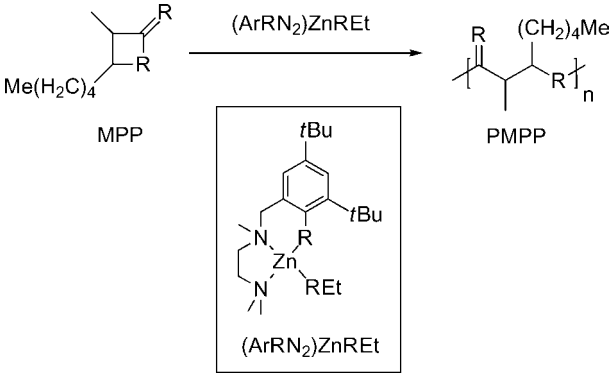

Scheme 11.26 Polymerization of (α-methyl-β-pentyl-β-propiolactone) using a zinc alkoxide.

from biorenewable resources. PMPP was targeted as a biodegradable, biorenewable alternative to polyethylene that is blended with PLA in order to increase the mechanical toughness of PLA.

Poly(3-hydroxybutyrate) (PHB), one of the most common PHAs, can be synthesized to give isotactic polyester through the use of optically pure (*R*)- or (*S*)-β-butyrolactone (BBL); however, syndiotactic PHB has been an elusive target. Notably, in a recent study, Carpentier and co-workers employed an yttrium isopropoxide complex $(ArO_2)Y(THF)OiPr$ (Scheme 11.27) to generate highly syndiotactic PHB in 1 min from *rac*-BBL [71]. The polymer contained 90% syndiotactic linkages and possessed an M_n of 23 000 g mol^{-1} and a PDI of 1.15. A decrease in temperature from 20 to −20 °C resulted in an increase in syndiotacticity to 94%.

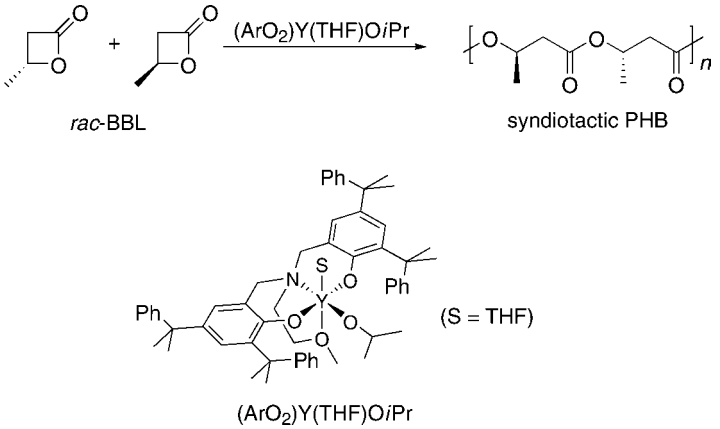

Scheme 11.27 Synthesis of syndiotactic PHB using yttrium catalyst $(ArO_2)Y(THF)OiPr$.

Another report of high activity in the polymerization of BBL comes from Coates and co-workers [72]. They used a β-diiminate zinc catalyst, (BDI-*i*Pr)ZnO*i*Pr, to effect the ROP of *rac*-BBL in 5 min at 70 °C to produce PHB with an M_n of 25 000 and a PDI of 1.14. At a monomer : initiator ratio of 2000 : 1, M_n values as high as 144 000 g mol^{-1} were achieved. Also, isotactic PHB was generated using optically pure (*R*)-BBL in the feed, although complete conversion was not realized as the highly crystalline polymer precipitated out of benzene solution at 67% conversion. It was also shown that the catalyst system is active for the ROP of β-valerolactone (BVL).

N-Heterocyclic carbenes (NHCs, Scheme 11.25) have also been shown by Hedrick and co-workers to effect the ROP of BBL [67]. They were able to polymerize 44 equiv. of BBL relative to pyrenebutanol initiator to afford PHB with a PDI of 1.15.

11.3.3 ROP of Other Cyclic Esters

In addition to LA and BBL, ε-caprolactone (CL) and similar lactones are suitable monomers for the synthesis of biodegradable aliphatic polyesters via well-defined

single-site catalysts. Hillmyer and co-workers recently reported the ROP of (−)-menthide (Scheme 11.28) using complex ($ArON_2$)ZnOEt (Scheme 11.26) [73]. Menthide is an ε-lactone readily synthesized from naturally occurring (−)-menthol (Scheme 11.28). This reaction gave M_n values in excess of 90 000 g mol^{-1} and narrow PDIs. More recently, the same group reported the copolymerization of menthide with *rac*-LA to form an ABA triblock thermoplastic elastomer from completely renewable resources [74]. This polymer has potential application in the biomedical and pharmaceutical fields.

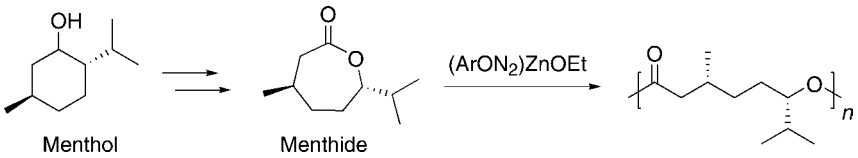

Scheme 11.28 Polymerization of menthide using a zinc alkoxide catalyst.

An *N*-heterocyclic carbene (Scheme 11.25) was also shown by Hedrick and co-workers to catalyze the ROP of CL [67]. They were able to achieve high conversions, albeit at longer times than for the previously mentioned ROP of LA (24 h instead of 2 h). In addition, star polyesters were synthesized using a six-arm hydroxyl-functionalized poly(propylene glycol) initiator. A guanidine base (Scheme 11.25) was also shown by Waymouth and co-workers to polymerize VL and CL [68]. In the ROP of VL, they used a slightly higher catalyst loading than with LA and achieved a polymer with a high M_n (16 000 g mol^{-1}) and narrow PDI (1.12) in 30 min at 25 °C. The ROP of CL, however, required much longer times in addition to higher catalyst loading. In 8 h, the ROP of CL catalyzed by the guanidine base resulted in an M_n of 21 000 g mol^{-1} and PDI of 1.16. Diblock copolymers were produced through the use of monohydroxy-functionalized macroinitiators such as poly(ethylene oxide). These block copolymers exhibited clean chain extensions.

11.3.4
Copolymerization of Epoxides and Cyclic Anhydrides

In addition to the ROP of cyclic esters, the alternating copolymerization of epoxides and cyclic anhydrides is a novel method for aliphatic polyester synthesis. This technique affords a polymer repeat structure identical to that of a condensation polyester, in which a diol and diacid are copolymerized via a polycondensation reaction (Scheme 11.18). However, the use of an anhydride and epoxide avoids the production of small-molecule byproducts and allows for the facile synthesis of high molecular weight polyesters. A number of anhydrides and epoxides are naturally occurring or can be readily synthesized from naturally occurring starting materials.

One of the first examples of epoxide–cyclic anhydride copolymerization came from Inoue and co-workers [75]. They employed an aluminum porphyrin–quaternary salt system, (TPP)AlCl–$EtPh_3PBr$, to copolymerize a variety of epoxides with phthalic

anhydride, including propylene oxide and cyclohexene oxide (Scheme 11.29). With a chloride initiator, polymers with M_n values up to 4000 g mol^{-1} were synthesized, while PDIs were as low as 1.08. The system was shown to be living by the addition of more epoxide to the growing poly(alkylene phthalate), which caused a noticeable increase in M_n while retaining the narrow PDI. However, one drawback to this system is the long reaction times required: 4–16 days were necessary to achieve full conversion of 25 equiv. of each monomer.

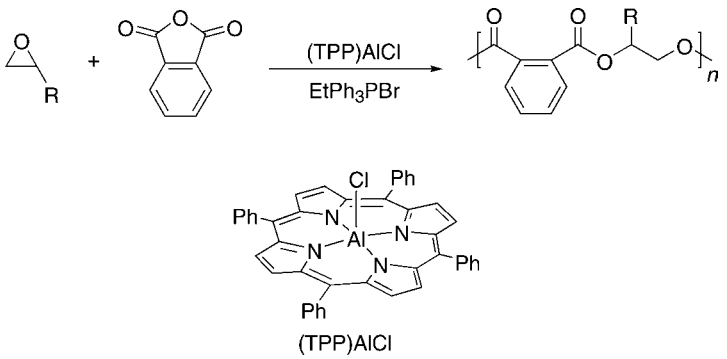

Scheme 11.29 Copolymerization of epoxides and maleic anhydride using (TPP)AlCl–$EtPh_3PBr$.

Recently, Coates and co-workers reported a more efficient method for the synthesis of aliphatic polyesters from epoxides and cyclic anhydrides using a β-diiminate (BDI) zinc complex, (CN-BDI)ZnOAc [76], which has been developed for use in ROP reactions over the past decade. This complex was active for a number of combinations of epoxides and cyclic anhydrides, including cyclohexene oxide and diglycolic anhydride (Scheme 11.30). M_n values in excess of 50 000 g mol^{-1} and PDIs as low as 1.11 were obtained. This system is noteworthy in that most ROPs can be performed in a matter of hours, instead of days, and can attain high molecular weight polymers while retaining low PDIs.

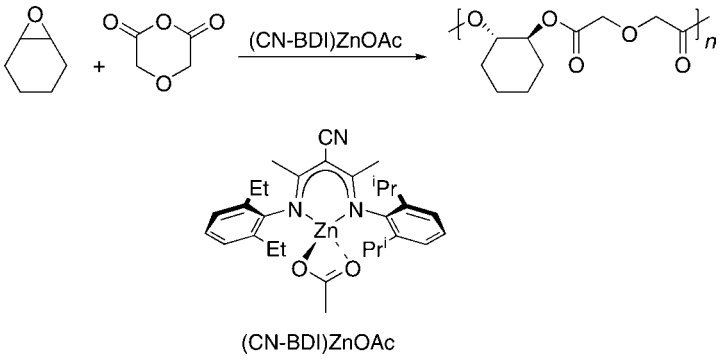

Scheme 11.30 Alternating copolymerization of epoxides and cyclic anhydrides using (CN-BDI)ZnOAc.

11.3.5 Summary

Interest in aliphatic polyesters has increased considerably over the past few decades, due in large part to their biodegradable properties and the biorenewable origin of many of the monomers. These materials have found many uses in today's society, from drug delivery systems, degradable tissue scaffolds and sutures, to commodity plastics and textiles. Although the cost of aliphatic polyesters has decreased, they are still more expensive than polyalkenes. With continuing research and an increasing public knowledge of, and interest in, this area, the cost of aliphatic polyesters is expected to become more competitive with polyalkenes. This development should be instrumental in lessening the environmental impact of our heavy dependence on non-biodegradable and non-biorenewable plastics.

References

1 Okada, M. (2002) *Progress in Polymer Science*, **27**, 87–133.

2 Stevens, E.S. (2002) *Green Plastics*, Princeton University Press, Princeton, NJ.

3 Gerngross, T.U. and Slater, S.C. (2000) *Scientific American*, **283** (2), 36–41.

4 Weisman, A. (2007) Polymers are forever, in *The World Without Us*, St Martins Press, New York, Chapter 9.

5 American Chemical Society . (1996) *Technology Vision 2020: the US Chemical Industry*, American Chemical Society, Washingtin, DC.

6 National Research Council of the National Academies . (2005) *Sustainability in the Chemical Industry: Grand Challenges and Research Needs – a Workshop Report*, National Research Council of the National Academies, New York.

7 Gerngross, T.U. and Slater, S.C. (2000) *Scientific American*, **283** (2), 36–41.

8 (a) Gross, R.A. and Kalra, B. (2002) *Science*, **297**, 803–807; (b) Okada, M. (2002) *Progress in Polymer Science*, **27**, 87–133.

9 (a) Leitner, W. (2000) *Comptes Rendus de l'Académie des Sciences - Series IIC - Chemistry*, **3**, 595–600; (b) Cooper, A.I. (2000) *Journal of Materials Chemistry*, **10**, 207–234.

10 (a) Jessop, P.G., Ikariya, T. and Noyori, R. (1999) *Chemical Reviews*, **99**, 475–493; (b) Kendall, J.L., Canelas, D.A., Young, J.L. and DeSimone J.M. (1999) *Chemical Reviews*, **99**, 543–563.

11 Coates, G.W. and Moore, D.R. (2004) *Angewandte Chemie – International Edition*, **43**, 6618–6639.

12 (a) For some other recent reviews, see: Kuran, W. (1981) *Progress in Polymer Science*, **23**, 919–992; (b) Darensbourg, D.J. and Holtcamp, M.W. (1996) *Coordination Chemistry Reviews*, **153**, 155–174; (c) Super, M.S. and Beckman, E.J. (1997) *Trends in Polymer Science*, **5**, 236–240; (d) Ochiai, B. and Endo, T. (2005) *Progress in Polymer Science*, **30**, 183–215; (e) Sugimot, H. and Inoue, S. (2004) *Journal of Polymer Science, Part A*, **42**, 5561–5573; (f) Darensbourg, D.J., Mackiewicz, R.M., Phelps, A.L. and Billodeaux, D.R. (2004) *Accounts of Chemical Research*, **37**, 836–844.

13 (a) Inoue, S., Koinuma, H. and Tsuruta, T. (1969) *Journal of Polymer Science, Part B*, **7**, 287–292; (b) Inoue, S., Koinuma, H. and Tsuruta, T. (1969) *Makromolekulare Chemie – Macromolecular Chemistry and Physics*, **130**, 210–220.

14 (a) Kuran, W., Pasynkiewicz, S., Skupinska, J. and Rokicki, A. (1976) *Makromolekulare Chemie – Macromolecular Chemistry and Physics*, **177**, 11–20; (b) Gorecki, P. and Kuran, W. (1985) *Journal of Polymer Science, Part C*, **23**, 299–304.

15 Soga, K., Imai, E. and Hattori, I. (1981) *Polymer Journal*, **13**, 407–410.

16 Kruper, W.J. and Dellar, D.V. (1995) *The Journal of Organic Chemistry*, **60**, 725–727.

17 Mang, S., Cooper, A.I., Colclough, M.E., Chauhan, N. and Holmes, A.B. (2000) *Macromolecules*, **33**, 303–308.

18 Stamp, L.M., Mang, S.A., Holmes, A.B., Knights, K.A., de Miguel, Y.R. and McConvey, I.F. (2001) *Chemical Communications*, 2502–2503.

19 Darensbourg, D.J. and Yarbrough, J.C. (2002) *Journal of the American Chemical Society*, **124**, 6335–6342.

20 Darensbourg, D.J., Rodgers, J.L. and Fang, C.C. (2003) *Inorganic Chemistry*, **42**, 4498–4500.

21 Darensbourg, D.J. and Mackiewicz, R.M. (2005) *Journal of the American Chemical Society*, **127**, 14026–14038.

22 Eberhardt, R., Allmendinger, M. and Rieger, B. (2003) *Macromolecular Rapid Communications*, **24**, 194–196.

23 Darensbourg, D.J., Yarbrough, J.C., Ortiz, C. and Fang, C.C. (2003) *Journal of the American Chemical Society*, **125**, 7586–7591.

24 Soga, K., Uenishi, K. and Ikeda, S. (1979) *Journal of Polymer Science, Polymer Chemistry Edition*, **17**, 415–423.

25 (a) Lu, X.B., Feng, X.J. and He, R. (2002) *Applied Catalysis A-General*, **234**, 25–33; (b) Lu, X.B., He, R. and Bai, C.X. (2002) *Journal of Molecular Catalysis A-Chemical*, **186**, 1–11.

26 Qin, Z.Q., Thomas, C.M., Lee, S. and Coates, G.W. (2003) *Angewandte Chemie – International Edition*, **42**, 5484–5487.

27 Lu, X.B., Liang, B., Zhang, Y.J., Tian, Y.Z., Wang, Y.M., Bai, C.X., Wang, H. and Zhang, R. (2004) *Journal of the American Chemical Society*, **126**, 3732–3733.

28 Lu, X.B. and Wang, Y. (2004) *Angewandte Chemie – International Edition*, **43**, 3574–3577.

29 Cohen, C.T., Chu, T. and Coates, G.W. (2005) *Journal of the American Chemical Society*, **127**, 10869–10878.

30 (a) Nakano, K., Kamada, T. and Nozaki, K. (2006) *Angewandte Chemie – International Edition*, **45**, 7274–7277; (b) Noh, E.K., Na, S.J., Sujith, S., Kim, S.W. and Lee, B.Y. (2007) *Journal of the American Chemical Society*, **129**, 8082–8083.

31 Cohen, C.T., Thomas, C.M., Peretti, K.L., Lobkovsky, E.B. and Coates, G.W. (2006) *Dalton Transactions*, 237–249.

32 Darensbourg, D.J. and Holtcamp, M.W. (1995) *Macromolecules*, **28**, 7577–7579.

33 Darensbourg, D.J., Holtcamp, M.W., Struck, G.E., Zimmer, M.S., Niezgoda, S.A., Rainey, P., Robertson, J.B., Draper, J.D. and Reibenspies, J.H. (1999) *Journal of the American Chemical Society*, **121**, 107–116.

34 Darensbourg, D.J., Wildeson, J.R., Yarbrough, J.C. and Reibenspies, J.H. (2000) *Journal of the American Chemical Society*, **122**, 12487–12496.

35 Koning, C., Wildeson, J., Parton, R., Plum, B., Steeman, P. and Darensbourg, D.J. (2001) *Polymer*, **42**, 3995–4004.

36 Dinger, M.B. and Scott, M.J. (2001) *Inorganic Chemistry*, **40**, 1029–1036.

37 Cheng, M., Lobkovsky, E.B. and Coates, G.W. (1998) *Journal of the American Chemical Society*, **120**, 11018–11019.

38 Moore, D.R., Cheng, M., Lobkovsky, E.B. and Coates, G.W. (2002) *Angewandte Chemie – International Edition*, **41**, 2599–2602.

39 (a) Chisholm, M.H., Huffman, J.C. and Phomphrai, K. (2001) *Journal of the Chemical Society-Dalton Transactions*, 222–224; (b) Chisholm, M.H., Gallucci, J. and Phomphrai, K. (2002) *Inorganic Chemistry*, **41**, 2785–2794.

40 Eberhardt, R., Allmendinger, M., Luinstra, G.A. and Rieger, B. (2003) *Organometallics*, **22**, 211–214.

41 (a) Zhang, M., Chen, L.B., Liu, B., Yan, Z., Qin, G. and Li, Z. (2001) *Polymer Bulletin*, **47**, 255–260; (b) Zhang, M., Chen, L.B., Qin, G. and Li, Z.M. (2001) *Acta Polymerica Sinica*, 422–424; (c) Zhang, M., Chen, L.B., Qin, G., Liu, B., Yan, Z. and Li, Z. (2003) *Journal of Applied Polymer Science*, **87**, 1123–1128.

42 Allen, S.D., Moore, D.R., Lobkovsky, E.B. and Coates, G.W. (2002) *Journal of the American Chemical Society*, **124**, 14284–14285.

43 Moore, D.R., Cheng, M., Lobkovsky, E.B. and Coates, G.W. (2003) *Journal of the American Chemical Society*, **125**, 11911–11924.

44 Lee, B.Y., Kwon, H.Y., Lee, S.Y., Na, S.J., Han, S.I., Yun, H.S., Lee, H. and Park, Y.W. (2005) *Journal of the American Chemical Society*, **127**, 3031–3037.

45 Nakano, K., Kosaka, N., Hiyama, T. and Nozaki, K. (2003) *Journal of the Chemical Society-Dalton Transactions*, 4039–4050.

46 Nozaki, K., Nakano, K. and Hiyama, T. (1999) *Journal of the American Chemical Society*, **121**, 11008–11009.

47 Nakano, K., Nozaki, K. and Hiyama, T. (2001) *Macromolecules*, **34**, 6325–6332.

48 Nakano, K., Nozaki, K. and Hiyama, T. (2003) *Journal of the American Chemical Society*, **125**, 5501–5510.

49 Cheng, M., Darling, N.A., Lobkovsky, E.B. and Coates, G.W. (2000) *Chemical Communications*, 2007–2008.

50 (a) Steinbüchel, A. and Doi, Y. (eds) (2002) *Biopolymers*, Vol. 4, Wiley-VCH Verlag GmbH, Weinheim; (b) Okada, M. (2002) *Progress in Polymer Science*, **27**, 87–133. (c) Dechy-Cabaret, O., Martin-Vaca, B. and Bourissou, D. (2004) *Chemical Reviews*, **104**, 6147–6176. (d) Müller, H.M. and Seebach, D. (1993) *Angewandte Chemie – International Edition*, **32**, 477–502.

51 Coulembier, O., Degée, P., Hedrick, J.L. and Dubois, P. (2006) *Progress in Polymer Science*, **31**, 723–747.

52 Williams, S.F. and Martin, D.P. (2002) in *Biopolymers, Vol. 4* (eds A. Steinbüchel, and Y. Doi), Wiley-VCH Verlag GmbH, Weinheim, pp. 91–127.

53 (a) Vink, E.T.H., Rábago, K.R., Glassner, D.A., Springs, B., OConnor, R.P., Kolstad, J. and Gruber, P.R. (2004) *Macromolecular Bioscience*, **4**, 551–564;(b) Gruber, P.R. and OBrien, M. (2002) *Biopolymers, Vol. 4* (eds A. Steinbüchel and Y. Doi), Wiley-VCH Verlag GmbH, Weinheim, pp. 235–250.

54 http://www.epa.gov/epaoswer/non-hw/muncpl/pubs/mswchar05.pdf.

55 Williams, S.F. and Peoples, O.P.(September (1996)) *Chemtech*, 38–44.

56 (a) Gupta, A.P. and Kumar, V. (2007) *European Polymer Journal*, **43**, 4053–4074; (b) OKeefe, B.J., Hillmyer, M.A. and Tolman, W.B. (2001) *Dalton Transactions*, 2215–2224.

57 (a) Odian, G. (2004) *Principles of Polymerization*, 4th edn John Wiley and Sons, Inc, Hoboken, NJ; (b) Seppälä, J.V., Korhonen, H., Kylmä, J. and Tuominen, J. (2002) *Biopolymers, Vol. 4* (eds A. Steinbüchel and Y. Doi), Wiley-VCH Verlag GmbH, Weinheim, pp. 327–369

58 Kamber, N.E., Jeong, W., Waymouth, R.M., Pratt, R.C., Lohmeijer, B.G.G. and Hedrick, J.L. (2007) *Chemical Reviews*, **107**, 5813–5840.

59 http://www.natureworksllc.com/.

60 Spassky, N., Wisniewski, M., Pluta, C. and Le Borgne, A. (1996) *Macromolecular Chemistry and Physics*, **197**, 2627–2637.

61 (a) Ovitt, T.M. and Coates, G.W. (1999) *Journal of the American Chemical Society*, **121**, 4072–4073; (b) Ovitt, T.M. and Coates, G.W. (2002) *Journal of the American Chemical Society*, **124**, 1316–1326.

62 (a) Radano, C.P. Baker, G.L. and Smith, M.R., III (2000) *Journal of the American Chemical Society*, **122**, 1552–1553. (b) Ovitt, T.M. and Coates, G.W. (2000) *Journal of Polymer Science, Part A: Polymer Chemistry*, **38**, 4686–4692.

63 (a) Zhong, Z., Dijkstra, P.J. and Feijen, J. (2002) *Angewandte Chemie – International Edition*, **41**, 4510–4513; (b) Zhong, Z., Dijkstra, P.J. and Feijen, J. (2003) *Journal of*

the American Chemical Society, **125**, 11291–11298.

64 Hormnirun, P., Marshall, E.L., Gibson, V.C., Pugh, R.I. and White, A.J.P. (2006) *Proceedings of the National Academy of Sciences of the United States of America*, **103**, 15343–15348, and references cited therein.

65 (a) Cheng, M., Attygalle, A.B., Lobkovsky, E.B. and Coates G.W. (1999) *Journal of the American Chemical Society*, **121**, 11583–11584; (b) Chamberlain, B.M., Cheng, M., Moore, D.R., Ovitt, T.M., Lobkovsky, E.B. and Coates, G.W. (2001) *Journal of the American Chemical Society*, **123**, 3229–3238.

66 Chmura, A.J., Chuck, C.J., Davidson, M.G., Jones, M.D., Lunn, M.D., Bull, S.D. and Mahon, M.F. (2007) *Angewandte Chemie – International Edition*, **46**, 2280–2283.

67 Connor, E.F., Nyce, G.W., Myers, M., Möck, A. and Hedrick, J.L. (2002) *Journal of the American Chemical Society*, **124**, 914–915.

68 Pratt, R.C., Lohmeijer, B.G.G., Long, D.A., Waymouth, R.M. and Hedrick, J.L. (2006) *Journal of the American Chemical Society*, **128**, 4556–4557.

69 Schreck, K.M. and Hillmyer, M.A. (2004) *Tetrahedron*, **60**, 7177–7185.

70 Williams, C.K., Breyfogle, L.E., Choi, S.K., Nam, W., Young, V.G., Hilmyer, M.A. and Tolman, W.B. (2003) *Journal of the American Chemical Society*, **125**, 11350–11359.

71 Amgoune, A., Thomas, C.M., Ilinca, S., Roisnel, T. and Carpentier, J. (2006) *Angewandte Chemie – International Edition*, **45**, 2782–2784.

72 Rieth, L.R., Moore, D.R., Lobkovsky, E.B. and Coates, G.W. (2002) *Journal of the American Chemical Society*, **124**, 15239–15248.

73 Zhang, D., Hillmyer, M.A. and Tolman, W.B. (2005) *Biomacromolecules*, **6**, 2091–2095.

74 Wanamaker, C.L., OLeary, L.E., Lynd, N.A., Hillmyer, M.A. and Tolman, W.B. (2007) *Biomacromolecules*, **8**, 3634–3640.

75 (a) Aida, T. and Inoue, S. (1985) *Journal of the American Chemical Society*, **107**, 1358–1364; (b) Aida, T., Sanuki, K. and Inoue, S. (1985) *Macromolecules*, **18**, 1049–1055.

76 Jeske, R.C., DiCiccio, A.M. and Coates, G.W. (2007) *Journal of the American Chemical Society*, **129**, 11330–11331.

12
The Aerobic Oxidation of *p*-Xylene to Terephthalic acid: a Classic Case of Green Chemistry in Action

Walt Partenheimer and Martyn Poliakoff

Although the ultimate aim of most green chemistry research is industrial implementation, the research is often perceived as being primarily an academic pursuit. This chapter is different. It focuses on the continuing development and improvement of a major commercial bulk chemical process, the oxidation of *p*-xylene. The two authors, W.P., a US industrial chemist with more than 30 years' experience of oxidation processes, and M.P., a UK academic green chemist, were first brought together by the oxidation of *p*-xylene in supercritical water, which forms the final section of this chapter. Their aim is to bring this story of this process to a wider chemical public. The chapter shows how apparently simple reactions can have unexpected mechanistic complexity and how this complexity offers fascinating opportunities for major innovation even in well-established processes. A key objective is to show that, despite the fact that the drivers continue to be largely commercial, the developments in this process have all the appearance of being guided by the Principles of Green Chemistry. Indeed, the oxidation of *p*-xylene may well be one of the best demonstrations that greener processes are more profitable.

12.1
Introduction

The commercial methods for the manufacture of terephthalic acid are based on dissolving *p*-xylene and the components of the catalyst into a given solvent and passing a source of molecular oxygen (O_2), usually air, through it (Scheme 12.1).

Most of the manufactured terephthalic acid is used to produce poly(ethylene terephthalate) (PET) by its reaction with ethylene glycol (Scheme 12.2).

One of the most visible forms of PET is in the manufacture of water bottles, although it has many other forms, including fibers, films and engineered plastics. Over 6 million tons per year were produced in the 2002 [1].

The structure of this chapter is based on the historical methods of preparation of terephthalic acid, demonstrating how the discovery of each method allowed for a large increase in greenness in the manufacturing process (Table 12.1). Each advance

Handbook of Green Chemistry, Volume 1: Homogeneous Catalysis. Edited by Robert H. Crabtree

ISBN: 978-3-527-32496-5

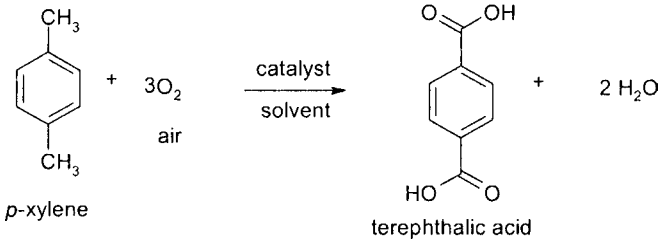

p-xylene terephthalic acid

Scheme 12.1

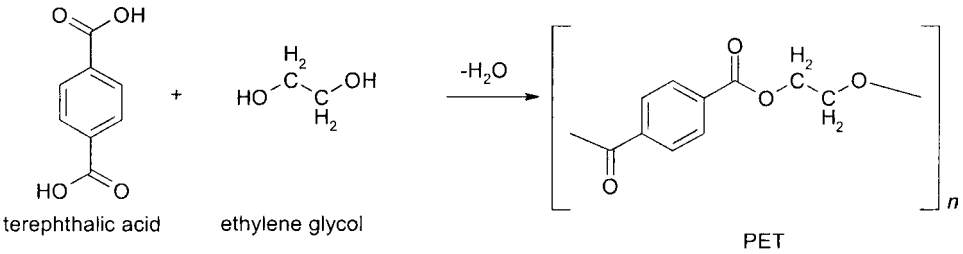

terephthalic acid ethylene glycol PET

Scheme 12.2

is based on the invention of new catalysts; small variants in these processes have been discussed elsewhere [2]. After a brief description of each process, the greenness of the process will be outlined and then the catalytic mechanisms responsible for the green aspects will be highlighted, ending with a discussion of the weaknesses in the process. Our discussion of greenness will be based on the 12 Principles of Green Chemistry and Engineering [3]; those that are relevant to this chapter are given in Table 12.2. Engineering aspects of these processes are beyond the scope of this chapter and have been discussed elsewhere [1, 2, 4–7].

The earliest methods for preparing terephthalic acid used stoichiometric reagents such as permanganate and dichromate salts. The first commercial manufacturing methods were initiated with the invention of the Co(II) acetate catalyst using acetic

Table 12.1 Past, present and future methods for manufacturing terephthalic acid from *p*-xylene.

	Catalyst	Solvent	Description[a]
Past	None – stoichiometric	—	—
Present	$Co(OAc)_2$	Acetic acid	Witten process. Autoxidation followed by esterification
Present	$Co(OAc)_2$	Acetic acid	Eastman process. Autoxidation with an organic co-oxidant
Present	$Co(OAc)_2$–$Mn(OAc)_2$–HBr	Acetic acid	Mid-Century process. Autoxidation
Future (?)	$MnBr_2$ (?)	Water	Autoxidation

[a]Autoxidation is defined as products obtained by reaction of a hydrocarbon using dioxygen as the primary oxidant.

Table 12.2 Selected Principles of Green Chemistry and Engineering used in this chapter (adapted and modified from [3]).

Principle[a]	Description
1	It is better to prevent waste than to treat or clean up waste
2	Atom economy; maximize all materials used into the desired product
3	Safer solvents; should be innocuous and made unnecessary if possible
4	Design for energy efficiency and simplicity
5	Use renewable feedstocks
6	Use catalysts, as selective as possible, rather than stoichiometric reagents
7	Avoid derivatization or masking of the reagents
8	Less hazardous chemical syntheses; methods should be designed to generate substances that have little or no toxicity.

[a]Note that the numbering of these principles has been changed from those used in [3].

acid as the solvent in 1938 [8]. There are two variants of this method based on aerobic oxidation with the products being separated and purified by esterification (Witten process) and air oxidation using a co-oxidant such as acetaldehyde (Eastman process). A giant step forward in terephthalic acid manufacture was the invention of metal–bromide catalysts, the most prominent being the combination of Co(II) and Mn(II) acetates with bromide salts in 1954 [4, 9, 10]. Finally, we discuss a possible future process based on changing the solvent from acetic acid to 'hot' water (250–374 °C) or supercritical water ($T_c = 374\,^{\circ}C$, $P_c = 221$ bar).

12.2 Methods of Making Terephthalic Acid Using Stoichiometric Reagents

Introductory textbooks in organic chemistry and also advanced treatises on oxidation chemistry teach the oxidation of methylaromatic compounds using permanganate and dichromate salts [11], e.g. Scheme 12.3.

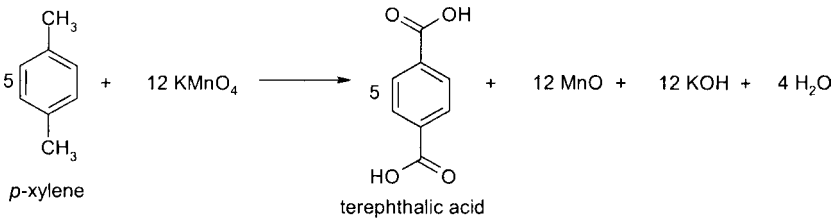

p-xylene

terephthalic acid

Scheme 12.3

The atom economy of the reaction in Scheme 12.1 to give terephthalic acid (Green Principle 2, Table 12.2), based on the moles of product and by-products produced [12, 13], is only 38% Current terephthalic acid plants often have a capacity of at least 1 billion lb per year. It is difficult to conceive of a process using potassium

permanganate and generating multi-million pounds of waste in the form of manganese(II) oxide and alkali metal hydroxide.

12.3 Methods for Preparing Terephthalic Acid Using Cobalt Acetate and Dioxygen in Acetic Acid

We begin by discussing the large increase in greenness in going from a stoichiometric preparation of terephthalic acid to a catalytic process using O_2 as the oxidant. Then we describe the catalytic mechanisms responsible for the increasing greenness. Finally, we explain the disadvantages of the Co–acetic acid-based chemical processes so that one can appreciate the value of the next advance in greenness – the invention of the Co−Mn−Br catalyst.

Principle 2 – Atom Economy
The Co catalyst allows for the direct incorporation of dioxygen into *p*-xylene in which the atom economy is increased from 38% in Scheme 12.3 to 82% in Scheme 12.1. The number of by-products is reduced from 3 in the stoichiometric oxidation to just simply water in Scheme 12.1. Although water is normally considered a green by-product, it is not 'green' in this instance since it deactivates the catalyst [14]; hence the energy-intensive separation of the water from the acetic acid eventually becomes necessary. This is one of the key driving forces for developing a process that uses water as a solvent.

Principle 5 – Renewable Feedstocks
Air, which contains 20.9% of O_2, is usually used as the source of O_2 in these processes. Air is a renewable resource since O_2 is generated biologically via photosynthesis. *p*-Xylene, however, is not renewable since it comes from petroleum refining.

Principle 4 – Design for Simplicity and Energy Efficiency
One outstanding green property of the acetic acid solvent is that terephthalic acid is highly insoluble in it, whereas all the other intermediates (shown in Scheme 12.4) and by-products produced are much more soluble. Thus, as *p*-xylene is being oxidized in acetic acid, the terephthalic acid preferentially precipitates. The product is thus separated from the by-products and catalyst as it is being produced. The solubility of terephthalic acid at 150 °C, the approximate operating temperature of these processes, is only 0.38 g per 100 g of acetic acid. Hence the one disadvantage of homogeneously catalyzed processes – that of separation of the product from the solvent and catalyst – is largely absent when acetic acid is used.

One of the great green advantages of this aerobic reaction is that the enthalpy change of the reaction in Scheme 12.1 is -336 kcal mol^{-1}. This enormous amount of heat can be captured by conversion of water to steam in heat exchangers and then used to provide energy in subsequent chemical steps – such as for the purification of the terephthalic acid or for conversion of terephthalic acid to PET. For example, one

method used to purify terephthalic acid is by recrystallization in water at around ~300 °C. The energy required to heat 1 mol of terephthalic acid from room temperature (25 °C) to 300 °C is 275 kcal mol^{-1}, which could be supplied by the heat of reaction.

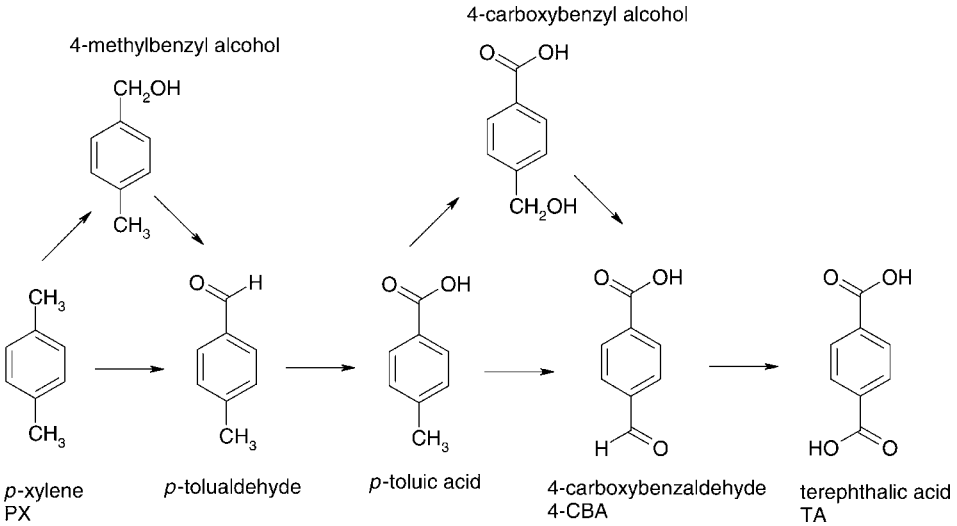

Scheme 12.4 Intermediates present during the autoxidation of *p*-xylene to terephthalic acid. For a more detailed description and the relative reactivities of the intermediates, see [21].

Principle 8 – Less Hazardous Chemical Synthesis Producing Substances with Little or No Toxicity

Both terephthalic acid and dimethyl terephthalate have low toxicity and cause only mild and reversible irritation to the skin, eyes and the respiratory system [16].

Principles 1 and 6 – Use Selective Catalysts to Reduce By-products

Co(II) acetate dissolved in acetic acid strongly activates molecular oxygen and also reduces undesirable by-products. Activation of oxygen is necessary because it exists in a triplet electronic spin state ($^3O_2$) and *p*-xylene is in a singlet spin state. This dissimilarity in spin produces a large activation energy barrier, which causes the reaction to be very slow [17]. Experimentally, this can be shown by heating toluene in acetic acid to 205 °C at 34 bar pressure for 25 min and obtaining only a trace of benzaldehyde [17, 18]. However, addition of Co(II) acetate immediately initiates a reaction and benzyl alcohol, benzaldehyde and benzoic acid are obtained. The increase in activity and selectivity that Co(II) imparts to this free radical chain mechanism has been demonstrated by oxidation in acetic acid of 4-methylbenzaldehyde (*p*-tolualdehyde) one of the intermediates in *p*-xylene oxidation [15]. The oxidizability of 4-methylbenzaldehyde is 340 times greater than that of *p*-xylene; consequently, its oxidation can be observed even in the absence of a catalyst. As shown in Scheme 12.5, addition of the cobalt catalyst increases the rate of reaction by

a factor of 2.5 and dramatically decreases the yields of the by-products. The yield of toluene is reduced by a factor of 10, that of *p*-tolyl formate is decreased by a factor of 300 and *p*-cresol falls to undetectable amounts. The amount of CO_2 is reduced by a factor of 7.4! *p*-Cresol is a very strong antioxidant, the concentration of which increases with time in the uncatalyzed reaction and eventually causes the reaction to terminate at a conversion of only 43%. In the presence of cobalt catalyst, the reaction continues to 100%, giving high yields of *p*-toluic acid [15].

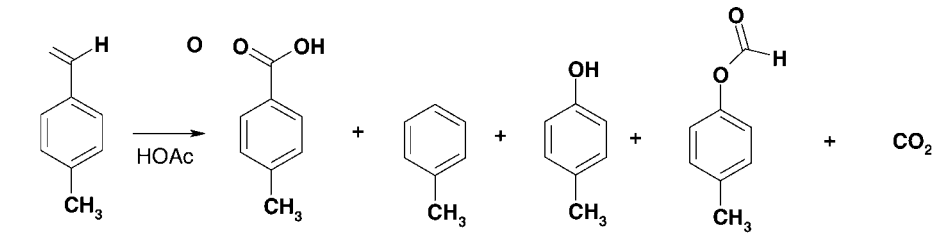

Without Co	rate = 1.2 x 10^{-4} s^{-1}	0.78% yield	0.63% yield	1.5% yield	0.82 mmol
With Co	rate = 4.2 x 10^{-4} s^{-1}	0.074% yield	0.0% yield	0.005% yield	0.11 mmol

Scheme 12.5 *p*-Toluic acid and by-products from the oxidation of *p*-tolualdehyde (4-methylbenzaldehyde) in 5% water–acetic acid with and without the presence of Co(II) acetate (at 10 m*M*).

The mechanistic rationale for the dramatic increase in reaction rate and selectivity is given in Scheme 12.6 (Reactions 12.1–12.16). The initiation, propagation and termination steps of the free radical chain mechanism are given in Reactions 12.1–12.4. The product of these reactions is 4-methylperoxybenzoic acid. The bond strengths of peroxides are weak ($\sim$25–30 kcal mol^{-1}) and, above 80 °C, the thermal dissociation of these bonds can occur to give the carboxyl radical and hydroxyl radicals, Reaction 12.5. The carboxyl radical readily undergoes decarboxylation, Reaction 12.9, to give the 4-methylphenyl radical. Hydrogen atom abstraction of this radical generates the observed by-product, toluene. The 4-methylphenyl radical will also react at a diffusion-controlled rate with O_2 and go through a series of reactions to generate the 4-methylcresol, Reaction 12.13. The hydroxyl radical, generated in Reaction 12.5, is *always* undesirable in selective oxidations, for two reasons. (i) It is highly energetic and reacts exothermically with virtually any available C−H bond; it reacts preferentially with the aromatic ring, with an enthalpy change of -15 kcal mol^{-1}, to form the cyclohexyldienyl radical, which subsequently rearranges to 2-hydroxyl-4-methylbenzaldehyde, Reaction 12.6. (ii) The reaction rates of the hydroxyl radical with organic substrates is often close to diffusion controlled; it reacts with *p*-xylene at a rate of 7.0×10^9 L mol^{-1} s^{-1}) [19]. The observed by-product, *p*-tolyl formate, forms via the Baeyer–Villiger rearrangement of the reaction of the 4-methylbenzaldehyde with the 4-methylperoxybenzoic acid, Reaction 12.11. The greenhouse gas CO_2 forms from the oxidation of the phenols, Reactions 12.8 and 12.15, and from the decarboxylation of the 4-methylbenzylcarboxyl radical,

Reaction 12.9. The cresols oxidize to the quinones, which are highly colored and hence undesirable, since one of the key specifications for commercial terephthalic acid is a high degree of whiteness.

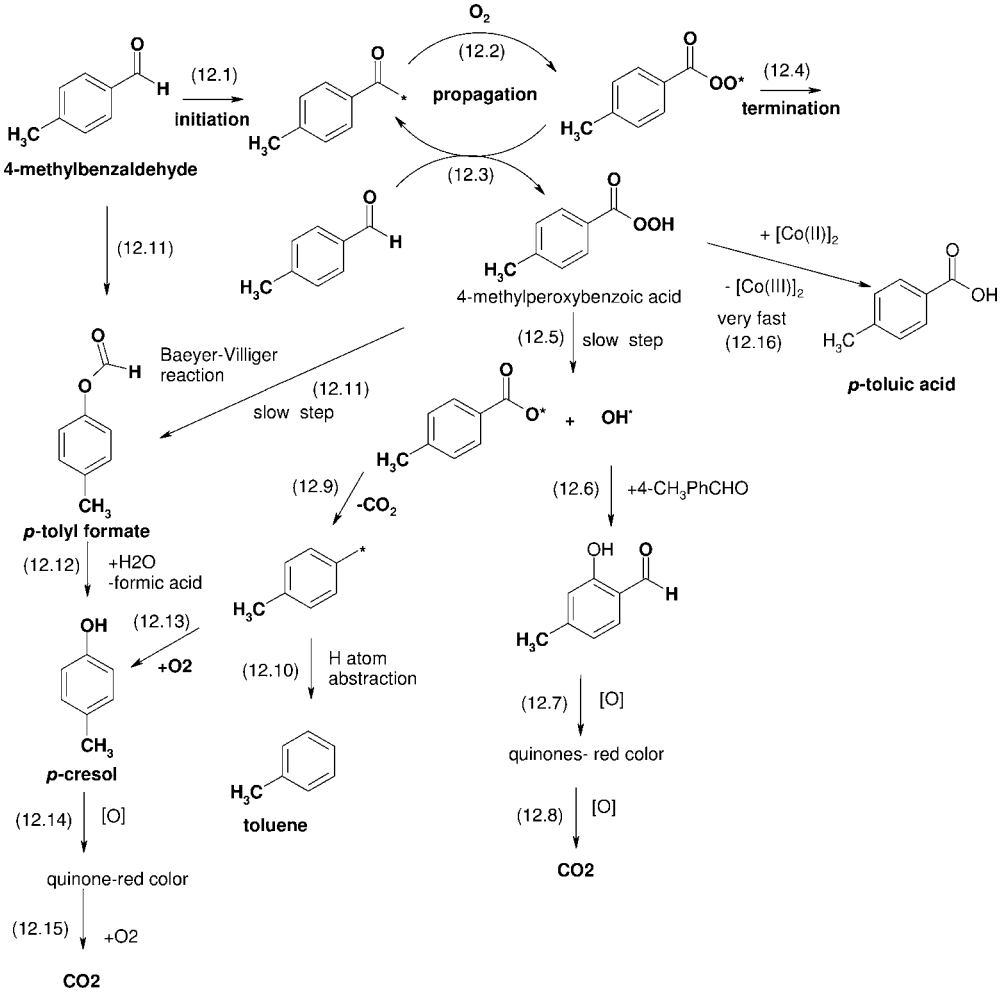

Scheme 12.6 The mechanism for the formation of toluene, *p*-cresol, *p*-tolyl formate and carbon dioxide from the autoxidation of 4-methylbenzaldehyde (*p*-tolualdehyde).

It is well established that Co(II) reacts with peroxyaromatic acids at a very high rate [15]. In acetic acid, the reaction of 3-chloroperoxybenzoic acid with Co(II) is 400 000 times faster than its thermal dissociation (Scheme 12.7). The reaction with Co(II) is also much more selective, giving higher yields to the carboxylic acid with significant decreases in the 4-chlorobenzene by-product (the equivalent of toluene formation in Scheme 12.6) and CO_2. Thus in Scheme 12.6, the reaction of Co(II) with

the 4-methylperoxyacid, Reaction 12.16, is much faster than both the thermal dissociation, Reaction 12.5, and the Baeyer–Villiger reaction, Reaction 12.11. The direct formation of the aromatic acid via Reaction 12.16 is therefore highly favored when a cobalt catalyst is added and is consistent with the large observed reduction in yield of the by-products, toluene, 4-methylcresol, *p*-tolyl formate and CO_2.

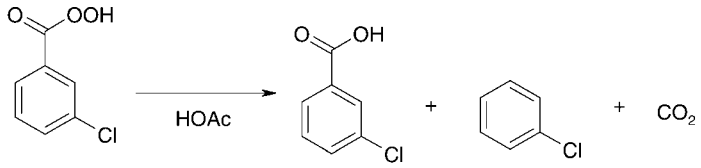

3-chloroperoxybenzoic acid 3-chlorobenzoic acid chlorobenzene

without Co(II)	$t_{1/2}$ = 900 s	87% yield	4.8% yield	0.70 mmol
with Co(II)	$t_{1/2}$ = 0.0023 s	100% yield	<0.7% yield	0.025 mmol

Scheme 12.7 A comparison of the thermal decomposition and stoichiometric oxidation of 3-chloroperbenzoic acid with Co(II) acetate in acetic acid at 60 °C in 10% water–acetic acid [20].

Co(II) acetate appears to be unique in its ability to catalyze autoxidations of this type. One of the fundamental problems with free radical chain mechanisms is how the initiation step occurs [18]. It has been shown that Co(II) acetate reacts with trace amounts of peroxides in acetic acid to generate small amounts of Co(III) and of products which are derived from the formation of the methyl radical (methyl acetate, CO_2 and CH_4). Both the methyl radical, $CH_3^{\bullet}$, and Co(III), are known to generate the benzylic radical ($CH_3PhCH_2^{\bullet}$) and hence initiate the reaction (Scheme 12.8a). Of all the first-row transition metals (Ti, V, Cr, Mn, Fe, Co, Ni, Cu and Zn), only Co has this ability. Similarly, Co is unique in its ability to catalyze the oxidation of *p*-toluic acid, one of the intermediates in *p*-xylene oxidation [18].

Not only is the Co(III) generated by trace amounts of peroxide but also, once the free radical chain mechanism is operational, Co(III) is generated from the peroxy acid, Reaction 12.16 (Scheme 12.6), and by reaction with the highly energetic hydroxyl radical. As discussed above, the reduction of the steady-state concentration of the hydroxyl radical in these reactions is highly desirable because of the lack of selectivity and high reactivity of $OH^{\bullet}$ toward virtually any organic substrate [19]. Co (II) and most other metals used in autoxidation react very quickly with the hydroxyl radical (Table 12.3), thereby lowering its concentration and hence increasing the selectivity of the process. The increase in selectivity imparts 'greenness' by decreasing waste.

This free radical mechanism explains how the conservation of electronic spin, which prevents the direct reaction of $^3O_2$ with hydrocarbons, can be overcome. In the propagation step of the free radical mechanism, the hydrocarbon is itself a radical species in a doublet spin state and reacts essentially at diffusion-controlled rates with O_2 to give the peroxy radical:

$$^2CH_3PhCH_2^{\bullet} + {}^3O_2 \rightarrow {}^2CH_3PhCH_2OO^{\bullet} \qquad (12.17)$$

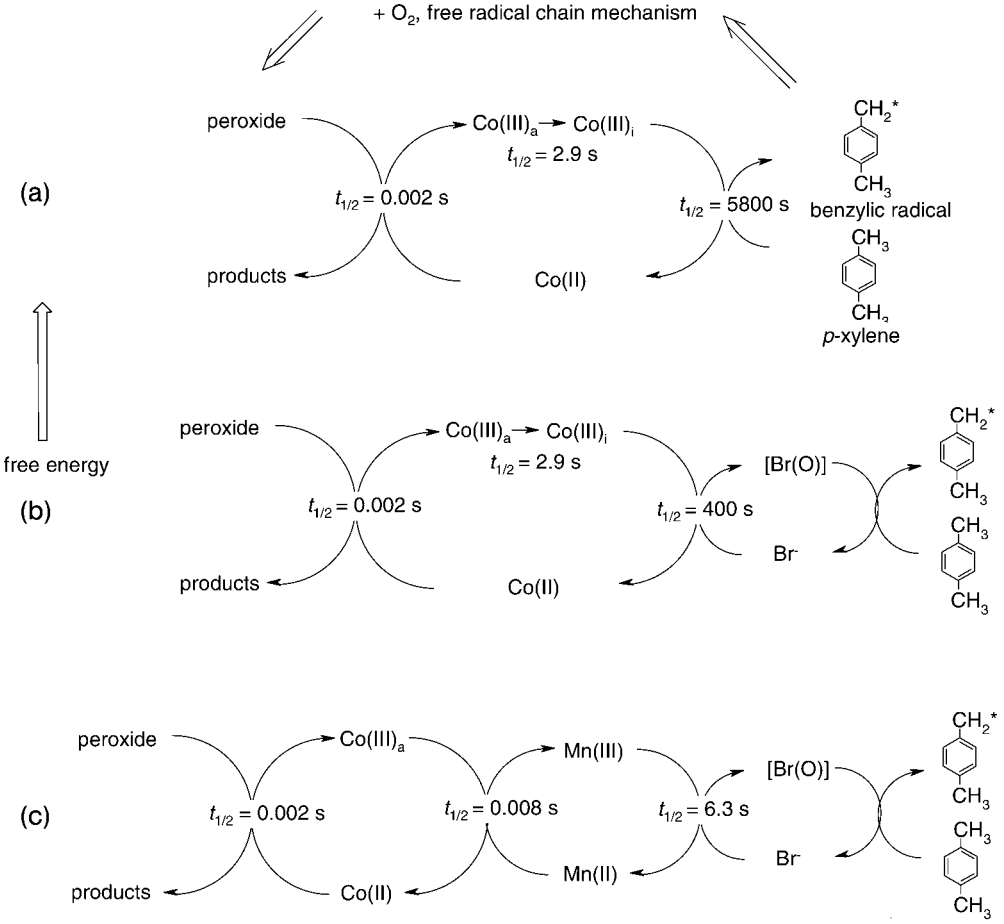

Scheme 12.8 The initiation of the oxidation of *p*-xylene with (a) Co, (b) Co–Br and (c) Co–Mn–Br catalysts. The $t_{1/2}$ data are from experiments at 60 °C in 10% water–acetic acid. Vertical distances between Co(II)–Co(III), Mn(II)–Mn(III) and Br(–1)–Br(0) are proportional to their redox potentials. $Co(III)_a$ and $Co(III)_i$ are different forms of Co(III) with the activity of $Co(III)_a$ being greater than that of $Co(III)_i$. Redrawn from [55].

Table 12.3 Rates of reaction of the hydroxyl radical with selected compounds in aqueous solution [19].

Species reacting with OH radical	Product of reaction	pH	Rate constant ($L\,mol^{-1}\,s^{-1}$)
Bromide ion	$BrOH^-$	1	1.1×10^{10}
Co(II)	Co(III)OH	7	8×10^{5}
Mn(II)	Mn(III)OH	6.7	2.9×10^{7}

We have seen how the aerobic autoxidation of *p*-xylene is superior in greenness to stoichiometric oxidation and how the cobalt catalyst imparts great selectivity in reducing many unwanted by-products. The problem with this chemistry, however, is that one is limited to low terephthalic acid yields of ~15% with large amounts of partially oxidized intermediates shown in Scheme 12.4. The reasons for this are complex but include the following:

- The reaction is sluggish even at high catalyst concentrations since Co(III) reacts slowly with *p*-xylene (Scheme 12.8a).
- Studies using the Hammett equation show that the transition state of Co(III) responds strongly to electron-withdrawing substituents on the ring, such as a carboxyl group, and hence *p*-toluic acid is 76 times less reactive than *p*-xylene [15, 21, 22].
- The steady-state concentration of Co(III) is high during the reaction, often 50–70% of the metal present [17, 23]. Co(III) is a very strong oxidant in acetic acid [Co(II)–Co(III) reduction potential = 1.8 V] and is known readily to decarboxylate aromatic and aliphatic acids [24].

The structure of the coordination compounds in acetic acid–water solutions has been discussed in detail [25]. The rates of ligand exchange of Co(II) are essentially instantaneous at room temperature and the coordination sphere contains acetic acid, acetate, water and oxygenated products such as benzaldehydes and carboxylic acids. Both acetic acid and *p*-toluic acid are decarboxylated by Co(III), generating the plethora of by-products shown in Scheme 12.9. The reaction is also strongly deactivated by the decarboxylation reaction because (i) the *p*-cresol formed is a strong antioxidant and (ii) Co(III) is in competition with the desired reaction, Reaction 12.21, which produces the benzylic radical as opposed to the undesired decarboxylations, Reactions 12.22 and 12.23 (Scheme 12.9).

Why can the rate of reaction not be increased by increasing the temperature so that the oxidation can be driven to completion giving terephthalic acid in high yield? The activation energy for the Co(III) decarboxylation is very high (42 kcal mol^{-1} in anhydrous acetic acid, 33 kcal mol^{-1} in 5% water–acetic acid and 28 kcal mol^{-1} in 10% water–acetic acid [26]). As the temperature increases, the importance of decarboxylation, Reactions 12.22 and 12.23 become dominant at ~120 °C and the relative rates of conversion to the desired aromatic acid decrease above this temperature [17, 23, 26].

Two strategies have been used to overcome the low terephthalic acid yields in the cobalt-catalyzed reaction. Both of these strategies use co-oxidation processes to drive the reaction of *p*-xylene to terephthalic acid to high yield. The Eastman process adds acetaldehyde to the oxidation reaction along with the *p*-xylene. The acetaldehyde is oxidized to peroxyacetic acid and this peroxy acid effectively oxidizes Co(II) to Co(III), which drives the reaction to completion. Large amounts of acetaldehyde are required (about 2 mol of acetaldehyde–*p*-xylene [27]), making the reaction stoichiometric in acetaldehyde. The process is a net producer of acetic acid. Similar processes have used paraldehyde [26] and 2-butanone [23] as the co-oxidants. In the Witten process, the initial oxidation mixture of *p*-toluic acid and terephthalic acid is esterified with methanol. The dimethyl terephthalate is separated from the monomethyl-*p*-toluic

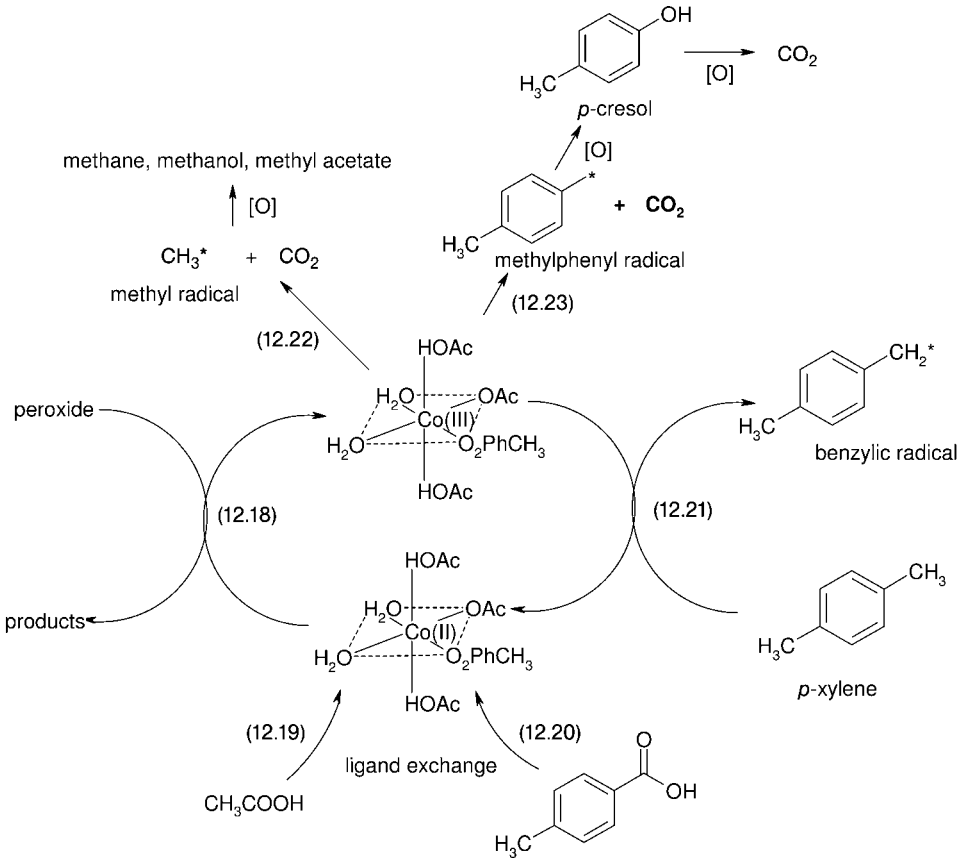

Scheme 12.9 Structure of possible coordination compounds of cobalt in water–acetic acid solutions, incorporating aromatic acids in the coordination sphere of Co(II), and some of the by-products from decarboxylation.

acid and the latter is recirculated back to the oxidation reactor. Then one has a co-oxidation of the more active *p*-xylene with the less reactive monomethyl-*p*-toluic acid to produce monomethyl terephthalate. Continuous oxidation followed by esterification and separation of the esters eventually produces dimethyl terephthalate with about 90% selectivity.

12.4 Adding Bromide to Improve Terephthalic Acid Production Using Cobalt and Manganese Acetates in Acetic Acid

A huge step forward in greening of this reaction occurred in 1954 with the discovery of metal–bromide catalysts by Landau, Saffer and Barker [10, 28]. Their initial

discovery was with an $MnBr_2$ catalyst with 1,4-diisopropylbenzene as the substrate. Although the Co–Mn–Br catalyst is much more active than the Mn–Br catalyst and the diisopropylbenzene substrate is significantly more difficult to oxidize to terephthalic acid than is *p*-xylene, a large boost in activity and yield was apparent and they immediately recognized the commercial significance of the discovery. Some of the more important characteristics of this momentous discovery are given in Table 12.4. The metal–bromide catalysts give a yield boost in terephthalic acid from 15% to >95%! Furthermore, even at typical operating temperatures of around 200 °C, the solubility of terephthalic acid is only 1.7 g per 100 g of acetic acid and the hence a large majority of it precipitates as it is formed in the reactor. The composition of the solids is typically >99% terephthalic acid.

Some of the enhancement in greenness includes the following.

Principles 1 and 6 – Prevent Waste. Use More Selective Catalysts

As seen in Table 12.4, addition of bromide to cobalt not only quadruples the rate of reaction, but simultaneously make it much more selective and also the rate of CO_2 generation decreases by a factor of 5.9. Addition of Mn to the Co–Br catalyst further increases it activity and selectivity (Table 12.4).

Principles 4 and 7 – Design for Energy Efficiency and Simplicity. Avoid Derivatization or Masking of the Reagents

In the Witten process, esterification, a masking of the carboxylic acid group, is used to separate and purify the terephthalic acid. Esterifications are slow, equilibrium-controlled reactions and the products are separated by distillation. Since the Witten process makes dimethyl terephthalate (DMT), MeOH is released during the

Table 12.4 Comparison of uncatalyzed with Co-, Co–Br- and Co–Mn–Br-catalyzed oxidation of *p*-xylene in acetic acid. Data from [4, 15, 17].

Description	No catalyst	Co catalyst	Co–Br catalyst	Co–Mn–Br catalyst
Terephthalic acid yield (%), on a per pass basis [17]	—	~15	~95	>95
Relative reactivity of catalyst [15, 17]	1.0	2.5	9.5	41
CO_2, relative, substrate = 4-methylbenzaldehyde (*p*-tolualdehyde) [15]	17	2.2	—	1
CO_2, relative, substrate = *p*-xylene [17]	—	5.9	1.0	—
Toluene, yield (%) [15]	0.078	0.071	—	0.0
Tolyl formate, yield (%) [15]	1.5	0.005	—	0.0
Reactivity, *p*-xylene/*p*-toluic acid	—	76	22	21
Steady-state [Co(III)] (%) [17]	—	11	<0.6	<0.6
Typical catalyst concentration (*M*)	—	~0.1	0.02/0.02	0.01/0.01/0.02
Range of operating temperatures (°C)	—	70–150	30–225	30–225

manufacture of PET and it must be captured and returned to the manufacturer of the DMT. All these extra energy-intensive steps can be eliminated with the use of the Co−Mn−Br catalyst. Similarly, the Eastman process generates an excess of acetic acid, which is avoided with the Co−Mn−Br catalyst.

Principle 4 – Design for Energy Efficiency and Simplicity

The fact that the product separates itself as it is being produced avoids the problem usually associated with homogeneously catalyzed processes, i.e. the separation of the product from the solvent and catalyst. Also, the process is sufficiently selective that a significant amount of the solvent containing the catalyst (mother liquor) can be directly recycled back to the oxidation reactor without purification. Various schemes have been developed to recycle the remaining catalyst metals. The metals can be precipitated from acetic acid as their oxalate [29] or carbonate salts [30]. The solid salts can be returned to the oxidation reactor since their dissolution in acetic acid and subsequent oxidation simply release CO_2. Also, methods have been developed to separate the cobalt and manganese from the corrosion metals, such as iron and chromium [31]. Since the Co−Mn−Br catalyst is much more active, much less catalyst needs to be used than for the Co catalyst alone; see Table 12.4 for typical catalyst concentrations. Finally, the capture of the energy released during the oxidation reaction is improved because the reactors can be operated at higher temperatures. For the cobalt catalyst the temperatures are 120–150 °C whereas for the Co−Mn−Br catalyst typical operating temperatures will range from 170 to 225 °C.

Principle 3 – Less Hazardous to the Environment

The Co−Br and Co−Mn–Br catalysts generate less CO_2 and toxic carbon monoxide than the Co catalyst (Table 12.4). Methods have been developed to destroy effectively the carbon monoxide and other organic species, in the vent gas streams. Also, the action of bacteria is often used in the plants to destroy all of the organic waste (acetic acid, terephthalic acid, intermediates and by-products). The resulting sludge can be dried and burned or spread on land [16, 32].

One key observation to explain the mechanism of the increased selectivity of the metal–bromide catalysts is the steady-state concentration of Co(III) in the reactor. In one example in Table 12.4, the concentration was reduced from 11% to <0.6% of the total cobalt in solution. This is readily observed when performing these oxidations in glass reactors. When the Co(II) acetate is initially dissolved with the *p*-xylene in acetic acid the color is light blue. After initiation of the reaction, the color is changed to deep green by the Co(III) that is formed. If one now adds an equimolar amount of sodium bromide to the cobalt in the flask, the color immediately reverts to light blue as nearly all of the Co(III) disappears. At the same time, the rate of reaction increases and the rates of CO_2 and toluene generation decrease significantly (Table 12.4). The reduction in by-product formation is expected because they are the result of Co(III) decarboxylation and now much less Co(III) exists in solution. There is a rapid reaction of Co(III) with Br^- to generate a bromine(0) species (Scheme 12.8b), which effectively lowers the concentration of Co(III) in solution. The bromine(0) rapidly abstracts a hydrogen atom from *p*-xylene to generate the benzylic radical, which propagates the free radical chain.

Also known are the rates of reaction when a peroxy acid is added to a mixture of Co(II), Mn(II) and bromide in acetic acid (Scheme 12.8c). The reaction of Co(III) with Mn(II) is faster than that of Br^-, hence Mn(II) is oxidized before Br^-. The very fast reaction of Mn(II) with Co(III) lowers the concentration of Co(III) even further than in the Co−Br catalyst, resulting in an even more selective system. Addition of Mn(II) to a Co−Br catalyst does not significantly change its color. Since Mn(II) is nearly colorless whereas Mn(III) is intense brown, both the steady-state concentration of Co and Mn are in their + II state. Finally, the Co, Mn and Br can lower the steady-state concentration of the unselective OH radicals which react spontaneously and very rapidly with OH (Table 12.3), to form catalytically active species, i.e. Co(III), Mn(III) and Br(0).

As discussed above, the maximum temperature of a Co catalyst is limited because the decarboxylation of the carboxylic acids via Co(III) becomes the predominant reaction at temperatures >120 °C. The lower steady-state concentrations of Co(III) and Mn(III) in a Co−Mn−Br catalyst allow one to operate at higher temperatures. As a consequence, *p*-xylene can be completely oxidized to terephthalic acid in a reasonably short, industrially acceptable, residence time.

There are, however, four drawbacks associated with the Co−Mn−Br-catalyzed autoxidation of *p*-xylene, three of which are associated with the acetic acid solvent. (i) Significant quantities of acetic acid are oxidatively destroyed; the exact amounts are proprietary to the commercial manufacturers of terephthalic acid but, in 1995, about 12% of the acetic acid (6.8×10^5 tons) sold worldwide was used to replenish the terephthalic acid plants that use acetic acid as a solvent [33]. (ii) Methyl bromide, a severe ozone-depleting chemical, is found in the vent gases; it is probably formed from the methyl radicals generated by acetic acid decarboxylation, Reaction 12.22 (Figure 12.6), with the reduced Br(0) species in solution. (iii) Water is a product of the oxidation of *p*-xylene(2 mol per mole of terephthalic acid) and this water must be separated from the acetic acid by a energy-intensive distillation step. (iv) Even though the product precipitates from the reaction in >99% purity, it contains ∼0.5% of 4-CBA, which is a chain stopper in the esterification needed for PET manufacture; the concentration of 4-CBA has to be lowered by further purification either via hydrogenation in water or by further oxidation at higher temperatures which causes a significant increase in solvent oxidative degradation [6].

12.5
Potential Processes Using Water as a Solvent

At this point, we switch to discussing a possible future development in xylene oxidation, namely switching from acetic acid to H_2O as the process solvent. These developments are not mere speculation; they based on results published in the open literature, particularly by Savage's group in Michigan and Poliakoff's group in Nottingham. Although xylene oxidation in high-temperature water is still at an early stage, there is a long history of commercial wet air oxidation and total oxidation in supercritical water has also been carried out commercially [58], albeit on a scale very modest compared with that of current terephthalic acid plants.

Three of the four problems described in the previous section are associated with the acetic acid solvent. Therefore, it is not surprising that attempts have been made in the past by terephthalic acid manufacturers to eliminate the acetic acid or to use water as a solvent. As early as 1961 there was a report by McIntyre and Ravens of ICI [34]. This was followed by a series of reports by Hronec and Ilavsky in 1982–83 [35, 36] and from Amoco in 1990 [37].

In 1996, work began at Nottingham on continuous selective partial oxidation in supercritical H_2O. Interest in high-temperature water was further stimulated by a paper by Holliday *et al.*, who demonstrated that selective batch oxidation could be performed on a small scale in sub-critical water at 300–355 °C [38]. This was followed by reports on continuous oxidation from the Nottingham team in collaboration with INVISTA [39–42] and from Savage's group in Michigan largely on batch reactions [43–46].

Partenheimer was introduced to this area by the 2002 report from Nottingham of the continuous oxidation of *p*-xylene using $MnBr_2$ as a catalyst in supercritical water to produce terephthalic acid in high yield (>80%) with *no* detectable 4-CBA in the product [39]. *This is particularly exciting because there is a possibility of simultaneously eliminating all four of the problems discussed above!* More specifically, if water were successfully employed as a solvent, one would have the following advancements in green chemistry.

Principles 1 and 8 – Prevent Waste and Generation of Hazardous Substances
The elimination of the products of the oxidative combustion of acetic acid (CO – toxic; CO_2 – greenhouse gas; and CH_3Br – ozone depleting).

Principle 3 – Safer Solvents
Acetic acid is susceptible to explosions whereas water is non-combustible.

Principle 4 – Design for Energy Efficiency and Simplicity
There would no need to separate water from the acetic acid. With no 4-CBA in the product, downstream purification steps, such as hydrogenation, may become unnecessary. If hydrogenation in water is necessary, then there is solvent compatibility and simplicity, since oxidation, hydrogenation and crystallization can be performed in the same solvent. Also, there is the advantage of operating at higher temperatures (300–400 °C) than either the Co- or Co−Mn−Br-catalyzed processes (∼150 and ∼190 °C, respectively), so that energy recovery would be more efficient.

Phenomenologically, the mechanism of terephthalic acid in sub- and supercritical water appears to be much the same as that in acetic acid, namely a catalyst-modified free radical chain mechanism. Similarities between the reactions in the two solvents include the following:

- The same product sequence as shown in Scheme 12.4 is reported in sub- and supercritical water [39, 45, 46].
- At these high temperatures, one can observe the *uncatalyzed* oxidation of *p*-xylene with the expected products (i.e. large amounts of toluene and cresols from the

thermal decomposition of the hydroperoxides; see Scheme 12.6); the cresols will prevent high yields of the aromatic acids. The uncatalyzed oxidation of *p*-xylene at 240–500 °C and 200–300 bar gives a maximum yield of only 22% terephthalic acid and up to a 64% yield of toluene [45, 46].

- Benzylic alcohols are always found in low yields (~1–5%) in metal-catalyzed oxidation in acetic acid because the catalyst metals not only operate as redox catalysts but also as Lewis acids to dehydrate the benzyl hydroperoxides to aldehydes very rapidly, thereby by-passing the formation of the benzylic alcohol [49, 50]:

$$PhCH_2OOH + M^{(+N)} \rightarrow PhCHO + M^{(+N)}(H_2O) \qquad (12.24)$$

  Hence one would expect relatively high amounts of the benzylic alcohols to be formed in *uncatalyzed* oxidation of *p*-xylene in water. This indeed has been reported where *p*-xylene was found to give a ~40% yield at 380 °C in water [46].

- Addition of the appropriate catalyst metal and bromide enhances the yield of aromatic acid and increasing the catalyst concentration increases the yield further, all of which suggests that oxidation in water is operating with the same mechanisms as in acetic acid [4, 38, 44, 45].

It is well established that the properties of water change greatly with increasing temperature. Gases and organic substrates are very soluble in supercritical water since its physical properties become similar to those acetone or anhydrous acetic acid. For example, the dielectric constant of water decreases from 80 at ambient temperature to 4 at the critical point. By comparison, at room temperature, the dielectric constant of acetone and anhydrous acetic acid are 1.3 and 6.2, respectively.

The structure of $MnBr_2$ in water has been determined at 25, 325 and 400 °C using EXAFS and XANES [51, 52]. As can be seen from Scheme 12.10, very little bromide is in the coordination sphere at room temperature, whereas at 325 °C, a mixture of tetrahedral and octahedral mono- and dibromo compounds exist with most of the bromide directly bonded to Mn. At 400 °C in supercritical water, only the tetrahedral $[Mn^{II}Br_2(H_2O)_2]$ is detected. This is consistent with the decreasing dielectric constant of the solvent since ionic species are becoming less favored. This is supported by the fact that the structure of $CoBr_2$ in acetone, $[CoBr_2\ (acetone)_2]$ [53], is essentially the same as that of $MnBr_2$ in supercritical water $[MnBr_2(H_2O)_2]$.

With water as a solvent, the catalyst is significantly less active at 200 °C than at 400 °C. At 200 °C, a 37 times higher concentration of the Co−Mn−Br catalyst was needed to obtain a yield of terephthalic acid similar to that obtained in acetic acid [37]. Much lower catalyst concentrations are required in water at 400 °C. The dielectric constant of water changes from 37 at 200 °C to 4 at 400 °C; hence there appears to be a correlation between the degree of metal–bromide bonds and catalytic activity. A similar relationship exists in acetic acid–water solutions between the degree of metal–bromide bonds with dielectric constant and catalytic reactivity (Table 12.5). A simple model has been devised to rationalize these relationships (Scheme 12.11) [52].

In autoxidation, the energetically difficult step is the initiation step where the benzylic radical $CH_3PhCH_2^{\bullet}$ is generated from *p*-xylene,. When the dielectric

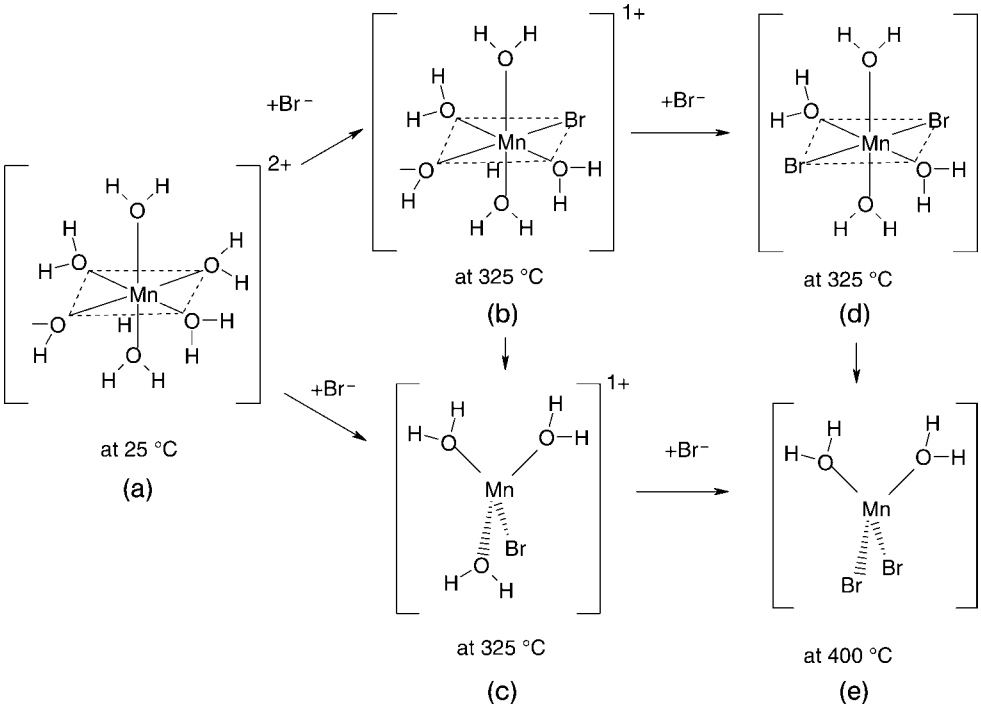

Scheme 12.10 Structure of $MnBr_2$ in water as a function of temperature as determined by Br and Mn EXAFS and XANES measurements [51, 52].

constant is high, the value of the equilibrium constant in Scheme 12.11 is small. The active catalyst is then generated via Reactions 12.25–12.28. Thus, Mn(II) is initially oxidized to Mn(III), ligand exchange occurs and bromide is incorporated into the Mn (III) coordination sphere. This coordination is followed by the intramolecular

Table 12.5 Relationship of catalytic activity of the Co−Mn−Br catalyst to the amount of metal–bromide bonds and dielectric constant in acetic acid–water mixtures. Data from [25, 56, 57].

Solvent	Dielectric constant	Metal as metal–bromide species (%)[a]	Rate of *p*-toluic acid with Co–Mn–Br catalyst (cm^3 O_2 min^{-1})
10% H_2O in HOAc	17	3	1.2
5% H_2O in HOAc	13	14	2.1
1% H_2O in HOAc	7.6	67	—
HOAc	6.2	89	4.8

[a]The percentage of the Co and Mn metals in solution that have a metal–bromide bond as determined using a bromide-selective electrode.

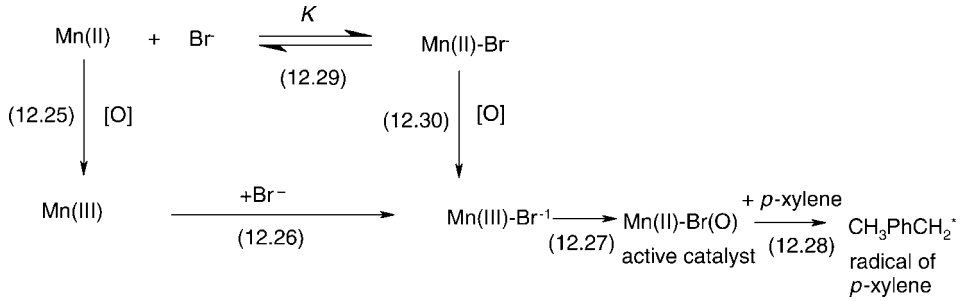

Scheme 12.11 A model to rationalize the activity of metal–bromide catalysts in acetic acid and water.

electron transfer, Reaction 12.27, to generate the active catalyst species which in turn generates the benzylic radical, Reaction 12.28. By contrast, when the dielectric constant is low the equilibrium constant is high and most of the manganese exists with an Mn(II)−Br bond. The active catalytic species is then generated via Reactions 12.30 and 12.27. There are two reasons for expecting the route via Reactions 12.25–12.27 to be slower than that via Reactions 12.30 + 12.27 because three reactions are needed to generate the active species via Reactions 12.25–12.27, whereas only two reactions are needed via Reactions 12.30 and 12.27 and the rate of incorporation of the bromide anion into the coordination sphere will be much slower for Mn(III) than that for Mn(II) [54]. The rate of generation of the active species is expected to be faster when the dielectric constant is low, in agreement with the experimental data in both water and acetic acid.

So far, discussion in this chapter has been entirely restricted to the oxidation of *p*-xylene. This is because current processes involve the upstream separation of the refinery C_8 aromatic stream, consisting of a mixture of the three isomeric xylenes with ethylbenzene, into its constituent compounds. Such separation is energy intensive because the physical properties of the C_8 components are rather similar. After separation, the isomers are oxidized in separate processes (Figure 12.1), because their rates of oxidation are substantially different. An interesting aspect of oxidation in supercritical water is that the rates of oxidation of the isomeric xylenes are very similar [41] and it is possible to co-oxidize them in a way which cannot easily be done in acetic acid (Table 12.6 and Figure 12.2). This opens up the exciting possibility of directly co-oxidizing the three xylenes *without separating them*; this is potentially important from a green chemistry perspective because the corresponding carboxylic acids have more widely differing properties and are more easily separated than the xylene precursors.

12.6
Summary and Final Comments

We have described how the preparation of terephthalic acid has been greened from the highly wasteful stoichiometric oxidation, to the Co(II) acetate catalyst in acetic acid which a renewable source of oxidant, O_2, can be used and which is able to drive

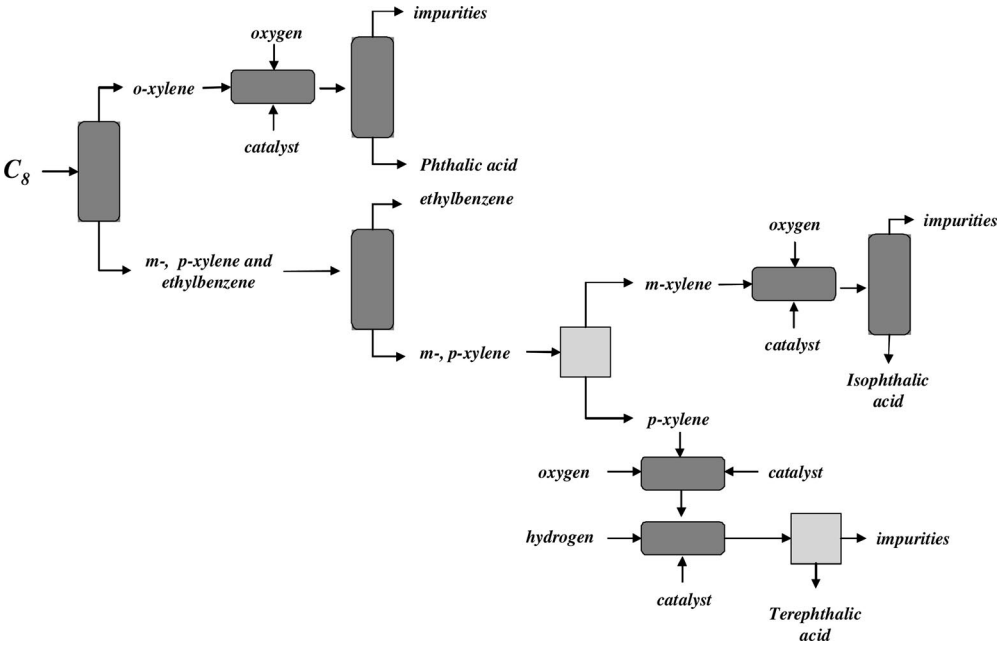

Figure 12.1 Schematic of current processes for separating the refinery C_8 aromatic stream into its components and oxidizing the different compounds to their corresponding acids. Reproduced with permission from [41], © The Royal Society of Chemistry.

the oxidation of *p*-xylene down selective pathways to terephthalic acid. Further greening was seen with the simple addition of Mn and Br to the Co catalyst to give a great boost in activity and selectivity, so that >95% yields could be obtained with >99% purity of the isolated terephthalic acid. These advances have enabled major

Table 12.6 Yields[a] observed in the continuous Mn–Br oxidation of mixed xylenes in supercritical H_2O. Adapted from [41].

o-:*m*-:*p*-Xylene[a] (*w*/W_t)	Di-CA: total yield (%)	*o*-Di-CA (%)[b]	*m*-Di-CA(%)[b]	*p*-Di-CA(%)[b]
33.3 : 33.3 : 33.3	59	47	62	69
66 : 17 : 17	60	58	65	67
17 : 66 : 17	52	34	58	47
17 : 17 : 66	47	39	50	48
100 : 0 : 0	52	52	-	-
0 : 100 : 0	66	-	66	-
0 : 0 : 100	61	-	-	61

[a]All calculated by HPLC (di-CA = dicarboxylic acid).
[b]Feed composition of the xylene mixture by weight. All the reactions were carried out under the same conditions; see [41] for details.

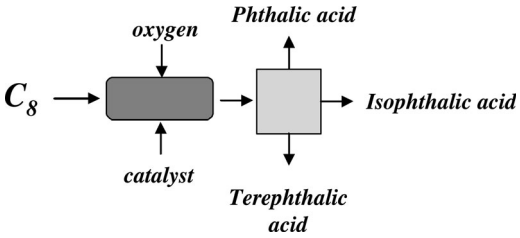

Figure 12.2 Schematic of a possible simultaneous oxidation process in supercritical H_2O for a mixture of all three isomeric xylenes to their corresponding acids. Reproduced with permission from [41], © The Royal Society of Chemistry.

process simplification to be implemented. In the future, a change in solvent from acetic acid to water could eliminate the wasteful oxidation of the acetic acid and possibly reduce the number of processing steps.

The use of water as an oxidation solvent is in infancy and many questions still need to be addressed. For example, the specifications for the terephthalic acid to be used in PET are very stringent. The terephthalic acid must be very white and not contain trace organic and inorganic impurities that may impart undesirable properties to the PET during its preparation. 'Hot' water can be very corrosive, so materials of construction will be important. Elimination of the oxidative destruction of acetic acid will eliminate one of the primary variable costs of the current process. However, one does not yet know how much of the *p*-xylene, its intermediates and terephthalic acid product will undergo this same oxidative destruction. One might expect that the 'burn' of *p*-xylene oxidation in water might be higher than in acetic acid because, for example, the hydroxyl radicals, which were destroying the acetic acid, will now attack the *p*-xylene, thereby increasing its rate of destruction. The use of water will have the challenging task of competing against a very mature terephthalic acid manufacturing industry which benefits from empirical learnings gathered over the last 50 years and also from good scientific and technological understanding.

References

1 Cornils, B. and Herrmann, W.A. (2002) Synthesis of dimethyl terephthalate/terephthalic acid and poly (ethylene terephthalate), in *Applied Homogeneous Catalysis with Organometallic Compounds*, 2nd edn (ed. D.A. Schiraldi), Wiley-VCH Verlag GmbH, Weinheim, pp. 544–552.

2 Raghavendrachar, P. and Ramachandran, S. (1992) Liquid-phase catalytic oxidation of *p*-xylene. *Industrial & Engineering Chemistry Research*, **31**, 453–462.

3 (a) Anastas, P.T. and Warner, J.C. (1998) *Green Chemistry: Theory and Practice*, Oxford University Press, New York, pp. 30; (b) Anastas, P.T. and Zimmerman, J.B. (2003) *Environmental Science & Technology*, **37**, 94.

4 Partenheimer, W. (1995) The methodology and scope of metal/bromide autoxidation of hydrocarbons. *Catalysis Today*, **23**, 69–158.

5 Cincotti, A., Orru, R. and Cao, G. (1999) Kinetic and related engineering aspects of catalytic liquid-phase oxidation of *p*-xylene to terephthalic acid. *Catalysis Today*, **52**, 331–347.

6 Suresh, A.K., Sharma, M.M. and Sridhar, T. (2000) Engineering aspects of industrial liquid-phase air oxidation of hydrocarbons. *Industrial & Engineering Chemistry Research*, **39**, 3958–3997.

7 Carra, S. and Santacesaria, E. (1980) Engineering aspects of gas–liquid catalytic reactions. *Catalysis Reviews: Science and Engineering*, **22**, 75.

8 Loder, D.J. (1938) (DuPont), US Patent 2 245 528.

9 Burney, D.E., Weisemann, G.H. and Fragen, N. (1959) Now – dibasic acids by direct oxidation. *Petroleum Refiner*, **38**, 186.

10 Landau, R. and Saffer, A. (1968) Development of the MC process. *Chemical Engineering Progress*, **64**, 20.

11 Hudlicky, M. (1990) *Oxidations in Organic Chemistry*, ACS Monograph No. 186, American Chemical Society, Washington, DC.

12 Sheldon, R.A. (1992) Organic synthesis – past, present and future. *Chemistry & Industry (London)*, 903.

13 Sheldon, R.A. (1994) Consider the environmental quotient. *Chemotherapy*, 38.

14 Partenheimer, W. (2004) The complex synergy of water in the metal/bromide autoxidation of hydrocarbons caused by benzylic bromide formation. *Advanced Synthesis and Catalysis*, **246**, 297–306.

15 Partenheimer, W. (2005) The complex synergy of water in metal/bromide autoxidations. Part II. Effect of water and catalyst on the aerobic oxidation of benzaldehydes and the effect of water on the elementary pathways. *Advanced Synthesis and Catalysis*, **347**, 580–590.

16 Sheehan, R.J. (1995) Terephthalic acid, dimethylterephthalate and isophthalic acid, in *Ullmann's Encyclopedia of Industrial Chemistry*, (eds B. Ehers, S. Hawkins and W. Russey), Wiley-VCH, Weinheim. Vol. A26, 193–226.

17 Partenheimer, W. (1990) A chemical model for the Amoco 'MC' oxygenation process to produce terephthalic acid, in *Catalysis of Organic Reactions*, (ed. D.W. Blackburn), Marcel Dekker, New York, Chapter 20.

18 Partenheimer, W. (1991) Characterization of the reaction of Co(II) acetate, dioxygen and acetic acid and its significance in autoxidation reactions. *Journal of Molecular Catalysis*, **67**, 35–46.

19 Buxton, G.V., Greenstock, C.L., Helman, W.P. and Ross, A.B. (1988) Critical review of rate constants for reactions of hydrated electrons, hydrogen atoms and hydroxyl radicals ($^{\bullet}OH/^{\bullet}O^{-}$) in aqueous solution. *Journal of Physical and Chemical Reference Data*, **17**, 513–886.

20 Partenheimer, W., and Gipe, R.K. (1993) Nature of the Co–Mn–Br catalyst in the methylaromatic compounds process: kinetic and thermodynamic studies, in *Catalytic Selective Oxidation*, (eds S.T. Oyama and J.W. Hightower), American Chemical Society, Washington, DC, 81–88.

21 Partenheimer, W. (2003) The effect of zirconium in metal/bromide catalysts on the autoxidation of *p*-xylene. Part I. Activation and changes in benzaldehyde intermediate formation. *Journal of Molecular Catalysis*, **206**, 105–119.

22 Partenheimer, W. (2004) The unusual characteristics of the aerobic oxidation of 3,4-dimethoxytoluene with metal/bromide catalysts. *Advanced Synthesis and Catalysis*, **347**, 1495–1500.

23 Brill, W.F. (1960) Terephthalic acid by single stage oxidation. *Industrial & Engineering Chemistry*, **52**, 837.

24 Lande, S.S. and Kochi, J.K. (1968) Formation and oxidation of alkyl radicals by Co(III) complexes. *Journal of the American Chemical Society*, **90**, 5196.

25 Partenheimer, W. (2001) The structure of metal/bromide catalysts in acetic acid/water mixtures and its significance in autoxidation. *Journal of Molecular Catalysis*, **174**, 29–33.

26 Nakaoka, K., Miyama, Y., Matsuhisa, S. and Wakamatsu, S. (1973) Preparation of

terephthalic acid using paradehyde promoter. *Industrial & Engineering Chemistry Product Research and Development*, **12**, 150.

27 Hull, D.C. (1957) (Eastman Kodak), US Patent 2 673 217.

28 Saffer, A. and Barker, R.S. (1958) (Mid-Century), US Patent 2 833 816.

29 Hobbs, C.C., Trebellas, J.C. and Huguet, J.L. (1974) (Celanese), US Patent 3 840 469; Feld, M. (1984) (Dynamit Nobel), US Patent 4 490 298; Brown, A.P. and Hundley, J.G. (1986) (Amoco), US Patent 4 487 355; Nowicki, N.R. and Thomka, D.E. (1988) (Amoco), US Patent 4 769 488; Holzhauer, J.K., Schammel, W.P. and Nowicki, N. R. (1988) (Amoco), US Patent 4 786 752; Lowry, J.D. Nowicki, N.R. and Partenheimer, W. (1989) (Amoco), US Patent 4 816 601.

30 Jeffery, I., and Whiston, K., (1998) (INVISTA), Patent WO98/08605, ICI; Trevillan, A.E. (1972) (Atlantic Richfield), US Patent 3,673,154.

31 (a) Trevillan, A.E. (1972) (Atlantic Richfield), US Patent 3 673 154; (b) Partenheimer, W. (1980) (Amoco), US Patent 4 228 091; (c) Partenheimer, W. (1980) (Amoco), US Patent 4 242 128.

32 Shelley, S. (1991) *Chemical Engineering*, **98**, 90–93.

33 Weissermel, K. and Arpe, H.J. (1997) *Industrial Organic Chemistry*, 3rd edn, Verlag Chemie, Weinheim, p. 178.

34 McIntyre, J.E. and Ravens, D.A.S. (1961) The oxidation of alkylaromatic compounds in aqueus hydrogen bromide. *Journal of the Chemical Society*, 4082.

35 Hronec, M. and Ilavsky, J. (1982) Oxidation of polyalkylaromatic hydrocarbons. XII. Technological aspects of p-xylene oxidation to terephthalic acid in water. *Industrial & Engineering Chemistry Product Research and Development*, **21**, 455.

36 Hronec, M. and Ilavsky, J. (1983) Effect of pyridine on cobalt bromide catalyzed oxidation of *p*-xylene in various solvents. *Oxidation Communications*, **3**, 303.

37 Nowicki, N.R. and Lowry, J.D. (1990) (Amoco), US Patent 4 892 970.

38 Holliday, R.L., Jong, B.W.M. and Kolis, J.W. (1998) Organic synthesis in subcritical water. Oxidation of alkylaromatics, *Journal of Supercritical Fluids*, **12** 1255.

39 Hamley, P.A., Ilkenhans, T., Webster, J.M., Garcia-Vedugo, E., Vernardou, E., Clarke, M.J., Auerbach, R., Thomas, W.B., Whiston, K. and Poliakoff, M. (2002) Selective partial oxidation in supercritical water: the continuous generation of terephthalic acid from *para*-xylene in high yield. *Green Chemistry*, **4**, 235–238.

40 Garcia-Verdugo, E., Vernardou, E., Thomas, W.B., Whiston, K., Partenheimer, W., Hamley, P.A. and Poliakoff, M. (2004) Is it possible to achieve highly selective oxidations in supercritical water? Aerobic oxidation of methylaromatic compounds. *Advanced Synthesis and Catalysis*, **346**, 307.

41 Garcia-Verdugo, E., Fraga-Dubreuil, J., Hamley, P.A., Thomas, W.B., Whiston, K. and Poliakoff, M. (2005) Simultaneous continuous partial oxidation of mixed xylenes in supercritical water. *Green Chemistry*, **7**, 294–300.

42 Fraga-Dubreuil, J. and Poliakoff, M. (2006) Organic reactions in high-temperature and supercritical water. *Pure and Applied Chemistry*, **78**, 1791–1982.

43 Dunn, J.B. and Savage, P.E. (2002) Terephthalic acid synthesis in high-temperature liquid water. *Industrial & Engineering Chemistry Research*, **41**, 4460.

44 Dunn, J.B. Urquhart, D.I. and Savage, P.E. (2002) Terephthalic acid synthesis in supercritical water. *Advanced Synthesis and Catalysis*, **341**, 385–392.

45 Dunn, J.R. and Savage, P.E. (2005) High-temperature liquid water: a viable medium for terephthalic acid synthesis. *Environmental Science & Technology*, **39**, 5427.

46 Dunn, J., Savage, P. and Yu, J. (2006) *Combustion Science and Technology*, Recent advances in catalytic oxidation in supercritical water, **178**, 443–465.

47 Kim, Y.-L., Chung, S.J., Kim, J.-D., Lim, J.S., Lee, Y.-W. and Yi, S.-C. (2002) Uncatalyzed partial oxidation of *p*-xylene and supercritical water. *Reaction Kinetics and Catalysis Letters*, **77**, 35–43.

48 Kim, Y.L., Kim, J.D., Lim, J.S., Lee, Y.W. and Yi, S.C. (2002) Reaction pathway and kinetics for uncatalyzed partial oxidation of *p*-xylene in sub- and supercritical water. *Industrial & Engineering Chemistry Research*, **71**, 5576–5583.

49 Partenheimer, W. (2003) The effect of zirconium in metal/bromide catalysts on the autoxidation of *p*-xylene. Part I. Activation and changes in benzaldehyde intermediate formation *Journal of Molecular Catalysis*, **206**, 105–119.

50 Partenheimer, W. (2003) The effect of zirconium in metal/bromide catalysts on the autoxidation of *p*-xylene. Part II. The effect in Co/metal/Br catalysts on manganese(IV) formation and precipitation with pyromellitic acid. *Journal of Molecular Catalysis*, **206**, 131–144.

51 Chen, Y., Fulton, J.L. and Partenheimer, W. (2005) XAFS study of hydration and ion pairing in ambient aqueous $MnBr_2$ solutions. *Journal of Solution Chemistry*, **4**, 993.

52 Chen, Y., Fulton, J.L. and Partenheimer, W. (2005) The structure of the homogeneous oxidation catalyst, $Mn(II)-Br(-I)_x$, in supercritical water: An X-ray absorption fine structure study. *Journal of the American Chemical Society*, **127**, 14085.

53 Sawada, K., Onoda, T. and Suzuki, T. (1983) Bromo-complexes of Co(II) in acetone. *Journal of The Chemical Society-Dalton Transactions*, 1565.

54 Gray, H.B. and Langford, C.H. (1968) *Chemical & Engineering News*, **46**, 68.

55 Jones, G.H. (1979) *p*-Xylene autoxidation studies. Oxidation Co(II) and manganese (II) acetates by peracids. *Journal of the Chemical Society. Chemical Communications*, 536.

56 Popov, A.I. (1970) in *The Chemistry of Nonaqueous Solvents III* (ed. J.J. Lagowski), Academic Press, New York. p. 214.

57 Sawada, K. and Tanaka, M. (1973) *Journal of Inorganic & Nuclear Chemistry*, **35**, 2455.

58 Bermejo, M.D. and Cocero, M.J. (2006) Supercritical water oxidation: a technical review. *AIChE Journal*, **52**, 3933–3951.